

491
2
11
A82X
NH

SILURIAN CYCLES

LINKAGES OF DYNAMIC STRATIGRAPHY WITH ATMOSPHERIC, OCEANIC, AND TECTONIC CHANGES

EDITED BY ED LANDING AND MARKES JOHNSON



JAMES HALL CENTENNIAL VOLUME

NEW YORK STATE MUSEUM

SILURIAN CYCLES

Account of some new or little
known species of fossils from
rocks of the age of the Niagara
Group.

By James Hall,
Geologist of the State of New-York.

THE UNIVERSITY OF THE STATE OF NEW YORK

Regents of The University

CARL T. HAYDEN, <i>Chancellor</i> , A.B., J.D.	Elmira
LOUISE P. MATTEONI, <i>Vice Chancellor</i> , B.A., M.A., Ph.D.	Bayside
JORGE L. BATISTA, B.A., J.D.	Bronx
J. EDWARD MEYER, B.A., LL.B.	Chappaqua
R. CARLOS CARBALLADA, <i>Chancellor Emeritus</i> , B.S.	Rochester
ADELAIDE L. SANFORD, B.A., M.A., P.D.	Hollis
DIANE O'NEILL MCGIVERN, B.S.N., M.A., Ph.D.	Staten Island
SAUL B. COHEN, B.A., M.A., Ph.D.	New Rochelle
JAMES C. DAWSON, A.A., B.A., M.S., Ph.D.	Peru
ROBERT M. BENNETT, B.A., M.S.	Tonawanda
ROBERT M. JOHNSON, B.S., J.D.	Lloyd Harbor
PETER M. PRYOR, B.A., LL.B., J.D., LL.D.	Albany
ANTHONY S. BOTTAR, B.A., J.D.	Syracuse
MERRYL H. TISCH, B.A., M.A.	New York
HAROLD O. LEVY, B.S., M.A. (Oxon.), J.D.	New York
ENA L. FARLEY, B.A., M.A., Ph.D.	Brockport

President of The University and Commissioner of Education

RICHARD P. MILLS

Chief Operating Officer

RICHARD H. CATE

Deputy Commissioner for Cultural Education

CAROLE F. HUXLEY

Assistant Commissioner for State Museum

LOUIS D. LEVINE

The State Education Department does not discriminate on the basis of age, color, religion, creed, disability, marital status, veteran status, national origin, race, gender, genetic predisposition or carrier status, or sexual orientation in its educational programs, services and activities. Portions of this publication can be made available in a variety of formats, including braille, large print or audio tape, upon request. Inquiries concerning this policy of nondiscrimination should be directed to the Department's Office for Diversity, Ethics, and Access, Room 152, Education Building, Albany, NY 12234. Requests for additional copies of this publication may be made by contacting Publications Sales N.Y.S. Museum, Albany, N.Y. 12230.

SILURIAN CYCLES

LINKAGES OF DYNAMIC STRATIGRAPHY WITH
ATMOSPHERIC, OCEANIC, AND TECTONIC CHANGES

JAMES HALL CENTENNIAL VOLUME

Edited by

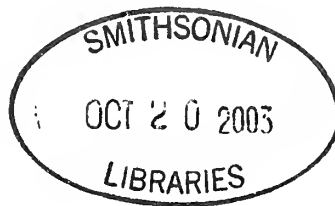
Ed Landing

*Geological Survey, New York State Museum
The State Education Department, Albany, New York 12230*

and

Markes E. Johnson

*Department of Geosciences, Williams College
Williamstown, Massachusetts 01267*



New York State Museum Bulletin 491

THE UNIVERSITY OF THE STATE OF NEW YORK
THE STATE EDUCATION DEPARTMENT

Copyright © 1998 The New York State Education Department

Printed in the United States of America

Copies may be ordered from:

Publication Sales
New York State Museum
Albany, New York 12230
Phone: (518) 449-1404

Library of Congress Catalog Card Number: 98-60308

ISSN: 0278-3355

ISBN: 1-55557-206-5

Typesetting: Cathleen Collins

This book is printed on acid-free paper.

Cover: James Hall (1811–1898) in 1856, from lithograph by Swinton; courtesy of New York State Historical Survey photographic collection.

Half title page: Copy of James Hall's handwritten manuscript "Relations of the Niagara Group with the Leclaire and Racine Limestones of Iowa and Wisconsin, and the Galt or Guelph Limestone of Canada West (1867, Twentieth Annual Report of the State Cabinet of Natural History); courtesy of New York State Archives.

CONTENTS

PREFACE	
<i>Markes E. Johnson and Ed Landing</i>	vii
PART I: PHYSICAL EVIDENCE FOR SILURIAN EUSTASY	
CALIBRATING SILURIAN EUSTASY BY EROSION AND BURIAL OF COASTAL PALEOTOPOGRAPHY	
<i>M.E. Johnson, Rong J.-y., and S. Kershaw</i>	3
ORDOVICIAN-SILURIAN GLACIATIONS AND GLOBAL SEA-LEVEL CHANGES	
<i>M.V. Caputo</i>	15
SILURIAN SEA-LEVEL CHANGE AT ARISAIG, NOVA SCOTIA: COMPARISON WITH THE STANDARD EUSTATIC PATTERN	
<i>R.K. Bambach</i>	27
EARLY SILURIAN STRATIGRAPHIC SEQUENCES OF EASTERN WISCONSIN	
<i>M.T. Harris, J.J. Kuglisch, R. Watkins, D.P. Hegrenes, and K.R. Waldhuetter</i>	39
EARLY SILURIAN STRATIGRAPHIC SEQUENCES OF THE EASTERN GREAT BASIN (UTAH AND NEVADA)	
<i>M.T. Harris and P.M. Sheehan</i>	51
EUSTATIC FLUCTUATIONS IN THE EAST SIBERIAN BASIN (SIBERIAN PLATFORM AND TAYMYR PENINSULA)	
<i>Yu.I. Tesakov, M.E. Johnson, N.N. Predtetchensky, V.G. Khromych, and A.Ya. Berger</i>	63
SILURIAN CYCLES, TEMPESTITE DEPOSITS, AND PROXIMALITY ANALYSIS	
<i>B.G. Baarli</i>	75
EARLY SILURIAN CONDENSED HORIZONS, IRONSTONES, AND SEQUENCE STRATIGRAPHY IN THE APPALACHIAN FORELAND BASIN	
<i>C.E. Brett, B.G. Baarli, T.M. Chowns, E. Cotter, S. Dreise, and M.E. Johnson</i>	89
TECTONIC COMPONENTS IN SILURIAN CYCLICITY: EXAMPLES FROM THE APPALACHIAN BASIN AND GLOBAL IMPLICATIONS	
<i>F.R. Ettensohn and C.E. Brett</i>	145
PART II: TEMPORAL FAUNAL PATTERNS RELATED TO EUSTASY	
GLOBAL DIVERSITY AND SURVIVORSHIP PATTERNS OF SILURIAN GRAPTOLOIDS	
<i>M.J. Melchin, T.N. Koren', and P. Štorch</i>	165
RECURRENT SILURIAN-LOWEST DEVONIAN CEPHALOPOD LIMESTONES OF GONDWANAN EUROPE AND PERUNICA	
<i>Jiri Kříž</i>	183
SILURIAN CEPHALOPOD BEDS FROM NORTH ASIA	
<i>Olga K. Bogolepova</i>	199
SPECIES DIVERSITY OF SILURIAN GASTROPODS RELATED TO ABIOTIC EVENTS	
<i>A.P. Gubanov</i>	209
SILURIAN-DEVONIAN TRILOBITE EVOLUTION AND DEPOSITIONAL CYCLICITY IN THE ALTAI-SALAIR REGION, WESTERN SIBERIA	
<i>E.A. Yolkin</i>	215

PART III: SHORT-TERM CYCLES

SILURIAN COASTAL SEDIMENTATION AND METER-SCALE CHANGES IN THE APPALACHIAN FORELAND BASIN OF PENNSYLVANIA <i>Edward Cotter</i>	229
SILURIAN OCEANIC EVENTS: SUMMARY OF GENERAL CHARACTERISTICS <i>Lennert Jeppsson</i>	239
SILURIAN OCEANIC EPISODES: EVIDENCE FROM CENTRAL NEVADA <i>William B.N. Berry</i>	259
SILURIAN REEF EPISODES, CHANGING SEASCAPES, AND PALEOBIOGEOGRAPHY <i>F.R. Brunton, L. Smith, O.A. Dixon, P. Copper, S. Kershaw, and H. Nestor</i>	265

PART IV: ISOTOPE STUDIES

HIGH-RESOLUTION SILURIAN $^{87}\text{Sr}/^{86}\text{Sr}$ RECORD: EVIDENCE OF EUSTATIC CONTROL OF SEAWATER CHEMISTRY? <i>S.C. Ruppel, E.W. James, J.E. Barrick, G.S. Nowlan, and T.T. Uyeno</i>	285
CORRELATION OF CARBON ISOTOPE EVENTS AND ENVIRONMENTAL CYCLICITY IN THE EAST BALTIC SILURIAN <i>D. Kaljo, T. Kiipli, and T. Martma</i>	297
EARLY SILURIAN CARBON AND OXYGEN STABLE-ISOTOPE STRATIGRAPHY OF ESTONIA: IMPLICATIONS FOR CLIMATE CHANGE <i>R.J. Heath, P.J. Brenchley, and J.D. Marshall</i>	313

PREFACE

MARKES E. JOHNSON AND ED LANDING

*Department of Geosciences, Williams College, Williamstown, MA 01267, and
New York State Geological Survey, The State Education Department, Albany, NY 12230*

This volume features part of the proceedings of the Second International Symposium on the Silurian System, which was held at the University of Rochester in Rochester, N.Y. on August 4–9, 1996. Convened under the primary sponsorship of the Subcommittee on Silurian Stratigraphy (a subdivision of the International Commission on Stratigraphy under the International Union of Geological Sciences), the Rochester conference attracted 75 participants from sixteen countries that represented all continents where Silurian strata are extensively exposed. A poster session and workshop on “Silurian Cycles: Linkages of Dynamic Processes in Atmosphere and Oceans” began the program. A broad range of evidence for eustatic changes, glacial episodes, geochemical cycles, extinction events, and changes in faunal diversity was exhibited, and their possible interconnections were debated during these sessions. The reports collected in this volume represent seventeen of the original posters presented at the Rochester conference, supplemented by four contributions on related topics that were solicited to round out the collection.

Geologists and paleontologists who study a wide variety of Silurian global cycles have been especially active during the last decade. The idea for a workshop to explore the form, timing, and interrelationships of a variety of Silurian global cycles was born from a feeling of frustration and hope. Lack of communication among the many researchers in this rapidly expanding area of research was the source of frustration. Hope was inspired by the opportunity to take advantage of this venue, the Second Symposium on the Silurian System, to assemble a diverse field of advocates in order to seek a common ground on the principal patterns of cyclicity in Silurian strata.

Part One of this volume assembles nine papers that treat the physical evidence for Silurian eustasy. The Brazilian geologist Mario Caputo has a long-held interest in the mid-Paleozoic glaciations of South America (Caputo and Crowell, 1985; Grahn and Caputo, 1992). His contribution to this volume provides an important review of hard-to-come-by data on Silurian glacial and interglacial stratigraphy from that sector of Gondwana. Ed Cotter and Carlton Brett are interested in Lower Silurian Clinton

ironstones and new applications of sequence stratigraphy in the northern Appalachian foreland (Cotter and Link, 1993; Brett et al., 1990). The article by Brett, Cotter, and others in this volume summarizes and updates what is known about the cyclicity and correlation of these ironstones from Alabama to New York. Steve Driese and his students injected into Silurian stratigraphy the concept of proximity analysis, in which the sedimentology of nearshore and offshore accumulations are contrasted (Easthouse and Driese, 1988; Bolton, 1990; Dorsch et al., 1994). Gudveig Baarli also applied this technique to Silurian sequences in southern Norway and Alabama (Baarli, 1988; Baarli et al., 1992). Her contribution in this volume provides an overview on proximity analysis with dual emphasis on the paleogeography of Silurian storm patterns and global cycles of sea-level change. Markes Johnson has pursued research on the global identity of Silurian sea-level cycles for many years. His recent summary on Silurian eustasy (Johnson, 1996) is corroborated and expanded through several contributions to this volume by Richard Bambach, Mark Harris and others, and Yuri Tesakov and others. Coastal paleotopography, a key to calibration of Silurian eustasy, brings a completely new approach to this complicated topic (Johnson et al., this volume). It should never be doubted that eustasy and tectonics are two competing sources of sea-level change. The paper by Frank Effensohn and Carlton Brett examines the global implications of tectonic changes in sea-level during the Silurian.

Part Two of this volume draws attention to the connection between temporal faunal patterns and Silurian eustasy. Reports on graptolites (Michael Melchin and others), cephalopods (Juri Kříž and Olga Bogolepova), gastropods (Alexander Gubanov), and trilobites (Evgeny Yolkin) lend a diverse taxonomic coverage to this topic.

Part Three of this volume shifts focus to short-term cycles, sometimes referred to as Milankovitch cycles or orbital-forcing cycles (House and Gale, 1995). Lennart Jeppsson and other colleagues have launched an initiative that relates climate-driven, oceanographic cycles to patterns of Silurian conodont extinction (Jeppsson, 1990;

Aldridge et al., 1994; Jeppsson et al., 1994). In this volume, Jeppsson provides a detailed summary of the short-term climatic and oceanographic changes he believes account for extinctions among conodonts and other taxa. Although the precise dating of these events in absolute years remains problematic, orbital forcing may be the best explanation. Related papers by W.B.N. Berry, and by Frank Brunton and others, assemble stratigraphic data in support of Jeppsson's oceanic episodes. Edward Cotter examines meter-scale rhythms recorded by Silurian coastal sediments that were deposited in the Appalachian foreland basin of Pennsylvania.

Once considered the exclusive domain of Quaternary geologists, technology has pushed open the window so far on isotope studies that even geochemists fixated on the Paleozoic may participate in the search for meaningful patterns. Recent ground-breaking reports on the Silurian by Bernd Wenzel and Michael Joachimski and Stephen Ruppel and his colleagues have attracted much attention (Wenzel and Joachimski, 1996; Ruppel et al., 1996). The fourth and final part of this volume draws together three papers that attempt to search for congruences between Silurian isotope patterns and those patterns attributed to glacial episodes, oceanographic episodes, and eustasy. Strontium data from sections in Europe and North America are reviewed by Stephen Ruppel and his colleagues. Whole-rock carbon data from the Silurian of Estonia is treated by Dimitri Kaljo and colleagues, and carbon and oxygen data of shelly material from Estonia is treated by Rachel Heath and colleagues.

No single individual or organization has previously attempted to sort out such a large corpus of research on cyclic patterns preserved in Silurian strata. Before issues of cause and linkage may be explored, it is necessary to determine the degree to which the various cycles are coeval. With its primary mission now largely accomplished in defining the Silurian series and stages by means of "golden spikes" at stratotype localities, the Subcommittee on Silurian Stratigraphy is at an excellent point in its history to encourage the charting of various stratigraphic cycles on a standard time scale. This role is further enhanced by the Subcommittee's adoption of a unified zonal scheme for graptolites, conodonts, and chitinozoans (Nolan, 1995; Koren' et al., 1996). Thus, a major source of frustration and potential confusion has already been eased by broad consensus on the definition of biostratigraphic boundaries within the Silurian System.

JAMES HALL MEMORIAL VOLUME

Following the tradition of the First International Symposium on the Silurian System, which was named in honor

of Roderick Murchison 150 years after publication of *The Silurian System* (1839), the Rochester symposium was designated to honor James Hall, the prominent 19th-century geologist and paleontologist from New York State and a contemporary of Roderick Murchison. It was largely under the zealous leadership of James Hall that the nomenclature of the Silurian System was promulgated and applied across a wide swath of the United States that extended from New York State through the Great Lakes region to the upper Mississippi River valley. Largely remembered as the first State Paleontologist of New York, Hall also served at various times as the State Geologist of Wisconsin and Iowa.

By any measure, Hall's monumental contribution was the 4,320 pages of taxonomic description accompanied by 980 illustrated plates contained in thirteen quarto volumes belonging to the *Paleontology of New York*. It was on September 1, 1846, 150 years before the convening of the Rochester meeting, that James Hall submitted to the governor of New York State, Silas Wright, the first of these famous volumes. The second volume, published in 1852, is devoted to the Silurian of New York State. The final volume was issued in 1894, and marks the conclusion of one of the longest-running contests of willpower between an often reticent legislature and a public servant determined to win state funding for science. The publication of this volume in 1998 takes place 100 years after the death of James Hall, the founder of the New York State Museum. Hence this volume, New York State Museum Bulletin 491, is dedicated to James Hall.

Given the worldwide economic mindset for corporate down-sizing and the political pressures for budget-trimming that have curbed spending on basic scientific research—in particular, in geology—James Hall may well be the obvious choice for canonization as "patron saint" of symposium conveners and volume organizers, who desire to promote international research in stratigraphic geology. James Hall prevailed through good times and lean times, and so can we if we are persistent and stubborn enough.

ACKNOWLEDGMENTS

Although the National Science Foundation encouraged the workshop that led to this volume, it could not help fund it. The Rochester symposium could not have taken place without the generous support of Williams College (through the President's Office) and timely grants from the Petroleum Research Fund of the American Chemical Society (through its Scientific Education Program), Saga Petroleum of Norway, and the International Science Foundation (through its Logovaz Conference Travel

Grant Program). We hope the end product of this volume will justify the financial faith expended on our collective behalf. J.C. Finley is gratefully acknowledged for the line editing of this volume. L. Van Aller Hernick obtained the negative for the portrait of James Hall on the cover of this volume from the New York State Historical Survey collections. K.E. Bartowski provided the copy of James Hall's hand-written manuscript used on the half-title page from the collections of the New York State Archives.

REFERENCES

- ALDRIDGE, R.J., L. JEPSSON, AND K.J. DORNING. 1993. Early Silurian oceanic episodes and events. *Journal of the Geological Society*, London, 150:501–513.
- BAARLI, B.G. 1988. Bathymetric co-ordination of proximity trends and level bottom communities: a case study from the Lower Silurian of central Oslo region, Norway. *Palaos*, 3:577–587.
- , S. BRANDE, AND M.E. JOHNSON. 1992. Proximity trends in the Red Mountain Formation (Lower Silurian) of Birmingham, Alabama. *Oklahoma Geological Survey Bulletin*, 145:1–17.
- BRETT, C.E., W.M. GOODMAN, AND S.T. LODUCA. 1990. Sequences, cycles, and basin dynamics in the Silurian of the Appalachian foreland basin. *Sedimentary Geology*, 69:191–244.
- BOLTON, J.C. 1990. Sedimentological data indicate greater range of water depths for *Costistricklandia litrata* in the Southern Appalachians. *Palaos*, 5:371–374.
- CAPUTO, M.V., AND J.C. CROWELL. 1985. Migration of glacial centers across Gondwana during Paleozoic Era. *Geological Society of America Bulletin*, 96:1020–1036.
- COTTER, E., AND J.E. LINK. 1993. Deposition and diagenesis of Clinton ironstones (Silurian) in the Appalachian Foreland Basin of Pennsylvania. *Geological Society of America Bulletin*, 105:911–922.
- DORSCH, J., R.K. BAMBAÇH, AND S.G. DRIESE. 1994. Basin-rebound origin for the "Tuscarora unconformity" in southwestern Virginia and its bearing on the nature of the Taconic Orogeny. *American Journal of Science*, 294:237–255.
- EASTHOUSE, K.A., AND S.C. DRIESE. 1988. Paleobathymetry of a Silurian shelf system: applications of proximity trends and ichnofacies distributions. *Palaos*, 3:473–486.
- GRAHN, Y., AND M.V. CAPUTO. 1992. Early Silurian glaciations in Brazil. *Palaogeography, Palaeoclimatology, Palaeoecology*, 99:9–15.
- HOUSE, M.R., AND A.S. GALE (eds.). 1995. *Orbital Forcing, Timescales, and Cyclostratigraphy*. Geological Society Special Publication No. 85, 210 p.
- JEPSSON, L. 1990. An oceanic model for lithological and faunal changes, tested on the Silurian record. *Journal of the Geological Society*, London, 147:663–674.
- , V. VIIRA, AND P. MANNIC. 1994. Silurian conodont-based correlations between Gotland (Sweden) and Saaremaa (Estonia). *Geological Magazine*, 131:201–218.
- JOHNSON, M.E. 1996. Stable cratonic sequences and a standard for Silurian eustasy, p. 203–211. *In* B.J. Witzke, G.A. Ludvigson, and J.E. Day (eds.), *Paleozoic Sequence Stratigraphy: Views from the North American Craton*. Geological Society of America Special Paper 306.
- KOREN', T.N., A.C. LENZ, D.K. LOYDELL, M.J. MELCHIN, P. ŠTORCH, AND L. TELLER. 1996. Generalized graptolite zonal sequence defining Silurian time intervals for global paleogeographic studies. *Lethaia*, 29:59–60.
- NOWLAN, G.S. (ed). 1995. Left hand column for correlation charts. *Silurian Times*, 3:7, 8.
- RUPPEL, S.C., E.W. JAMES, J.E. BARRICK, G. NOWLAN, AND T.T. UYENO. 1966. High-resolution $^{87}\text{Sr}/^{86}\text{Sr}$ chemostratigraphy of the Silurian: implications for event correlation and strontium flux. *Geology*, 24:831–834.
- WENZEL, B., AND M.M. JOACHIMSKI. 1996. Carbon and oxygen isotopic composition of Silurian brachiopods (Gotland/Sweden): paleoceanographic implications. *Palaogeography, Palaeoclimatology, Palaeoecology*, 122:143–166.

PART I: PHYSICAL EVIDENCE FOR SILURIAN EUSTASY

CALIBRATING SILURIAN EUSTASY AGAINST THE EROSION AND BURIAL OF COASTAL PALEOTOPOGRAPHY

MARKES E. JOHNSON¹, RONG JIA-YU², AND STEPHEN KERSHAW³

¹Department of Geosciences, Williams College, Williamstown, Massachusetts 01267,

²Nanjing Institute of Geology and Palaeontology, Academia Sinica, Nanjing, 21008 China, and

³Department of Geography and Earth Sciences, Brunel University, Borough Road, Isleworth, Middlesex, TW7 5DU, U.K.

ABSTRACT—Rocky shores and coastal valleys undergo sub-aerial and/or some degree of intertidal erosion. Burial of coastal topography with rise in sea-level results in the formation of unconformities. If the tectonic component of relative sea-level change can be identified, the minimum eustatic rise may be determined from the maximum topographic relief covered by marine strata. Data of this kind are reviewed for a dozen Silurian rocky-shore localities and from four regions that preserve Silurian paleovalleys. Palecontinents on which these coastal features are known include Gondwana, Laurentia, Avalonia, Baltica, and North and South China.

All purported global rises in Silurian sea-level are associated with burial of Silurian coastal topography. The best documented examples are for the Rhuddanian (+70 m) and Aeronian (+65 m) events in the Early Silurian. Other unconformities that resulted from onlap across Silurian rocky shores are correlated with the early and late Telychian, middle Sheinwoodian, early Gorstian, middle Ludfordian, and Pridoli transgressions. Available descriptions of these features are less informative with regard to the extent of paleotopographic relief. The regional relief of karst surfaces buried during the late Llandovery and early Pridoli in Laurentia is 30–53 m. Improved understanding of this topic relies on more thorough outcrop observations, greater use of subsurface data, and better dating of the time of formation of rocky shores and paleovalleys.

three highstands and three lowstands in the Late Silurian (Ludlow and Pridoli Series). These events are regarded as eustatic in nature, based primarily on carbonate sequences from relatively stable cratonic platforms, where the preservation of marine invertebrate communities shows repetitive stratigraphic patterns. By comparison with global sea-level curves proposed for most other intervals in the Paleozoic, these events are well-dated and correlated with internationally accepted definitions of Silurian series and stage boundaries (Holland and Bassett, 1989).

More difficult to establish than the relative age of a given event, however, is the actual vertical extent of Silurian sea-level rise or fall. Typical estimates of absolute water depths under which key Silurian communities lived and died revolve around arguments over associated sedimentary structures, post-mortem development of shell beds, and the depth range of biota as controlled by the diminution of sunlight in sea water (Baarli, 1988; Johnson, 1989; Brett et al., 1993). This report applies an entirely independent method to the determination of absolute water depths of the Silurian sea-level curve. Our approach emphasizes the importance of coastal paleotopography, specifically its erosion during stable or falling sea-level and its burial during rising sea-level.

The two types of paleotopographic elements employed in this study are rocky shorelines and coastal valleys. Both are readily discernible through study of unconformities in the stratigraphic record. The most recent bibliography on ancient rocky shores (Johnson, 1992) lists only seven studies for the Silurian, most of which concern localities in the Welsh Borderland. Several other sources of published information on Silurian rocky shorelines are incorporated herein. A study by McClure (1978) was among the first to describe paleovalleys formed in association with the glaciation and deglaciation of

INTRODUCTION

A global sea-level curve constructed for the Silurian from many localities around the world (Johnson et al., 1991; Johnson and McKerrow, 1991) has been expanded through the entire system (Johnson, 1996). This curve emphasizes five major highstands and five lowstands in the Early Silurian (Llandovery and Wenlock Series) and

Ordovician–Silurian Gondwana. This report, however, utilizes additional localities from the Middle East, as well as other regions in North America and the British Isles, that are only indirectly linked to the effects of Gondwanan glaciation. In all cases, it is the burial of paleotopography that enables determination of the range of local, coastal sea-level change.

USE OF TOPOGRAPHIC MODELS

Coastal topography is affected by a variety of dynamics related to relative fluctuations in sea-level. Several models of these dynamics are shown in Figure 1. The relief of rocky shores or coastal valleys may be eroded and buried when: 1) the land remains tectonically fixed, but global sea-level falls and rises (Figure 1.1); 2) sea-level is fixed, but the land surface is tectonically raised and lowered (Figure 1.2); and 3) minor uplift or subsidence occurs and major eustatic fluctuations occur at the same time (Figure 1.3). Coastal relief may develop, but will only be partly buried when major tectonic uplift is associated with minor eustatic rise (Figure 1.4). As a result, coastal relief may develop, but will not be buried when major tectonic uplift is associated with major eustatic drop, or is balanced against a global rise in sea-level of equal magnitude (Figure 1.5). Important topographic relief is unlikely to develop when minor eustatic fluctuations are associated with major tectonic subsidence of the shoreline (Figure 1.6).

In principle, two or more of these models might operate simultaneously at different places around the planet due to the irregular shape of the geoid (Mörner, 1976) and with differences in vertical tectonic motion in different areas or variations in the geometry of oceans and seas. The strategy of determining global Silurian sea-level fluctuations on the basis of cyclic carbonates from stable cratons (Johnson, 1996) features the model in Figure 1.1, in which tectonism is quiescent over extensively flooded platforms on several paleocontinents. Transgression and burial of coastal topography by marine sediments under such conditions would seem to provide an ideal estimate of absolute changes in water depth. The greatest challenge to overcome, in this case, is proof of tectonic quiescence. In reality, relative change in sea-level at any one time or place is most likely due to some combination of eustatic and tectonic effects (Figure 1.3–1.6). The most convincing situation by which to gauge eustatic change is a variant of the model in Figure 1.3, in which a major eustatic rise drowns coastal topography that is undergoing modest tectonic uplift. The disadvantage in this model is that measurement of eustatic change is obscured by the additive but weaker component of tectonic

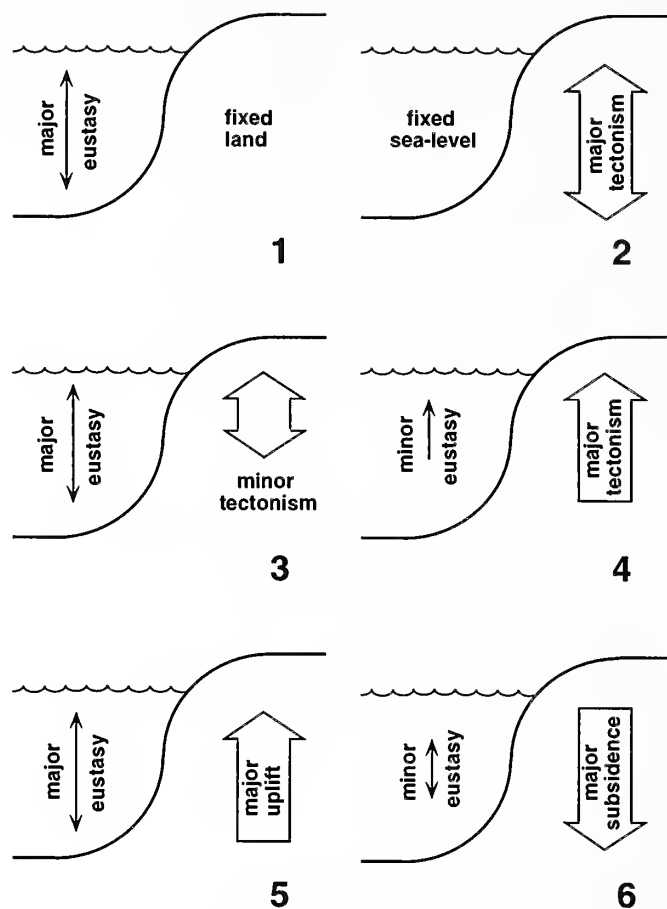


FIGURE 1—Six models (1–6) of the variable dynamics that control fluctuations in relative sea-level, where the two components are eustasy and tectonism. Under ideal conditions (model 1), erosion and burial of coastal topography serve as a measure of eustatic rise when the tectonic component is quiescent. The most favorable condition to measure eustatic rise is that in which a minor but detectable component of tectonic uplift is offset by a major eustatic rise (variant of model 6).

change. The advantage, however, is positive identification and limitation of the role of the tectonic component.

Certain assumptions regarding the development and burial of coastal topography must be made in order to apply the following data to the calibration of Silurian eustasy. Rocky shorelines are considered durable markers of paleoshorelines that form during episodes of relative fall or standstills in sea-level. Rocky shorelines may continue to erode during relative rise in sea-level, but the burial or overstepping of rocky shores by marine sediments is the critical result of a rapid rise in relative sea-level. Similarly, coastal valleys form primarily during episodes of relative sea-level fall when downcutting is stimulated by changes in stream gradient. Coastal valleys are prone to fill with terrestrial sediments during a stillstand in relative sea-level, but ultimately should fill with marine sediments during a rapid rise in relative

TABLE 1—Summary of Silurian coastal topography.

Global event	Feature	Relief	Location	Paleocontinent	Reference
8	Rocky shore	30 m	Ohio	Laurentia	Kahle (1988)
8	Rocky shore	>23 m	Inner Mongolia	North China	Li et al. (1984)
7	Rocky shore	?	Gotland	Baltica	Cherns (1982)
7	Rocky shore	1-2 m	Gotland	Baltica	Keeling & Kershaw (1994)
6	Rocky shore	?	Inner Mongolia	North China	Li et al. (1984)
6	Rocky shore	?	Czech Republic	Perunica	Kříž (1992)
5	Rocky shore	2 m	Gotland	Baltica	Riding & Watts (1991)
4	Rocky shore	53 m	Illinois & Wisconsin	Laurentia	Kluessendorf & Mikulic (1996)
3	Rocky shore	2m	Welsh Borderland	Avalonia	Reading & Poole (1961)
3	Rocky shore	?	Welsh Borderland	Avalonia	Whittard (1932)
2	Paleovalley	65 m	WeBh Borderland	Avalonia	Ziegler et al. (1968)
2	Rocky shore	63 m	Guizhou Province	South China	Rong & Johnson (1996)
1	Paleovalley	41 m	Iowa	Laurentia	Brown & Whitlow (1963)
1	Paleovalley	70 m	Iowa & Illinois	Laurentia	Du Bois (1945); Parker (1971)
1	Paleohill	70 m	Dalarna	Baltica	Brenchley & Newall (1980)
1	Paleovalley	275 m	Saudi Arabia	Gondwana	Vaslet (1990)
1	Paleovalley	50 m	Jordan	Gondwana	Powell et al. (1994)
1	Paleovalley	10m	Ireland	Avalonia?	Parkes (1993)
1	Rocky shore	?	Wales	Avalonia	Cave & Dixon (1993)

sea-level. Calibrating the depth gradient of the global Silurian sea-level curve is essentially a matter of correlating specific unconformities with the given lowstands or onlap events considered to be eustatic in origin. Biostratigraphic precision relies on the ability of the onlap sediments to preserve key zone fossils, and such precision is likely to be variable. Given an appropriate biostratigraphic correlation, the depth to which coastal topographic relief is buried by onlapping marine sediments during a global event provides only a minimum estimate of sea-level rise. Multiple sources of comparable data from different paleocontinents increase the reliability of the eustatic calibration.

LITERATURE REVIEW

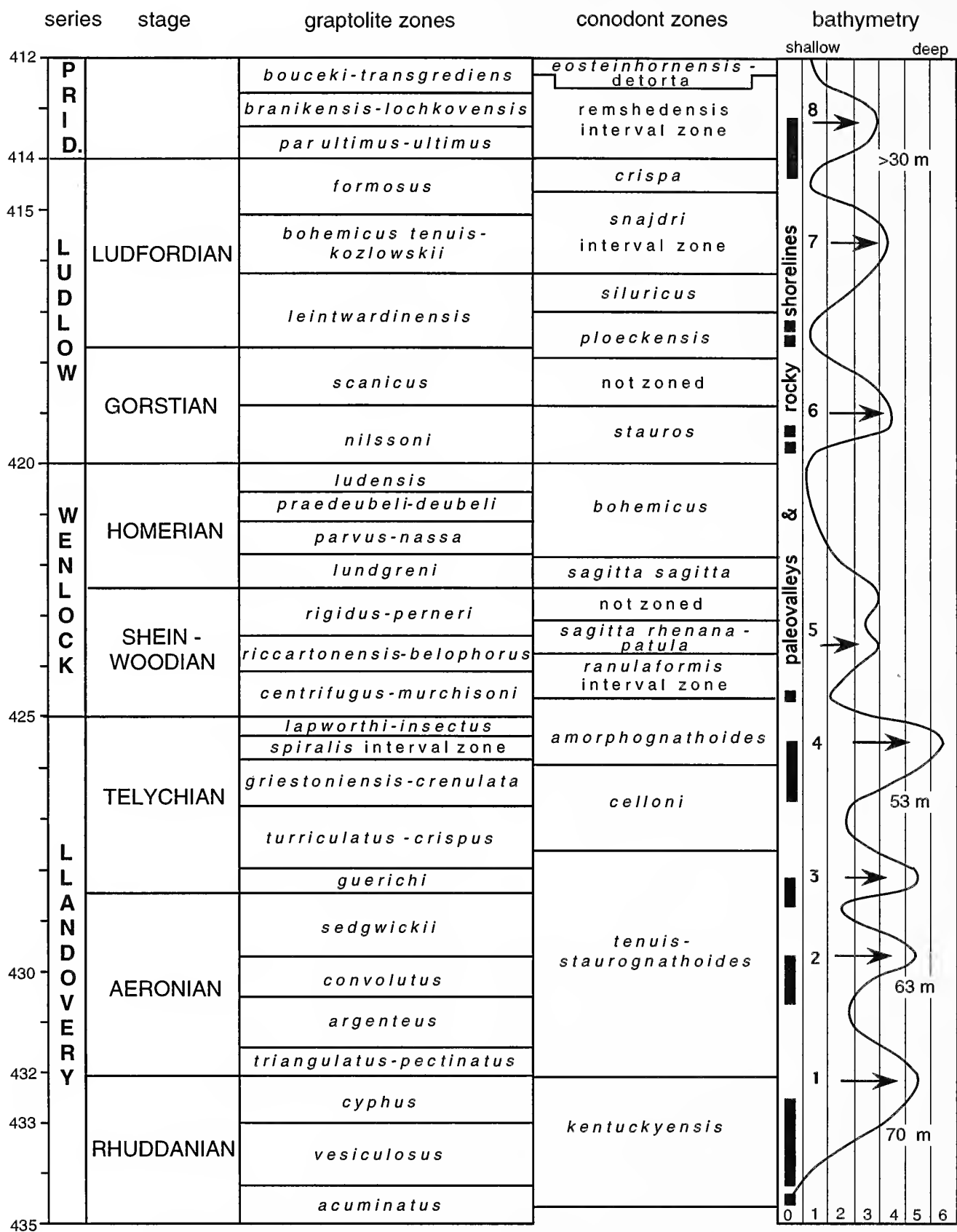
The Silurian sea-level curve of Johnson (1996) is modified in Figure 2, with additional range lines that mark the association of coastal paleotopography with eustatic events. Data from specific sites that preserve paleotopography are related to each of eight different highstands in sea-level (or the immediately preceding lowstand). References to the original literature are provided in Table 1. These data are summarized below, with a division of the Silurian System into its lower and upper parts and their component stages.

The Lower Silurian consists of the Llandovery and Wenlock Series (Holland and Bassett, 1989). The Llandovery records four eustatic highstands that correspond

to events preserved in the Rhuddanian, Aeronian, lower Telychian, and upper Telychian Stages (Johnson, 1996; Figure 2). The Wenlock contains evidence of a pair of closely related but minor highstands at the middle and top of the Sheinwoodian Stage.

RHUDDANIAN TRANSGRESSIVE EVENT.—Paleovalleys associated with the Ordovician–Silurian unconformity provide a wealth of topographic information. McClure (1978, p. 323) mapped the Jebel Sarah paleovalley in north-central Saudi Arabia over a distance of 25 km. Although he indicated that this valley cuts through a thick sequence of Ordovician (Arenig–Caradoc Series) strata, he did not attempt to quantify topographic relief. Vaslet (1990) described eighteen additional valleys associated with the Jebel Sarah paleovalley, some up to 50 km in length. The paleovalley floors are often glacially striated. Assigned to the Jebel Sarah Formation, the valley fill has a maximum thickness of 300 m in its downstream part, and consists of medium-grained, cross-bedded sandstone interbedded with layers of reworked tillite. A second glacial advance may be represented by the 54 m-thick Hawban Member at the top of the Jebel Sarah Formation. An assemblage of unspecified Early Silurian acritarchs and chitinozoans is said to occur in the upper part of the Jebel Sarah Formation (Vaslet, 1990, p. 155), which suggests that the Ordovician–Silurian boundary occurs within this unit.

A cross-section of paleovalleys drawn to scale by Vaslet (1990, p. 152) may be open to interpretation, but



the relief appears to have been no less than 275 m. Similar Late Ordovician–Early Silurian glacio-fluvial deposits are documented in southern Jordan by Powell et al. (1994). The minimum known topographic relief of these valleys is 50 m. Clearly, downcutting of the Saudi Arabian and Jordanian valleys occurred during one or more episodes of Late Ordovician glaciation. Partial infill by terrestrial sediments also took place during the Late Ordovician.

The far-reaching effect of lowered sea-level due to the Late Ordovician glaciations is placed in perspective by considering paleovalleys that formed on paleocontinents remote from Gondwana. In North America, the Upper Ordovician Maquoketa Shale is a marine unit that is widespread in the subsurface of Iowa and Illinois. Whitlow and Brown (1963, p. C11) studied Ordovician–Silurian boundary outcrops in Dubuque County, eastern Iowa, where they reported “an ancient erosion surface on the Maquoketa Shale” with 41 m of relief. According to isopach maps of the Maquoketa Shale for Illinois and Iowa (Du Bois, 1945; Parker, 1971), maximum thickness of the formation is somewhat greater than 100 m and minimum thickness (exclusive of post-Silurian erosion) is somewhat more than 30 m. This means that the maximum relief of paleovalleys that were subaerially eroded into the Maquoketa Shale and subsequently capped by Silurian marine sediments was on the order of 70 m. In Iowa, the largest valleys appear to have been 100 km in length (see Parker, 1971, map 1).

No paleovalleys are known at the Ordovician–Silurian boundary in western New York, although the Cherokee Unconformity is a well-defined erosion surface that stretches 500 km west from the Middle Ordovician–Silurian Taconic orogen (Brett et al., 1990; Goodman and Brett, 1994). The Silurian of western New York is divided into six major sequences, the first of which includes the 42 m-thick Medina Group, which is truncated by the Cherokee Unconformity (Brett et al., 1990, p. 201). Compaction of muddy sediments is not considered a factor here, nor is uplift of the Taconic orogen, and the actual rise in sea-level during deposition of the Rhuddannian Medina Group was certainly more than 42 m.

Paleokarst formed on the top of the Upper Ordovician Portrane Limestone Formation is unconformably

overlain by purported Wenlock strata on the coast of eastern Ireland (Parkes, 1993). A paleorelief of 10 m is attributed to erosion during a drop in sea-level with the Late Ordovician glaciation of Gondwana.

A rocky shore of Rhuddanian Age occurs in central Wales at Welshpool, where the Silurian Powis Castle Conglomerate rests against columnar-jointed, igneous rocks of an oligoclase–trachyte composition (Cave and Dixon, 1993). It is evident that the igneous rock was the source of cobble- to boulder-sized clasts in this Lower Silurian conglomerate. No information is available on the thickness of the conglomerate or the topographic relief of the igneous cliffs.

Karstified rocky islands formed on the Boda Limestone were subaerially exposed in Dalarna, southern Sweden, at the end of the Ordovician. These features probably persisted as topographic highs during the earliest Silurian. Fissures reach down to a depth of more than 30 m from the top of the mound-like islands. They exhibit calcite linings that resemble speleothem drip-stone (Brenchley and Newall, 1980). If the tops of the mounds were at or just below wave base prior to the Late Ordovician regression, “the total fall in sea level at the end of the Ordovician would have been in the order of 70 m” (Brenchley and Newall, 1980, p. 34).

A maximum of 70 m of eustatic fall and rise appears to be a reasonable estimate for the Ashgill regressive and Rhuddanian transgressive events in North America and Scandinavia. Ordovician–Silurian paleovalleys in the Middle East show much more topographic relief than the hills on the Maquoketa Formation in Laurentia or the Boda Limestone mounds of Baltica, but ice loading on Gondwana and isostatic rebound was likely to have been a contributing factor.

AERONIAN TRANSGRESSIVE EVENT.—The second Silurian highstand in sea-level is recorded in the Aeronian, and is coincident with the lower *Monograptus sedgwickii* Zone (graptolites) (Johnson, 1996; Figure 2). An example of a small Ordovician–Silurian paleovalley cut during this global event is Hope Valley in the Welsh Borderland (Whittard, 1932, p. 893–895; Ziegler et al., 1968, p. 743; Bridges, 1975, p. 80). The 1 km-wide valley contains remnants of the Silurian Venusbank Formation, which sits unconformably at various elevations on the Lower Ordovician (Llanvirn) Hope Shales. Now exhumed to its original pre-Aeronian dimensions, the modern valley retains enough of the Venusbank Formation to suggest that this formation filled the valley to a depth of 65 m. Fossils in this sandstone unit include brachiopods transitional between *Stricklandia lens intermedia* and *S. lens progressa* (Ziegler et al., 1968, p. 744), and provide a precise correla-

FIGURE 2—(opposite) Silurian eustatic curve with the burial history of particular paleovalleys and rocky shorelines marked by black vertical bars under the zero column that indicates land (revised from Johnson, 1996). Relative bathymetry of sea-level curve is indicated by numbers 1 (shallow) to 6 (deep), which represent benthic assemblage zones. Definition of series and stage boundaries in Holland and Bassett (1989).

tion with the Aeronian transgressive event (see Bassett, 1989, p. 234).

An exceptional example of a karstic and rocky shoreline buried during this global event is found near the village of Wudang in central Guizhou Province, south China (Rong and Johnson, 1996). The Silurian Kaochaitien Formation near Wudang oversteps a 63 m-high escarpment that was eroded in the Ordovician Huanghuachong and underlying Guniutan Formations. The local unconformity at the Ordovician–Silurian boundary is variable in depth over a distance of only 0.8 km, and cuts out all or parts of the Ordovician Llanvirn, Caradoc, and Ashgill Series, as well as all or parts of the Lower Silurian Rhuddanian and Aeronian Stages. Much of the Ashgill, all of the Rhuddanian, and much of the Aeronian are absent in the Wudang area. This gap gradually closes north over a distance of 250 km, which indicates that central Guizhou underwent modest tectonic uplift and subaerial erosion during the missing interval. The actual eustatic rise must have been somewhat more than 63 m, because it overtook minor tectonic uplift at this locality. This example depicts one variant of the model shown in Figure 1.3. Although located on paleocontinents widely separated from one another, Hope Valley (Avalonia) and the Wudang escarpment (South China) experienced comparable submergence during the same interval of time.

EARLY TELYCHIAN TRANSGRESSIVE EVENT.—The third Silurian highstand in sea level is recorded in the lower Telychian Stage, and is coincident with the *Spirograptus guerichi* Zone (graptolites) (Loydell, 1994; Figure 2). The time of transgression of a rocky shoreline that is exposed at the Gullet Quarry in the Malvern Hills of the Welsh Borderland matches this interval. Literature on the Malvern Line as a Silurian coastline is extensive, but the best descriptive reports are those by Reading and Poole (1961, 1962) and Brooks and Druce (1965). At the Gullet Quarry, basal conglomerate and sandstone layers of the Silurian Wyche Beds rest unconformably at a steep angle against tilted Precambrian pegmatitic gneiss and schists. The optimal exposure of this unconformity in the early 1960s showed a thin cover of Silurian on a “very irregular” surface of Precambrian basement rocks with an area of approximately 250 m². This surface featured Precambrian knobs that protrude through the overlying Silurian strata as “sea shore stacks” (Reading and Poole, 1962, p. 378). No measurements of these Silurian sea stacks were made, and the outcrop photo published by Reading and Poole (1961, pl. 15) indicates only 75 cm of topographic relief on the unconformity. Brooks and Druce (1965, p. 372) described a 20 cm-wide “neptunian dyke” that could be followed 1.25 m “below the Pre-Cambrian surface.” Combining these two elements, a minimum of 2 m of

relief existed prior to the Silurian transgression. Conodonts, including *Apsidognathus tuberculata*, were recovered from the basal Silurian at this locality (Brooks and Druce, 1965). The same beds also have the brachiopod *Eocoelia curtisi* (Ziegler et al., 1968, p. 757). Although Brooks and Druce (1965) regarded the biostratigraphy indicated by their conodont data as being at odds with the brachiopod data, all occurrences are consistent with an early Telychian Age (Bassett, 1989, p. 234; Aldridge and Schönlaub, 1989, p. 276).

Whittard (1932, p. 866, 867) described basal Silurian deposits of conglomerate and pebbly grit that rest on Precambrian Purple Slates in the Plowdon area adjacent to the Long Mynd in the Welsh Borderland. The conglomerates have subangular clasts of Precambrian slate, and the name “Kenley Grit” was applied by Ziegler et al. (1968, p. 745), who estimated a maximum thickness of 20 m. Whittard (1932, p. 893) pointed out that “islets or sea-stacks” are surrounded by Silurian pebble banks. The amount of topographic relief on an islet is shown by a field photo of the excavated unconformity from a site in one of the abandoned quarries in Park Plantation (Whittard, 1932, pl. 58). The age of this transgression is more difficult to assess, but Whittard (1932, p. 873) also recognized “a gradation along strike from arenaceous to argillaceous sediments” and reported graptolites of the *Monograptus turriculatus* Zone immediately above the unconformity. In a review of these data, Ziegler et al. (1968, p. 746) accepted a “fairly rapid increase in depth westwards from the Long Mynd” through the Aeronian–Telychian transition.

The standard sea-level curve (Johnson, 1996; Figure 2) suggests that the second and third highstands of the Early Silurian were equal in eustatic effect. Unfortunately, the best understood unconformities along the Welsh Borderland at Gullet Quarry and at Plowdon provide insufficient exposure to test this prediction.

LATE TELYCHIAN TRANSGRESSIVE EVENT.—The global sea-level curve (Johnson, 1996; Figure 2) indicates that the fourth highstand, as recorded in the upper Telychian, represents the maximum rise in sea-level of the entire Silurian. This interpretation is based on evidence derived from community-replacement patterns in the stratigraphic sequence.

A regional karstic unconformity associated with transgressive strata is referable to this interval and forms a prominent sequence boundary in the Lower Silurian of Illinois and Wisconsin. Part of a gently sloping, 8 m-high paleoscarp at Waukesha, Wisconsin was illustrated by Klussendorf and Mikulic (1996, p. 179) at a quarry that exposes the basal Brandon Bridge Group. The Brandon Bridge wedges out over a distance of

100 m against a beveled surface on the older Byron and Schoolcraft Formations. This paleoscarp forms steps on the lower, more resistant Byron Formation at other localities. The age of the overlying Brandon Bridge Group is constrained by conodonts of the *Pterospirifer celloni* and *P. amorphognathoides* Zones. Based on regional variations in the thickness of strata above and below the unconformity, the minimum topographic relief along a north-south transect is taken as approximately 53 m (J. Kluessendorf, personal commun., 1996). This estimate is of the same order of magnitude as that calculated for the earlier Aeronian transgressive event, but smaller than predicted by the global sea-level curve based on community replacement patterns.

MIDDLE WENLOCK TRANSGRESSIVE EVENTS.—A small global rise in sea-level is suggested by two closely related peaks that have been grouped together for convenience as a fifth eustatic event in the middle-late Sheinwoodian (Johnson, 1996; Figure 2). On the island of Gotland, Sweden, the Kopparsvik Formation of Riding and Watts (1991), or Tofta Limestone in the older literature, features several erosion surfaces in the lower Sheinwoodian that predate these highstands. The channelled erosion surface on which the Halsjarnet Member rests cuts through two underlying members of the Kopparsvik Formation. The Halsjarnet Member fills approximately 2 m of topographic relief that is exposed in quarry walls near Visby (Riding and Watts, 1991, p. 361). The upper part of the Halsjarnet Member is beveled by another erosion surface. The biostratigraphy at these levels (Jeppsson et al., 1994) is consistent with the early Sheinwoodian lowstand. The succeeding Slite Beds probably represent the culmination of the fifth transgressive event, as recorded on Gotland.

The Ludlow and Pridoli Series comprise the Upper Silurian (Holland and Bassett, 1989). The lower Gorstian and middle Ludfordian Stages of the Ludlow record the sixth and seventh highstands in Silurian sea-level, with an intervening lowstand that is coincident with the *Saetograptus leintwardinensis* Zone (graptolites) (Johnson, 1996; Figure 2). The eighth highstand in global sea level is interpreted to be midway through the Pridoli Series.

EARLY GORSTIAN TRANSGRESSIVE EVENT.—Basalts and volcanoclastics from the uppermost Wenlock and lowermost Ludlow are associated with the major eruptions of the Svatý Jan volcanic center in Bohemia. On the Berounka River, lower Gorstian limestone with a moderately rich brachiopod and trilobite fauna rests unconformably on basalt. Corals are attached directly to the unconformity surface (Kříž 1992, p. 70).

Ordovician quartz diorites in the Bateobao area of Inner Mongolia on the North China paleocontinent are overlain by basal conglomerates and limestone of the Bateobao Formation (Li et al., 1984). Maximum thickness of the basal conglomerate is 5 m. Considered to be late Wenlock to early Ludlow, the limestone includes such brachiopods as *Conchidium* and such tabulate corals as *Favosites*.

The paleorelief is unknown at these localities in the Czech Republic and China. However, the unconformities lay at an elevation that was inundated by a transgression near the start of Ludlow time.

LUDFORDIAN TRANSGRESSIVE EVENT.—The initial transgressive stages of this event may be recorded by burial of karstic unconformities within and on the Hemse Group on the island of Gotland, Sweden. On the east shore of Gotland at Kuppen, an unconformity with a 1–2 m-high cliff is preserved as a karst surface within the upper Hemse (Keeling and Kershaw, 1994). A similar karstic unconformity occurs at the boundary between the Hemse Group and overlying Eke Formation about 20 km southwest of Kuppen (Cherns, 1982). These levels in the upper part of the Hense Group fall within the *Polygnathoides siluricus* Zone (conodonts), which is equivalent to the upper *Saetograptus leintwardinensis* Zone (graptolites) (Jeppsson et al., 1994). Lowstands in sea-level clearly promoted the erosion of Silurian karstic shorelines during this interval and were followed by sea-level rises that led to their burial.

PRIDOLIAN TRANSGRESSIVE EVENT.—The lowstand preceding this event may have occurred before the end of Ludlow time, with the ensuing transgressive event spanning the Ludlow–Pridoli boundary but peaking well into Pridoli time (Johnson, 1996; Figure 2). A significant paleokarst occurs around this boundary in Ohio on the Findlay Arch of the Laurentian paleocontinent. According to Kahle (1988, p. 250), “The Lockport/Peebles and Greenfield contact in western Ohio is a major, regional, subaerial unconformity even though as seen in quarry walls this contact never has over 3 m of erosional relief.” Kahle (1988) predicted that subsurface data will eventually show this contact to have over 30 m of erosional relief. The Greenfield is a dolostone, which is partly upper Ludlow on the occurrence of the brachiopod *Plicocaelina occidentalis* just above the unconformity (Boucot and Johnson, 1966). This relationship appears to be another example of the model in Figure 1.3, in which eustatic rise overcame regional tectonic uplift of a lesser magnitude.

South of Gashaomia in the Bateobao area of Inner Mongolia, northern China, Pridoli deposits of the Xibiehe

Formation include a sequence of conglomerate and intercalated shale and limestone lenses that rests unconformably on granodiorite of Ordovician age. Published outcrop photos (Li et al., 1984) hint at the paleorelief inundated by this transgression, but this relief has not been measured. It may be useful to note, however, that the basal conglomerate of the Xibiehe Formation is 23 m thick. This thickness clearly indicates a ready source of eroded clasts, and implies a significant paleorelief. The succeeding shales and limestone lenses yield an abundant, relatively low-diversity brachiopod fauna with *Atrypodea*, *Gypidula*, *Howellella*, *Linguopugnoides*, *Retziella*, and *Stegerhynchus*. These indicate a position in the upper subtidal range.

DISCUSSION

The realization that ancient shorelines may be used to recognize and gauge minimum relative changes in sea-level has a long history dating back to works by Benoit De Maillet and Robert Chambers in the 18th and 19th centuries (Johnson, 1992). Data on rocky shores from intervals older than the Pleistocene, however, are difficult to find in the published literature. Two reasonable explanations for this situation are possible. One inference concedes the incompleteness of the stratigraphic record. Excluding glaciated coasts, the majority of modern rocky shores are associated with active continental margins, island arcs, and island hot spots (Johnson, 1988). These environments are susceptible to tectonic uplift and erosional degradation over short periods of geological time. Much of the surviving Paleozoic record involves epicontinental deposits well-removed from active plate boundaries. Ordovician–Silurian sea-level also was much higher than today, and the length of earth's epicontinental shorelines (tectonically stable or not) was accordingly smaller. Another inference draws not on the limitations of the stratigraphic record, but on our ability to extract useful data from the available record. An ancient rocky shore may become an unconformity, wherein a sharp boundary exists between a resistant substrate overlain by littoral deposits. The stratigraphic record is replete with unconformities, many of which undoubtedly fit this narrow definition. Silurian rocky shorelines, as those dating from any other time interval, are probably "more overlooked than rare" (Johnson, 1992, p. 804). The same argument certainly reflects on coastal paleovalleys as yet another variant of geological unconformity.

It is not the intent of this review to insist that all examples of Silurian rocky shores or all coastal valleys must exhibit burial histories consistent with patterns of global

flooding events. The Panuara hiatus in central New South Wales, for example, involves various unconformities among marine sedimentary rocks that completely cut out the time–rock intervals belonging to the *Mono-graptus convolutus* and succeeding *M. sedgwickii* Zones (Jell and Talent, 1989, p. 188). These two zones encompass the second transgressive–regressive cycle in the sequence of Silurian global events (Johnson, 1996; Figure 2). The nonalignment of this particular hiatus does not invalidate arguments for a Silurian highstand coeval with the *M. sedgwickii* Zone. The widespread Panuara hiatus merely demonstrates that regional uplift in New South Wales was more significant than coeval changes in global sea-level. The Panuara hiatus is a good example of the model in Figure 2.4, in which a relative drop in sea-level is linked with a coeval major episode of tectonic uplift and a comparatively weak eustatic rise. Although the Panuara hiatus obscures evidence for the postulated Aeronian highstand in sea-level, it is worthy to note that basal units of the Waugoola Group above the Panuara unconformity show an early Telychian rise in sea-level (Jell and Talent, 1989, p. 188). This relationship suggests that the episode of regional tectonic uplift associated with the Panuara hiatus eventually ran its course and was followed by the next global rise in sea-level at the beginning of Telychian time (Johnson, 1996; Figure 2).

A model in which a global drop in sea-level results in a local transgression due to stronger regional subsidence of the adjacent coastline (Figure 1.6) is equally valid as a possible scenario. We are not aware of a Silurian example, but such a situation would be seen as a local onlap inconsistent with sea-level changes that show the global lowstand elsewhere. There are exceptions to every rule, and the eustatic curve interpreted for the Silurian should be regarded only as a general guideline.

The fact that some Silurian rocky shores may have only low relief, as do the karst features on Gotland (Cherns, 1982; Riding and Watts, 1991; Keeling and Kershaw, 1994), has some bearing on the length of time represented by the unconformity. Simply because these rocky shores may have been quite low, however, does not mean the transgressions that enveloped them were minor. A substantial rise in sea-level will more easily inundate low-relief coasts than those with higher relief. The end result is that a low-relief coast is drowned more rapidly and to a greater extent. It may be less useful than a coast of high relief in determining the depth of submergence, but it still marks the local time of transition between regression and transgression.

Much future work is necessary to expand and strengthen insights on the absolute range of water depth represented by global changes in Silurian sea-level. The

extensive, older literature from the Silurian type areas in Wales and the Welsh Borderland provides mostly anecdotal information on unconformities on ancient rocky shorelines. No focused attempt was made to measure the topographic relief buried at the Ordovician–Silurian boundary or at intra-Silurian unconformities. Whatever the coverage, traditional stratigraphical–paleontological reports tend to regard unconformities of any age merely as convenient boundaries that separate rock units. Only rarely are the thicknesses of rock units above and below an unconformity surface given spatial consideration and related to one another in order to reconstruct paleotopography. Only three studies cited herein were undertaken explicitly as descriptions of Silurian rocky-shore features (Cherns, 1982; Keeling and Kershaw, 1994; Rong and Johnson, 1996). Most other references to the rocky-shore localities reviewed herein merit additional investigation in order to recover more useful information. Other outstanding localities bearing on this topic surely await discovery and description.

Only three studies cited herein are devoted mainly to the description of Silurian paleovalleys (Whitlow and Brown, 1963; Vaslet, 1990; Powell et al., 1994). The Saudi Arabian and Jordanian studies take advantage of outcrop-scale observations, in which well-cemented sandstones that represent valley fill are sometimes exposed in relief and are unobscured by the softer valley walls that originally cradled them. Isopach maps routinely consider spatial variations in the thicknesses of rock units, but seldom detail unconformities that are preserved in paleovalleys. More attention should be paid to isopach studies that span the Ordovician–Silurian boundary, particularly in regions on ancient continents remote from the Gondwanan ice margin.

Expansion of this data set on Silurian coastal topography has ramifications beyond calibration of the Silurian sea-level curve. Intercontinental comparison of data may further substantiate differences in hypsometry, especially those related to the ice loading of Gondwana. This, in turn, may tell us something about the thickness of the ice margin around parts of Gondwana. Data on Silurian topography and its burial may help to settle conflicting estimates on the absolute water depths at which Silurian benthic communities lived. Observations on the recurrent stratigraphic patterns of key communities played an important role in the definition of Silurian transgressive–regressive cycles (Johnson, 1987), but statements on absolute water depths based on their ecology are questionable (Brett et al., 1993). By establishing a better quantification of fluctuating water depths on extensive Silurian epicontinental platforms, it may also be possible to clarify models for changing patterns of oceanic circulation connected

to extinction and diversity patterns (Jeppsson, 1990; Aldridge et al., 1993).

CONCLUSIONS

Limited as it is, this summary of available data on coastal erosion and marine onlap of paleotopography leads to at least six conclusions on the repetition and vertical extent of sea-level fluctuations recorded widely throughout the Silurian world:

- 1) All eight known Silurian events (i.e., those beginning with a lowstand and culminating with a highstand) are associated with the burial of coastal topography at unconformities preserved in the stratigraphic record.
- 2) Although paleovalleys associated with the ice margins of Gondwana were more deeply eroded (perhaps due to the effect of submarine ice), the maximum drawdown of global sea-level at the end of the Ordovician and the maximum rise during the Early Silurian (Rhuddanian) was approximately 70 m. This figure is derived from buried paleotopography on two paleocontinents (Laurentia and Baltica).
- 3) A rise in sea-level of no less than 65 m occurred during Aeronian time, and is recorded by the coeval burials of a paleovalley in the Welsh Borderland (Avalonia) and a rocky escarpment in South China.
- 4) Modest tectonic uplift in South China preceded and accompanied the Aeronian rise in sea-level. Evidence for a tectonic component in relative sea-level change makes identification of the eustatic component more reliable when linked with other inter-regional data. When local topography underwent minor tectonic uplift, eustasy is the only possible cause for a coeval, substantial rise in sea-level.
- 5) Unconformities that show burial of rocky shorelines are correlated with the early Telychian, late Telychian, middle Sheinwoodian, early Gorstian, middle Ludfordian, and Pridoli transgressions. In most cases, descriptions of these features in the Welsh Borderland, Sweden, China, and the United States provide little or no information on paleorelief. The minimal regional relief of a karst surface buried during the late Telychian in Laurentia is approximately 53 m; the minimum relief of a similar karst surface buried during the early Pridoli in Laurentia is 30 m.
- 6) Rocky shorelines with low relief are better suited as markers of the transition between local regres-

sions and transgressions than as checks against the depth of major onlaps.

Constraints on the three-dimensional exposure of unconformities make it difficult to determine the full paleorelief from local field observations. More sophisticated use of subsurface data is one solution to this problem. A greater awareness of the interesting applications to which a comprehensive physical description of paleovalleys and rocky shorelines may be applied will improve the quality of data extracted from the stratigraphic record. Unusually well-preserved examples of these features remain to be redescribed based on hints in the existing literature, or will be discovered as a result of entirely new initiatives. Refinements in our comprehension of the Silurian eustatic curve will continue to unfold and provide insight on the interplay of lithospheric, oceanic, and atmospheric cycles chronicled in the stratigraphic record.

ACKNOWLEDGMENTS

The authors are grateful to E. Landing for his thorough technical review and to G.T. Moore and W.N. Orr for their manuscript reviews. Their efforts improved the clarity of our contribution to this volume.

REFERENCES

- ALDRIDGE, R.J., AND H.P. SCHÖNLAUB. 1989. Conodonts, p. 274–279. In C.H. Holland and M.G. Bassett (eds.), *A Global Standard for the Silurian System*. National Museum of Wales, Geological Series Number 9.
- , L. JEPSSON, AND K.J. DORNING. 1993. Early Silurian oceanic episodes and events. *Journal of the Geological Society of London*, 150:501–513.
- BAARLI, B.G. 1988. Bathymetric co-ordination of proximity trends and level-bottom communities: a case study from the Lower Silurian of Norway. *Palaio*, 3:577–587.
- BASSETT, M.G. 1989. Brachiopods, p. 232–242. In C.H. Holland and M.G. Bassett (eds.), *A Global Standard for the Silurian System*. National Museum of Wales, Geological Series Number 9.
- BOUCOT, A.J., AND M.G. JOHNSON. 1966. *Lissocoelina* and its homeomorph *Plicocoelina* n. gen. (Silurian Pentameracea). *Journal of Paleontology*, 40:1037–1042.
- BRENCHLEY, P.J., AND G. NEWALL. 1980. A facies analysis of Upper Ordovician regressive sequences in the Oslo region, Norway—a record of glacio-eustatic changes. *Palaogeography, Palaeoclimatology, Palaeoecology*, 31:1–38.
- BRETT, C.E., W.M. GOODMAN, AND S.T. LODUCA. 1990. Sequences, cycles, and basin dynamics in the Silurian of the Appalachian foreland basin. *Sedimentary Geology*, 69:191–244.
- , A.J. BOUCOT, AND B. JONES. 1993. Absolute depths of Silurian benthic assemblages. *Lethaia*, 26:25–40.
- BRIDGES, P.H. 1975. The transgression of a hard substrate shelf: the Llandovery (Lower Silurian) of the Welsh Borderland. *Journal of Sedimentary Petrology*, 45:79–94.
- BROOKS, M., AND E.C. DRUCE. 1965. A Llandovery conglomeratic limestone in Gullet Quarry, Malvern Hills, and its conodont fauna. *Geological Magazine*, 102:370–382.
- CAVE, R., AND R.J. DIXON. 1993. The Ordovician and Silurian of the Welshpool area, p. 61–64. In N.H. Woodcock and M.G. Bassett (eds.), *Geological Excursions in Powys, Central Wales*. University of Wales Press, National Museum of Wales, Cardiff.
- CHERNS, L. 1982. Palaeokarst, tidal erosion surfaces and stromatolites in the Silurian Eke Formation of Gotland, Sweden. *Sedimentology*, 29:819–833.
- DU BOIS, E.P. 1945. Subsurface relations of the Maquoketa and “Trenton” Formations in Illinois. *Illinois Geological Survey Report of Investigations*, 105:7–16.
- GOODMAN, W.M., AND C.E. BRETT. 1994. Roles of eustasy and tectonics in development of Silurian stratigraphic architecture of the Appalachian foreland basin. *SEPM Vol. 4, Concepts in Sedimentology and Paleontology (Society of Sedimentary Geology)*, 4:147–169.
- HOLLAND, C.H., AND M.G. BASSETT (EDS.). 1989. *A Global Standard for the Silurian System*. National Museum of Wales, Geological Series Number 9, Cardiff.
- JELL, J.S., AND J.A. TALENT. 1989. Australia: the most instructive sections, p. 183–200. In C.H. Holland and M.G. Bassett (eds.), *A Global Standard for the Silurian System*. National Museum of Wales, Geological Series Number 9, Cardiff.
- JEPSSON, L. 1990. An oceanic model for lithological and faunal changes, tested on the Silurian record. *Journal of the Geological Society of London*, 147:663–673.
- , V. VIIRA, AND P. MÄNNIK. 1994. Silurian conodont-based correlations between Gotland (Sweden) and Saaremaa (Estonia). *Geological Magazine*, 131:201–218.
- JOHNSON, M.E. 1987. Extent and bathymetry of North American platform seas in the early Silurian. *Paleoceanography*, 2:185–211.
- . 1988. Why are ancient rocky shores so uncommon? *Journal of Geology*, 96:469–480.
- . 1989. Tempestites recorded as variable *Pentamerus* layers in the Lower Silurian of southern Norway. *Journal of Paleontology*, 63:195–205.
- . 1992. Studies on ancient rocky shores. *Journal of Coastal Research*, 8:797–812.
- . 1996. Stable cratonic sequences and a standard for Silurian eustasy, p. 203–211. In B.J. Witzke, G.A. Ludvigson, and J.E. Day (eds.), *Paleozoic Sequence Stratigraphy: Views from the North American Craton*. Geological Society of America, Special Paper 306.
- , D. KALJO, AND RONG J.-Y. 1991. Silurian eustasy, p. 145–163. In M.G. Bassett, P.D. Lane, and D. Edwards (eds.), *The Murchison Symposium: Proceedings of an International Conference on the Silurian System*. Special Papers in Palaeontology, 44.
- , AND W.S. MCKERROW. 1991. Sea level and faunal changes during the latest Llandovery and earliest Ludlow (Silurian). *Historical Geology*, 5:153–169.
- KAHLE, C.F. 1988. Surface and subsurface paleokarst, Silurian Lockport, and Peebles Dolomites, western Ohio, p. 229–255. In N.P. James and P.W. Choquette (eds.), *Paleokarst*. Springer-Verlag, New York.
- KEELING, M., AND S. KERSHAW. 1994. Rocky shore environments in the Upper Silurian of Gotland, Sweden. *Geologiska Föreningens i Stockholm Förhandlingar*, 116:69–74.
- KLUESSENDORF, J., AND D.G. MIKULIC. 1996. An Early Silurian sequence boundary in Illinois and Wisconsin, p. 177–185. In B.J. Witzke, G.A. Ludvigson, and J.E. Day (eds.), *Paleozoic Sequence*

- Stratigraphy: Views from the North American Craton. Geological Society of America, Special Paper 306.
- KŘÍŽ, J. 1992. Silurian Field Excursions—Prague Basin (Barrandian), Bohemia. National Museum of Wales, Geological Series Number 13.
- LI W.-G., RONG J.-Y., DONG D.-Y., YANG D.-R., SU Y.-Z., AND WANG Y.-F. 1984. Silurian and Devonian rocks of the Bateaobao area in Darhan Mumingan Joint Banner, Inner Mongolia, p. 1–25. *In* Li W.-G., Rong J.-Y., and Dong D.-Y. (eds.), *Silurian and Devonian Rocks and Faunas of the Bateaobao Area in Darhan Mumingan Joint Banner, Inner Mongolia*. The People's Publishing House of Inner Mongolia.
- LOYDELL, D.K. 1994. Early Telychian changes in graptoloid diversity and sea level. *Geological Journal*, 29:355–368.
- MCCLURE, H.A. 1978. Early Paleozoic glaciation in Arabia. *Palaeogeography, Palaeoclimatology, Palaeoecology*, 25:315–326.
- MÖRNER, N.-A. 1976. Eustasy and geoid changes. *Journal of Geology*, 84:123–151.
- PARKER, M.C. 1971. The Maquoketa Formation (Upper Ordovician) in Iowa. Iowa Geological Survey, Miscellaneous Map Series 1, 6 maps.
- PARKES, M.A. 1993. Palaeokarst at Portrane, County Dublin: evidence for Hirnantian glaciation. *Irish Journal of Earth Sciences*, 12:75–81.
- POWELL, J.H., B.K. MOH'D, AND A. MASRI. 1994. Late Ordovician–Early Silurian glaciofluvial deposits preserved in palaeovalleys in south Jordan. *Sedimentary Geology*, 89:303–314.
- READING, H.G., AND A.B. POOLE. 1961. A Llandovery shoreline from the southern Malverns. *Geological Magazine*, 98:295–300.
- , AND ———. 1962. Correspondence. *Geological Magazine*, 99:377–379.
- RIDING, R., AND N.R. WATTS. 1991. The lower Wenlock reef sequence of Gotland: facies and lithostratigraphy. *Geologiska Föreningens i Stockholm Förhandlingar*, 113:343–372.
- RONG J.-Y., AND M.E. JOHNSON. 1996. A stepped karst unconformity as an Early Silurian rocky shoreline in Guizhou Province (south China). *Palaeogeography, Palaeoclimatology, Palaeoecology*, 121:115–129.
- VASLET, D. 1990. Upper Ordovician glacial deposits in Saudia Arabia. *Episodes*, 13:147–161.
- WHITLOW, J.W., AND C.E. BROWN. 1963. The Ordovician–Silurian contact in Dubuque County, Iowa. U.S. Geological Survey, Professional Paper 475-C:11–13.
- WHITTARD, W.F. 1932. The stratigraphy of the Valentian rocks of Shropshire, the Longmynd-shelve and Breidden outcrops. *Quarterly Journal of the Geological Society of London*, 88:859–902.
- ZIEGLER, A.M., L.R.M. COCKS, AND W.S. MCKERROW. 1968. The Llandovery transgression of the Welsh Borderland. *Palaeontology*, 11:736–782.

ORDOVICIAN–SILURIAN GLACIATIONS AND GLOBAL SEA-LEVEL CHANGES

MARIO V. CAPUTO

*Universidade Federal do Pará, Campus Universitário do Guama, Centro de Geociencias,
Departamento de Geologia, Belem CEP 66075-970, Pará, Brazil*

ABSTRACT—Filling of the intracratonic basins of South America was initiated by fluvial deposition, followed by Late Ordovician shallow-marine sedimentation. Continental sedimentation succeeded shallow-marine deposits with sea-level falls due to Hirnantian glaciation in Africa. Melt water from Hirnantian ice caps carried coarse-grained siliciclastics into the Accra (Africa) and Brazilian Parnaíba and Paraná basins. Glacials and interglacials alternated until the early Wenlock, when the ice caps migrated to central South America and deposited continental and marine diamictites. Silurian glacial deposits occur in the Amazon, Parnaíba, and Paraná Basins in Brazil and the Andean basins of Argentina, Bolivia, and Peru. In the Amazon Basin, three Silurian glaciations deposited diamictites and fluvial sandstones above littoral and shoreface sedimentary rocks (Nhamundá Formation). Subglacial deposits in this area are quartzose subgraywackes with ice-push and -shear features. In the Parnaíba Basin, there is no fossil control on Silurian diamictites (Ipu Member), although an early–late Llandovery age for marine shales of the overlying Tianguá Formation is known. The Iapó Formation in the Paraná Basin is composed of glacial diamictites, and is likely Hirnantian, as are those in the Cape Basin, South Africa (Pakhuis Tillite), and Argentina (Don Braulio Formation). In Bolivia and Peru, the Cancañiri Formation has glacial sedimentary rocks and resedimented siliciclastics. The Cancañiri Formation is latest Llandovery–earliest Wenlock. Silurian ice movement was probably from upland shield areas to basin margins in southeast Andean areas, Brazil, and Africa, and from the Pampean and Arequipa massifs into the Andean basins.

INTRODUCTION

The Silurian geology of South America is less known than that of other continents, but the most interesting feature is the presence of tillites at its base in several sedimentary basins. Ordovician–Silurian glacial deposits are

known from Argentina, Bolivia, Brazil, and Peru (Figure 1). The first recognition of latest Ordovician glaciation in South America was based on study of the Don Braulio Formation in Argentina (Büggisch and Astini, 1993; Astini and Büggisch, 1993) and the Iapó Formation in the Paraná Basin in Brazil (Caputo and Lima, 1984; Zalan et al., 1987; Grahn and Caputo, 1992).

Although no direct evidence of glaciation is currently known in the Silurian of Paraguay on the western border of the Paraná Basin, conglomeratic units of this age may be related to glaciation in nearby regions. In northern Andean countries, the climate was warm enough to prevent Silurian glaciation.

Three short-lived, Silurian glacial episodes (early Aeronian, latest Aeronian–early Telychian, and latest Telychian–earliest Wenlock) are recorded in the Nhamundá Formation of the Trombetas Group in Brazil (Caputo, 1984; Grahn and Caputo, 1992; Grahn, 1996). In the Amazon Basin, the Trombetas Group comprises four units: the Autás-Mirim, Nhamundá, Pitinga, and Manacapuru Formations. This group was deposited after rifting of the Amazon Basin. It is considered to have been the earliest Paleozoic sequence deposited in the Amazon Basin. Maximum thickness is estimated to be over 800 m in the central parts of the basin. The sea encroached upon the basin from the east at the same time as the northwest African transgressions. Sediment deposition occurred all the way to the eastern flank of the Purus Arch, which separates the Amazon Basin from the Solimões Basin in the westernmost part of the country.

With many gaps in the section, a Late Ordovician–Early Devonian age based on chitinozoans is assigned to the Trombetas Group (Grahn and Paris, 1992). In the Paraná Basin of south Brazil, a shale interval in the Vila Maria Formation immediately overlies diamictites of the Iapó Formation, and probably records a transgressive peak that is synchronous with the latest Aeronian–early Telychian deglaciation. Therefore, this interval can be

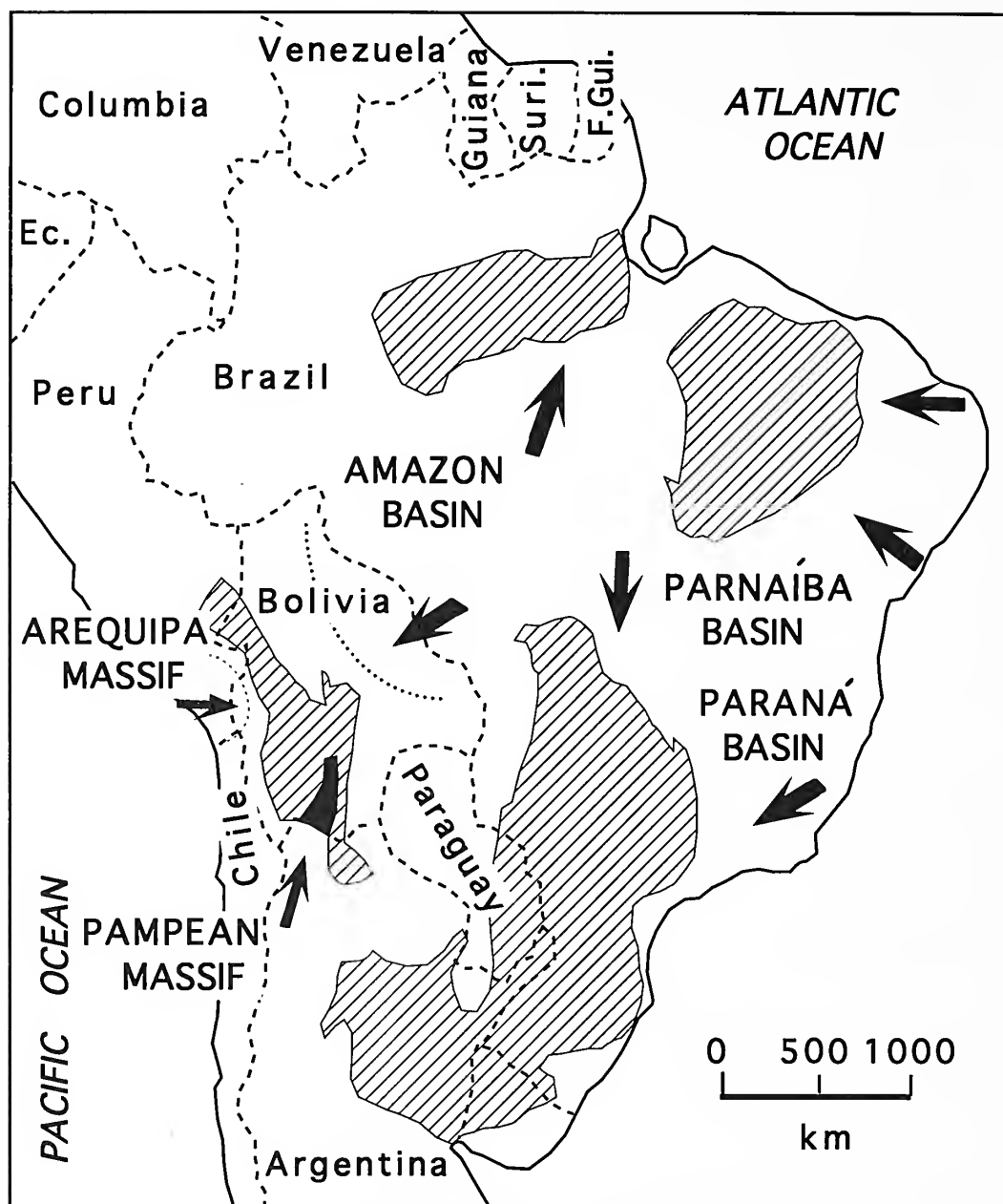


FIGURE 1—Map showing Paleozoic basins (in grey shading), after Grahn and Caputo (1992) and Crowell et al. (1980). Arrows show ice sheet movements. Diamictites in the Parnaíba Basin lack fossil control.

correlated with the Vargas Peña Shale in Paraguay (Grahn, 1993). On the other hand, the underlying diamictites are probably of the same Hirnantian Age as those in the Cape Basin (Pakhuis tillite; Rust, 1973, 1981) and in Argentina (Dom Braulio Formation; Astini and Büggisch, 1993).

In Bolivia, the Cancañiri Formation has yielded fossils from a few sites in the Cochabamba area that contain glacial sedimentary rocks. The age of the Cancañiri Formation in Bolivia and Peru has been regarded as latest Llandovery–earliest Wenlock, based on chitinozoans and

acritarchs (Crowell et al., 1980). Therefore, two glaciations may be recorded in the Andean area: Ashgillian (Argentina) and latest Llandovery–earliest Wenlock (Bolivia, Peru, and Argentina).

STRATIGRAPHY OF THE AMAZON BASIN

AUTÁS-MIRIM FORMATION.—The Amazon Basin covers an area of approximately 400,000 km². It is bounded on the west by the Purus Arch and on the east by the Gurupa

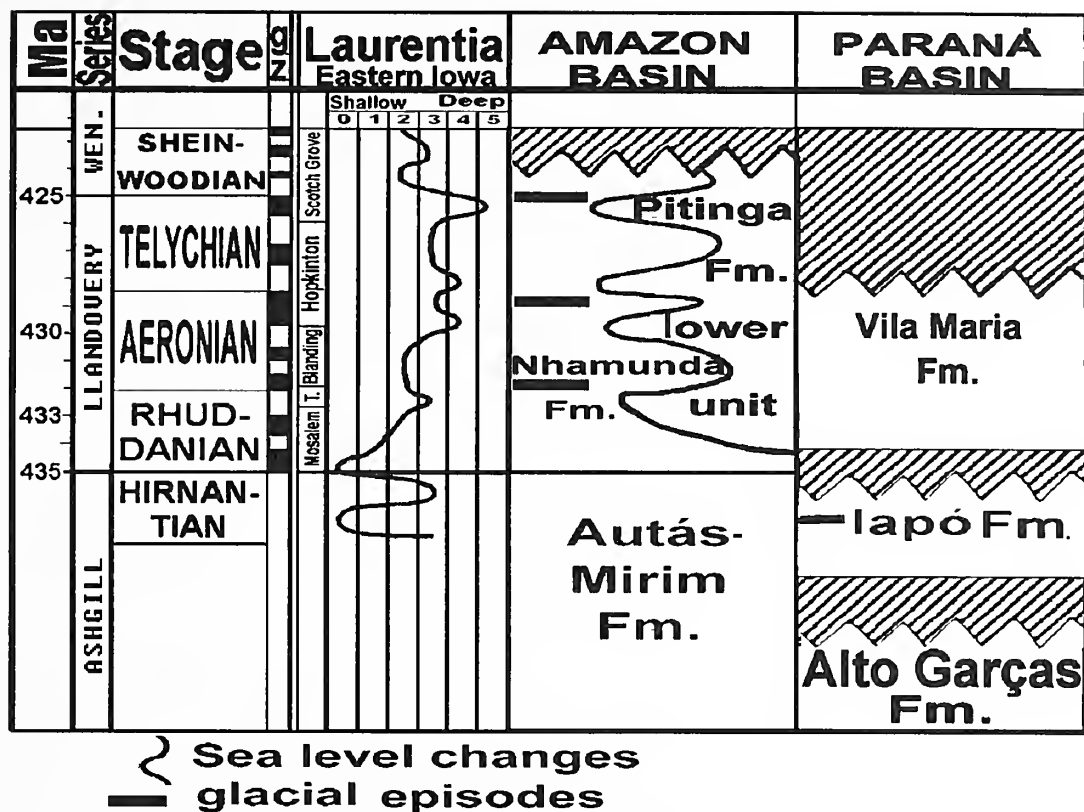


FIGURE 2—Correlation of sea-level changes and glaciations in the Late Ordovician–Early Silurian. Laurentian data after Johnson and McKerrow (1991). Black horizontal bars are diamictites.

Arch. The Autás-Mirim Formation (oldest unit in the Trombetas Group) is present only in the subsurface (Figure 2). This formation consists of micaceous, feldspathic sandstone beds which are mainly fine-grained, commonly well-rounded, and red, light green, and brown at the base of the section but predominantly white in the middle and upper part. The beds are mainly cross-bedded at the base and top of the section, and chiefly parallel-laminated in the middle. A kaolinitic matrix predominates, and the beds are well-indurated. Siltstones and shales are subordinate in the unit. The siltstones are light green to greenish gray, highly micaceous and feldspathic, well-indurated, and laminated. Minor bioturbation is present. The shales are micaceous and dark gray, have few biogenic structures, and are well-indurated. The maximum thickness of the formation is about 350 m. It unconformably overlies Precambrian formations of the basement complex. The Nhamundá Formation probably overlies the Autás-Mirim Formation conformably. In some sections, the Autás-Mirim Formation contains poorly preserved chitinozoans and *Skolithos* traces. These indicate a Late Ordovician age and a very shallow marine environment during part of the unit's sedimentation. The Autás-Mirim Formation represents a continental-marine-continental cycle that slowly onlapped the basin flanks. The continental sandstone suggests deposi-

tion in a fluvial-braided environment with some aeolian reworking.

NHAMUNDÁ FORMATION.—Up to 450 m-thick, this formation crops out only in the northwest of the Amazon Basin, but is also present in the subsurface throughout the basin (Figure 3). The Nhamundá Formation consists of quartzites (dominant), quartzitic subgreywackes, quartzitic wackes, and diamictites (Carozzi et al., 1973). The outcrops can be subdivided into three units (Swan, 1957). In the lower part, a micaceous, cream-colored, silty sandstone occurs, and is overlain by pink, fine- and medium-grained, kaolinitic, and highly cross-bedded sandstone beds with angular grains. The middle part of the formation consists of light gray, hummocky cross-stratified and ripple cross-laminated sandstone with *Skolithos*, scattered medium- and coarse-grained rounded quartz, and minor gray carbonaceous shale interbeds. In the upper part, the beds are silty and increasingly argillaceous sandstones, with marked development of thin, gray silty shale interbeds, stylolites, and trace fossils. This upper section contains three diamictite horizons (Carozzi et al., 1973). The upper diamictite beds and associated graywackes (Figure 3) were mapped in the Carabinani River by Caputo and Saad (1974).

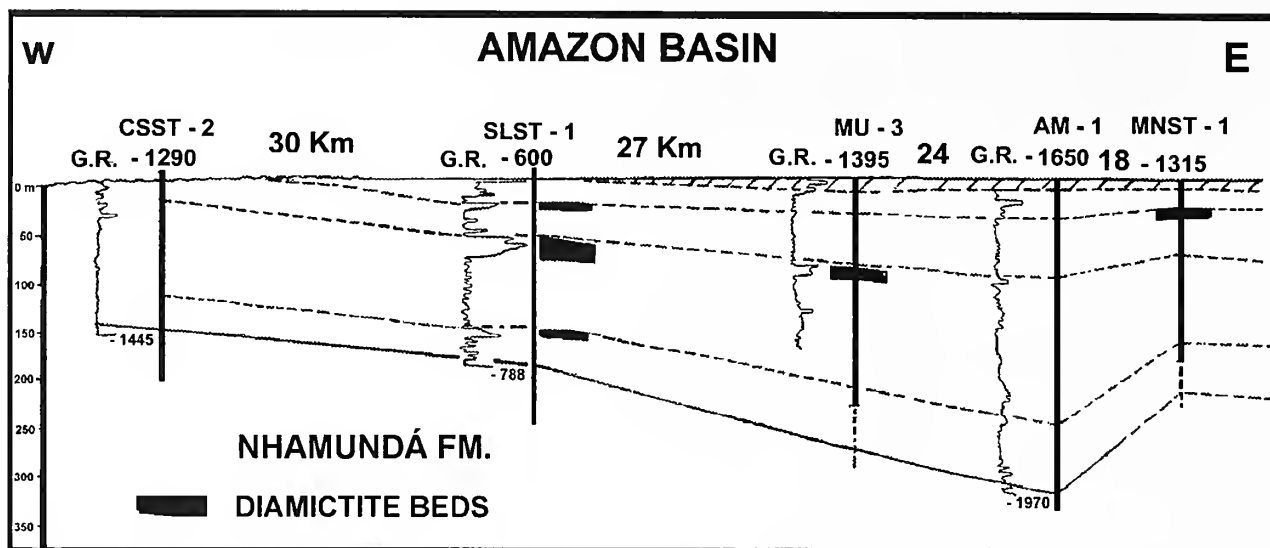


FIGURE 3—Silurian diamictites identified in wells from the north flank of the Amazon Basin.

The upper part of the Nhamundá Formation consists of diamictites and associated graywackes. The diamictites have a hard, dark grayish, structureless massive clay and silt matrix that supports coarse-grained sand grains and granules and pebbles of quartz, quartzite, shale, and crystalline rocks. The clasts vary considerably in size and roundness, as observed in core and outcrop. The diamictites from the northern margin are predominantly composed of sedimentary rock clasts, but on the southern margin are made of igneous, metamorphic, and sedimentary rocks. This diversity indicates varied source areas. In surface exposures, the diamictites weather to white, yellow, and red. X-ray diffraction shows that the matrix of the diamictites is mainly chlorite and subordinate illite (Carozzi, 1979). The clay is recrystallized to muscovite. The uppermost beds of the Nhamundá Formation consist of thin, subrounded, greenish gray, medium- and coarse-grained sandstone beds that contain dispersed pyrite, green sandy clay partings, and siliceous bands or beds. Sideritic, hematitic, and chamositic strata are common in the section. The transition zone at the top of the Nhamundá sandstones indicates low sediment supply from the continent, with predominant chemical deposition. The diamictite levels are interpreted to be a result of glacial activity, on the basis a heterogeneous grain size and pebbles of great petrographic variety that float in a silty to argillaceous matrix. Paleogeographic considerations reinforce the glacial interpretation, because basement clasts rest on a subhorizontal shelf substrate (original dip less than 0.5°) in wells 150 km away from outcrops of the basement. Because of their occurrence as distinct lobes that are intercalated in sandstones, the diamictites appear to have formed by in situ wasting of debris-laden ice, rather than

by subaqueous mudflow (Carozzi, 1979). This Silurian glaciation is less well exposed in the Amazon Basin than its Devonian counterpart (Caputo and Crowell 1985), which features similar rock texture but provides better evidence of a glacial origin (Caputo, 1985).

Subglacial beds often display deformational features that were probably induced by ice-push and -shear (Nogueira et al., In press). The Nhamundá Formation is composed mainly of sandstones that grade laterally into and are overlain by shales of the lowermost Pitinga Formation (Figures 2, 4). The latter formation is dated by chitinozoans and graptolites as middle Llandovery (*Cornograptus gregarius* graptolite Zone) to earliest Wenlock (Grahns and Paris, 1992). Except for trace fossils (e.g., *Skolithos*) from the middle and upper parts, no macrofossils are recorded in the Nhamundá Formation. The shales of the Nhamundá Formation contain the same chitinozoan assemblage as in the lower Pitinga Formation (*Angochitina longicollis* [Eisenack, 1959], *Margachitina margaritana* [Eisenack, 1937], *Cyathochitina* sp. B Paris, 1981, *Pogonochitina djalmai* [Somme and van Broekel, 1965]), according to Grahns and Paris (1992). The unit records a general transgression, during which basal sediments, characterized by fine- and medium-grained, cross-stratified sandstones with bioturbated sandstone interbeds, may have been laid down on the upper shoreface. Storm swells and fair-weather waves may have been the dominant wind-induced physical processes that shaped the shoreline deposits, and caused reworking of older aeolian dunes and backshore deposits during transgression.

The middle part of this unit has beds with hummocky cross-stratification, which represent lower shoreface sedimentation and frequent storm activity (Harms et

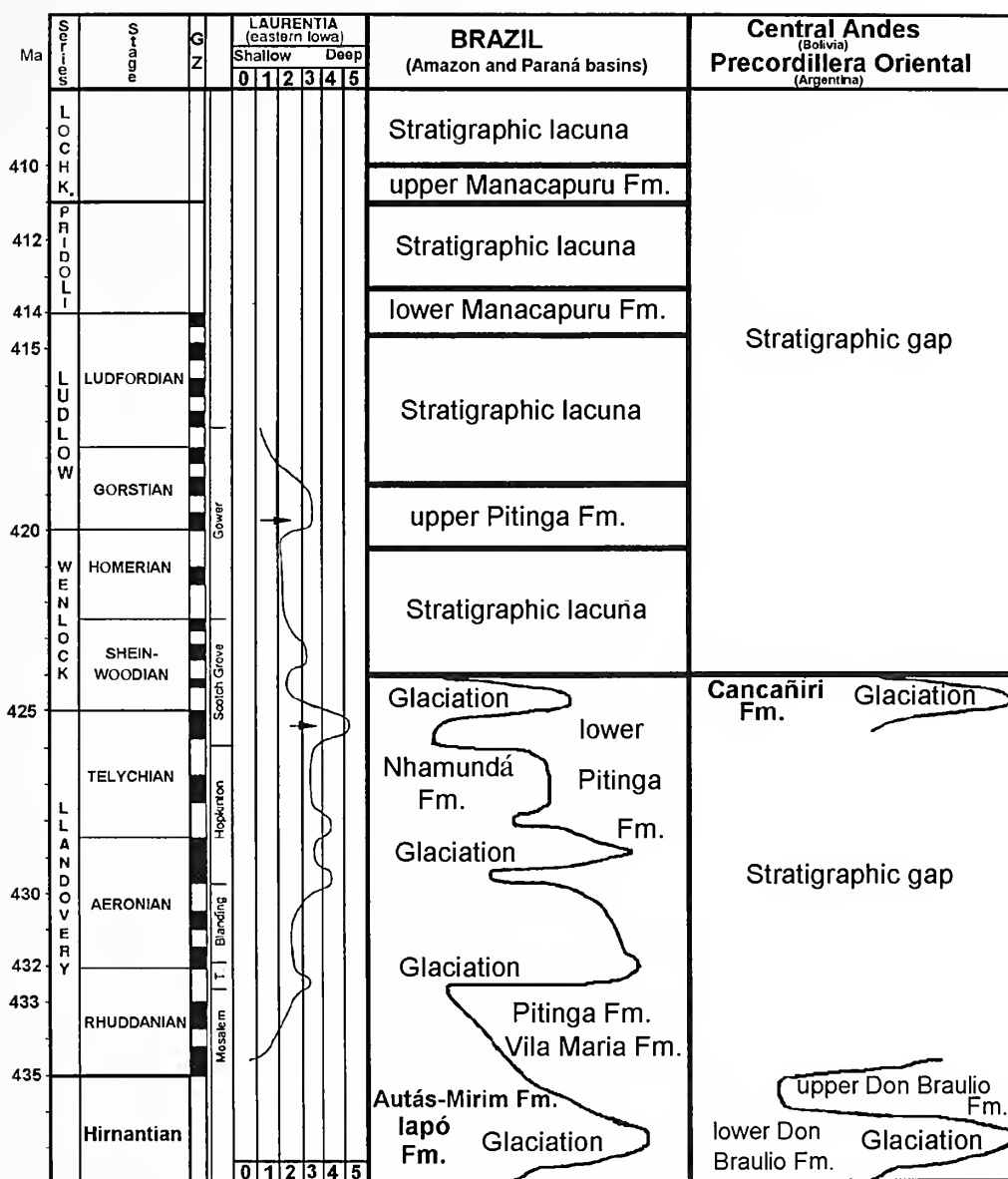


FIGURE 4—Correlation between Late Ordovician and Silurian sea-level changes and glaciation, after Johnson and McKerrow (1991) and Grahn and Caputo (1992).

al., 1975). It is supposed that anticyclonic winds in circumpolar regions acted with great vigor in the past, as they do today in high-latitude periglacial areas. The upper part of this unit is thought to represent an alternation between lower shoreface and subaereal deposits, with a rapid fall in sea-level during glacial episodes that resulted in consequent exposure of older sediments.

PITINGA FORMATION.—The lower Pitinga Formation consists of green-gray to dark gray, micaceous, laminated, soft, carbonaceous, pyritic, locally sideritic shale with interbedded shaley siltstone and hematite lenses. Thin conglomerates with shale pebbles or exotic rocks are also

present. The upper Pitinga Formation comprises very fine-to fine-grained, thin sandstone beds, as well as some chert and nodular interbeds that occur through the unit. Paleontological studies (Grahn and Paris, 1992) show a depositional gap between the lower and upper parts of the formation in the basin-shelf area.

The formation interfingers with the Nhamundá Formation and overlies it (Figure 2). The Pitinga Formation also onlaps underlying units and rests on the Precambrian Prosperanca Formation and Uatumã Group on the basin flanks. At several places on the southern margin, Pitinga shales directly overlie the Uatumã Group with no intervening sandstone or basal conglomerate.

This suggests a rapid transgression under low-energy conditions. The Pitinga Formation's upper contact is unconformable with the Manacapuru Formation (Figure 4). At different places along the basin edge, the Pitinga is unconformably overlain by younger formations.

The Pitinga Formation has yielded graptolites, chitinozoans, algae, sponge spicules, brachiopods, mollusks, scolecodonts, foraminiferans, crustaceans, and other fossil groups. Graptolites (*Climacograptus innotatus brasiliensis* Ruedemann, 1929, and *Monograptus* sp. cf. *M. gregarius*) are known from the lower unit (Caputo and de Andrade, 1968). Jaeger (1976) suggested a middle Llandovery age (*Monograptus gregarius* Zone) for the lowest shales. The graptolites occur in siltstone beds immediately above a diamictite layer exposed on the Trombetas River. The biota in the lower unit of the Pitinga Formation, according to Grahn and Paris (1992), also includes *Cyathochitina* sp. cf. *C. canoabykaefirius* (Eisenack, 1931) and *Conochitina* sp. cf. *C. iklaensis* Nestor, 1980, and indicates a late Llandovery age for most of the lower Pitinga shales. The upper part of the lower unit is characterized by *Bursachitina wilhelmi* Costa, 1970; *Pogonochitina monterrosae* (Cramer, 1969); *P.* sp. aff. *P. inornata* Costa, 1971; *P. djalmi* (Sommer and van Boekel, 1965); *Cyathochitina caputoi* Costa, 1971; *C.* sp. cf. *C. acuminata* Eisenack, 1959; *C. proboscifera* Eisenack, 1937; *Cyathochitina* sp.; *Densochitina densa* (Eisenack, 1962); *Ancyrochitina* sp.; *A. primitiva*? Eisenack, 1964; *Conochitina cruzi* Costa, 1970; *Cingulochitina* sp. aff. *C. serrata* (Taugourdeau and Jekhowsky, 1960); *Lagenochitina* n. sp. aff. *L. navicula* Taugourdeau and Jekhowsky, 1960; *Angochitina* sp. A; and *Margachitina margaritana* (Eisenack, 1937). This chitinozoan assemblage indicates a middle Llandovery–earliest Wenlock age for the lower Pitinga Formation (Grahn and Paris, 1992).

A hiatus corresponding approximately to the late early–early middle Wenlock separates the lower and upper parts of the unit. The most common chitinozoans in the upper unit are *Conochitina tuba* Eisenack, 1932; *C. pachycephala* Eisenack, 1964; *Ancyrochitina brevis* Taugourdeau and Jekhowsky, 1960; *A.* n. sp.; *Tanuchitina* sp. aff. *T. cylindrica* (Taugourdeau and Jekhowsky, 1960, sensu Boumendjel, 1987); *T. elenitae* (Cramer, 1964); *Angochitina* sp. cf. *A. echinata* Eisenack, 1931; *Rhabdochitina conocephala*? Eisenack, 1934, sensu Boumendjel, 1987; and *Gotlandochitina* sp. These chitinozoan assemblages suggest a late Wenlock to early Ludlow age for the upper Pitinga Formation.

The Pitinga Formation features an interval of predominantly muddy shoreface and offshore deposits formed during the marine onlap that resulted from melting of widespread ice caps in Africa and South America. The well-developed laminations and fine-scale bedding

are suggestive of relatively quiet-water deposition. Some thin sandstones in the lower part of the formation contain *Lingula* and *Arthropycus*, and suggest shallow nearshore to paralic deposition. Shale pebble beds up to 5 cm in thickness are present, and are interpreted as conglomerates that resulted either from exposures of the basal unit during sea-level falls or from storm activity. Climatic warming may have enhanced chemical weathering, which produced a large amount of clay minerals. Marine onlap may have caused the deposition of coarse-grained clastic sediments in estuaries and river valleys. In turn, this may have been offset by significant sedimentation of silt and clay in the sediment-starved seas during Pitinga Formation deposition.

In the lower part of the Pitinga Formation, illite predominates, while in the upper part kaolinite dominates (Rodrigues et al., 1971). This relationship suggests that a change in weathering in the transition from a glacial to a post-glacial climate may have occurred during deposition of the Pitinga Formation. These clay minerals contain low boron content (Carozzi et al., 1973), and indicate a low salinity compatible with a great fresh water influx into the basin.

MANACUPURU FORMATION.—This unit was uplifted and exposed in the northwestern outcrop belt during the Late Paleozoic. In the southern part of the Paleozoic outcrop belt, the Manacapuru Formation is unexposed, because it is overlapped by Devonian sandstones. The Manacapuru Formation is now subdivided into two units, based on the discovery of an unconformity within the succession (Grahn and Paris, 1992). The Manacapuru Formation consists of sandstones with shale, siltstone, and ironstone interbeds. In exposure, it appears as white and buff, fine- to very fine-grained, well-sorted, friable, highly cross-bedded sandstones with brownish gray, very soft argillaceous shale and siltstone interbeds. In the subsurface, the sandstones are mainly parallel laminated, fine-grained, micaceous, and bioturbated, with beds 5–20 cm in thickness that are interrupted by siltstone interbeds. Three main sandstone bodies separated by shale–siltstone bodies are present in many wells.

Sandstone beds with a clay–ferruginous matrix and oolitic ironstone beds (siderite, chamosite, hematite) are well-developed on the margin and in the western part of the basin. Small white peloids of collophane and kaolinite–chamosite are scattered through the oolites (Carozzi, 1979). The upper unit of the Manacapuru Formation consists of bioturbated, brown sideritic mudstone with a few layers of ferruginous, micaceous siltstone that contain scattered, white, phosphatic, kaolinite peloids. The Manacapuru Formation rests unconformably on the Pitinga Formation (Figure 4), and is overlain at a low

angle unconformity by Lower Devonian and younger formations. At the base of the Manacapuru Formation, the presence of *Arthropycus* sp. and *Lingula* sp. (Lange, 1967) suggests a shallow, sometimes brackish nearshore environment. The unit was dated as early Llandovery by Lange (1967) and Daemon and Contreiras (1971a, 1971b), based on palynological studies. Grahn and Paris (1992), however, recognized the presence of an unconformity within the formation and assigned a younger age to both intervals.

Chitinozoan of the lower interval include *Desmochitina corinnae* Jaglin, 1986; *Eisenackitina granulata* (Cramer, 1964); *Gotlandochitina* sp. A; *Ancyrochitina floris* Jaglin, 1986; *Pterochitina perivelata* (Eisenack, 1937); *Fungochitina kosoviensis* Paris and Kříž, 1984; *Angochitina* n. sp. aff. *A. cyrenaicensis* Paris, 1988; and *Conochitina gordonensis* Cramer, 1964. This assemblage indicates a late Ludlow to earliest Pridoli age. Characteristic chitinozoan species in the upper unit are *Margachitina catenaria catenaria* (Obut, 1973); *Ancyrochitina fragilis* Eisenack, 1955; *A. cantabrica* Cramer and Diez, 1978; *Angochitina filosa* Eisenack, 1955; *A. strigosa* Boumendjel, 1987; *Cingulochitina ervensis ervensis* (Paris, 1979); and *Eisenackitina* sp. cf. *E. boherochitina* (Eisenack, 1934). The chitinozoans indicate an Early Devonian, Lochkov age (Grahn and Paris, 1992).

The Manacapuru Formation records a general regression in the Amazon Basin with some transgressive oscillations. In the westernmost part of the basin, fine-grained, cross- and parallel-laminated, micaceous, argillaceous, bioturbated (*Skolithos*) sandstones are interpreted as deposited in a littoral environment. Medium-grained, cross-stratified sandstone beds are considered to have been deposited in fluvial and deltaic distributary channels. Carbonaceous shales may have been deposited in interdistributary lakes and bays. On the north and south flanks of the Amazon Basin, deltaic and fluvial deposits are locally preserved. The fine-grained, micaceous, cross-stratified and cross-laminated sandstones and shale interbeds were deposited in a low-energy shoreface environment. In the central parts of the basin, there is no subsurface control, but an offshore environment is postulated. The presence of ironstones suggests deposition in shallow water at the margins of the basin. Distributary delta abandonment or the onset of transgressive cycles may have inhibited clastic influx, and resulted in the concentration of ironstones in sand-starved environments. During regressive phases, the ironstones may have been eroded and redeposited with sandstones in a high-energy regressive environment.

It is interesting to note that shallowing phases (Johnson, 1987) in North America correspond to unconformities and glaciations in the Amazon Basin. This

may mean that Early Silurian water depth was consistently shallower in the intracratonic Amazon Basin than in North American epicontinental seas.

AGE OF THE TILLITES.—Diamictite horizons are dated by graptolites and chitinozoans in the Amazon Basin. The oldest Silurian diamictites (2–10 m thick) in the Amazon Basin record the advance of continental ice during the early middle Llandovery (early Aeronian, *Monograptus gregarius* Zone). Fossil evidence is available from the northern outcrop belt of the Amazon Basin from strata immediately above the lowest diamictite layer on the banks of the Trombetas River (Grahn and Caputo, 1992). This age determination is further strengthened by the presence of *Cyathochitina* sp. cf. *C. campanulaeformis* and *Conochitina* sp. cf. *C. iklaensis* (Grahn and Paris, 1992).

The next ice advance occurred during latest Aeronian–early Telychian (late Llandovery) time. Shale lateral to the tillites (locally 5–10 m-thick) yields an early Telychian chitinozoan fauna. *Cyathochitina* sp. B Paris, 1981, and *Pogonochitina djalmai* Sommer and van Boeckel, 1965, are common and reliable indicators of the early Telychian. *Cyathochitina* sp. B Paris, 1981, does not occur in beds younger than the *Monograptus turriculatus* Zone in Gondwana (Y. Grahn, personal commun., 1996).

The youngest tillites are dated as latest Telychian to earliest Wenlockian, based on the chitinozoans *Desmochitina densa* Eisenack, 1962; *Margachitina margaritana* (Eisenack, 1937); and *Salopochitina* (= *Pogonochitina*) *monterrosae* (Cramer, 1969). These species have ranges that begin in the upper Telychian. *Margachitina margaritana* disappeared in the early Wenlock.

From the Wenlock onwards, no evidence of glaciation is known until the Late Devonian. Only a small area of Silurian outcrops has yet been investigated. Perhaps more research may reveal additional glacial evidence, and this may explain other gaps through the Silurian.

STRATIGRAPHY OF THE PARANÁ BASIN

The Ordovician–Silurian in the Paraná Basin corresponds to the Rio Ivaí Group and includes the Alto Garças, Iapó, and Vila Maria Formations (Assine et al., 1994). As originally proposed by Faria (1982), in the northern part of the Paraná Basin the Vila Maria Formation is based on a section that consists of basal diamictites and overlying shales that are capped by sandstones. The Vila Maria Formation now corresponds only to the shale and sandstone section, while the underlying diamictites are referred to the Iapó Formation. As noted by Assine et al. (1994), this latter name was first proposed by Maack (1947). The basal part of the sequence is attributed to the

Alto Garças Formation. The maximum thickness of the Rio Ivaí Group is about 400 m, but in Paraguay in the western outcrop belt of the Paraná Basin the maximum thickness is about 600 m (Wiens, 1990).

ALTO GARÇAS FORMATION.—This formation consists of a basal conglomerate followed by feldspathic and quartzitic sandstones in its upper part. At the base of the lower sequence, there are conglomerate beds up to 30 m-thick with a feldspathic matrix and clasts composed mainly of quartz pebbles. The conglomeratic section is followed by cross-bedded; white, yellowish white, and red; sub-angular to subrounded; feldspathic; conglomeratic sandstone beds with the proportion of pebbles decreasing upwards. The upper section is composed of tabular cross-stratified white and pink, subangular to rounded, friable, fine- to coarse-grained sandstone beds. Cores through the formation only yield trace fossils that are not useful for dating. These trace fossils indicate only a shallow-marine depositional environment for the upper part of the unit. The lower section has characteristics of fluvial deposition. The Alto Garças Formation rests on volcanic rocks as old as 466 ± 7 Ma (Moro, 1993). It is overlain unconformably by the Iapó Formation of probable middle Hirnantian age.

IAPÓ FORMATION.—Along its outcrop belt in the southeastern part of the Paraná Basin, this unit is 15–20 m-thick, but it is more than 150 m-thick in the subsurface. This tillite has abundant angular to subrounded clasts up to 25 cm in diameter that are supported by a structureless sandy to clayey matrix. Pebbles in the tillite commonly consist of granite, gneiss, rhyolite, and quartzite, all apparently derived from older igneous and metamorphic basement rocks. Other sedimentary and metamorphic clasts, including quartz, chert and phyllite, appear in smaller percentages. The tillite shows a vague stratification in some places, but generally it is unstratified. The matrix is red and yellow-brown in color, and turns grey in its basal part in cores.

Some clasts are faceted and striated (Maack, 1947; Assine et al., 1994). The rock texture and the occurrence of striated and faceted pebbles suggest that the Iapó Formation is a tillite deposited directly from ice sheets. In the northern part of the Paraná Basin, the diamictites are greenish-grey, unsorted and have polymictic coarse clasts that range from granule to boulder size (1 m across). The smaller clasts are mainly angular, and the larger ones are chiefly subrounded. These clasts consist of granite, gneiss, quartz, quartzite, rhyodacite, phyllite, metamorphosed tuff, and basic rocks that are supported by a sandy or silty and clayey matrix. Interbeds of laminated, micaceous, and gray-greenish shales also occur (Faria,

1982). The glacial nature of the diamictites in the northern belt of the Paraná Basin was recognized by Caputo and Lima (1984).

AGE OF THE TILLITES.—No fossils are present in the Iapó diamictites, and their age is inferred by the fossiliferous early to middle Llandovery shales of the overlying Vila Maria Formation. Interpretation of a middle Hirnantian age for these tillites is reinforced by their stratigraphic position and a glacial character that closely matches South African glacial deposits in the Cape Ranges and Argentina.

VILA MARIA FORMATION.—This formation consists of lower shales and upper sandstones. The lower unit includes black, greenish-gray to brown and red, calcareous, fossiliferous shale and siltstone interbeds with bivalves, gastropods, ostracodes, and inarticulate brachiopods (Faria, 1982). The upper unit is composed of yellow-white and pink, fine-grained, well-sorted, cross-bedded, and cross-laminated sandstones with pink siltstone interbeds with shell molds. Mud cracks and bioturbation are common. The unit is thin but widespread in the Paraná Basin. Burjack and Popp (1981) described *Arthrophyucus harlani*, an indicator of an Early Silurian age, from the Vila Maria Formation, and Gray et al. (1985) observed such early Llandovery microfossils as tetrahedral tetrads, acritarchs, and prasinophytes. According to Grahn (1993), the age of the Vila Maria Formation is late Aeronian–early Telychian based on chitinozoans (e.g., *Cyathochitina* sp. B of Paris, 1981). The environment of deposition was shallow marine and tidal flats.

ARGENTINE PRECORDILLERA

DON BRAULIO FORMATION.—New evidence from the lower Don Braulio Formation of the Argentine Precordillera supports the presence of a Late Ordovician glacial event in southern South America (Astini and Büggisch, 1993). The lower Don Braulio Formation consists of diamictite, conglomerate, sandstone, and shale. The thickness in outcrops is about 20 m. The diamictite includes a micaceous, light to dark gray, massive, clayey and silty matrix with scattered sand-sized grains, granules, cobbles, and pebbles, some of them faceted, polished, and striated. In the middle part, the section is composed of coarse-grained sandstone and conglomerate beds. The composition of clasts is about 50% meta-sandstone, 20% sandstone, 20% igneous rock, and 10% clasts of a wide variety of rock types. Sandstone and shale interbeds with dropstones show varve-like features. The main facies association in the lower and upper portion of

the section corresponds to melt-out tills. In the middle Don Braulio Formation, proglacial channels and lacustrine facies suggest an interglacial stage. The lower member is succeeded by a fossiliferous basal conglomerate and overlying shale beds of the upper Don Braulio Formation. These transgressive strata and overlying shale beds contain a rich Hirnantian fauna (Astini and Büggish, 1993) that suggest an early to middle Hirnantian age for the glacial event in the Argentine Precordillera.

HIGH EASTERN ANDES OF BOLIVIA AND PERU

CANCAÑIRI FORMATION.—In the eastern Andes and Andean foothills, glaciogenic units of Early Silurian age crop out along a belt that extends about 1,500 km from northern Argentina across Bolivia and into Peru (Crowell et al., 1980, 1981; Suarez-Soruco, 1995). Names applied to this interval include the Zapla (Schlangtweit, 1943), Cancañiri, and Sacta Formations in Bolivia; San Gaban Formation in Peru; and Mecoyita Formation in Argentina. This glaciogenic interval unconformably overlies several Ordovician formations that include Caradoc strata in Bolivia to Tremadoc beds in northern Argentina. The Cancañiri Formation is conformably overlain by the Kirusilhas Formation, which is largely dark gray shale with interbedded sandstone layers (Crowell et al., 1980, 1981). The Cancañiri includes structureless, micaceous diamictite that is intercalated with sandstone, conglomerate, and marine black shale. The diamictite is dark brown and is locally unstratified with an argillaceous to sandy matrix and scattered clasts of great petrographic variety. A few of these clasts are striated, faceted, and polished. Small sand lenses, which average 2 m thick and about 10 m in length, are cigar-shaped and deformed. Oversized clasts are abundant in some portions and rare in other sections of the Cancañiri Formation, and include quartz, quartzite, granite, gneiss, slate, conglomerate, sandstone, and shale fragments. The sedimentary clasts came from the Cancañiri and older formations. Black micaceous shale interbeds are also present. Slump and convolute structures are common. The thickness of the formation ranges from about 20 to 700 m, and reaches over 1,000 m in the Lake Titicaca area.

Because of the syntectonic character of the Cancañiri Formation, most fossils were reworked by erosion and resedimentation of older Ordovician units (Suarez-Soruco, 1995). The reworked taxa found in this section range from Early Ordovician in southern Bolivia to Late Ordovician in central Bolivia.

Palynological investigations indicate a Wenlock age (*Duvernaysphaera jelint* Zone) based on acritarchs and chitinozoans (Crowell et al., 1980, 1981). There are well-preserved trilobites, corals, mollusks, and brachiopods in shale beds that are intercalated between diamictite horizons. The trilobite *Paraencrinus boliviensis* suggests a Llandovery age. According to Suarez-Soruco (1995), acritarchs and chitinozoans found in these outcrops indicate an age close to the Llandovery–Wenlock boundary. Considering the reworked character of the unit and the age indicated by the youngest taxa, an early–late Early Silurian age is suggested for the Cancañiri Formation. It is thought that ice locally rimmed a marine basin, and that glaciers on the Brazilian Shield to the east and on highlands to the south and west contributed glacial debris. The Cordilleran orogenic cycle of Bolivia (Silurian–Early Carboniferous) featured the infill of a foreland basin with erosion of a fold–thrust belt located to the west and south related to east-dipping oblique subduction. Overthrusting of an accretionary prism was the probable cause for increased subsidence, sediment supply, and tectonic instability that led to sediment gravity flows and featured a development of topographic relief that allowed the glaciation reflected in the Cancañiri Formation (Diaz et al., 1996).

ORDOVICIAN–SILURIAN SEA-LEVEL CHANGES

The net growth of continental ice sheets and their advance towards the sea during cooling events are accompanied by sea-level falls, and the melting of continental ice promotes sea-level rises. In glaciated areas this relationship is very complex, because isostatic adjustments, which take place in response to variations in the ice load, are not synchronous with sea-level changes. In non-glaciated areas, the relationship between sea-level changes and glacial and interglacial phases is clearer.

The identification of latest Ordovician–Early Silurian glaciations in Western Gondwana may help to explain coeval sea-level falls that are documented in such continents as Laurentia, South China, and Baltica (Johnson et al., 1984, 1991; Johnson and McKerrow, 1991; Johnson 1996). A possible correlation of eustasy with glacial and interglacial episodes is offered in Figure 4. The sea-level curve of Figure 4 is for eastern Iowa on the Laurentian platform (from Johnson and McKerrow, 1991, fig. 3). This curve features four distinct highstands in sea-level recorded in the Llandovery Series. The eustatic nature of the Iowa sea-level curve is corroborated by correlation with several other areas in North America

(Johnson, 1987), China (Johnson et al., 1985), Scandinavia and the Baltic region (Johnson et al., 1991), and central Europe and Australia (Johnson, 1996).

CONCLUSIONS

Global sea-level fluctuations on the order of few meters up to 50 m occurred during the Silurian, according to many researchers. Indirect evidence of glaciation and cold temperatures includes rapid sea-level changes due to the transfer of water between ice sheets and oceans. Sea-level changes during glacial episodes are difficult to recognize in the Phanerozoic. However, during the Late Ordovician–Early Silurian, regressions and increased clastic supply correlate with glacial events (Figure 3). Eustatic falls may be caused by many different phenomena. When they are synchronous with proven glaciations, however, it is reasonable to interpret them as a result of water withdrawal with formation of continental ice caps. Sea-level drops during the Silurian after the early Wenlock seem to be related to other causes, because there are no presently known glacial events with which they could correlate.

Four short-lived glacial events in South America (Figure 2) correlate with shallowing events recorded on the North American craton and elsewhere. The study area in Brazil (Figure 1) is small, and more research is needed to interpret younger Silurian and Devonian stratigraphic gaps. Massive biotic extinctions and faunal changes have been attributed to a number of different causes, and different extinction events may have different causes, but the Late Ordovician–Early Silurian, latest Devonian, and Eocene–early Oligocene extinctions may have been due to coeval glacial episodes (Caputo, 1985) and resultant changes in sea-level during a glacial cycle.

ACKNOWLEDGMENTS

The author is grateful to J.H.G. de Melo, L. Borghi, Y. Grahm, and M.E. Johnson for discussions, suggestions, and revisions to this report. The Universidade Federal do Pará made this study possible. Peer reviews were supplied by C.R. Barnes and S.M. Bergstrom.

REFERENCES

- ASSINE, M.L., P.C. SOARES, AND E.J. MILANI. 1994. Sequências tectono-sedimentares Mesopaleozóicas da Bacia do Paraná, sul do Brasil. *Revista Brasileira de Geociências*, 24:77–89.
- ASTINI, R.A., and W. BÜGGISCH. 1993. Aspectos sedimentológicos y paleoambientales de los depósitos glaciogénicos de la Formación Don Braulio, Ordovícico tardío de la Precordillera Argentina. *Revista de la Asociación Geológica Argentina*, 48:217–232.
- BOUMENDJEL, K. 1987. Les chitinozoaires du Silurien supérieur et du Dévonien du Sahara Algérien (cadre géologique, systématique, biostratigraphie). Unpublished Ph.D. dissertation, University of Rennes, Rennes, 181 p.
- BÜGGISCH, W., and R.A. ASTINI. 1993. The Late Ordovician ice age: new evidence from the Argentine Precordillera, p. 439–447. In R.H. Findley, R. Unrug, M.R. Banks, and J.J. Veivers (eds.), *Gondwana Eight—Assembly, Evolution and Dispersal*. Balkena, Rotterdam.
- BURJACK, M.I., and M.I.B. POPP. 1981. A ocorrência do icnogênero *Arthropycus* no Paleozóico da Bacia do Paraná. *Pesquisas*, 14:163–168.
- CAPUTO, M.V. 1984. Stratigraphy, tectonics, paleoclimatology and paleogeography of northern basins of Brazil. Unpublished Ph.D. dissertation, University of California, Santa Barbara.
- . 1985. Late Devonian glaciation in South America. *Palaeogeography, Palaeoclimatology, Palaeoecology*, 51:291–317.
- , AND J.C. CROWELL. 1985. Migration of glacial centers across Gondwana during the Paleozoic Era. *Geological Society of America Bulletin*, 96:1020–1036.
- , and F.G. DE ANDRADE. 1968. Geologia em Semidetalhe do Flanco Sul da Bacia Amazônica, Entre os Rios Cupari e Abacaxis. *Petrobrás Internal Report No 598-A*, Belém, Brazil.
- , and E.C. LIMA. 1984. Estratigrafia, idade e correlação do Grupo Serra Grande-Bacia do Parnaíba. *Anais 33 Congresso Brasileiro de Geologia (Rio de Janeiro)*, Sociedade Brasileira de Geologia, 2:740–753.
- , and A.R.C. SAAD. 1974. Geologia do Baixo Rio Negro e Trecho da Estrada Br-174. *Petrobrás Internal Report No. 675-A*, Belém, Brazil.
- CAROZZI, A.V. 1979. Petroleum geology in the Paleozoic clastics of the middle Amazon Basin, Brazil. *Journal of Petroleum Geology*, 2:55–74.
- , H.R.P. PAMPLONA, J.C. CASTRO, and C.J.A. CONTREIRAS. 1973. Ambientes depocionais e evolução tectosedimentar da seção clástica paleozóica da bacia do Médio Amazonas. *Anais 27 Congresso Brasileiro de Geologia (Aracaju)*, Sociedade Brasileira de Geologia, 3:279–314.
- CROWELL, J.C., A.C. ROCHA-CAMPOS, and R. SUAREZ-SORUCO. 1980. Silurian glaciation in central South America, p. 105–110. In M. Cresswell and P. Vela (eds.), *Gondwana Five: Selected Papers and Abstracts of Papers Presented at the Fifth International Gondwana Symposium*. Balkena, Rotterdam.
- , and ———. 1981. The Silurian Cancañiri (Zapla) Formation of Bolivia, Argentina, and Peru, p. 902–907. In M.J. Hambrey and W.B. Harland (eds.), *Earth's Pre-Pleistocene Glacial Record*. Cambridge University Press.
- DAEMON, R.F., and C.J.A. CONTREIRAS. 1971. Zoneamento palinológico da Bacia do Amazonas. *Anais 25 Congresso Brasileiro de Geologia*, Sociedade Brasileira de Geologia, 3:79–92.
- DIAZ, E., R. LIMACHI, V.H. GOITIA, D. SARMIENTO, O. ARISPE, and R. MONTECINOS. 1996. Inestabilidad tectonica relacionada con el desarrollo de la Cuenca de Antepaís Paleozóica de los Andes Centrales de Bolivia, p. 299–308. In 1 Simposio Sul Americano do Siluro–Devoniano. *Estratigrafia e Paleontologia*. Anais do 1. Simposio Sul Americano do Siluro–Devoniano: *Estratigrafia e Paleontologia*, Ponta Grossa, Pr. Gráfica Planeta.

- FARIA, A. 1982. Formação Vila Maria-Nova unidade litoestratigráfica siluriana da Bacia do Paraná. *Ciências da Terra*, 3:12–15.
- GRAHN, Y. 1993. Chitinozoan biostratigraphy of the Parana Basin. *In* Simpósio Sobre a Cronoestratigrafia da bacia do Parana, 1, Rio Claro. Resumos, Rio Claro, UNESP, p. 10–12.
- . 1996. Ordovician and Silurian glaciations in Brazil. Abstract, p. 299–308. *In* 1 Simposio Sul Americano do Siluro-Devoniano—Estratigrafia e Paleontologia. Anais do 1 Simpósio Sul Americano do Siluro-Devoniano: Estratigrafia e Paleontologia, Ponta Grossa, Pr. Gráfica Planeta.
- , and M.V. CAPUTO. 1992. Early Silurian glaciations in Brazil. *Palaeogeography, Palaeoclimatology, Palaeoecology*, 99:9–15.
- , and F. PARIS. 1992. Age and correlation of the Trombetas Group. Amazonas Basin, Brazil. *Review of Micropaleontology*, 35:20–32.
- GRAY, Y., G.K. COLBATH, A. FARIA, A.J. BOUCOT, and D.M. ROHR. 1985. Silurian age fossils from the Paleozoic Paraná Basin, southern Brazil. *Geology*, 13:521–525.
- HARMS, J.C., D.R. SPEARING, J.B. SOUTHARD, and R.G. WALKER. 1975. Depositional Environments as Interpreted from Primary Sedimentary Structures and Stratification Sequences. Society of Economic Paleontology and Mineralogy, Short Course 2.
- JAEGGER, H. 1976. Das Silur und Unterdevon von Thüringischer typ in Sardinien und seine regionalgeologische Bedeutung. *Nova Acta Leopoldina*, 45(224):263–299.
- JOHNSON, M.E. 1987. Extent and bathymetry of North American platform seas in the Early Silurian. *Paleoceanography*, 2:185–211.
- . 1996. Stable cratonic sequences and a standard for Silurian eustasy, p. 203–211. *In* B.J. Witzke, G.A. Ludvigson, and J.E. Day, (eds.), *Paleozoic Sequence Stratigraphy: Views from the North American Craton*. Geological Society of America Special Paper 306.
- , and W.S. MCKERROW. 1991. Sea level and faunal changes during the latest Llandovery and earliest Ludlow (Silurian). *Historical Biology*, 5:153–169.
- , B.G. BAARLI, H. NESTOR, M. RUBEL, and D. WORSLEY. 1991. Eustatic sea-level patterns from the Lower Silurian (Llandovery Series) of southern Norway and Estonia. *Geological Society of America Bulletin*, 103:315–335.
- , RONG J.-Y., AND YANG X. 1984. Intercontinental correlation by sea-level events in the Early Silurian of North America and China. *Geological Society of America Bulletin*, 96:1384–1397.
- LANGE, F. W. 1967. Subdivisão bioestratigráfica e revisão da coluna Siluro-Devoniana da Bacia do Baixo Amazonas, p. 215–236. *In* Atas do Simpósio Sobre a Biota Amazonica, V. 1, Geociências.
- MAACK, R. 1947. Breves notícias sobre a geologia dos estados do Paraná e Santa Catarina. *Arquivos do Biologie e Technologie*, 2:63–154.
- MORO, R.X. 1993. A bacia Ordoviciano do Grupo Castro—PR. Rio Claro. M.Sc. thesis, IGCE-UNESP, 157 p.
- NOGUEIRA, A., E. SOARES, V. SOUZA, W. TRUCKENBRODT, and M.V. CAPUTO. *In press*. Estruturas glaciectônicas na Formação Nhamundá, Siluriano da Bacia do Amazonas.
- PARIS, F. 1981. Les Chitinozoaires dans le Paléozoïque du Sud-Ouest de l'Europe (Cadre Géologique, Etude Systématique, Biostratigraphie). *Mémoire du Societe géologique y mineralogique Bretagne*, Rennes, 26, 496 p.
- RODRIGUES, R., D.N.N. VASCONCELOS, and M.V. CAPUTO. 1971. Sedimentologia das Formações Pre-Pensilvanianas da Bacia do Amazonas. Petrobrás Internal Report No. 273-A.
- RUST, I.C. 1973. The evolution of the Paleozoic Cape Basin, southern margin of Africa, p. 247–276. *In* A.E.M. Nairn and F.G. Stehli (eds.), *The Ocean Basins and Margins*. Vol 1: South Atlantic. Plenum Press, New York.
- . 1981. Early Palaeozoic Pakhuis tillite, South Africa, p. 113–117. *In* M.J. Hambrey and W.B. Harland (eds.), *Earth's Pre-Pleistocene Glacial Record*. Cambridge University Press, Cambridge.
- SCHLANTWEIT, O. 1943. La posición estratigráfica del yacimiento de hierro de Zapla y la difusión del horizonte glacial de Zapla en la Argentina y en Bolivia. *Revista Minera*, 13:115–127.
- SUAREZ-SORUCO, R. 1995. Comentarios sobre la edad de la Formación Cancañiri. *Revista Técnica de Yacimientos Petrolíferos Fiscales Bolivianos*, 16:51–54.
- SWAN, A.G. 1957. Geology of the Paleozoics on Urubu River. Petrobrás Internal Report No. 197-A, Belém, Brazil.
- WIENS, F. 1990. Estratigrafia Fanerozoica Resumida del Paraguay. Geoconsultores, Asunción, (Internal report).
- ZALAN, P.V., S. WOLFF, J.C.J. CONCEIÇÃO, I.S. VIEIRA, M.A.M. ASTOLFI, V.T. APPI, and O.A. ZANOTTO. 1987. A divisão tripartite do Siluriano da Bacia do Paraná. *Revista Brasileira de Geociências*, 17:242–252.

SILURIAN SEA-LEVEL CHANGE AT ARISAIG, NOVA SCOTIA: COMPARISON WITH THE STANDARD EUSTATIC PATTERN

RICHARD K. BAMBACH

Department of Geological Sciences, Virginia Polytechnic Institute and State University, Blacksburg, VA 24061

ABSTRACT—The Arisaig Group, a siliciclastic sequence that extends from the base of the Silurian into the Lower Devonian, was deposited predominantly in marine-shelf environments. Fluctuation in the abundance and thickness of tempestites and changes in the relative abundance of deposit-feeding and byssate suspension-feeding bivalves indicate intervals of shallower and deeper water. Other diagnostic features record occasional shifts to very shallow, to non-marine, or to deep-shelf and basinal depths. The Arisaig Group records six or seven highstands and seven lowstands of sea-level. These appear to correspond to seven of the eight highstands and seven of the nine lowstands of sea-level identified by Markes Johnson in his proposed Silurian standard eustatic sea-level curve.

INTRODUCTION

The Arisaig Group is the most complete section of Silurian rocks in the Appalachian-Caledonian mountain system and one of the most complete in the world (Boucot et al., 1974). Almost every stage and substage of the Silurian is probably represented. The Arisaig Group was deposited in the Avalonian suspect terrane and is now preserved in fault blocks in the Antigonish Highlands of northern mainland Nova Scotia. The best known outcrops occur between the Hollow Fault Zone on the south and Northumberland Strait on the north, with the most completely exposed section in low shoreline cliffs along the coast near the town of Arisaig, approximately 30 kilometers southwest of Cape George (Figure 1). Tectonism in the Middle and Late Paleozoic deformed the Antigonish Highlands area, and the outcrop belt is cut by numerous faults. Despite the probable representation of most stratigraphic subdivisions of the Silurian, no formation is preserved in a continuous, unbroken section. Lateral compression and folding have also caused internal

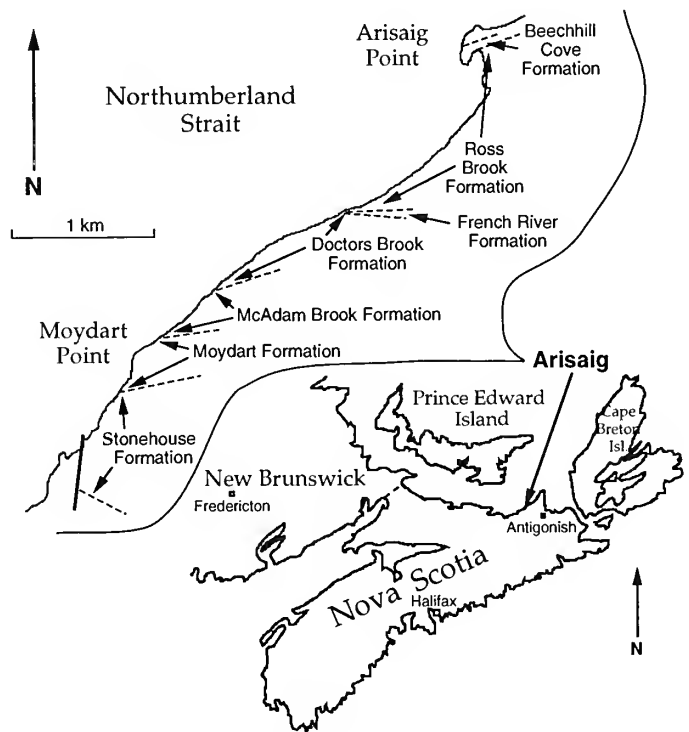


FIGURE 1—Index map of Nova Scotia with location of coastal outcrop of the Arisaig Group and enlarged map showing outcrop of each formation along the shore of Northumberland Strait. Section access is from a road to the pier at Arisaig Point that branches from Route 245 at the village of Arisaig, or by walking from Route 245 to the coastal outcrop of the Stonehouse Formation.

shearing and incipient reticulate cleavage (Bambach, 1973). This body deformation has also affected the thickness of the section (Waldron et al., 1996). Nonetheless, despite the significant deformation in the section, the general stratigraphic sequence is unambiguous, and the rocks are reasonably well-placed in age by the combination of fossils, stratigraphic position, and apparently continuous sedimentation, with no detected unconformities.

The preserved sedimentological and faunal characteristics are quite distinctive for the range of sedimentary environments represented in the sequence.

The Arisaig Group is predominantly fine-grained siliciclastic sediments (siltstones and mudstones). Only a few strata contain sand-size material; no conglomerate occurs above the basal beds of the section, and no pure limestones are present. Over 90% of the section are mudstones and interbedded tempestites. The section is fossiliferous throughout. With one exception, the only carbonate sediment in the section is derived from fossil debris. On the basis of sedimentological characteristics and faunal interpretation, the bulk of the section was deposited in mid- to shallow-shelf environments, with only one interval of deeper basinal deposition (including fissile, graptolitic shales) and one subaerial interval (a red bed with carbonate nodules interpreted as a warm-climate soil). The predominantly marine Arisaig Group is bracketed between non-marine sediments and volcanics of Late Ordovician age at the base and non-marine redbeds of Early Devonian age at the top.

The section was measured in detail in 1964 and 1965, with corrections for fault displacement made by matching key beds across faults where possible. Collections of bivalves were taken at 368 stratigraphic levels in the 1,200 meter-thick section (Bambach, 1969). Boucot et al. (1974), Watkins and Boucot (1975), Lane and Jensen (1975), Cant (1980), Pickerill and Hurst (1983), and Hurst and Pickerill (1986) provide supplementary data on all or parts of the section. Since all these data were obtained before the study of sea-level became the focus of modern stratigraphy, they provide an unusual opportunity to see if change in sea-level is apparent in a data set collected when detection of sea-level change was not a goal. In addition, the data allow an evaluation of whether or not this remarkable section of siliciclastic rocks records any readily detectable signals of the eustatic changes during the Silurian Period documented by Markes Johnson and colleagues from carbonate sections (Johnson, 1996, and references therein). Variation in bathymetry is easily detected in tempestite-rich sections (Kreisa, 1981; Aigner, 1985), and bivalve mollusks are particularly good environmental indicators that provide a further monitor of variation in depositional conditions because of their range of distinctive interactions with both sediment type and food supply in different benthic environments (Stanley, 1970, 1972; Levinton and Bambach, 1975; Bennington, 1995).

The criteria for identifying different bathymetric conditions will be discussed in the next section of the paper. No effort has been made to quantify depths; only relative terms are used. This is because the data are from a single section, and were obtained with no intention of

defining or calculating absolute depths. It would be pure speculation to attempt absolute depth estimates with the data available, but relative comparisons within the section are warranted. After the criteria for different bathymetric interpretations have been noted, the stratigraphic section at Arisaig will be described from bottom to top, with notes on the most probable age correlations and apparent changes in sea-level. Finally, the bathymetric changes observed at Arisaig will be compared to the standard for eustasy through the Silurian.

INDICATORS OF GENERAL BATHYMETRIC CONDITIONS

The Arisaig section was deposited predominantly in shallow-shelf environments (Bambach, 1969; Boucot et al., 1974; Watkins and Boucot, 1975). Variation does exist, however, and a number of environments are present in the Arisaig section. These environments are all described with reference to the predominant shallow-shelf marine setting, and the diagnostic criteria used to differentiate the different environments from the "norm" in the section are noted.

Marine environments occur throughout the Arisaig section. They are identified by the presence of a variety of marine fossils (articulate brachiopods; palaeotaxodont, pteriomorph, palaeoheterodont, and heterodont bivalves; gastropods; cephalopods; trilobites; crinoids; bryozoans; and graptolites). Tempestites are typical of shelf-depth, marine environments (Kreisa, 1981; Einsele and Seilacher, 1982; Aigner, 1985). Tempestite-related bedding characterizes the entire section, with the exception of the basal beds of the Beechhill Cove Formation, the 30 meter-thick lower member of the Ross Brook Formation, and the upper (red) member of the Moydart Formation (Figure 2). None of the graded beds in the Arisaig Group have the characteristics of turbidites. All seem to be tempestites (Bambach, 1969; Cant, 1980). Studies by Kreisa (1981), Kreisa and Bambach (1982), and Aigner (1985) update the conclusions about storm processes in Cant (1980). The coarse fraction of most Arisaig tempestites is reworked in situ, not transported, material introduced into the shelf environment during the storms that formed the beds. Similarly, the fossils in coquinities at the bases of the tempestites are also reworked, but are derived from the local environment (Kreisa and Bambach, 1982).

SHALLOW SHELF.—Abundant bivalves characterize shelf faunas during much of the Paleozoic (Ziegler, 1965; Ziegler et al., 1968; Bretsky, 1969; Calef and Hancock, 1974; Boucot, 1975). Mixed bivalve faunas, containing a

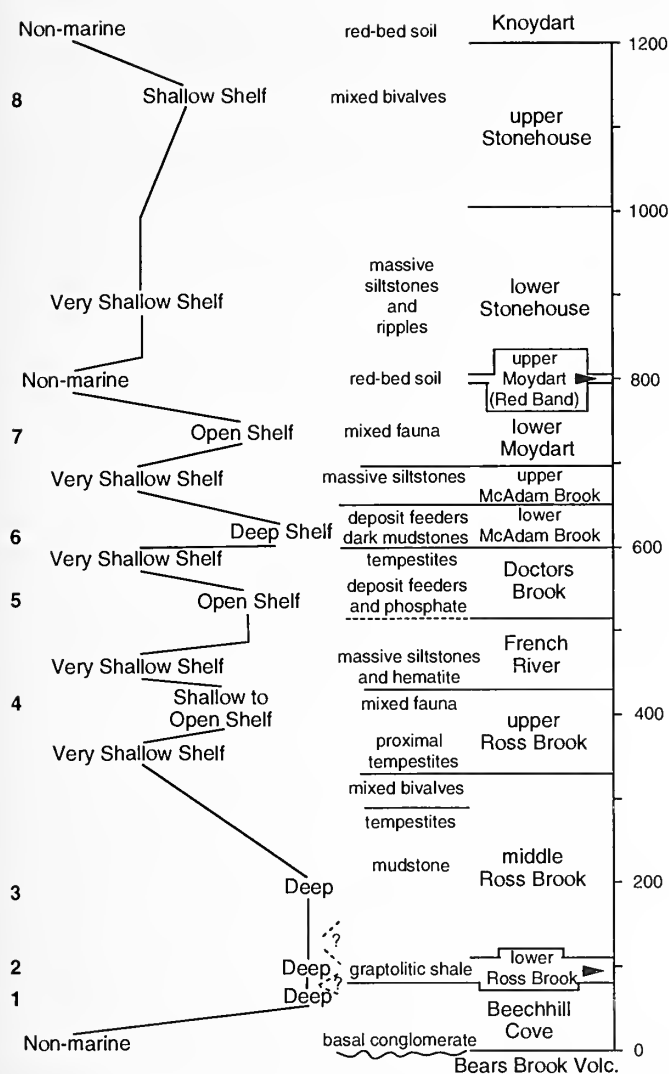


FIGURE 2—Stratigraphy of Arisaig sequence (on the right with thickness in m) and notes on the evidence that indicates lowstand and highstand conditions. Diagram of bathymetric changes through the Arisaig Group in the left-hand column with interpretations of environmental setting for highest and lowest sea-level stands and lines that indicate sea-level trends (shallower on left, deeper on right). Numerals 1–8 mark highstands that may correlate to the Silurian standard eustatic curve (Johnson, 1996).

mixture of deposit- and suspension-feeders, are abundant in parts of the middle and upper members of the Ross Brook Formation, the middle and upper parts of the lower member of the McAdam Brook Formation, and the upper member of the Stonehouse Formation (Table 1). These parts of the Arisaig Group are regarded as representing relatively shallow, marine-shelf environments. Thin tempestites (2–10 cm-thick) characterize these same parts of the Arisaig Group, and also indicate shelf environmental conditions below “fair-weather” wave base, but were shallow enough that major storms frequently

reworked the sediments to a depth of several centimeters (as described in Kreisa, 1981, and Aigner, 1985). Comparisons of other bedding and faunal characteristics with the features of the shallow-shelf setting are used to identify parts of the Arisaig Group that represent shallower- or deeper-water environments and, therefore, fluctuation in relative (and possibly global) sea-level.

VERY SHALLOW SHELF.—In the Arisaig section, very-shallow-shelf conditions are represented by intervals characterized by thicker tempestites (up to 30–50 cm) that include some amalgamated beds and thinner mudstone interbeds between tempestites. In very-shallow-shelf deposits, the bivalve fauna often has a lower proportion of deposit-feeders because the higher-energy ambient conditions associated with shallower water kept organic matter in suspension, and it did not accumulate in the sediment to provide an abundant food supply for deposit feeders (Bambach, 1969; Bennington, 1995). Byssate, suspension-feeding bivalves, such as species of the Paleozoic mussel genus *Modiolopsis*, are the common forms in these more energetic habitats. Two less common sedimentary features also characterize these very shallow settings: 1) massive siltstones with load casts (produced by rapid influx of large amounts of coarser-grained sediment onto uncompacted muds) in the upper members of the Ross Brook and McAdam Brook Formations; and 2) abundant interference ripples on siltstones in the thick-bedded lower members of the Moydart and Stonehouse Formations.

DEEPER OPEN SHELF.—Somewhat deeper but still normal shelf environments are represented in the Arisaig section by moderately thick (up to 1 m), extensively bioturbated beds, and less common, relatively thin, distinct tempestites. The stratification suggests that the somewhat lower sediment accumulation rates characteristic of distal-shelf environments permitted more complete homogenization by bioturbation. The presence of allogenic sediments (an oolitic hematite bed up to 1.0 m-thick in the French River Formation, and phosphatic nodules in the Doctors Brook Formation) also suggest lower rates of clastic influx. Bivalves are still fairly abundant in the intervals transitional from shallow-shelf to deeper, open-shelf settings, with pteriods commoner than modiolopsids among suspension-feeders, and deposit-feeders usually predominating in abundance (Table 1). Faunas in the deeper, open-shelf deposits have far fewer bivalves than the shallow-shelf faunas, but include articulate brachiopods that Watkins and Boucot (1975) placed in “benthic assemblage 3 or 4”. Crinoids, indicative of clear water and invariant normal marine salinities, also become a noticeable part of the fauna in the Doctors Brook

TABLE 1—Composition of bivalve assemblages through the Arisaig Group at Arisaig, Nova Scotia. Intervals without data are parts of sequence that are nearly devoid of bivalve fossils. The depositional environment of the lower Ross Brook Formation was too deep for bivalves; other intervals in the Arisaig Group were so shallow that bottom conditions were too unstable for most bivalves. No collections have been processed from the Beechhill Cove Formation. Abbreviations: *Aris.*, *Arisaigia*; *Mod.*, *Modiolopsis*; *Nuc.*, *Nuculites*; *Pal.*, *Palaconeilo*; *Pter.*, *Pterinea*.

[illegible]

Formation and in the middle of the lower (green) member of the Moydart Formation.

DEEP WATER.—Sediments lacking tempestites must have been deposited in water deep enough that the bottom was little disturbed by major storms. Two relatively deep-water intervals occur at Arisaig. Deep outer-shelf conditions are recorded in the lower part of the lower member of the McAdam Brook Formation. The sediments are dark gray, massive mudstones with only a few, thin traces of storm-winnowed silts. The environment of deposition was sufficiently calm that abundant organic matter accumulated in the sediment, and the fauna contains common deposit-feeding bivalves even though it was not a typical setting for common bivalves in the Paleozoic. Basinal conditions are recorded by the fissile, dark-colored, graptolitic shales of the lower member of the Ross Brook Formation and the papery shales of the lower part of the middle member of the Ross Brook Formation. Benthic shelly fossils have been reported from only one horizon in these units.

NON-MARINE.—Weathered horizons on the tops of lava flows in the Bears Brook Volcanic Group that underlies the Arisaig Group have been interpreted as lateritic soils (Boucot et al., 1974). These features are further discussed by Johnson and Van Der Voo (1990). The unconformity surface at the contact of the Bears Brook Volcanic Group with the Arisaig Group also represents subaerial exposure and erosion. The upper (red) member of the Moydart Formation contains blocky red silty mudstones with calcareous nodules suggestive of some warm climate soils. Red beds with feldspathic sandstones and fossils of freshwater fish characterize the bulk of the Early Devonian Knydart Formation that conformably overlies the Stonehouse Formation.

THE ARISAIG GROUP AND ITS RELATIVE BATHYMETRY

The left side of Figure 2 shows the variation from shallower to deeper conditions throughout the Arisaig Group, with stratigraphic thickness for the vertical scale. The units are discussed in stratigraphic order below. All otherwise unreferenced descriptions are taken from Bambach (1969).

BEARS BROOK VOLCANIC GROUP.—The volcanic and sedimentary rocks that underlie the Arisaig Group are Ordovician (Boucot et al., 1975; Johnson and Van Der Voo, 1990). Lateritic soils on some of the lava flows dem-

onstrate that at least some of the volcanics in the Bears Brook Volcanic Group erupted subaerially, and the unconformity on which the Beechhill Cove Formation was deposited is a subaerial erosion surface of latest Ordovician age. Therefore, deposition of the Arisaig Group began at or slightly above sea-level.

BEECHHILL COVE FORMATION.—Pickerill and Hurst (1983) made a definitive study of the facies and brachiopod faunas of the Beechhill Cove Formation. The Beechhill Cove Formation is reported as 73 m-thick in a complete section at Doctors Brook (Pickerill and Hurst, 1983), but about 90 m were measured at Beechhill Cove without reaching the base (Bambach, 1969; Boucot et al., 1974). Brachiopods suggest an early Llandovery (Rhuddanian) age for the unit, but the recent report of Ashgill acritarchs from the Beechhill Cove Formation (Beck, 1996) raises the possibility that all or part of the formation may be latest Ordovician. The formation rests on an erosion surface and begins with a thin basal conglomerate that is succeeded by a red shale with marine trace fossils. The bulk of the formation is bioturbated mudstones and thin siltstones. These facies contain linguloid brachiopods, and several horizons are characterized by several different articulate brachiopods. Some crinoid columnals and several bivalves have also been reported (Bambach, 1969). About 1.5 m of laminated black shale that lacks both shelly fauna and bioturbation occur about 7–10 m below the top of the formation. Pickerill and Hurst (1983) reported *Dalmanella*-dominated brachiopod assemblages from the 2.0 m just below the black shale bed at Beechhill Cove. Springer and Bambach (1985) documented that dalmanellids commonly dominate muddy deep-shelf environments in the Late Ordovician. The uppermost part of the formation returns to bioturbated mudstones and tempestite siltstones. It is obvious that this sequence represents a deepening interval in the end-Ordovician–Rhuddanian that progresses from subaerial exposure to basinal depths, and concludes with a brief shallowing interval before the profound deepening that starts the succeeding Ross Brook Formation.

ROSS BROOK FORMATION.—Hurst and Pickerill (1986) discussed the facies and brachiopod faunas of the Ross Brook Formation in detail. Their work clarified stratigraphic details not completely recorded in Bambach (1969) or Boucot et al. (1974). But they apparently followed the standard practice of brachiopod specialists by collecting primarily from coquinites and shell clusters, and therefore did not adequately document the bivalve fauna in the formation. Data on the abundant bivalve fauna from Arisaig are available in Bambach (1969). In the Paleozoic, bivalve shells were predominately arago-

nitic and dissolved quickly after burial, often before lithification of the enclosing sediment. This means Paleozoic bivalves are commonly preserved as composite molds (McAlester 1962; Bambach, 1973). Molds in unlithified sediment cannot be reworked, and, because most coquinites are formed by reworking in storm events, the reworked fossils preserved in storm deposits are biased in favor of such calcitic forms as articulate brachiopods. However, studies of shelf tempestites (Kreisa and Bambach, 1982; Springer and Bambach, 1985; Bennington, 1995) indicate that tempestite coquinites, such as those throughout the Arisaig Group, usually represent reworked local faunas rather than transported shells. The Ross Brook Formation is 310–340 m-thick and comprises three members.

LOWER MEMBER OF ROSS BROOK FORMATION.—The lower member of the Ross Brook Formation is a black, fissile, graptolitic shale about 30 m-thick that starts abruptly at the contact with the Beechhill Cove Formation. It lacks a significant benthic fauna. Waldron et al. (1996) reported that the graptolites in the shale span most of the middle Llandovery (Aeronian). The lower member represents renewed deep-water conditions during the Aeronian after the end-Ordovician (Rhuddanian) deepening and slight shallowing at the top of the Beechhill Cove Formation.

MIDDLE MEMBER OF ROSS BROOK FORMATION.—The middle member of the Ross Brook Formation is predominantly mudstone with thin siltstones in the middle and upper portions of the unit. The thickness of approximately 180–200 m is not known accurately because of structural complications and incomplete exposure of the lower part along the primary coastal exposure. Graptolites and brachiopods indicate that the unit probably ranges from the end of the middle Llandovery (Aeronian) to the late Llandovery (Telychian). Deeper-water shales low in the member give way to mudstones with thin tempestites in the middle to upper parts of the member. *Eocoelia*, a dominant shallow-shelf brachiopod genus (Ziegler, 1965; Ziegler et al., 1968), is common in most of the middle and upper parts of the member (Watkins and Boucot, 1975; Hurst and Pickerill, 1986). Rare occurrences of deposit-feeder-dominated bivalves also occur in shales in the middle of the member. A 5.0 m interval of frequent tempestites (50% of the section) about 25 m below the top of the member lacks bivalves, and the top 10 m of the member contain fewer and thinner tempestites and thicker mudstones, with a more diverse fauna that includes bivalves dominated by suspension-feeding modiolopsids. The sequence represents shoaling from deep-water through deeper, open-shelf to very shallow-shelf conditions in the early to middle Telychian.

UPPER MEMBER OF ROSS BROOK FORMATION.—The upper member of the Ross Brook Formation is later Telychian in age. Faulting prevents an accurate determination of the thickness of this member. It is a minimum of 100–110 m-thick, but faults in the lower middle part prevent complete resolution of the stratigraphic succession (some small intervals are probably faulted out). The top of the member is missing along the coast because it is faulted against the overlying French River and Doctors Brook Formations. The upper member is entirely late Llandovery (later Telychian). The lower and middle parts of the member were deposited in very shallow-shelf environments characterized by numerous thicker tempestites (up to 45 cm), and load casts and scour marks are present on the bases of many of the thicker siltstones in the middle of the member. The bivalve portion of the fauna in the lower part of the member is strongly dominated by just three species of byssate suspension-feeders, with only sporadic occurrences of other species. The bivalves are common only in a 10 m interval in the middle of the lower part of the member. Much of the top 20 m of the member exposed along the coast is composed of thick, massive, heavily bioturbated mudstones with a diverse fauna that includes both deposit-feeding and suspension-feeding bivalves. Cephalopods and gastropods also become common in the top 20 m of the upper member. At the highest exposures, the molluscan component of the fauna decreases, and brachiopods and graptolites are the most common fossils. The environments represented in the upper member of the Ross Brook Formation start with very shallow-shelf in the lower and middle parts of the member, deepen to shallow-shelf, and then are replaced by marginally deeper, open-shelf conditions at the top of the coastal exposure of the member. As *Eocoelia sulcata* is common in the highest coastal exposures (Hurst and Pickerill, 1986), the deepening high in the upper member of the Ross Brook Formation is very late Telychian (C6 Llandovery).

FRENCH RIVER FORMATION.—The French River Formation is the poorest exposed formation in the Arisaig Group at Arisaig, Nova Scotia. It is not exposed in the classic coastal section, and faulting complicates its stratigraphic expression in stream sections in the area. The formation appears to be 40–80 m-thick. It is composed predominantly of siltstones from 5–40 cm-thick with accompanying thin shales. A bed of oolitic hematite is present in the middle of the unit at several sections. Because the formation overlies the later late Llandovery upper member of the Ross Brook Formation and contains fossils known to range from the late Llandovery into the Wenlock, the French River Formation is probably mostly early Wenlock (Sheinwoodian). In stream sections, the

contact with the Ross Brook Formation is conformable, but the lithology changes dramatically from dark mudstones into light-colored siltstone. The shift to primarily winnowed sediments indicates a marked shallowing. The bed of oolitic hematite (up to 1.0 m-thick) indicates a further decrease in siliciclastic sediment supply. A complex interaction of tectonic movement and eustatic change seems to have been involved in deposition of the formation. Although the sediments are clearly related to higher energy deposition associated with fairly shallow water, the fauna in the iron ore and scattered through the siltstones indicates open-shelf, not shallow-shelf, environments (benthic assemblage 3–4 according to Watkins and Boucot, 1975). Bambach (1969) observed trilobites and nautiloids, as well as brachiopods and a mixed fauna of shallow-burrowing deposit-feeding and byssate suspension-feeding bivalves, at the type section of the formation about 30–35 km southwest of Arisaig, which is also consistent with open-shelf environments. Apparently after the initial shallowing at the base of the formation, subsidence was slow and sedimentation continued in shallow, high-energy conditions. However, sea-level rose enough by the middle of the formation to flood the source of clastic sediments, and only fossils and allogenic precipitates accumulated in open-shelf conditions during the deposition of the hematite bed.

DOCTORS BROOK FORMATION.—The Doctors Brook Formation is approximately 85 m-thick, but faulting repeats parts of the lower half of the formation along the coast section at Arisaig and prevents a precise determination of the thickness. Although no distinctive, biostratigraphically useful fossils have been recorded from the formation, the age of the Doctors Brook Formation is inferred to be late Wenlock (Homerian) because it underlies the lower member of the McAdam Brook Formation, which contains distinctive early Ludlow graptolites (Boucot et al., 1974), and overlies the earlier Wenlock French River Formation. The lithology is predominantly blocky, medium- to thick-bedded (up to 50 cm) mudstones with thin-bedded (10 cm or less) siltstone and coquinite tempestites. Phosphatic nodules are present in some of the siltstones and coquinites. The brachiopod fauna is similar to that in the French River Formation (benthic assemblage 3–4 according to Watkins and Boucot, 1975), but fossils are far more common than in the French River Formation. Crinoid columnals are abundant in some beds, even forming a few crinoidal coquinites, and deposit-feeding bivalves are common in the thick mudstone beds of the lower part of the formation. Mudstones decrease in thickness as thicker siltstones with interference ripples become common in the upper 30 m of the formation. The lower and middle parts of the formation represent open-shelf environments, as

suggested by the nature of the brachiopod fauna, prevalence of deposit-feeding bivalves, and the presence of crinoids and phosphatic nodules. The environment shallowed through the upper middle part of the formation, and the upper part of the unit represents shallow- to very shallow-shelf environments.

MCADAM BROOK FORMATION.—The McAdam Brook Formation is about 95 m-thick. All but about 10 m of the formation is exposed continuously along the coast section. Although the section is cut by numerous small normal faults, the section can be precisely reconstructed by tracing key beds across different fault blocks (Bambach, 1969). This revealed a nearly continuous, gradational change in facies and faunas from the bottom to the top of the formation. The lithologies change upward from blocky, dark gray mudstones with no tempestites through interbedded, dark gray mudstones and silty tempestites to massive siltstones with large load casts. Levinton and Bambach (1975) documented the faunal sequence of bivalves and its environmental setting. The formation is dated as early Ludlow (Gorstian), based on graptolites (Boucot et al., 1974).

LOWER MEMBER OF MCADAM BROOK FORMATION.—On the coast, the contact of the Doctors Brook and McAdam Brook Formations displays a sharp change from light gray, silty mudstone to dark gray mudstone. At the contact, burrows into the top bed of the Doctors Brook Formation are filled with dark-colored mudstone of the basal McAdam Brook Formation. This seems to represent a rapid deepening from very shallow to deep open-shelf conditions. At several other localities, Boucot et al. (1974) reported the contact as gradational. The lithology of the lower member changes from massive mudstones to mudstones with thin siltstone laminae that represent slight winnowing from storm events in deep water to thick mudstones and thin tempestites to mudstones with regularly interbedded tempestites up to 6 cm-thick. This whole sequence represents a sudden deepening to deep open-shelf conditions at the contact with the underlying Doctor's Brook Formation that was followed by near-continuous shallowing to shallow-shelf conditions at the top of the lower member. The bivalve fauna reflects this environmental change as well. The bivalves change from a fauna of non-siphonate deposit-feeders adapted to life in seldom disturbed, quiet, soupy, deep-water muds to siphonate deposit-feeders adapted for burrowing in the coherent muds of shallower waters that were swept clear of a soupy overlayer by frequent currents. Levinton and Bambach (1975) documented parallel changes in this Silurian sequence and in modern deposit-feeding bivalve communities.

UPPER MEMBER OF MCADAM BROOK FORMATION.—The lithology of the upper member is massive siltstones and silty mudstones in beds up to 60 cm-thick. Large loadcasts occur in the middle of the member and indicate rapid deposition of the overlying siltstone beds on still uncompacted mudstones. A shelly fauna is not abundant in this member. Interference ripples mark the tops of the siltstones in the upper part of the member. These features indicate that the environment of deposition of the upper member was very shallow-shelf, and that the shallowing that characterizes the lower member continued through the deposition of the upper member of the McAdam Brook Formation.

MOYDART FORMATION.—The Moydart Formation is 115 m-thick and is divided into two distinctive but unequal members. The lower (green) member is 105 m-thick, whereas the upper (red) member is only 10 m-thick. The Moydart overlies the well-dated early Ludlow (Gorstian) McAdam Brook Formation, and late Ludlow (Ludfordian) fish remains have been reported from the upper (red) member (Boucot et al., 1974), so it appears that the formation is late Ludlow (Ludfordian).

LOWER (GREEN) MEMBER OF MOYDART FORMATION.—The lower member is composed of massive silty mudstones and siltstones in beds up to 1.25 m-thick. Vertical burrows are common in the lowest 10 m and the top 15 m of the member, and intense bioturbation, more obvious than in any other part of the section, has disrupted much of the primary lamination in many of the beds. Interference ripples are common in all but the middle third of the member. Fossils are concentrated primarily in coquinites in the lower and upper parts of the unit, but are dispersed in the finer-grained beds in the middle part of the member, the only part of the member where bivalves occur. The bivalves are mostly byssate suspension-feeders. Bryozoans and articulated crinoid calyces are also found in the middle of the member. Intermittent high sedimentation rates are evident in the lower part of the unit. Articulated crinoid stems up to 40 cm in length are preserved vertically in life position in one bed. The lower part of the lower member of the Moydart Formation was deposited in very shallow-shelf environments, with these very shallow conditions that persisted from the upper member of the McAdam Brook Formation. Conditions then deepened to open-shelf in the middle of the member, and returned to very shallow-shelf in the upper part of the unit.

UPPER (RED) MEMBER OF MOYDART FORMATION.—The 10 meter-thick upper (red) member of the Moydart Formation is composed of red silty mudstone. The basal and uppermost meters each contain thin laminations. Dineley

(1963) reported linguloid brachiopods and fish spines from the basal laminated portion. The lamination at the contact with the overlying Stonehouse Formation suggests intertidal cryptalgal laminae. The features at both the base and top of the unit are consistent with a transition from marine to non-marine conditions. The bulk of the unit appears to be non-marine, with pedogenic carbonate nodules.

STONEHOUSE FORMATION.—The highest marine unit in the Arisaig Group is the 425 m-thick Stonehouse Formation. The formation is dated as Pridoli on the basis of both conodonts and brachiopods (Boucot et al., 1974). The overlying Knoydart Formation is dated as Gedinian (Boucot et al., 1974), and the top 20 or 30 m of the Stonehouse Formation, which is exposed only in streams inland of the coast section, also may be earliest Devonian (Bambach, 1969). There are two members of the formation, each a bit over 200 m-thick.

LOWER MEMBER OF STONEHOUSE FORMATION.—The lithology of the lower member of the Stonehouse Formation is very similar to the lower and upper parts of the lower member of the Moydart Formation. Massive, thoroughly bioturbated silty shales up to 1.25 m-thick and laminated siltstones up to 30 cm thick with extensive interference ripple-marked surfaces comprise the whole unit. The only shelly fossils are found in coquinites at the bottoms of some of the laminated siltstones. The entire 205 m of the member represent very shallow-shelf environments. Fragmentary remains of freshwater fish have also been identified in this unit, and further indicate proximity to shore (Bambach, 1969).

UPPER MEMBER OF STONEHOUSE FORMATION.—A deepening and shallowing occurred between the very shallow-shelf environments of the lower member and the transition to non-marine conditions in the overlying Knoydart Formation. The 210–215 m of the upper member of the Stonehouse Formation are interbedded thin mudstones and tempestites. The thickest mudstones are about 50–60 cm-thick, and the thickest tempestites are about 30 cm-thick, but many of each are thinner. The beds are richly fossiliferous. The entire unit represents shallow-shelf environments. Variation in the bivalve fauna in the upper member reveals that the maximum depth produced by the deepening event in the upper member of the Stonehouse was reached in a 15 m-thick interval about 60–70 m below the top of the formation. In this interval, the proportion of deposit-feeders rises to about 55% of the bivalve fauna, compared to the 55–60% proportion of suspension-feeders both below and above this deepest-water segment of the section (Table 1). As noted

above, the proportions of suspension-feeding and deposit-feeding bivalves are often related to depth. The accumulation of low specific gravity organic particles in the sediment that the deposit-feeders utilized for food is inversely correlated to the frequency and intensity of agitation, which decreases with increasing water depth.

KNOYDART FORMATION.—Conformably overlying the Stonehouse Formation is the Knoydart Formation. The contact, which is only exposed inland in small stream valleys, is gradational, with the beds changing from fossiliferous coquinites to barren, micaceous, fine-grained sandstones to red sandstones and siltstones with calcareous nodules similar to the lithology of the upper (red) member of the Moydart Formation. Fining-upward cycles above this transition are apparently fluvial sequences, and at least three horizons have produced fossils of freshwater fish of definite Gedinnean age (Boucot et al., 1974). The Arisaig section ends in deposits formed above sea-level in the Early Devonian.

COMPARISON OF ARISAIG BATHYMETRY AND SILURIAN EUSTASY

Johnson (1996) established a standard eustatic curve for the entire Silurian. The curve was developed after numerous studies and in collaboration with several other workers; references are listed in Johnson (1996). Johnson listed eight major highstand events and nine lowstands (including the lowstands that bound the Silurian System). Four of the highstands occur in the Llandovery, with one at the Rhuddanian–Aeronian boundary, a second in the Aeronian, the third early in the Telychian, and the fourth near the end of the Telychian. The fifth highstand is a complex one in the early to middle Wenlock (Johnson [1996] diagramed some fluctuation in sea-level during this highstand). The sixth and seventh highstands are Ludlow, one at the base of the Gorstian and the other in the middle Ludfordian. The eighth Silurian highstand occurs in the Pridoli. The nine lowstands occur at the beginning of the Silurian (related to the Ashgill glacial event), between each of the highstands, and in the Early Devonian.

As shown in Figures 2 and 3, there is nearly a one-to-one correspondence of highstands in the Arisaig Group with those in Johnson's Silurian standard eustatic curve. The only part of the eustatic curve that is not well-represented is in the early and middle Llandovery. There are doubts about the exact age of the Beechhill Cove Formation, although the unit almost certainly represents a deepening sequence likely to represent the sea-level rise after the Ashgill glaciation, but it is not clear that the

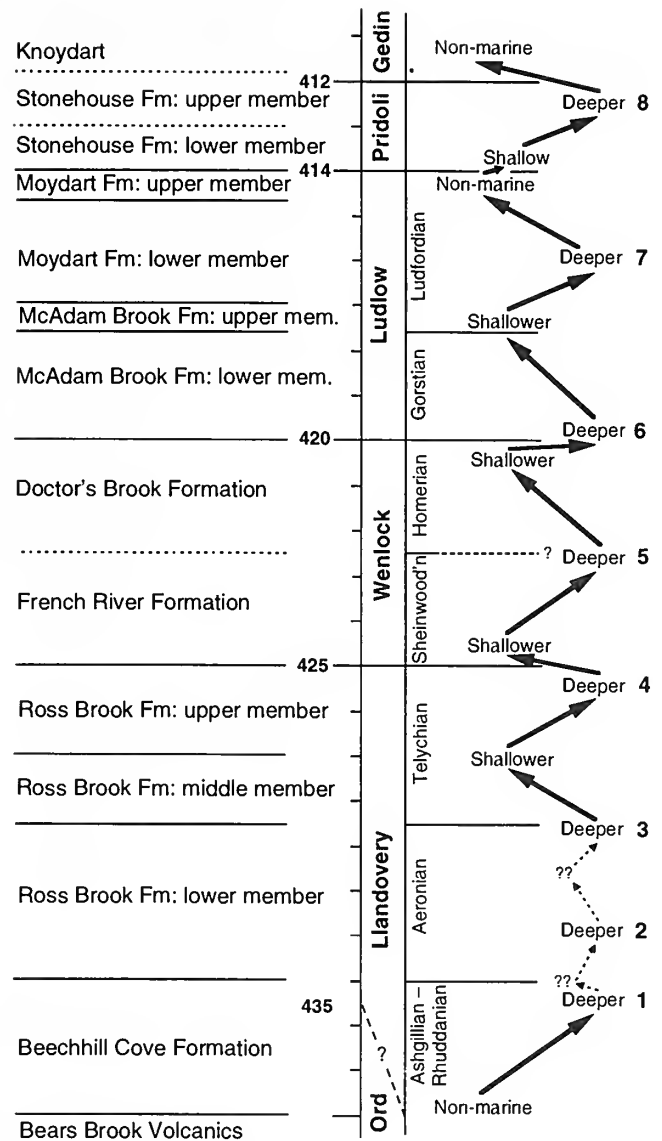


FIGURE 3—Suggested temporal positions of the eight sea-level highstands in the Arisaig section and correlation with highstands of the Silurian standard eustatic curve (Johnson, 1996). Numbers as in Figure 2. Beechhill Cove Formation, members of the Ross Brook Formation, lower member of the McAdam Brook Formation, upper member of the Moydart Formation, and Stonehouse Formation are dated by fossils. Lowstands between highstands 1–3 are not unambiguously identifiable in deep basinal facies of upper Beechhill Cove Formation and lower member of Ross Brook Formation.

highstand near the top of the unit is the Rhuddanian–Aeronian highstand. Deep basinal conditions occur in the Aeronian lower member of the Ross Brook Formation. Tectonic subsidence as well as sea-level rise is associated with this maximum highstand record at Arisaig. Continued deep-water conditions related to tectonic subsidence may have prevented the lowstand between the first two highstands in the Silurian from being recorded at Arisaig, and also may obscure the difference between the middle

Aeronian highstand and the Aeronian–Telychian boundary highstand. However, it is clear that the Arisaig section records high sea-level during the Aeronian (eustatic highstands 1 to 3), and the shallowing in the middle of the Ross Brook Formation corresponds with the middle Telychian shallowing in Johnson's eustatic curve. From then on, the Silurian section at Arisaig, within the current available limits on precise dating, is remarkable in its apparent faithful recording of eustatic fluctuations in a siliciclastic section.

Because the Arisaig area was tectonically active (Waldron et al., 1996), tectonism could have controlled sea-level in the area and obscured eustatic effects. However, the correspondence in number and the plausibility of timing of the pattern of shallowing and deepening parallel to Johnson's eustatic curve is striking. Waldron et al. (1996) have estimated subsidence curves for the Arisaig Group that show variation in subsidence rate through the Silurian at Arisaig. High subsidence rates are recorded for the Beechhill Cove, Doctors Brook, and Stonehouse Formations, and low rates are noted for the French River, McAdam Brook, and Moydart Formations. Sediment supply also varied. Relatively less sediment accumulated in the Beechhill Cove, French River, Doctors Brook, and Moydart Formations, and more sediment accumulated in the Stonehouse Formation than would be expected if sediment accumulation and the passage of time had been in balance throughout the section. The item of interest for this report is that, except for the Aeronian, the rate of sediment supply was almost always closely balanced with accommodation space at Arisaig during the Silurian, despite variations in subsidence rate. General depositional conditions remained in relatively shallow-shelf environments most of the time. It is this remarkable balance between sediment supply and accommodation space that permitted the section to record the effects of eustatic change.

ACKNOWLEDGMENTS

Data for this report were compiled for a dissertation submitted in partial fulfillment of the requirements for the Ph.D. at Yale University in 1969. I am still indebted to my doctoral advisory committee (A.L. McAlester, Chair) and, for many discussions of this work as it was compiled and for the learning experience of interactions in the field as the work was done, to A. Boucot, J. Dewey, S. McKerrrow, D. Rhoads, J. Rodgers, and A. M. Ziegler. In recent years, M.E. Johnson has encouraged me to unearth my old data and cast it in this more modern form. The manuscript was much improved by suggestions from M. Melchin, E. Landing, and an anonymous reviewer.

REFERENCES

- AIGNER, T. 1985. Storm Depositional Systems. Lecture Notes in Earth Sciences 3, Springer-Verlag, Berlin.
- BAMBACH, R.K. 1969. Bivalvia of the Siluro-Devonian Arisaig Group, Nova Scotia. Unpublished Ph.D. dissertation, Yale University, 376 p.
- , 1973. Tectonic deformation of composite-mold fossil Bivalvia (Mollusca). *American Journal of Science (Cooper Volume)*, 273—A:409–439.
- BECK, J.H. 1996. Bioevents in the Silurian Arisaig Group: a palynological perspective. Abstracts for the James Hall Symposium: Second International Symposium on the Silurian System. University of Rochester, August 4–9, 1996, p. 29.
- BENNINGTON, J.B. 1995. Community persistence and the pattern of community variability over time: a test using fossil assemblages from four marine transgressions in the Breathitt Formation (Middle Pennsylvanian) of eastern Kentucky. Unpublished Ph.D. dissertation, Virginia Polytechnic Institute and State University, Blacksburg, 436 p.
- BOUCOT, A.J. 1975. *Evolution and Extinction Rate Controls*. Elsevier, Amsterdam.
- , J.F. DEWEY, D.L. DINELEY, R. FLETCHER, W.K. FYSON, J.G. GRIFFIN, C.F. HICKOX, W.S. MCKERROW, AND A.M. ZIEGLER. 1974. Geology of the Arisaig Area, Antigonish County, Nova Scotia. *Geological Society of America Special Paper* 139.
- BRETSKY, P.W., Jr. 1969. Evolution of Paleozoic benthic marine invertebrate communities. *Palaeogeography, Palaeoclimatology, Palaeoecology*, 6:45–59.
- CALEF, C.E., AND N.J. HANCOCK. 1974. Wenlock and Ludlow marine communities in Wales and the Welsh Borderland. *Palaeontology*, 17:779–810.
- CANT, D.J. 1980. Storm-dominated shallow marine sediments of the Arisaig Group (Silurian–Devonian) of Nova Scotia. *Canadian Journal of Earth Sciences*, 17:120–131.
- DINELEY, D.L. 1963. The "Red Stratum" of the Silurian Arisaig series, Nova Scotia, Canada. *Journal of Geology*, 71:523–524.
- EINSELE, G., AND A. SEILACHER (eds.). 1982. *Cyclic and Event Stratification*. Springer-Verlag, Berlin.
- HURST, J.M., AND R.K. PICKERILL. 1986. The relationship between sedimentary facies and faunal associations in the Llandoverly siliciclastic Ross Brook Formation, Arisaig, Nova Scotia. *Canadian Journal of Earth Sciences*, 23:705–726.
- JOHNSON, M.E. 1996. Stable cratonic sequences and a standard for Silurian eustasy, p. 203–211. In B.J. Witzke, G.A. Ludvigson, and J.E. Day (eds.), *Paleozoic Sequence Stratigraphy: Views from the North American Craton*. Geological Society of America Special Paper 306.
- JOHNSON, R.J.E., AND R. VAN DER VOO. 1990. Pre-folding magnetization reconfirmed for the Late Ordovician–Early Silurian Dunn Point volcanics, Nova Scotia. *Tectonophysics*, 178:193–205.
- KREISA, R.D. 1981. Storm-generated sedimentary structures in subtidal marine facies with examples from the Middle and Upper Ordovician of southwest Virginia. *Journal of Sedimentary Petrology*, 51:823–848.
- , AND R.K. BAMBACH. 1982. The role of storm processes in generating shell beds in Paleozoic shelf environments, p. 200–207. In G. Einsele and A. Seilacher (eds.), *Cyclic and Event Stratification*. Springer-Verlag, Berlin.
- LANE, T.E., AND L.R. JENSEN. 1975. Stratigraphy of the Arisaig Group. *Maritime Sediments*, 11:119–140.

- LEVINTON, J.S., AND R.K. BAMBACH. 1975. A comparative study of Silurian and Recent deposit-feeding bivalve communities. *Paleobiology*, 1:97-124.
- MCALESTER, A.L. 1962. Mode of preservation in Early Paleozoic pelecypods and its morphologic and ecologic significance. *Journal of Paleontology*, 36:69-73.
- PICKERILL, R.K., AND J.M. HURST. 1983. Sedimentary facies, depositional environments, and faunal associations of the lower Llandovery (Silurian) Beechill [sic, read Beachhill] Cove Formation, Arisaig, Nova Scotia. *Canadian Journal of Earth Sciences*, 20:1761-1779.
- SPRINGER, D.A., AND R.K. BAMBACH. 1985. Gradient versus cluster analysis of fossil assemblages: a comparison from the Ordovician of southwestern Virginia. *Lethaia*, 18:181-198.
- STANLEY, S.M. 1970. Relation of shell form to life habits of the Bivalvia (Mollusca). *Geological Society of America Memoir* 125.
- . 1972. Functional morphology and evolution of byssally attached bivalve mollusks. *Journal of Paleontology*, 46:165-212.
- WALDRON, J.W.F., J.B. MURPHY, M.J. MELCHIN, AND G. DAVIS. 1996. Silurian tectonics of western Avalonia: strain-corrected subsidence history of the Arisaig Group, Nova Scotia. *Journal of Geology*, 104:677-694.
- WATKINS, R., AND A.J. BOUCOT. 1975. Evolution of Silurian brachiopod communities along the southeastern coast of Acadia. *Geological Society of America Bulletin*, 86:243-254.
- ZIEGLER, A.M. 1965. Silurian marine communities and their environmental significance. *Nature*, 207:270-272.
- , L.R.M. COCKS, AND R.K. BAMBACH. 1968. The composition and structure of Lower Silurian marine communities. *Lethaia*, 1:1-27.

EARLY SILURIAN STRATIGRAPHIC SEQUENCES OF EASTERN WISCONSIN

MARK T. HARRIS¹, JEFFREY J. KUGLITSCH², RODNEY WATKINS³,
DANIEL P. HEGRENES¹, AND KURT R. WALDHUETTER¹

¹Department of Geosciences, University of Wisconsin–Milwaukee, Milwaukee, WI 53201,

²Department of Geology and Geophysics, University of Wisconsin–Madison, Madison, WI 53706, and

³Milwaukee Public Museum, 800 W. Wells Street, Milwaukee, WI 53233.

ABSTRACT—Lower Silurian strata of eastern Wisconsin include inner- and middle-shelf deposits in the north and outer-shelf and ramp deposits in the south. Water-depth curves constructed from sedimentological and paleontological data show depositional sequences of early Rhuddanian, late Rhuddanian–early Aeronian, early–middle Aeronian, late Aeronian–early Telychian, Telychian, and late Telychian–early Sheinwoodian age. These sequences correlate to sea-level cycles described from several other regions, and this suggests strong eustatic control. Depositional sequences are easily recognized in shallow-water deposits of northeastern Wisconsin, where exposure surfaces are well-developed, and sedimentary facies and faunas are sensitive to changes in water depth. In contrast, the deeper setting of southeastern Wisconsin masks the sea-level cycles because water depth changes are not readily resolvable.

INTRODUCTION

Silurian strata underlie eastern Wisconsin adjacent to Lake Michigan (Figure 1), although Pleistocene sediments cover most of the outcrop belt. The most abundant natural exposures occur at the northern end of this belt in the Door Peninsula (Door and Brown Counties; Figure 2). Scattered quarry outcrops occur throughout eastern Wisconsin, and were the only data sources available for the Waukesha County study area, 200 km south of the Door Peninsula. The two study areas lie on a line oblique to depositional strike, and lie between the Wisconsin Arch (to the west and northwest) and the Michigan Basin (to the east and southeast).

Different stratigraphic nomenclatures have been used for the two areas since the work of Chamberlin (1877). In the Door Peninsula, Shrock (1940) applied the northern Michigan nomenclature (Ehlers and Kesling, 1957; Ehlers, 1973), and its use has continued with minor

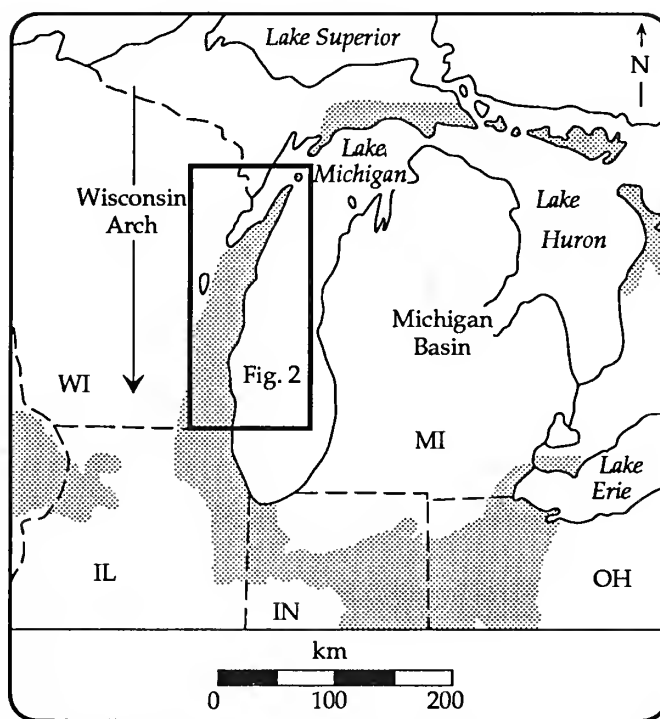


FIGURE 1—Generalized Silurian outcrop (or pre-Pleistocene subcrop) in the Great Lakes region (shaded areas). Location of Figure 2 shown. Modified from Lowenstam (1950).

modifications (Stieglitz, 1989; Kluessendorf and Mikulic, 1989; Harris and Waldhuetter, 1996). Chamberlin's (1877) stratigraphic nomenclature for southeast Wisconsin has been variously modified by Alden (1918), Mikulic (1977), and Mikulic and Kluessendorf (1988). Rovey (1990) and Kluessendorf and Mikulic (1996) introduced names for stratigraphic units defined in Illinois (Willman, 1973) and northern Michigan. Our column for Waukesha County is a hybrid of Wisconsin and Michigan nomenclature and is discussed below. Figure 3 summarizes the relationship between the stratigraphic units of the two areas.

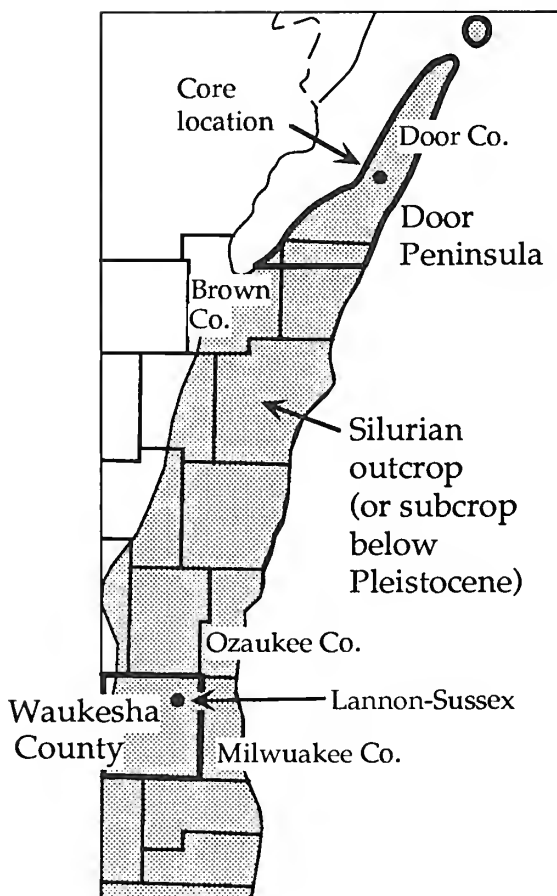


FIGURE 2—Study areas in the Door Peninsula and Waukesha County, Wisconsin. See Harris and Waldhuetter (1996), Hegrenes (1996) and Kuglitsch (1996) for locality data. Location of Door Peninsula core (Figure 6) and Lannon-Sussex area (Figure 9) given.

This contribution reviews our recent work in these two areas and uses new biostratigraphic data (detailed below) to correlate the five Llandovery depositional sequences recognizable in the updip Door Peninsula with the downdip Waukesha County outcrops. In addition, at least two younger (Wenlock) sequences are present in Waukesha County sections. The sequences (informally termed S1–S7) provide a stratigraphic framework for interpreting relative sea-level changes from facies. The relative sea-level curve established in the Door Peninsula is correlative with those described from other regions, and suggest a strong control by eustatic changes in their generation.

SILURIAN FACIES AND BENTHIC ASSEMBLAGES

Depositional facies are informal rock units characterized by lithologic fabrics, sedimentary structures, and faunas indicative of a shared depositional environment (Figure

System	Series	Stage	Door Peninsula	Sequen.	Waukesha County
SILURIAN	Wenlock	Ludlow			
	Llandovery	Telychian			Racine Formation
					Waukesha Formation
			Engadine Dolostone	S6	Brandon Bridge Form.
			Manistique Formation	S5	Manistique Formation
	Llandovery	Aeronian	Cordell Member		
			Schoolcraft Member	S4	
			Hendricks Dolostone	S3	Burnt Bluff Group
	Rhuddanian	Rhuddanian	Byron Dolostone		
			Mayville Dolostone	S2 S1	Mayville Dolostone
ORDOV.			Maquoketa Formation		Maquoketa Shale

FIGURE 3—Stratigraphy and correlation of the study areas. Nomenclature for Waukesha County is tentative. Brandon Bridge Formation equivalent to part of the Waukesha Formation and is not present in Lannon-Sussex area (see Figure 9). Unconformities indicated in the sequence column. Rhudd. is Rhuddanian Stage. Data from Ehlers and Kesling (1957), Ehlers (1973), Willman (1973), Mikulic (1977), Mikulic and Klusendorf (1988), Stieglitz (1989, 1991), Johnson and Stieglitz (1990), Rovey (1990), Kleffner et al. (1994), Kuglitsch (1994, 1996), Waldhuetter (1994), Watkins et al. (1994), Harris and Waldhuetter (1996), Hegrenes (1996), and Watkins and Kuglitsch (1997).

Facies & Environment	Depositional textures	Common sedimentary structures	Benthic assemblage
Laminite Tidal flat	mudstone, wackestone	flat, wavy and crinkly laminations, burrows	BA 1
Packstone Shallow shelf	packstone, wackestone, boundstone	ripples, burrows	BA 2
Burrowed Deeper shelf	wackestone, mudstone, packstone	burrows, bioturbation	BA 3
Grainstone Shelf margin	grainstone, packstone, boundstone	ripples, cross-beds, reefs	BA 2-3
Mudstone Slope	mudstone, wackestone	flat to wavy beds, intraclasts, graded beds	BA 4-5

FIGURE 4—Lithology and benthic assemblages of the Silurian of eastern Wisconsin. Depositional textures listed in order of decreasing abundance.

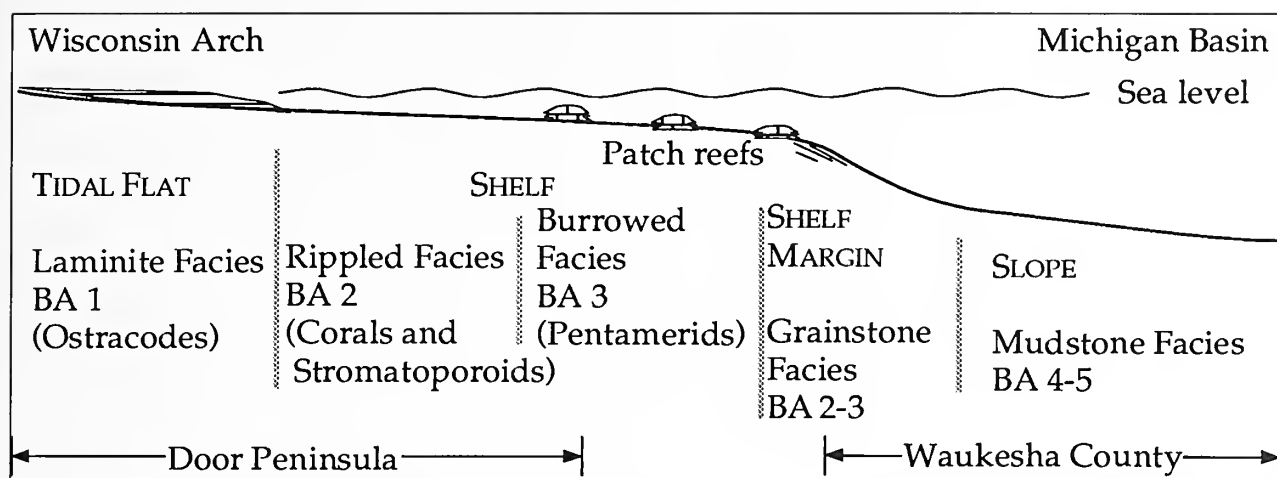


FIGURE 5—Facies model for the Silurian of eastern Wisconsin. Study areas projected into transect from the Wisconsin Arch to the Michigan Basin.

4) (Demicco and Hardie, 1994). In the Silurian of Wisconsin, depositional facies closely parallel the Benthic Assemblage (BA) classification of Boucot (1975). Boucot's classification ranges from BA 1 (intertidal facies) to BA 6 (deep basinal facies). For example, a tidal flat environment is represented by a laminite facies with a BA 1 fauna. Brett et al. (1993) concluded that most Silurian benthos inhabited the photic zone, with outer shelf faunas of BA 4 occupying water depths no greater than 60 m.

Depositional facies and benthic assemblages indicate that the Door Peninsula section consists of inner- to middle-shelf deposits (Harris and Waldhuetter, 1996; Harris et al., 1996), whereas the Waukesha County strata accumulated in an offshore setting (Kuglitsch, 1996). Watkins and Kuglitsch (1997) documented a similar lateral facies change from tidal flat (BA 1) to basin (BA 4–5) in time-equivalent Aeronian strata of Wisconsin and Michigan. Our generalized facies model for eastern Wisconsin features a projection of the outcrop areas into a single cross-section (Figure 5).

The sequences that comprise the Door Peninsula sections consist of stacked transgressive–regressive couplets. The transgressive systems tracts (TST) ideally consist of a deepening succession of laminite–packstone–burrowed facies, although most are incomplete. The highstand systems tracts (HST) are generally thicker than TSTs, and contain the same facies arranged in a shallowing succession capped by exposure surfaces. Sequence boundaries do not necessarily coincide with existing formation or facies boundaries. In Waukesha County to the south, sequence boundaries are obscure because of the deeper water setting.

Correlation of the stratigraphic units and sequences between the two areas is based on conodont biostratigra-

phy. Conodont abundance in Wisconsin Silurian dolostones is very low. For the Waukesha County section, 262 kg of dolostone from the Burnt Bluff Group through the Racine Formation were digested to yield 1,550 conodont elements (Kuglitsch, 1996). For the Door Peninsula and the equivalent section in northern Michigan, 387 kg of dolostone from the Byron through the Engadine were digested, and yielded 1,815 conodont elements (Watkins and Kuglitsch, 1997; J.L. Kuglitsch, unpublished data). These low conodont yields impose limits on biostratigraphic resolution, and zone boundaries can only be approximately located.

DOOR PENINSULA.—The Door Peninsula section consists of five well-defined Llandovery depositional sequences (Harris and Waldhuetter, 1996; Harris et al., 1996; see Figure 6). In cores (Hegrenes, 1996), the Silurian overlies an exposure surface that represents the Hirnantian (latest Ordovician) hiatus. Sequence S1 consists of a transgressive–regressive succession that constitutes the bulk of the Mayville Dolostone, and is capped by a weathered zone located within an interval of laminite facies. The upper Mayville and part of the Byron Dolostone comprise sequence S2; this sequence is predominantly a laminite facies with a thin burrowed facies interval that represents the transgressive maximum. The age assignments of these two sequences is largely based on the occurrence of the brachiopod *Virgiana mayvillensis* in the upper part of the Mayville Dolostone, and is Rhuddanian, based on the range of *Virgiana* in Canada (Jin et al., 1993). The precise position of the Rhuddanian–Aeronian boundary is uncertain.

Sequence S3 consists entirely of laminite facies and forms the uppermost Byron Dolostone and almost all of

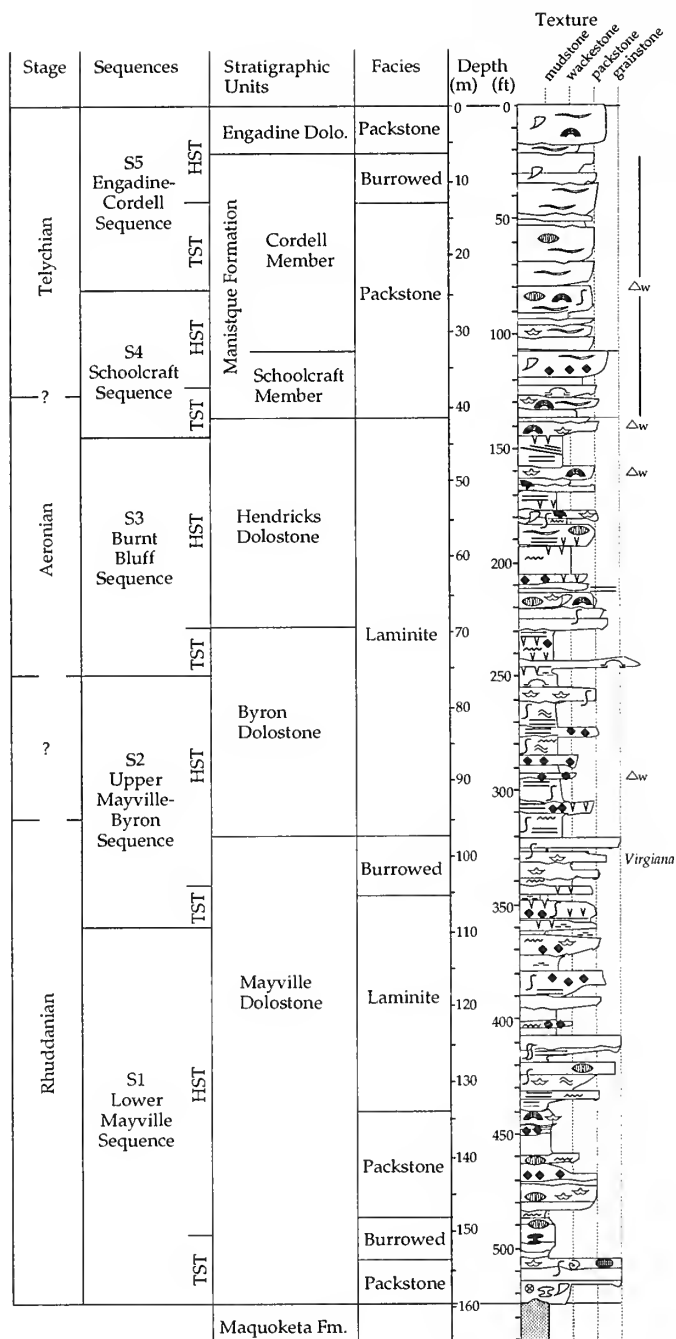


FIGURE 6—Jarmen Road core, Door County (Hegrenes, 1996). See Figure 7 for explanation of symbols in column.

the overlying Hendricks Dolostone. A low-angle truncation surface marks the top of the sequence in outcrop. Age control is provided by conodonts in the upper part of the Byron Dolostone (a few meters above the base of sequence S3) that range upward to the top of the Hendricks Dolostone. The conodonts include *Icriodella deflecta*, *I. discreta*, *Kockelella manitoulinensis*, *Oulodus* spp., *Ozarkodina oldhamensis*, *Ozarkodina* sp. A and *Ozarkodina* sp. B of

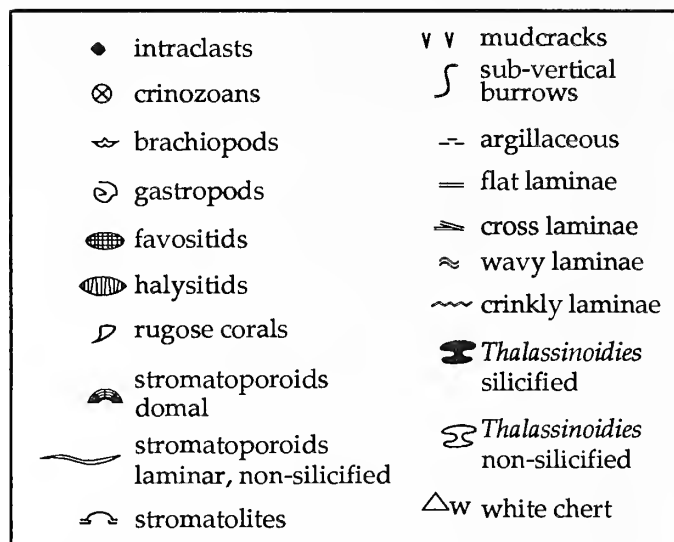


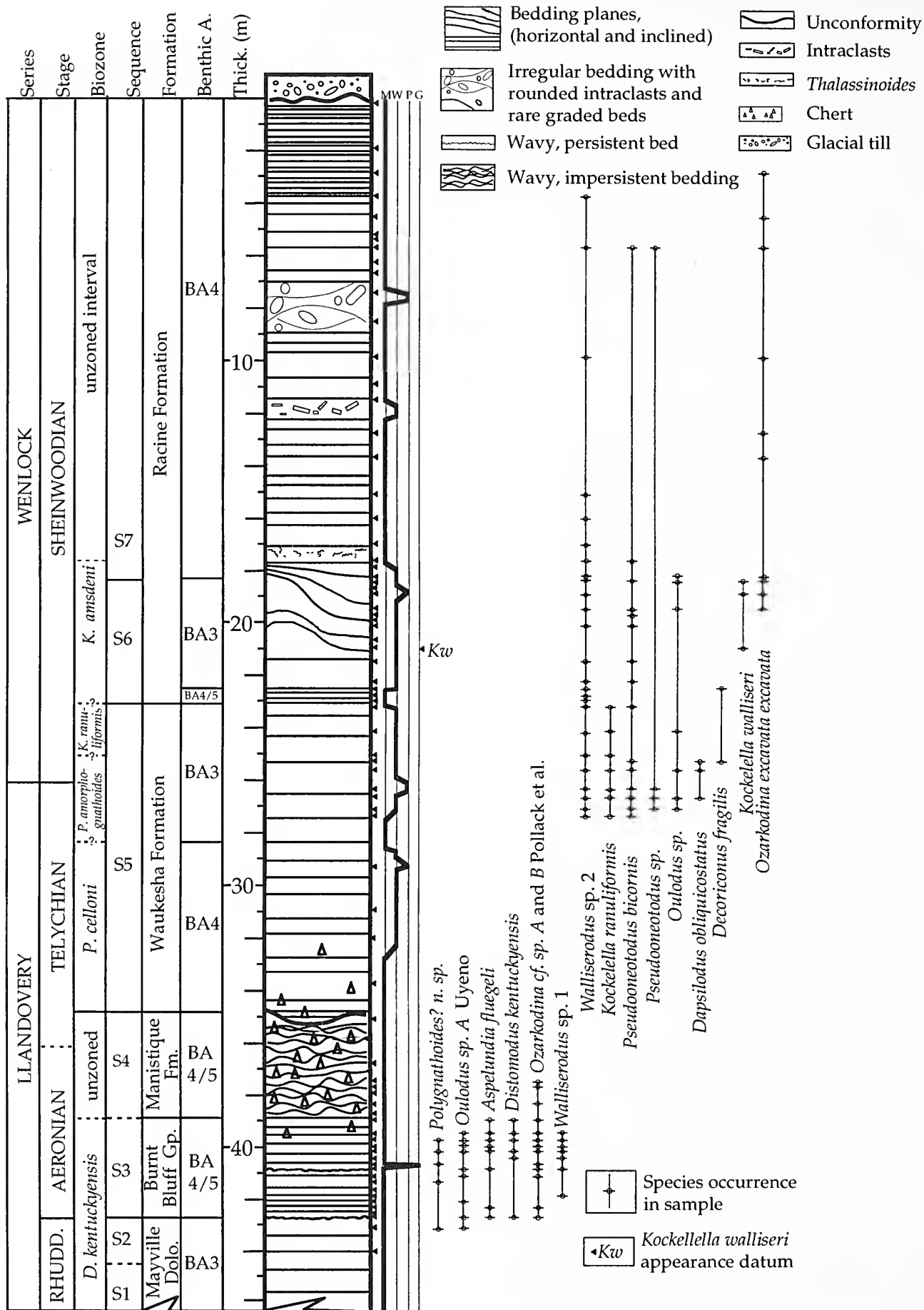
FIGURE 7—Explanation of symbols in Figure 6.

Pollack et. al. (1970), and *Panderodus* sp. (see Watkins and Kuglitsch, 1997). These taxa represent the upper part of the *Icriodella discreta*-*Icriodella deflecta* Zone, which indicates an early to middle Aeronian Age (Aldridge, 1972; Uyeno and Barnes, 1983).

The Manistique Formation and the Engadine Dolostone make up sequences S4 and S5. The Manistique has not yielded diagnostic conodonts, but contains *Pentamerus oblongus* and *Pentameroides bisinuatus* of possible late Aeronian through Telychian Age (Watkins, 1994). The Engadine Dolostone contains the conodont *Aulacognathus bullatus*, which indicates a Telychian to possible earliest Sheinwoodian Age (Kuglitsch, 1994). These data permit rough age assignments, but do not allow precise location of the stage boundaries (Figure 6). The depositional facies and the benthic assemblages indicate predominantly shelf conditions (BA 2 and 3), although shallowing and possible exposure is indicated at the top of sequence S4 in the northern Door Peninsula (Harris and Waldhuetter, 1996) and the adjacent Upper Peninsula of Michigan (Johnson and Campbell, 1980).

We base the water depth curve for the Door Peninsula (Figure 8) on the depositional facies and the benthic assemblages (see Figure 5). The generally shallow depths (BA 1–3) reflect a geological setting adjacent to the Wisconsin Arch.

WAUKESHA COUNTY.—The Silurian in Waukesha County (Figure 9) consists mainly of outer-shelf and ramp deposits (Kuglitsch, 1996; Watkins and Kuglitsch, 1997). The water-depth curve for this area (Figure 8) is based largely on benthic assemblages. These assemblages indicate greater water depths than in the Door Peninsula, and are consistent with a more basinal setting.



of the undifferentiated Burnt Bluff and the Mayville represents a deepening event that is correlated with the base of sequence 3 in Door County. In Waukesha County, the Burnt Bluff Group contains conodonts of the upper part of the *Distomodus kentuckyensis* Zone and the lower *Aspelundia fluegeli* Zone of Armstrong (1990); this indicates an early to middle Aeronian Age (Kuglitsch, 1996; Watkins and Kuglitsch, 1997).

The Burnt Bluff is conformably overlain by a unit of bioturbated mudstone with common chert-replaced *Thalassinoides*. This cherty unit has been called the "Franklin Member" of the Manistique Formation (Rovey, 1990) and the "Schoolcraft Dolomite" (Kluessendorf and Mikulic, 1996). Aside from its chert content, the unit is not lithologically similar to the Schoolcraft of Door County, and we refer to it simply as the Manistique Formation. The Manistique of Waukesha County contains the same diverse BA 4–5 fauna as the underlying Burnt Bluff Group (Watkins and Kuglitsch, 1997). Conodonts are rare, and recovered taxa (Figure 9) are not diagnostic of age. The base of sequence 4 has not been recognized.

In the section in the Lannon–Sussex area (Figure 9), the Manistique Formation is disconformably overlain by the Waukesha Formation, and the contact of these units is an erosional surface at the base of sequence 5. Eight km to the south at the Waukesha Lime and Stone Company quarry, this same erosional surface is overlain by a unit of argillaceous dolostone known as the Brandon Bridge Formation (Kluessendorf and Mikulic, 1996). The Brandon Bridge, which pinches out south of the study area, contains conodonts of the *Pterospathodus celloni* Zone and the lower part of the *Pterospathodus amorphognathoides* Zone, and is Telychian (Watkins et al., 1994; Kleffner, 1995). Kluessendorf and Mikulic (1996) interpreted the erosional surface beneath the Brandon Bridge Formation to mark the position of a significant hiatus. However, they presented no data on the precise age of the underlying Manistique. While we accept this surface as a sequence boundary, we do not believe that a temporal gap of conodont-zone magnitude is present.

In the Lannon–Sussex area, the Waukesha Formation above the base of sequence 5 is dominated by mudstone and wackestone with a sparse, probable BA 4 fauna of crinozoans, brachiopods, and bryozoans (Kuglitsch, 1996). We correlate this part of the Waukesha with the Brandon Bridge Formation to the south (Figure 3). The absence in the Lannon–Sussex area of conodonts diagnostic of the *Pterospathodus celloni* Zone and the lower part of the *Pterospathodus amorphognathoides* Zone may reflect an inadequate sampling and low conodont yields (0.2 elements per kg of sample).

The upper part of the Waukesha Formation in the Lannon–Sussex area is characterized by crinozoan wackestones, although minor mudstones and packstones are also present. These beds, which locally exhibit large-scale, low-angle cross-stratification, also contain corals, stromatoporoids, brachiopods (including unidentified pentamerids), and mollusks that represent a BA 3 fauna. The upper part of the Waukesha contains early Sheinwoodian conodonts that are tentatively assigned to the uppermost *Pterospathodus amorphognathoides* Zone and *Kockelella ranuliformis* Zone (Figure 9). This is consistent with the highest occurrence of *P. amorphognathoides* within the basal 1.5 m of the Waukesha Formation above the Brandon Bridge Formation at the Waukesha Lime and Stone Company quarry to the south (Kleffner, 1995). The recovery of a *Distomodus* Pa element (probably *D. staurognathoides*) from crinozoan wackestone at Sussex supports assignment to the *Pterospathodus amorphognathoides* Zone (Kuglitsch, 1996). The uppermost beds of the Waukesha Formation are assigned to the *Kockelella ranuliformis* Zone because of the presence of *K. ranuliformis*, absence of *Distomodus* elements, and their stratigraphic position slightly below the first occurrence of *Kockelella walliseri*.

The base of the overlying Racine Formation is marked by a laterally persistent bed of dense mudstone that contains scattered large cephalopods (Mikulic, 1977; Kuglitsch, 1996). This mudstone indicates a deepening event, and its lower contact represents the base of sequence 6. Above the cephalopod bed is a unit of crinozoan wackestone and packstone with horizontal stratification defined by partial sorting of ossicles. This unit contains a diverse BA 3 fauna dominated by robust crinoids, the cystoid *Caryocrinites*, platycerid gastropods, and brachiopods (Kuchta et al., 1997). The crinozoan beds contain conodonts typical of the *Kockelella amsdeni* Zone of Barrick and Klapper (1976), which is equivalent to the upper *Ozarkodina sagitta rhenana* Zone of Aldridge and Schönlaub (1989). These beds contain *Kockelella walliseri*, a species believed to have originated from *Kockelella ranuliformis* in the Sheinwoodian (Aldridge and Schönlaub, 1989; Kleffner, 1989, 1994). The short stratigraphic

FIGURE 9—(opposite) Ranges of selected conodonts in Lannon–Sussex composite section, Waukesha County (Kuglitsch, 1996). Omitted are *Panderodus* sp. (present in almost every sample), *Distomodus stenolophata* (single occurrence in Burnt Bluff), *Aspelundia petila* (small number of elements in Burnt Bluff), and *Distomodus* sp. (single occurrence in the upper Waukesha). Samples indicated by small triangles between the graphic log and the Dunham texture log. See text for discussion of assignment of faunal zones. Sub-Waukesha–Brandon Bridge disconformity shown in graphic log by thick line at Manistique–Waukesha contact.

interval between the first appearance of *K. walliseri* and the last appearance of *K. ranuliformis* (Figure 9) is assumed to include the interval of this speciation event.

The crinozoan beds are overlain by a unit of the Racine Formation that consists of well-bedded, bioturbated mudstone. The base of this mudstone unit is the base of sequence 7 and marks a deepening event. The fauna and age of this part of the Racine have been studied in areas to the west and north of Waukesha County, as discussed below.

RACINE FORMATION IN MILWAUKEE AND OZAUKEE COUNTIES.—In Milwaukee County, burrow-churned, well-bedded, argillaceous dolomitic mudstone of the Racine Formation is stratigraphically equivalent to the portion of the Waukesha section above the base of sequence 7. These beds include an ichnofauna dominated by *Palaeophycus*, *Chondrites*, *Planolites*, and locally silicified *Thalassinoides* (Watkins, 1991; Watkins and Coorrough, 1997a). Skeletal material in the mudstone is dominated by small crinozoan ossicles, and spicules of lithistid, hexactinellid and heteractinid sponges are locally common (Watkins and Coorrough, 1997b). Diverse small brachiopods, inclusive of *Dicoelosia*, *Skenidioides*, *Leangella* and *Resserella*, represent BA 5 (Watkins, 1991; Coorrough and Watkins, 1997). Less common taxa include over 50 species of receptaculitids, corals, bryozoans, molluscs, cornulitids, annelids, ostracods, trilobites, and dendroid graptolites. Reefs in the upper part of the Racine Formation contain a very diverse, stromatoporoid–coral–crinozoan-dominated fauna (Watkins, 1993, 1997).

In Milwaukee County, the Racine Formation has yielded a single graptoloid that indicates a Wenlock age no younger than Homerian (Watkins, 1991). At Grafton, Ozaukee County, mudstone beds near the top of the Racine yield *Ozarkodina sagitta sagitta* (Kuglitsch, 1994, 1996). This conodont species indicates the *Ozarkodina sagitta sagitta* Zone of Walliser (1964). Equivalent to the *Ozarkodina sagitta sagitta* Zone of Aldridge and Schönlaub (1989), this zone ranges from the Homerian to earliest Gorstian. The Racine is overlain by the Waubakee Formation, a laminated mudstone of intertidal and supratidal origin with a fauna not indicative of a precise age (Mikulic and Kluessendorf, 1988).

DISCUSSION

Biostratigraphic data permit correlation of the Door Peninsula and Waukesha County sections (Figures 3, 8). A comparison of the two areas indicates that the exposure surfaces and shallowing–deepening cycles that characterize sequence boundaries are most clearly expressed in

updip positions (such as the Door Peninsula). Both the depositional facies and the benthic assemblages are most sensitive to changes in sea-level at the shallow end of the depositional profile. By contrast, shallowing events are poorly resolved in coeval basinward sections (Waukesha County), because deeper water benthic associations have broader depth ranges.

The biostratigraphic data also allow correlation of the Wisconsin sequences and sea-level curves to other regions in Laurentia (Figure 10). Similar Llandovery cycles have been recognized in the Michigan Basin (i.e., in the Upper Peninsula of Michigan (Johnson and Campbell, 1980) and Manitoulin Island (Johnson, 1981), as well as in the Appalachian Basin (Brett et al., 1990a, 1990b), Midcontinent (Johnson, 1975, 1996; Ross and Ross, 1996; Witzke and Bunker, 1996), Willison Basin (Johnson and Lescinsky, 1986), Great Basin (Harris and Sheehan, 1996, 1998), and western Canada (Lenz, 1982). These cycles have been correlated to other continents (Johnson et al., 1985, 1991; Johnson and McKerrow, 1991; Johnson, 1996; Ross and Ross, 1996). The similarity in the sea-level curves in these areas indicate a eustatic control on cyclicity. The middle Rhuddanian sea-level fall is less widely recognized but appears in New York (Brett et al., 1990a, 1990b), the Great Basin (Harris and Sheehan, 1996; this volume), and Estonia (Johnson, 1996), and this suggests it was of lesser magnitude than the others.

Future revisions of the Silurian stratigraphy of the Great Lake region could make use of the eustatic control on cyclicity, as implied by Shaver (1996). Sequence stratigraphy is most useful in shelf settings as a tool for integrating biostratigraphic, sedimentologic, and paleontologic data. Sequence correlations could assist the recognition of stratigraphic equivalents throughout the region. In a broader perspective, use of sedimentological data (as in the Door Peninsula) improves the recognition and correlation of Silurian cycles.

CONCLUSIONS

Early Silurian water-depth curves for eastern Wisconsin can be derived from the integration of depositional facies and benthic assemblages. Conodont biostratigraphy has clarified correlations and stratigraphic relationships between the Door Peninsula and Waukesha County areas. Stratigraphic sequences are readily resolvable in shallow inner-shelf sections (Door Peninsula). In equivalent basinward sections (Waukesha County), the sequences are not clearly recognizable, because facies changes do not closely reflect changes in water depth. The eastern Wisconsin sequences are correlative with

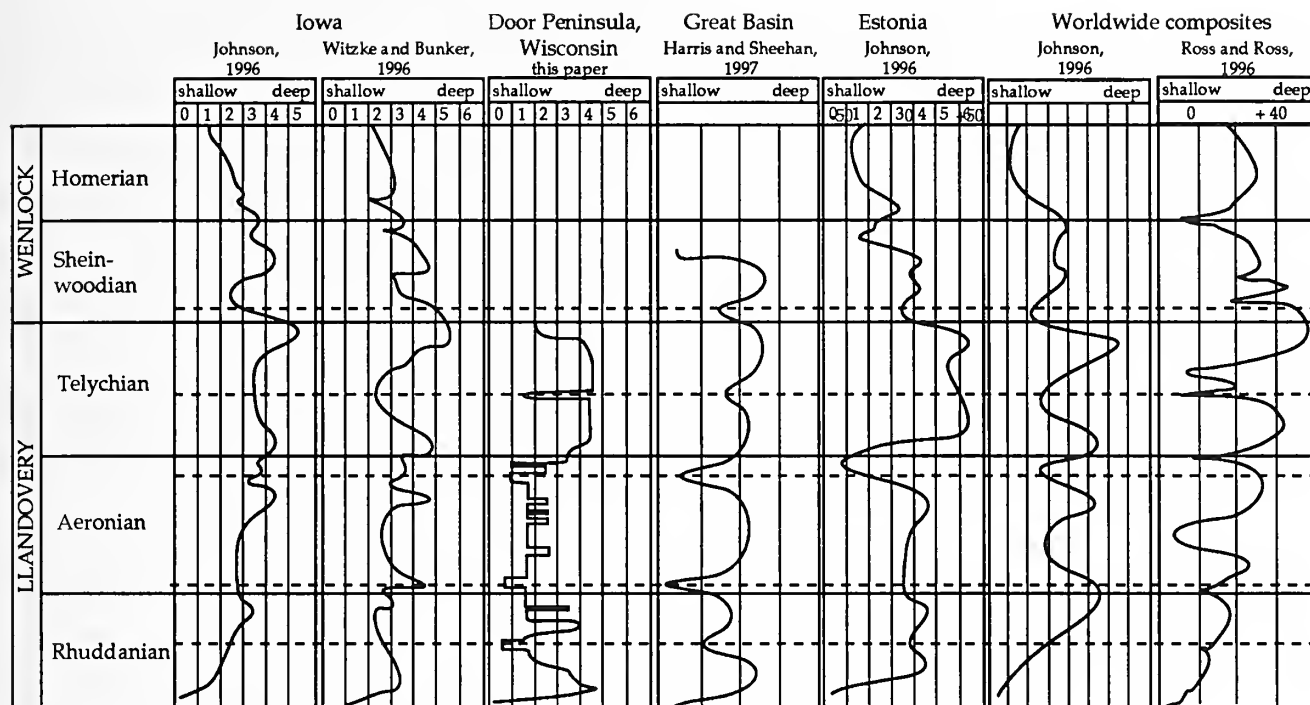


FIGURE 10—Comparison of Early Silurian sea-level curves for Iowa, the Door Peninsula, the Great Basin, and Baltica with global composite of Johnson (1996) and Ross and Ross (1996). Dashed lines show approximate position of sequence boundaries recognized in Door Peninsula. Sea-level curves for Iowa, Wisconsin, and Estonia are tied to benthic assemblages, but Great Basin and Ross and Ross (1991) curves are in meters. Johnson intentionally did not label depth zones in his global composite.

those identified elsewhere, and this suggests a strong eustatic control on their development.

ACKNOWLEDGMENTS

We thank the State of Wisconsin for supporting the Door Peninsula studies, and Ken Staats for permission to drill the Door Peninsula core. The Halquist Stone Company kindly provided access to study areas in Waukesha County. Reviews by E. Landing, R.H. Shaver, and B.J. Witzke considerably improved the clarity and content of this contribution.

REFERENCES

ALDEN, W.C. 1918. The Quaternary Geology of Southeastern Wisconsin with a Chapter on the Older Rock Formations. United States Geological Survey Professional Paper 106.

ALDRIDGE, R.J. 1972. Llandovery conodonts from the Welsh Borderland. *Bulletin of the British Museum (Natural History)*, 22:127–231.

———. 1976. Comparison of macrofossil communities and conodont distribution in the British Silurian, p. 91–104. In C.R. Barnes (ed.), *Conodont Paleocology*. Geological Association of Canada, Special Paper 15.

———, AND H.P. SHÖNLAUB. 1989. Conodonts, p. 274–279. In C.H. Holland and M. G. Bassett (eds.), *A Global Standard for the Silurian System*. National Museum of Wales, Geological Series 9.

ARMSTRONG, H.A. 1990. Conodonts from the Upper Ordovician–Lower Silurian carbonate platform of North Greenland. *Grønlands Geologiske Undersøgelse, Bulletin* 159.

BARRICK, J.E. 1977. Multielement simple-cone conodonts from the Clarita Formation (Silurian), Arbuckle Mountains, Oklahoma. *Geologica et Palaeontologica*, 11:47–68.

———, AND G. KLAPPER. 1976. Multielement Silurian (late Llandoveryan–Wenlockian) conodonts of the Clarita Formation, Arbuckle Mountains, Oklahoma, and phylogeny of *Kockelella*. *Geologica et Palaeontologica*, 10:59–100.

BOUCOT, A.J. 1975. *Evolution and Extinction Rate Controls*. Elsevier, Amsterdam.

BRETT, C.E., A.J. BOUCOT, AND S.T. LODUCA. 1990a. Sequence Stratigraphy of the type Niagarian Series (Silurian) of western New York and Ontario. New York State Geological Association, 62nd Annual Meeting, Field Trip Guidebook, p. C1–C71.

———, ———, AND ———. 1990b. Sequences, cycles, and basin dynamics in the Silurian of the Appalachian Foreland Basin. *Sedimentary Geology*, 69:191–244.

CHAMBERLIN, T.C. 1877. *Geology of Wisconsin*. Geological Survey of Wisconsin, Survey of 1873–1877, 2:327–394.

COOPER, B.J. 1976. Multielement conodonts from the St. Clair Limestone (Silurian) of southern Illinois. *Journal of Paleontology*, 50:205–217.

COOROUGH, P.J., AND R. WATKINS. 1997. Silicified *Dicoelosia* community from the Silurian Racine Formation, Milwaukee subsurface, Wisconsin. *Geological Society of America, Abstracts with Programs*, 29(4):11.

- DEMICO, R.V., AND L.A. HARDIE. 1994. Sedimentary Structures and Early Diagenetic Features of Shallow Marine Carbonates. SEPM (Society for Sedimentary Geology), Atlas Series Number 1.
- EHLERS, G.M. 1973. Stratigraphy of the Niagaran Series of the Northern Peninsula of Michigan. University of Michigan Museum of Paleontology, Papers on Paleontology, No. 3.
- , AND R.V. KESLING. 1957. Silurian Rocks of the Northern Peninsula of Michigan. Michigan Geological Society, Michigan Basin Geological Society Annual Geological Excursion.
- HARRIS, M.T., D.P. HEGRENES, AND M.A. MULDOON. 1996. Jarmen Road core study, p. 39–71. In M.T. Harris, M.A. Muldoon, and R.D. Stieglitz (eds.), The Silurian Dolomite Aquifer of the Door Peninsula: Facies, Sequence Stratigraphy, Porosity and Hydrogeology. Guidebook for the Fall 1996 Field Conference of the Great Lakes Section of SEPM.
- , AND P.M. SHEEHAN. 1996. Upper Ordovician–Lower Silurian sequences determined from inner shelf sections, Barn Hills and Lakeside Mountains, eastern Great Basin, p. 161–176. In B.J. Witzke, G.A. Ludvigson, and J.E. Day (eds.), Paleozoic Sequence Stratigraphy: North American Perspectives—Views from the North American Craton. Geological Society of America Special Publication 306.
- , AND ———. 1998. Early Silurian stratigraphic sequences of the eastern Great Basin (Utah and Nevada). New York State Museum Bulletin 491 (this volume).
- , AND K.R. WALDHUETTER. 1996. Silurian of the Great Lakes Region, Part 3: Llandovery Strata of the Door Peninsula, Wisconsin. Milwaukee Public Museum Contributions in Biology and Geology, No. 90.
- HEGRENES, D.P. 1996. A core study of the sedimentology, stratigraphy, porosity, and hydrogeology of the Silurian aquifer in Door County, Wisconsin. Unpublished M.Sc. thesis, University of Wisconsin–Milwaukee, 156 p.
- JIN J., W.G.E. CALDWELL, AND B.S. NORFORD. 1993. Early Silurian Brachiopods and Biostratigraphy of the Hudson Bay Lowlands, Manitoba, Ontario, and Quebec. Geological Survey of Canada, Bulletin 457.
- JOHNSON, M.E. 1975. Recurrent community patterns in eperic seas: the Lower Silurian of eastern Iowa. Iowa Academy of Science Proceedings, 82:130–139.
- . 1981. Correlation of Lower Silurian strata from the Michigan Upper Peninsula to Manitoulin Island. Canadian Journal of Earth Sciences, 18:869–883.
- . 1996. Stable cratonic sequences and a standard for Silurian eustasy, p. 203–211. In B.J. Witzke, G.A. Ludvigson, and J.E. Day (eds.), Paleozoic Sequence Stratigraphy: North American Perspectives—Views from the North American Craton. Geological Society of America, Special Publication 306.
- , AND G.T. CAMPBELL. 1980. Recurrent carbonate environments in the Lower Silurian of northern Michigan and their inter-regional correlation. Journal of Paleontology, 54:1041–1057.
- , D. KALJO, AND RONG J.-Y. 1991. Silurian eustasy. Special Papers in Palaeontology (Palaeontological Association), 44:145–163.
- , AND H.L. LESCINSKY. 1986. Depositional dynamics of cyclic carbonates from the Interlake Group (Lower Silurian) of the Williston Basin. Palaios, 1:111–121.
- , AND W.S. MCKERROW. 1991. Sea level and faunal changes during the latest Llandovery and earliest Ludlow (Silurian). Historical Biology, 5:153–169.
- , RONG J.-Y., AND YANG X.-C. 1985. Intercontinental correlation by sea-level events in the Early Silurian of North America and China (Yangtze Platform). Geological Society of America Bulletin, 96:1384–1397.
- JOHNSON, S.B., AND R.D. STIEGLITZ. 1990. Karst features of a glaciated dolomite peninsula, Door County, Wisconsin. Geomorphology, 4:437–54.
- KLEFFNER, M.A. 1989. A conodont-based Silurian chronostratigraphy. Geological Society of America Bulletin, 101:904–912.
- . 1994. Conodont biostratigraphy and depositional history of strata comprising the Niagaran sequence (Silurian) in the northern part of the Cincinnati Arch region, west-central Ohio, and evolution of *Kockelella walliseri* (Helfrich). Journal of Paleontology, 68:141–153.
- . 1995. Conodont distribution and preliminary conodont chronostratigraphy of Lower Silurian strata in southeastern Wisconsin. Geological Society of America, Abstracts with Programs, 27(3):65.
- , R.D. NORBY, J. KLUESSENDORF, AND D.G. MIKULIC. 1994. Conodont biostratigraphy of the Brandon Bridge and associated Silurian Waukesha *Lagerstatte* in Waukesha County, Wisconsin. Geological Society of America, Abstracts with Programs, 26(5):23.
- KLUESSENDORF, J., AND D.G. MIKULIC. 1989. Bedrock geology of the Door Peninsula of Wisconsin, p. 12–31. In J.C. Palmquist (ed.), Wisconsin's Door Peninsula: A Natural History. Perin Press, Appleton, Wisconsin.
- , AND ———. 1996. An Early Silurian sequence boundary in Illinois and Wisconsin, p. 177–195. In B.J. Witzke, G.A. Ludvigson, and J.E. Day (eds.), Paleozoic Sequence Stratigraphy: North American Perspectives—Views from the North American Craton. Geological Society of America, Special Publication 306.
- KUCHTA, M.A., R. WATKINS, AND G.L. SMITH. 1997. A Silurian crinoid-dominated community in the lower Racine Formation, Waukesha County, Wisconsin. Geological Society of America, Abstracts with Programs, 29(4):28.
- KUGLITSCH, J.J. 1994. Conodont biostratigraphy of the Silurian Waukesha, Racine and Engadine Formations, eastern Wisconsin. Geological Society of America, Abstracts with Programs, 26(5):49.
- . 1996. Conodont biostratigraphy of the Silurian Racine and Waukesha Formations of northeastern Waukesha County, Wisconsin. Unpublished M.Sc. thesis, University of Wisconsin–Milwaukee, 231 p.
- LE FÈVRE, J.L., C.R. BARNES, AND M. TIXIER. 1976. Paleogeology of Late Ordovician and Early Silurian conodontophorids, Hudson Bay Basin, p. 69–89. In C.R. Barnes (ed.), Conodont Paleogeology. Geological Association of Canada, Special Paper 15.
- LENZ, A.C. 1982. Ordovician to Devonian sea-level changes in western and northern Canada. Canadian Journal of Earth Sciences, 19:1919–1932.
- LOWENSTAM, H.A. 1950. Niagaran reefs of the Great Lakes area. Journal of Geology, 58:430–487.
- MCCRACKEN, A.D., AND C.R. BARNES. 1981. Conodont biostratigraphy and paleogeology of the Ellis Bay Formation, Anticosti Island, Quebec, with special reference to Late Ordovician–Early Silurian chronostratigraphy and the systemic boundary. Geological Survey of Canada Bulletin, 329(2):51–134.
- MIKULIC, D.G. 1977. A preliminary revision of the Silurian stratigraphy of southeastern Wisconsin, p. A6–A34. In K.G. Nelson (ed.), Geology of Southeastern Wisconsin, 41st Annual Tri-State Field Guidebook, University of Wisconsin–Milwaukee.
- , AND J. KLUESSENDORF. 1988. Subsurface stratigraphic relationships of the Upper Silurian and Devonian rock of Milwaukee County, Wisconsin. Geoscience Wisconsin, 12:1–23.
- NOWLAN, G.S. 1983. Early Silurian conodonts of eastern Canada. Fossils and Strata, 15:95–110.

- POLLACK, C.A., C.B. REXROAD, AND R.S. NICOLL. 1970. Lower Silurian conodonts from northern Michigan and Ontario. *Journal of Paleontology*, 44:743–764.
- ROSS, C.A., AND J.R.P. ROSS. 1996. Silurian sea-level fluctuations, p. 187–192. In B.J. Witzke, G.A. Ludvigson, and J.E. Day (eds.), *Paleozoic Sequence Stratigraphy: North American perspectives—Views from the North American Craton*. Geological Society of America Special Publication 306.
- ROVEY, C.W., II. 1990. Stratigraphy and sedimentology of Silurian and Devonian carbonates, eastern Wisconsin, with implications for ground-water discharge into Lake Michigan. Unpublished Ph.D. dissertation, University of Wisconsin–Milwaukee, 427 p.
- SCOTese, C.R., AND W.S. MCKERROW. 1990. Revised world maps and introduction, p. 1–21. In W.S. McKerrrow and C.R. Scotese (eds.), *Paleozoic Palaeogeography and Biogeography*. Geological Society Memoir 12.
- SHAYER, R.H. 1996. Silurian sequence stratigraphy in the North American craton, Great Lakes area, p. 193–202. In B.J. Witzke, G.A. Ludvigson, and J.E. Day (eds.), *Paleozoic Sequence Stratigraphy: North American Perspectives—Views from the North American Craton*. Geological Society of America, Special Publication 306.
- SHROCK, R.R. 1940. Geology of Washington Island and its neighbors, Door County, Wisconsin. *Transactions of the Wisconsin Academy of Sciences, Arts and Letters*, 32:199–228.
- STIEGLITZ, R.D. 1989. The geological environment and water quality in Wisconsin's Door Peninsula, p. 82–97. In J. C. Palmquist (ed.), *Wisconsin's Door Peninsula: A Natural History*. Perin Press, Appleton, Wisconsin.
- . 1991. The geologic foundation of Wisconsin's Door Peninsula: the Silurian of Door County, p. 1–12. In *Wisconsin Section of American Institute of Professional Geologists, North Central Section, 1991 Fall Field Trip Guidebook*.
- UYENO, T.T., AND C.R. BARNES. 1983. Conodonts of the Jupiter and Chicotte Formations (Lower Silurian), Anticosti Island, Quebec. *Geological Survey of Canada, Bulletin* 335.
- WALDHUETTER, K.R. 1994. Stratigraphy, sedimentology, and porosity distribution of the Silurian aquifer, the Door Peninsula, Wisconsin. Unpublished M.Sc. thesis, University of Wisconsin–Milwaukee, 210 p.
- WALLISER, O.H. 1964. Conodonten des Silurs. *Abhandlungen des Hessischen Landesamtes für Bodenforschung*, 41:1–106.
- WATKINS, R. 1991. Guild structure and tiering in a high-diversity Silurian community, Milwaukee County, Wisconsin. *Palaaios*, 6:465–478.
- . 1993. The Silurian (Wenlockian) reef fauna of southeastern Wisconsin. *Palaaios*, 8:325–338.
- . 1994. Evolution of Silurian pentamerid communities in Wisconsin. *Palaaios*, 9:488–499.
- . 1997. Paleocology of Silurian reef bivalves, Racine Formation, North America. *Lethaia*, 29:171–180.
- , AND P.J. COOROUGH. 1997a. Silurian *Thalassinoides* in an offshore carbonate community, Wisconsin, USA. *Palaeogeography, Palaeoclimatology, Palaeoecology*, 129:109–117.
- , AND ———. 1997b. Silurian sponge spicules from the Racine Formation, Wisconsin. *Journal of Paleontology*, 71:208–214.
- , AND J.J. KUGLITSCH. 1997. Lower Silurian (Aeronian) megafaunal and conodont biofacies of the northwestern Michigan Basin. *Canadian Journal of Earth Sciences*, 34:753–764.
- , ———, AND P.E. MCGEE. 1994. Silurian of the Great Lakes Region, Part 2: Paleontology of the upper Llandoverly Brandon Bridge Formation, Walworth County, Wisconsin. *Milwaukee Public Museum Contributions in Biology and Geology*, No. 87.
- WILLMAN, H.B. 1973. Rock Stratigraphy of the Silurian System in Northeastern and Northwestern Illinois. *Illinois State Geological Survey, Circular* 479.
- WITZKE, B.J., AND B.J. BUNKER. 1996. Relative sea-level changes during Middle Ordovician through Mississippian deposition in the Iowa area, North American craton, p. 307–330. In B.J. Witzke, G.A. Ludvigson, and J.E. Day (eds.), *Paleozoic Sequence Stratigraphy: North American Perspectives—Views from the North American Craton*. Geological Society of America, Special Publication 306.

EARLY SILURIAN STRATIGRAPHIC SEQUENCES OF THE EASTERN GREAT BASIN (UTAH AND NEVADA)

MARK T. HARRIS¹ AND PETER M. SHEEHAN²

¹Department of Geosciences, University of Wisconsin-Milwaukee, Milwaukee, WI 53201, and

²Milwaukee Public Museum, 800 W. Wells Street, Milwaukee, WI 53233.

ABSTRACT—The Silurian succession of the eastern Great Basin includes six Lower Silurian (Llandovery–Wenlock) sequences that are preserved in shelf, shelf margin, and basinal areas. The sequence ages are early Rhuddanian, late Rhuddanian–earliest Aeronian, Aeronian, late Aeronian–early Telychian, late Telychian–early Sheinwoodian, and Sheinwoodian. The lower three sequences accumulated on a westward-dipping carbonate ramp that steepened in the latest Aeronian into a westward-prograding, rimmed shelf that persisted into the Early Devonian.

Detailed measured sections that incorporate sedimentological and paleontological data allow the estimation of water depth curves for individual sections along shelf-to-basin transects. Along these transects, maximum flooding intervals establish the maximum shelf water depths and aid in restoration of paleotopographic profiles. The downdip extent of exposure surfaces and lowstand facies reflect the magnitude of sea-level falls. These factors delineate an Early Silurian sea-level curve for the Great Basin region. The sea-level cycles are similar to those identified elsewhere, and suggest strong eustatic control, although the middle Rhuddanian sequence boundary has been less commonly recognized in other areas. Shelf facies indicate that the maximum Silurian transgression occurred in the late Telychian, as suggested in earlier reports.

INTRODUCTION

Lower Silurian (Llandovery–Wenlock) carbonates of the eastern Great Basin consist of a succession of six stratigraphic sequences that can be correlated regionally. Sedimentological and paleontological data allow calibration of water depth curves for individual sections. Two representative shelf sections are illustrated herein. A general sea-level curve can be derived by comparing water depth curves across transects from inner shelf to slope sections.

GEOLOGICAL SETTING AND DATA BASE

The Silurian strata of the Great Basin accumulated along the western margin of Laurentia (Figure 1) and are preserved between the Sonoma (Permian–Triassic) and Sevier (Cretaceous) deformed belts (Figure 2) (Sheehan and Boucot, 1991; Poole et al. 1992). The Silurian shelf margin trends roughly north–south (present orientation), although it swings east–west north of the Tooele Arch, a Paleozoic basement feature that divides the shelf into a northern Tristate Basin and a southern Ibex Basin (Figure 3) (Webb, 1958; Sheehan, 1980; Budge and Sheehan, 1980a; Hintze, 1982; Poole et al., 1992).

A west-dipping carbonate ramp persisted from Late Ordovician through the middle Llandovery (Carpenter et al., 1986). Llandovery (late Aeronian) tectonic collapse, probably due to basement faulting, converted the ramp into a rimmed margin that continued into the Early Devonian (Johnson and Potter, 1975; Hurst et al., 1985; Hurst and Sheehan, 1985; Carpenter et al., 1985).

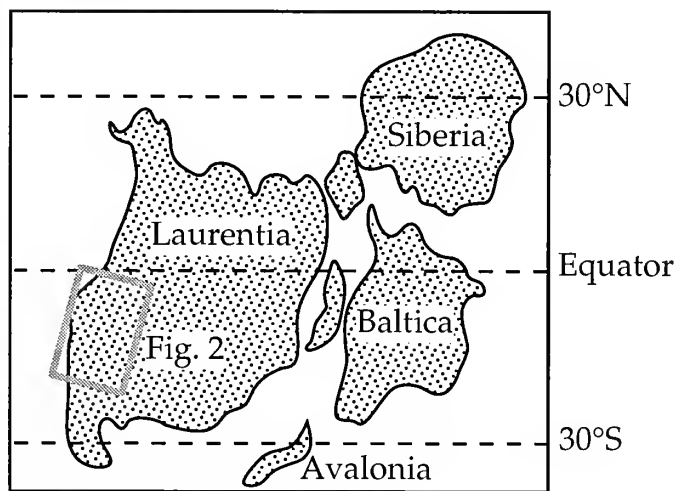


FIGURE 1—Early Silurian (Llandovery) continental positions. Location of Figure 2 indicated. Modified from Scotese and McKerrow (1990).

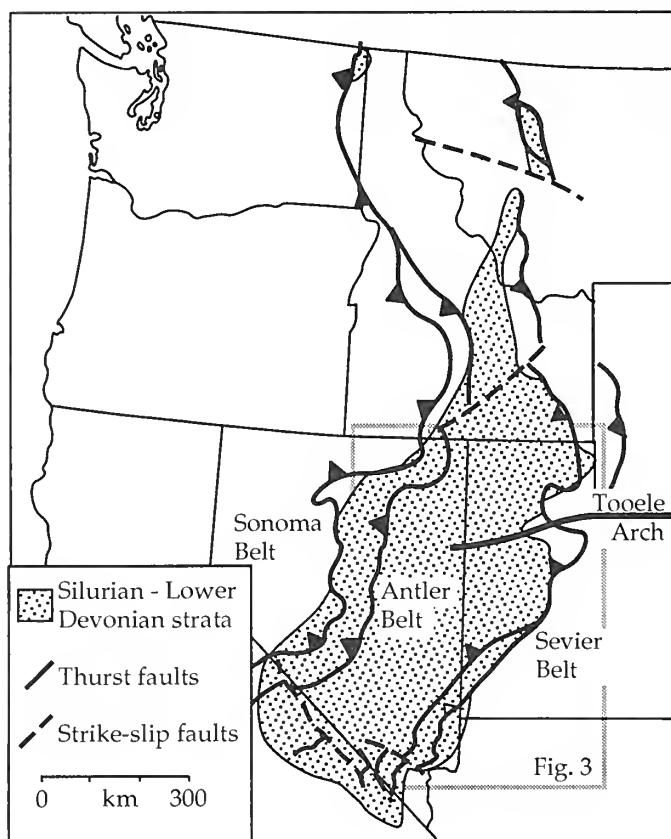


FIGURE 2—Distribution of Silurian-Lower Devonian strata in the western USA; figure ignores Middle Paleozoic roof pendants in California. Location of Figure 3 indicated. Modified from Poole et al. (1992).

This report focuses on Llandovery-Wenlock strata (Figure 4) and is based upon twelve measured sections (Figure 3). These localities are supplemented by less-detailed sections, faunal collections, and personal observations at several dozen additional localities. Two sections (Barn Hills and Lakeside Mountains) are used to illustrate water depth changes in shelf areas (Ibex and Tristate Basins). The regional sea-level curve is based upon the entire set of detailed sections.

DEPOSITIONAL FACIES

The studied sections are distributed across inner shelf to deep ramp/slope environments. Shelf facies are similar throughout the Silurian (Sheehan, 1990; Harris and Sheehan, 1996), but to the west, facies reflect the shift in the depositional profile from the early-middle Llandovery ramp to the overlying late Llandovery-Early Devonian rimmed margin (Figure 5) (Winterer and Murphy, 1960; Johnson and Potter, 1975; Matti et al., 1975; Matti and McKee, 1977; Nichols and Silberling, 1977; Cook,

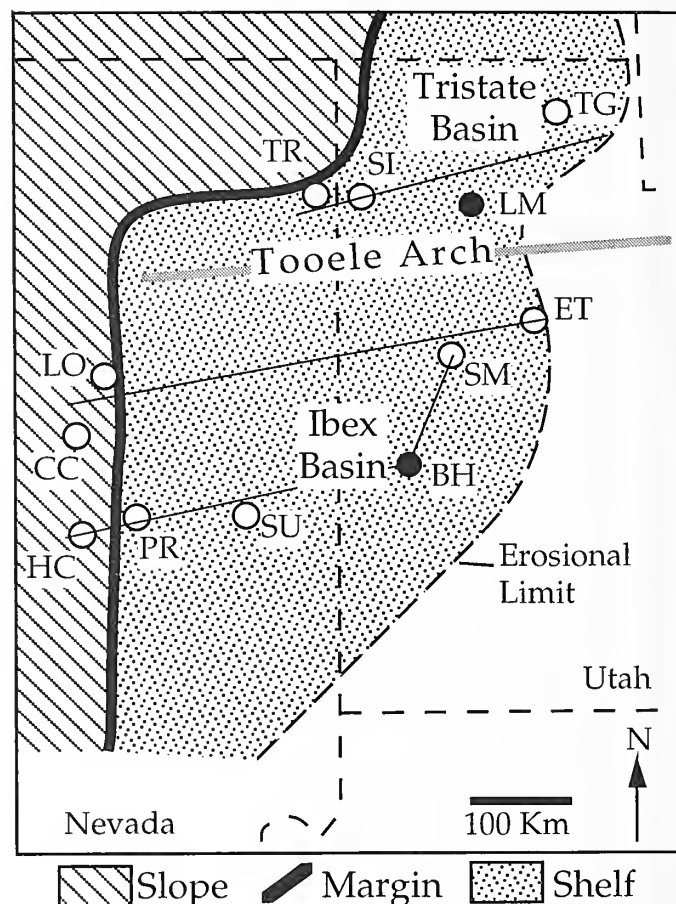


FIGURE 3—Generalized Early Silurian paleogeography of the Great Basin. Locations of detailed measured sections are shown. Barn Hills (BH) and Lakeside Mountains (LM) sections portrayed in Figure 8 are represented by solid circle. Other localities (open circles): Copenhagen Canyon (CC), East Tintics (ET), Hot Creek Range (HC), Lone Mountain (LO), Pancake Range (PR), Silver Island Range (SI), Southern Egan Range (SE), Spors Mountains (SM), Toano Range (TR), and Tony Grove Lake (TG). Positions of transects used to estimate sea-level curve (Figure 4) indicated by thin east-west trending lines. See Budge and Sheehan (1980a, 1980b) and Carpenter et al. (1986) for section locations and data on additional localities.

1984; Hurst and Sheehan, 1985; Sheehan, 1986). Murphy et al. (1979) suggested that an erosive unconformity occurs between the latest ramp deposits (Hanson Creek Dolostone) and the overlying slope strata (Roberts Mountains Formation). However, we interpret the facies changes and biostratigraphic gaps at the contact by fracturing, slumping, erosion, and sediment redeposition associated with downdropping of the shelf along basement faults (Hurst et al., 1985; Carpenter et al., 1986).

Silurian strata consist of five facies, each of which corresponds to a specific depositional environment (Figure 5). Shelf sections include laminite, cross-bedded, and bioturbated facies (Harris and Sheehan, 1996). The laminite facies (tidal flats) is characterized by laminite-

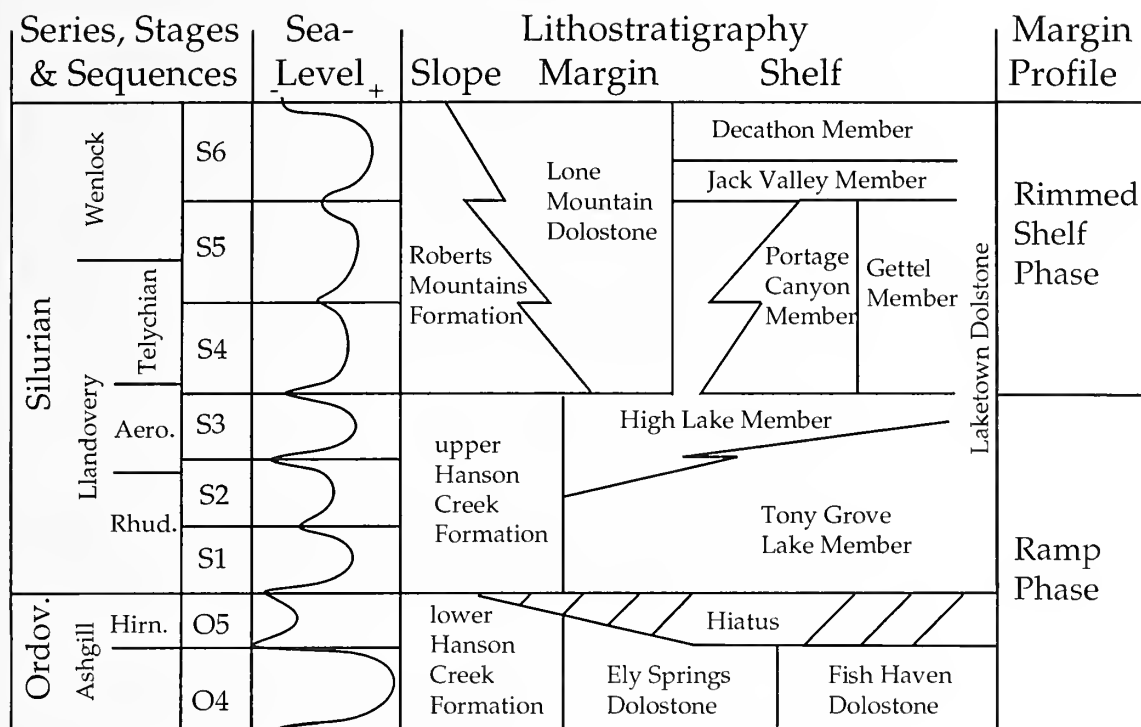


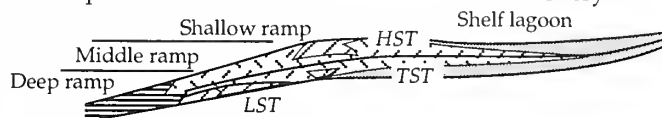
FIGURE 4—Stratigraphic summary of the Silurian of the eastern Great Basin. Relative sea-level curve derived from the method shown in Figure 10. Magnitude of sea-level fall at the beginning of the Hirnantian is ca. 100 m. Abbreviations for Llandovery stages: Rhud., Rhuddanian; Aeron., Aeronian.

capped cycles. The cross-bedded facies (subtidal shoals) is marked by coarsening-upward and shallowing-upward cycles capped by cross-bedded oolitic or oncoidal grainstone. The bioturbated facies (subtidal shelf and ramp) contains abundant burrows with scattered storm beds; textures range from grain-supported to mud-supported, and reflect varied energy levels.

Deeper water settings are represented by bioturbated, bedded, and basinal facies. The bioturbated facies is a mud-supported lithology that typifies deep ramp settings. The bedded facies is characterized by turbidities and other redeposited sediments representative of a slope environment (Hurst and Sheehan, 1985). The basinal facies consists of laminated shales, siltstones, and carbonate mudstones (Hurst and Sheehan, 1985).

RAMP FACIES (EARLY-MIDDLE LLANDOVERY).—Shelf facies (Fish Haven, Ely Springs and lower Laketown Dolostones) are dominated by laminite cycles and subtidal, bioturbated facies (Figure 6) (Sheehan, 1990; Harris and Sheehan, 1996). Tidal flats prograded from the inner shelf shoreline and the Tooele Arch, and underwent complete exposure at the end of each sequence. To the west, shallow ramp/outer shelf facies consist of a mixture of oolitic and oncoidal, grain-supported shoals and fossiliferous wackestones and packstones. Farther west

1. Ramp Phase: Late Ordovician to middle Llandovery



2. Rimmed-Shelf Phase: late Llandovery to Wenlock

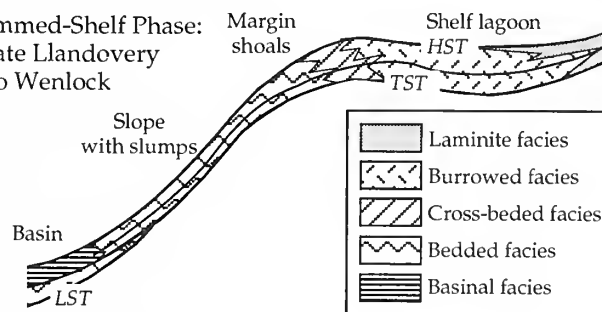


FIGURE 5—Sequence-keyed facies models for ramp margin (1) and rimmed shoal margin (2) phases. Facies discussed in the text. Systems tracts abbreviations are: LST, lowstand systems tract; TST, transgressive systems tract; HST, highstand systems tract.

(Hanson Creek Formation), ramp facies are progressively more muddy with fewer primary physical structures; these features reflect deeper water conditions above and below the storm-wave base. The most distal sections are starved-basin mudstones and shales. We follow Carpenter et al. (1986) in interpreting the central Nevada sections

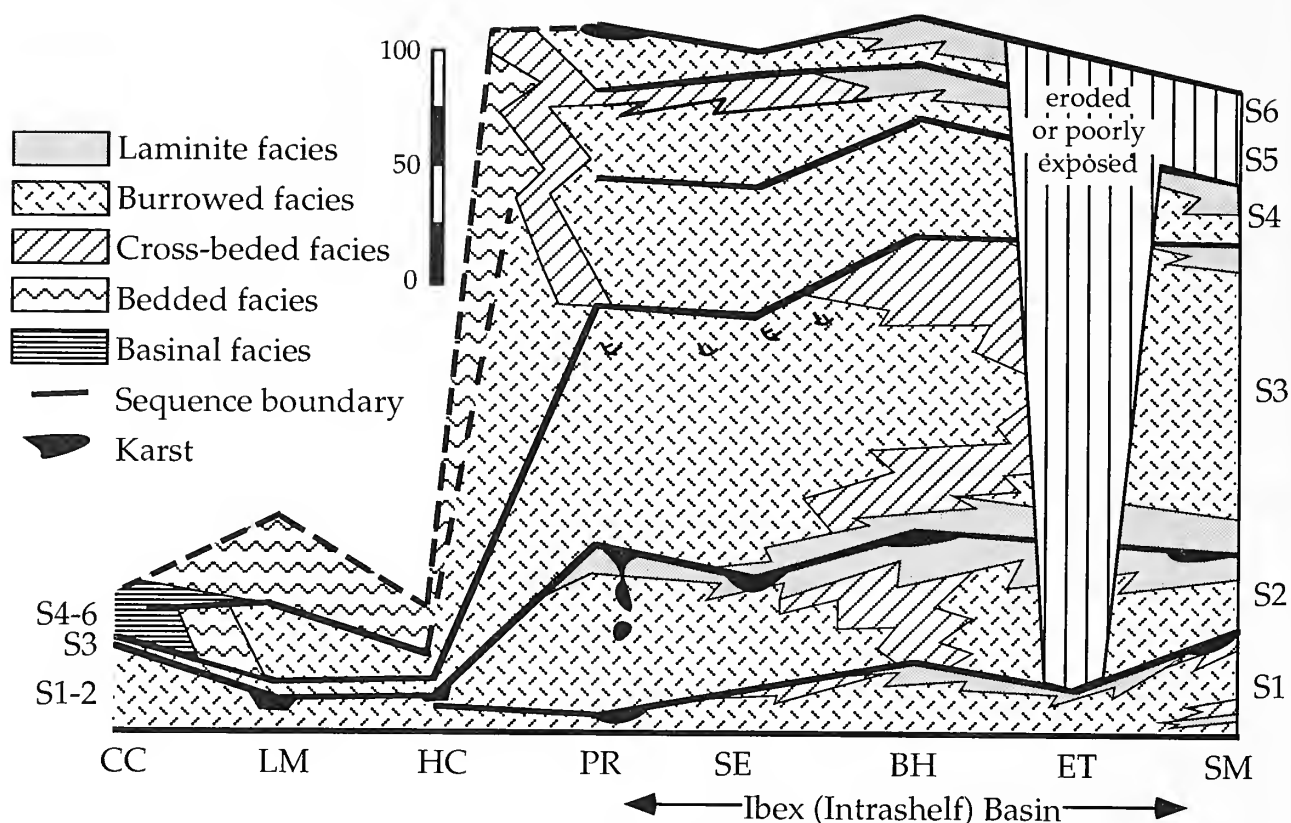


FIGURE 6—Silurian facies across the Ibex Basin. Section locations (bottom) are illustrated in Figure 1. Note that the horizontal scale varies.

(Lone Mountain, Copenhagen Canyon) as middle to deep ramp deposits, instead of lagoonal deposits as suggested by Dunham (1977) and Dunham and Olson (1980).

Ramp facies patterns relate to depositional sequences (Figure 5.1). In deep to middle ramp settings, oncoidal shoals mark lowstand systems tracts. In shallow ramp-to-shelf sections, laminite facies occur at the base of the transgressive systems tract and cap the highstand systems tract, so that laminite tongues bracket sequence boundaries.

RIMMED-MARGIN FACIES (LATE LLANDOVERY-WENLOCK).—Shelf facies are similar to those in the ramp phase and represent tidal flat and shallow shelf settings (Figure 6) (Sheehan, 1990; Harris and Sheehan, 1996). Shelf faunas were adapted for low-energy, soft-substrate conditions in a broad lagoon behind the shelf margin (Harris and Sheehan, 1997). The margin (Lone Mountain Dolostone) consists of stacked shoals that prograded over slope carbonates (Roberts Mountains Formation) (Hurst et al., 1985; Hurst and Sheehan, 1985). Proximal slope carbonates are marked by slumps and thick carbonate turbidites; distal deposits are argillaceous carbonates with thin turbidite beds (Matti et al., 1975; Hurst and Sheehan, 1985).

As in ramp sequences, laminite tongues bracket sequence boundaries in shelf settings (Figure 5.2). The sharply delineated margin-slope-basin geometry limited lateral facies migration by comparison to the gentler ramp profile. Exposure features (karst) allow identification of sequences in the margin and shallow slope, but in deeper water environments, differentiation of systems tracts is not possible, due to more uniform depositional conditions and slumping.

SEQUENCES AND RELATIVE SEA-LEVEL CYCLES

The Llandovery-Wenlock section consists of six sequences bounded updip by exposure surfaces that extend across all or part of the shelf (Figure 6, 7). Some sequence boundaries extend downdip into middle to deep ramp settings as karst surfaces; others pass into conformable sections with shallower facies that are interpreted as lowstand deposits. Criteria used to identify sequence boundaries include karst surfaces, soils, facies successions, cycle stacking patterns, erosional surfaces, redeposited debris, and lowstand shoals (Harris et al., 1995; Harris and Sheehan, 1996).

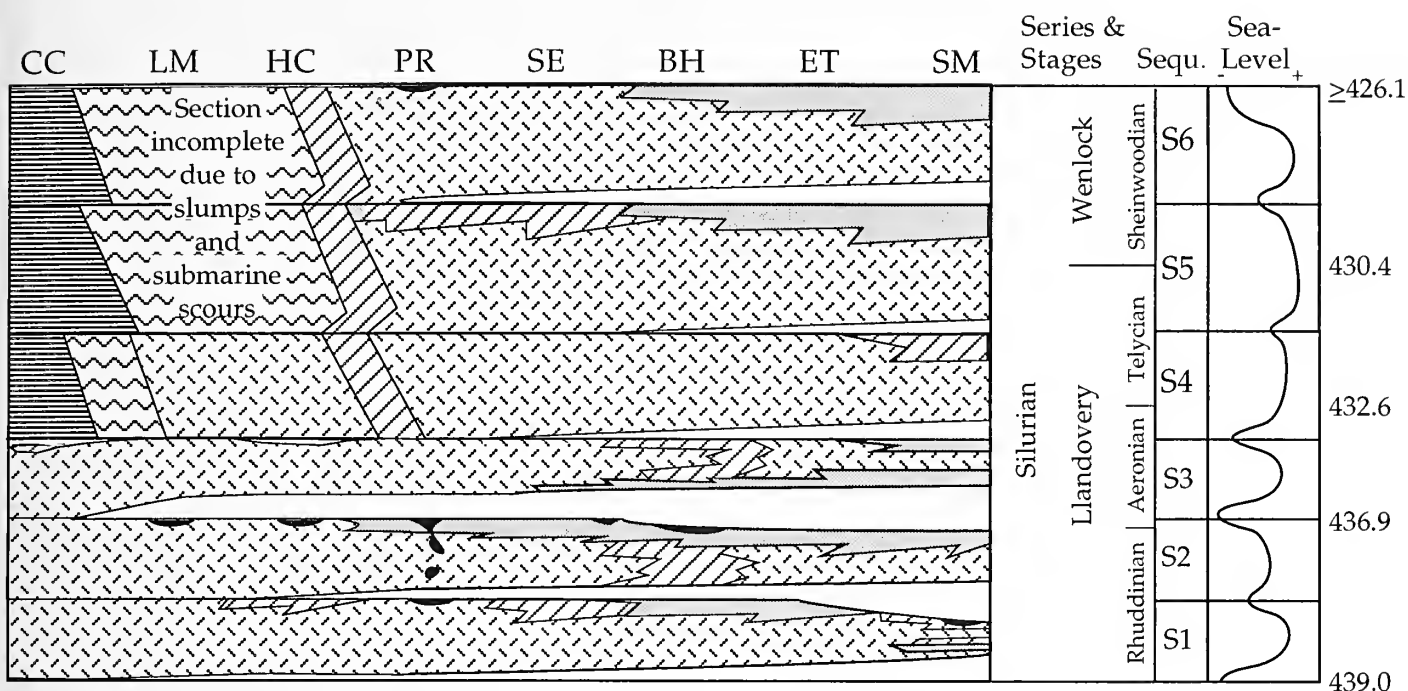


FIGURE 7—Time-space plot for the Ibex Basin transect to clarify the sequence stratigraphic interpretation. Facies explanation in Figure 6. Section locations (top) in Figure 1. Note that the horizontal scale varies. Sea-level curve from Figure 4. Ages (in Ma) in Harland et al. (1990). Section may not include uppermost Sheinwoodian.

In deeper water settings, the Silurian overlies Hirnantian (latest Ordovician) strata that are absent in shelf settings (Figure 4). Quartz sand is common (Mullens and Poole, 1972), and its influx is interpreted as the result of the sea-level lowstands. Similar lowstand sands are widely distributed in Ordovician rocks of Laurentia (Read and Goldhammer, 1988; Goldhammer et al., 1993). The overlying ramp sequences (S1–S3) are largely bioturbated facies with scattered cross-bedded facies units in shelf sections. Laminite facies tongues extend across the shelf and contain karst surfaces, most notably at the top of sequence S2.

The rimmed shelf sequences (S4–S6) are marked by sharper lateral facies changes than underlying ramp sequences. The rimmed shelf sequences consist of low-energy shelf (bioturbated facies), high-energy shelf rim (cross-bedded facies), and slope (bedded facies) deposits. Laminite facies tongues are restricted to the inner and middle shelves.

Available macrofaunal (Berry and Murphy, 1975; Harris and Sheehan, 1997; Sheehan and Harris, In press) and microfaunal (Ross et al., 1979; Murphy, 1989; Kleffner, 1995; Finney et al., 1995) data indicate that the sequences are correlative across the region. We should note that we have been able to better date the lowest two Silurian sequences since our earlier report (Harris and Sheehan, 1996).

Changes in relative sea-level are well-developed in middle shelf locations within the intra-shelf basins, as illustrated by the Barn Hills (Ibex Basin) and Lakeside Mountains (Tristate Basin) sections (Figure 8). The depth curves for these sections are keyed to benthic faunal assemblages to follow the scheme adopted by Johnson (1996, and references therein). However, we have based our curves upon depositional facies and benthic faunal assemblages (Figure 9). Environmental factors such as wave energy and restricted circulation influenced both categories of features (Brett et al., 1993). For example, we equate the laminite facies with benthic assemblage 1, and the cross-bedded facies with benthic assemblage 3. The bioturbated facies is more variable, because it occurs in both restricted shelf settings (benthic assemblage 2) or below wave base (benthic assemblage 4 and 5). The addition of sedimentological criteria allows extension of the water depth model to intervals with poor fossil recovery, and thus permits construction of a continuous water depth curve (Figure 8).

The assignment of water depths to Silurian benthic assemblages is problematic and we suggest using a slight modification of the water depth estimates proposed by Brett et al. (1993). We used their deeper depth estimates for the oceanic margin and their shallower estimates for inner shelf and middle shelf sections (Figure 9). The water depth range of benthic assemblage 2 is constrained by

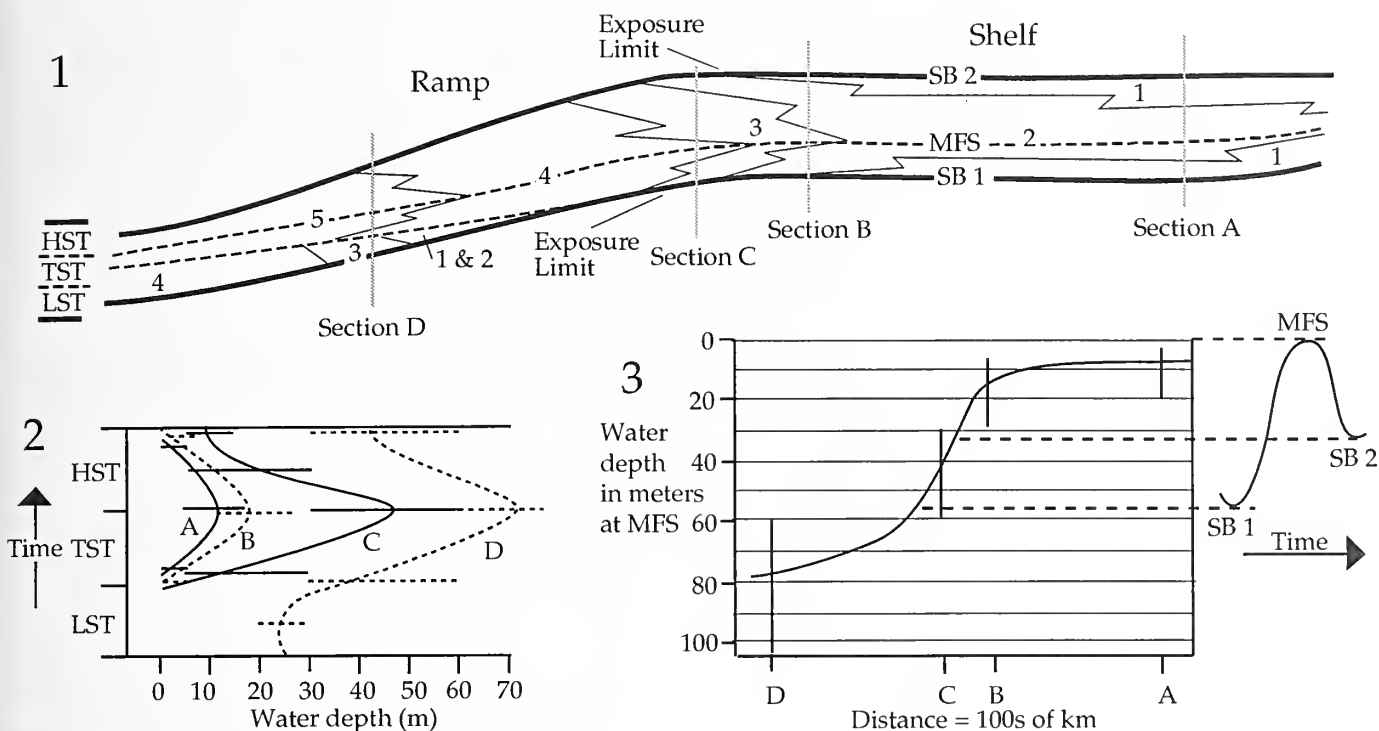


FIGURE 10—Model to estimate relative sea-level changes. 1, Idealized ramp facies model keyed to benthic associations 1–5 with lowstand (LST), transgressive (TST) and highstand (HST) systems tracts labeled. Positions of hypothetical sections A–D are marked. Note that the horizontal scale is several hundred km. 2, Water depth curves for sections A–D drawn through midpoints of depth ranges (Figure 9). Sections A–C were exposed during LST deposition; upper sequence boundary marked by exposure at sections A and B. 3, Depth profile along MFS with approximate positions of the downdip exposure limits on SB 1 and SB 2 indicated. Water depth curve derived from limits on maximum rise (MFS facies) and maximum fall (LST facies and SB exposure).

its occurrence in restricted shelf settings. We infer a depth below that assigned to tidal flats (i.e., less than 3 m), and a maximum depth of perhaps 20 m to reflect the intertonguing with tidal systems in innermost shelf settings. One drawback of the use of benthic assemblages for estimating water depths is that they are not linearly distributed in depth (i.e., the base of benthic assemblage 5 is not five times the depth of the base of benthic assemblage 1). The scale does, however, reflect the greater sensitivity of shallow environments to small changes in water depth (Brett et al., 1993). Consequently, any single section provides the most precise information on depth changes in the range of benthic assemblages 1–4. A second limitation is that benthic assemblages reflect more parameters than absolute water depth. For example, variations in water depth interpretations for different benthic assemblages (Brett et al., 1993) may relate to variable depths of wave base.

Interpretation of sea-level changes can be improved by comparing the water depth curves along shelf-to-basin transects (Figure 3). The basic approach can be illustrated by using the facies model for a ramp sequence (Figure 10.1). In any single section, the succession of facies and benthic assemblages defines a water depth

curve, as illustrated for the Barn Hills and Lakeside Mountains sections (Figure 8). Using the estimated water depths (Figure 9), these curves can be transformed into more quantified curves (in this example, Figure 10.2 illustrates water depth curves at the locations of sections A–D). The caveat is that during lowstand intervals, exposed sections (sections A and B) provide no data on the extent of a sea-level drop.

The sequence interpretation provides two additional time lines per sequence that correspond to maximum shelf inundation (maximum flooding surfaces or MFS) and maximum exposure (sequence boundaries or SB). The MFS provides a time line that allows the estimation of relative water depths across the shelf, and thus a reconstruction of the depositional profile (Figure 10.3). Water depth estimates for deeper water environments are less precise than those for shelf sections, as reflected by the larger depth ranges indicated in Figure 10.3. The MFS also defines the maximum flooding of the shelf, and provides an estimate of the maximum shelf water depth.

The extent of downdip exposure features and depth-dependent lowstand facies along a sequence boundary (SB) constrains the extent of sea-level fall. The profile reconstructed along the MFS provides a template

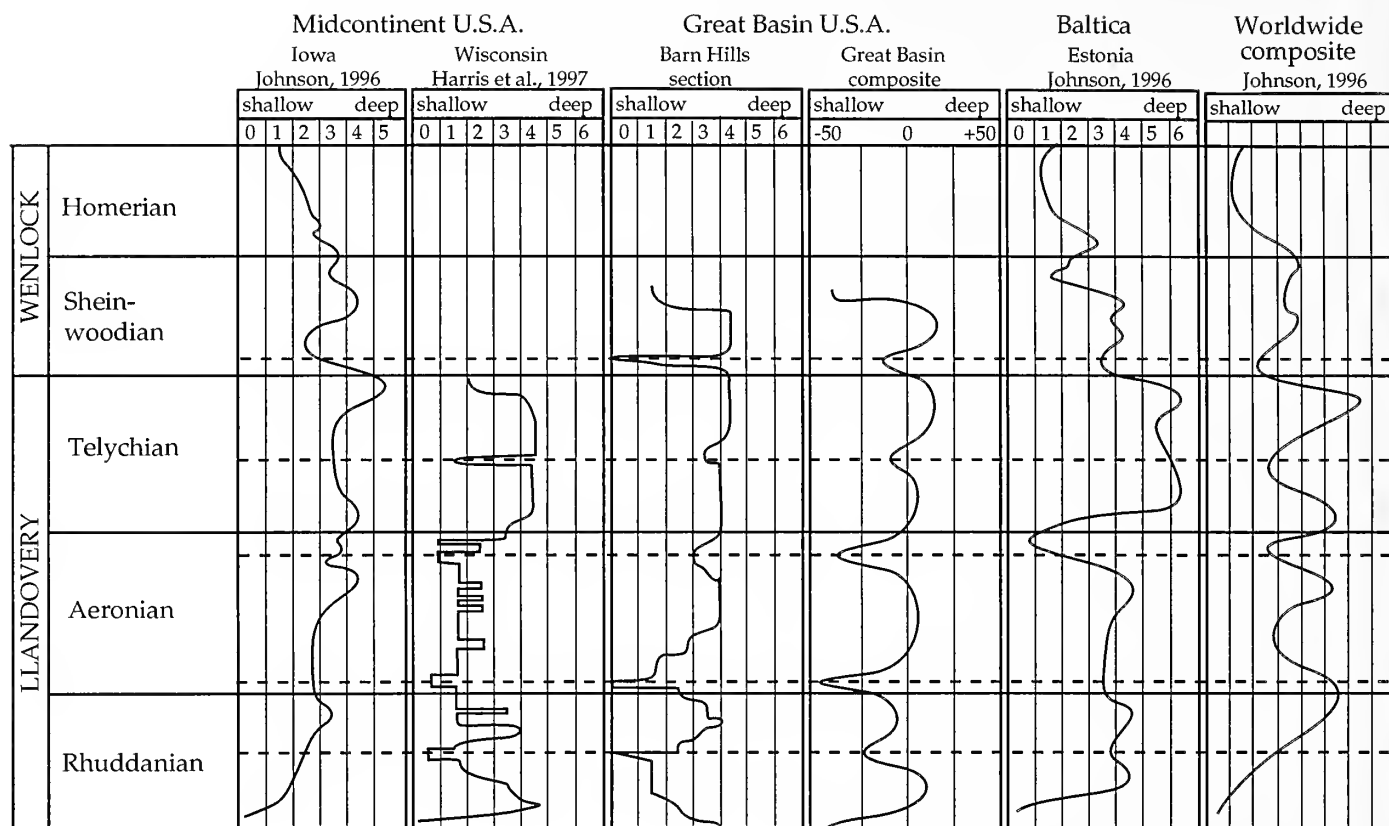


FIGURE 11—Comparison of Early Silurian sea-level curves for the midcontinent United States, the Great Basin, and Baltica with global composite of Johnson (1996). Note that Iowa, Wisconsin, Barn Hills, and Estonia sections are tied to benthic associations, but Great Basin composite is in meters; Johnson (1996) did not label the zones in his global composite.

on which to plot exposure features and depth-related lowstand features. The occurrence down dip of lowstand oncoidal shoals interbedded with benthic assemblage 4–5 (Figures 6, 7) provides an additional constraint on the magnitude of sea-level falls. These considerations allow the estimation of a relative sea-level curve along a profile (Figure 10.3).

The detailed sections can be aligned into three profiles (Figure 3) and the results averaged to produce a regional sea-level curve (Figure 4). This sea-level curve is only a rough estimate (subsidence and compaction effects have not been considered), but it indicates the relative magnitude of Silurian sea-level changes in this region. We must also note that the temporal position of the maximum water depth within each sequence (Figure 4) is not well-constrained because the timing of the MFS is a complex function of subsidence, eustasy, and sediment accumulation.

The result of this procedure is the identification of six Llandovery–Wenlock sea-level cycles in the Great Basin. These cycles are regional in extent, and their sediment record can be recognized in all shelf and shallow ramp sections measured to date.

CORRELATION TO OTHER REGIONS

The six Lower Silurian sea-level cycles identified in the Great Basin appear correlative to those recognized elsewhere in Laurentia (Figure 11). These include sections in the Williston Basin (Johnson and Lescinsky, 1986), Michigan Basin (Johnson and Campbell, 1980; Johnson, 1981; Harris and Waldhuetter, 1996; Harris et al., 1998), Illinois Basin (Ross and Ross, 1996), Iowa (Johnson, 1975; Witzke and Bunker, 1996), and Appalachian Basin (Brett et al., 1990a, 1990b). Similar sea-level cycles are recognized other areas outside of Laurentia (Johnson et al., 1985, 1991; Johnson and McKerrow, 1991; Johnson, 1996). The implication of this interregional sequence correlation is that the sea-level cycles are of eustatic origin, as suggested by McKerrow (1979).

Figure 11 illustrates this point by comparing the Great Basin sea-level curves (using both the Barn Hills section and the Great Basin composite) to similar curves for the midcontinental United States (Iowa section by Johnson, 1996; Wisconsin section by Harris et al., 1998) and Estonia (Johnson, 1996) and to Johnson's (1996) worldwide composite. Johnson (1996) also presented

similar sea-level curves for Avalonia, Bohemia, Cathaysia, and Gondwana. The Great Basin sea-level highstands that occur in the late Rhuddanian, middle-late Aeronian, early Telychian, late Telychian, and middle Sheinwoodian are the same as those that Johnson and co-workers (Johnson and McKerrow, 1991; Johnson et al., 1991; Johnson, 1996) recognized and interpreted as due to eustasy.

In contrast, the early Rhuddanian sea-level highstand is less widely recognized, although it may occur in the New York portion of the Appalachian Basin (Brett et al., 1990a, 1990b), the northwestern flank of the Michigan Basin (Johnson and Campbell, 1980; Harris and Waldhuetter, 1996; Harris et al., 1997), and Estonia (Johnson, 1996). We suggest two possible interpretations of the middle Rhuddanian sequence boundary: 1) if eustatic, the sea-level drop was small and only expressed in marginal marine settings (shallow shelf, tidal flats); or 2) the relative sea-level fall was due to local tectonic activity. We currently favor the first interpretation, because the sequence boundary appears to occur in four regions.

The Llandovery–Wenlock sea-level curves appear to support Johnson’s (1996) comment that the maximum Silurian transgression occurred in the late Telychian. Telychian sea-levels were generally high (Figure 11), and in the Great Basin, Telychian sequences 4 and 5 are marked by low-energy shelf lagoons (Gettel Member). A transgressive maximum in the late Telychian is suggested by the prominence of mudstone in shelf sections of sequence 5 (Figure 8).

CONCLUSIONS

Six Lower Silurian (Llandovery–early Wenlock) sequences can be correlated throughout the eastern Great Basin. Water depth curves for individual sections may be constructed from sedimentological and paleontological information. Comparison of curves along shelf-to-basin transects allows estimation of shelf paleotopography and of the magnitude of sea-level changes in the study area. Comparisons to other areas suggest a eustatic control over the sea-level cycles.

ACKNOWLEDGMENTS

This study was funded by grants (EAR-9303966 and EAR-9317719) from the National Science Foundation. We want thank J. Awe for his field assistance and Rod Watkins for fruitful discussions. Reviews by C.A. Ross, E. Landing, and an anonymous reviewer considerably helped the clarity of the manuscript.

REFERENCES

- BERRY, W.B.N., AND M.A. MURPHY. 1975. Silurian and Devonian Graptolites of Central Nevada. University of California Publications in Geological Sciences, 110.
- BRETT, C.E., A.J. BOUCOT, AND B. JONES. 1993. Absolute depths of Silurian benthic assemblages. *Lethaia*, 26:25–40.
- , ———, AND S.T. LODUCA. 1990a. Sequence stratigraphy of the type Niagarian Series (Silurian) of western New York and Ontario. New York State Geological Association, 62nd Annual Meeting, Field Trip Guidebook, p. C1–C71.
- , ———, AND ———. 1990b. Sequences, cycles, and basin dynamics in the Silurian of the Appalachian Foreland Basin. *Sedimentary Geology*, 69:191–244.
- BUDGE, D.R., AND P.M. SHEEHAN. 1980b. The Upper Ordovician Through Middle Silurian of the Eastern Great Basin, Part 1—Introduction: Historical Perspective and Stratigraphic Synthesis. Milwaukee Public Museum Contributions in Biology and Geology, No. 28.
- , AND ———. 1980b. The Upper Ordovician Through Middle Silurian of the Eastern Great Basin, Part 2—Lithologic Descriptions. Milwaukee Public Museum Contributions in Biology and Geology, No. 29.
- CARPENTER, R.M., J.M. PANDOLFI, AND P.M. SHEEHAN. 1986. The Late Ordovician and Silurian of the Eastern Great Basin, Part 6—The Upper Ordovician Carbonate Ramp. Milwaukee Public Museum Contributions in Biology and Geology, No. 69.
- COOK, H.E. 1984. Ancient carbonate platform margins, slopes and basins, p. 5.1–5.189. In H.E. Cook, A.C. Hine, and H.T. Mullins (eds.), *Platform Margin and Deep Water Carbonates*. Society of Economic Paleontologists and Mineralogists, Short Course Notes, 12.
- DUNHAM, J.B. 1977. Depositional environments and paleogeography of the Upper Ordovician, Lower Silurian carbonate platform of central Nevada, p. 157–164. In J.H. Stewart, C.H. Stevens, and A.E. Fritsche (eds.), *Paleozoic Paleogeography of the Western United States*, Pacific Coast Paleogeography Symposium 1. Society of Economic Paleontologists and Mineralogists, Pacific Basin Section, 7.
- , E.R. OLSON. 1980. Shallow subsurface dolomitization of subtidally deposited carbonate sediments in the Hanson Creek Formation (Ordovician–Silurian) of central Nevada, p. 139–161. In D.H. Zenger, J.B. Dunham, and R.L. Ethington (eds.), *Concepts and Models of Dolomitization*. Society of Economic Paleontologists and Mineralogists, Special Publication 28.
- FINNEY, S.C., W.B.N. BERRY, AND M.A. MURPHY. 1995. Post-meeting trip: Great Basin graptolites, p. 133–151. In J.D. Cooper (ed.), *Ordovician of the Great Basin: Fieldtrip Guidebook and Volume for the Seventh International Symposium on the Ordovician System*. Society of Economic Paleontologists and Mineralogists, Pacific Basin Section, 78.
- GOLDHAMMER, R.K., P.J. LEHMANN, AND P.A. DUNN. 1993. The origin of high-frequency platform carbonate cycles and third-order sequences (Lower Ordovician El Paso Group, west Texas): constraints from outcrop data and stratigraphic modeling. *Journal of Sedimentary Petrology* 63:318–359.
- HARRIS, M.T., L.A. SEXTON, AND P.M. SHEEHAN. Submitted. Sequence boundary criteria in shelf to middle ramp carbonates: Upper Ordovician–Lower Silurian of the eastern Great Basin. *Journal of Sedimentary Research*.
- , AND P.M. SHEEHAN. 1996. Upper Ordovician–Lower Silurian sequences determined from inner shelf sections, Barn Hills and Lakeside Mountains, eastern Great Basin, p. 161–176. In B.J.

- Witzke, G.A. Ludvigson, and J.E. Day (eds.), *Paleozoic Sequence Stratigraphy: North American Perspectives—Views from the North American Craton*. Geological Society of America, Special Publication 306.
- , AND ———. 1997. Trip #21: carbonate sequences and fossil communities from the Upper Ordovician–Lower Silurian of the eastern Great Basin. 105–128. In P. Link and B. J. Kowallis (eds.), *Proterozoic to Recent Stratigraphy, Tectonics, and Volcanology*, Utah, Nevada, southern Idaho, and central Mexico. Brigham Young University, Geology Studies, 42(1).
- , AND K.R. WALDHUETTER. 1996. Silurian of the Great Lakes Region, Part 3: Llandovery Strata of the Door Peninsula, Wisconsin. Milwaukee Public Museum Contributions in Biology and Geology, No. 90.
- , L.A. SEXTON, AND P.M. SHEEHAN. 1995. Contrasting expressions of sequence boundaries across Upper Ordovician–Lower Silurian carbonate shelf and shallow ramp facies of the eastern Great Basin (Utah and Nevada, p. 39. In American Association of Petroleum Geologists, Annual Meeting, Abstract Volume.
- , J.J. KUGLITSCH, R. WATKINS, D.P. HEGRENES, AND K.R. WALDHUETTER. 1998. Early Silurian stratigraphic sequences of eastern Wisconsin. New York State Museum Bulletin 491 (this volume).
- HINTZE, L.F. 1982. Geological History of Utah. Brigham Young University Geology Studies, 20(3).
- HURST, J.M., and P.M. SHEEHAN. 1985. Depositional environments along a carbonate shelf to basin transect in the Silurian of Nevada, U.S.A. *Sedimentary Geology*, 45: 143–171.
- , ———, AND J.M. PANDOLFI. 1985. Silurian carbonate shelf and slope evolution in Nevada—a history of faulting, drowning and progradation. *Geology* 13:185–188.
- JOHNSON, J.G., AND E.C. POTTER. 1975. Silurian (Llandovery) downdropping of the western margin of North America. *Geology* 3:331–334.
- JOHNSON, M.E. 1975. Recurrent community patterns in eperic seas: the Lower Silurian of eastern Iowa. *Iowa Academy of Science Proceedings*, 82:130–139.
- . 1981. Correlation of Lower Silurian strata from the Michigan Upper Peninsula to Manitoulin Island. *Canadian Journal of Earth Sciences*, 18:869–883.
- . 1996. Stable cratonic sequences and a standard for Silurian eustasy, p. 203–211. In B.J. Witzke, G.A. Ludvigson, and J.E. Day (eds.), *Paleozoic Sequence Stratigraphy: North American Perspectives—Views from the North American Craton*. Geological Society of America, Special Publication 306.
- , AND G.T. CAMPBELL. 1980. Recurrent carbonate environments in the Lower Silurian of northern Michigan and their inter-regional correlation. *Journal of Paleontology*, 54:1041–1057.
- , D. KALJO, AND RONG J.-Y. 1991. Silurian eustasy, p. 145–163. In *Special Papers in Palaeontology*, 44.
- , AND H.L. LESCINSKY. 1986. Depositional dynamics of cyclic carbonates from the Interlake Group (Lower Silurian) of the Williston Basin. *Palaios*, 1:111–121.
- , AND W.S. MCKERROW. 1991. Sea level and faunal changes during the latest Llandovery and earliest Ludlow (Silurian). *Historical Biology*, 5:153–169.
- , RONG J.-Y., AND YANG X. 1985. Intercontinental correlation by sea-level events in the Early Silurian of North America and China (Yangtze Platform). *Geological Society of America Bulletin*, 96:1384–1397.
- KLEFFNER, M.A. 1995. A conodont- and graptolite-based Silurian chronostratigraphy, p. 159–176. In K.O. Mann and H.R. Lane (eds.), *Graphic Correlation*. SEPM Society for Sedimentary Geology, Special Publication 53.
- MCKERROW, W.S. 1979. Ordovician and Silurian changes in sea level. *Journal of the Geological Society of London*, 136:137–145.
- MATTI, J.C., AND E.H. MCKEE. 1977. Silurian and Lower Devonian paleogeography of the outer continental shelf of the Cordilleran miogeosyncline, east-central Nevada, p. 181–215. In J.H. Stewart, C.H. Stevens, and A.E. Fritsche (eds.), *Paleozoic Paleogeography of the Western United States*, Pacific Coast Paleogeography Symposium 1. Society of Economic Paleontologists and Mineralogists, Pacific Basin Section, 7.
- , M.A. MURPHY, AND S.C. FINNEY. 1975. Silurian and Lower Devonian Basin and Basin-Slope Limestones, Copenhagen Canyon, Nevada. Geological Society of America, Special Paper 159.
- MULLENS, T.E., AND F.G. POOLE. 1972. Quartz sand-bearing zone and Early Silurian age of upper part of the Hanson Creek Formation in Eureka County, Nevada. United States Geological Survey Professional Paper 800-P:21–24.
- MURPHY, M.A. 1989. Central Nevada, p. 171–177. In C.H. Holland and M.G. Bassett (eds.), *A Global Standard for the Silurian System*. National Museum of Wales, Geological Series 9.
- , J.B. DUNHAM, W.B.N. BERRY, AND J.C. MATTI. 1979. Late Llandovery unconformities in central Nevada. Brigham Young University Geology Studies 26:21–36.
- NICHOLS, K.M., AND N.J. SILBERLING. 1977. Depositional and tectonic significance of Silurian and Lower Devonian dolomites, Roberts Mountains and vicinity, east-central Nevada, p. 217–240. In J.H. Stewart, C.H. Stevens, and A.E. Fritsche (eds.), *Paleozoic Paleogeography of the Western United States*, Pacific Coast Paleogeography Symposium 1. Society of Economic Paleontologists and Mineralogists, Pacific Basin Section, 7.
- POOLE, F.G., J.H. STEWARD, A.R. PALMER, C.A. SANDBERG, R.J. MADRID, R.J. ROSS, JR., L.F. HINTZE, M.M. MILLER, AND C.T. WRUCKE. 1992. Latest Precambrian to latest Devonian time: development of a continental margin, p. 9–56. In B.C. Burchfiel, P.W. Lipman, and M.L. Zoback (eds.), *The Cordilleran Orogen: Coterminous U.S. The Geology of North America*, V. G-3. Geological Society of America, Boulder.
- READ, J.F., AND R.K. GOLDHAMMER. 1988. Use of Fisher plots to define third-order sea-level curves in Ordovician peritidal cyclic carbonates, Appalachians. *Geology* 16:895–899.
- ROSS, C.A., AND J.R.P. ROSS. 1996. Silurian sea-level fluctuations, p. 187–192. In B. J. Witzke, G.A. Ludvigson, and J.E. Day (eds.), *Paleozoic Sequence Stratigraphy: North American Perspectives—Views from the North American Craton*. Geological Society of America, Special Publication 306.
- ROSS, R.J., JR., T.B. NOLAN, AND A.G. HARRIS. 1979. The Upper Ordovician and Silurian Hanson Creek Formation of Central Nevada. United States Geological Survey Professional Paper 1126-C.
- SCOTese, C.R., AND W.S. MCKERROW. 1990. Revised world maps and introduction, p. 1–21. In W.S. McKerrrow and C.R. Scotese (eds.), *Palaeozoic Palaeogeography and Biogeography*. Geological Society of London, Memoir 12.
- SHEEHAN, P.M. 1980. Paleogeography and marine communities of the Silurian carbonate shelf in Utah and Nevada, p. 19–37. In T.D. Fouch and E.R. Magatham (eds.), *Paleozoic Paleogeography of West-Central United States*, West-Central United States Paleogeography Symposium 1. Society of Economic Paleontologists and Mineralogists, Rocky Mountain Section.
- . 1986. The Upper Ordovician through Middle Silurian of the Eastern Great Basin, Part 7—Late Ordovician and Silurian Carbonate-Platform Margin Near Bovine and Lion Mountains,

Northeastern Utah. Milwaukee Public Museum Contributions in Biology and Geology, No. 70.

———. 1990. Late Ordovician and Silurian paleogeography of the Great Basin. Contributions to Geology, The University of Wyoming 27:41–54.

———, AND A.J. BOUCOT. 1991. Silurian paleogeography of the western United States, p. 51–82. In J.D. Cooper and C.H. Stevens (eds.), Paleozoic Paleogeography of Western United States, Revised Edition. Society of Economic Paleontologists and Mineralogists, Pacific Section, 67.

———, AND M.T. HARRIS. In press. Upper Ordovician–Silurian macrofossil biostratigraphy of the eastern Great Basin—Utah and Nevada, Part C. In M.E. Taylor (ed.), Early Paleozoic Biochronology of the Great Basin, Western United States. United States Geological Survey, Professional Paper 1579.

WEBB, B.W. 1958. Middle Ordovician stratigraphy in eastern Nevada and western Utah. American Association of Petroleum Geologists Bulletin, 42:2335–2377.

WINTERER, E.L., AND M.A. MURPHY. 1960. Silurian reef complex and associated facies, central Nevada. Journal of Geology, 68:117–139.

WITZKE, B.J., AND B.J. BUNKER. 1996. Relative sea-level changes during Middle Ordovician through Mississippian deposition in the Iowa area, North American craton, p. 307–330. In B.J. Witzke, G.A. Ludvigson, and J.E. Day (eds.), Paleozoic Sequence Stratigraphy: North American Perspectives—Views from the North American Craton. Geological Society of America, Special Publication 306.

EUSTATIC FLUCTUATIONS IN THE EAST SIBERIAN BASIN (SIBERIAN PLATFORM AND TAYMYR PENINSULA)

YU.I. TESAKOV¹, M.E. JOHNSON², N.N. PREDTETCHENSKY³, V.G. KHROMYCH¹, AND A.YA. BERGER³

¹United Institute for Geology, Geophysics and Mineralogy, Siberian Division of the RAS, 630090, Novosibirsk, Universitetskoy prospect 3, Russia,

²Department of Geosciences, Williams College, Williamstown, MA 01267, and

³All Russian Research Geological Institute, 199026, St. Petersburg, Sredniy prospect, 74, Russia

ABSTRACT—The east Siberian Silurian was deposited in a cratonic basin with facies that range from deep-water graptolitic to shallow foreshore and lagoonal with linguloids and fish. A detailed regional stratigraphy and analysis of local and regional tectonic and sedimentary cycles allow determination of bathymetry, submarine relief, and eustasy. Shoreline features were overlapped by transgressive sediments, and this allows interpretation of topography marginal to the basin and a quantitative measurement of sea-level rise. On the carbonate margins of the shallow shelf where rich, benthic faunal assemblages are regularly overlapped by pelagic assemblages, eustatic fluctuations are most clearly identifiable. The Moyero, Turukhansk, and Middendorf regions are most representative of this situation and allow creation of a sea-level curve for east Siberia. This standard is supported by local events that show the appearance of pelagic assemblages only on the deeper part of the shallow shelf. The deep-shelf sea-level curve is less dramatic. It is recognized only by the quantitative characters of graptolite and rarer pelagic brachiopod and ostracode faunas. The sea-level record of the east Siberian Silurian includes nine highstands, which are clearly recognized and conform to the eustatic standard. These highstands are: 1) late Moyeroceanian (late Rhuddanian), 2) late Khaastyrian (middle Aeronian), 3) early Agideian (early Telychian), 4) late Agideian (late Telychian), 5) early Khakomian (late Sheinwoodian), 6) late Tukalian (early Gorstian), 7) early Postnichian (late Ludfordian), and 8) late Postnichian (Pridoli). Another early Moyeroceanian highstand (1a) is related to the earliest, most extensive, and most rapid Silurian transgression after latest Ordovician regression.

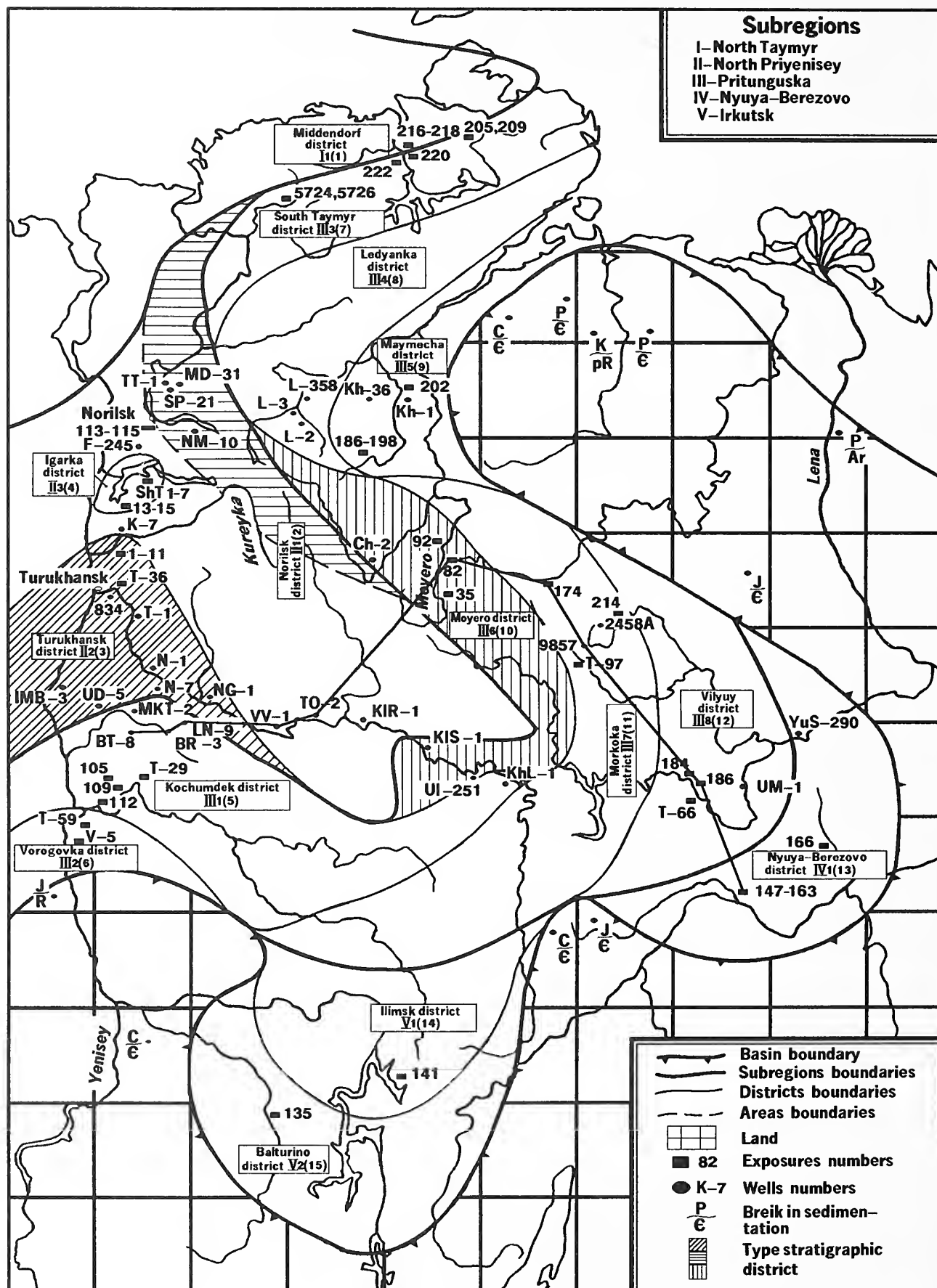
INTRODUCTION

Silurian eustasy was reviewed by Johnson (1996), who showed that recognition of coeval highstands in global sea-level depends on the study of local sea-level curves

established in cratonic (epeiric) seas. This report documents the major Silurian highstands recorded in the east Siberian epicontinental basin and compares them to the standard eustatic curve proposed by Johnson (1996) for the Silurian.

The east Siberian epicontinental basin occupied a vast area of not less than 3 million km² that lies between the courses of the Yenisey and Lena Rivers on the Siberian Platform and includes the Taymyr Peninsula and Severnaya Zemlya Archipelago (Figure 1). The initial task was to delineate this sedimentary basin and develop a stratigraphic zonation of its sediments (Tesakov et al., 1979, p. 11–14, fig. 1). Subsequent study of Silurian sequences on the Taymyr Peninsula suggested that they were most similar to those on the Siberian Platform (Tesakov et al., 1995). Therefore, the border of the East Siberian Basin was extended, and its boundaries and stratigraphic zonation have been revised (Figure 1). Additional tasks included the study of the history of sedimentation in the East Siberian Basin, its biota, and its regional sea-level fluctuations. For this purpose, a synthesis of Silurian litho-, bio-, chrono-, cyclo- and seismostratigraphy was undertaken.

The litho- and chronostratigraphic approach included bed-by-bed descriptions of all sections. In addition, a more detailed definition of units at the local level (formations, local faunal zones), regional level (horizons [i.e., a Russian rock-unit characterized by a distinctive fauna and commonly of formation or stage magnitude] and regional chronozones), and global level (substages and global chronozones) and their correlation were undertaken. Definition of unit stratotypes and their correlation was a fundamental step. The fundamental units are chronozones that are apparent on various geographic scales (local, regional, global). The geochronology of zonal stratotypes was estimated on the basis of two basic parameters. This included determination of stages and



faunal zones, which McKerrow et al. (1980) estimated at approximately 500 Ka. From this, an east Siberian zonal scheme was proposed (Tesakov et al., 1985, 1992, 1996b; Tesakov, 1996). This was incorporated into a stratigraphic chart for east Siberia (Tesakov et al., 1979, 1980, 1996a), where local units are correlated at the zonal level.

Biostratigraphy was based on bed-by-bed study at all sections. This allowed definition of the stratigraphic range of all species in terms of a zonal scheme for different areas (i.e., structural facies zones) in the East Siberian Basin, and correlation into a time scale. The species distribution by zone for the Moyero (Tesakov et al., 1985), Morkoka (Tesakov et al., 1992), and Igarka and Turukhansk (Tesakov et al., 1980) regions are published, and that for the entire east Siberia region is in preparation.

This lithofacies–biostratigraphic synthesis required definition of biogeocoenoses [i.e., facies associations of fossil assemblages] (Sukachev, 1945, 1949; Tesakov, 1978) based on the analysis of lithologies (Tesakov et al., 1980) and oryctocoenoses (Efremov, 1950), with the description of their structure, sediment type, biocoenoses, possible salinity, proposed wave and current dynamics, and location of the biogeocoenoses within the basin (Tesakov et al., 1986). This allowed an understanding of potential models for lithofacies development through time and space on the East Siberian Basin. Stratigraphic profiles (Tesakov et al., 1979, 1985; Tesakov, 1981) and sea-level curves for specific sections (Tesakov et al., 1986, 1992) have been published.

Cyclo-seismostratigraphy [i.e., seismic stratigraphy] produced seismic records used to evaluate cyclic and sequence stratigraphy at surface sections. These records were compared with subsurface logs.

Creation of a standard sea-level curve for the East Siberian Basin by these techniques led to problems in relating the different procedures. The first of these problems concerned the change in geochronologic scales. Initially, Tesakov et al. (1985, 1992) and Tesakov (1996) used the scale of McKerrow et al. (1980). Subsequently, revised ages were proposed by McKerrow et al. (1985) and Tucker and McKerrow (1995). Johnson (1996) used the dates of McKerrow et al. (1985) in his eustatic curve. Silurian faunal zones have an average duration of approximately 500 Ka by the 1980 scale. However, average faunal zone duration is demonstrated to be quite variable by the

1985 scale: Rhuddanian Stage, about 300 Ka/zone; Aeronian, about 400 Ka/zone; Telychian, about 700 Ka; Sheinwoodian, about 500 Ka; Homerian, about 400 Ka; Gorstian, over 200 Ka; Ludfordian, about 1.2 Ma; and Pridoli, about 400 Ka. Thus, it has been possible to retain the succession of the earlier scale, while using the later one (Figures 2 and 3, left side).

The second problem involves the correlation of biotic zones (Silurian Times, 1993, 1995; Johnson, 1996) (Figure 2, columns 3–6) and the chronozones used in Siberia (Tesakov et al., 1985, 1992, 1996c; Tesakov, 1996) (see Figure 3, column 3). The first approach is based on biological features not tied to local stratigraphy. The second is founded on stratotypes with boundaries in specific rock sequences, and can always be tested. Biostratigraphic zonations based on particular biotic groups cannot be applied everywhere because of biofacies constraints. A chronostratigraphy implies the ability to correlate between sections, even those that lack biological remains. The problem of correlation between biozones and chronozones appears to be so complicated that it cannot be solved in this report. Therefore, an attempt is made here only to correlate Johnson's (1996) eustatic curve with the Silurian standard curve for the East Siberian Basin and to relate the chronostratigraphic scale to the appearance of graptolite and conodont species (Figure 3). The non-coincidence of the lower boundaries of zones and the levels of occurrence of important species is evident in Figures 2 and 3. For example, the *Monograptus sedgwicki* Zone is confined to the middle Aeronian in the global and east Siberian faunal schemes. However, the *Monograptus convolutus* Zone is in the middle Aeronian in the global standard (Figure 2), but in the lowest part of the stage in the East Siberia Basin (Figure 3). In either case, the lowest appearance of the eponymous species is a guide to the lower Aeronian. A similar discrepancy exists with the eponymous species of the *Monograptus bouceki* Zone, which appears at the base of the second Pridoli zone in the East Siberia Basin (see Figure 3, correlation level (=CL) 51, and Kříž, 1989, fig. 67, bed 106), rather than in the upper part of the Pridoli in the global standard (Figure 2, column 4). Similarly, discrepancies may exist between the earliest appearance of key conodonts in Siberia, such as *Pterospirifer celloni* and *P. amorphognathoides*.

A third problem involves the comparison of various types of basin faunal sequences to produce a standard sea-level curve for the East Siberian Basin. This required the comparison of coenozones [i.e., benthic associations] based on brachiopods (see Ziegler, 1965; Ziegler et al., 1968; Boucot, 1975) that allowed the construction of the standard eustatic curve (Johnson, 1996) with facies complexes (Wilson, 1974; Tesakov et al., 1979) and shelf lithostratigraphy. This technique allowed the creation of

FIGURE 1—(opposite) Silurian East Siberian Basin. Sections at Bakhta River (boreholes BT-8, BR-3, LN-9), middle Nizhnyaya Tunguska River (boreholes VV-1, TO-2), Moyero River (section 82), Nizhnyaya Bolshaya Kuonda River (section 174), upper Alakit River (borehole 9857), middle Vilyuy River (sections 184, 186), lower Nyuya River (sections 147–163).

(McKerrow et al., 1985)	(Holland, Bassett, eds., 1989)		(Johnson, 1996)	(Silurian Times, 1995)	(Johnson, 1996)	(Silurian Times, 1995)		
	Series	Stage	Graptolite zones	Graptolite zones	Conodont zones	Conodont zones		
1	2		3	4	5	6		
412 Ma	P R I D.		seven zones	<i>bouceki</i> – <i>transgrediens</i>	<i>w. woschmidtii</i>	<i>eosteinhornensis</i> – <i>detorta</i>		
				<i>branikensis</i> – <i>lohkovensis</i>	<i>r. eosteinhornensis</i>	<i>remscheidensis</i> interval zone		
				<i>parultimus</i> – <i>ultimus</i>				
414 Ma	L U D L O W	Ludfordian	<i>balticus</i> / <i>caudatus</i>	<i>formosus</i>	<i>crispa</i>	<i>crispa</i>		
			<i>kozlowskii</i>					
415 Ma			<i>inexpectatus</i>	<i>bohemicus tenuis</i> – <i>kozlowskii</i>	<i>snajdri</i>	<i>snajdri</i> interval zone		
			<i>auriculatus</i>					
			<i>cornutus</i>					
		<i>precornutus</i> / <i>bohemicus</i>	<i>leintwardiensis</i>	<i>siluricus</i>	<i>siluricus</i>			
		<i>aversus</i>						
		<i>leintwardienensis</i>						
		<i>hemiaversus</i> / <i>tumescens</i>	<i>scanicus</i>	<i>ploeckensis</i>	<i>ploeckensis</i>			
		<i>invertus</i>						
		<i>scanicus</i>						
		<i>progenitor</i>	<i>nilssoni</i>					
		<i>nilssoni</i>						
420 Ma	W E N L O C K	Homerian	<i>ludensis</i>	<i>ludensis</i>	<i>praedeubell</i> – <i>deubell</i>	<i>bohémica bohémica</i>		
			<i>nassa</i>				<i>parvus</i> – <i>nassa</i>	
			<i>lundgreni</i>					<i>lundgreni</i>
		Shein- woodian	<i>ellesae</i>	<i>rigidus</i> – <i>perneri</i>	<i>sagitta sagitta</i>	<i>sagitta sagitta</i>		
			<i>flexilis</i>				<i>riccartonensis</i> – <i>belophorus</i>	<i>sagitta rhenana</i>
			<i>rigidus</i>					
			<i>riccartonensis</i>	<i>centrifugus</i>	<i>amorphognathoides</i>			
			<i>murchisoni</i>			<i>lapworthi</i> – <i>insectus</i>	<i>amorphognathoides</i>	
425 Ma			<i>centrifugus</i>	<i>spiralis</i> interval zone	<i>celloni</i>			
		L L A N D O V E R Y	Telychian			<i>crenulata</i>	<i>griestoniensis</i> – <i>crenulata</i>	<i>celloni</i>
	<i>griestoniensis</i>							
	<i>crispus</i>			<i>turriculatus</i> – <i>crispus</i>	<i>staurognathoides</i>			
	<i>turriculatus</i>							
	<i>guerichi</i>					<i>guerichi</i>		
430 Ma	Aeronian		<i>sedgwickii</i>	<i>sedgwickii</i>	<i>tenuis</i> – <i>staurognathoides</i>			
			<i>convolutus</i>	<i>convolutus</i>				
			<i>argenteus</i>	<i>argenteus</i>				
			<i>magnus</i>					
432 Ma	Rhuddanian		<i>triangulatus</i>	<i>triangulatus</i> – <i>pectinatus</i>	<i>kentuckyensis</i>	<i>kentuckyensis</i>		
433 Ma		<i>cyphus</i>	<i>cyphus</i>					
		<i>acinaces</i>	<i>vesiculosus</i>					
		<i>atavus</i>						
		<i>acuminatus</i>	<i>acuminatus</i>					
435 Ma					<i>nathani</i>			

FIGURE 2—(above) Correlation of Silurian graptolite- and conodont-based zones.

FIGURE 3—(opposite) Standard sea-level curve for Silurian East Siberian Basin and comparison with global curve. In columns 4 and 5, plus sign (+) is level of first biostratigraphic occurrence. Some key conodont species have their have occurrences earlier than commonly reported elsewhere (Figure 2). In column 7, dashed curves indicate intervals where graptolite facies overlap carbonates of the East Siberian Basin.

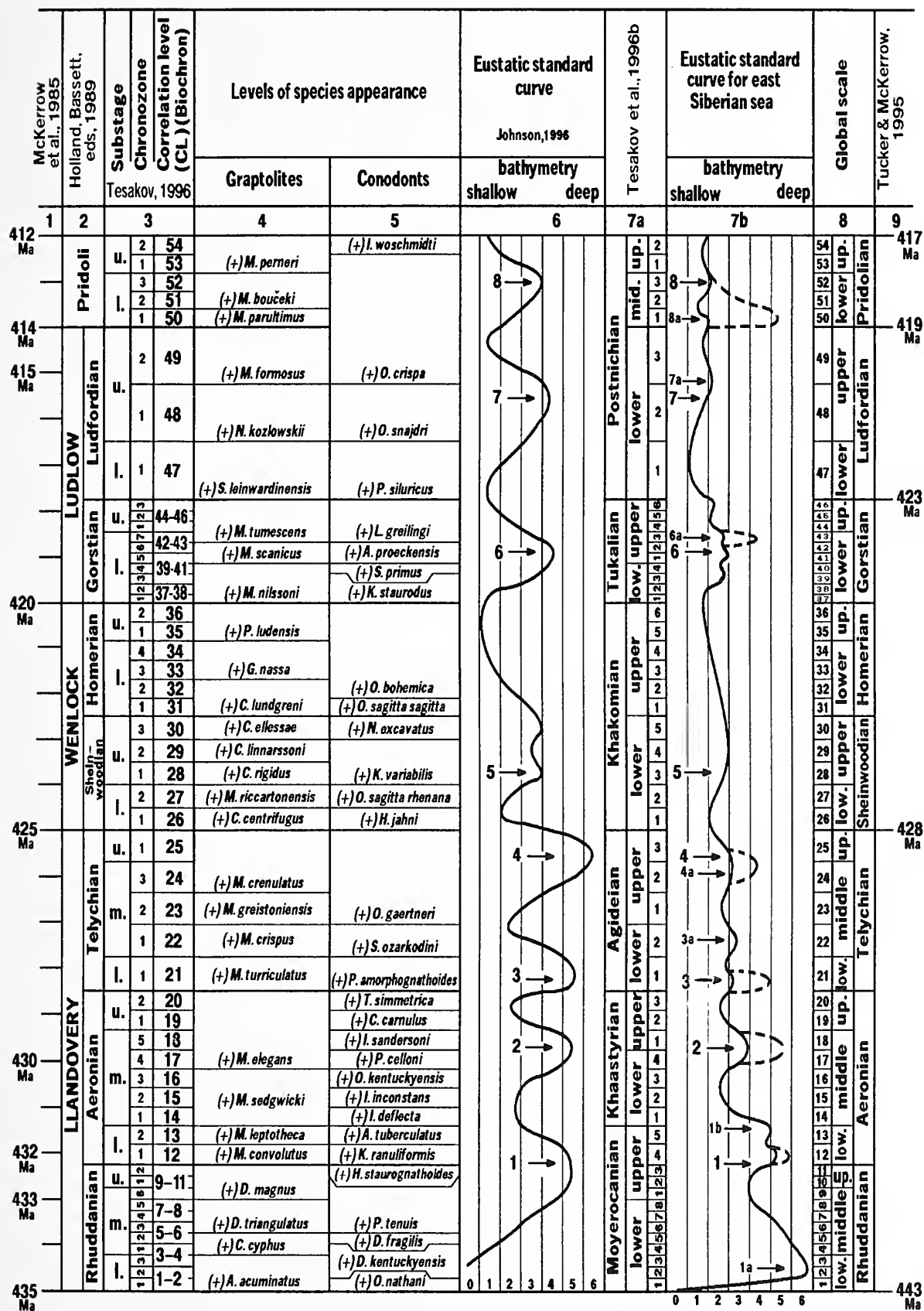


TABLE 1—Comparison of nomenclature for Silurian communities and benthic assemblages of Boucot (1975) and Johnson (1996) with Siberian depositional setting terminology applied in this report.

Boucot (1975)	Johnson (1996)	This report
1. <i>Lingula</i> community	Benthic assemblage 1	Nearshore area
2. <i>Eocoelia</i> community	Benthic assemblage 2	Upper shelf (fair-weather wave base)
3. <i>Pentamerus</i> community	Benthic assemblage 3	Middle shelf (storm wave-base)
4. <i>Stricklandia</i> community	Benthic assemblage 4	Outer shelf
5. <i>Clorinda</i> community	Benthic assemblage 5	Outer shelf
6. Graptolite community	Benthic assemblage 6	Deep shelf

sea-level curves for the Silurian of Podolia based on coral assemblages (Sokolov and Tesakov, 1984, 1986) and for the Silurian of the Moyero and Kuonda River basins based on analyses of benthic biocoenoses (Tesakov et al., 1986, 1992). The first attempt at a global comparison of Silurian benthic communities from proximal to distal settings was made by M.E. Johnson and Yu.I. Tesakov in 1993 in Novosibirsk (Johnson et al., 1997), and is summarized in Table 1.

SEA-LEVEL STANDARD FOR EAST SIBERIAN BASIN

A regional sea-level curve was based on analysis of sections in the Moyero, Turukhansk, and Norilsk areas, with allowances for local developments in the Middendorf region and elsewhere in the East Siberian Basin (Figure 4). This curve is the sea-level standard for east Siberia (Figure 3, column 7). It can be compared to the Silurian standard eustatic curve (Johnson, 1996) in Figure 3, column 6. Highstands in the Silurian standard curve (1–8) are indicated by arrows in both columns. Levels that deviate from the standard are lettered. The main deepening events of the East Siberian Basin are: 1a, early Moyerocanian (early Rhuddanian); 1, late Moyerocanian (Rhuddanian–Aeronian boundary); 1b, late Moyerocanian (early Aeronian); 2 middle Khaastyrrian (middle Aeronian); 3, earliest Agidean (early Telychian); 3a, late early Agidean (middle Telychian); 4a, late Agidean (late Telychian); 5, early Khakomian (late Sheinwoodian); 6, late Tukalian (early Gorstian); 7a, early Postnichian (late Ludfordian); 8a and 8, middle Postnichian (early Pridoli). The relative magnitude of transgressions are shown in Figure 3 (column 7) where the major highstands are Rhuddanian, Aeronian, Telychian, Gorstian, and early Pridoli. These levels (dashed lines) show the appearance of relatively deep-water, graptolitic sediments in more proximal areas of the basin.

HIGHSTAND 1A (EARLY RHUDDANIAN [EARLY MOYEROCANIAN]).—This rise in east Siberian sea-level (CL 2, 3) is probably associated with deglaciation during the latest Ordovician–Early Silurian (Beuf et al., 1971; McClure, 1978; Grahn and Caputo, 1992) and a subsidence of the Siberian paleocontinent that was complicated by regional and local tectonic movements (Tesakov et al., 1979; Tesakov, 1981). The early Rhuddanian transgression was so rapid that virtually the entire Siberian Platform was quickly inundated. The age of this event is supported by identification of the graptolite *Akidograptus acuminatus* and the conodont *Oulodus natani* from the base of the Silurian sections in Siberia.

The northwest region of the Siberian Platform features a contact between eroded Ordovician deposits and overlying, relatively deep-water Silurian deposits. The Ordovician was eroded after Late Ordovician uplift (Tesakov, 1967). On the remainder of the Siberian Platform and in the southern Taymyr Peninsula, Ordovician deposits were eroded and peneplaned after tectonic activity indicated in some sections by angular unconformities (Tesakov, 1967). Early Rhuddanian sea-level rise is considered to be significant because of the wide distribution of relatively deep-water sedimentary rocks with graptolites, which rest on Late Ordovician shallow marine rocks in the central and northwest areas of the Siberian Platform and the northern Taymyr Peninsula. The rise in early Rhuddanian sea-level inundated a rugged topography that developed in the latest Ordovician and earliest Silurian. This included small hills on the northwest Siberian Platform, which were not completely covered by the lowest Silurian sediments. Other features include high islands along the middle part of the Vilyuy River; rocky shores in the southern Taymyr Peninsula (Tesakov et al., 1995) and on the west side of the Anabar massif (Johnson et al., 1997); and gently sloping canyons formed by tectonic activity and subaerial erosion at the north-west margin of the Tunguska basin (Tesakov, 1967; Johnson et al., 1997). In the stratotype section located in the Moyero River basin at the mouth of the Moyerocanian

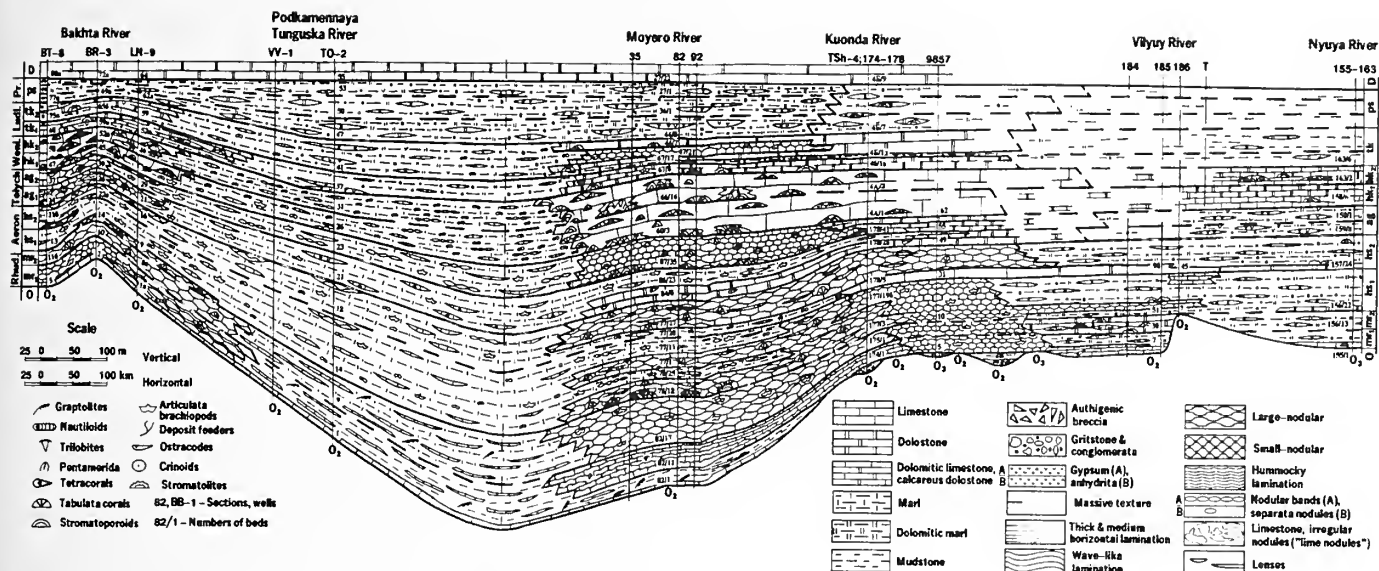


FIGURE 4—Silurian stratigraphy in central East Siberian Basin (locations in Figure 1). Abbreviations: Ludl., Ludlow; Pr., Pridoli; Rhud., Rhuddanian; Wenl., Wenlock. Horizon (i.e., regional stages in Siberia) and subhorizons: ag₁, lower Agideian; ag₂, upper Agideian; hk₁, lower Khakomian; hk₂, upper Khakomian; hs₁, lower Khaastyrian; hs₂, upper Khaastyrian; mr₁, lower Moyerocanian; mr₂, upper Moyerocanian; ps, Postnichian; tk₁, lower Tukalian; tk₂, upper Tukalian.

River (Tesakov et al., 1985), the onset of early Rhuddanian deepening is recorded by dark bituminous limestones with small phytolites [i.e., ooids and oncoids], brachiopods, and trilobites that rest on shallow-marine, Ordovician dolostone. This onlap flooded a peneplane on Ordovician rocks that are truncated at a low angle and overlain by monotonous Silurian strata (Tesakov et al., 1985, fig. 31). The different depths of erosion on the Ordovician and variable thickness of the lowermost Silurian shows that the sea-level rise inundated a tectonically active area, which subsided locally at different rates.

This sea-level highstand in the East Siberian standard section is substantiated by a wedging-out of dark, graptolitic mudstones within regional chronozone 2 on the upper (inner) part of the deep shelf, although they persist in regional chronozones 1–3 on the lower (outer) part of the deep shelf in the northwest of the platform. The age of this mudstone is early *Coronograptus cyphus* Chron. The eponymous species of this chron appears in the standard section only in the fourth chronozone.

Because Silurian deposits on a large part of the Siberian Platform consist of relatively deep-water rocks with graptolites and lie on an erosion surface, sea-level during this first highstand rose not less than 50–100 m. It might be noted that Silurian sea-level was, on average, 300 m higher than today (Harland et al., 1985, fig. 5.7).

The initial onlap (Figure 2, level 1a) is recorded in the Siberian standard section by graptolite assemblages (*Metabolograptus moyeroensis* Zone) that accumulated in soft argillaceous muds. Subsequent regression is recor-

ded by the successive *Coronograptus cyphus* and *Paraclimacograptus innotatus* Zones that occur in soft siliciclastic mudstones with carbonate mudstone lenses (CL 3–6). Succeeding faunas include the trilobite *Acernaspis superciliexilis* on firm carbonate mud bottoms (CL 7), the brachiopod *Clorinda undata* on firm carbonate mud (CL 8), and then the brachiopod *Sibiritia wiluensis* on firm argillaceous, carbonate mud bottoms (CL 9). A later, modest highstand with brachiopod (*Septatrypa antiquata* and *Zygospira duboisi*) assemblages in firm, argillaceous carbonate mud (CL 10, 11) is known.

HIGHSTAND 1 (RHUDDANIAN–AERONIAN BOUNDARY [LATE MOYEROCANIAN]).—This sea-level highstand is indicated in the standard section by assemblages with the brachiopod *Isorthis neocrassa* on calcareous, siliciclastic mudstone with *Stricklandia*. An abundance of graptolites is observed through the basin at this level. This highstand is modest in magnitude and gradual, because the change in brachiopod assemblages and the increase in clay-size siliciclastic sediment proceeded gradually at its beginning and end. The following minor regression (CL 13) is indicated by assemblages with the brachiopods *Zygospiraella duboisi* and *Z. planoconvexa* and crinoids.

HIGHSTAND 1B (EARLY MIDDLE AERONIAN [EARLIEST KHAASTYRIAN]).—This highstand is characterized by the appearance in the Siberian type area of coral assemblages with *Quadralites quadratus* on firm, argillaceous, carbonate mud. The coral bioherms occur on the middle part of

a shallow shelf. Among brachiopods, the highest *Borealis nanus* was identified here. Deep-water siliciclastic mudstones are common through the basin. The most dramatic feature of this time was a complete inundation of the highest island in the central East Siberian Basin (located in the middle part of the Vilyuy River), as well as rocky shorelines of the southern Gorny Taymyr and western Anabar region. The depth of the water on the middle shelf is indicated by a shallow pentamerid community. The graptolite-based age of this event corresponds to the *Monograptus sedgwickii* Chron.

Subsequent regression (CL 15 and 16) is recorded in the Siberian stratotype area by a number of alternating biogeocoenoses that represent a very shallow shelf environment. These include the corals *Calamopora alveolaris* and *Favosites gothlandicus gothlandicus* on firm mud and *Eocoelia hemisphaerica* on soft argillaceous mud.

HIGHSTAND 2 (MIDDLE AERONIAN [MIDDLE KHAASYRIAN]).—This highstand is easily recognizable in Johnson's (1996) curve by areally extensive assemblages with *Pentamerus oblongus*. In the Siberian type area, it is defined by lateral transitions from biogeocoenoses with *P. oblongus* that occur on soft argillaceous mud to biogeocoenoses with *Eocoelia hemisphaerica* that also occur on soft argillaceous mud with lenses of firm carbonate mud. In the transition area between the carbonate shelf and basin facies, carbonate facies at highstand 2 are overlapped by basinal facies with particularly diverse graptolites. This highstand is bracketed by an acme of *P. oblongus* and the lowest occurrence of the conodont *Pterospirifer ozarkodini*.

The ensuing regression (CL 19 and 20) is recorded in the Siberian stratotype area by the appearance of biogeocoenoses with *Favosites gothlandicus gothlandicus* on firm carbonate mud, and subsequent biogeocoenoses with *Eocoelia hemisphaerica* on soft argillaceous mud. The end of the regressive cycle (CL 20) is characterized by geographically extensive, coral biogeocoenoses with *F. gothlandicus gothlandicus* on firm, argillaceous-carbonate mud, and then by biogeocoenoses with *F. gothlandicus gothlandicus*, *Parastriatopora rhizoides*, and *P. tchernichevi* on rigid carbonate mud on the upper part of the shallow shelf.

HIGHSTAND 3 (EARLY TELYCHIAN [EARLY AGIDEAN]).—This highstand is recognized in the east Siberian type area by the appearance of biogeocoenoses with *Anabaria rara*, *Cytherellina oviformis*, and *Bystowicrinus quinquelobatus* in shallow-water assemblages with *Herrmannina moieroensis* on firm mud. This highstand cannot be recognized readily in east Siberia. It is evident mainly in west

and northwest areas of the Siberian Platform and in the northern Gorny Taymyr, where this interval is dominated by graptolitic basin facies. The marginal areas of the East Siberian Basin become shallower from this time on. The lowest appearance of the conodont *Pterospirifer amorphognathoides* suggests the age of this event.

Subsequent regression in the east Siberian stratotype area is indicated by shallow-water biogeocoenoses with *Herrmannina moieroensis*. These appeared on firm lime mud with patches of rigid mud with stromatolites.

HIGHSTAND 3A (EARLY MIDDLE TELYCHIAN [LATEST EARLY AGIDEAN]).—This highstand is recorded in the east Siberian type area by the appearance of biogeocoenoses with *Cytherellina oviformis*. These brachiopods lived on soft argillaceous mud, and are followed by assemblages with *Mendacella tungussensis* that also occurred on soft argillaceous mud. The shallow-water form *Pentamerus oblongus* appears in *M. tungussensis* assemblages on small carbonate banks. Highstand 3a is indicated by graptolitic mudrocks that extend onto the carbonate platform. The correlation of this highstand (CL 22) is provided by the lowest local appearance of the conodont *Spathognathodus ozarkodini*.

The subsequent regression (CL 23) is associated in the east Siberian type area by coral assemblages with *Multisolenia tortuosa* and *Favosites gothlandicus moyeroensis*. These taxa occurred on firm lime mud.

HIGHSTAND 4A (MIDDLE-EARLY LATE TELYCHIAN [MIDDLE LATE AGIDEAN]).—This highstand is indicated in east Siberia by the appearance of assemblages with *Alispira rotundata* that lived on soft argillaceous mud within shallow-water, carbonate shelf sequences with crinoids, ostracodes, deposit feeders, and stromatoporoids. This highstand features the youngest Llandovery graptolites (*Streptograptus nodifer*) on the Siberian Platform.

HIGHSTAND 5 (MIDDLE LATE SHEINWOODIAN [MIDDLE EARLY KHAKOMIAN]).—This modest rise in early Wenlock sea-level is recorded in the east Siberian stratotype area by the appearance within shallow-water sequences of deeper-water assemblages with *Neobeatricea nikiforovae* that lived on plastic lime mud and assemblages with *Dalejina rybnayaensis* that lived on soft argillaceous mud. In the early Sheinwoodian, the shallower-water facies includes a lower assemblage with *Labechia condensa* on rigid carbonate mud, and in areally extensive biostromes. Later shallow-water assemblages with *Beyrichia mirabilis* developed on firm, calcareous-dolomitic mud with numerous stromatolites. Still higher in

the sequence, the highstand assemblages are overlain by shallow-water, reef, and interbioherm assemblages with *Yavorskiina membrosa*, *Bystrowicrinus bilobatus*, *Clavidictyon cylindricum*, *Morynorhynchus proprius*, *Murchisonia cingulata*, and *Stelodictyon moieroensis* in the uppermost Sheinwoodian–Homerian, and by algal buildups in the lowest Gorstian.

HIGHSTANDS 6 AND 6A (GORSTIAN [TUKALIAN]).—The Gorstian records a minor sea-level rise and frequent fluctuations in east Siberia. In the Turukhansk stratotype area, this event is recorded by the appearance of assemblages with *Hyattidina acutisummatatus* (in CL 39 and 41), *Beyrichia quadricornuta* (CL 43), and *Parastriatopora kureikiana* (CL 46) in typical algal buildup assemblages in a lagoonal lithofacies. These highstands record the last appearance of graptoloids on the Siberian Platform in the Norilsk region during CL 43.

HIGHSTANDS 8 AND 8A (EARLY PRIDOLI [MIDDLE POSTNICHIAN]).—Two modest rises in east Siberian sea-level (CL 50 and 52) are recorded in the Norilsk stratotype area. The rises are indicated, as earlier in the Ludfordian, by the appearance of algal buildups in gypsum–dolostone–marl lithofacies. In the area north of the Gorny Taymyr, a single highstand is defined by the sharp transition from underlying shallow-shelf carbonates into relatively deep-water, graptolitic mudstones that were deposited as soft argillaceous mud.

DISCUSSION

The regional sea-level standard for the Silurian of east Siberia offered here matches fairly well with the global standard for Silurian eustasy proposed by Johnson (1996). If we consider these curves against the background of biozones (Figure 2, columns 3–6; Figure 3, columns 4, 5) rather than stages, substages, and global chronozones (Figure 3, column 3), then these events show significant variation in timing. One of the principal intervals with pentamerid brachiopods (Figure 3, level 2), for example, corresponds to the middle parts of the *Monograptus sedgwickii* and *Distomodus staurognathoides* Zones. It also should be noted that the *Pterospirifer celloni* and *P. amorphognathoides* Zones are interpreted to be earlier in Siberia than elsewhere. Some of the available Siberian graptolite and conodont data are in conflict. For example, *P. amorphognathoides*, which is normally considered to be upper Telychian, makes its first appearance in Siberia in the lower Telychian at the level of the *Monograptus turriculatus* Zone. Based on the conodont

data alone, many of the Llandovery highstands in Siberian sea-level (Figure 3, column 7) would normally be adjusted upward in position by one cycle. It is conceivable that the correlation between the east Siberian scheme and the global scheme is incorrect, and as a result many zonally important index species are recorded at lower levels than in the standard scheme of correlation (Figure 2, columns 3–6). This problem requires further study, but emphasizes once again that correlation of species' appearances should be defined with respect to global chronozones.

CONCLUSIONS

The East Siberian Basin is located on the Siberian Platform, the Taymyr fold belt, and the Severnaya Zemlya Archipelago. The Silurian depositional record includes deep-shelf siliciclastics in the northwest part of the basin, shallow-shelf carbonates in the central area, and shallow-shelf siliciclastics at the southeast margin. Silurian deposition featured onlap–offlap cycles that began with a major, earliest Silurian transgression. In the Late Silurian, virtually the entire basin featured restricted marine conditions. Fluctuations in sea-level are more clearly recognizable in the central carbonate area, where shallow-shelf facies were overlapped by deeper-water facies. The following regions were chosen for construction of a standard sea-level curve for east Siberia: Moyero (Llandovery–Wenlock), Turukhansk (Ludlow), and Norilsk and Middendorf (Pridoli). In the deeper part of the basin, highstand–lowstand fluctuations can be recognized only on the basis of increased carbonate content and more diverse faunas at lowstands. On the shelf, lowstands correspond to gaps in the sedimentary rock record.

In east Siberia, nine major highstands in sea-level are recognized. The first is early Rhuddanian. The second is early Aeronian, and the third is associated with a middle Aeronian acme in pentamerids. The fourth through sixth are early and late Telychian and Sheinwoodian, respectively. The seventh (Gorstian) features a number of changes in relative sea-level, and the eighth (Ludfordian) features only a modest rise in sea-level. The ninth is clearly recognizable only on the Taymyr Peninsula and is early Pridoli. All of these highstands match Johnson's (1996) standard Silurian eustatic curve. The somewhat younger or older ages of highstand in east Siberia, by comparison with the standard curve, are likely related to ambiguities in inter-regional correlation. The main divergence from the standard Silurian eustatic curve is the presence of an early Rhuddanian highstand, which correlates well with a coeval highstand in the

Baltic and Prague regions. This event, which inundated low topographic relief areas in east Siberia, seems to be related to the initial Silurian transgression. This earliest Silurian event may be part of a yet unrecognized global sea-level standard for the Silurian.

ACKNOWLEDGMENTS

Studies on Silurian eustasy were carried out during joint projects in the United States and Russia in 1993–1995. G.V. Lugovtsova prepared an original English language manuscript. The work was supported by the Russian Foundation for Fundamental Research (project 05-95-15564), as well as by the National Geographic Society (grant #5251-94). P.M. Sheehan and B.J. Witzke reviewed of an earlier draft of the manuscript.

REFERENCES

- BENEDICT, G.L., III, AND K.R. WALKER. 1978. Paleobathymetric analysis in Paleozoic sequences and its geodynamic significance. *American Journal of Science*, 278:579–60.
- BEUF, S., B. BIJU-DURAL, O. DECHARPAL, R. ROGON, O. GARIEL, AND A. BENNECEF. 1971. Les Gres du Paleozoique au Sahara—Sedimentation et Discontinuites, Evolution Structural d'un Craton. Publications de l'Institut Francais du Petrole, Collection "Science et Technique du Petrole," 18.
- BOUCOT, A.J. 1975. *Evolution and Extinction Rate Controls*. Elsevier, New York.
- COCKS, L.R.M. 1989. The Llandovery Series in the Llandovery area, p. 36–50. In C.H. Holland and M.G. Bassett (eds.), *A Global Standard for the Silurian System*. National Museum of Wales, Geology Series 9.
- EFREMOV, I.A. 1950. Taphonomy and geological record. In *Burial of Terrestrial Fauna in the Middle and Late Paleozoic*. Proceedings of the Paleontological Institute of the USSR Academy of Sciences, 24 (in Russian).
- GRAHN, Y., AND M.V. CAPUTO. 1992. Early Silurian glaciations in Brazil. *Palaeogeography, Palaeoclimatology, and Palaeoecology*, 99:9–15.
- HARLAND, W.B., A.V. COX, P.G. LEWELLYN, C.A.G. PICTON, A.G. SMITH, AND R. WALTER. 1985. *A Geologic Time Scale*. M. Mir (Russian translation).
- HOLLAND, C.H., AND M.G. BASSETT (EDS.). 1989. *A Global Standard for the Silurian System*. National Museum of Wales, Geology Series 9.
- JOHNSON, M.E. 1996. Stable cratonic sequences and a standard for Silurian eustasy, p. 203–211. In B.J. Witzke, G.A. Ludvigsen, and J.E. Day (eds.), *Paleozoic Sequence Stratigraphy: Views from the North American Craton*. Geological Society of America, Special Paper 306.
- , D. KALJO, AND RONG J.-Y. 1991. Silurian eustasy, p. 145–163. In M.G. Bassett, P.D. Lane, and D. Edwards (eds.), *The Murchison Symposium: Proceedings of an International Conference on the Silurian System*. Special Papers in Palaeontology, 44.
- , AND W.S. MCKERROW. 1991. Sea level and faunal changes during the latest Llandovery and earliest Ludlow (Silurian). *Historical Geology*, 5:153–169.
- , YU.I. TESAKOV, N.N. PREDTETCHENSKIY, AND B.G. BAARLI. 1997. Comparison of Lower Silurian shores and shelves in North America and Siberia. In G. Klapper, M.A. Murphy, and J.A. Talent (eds.), *Paleozoic Sequence Stratigraphy, Biostratigraphy, and Biogeography: Studies in Honor of J. Granville ("Jess") Johnson*. Geological Society of America Special Papers 321, 23–46.
- KOREN', T.N., A.C. LENZ, D.K. LOYDELL, M.J. MELCHIN, P. ŠTORCH, AND L. TELLER. 1995. Generalized graptolite zonal sequence defining Silurian time intervals for global paleogeographic studies. *Lethaia*, 28:137–138.
- KŘÍŽ, J. 1989. The Pridoli Series in the Prague Basin (Barrandian area, Bohemia), p. 90–100. In C.H. Holland and M.G. Bassett (eds.), *A Global Standard for the Silurian System*. National Museum of Wales, Geology Series 9.
- MCKERROW, W.S., R.ST.J. LAMBERT, AND V.E. CHAMBERLAIN. 1980. The Ordovician, Silurian, and Devonian time scales. *Earth and Planetary Science Letters*, 51:1–8.
- , AND L.R.M. COCKS. 1985. The Ordovician, Silurian, and Devonian Periods, p. 73–80. In N.J. Snelling (ed.), *The Chronology of the Geological Record*. Geological Society of London, Memoir 10.
- MCCLURE, H.A. 1978. Early Paleozoic glaciation in Arabia. *Palaeogeography, Palaeoclimatology, and Palaeoecology*, 25:315–326.
- SILURIAN TIMES. 1993. A newsletter of the Silurian Subcommittee. New left hand side for correlation diagrams, p. 6, 7.
- . 1995. A newsletter of the Silurian Subcommittee. Left hand column for correlation charts, p. 7, 8.
- SOKOLOV, B.S., AND YU.I. TESAKOV. 1984. Population, Biocoenotic, and Biostratigraphic Analysis of Tabulate Corals. The Podolian Model. NAIKA, Novosibirsk (in Russian).
- , AND ———. 1986. Tabulate Communities from Podolia. NAIKA, Novosibirsk (in Russian).
- SUKACHEV, V.N. 1945. Biogeocoenosis and phytocoenosis. *DAN SSSR*, 47:447–449 (in Russian).
- . 1949. The relationship between the notions of "geographic landscape" and "biocoenosis," p. 45–60. In *Problems of Geography*. State Publishers of Geographic Literature, Moscow.
- TESAKOV, YU.I. 1967. Ordovician–Silurian boundary on the Siberian Platform, p. 65–74. In *New Data on Lower Paleozoic Biostratigraphy of the Siberian Platform*. NAIKA, Novosibirsk (in Russian).
- . 1978. Tabulata. Population, Biocoenotic, and Biostratigraphic Analysis. NAIKA, Moscow (in Russian).
- . 1981. Ecosystem development in ancient platform sedimentary basins, p. 186–199. In *Problems of Geological Processes Evolution*. NAIKA, Siberian Division, Issue 517.
- . 1996. A new global chronostratigraphical scale for the Silurian, p. 94, 95. In *The James Hall Symposium*, University of Rochester.
- , N.N. PREDTETCHENSKIY, A.YA. BERGER, AND V.G. KHROMYCH. 1996. Silurian stratigraphy and paleogeography of East Siberia, p. 96, 97. In *The James Hall Symposium*, University of Rochester.
- , ———, ———, ———, E.O. KOVALEVSKAYA, AND N.N. SOBOLEV. 1995. Silurian stratigraphy of Gorny Taymyr, p. 123–141. In *Details of Taymyr-land*. VSEGEI, St. Petersburg (in Russian).
- , ———, V.G. KHROMYCH, AND A.YA. BERGER. 1996a. Re-

- gional chronostratigraphic scale for the Silurian of east Siberia, p. 96, 97. *In* The James Hall Symposium, University of Rochester.
- , ———, ———, AND ———. 1996b. Global chronostratigraphic scale and regional chronostratigraphic scale for the Silurian of east Siberia, p. 180–184. *In* Geodynamics and Evolution of the Earth. SB RAS, SPC UIGGV, Novosibirsk (in Russian).
- , ET AL. (23 authors). 1979. Silurian of the Siberian Platform. New Regional and Local Stratigraphic Subdivisions. NAUKA, Siberian Division, Novosibirsk, 410 (in Russian).
- , ET AL. (18 authors). 1980. Silurian of the Siberian Platform. Reference Sections in the Northwestern Siberian Platform. NAUKA, Siberian Division, Novosibirsk, 446 (in Russian).
- , ET AL. (26 authors). 1985. The Silurian Reference Section on the Moyero River, Siberian Platform. NAUKA, Novosibirsk, 629 (in Russian).
- , ET AL. (14 authors). 1986. Silurian Fauna and Flora from the Polar Regions of the Siberian Platform. NAUKA, Novosibirsk, 666 (in Russian).
- , ET AL. (22 authors). 1992. Silurian Sections and Fauna in the North of the Tunguska Syncline. NAUKA, Novosibirsk, 789 (in Russian).
- TUCKER, R.D., AND W.S. MCKERROW. 1995. Early Paleozoic chronology: a review in light of new U-Pb zircon dates from Newfoundland and Britain. *Canadian Journal of Earth Sciences*, 32:368–379.
- WILSON, J.L. 1975. Carbonate Facies in Geologic History. Springer-Verlag, Berlin.
- ZIEGLER, A.M. 1965. Silurian marine communities and their environmental significance. *Nature*, 207:270–272.
- , L.R.M. COCKS, AND R.K. BAMBACH. 1968. The composition and structure of Lower Silurian marine communities. *Lethaia*, 1:1–27.

SILURIAN CYCLES AND PROXIMALITY-TREND ANALYSIS OF TEMPESTITTE DEPOSITS

B. GUDVEIG BAARLI

Department of Geosciences, Williams College, Williamstown, Massachusetts 01267

ABSTRACT—Proximity-trend analysis records the occurrence of tempestite cycles on storm-dominated coasts. Most authors who use this method link their first-order proximity cycles to the third-order eustatic cycles of Vail et al. Data for the Llandovery Series illustrate a good fit between sea-level curves derived from proximity trends and the Silurian standard sea-level curve. Proximity-trend analysis is therefore deemed to be a valid method for detecting sea-level changes. Caution should be exercised, however, in situations of sediment by-pass and sediment trapping or starvation due to transgression or tectonic movement.

Areas for the Silurian System where this method has been or might be used were identified by literature search and paleoclimatic simulation. The literature search found 63 areas with tempestites that were described mostly in English-speaking countries. This result implies a bias in the literature, but the possibility of limited emphasis on storm deposits in different countries or lack of detailed studies is also possible. The paleoclimatic model predicted many additional sites for tempestite deposition. A closer investigation revealed that most of these were either areas of non-deposition or deeper facies. Kolyma, southeast Australia, south-central Europe, and probably Siberia and Kazakhstan, however, are the most likely places to find additional tempestite deposits. The South China Platform and areas on the west side of the Taconic orogen in Laurentia have tempestites, although none were predicted from the climatic simulation. Hurricane nucleation on the epicontinental platform or alternative paleogeographic reconstructions may explain this.

INTRODUCTION

Tempestites or storm deposits will vary with intensity of storm, direction of storm-generated currents, type of shelf, and distance from shoreline or intra-shelf sediment source (Johnson and Baldwin, 1996). Each separate tempestite bed displays a succession that reflects change in intensity of a single storm. On a larger scale,

tempestites tend to occur in a hierarchy of cycles that reflect climatic and eustatic changes.

One way to identify these cycles is to use proximity-trend analysis, as defined by Aigner (1985). He tested the model on the Triassic Muschelkalk of Germany and found it to be a sensitive indicator of paleobathymetry. This report will first review and evaluate studies where this approach was applied, in order to determine whether the method is valid for interpreting paleodepth and constructing sea-level curves. Secondly, it will concentrate on the use of proximity-trend analysis for Silurian sequences and relate the resulting cycles to the orders of sea-level cycles recognized by Vail et al. (1977). Finally, it will identify potential sites for future application of the analysis. Identification of potential sites is approached in the following way: The results of a literature study of Silurian storm deposits are plotted on a Silurian paleogeographic map. The distribution is then compared with existing Silurian climate models and the most storm-affected coasts revealed by those models.

HISTORY AND USE OF PROXIMALITY-TREND ANALYSIS

The term "proximity-trend analysis" was first formalized by Aigner and Reineck (1982) in a study on modern storm deposits in the Heligoland Bight. Aigner (1985) later elaborated the method by using modern examples from south Florida and the North Sea, as well as an example from the Middle Triassic of the South German Basin.

A literature search using Georef identified nine other studies, in addition to the four examples mentioned above, where the technique was adopted. Five studies were conducted on Silurian strata (Baarli, 1988; Easthouse and Driese, 1988; Baarli et al., 1992; Sami and Desrochers, 1992; and Bourker and Holland, 1996), and two were conducted on Cretaceous strata (Rowdan and

Brenner, 1985; Miskell-Gerhardt, 1987). Two other studies on the Cambrian (Myrow, 1992) and modern sediments (Bush, 1991) found conflicting proximality trends to the predicted onshore-offshore model of Aigner (1985).

As defined by Aigner (1985), proximality-trend analysis may be used to examine tempestite deposits either on sandy coastlines or on carbonate shelves with abundant shell material. The analysis assumes that storm deposits were laid down by offshore geostrophic currents that resulted from wind-driven surface currents that moved towards shore or across shoals. As the currents waned with increased depth, the characteristics of the deposits changed. These changes may easily be quantified. Grain size, thickness, and amalgamation of beds decrease, while bioturbation increases gradually offshore (Figure 1). The frequency of tempestite beds and amount of cross-lamination, however, show a maximum somewhere between normal wave base and normal storm-wave base in what is called the "transition zone" by Reineck and Singh (1975, p. 285, fig. 410). For a more complex view of storm-depositional processes, see Myrow and Southard (1996), who claimed that non-actualistic storm processes are sometimes needed to explain the distribution and unusual thicknesses of ancient tempestites. These authors did not, however, deny that geostrophic currents are important in tempestite deposition, but add that density-induced or excess-weight forces may be more important than previously imagined because the present low-angle continental slope may be a poor analog for many ancient shelves.

Proximality-trend analysis requires a centimeter-by-centimeter description of tempestites and their characteristics in cores or vertical sections. This record is then treated statistically for grain size, frequency, mean, and maximum number and thickness of tempestite beds per meter. Occurrence of amalgamated beds, cross-lamination, and bioturbation is also included. The statistical approach "evens out" the variability of storm parameters (e.g., a single major storm may show the same sedimentary effect in offshore areas as a weaker storm near shore). The analysis clearly distinguishes the transition zone, and thus divides the shelf into three zones.

There are many studies on storm deposits that approach the method of Aigner (1985), where a proximal-distal analysis is utilized. Examples include those by Chowns and McKinney (1980), Brenchley et al. (1986), and Brett et al. (1986). These authors typically published the percentage of sandstone per meter and conducted a careful analysis of many other criteria to determine proximality of storm beds. They did not, however, follow Aigner's (1985) method, and their studies are thus excluded from the list of proximality-trend analyses cited above.

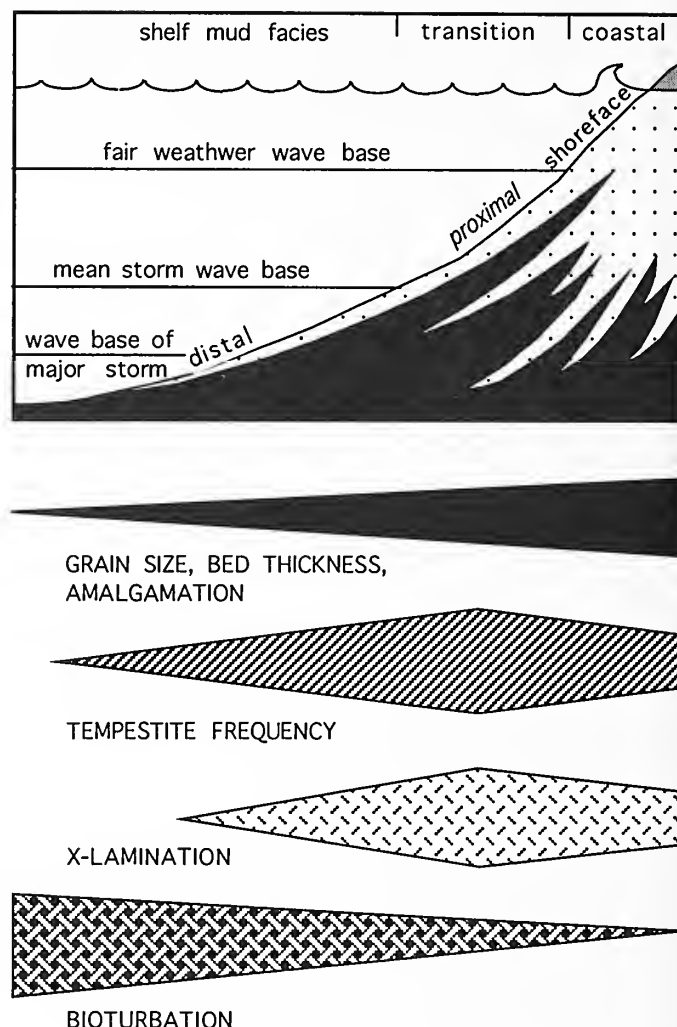


FIGURE 1—Proximality trends on a storm-dominated shelf. Modified from Aigner (1985, fig. 27a).

PROXIMALITY TRENDS AND SEA-LEVEL CURVES

Proximality trends are primarily dependent on depth and distance from shore, and thus record transgressive and regressive events. Proximality-trend analysis based on tempestite cycles of storm-dominated coasts, therefore, may provide corroboration of sea-level curves based on other criteria.

There are several ways to construct sea-level curves. Interpretation of sedimentary structures, preferably combined with paleontological information, has been the traditional basis. More specific methods include the use of benthic assemblages (Boucot, 1975), which are widely applied for determining depth changes during the Silurian (e.g., Johnson et al., 1991a). These Silurian benthic assem-

blages are found to occur in shoreline-parallel belts, and there is general agreement that they were controlled by depth-related factors (Brett et al., 1993). An overview by Brett et al. (1993) related benthic assemblages to absolute depth, and argued that although benthic assemblages may occupy somewhat different depth ranges in different depositional environments, the limits proposed by different lines of evidence are remarkably concordant and do not differ by an order of magnitude. Another paleontological technique employs depth-related ichnofossil assemblages, as outlined by Pemberton and Frey (1984). From a sedimentological point of view, sequence stratigraphy results in sea-level curves, but only proximity-trend analysis represents a quantified sedimentological method for depth analysis.

The majority of studies where proximity-trend analysis was used claim that the method works satisfactorily in constructing sea-level curves. Baarli (1988) and Easthouse and Driese (1988) tested and supplemented their proximity-trend studies with alternative methods for interpreting bathymetry. Baarli (1988) used level-bottom benthic communities (after Boucot, 1975), while the latter authors used ichnofossil analysis (see Pemberton and Frey, 1984). They found that the two methods complemented each other. The most convincing evidence, however, is derived from comparisons with standard eustatic curves. Both for the Silurian and Cretaceous, use of standard eustatic curves has a long-standing tradition (Johnson et al., 1991a; Hallam, 1992). Silurian curves are mainly based on depth-related benthic communities, but are supported by an array of other methods to determine water depth. When proximity-trend analysis yields curves that coincide with the standard sea-level curves, there are compelling reasons to believe that the analysis is valid. Data for the Llandovery Series (Figure 2) illustrate the close fit of sea-level curves derived from proximity-trend analysis with the Silurian standard sea-level curve (Johnson, 1996).

Available studies of proximity-trend analysis also point out that there may be complications and situations where the analysis is invalid as a method to construct sea-level curves. Sediment bypass is the explanation suggested by Bush (1991) and Myrow (1992) for conflicting results with proximity trends that result from the application of Aigner's (1985) model. The onshore-offshore pattern was one of muddy, fine-grained sediment near shore and coarser, thicker interbeds offshore, before the grain size and thickness decreased again further offshore. The current regime, however, was highest near shore, as indicated by abundant gutter casts in the fine-grained near-shore sediments (Myrow, 1992). There are a few additional examples of near-shore sediment bypass

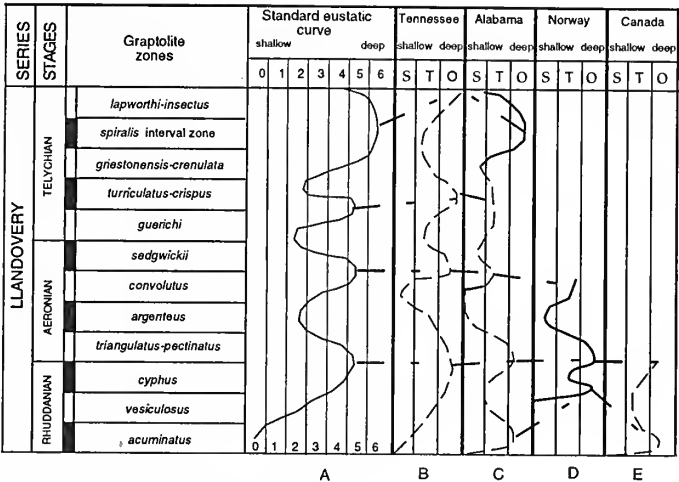


FIGURE 2—Comparison of standard Llandovery sea-level curve (A) from Johnson (1996) with sea-level curves created by proximity-trend analysis. Curve B from Green Gap, Tennessee (after Easthouse and Driese, 1988). Curve C from Birmingham, Alabama (after Baarli et al., 1992). Curve D from Sylling, Norway (after Baarli, 1988); curve E from Anticosti Island, Quebec (after Sami and Desrochers, 1992). Numbers 1–6 in curve A stand for Benthic Assemblages 1–6. Letters S, T, and O stand for shoreface, transition zone, and offshore, respectively. Dotted lines mean no fixed biostratigraphic points; unbroken line means good biostratigraphic control. Curves without biostratigraphic control are drawn according to stratigraphic thickness.

reported from modern shelves, but fewer ancient examples (Kidwell, 1989; Leckie et al., 1990). Clearly this is an important shelf situation, but not the norm.

Sediment trapping or starvation due to transgressions or tectonic movements may be more important to identify as a complication of proximity-trend analysis. The Red Mountain Formation at Birmingham, Alabama was the subject of a proximity-trend study by Baarli et al. (1992). They found inconsistencies in proximity trends in the middle parts of the Red Mountain Formation (interval E of Baarli et al., 1992). The thin, infrequent sandstones and oolitic ironstone interbeds in shale indicate inner offshore conditions. The inferred current energy, however, was high, and the presence of thin, condensed fossil lags and common shale clasts also indicate shallower conditions. An overview article by Chowns (1996) interpreted the sequence stratigraphy of the Red Mountain Formation. He identified interval E as occurring immediately above a major flooding surface indicated by the thick, condensed ironstone beneath interval E. Interval E was, thus, at the start of a transgressive system tract. Sediments from the source area were cut off by flooding of the source, while the depositional site was still within the shoreface. Flooding surfaces may, therefore, create situations where the normal proximity trends break down. Another example of trapping of coarse-grained sediment was documented in an article on

the Llandovery of the Oslo region in Norway (Baarli, 1988). Again, the thickness and frequency trends were in conflict with trends in grain size and the current regime. Baarli (1990) explained this transition by movements of a peripheral bulge across the region. The bulge cut off the former siliciclastic sediment source, and subsequent sedimentation in the area consisted of carbonate deposition derived from the top of the bulge.

In the same article, Baarli (1988) cited one example from a composite section where a small tectonic high or horst locally affected the area. The few and very thin, coarser-grained interbeds give an impression of deeper offshore conditions on the top of the horst, but this is contradicted by the coarse shell-lags, high current regime, and the fossil communities. Again, the proximality trends do not follow the scheme of Aigner (1985). Thus tectonically active coasts may not be ideal for this kind of analysis.

EUSTATIC VERSUS PROXIMALITY-TREND CYCLES

For Paleozoic times, relative changes in sea-level may be observed globally, as discussed by Vail et al. (1977). When these authors plotted Paleozoic sea-level curves, they observed three orders of eustatic cycles. Cycles of first-, second-, and third-order are considered to have durations of 200–300 Ma, 10–80 Ma, and 1–10 Ma years, respectively. Other workers have expanded on the work of Vail et al. (1977) and identified smaller, fourth- and fifth-order cycles. Ryer (1983) identified fourth-order cycles from the Cretaceous as being on the order of a few hundred thousand years in duration. Read and Goldhammer (1988) linked their smaller fifth-order eustatic cycles to Milankovitch climatic cycles with a duration of 20–100 Ka.

Tempestite deposition may also occur in cycles, and all the studies that use proximality-trend analysis have linked their major cycles to eustatic cycles. Most workers that conduct proximality-trend analyses distinguish two to three temporal orders of tempestite cycles. Because of their scope of study, typically one or two formations, first-order tempestite cycles are linked to the third-order cycle of Vail et al. (1977). Aigner (1985), in his investigation of the Triassic upper Muschelkalk, and Sami and Desrochers (1992), in their work on the Lower Silurian of Anticosti Island, both estimated a duration of 5 Ma for this cycle. Cotter (1988) worked on tempestite cycles through most of the Silurian Clinton Group in Pennsylvania. His first-order cycles were estimated to last an average of 2.5 Ma. All the Silurian workers that apply proximality analysis have compared their cycles to the

Silurian standard eustatic curve recently expanded by Johnson (1996), who estimated an average 2.5 Ma duration for Silurian cycles. Johnson (1996) also linked his eustatic cycles to the third-order cycle of Vail et al. (1977). It is worth noting that the deviation in age durations between is due to the adoption of different absolute-age scales. Johnson (1996) and Cotter (1988) used the time scale of McKerrow et al. (1985) that indicates a 3-Ma duration for the Rhuddanian Stage. Sami and Desrochers (1992) arrived at a 5 Ma duration for the Rhuddanian by using the less detailed time scale of Palmer (1983).

The first-order cycles described by Sami and Desrochers (1992) consist of an initial deepening succeeded by a middle Aeronian shallowing and deepening. This middle Aeronian deepening cycle is not noted in the standard Silurian sea-level curve of Johnson (1996). Using proximality-trend analysis, however, this additional Rhuddanian cycle is also found in Norway (Baarli, 1988) and Alabama (Baarli et al., 1992). In an overview of the Silurian bathymetry of North America, Johnson (1987) showed this cycle in sequences from central Manitoba, Anticosti Island, northern Michigan, Manitoulin Island, and New York. The same minor cycle was subsequently reported from Illinois (Ross and Ross, 1996), and from the Great Basin in Utah (Harris and Sheehan, 1996). It is also found in Estonia (Johnson, 1996). This middle Rhuddanian cycle must be an additional minor eustatic cycle not well developed everywhere, and therefore omitted from the standard curve. The fact that three out of the four studies (from Norway, Alabama, and Anticosti, Canada) that applied proximality-trend analysis recognized this minor cycle suggests proximality-trend analysis to be a sensitive tool for sea-level analysis.

Higher-order cycles are shown, but not defined by most studies on tempestite-dominated sections. Sami and Desrochers (1992) and Cotter (1988) distinguished two and one additional order of cycles, respectively. Both of these reports compared their highest order cycles, with an estimated duration of 80–100 Ka, to Milankovitch sea-level cycles. The second-order sea-level fluctuations of Sami and Desrochers (1992) averaged 1 Ma. Higher-order cycles may also have had a eustatic origin, but at such a high degree of temporal resolution, slight adjustments in local depositional conditions may have easily interfered with and overprinted possible eustatic signals.

In summary, the major cycles derived from Silurian proximality analysis coincide well with the standard eustatic curves, which are linked to eustatic third-order cycles of Vail et al. (1977). The resolution obtained by proximality analysis, however, may be considerably higher and surpass those obtained by lithofacies and paleontological methods. With an increased understanding of the processes that control storm deposition, the analy-

sis may prove to be a powerful tool for investigation of storm-dominated basins in the future.

OCCURRENCE OF SILURIAN TEMPESTITES

Used with caution, proximity analysis may produce valuable information on the bathymetry of storm-dominated coasts. Therefore, it may be important to identify areas with abundant tempestite deposition, and where the method can be used. It is logical first to identify areas where tempestites are known through a literature survey. The result of the literature survey is then compared with existing paleoclimatic models for the Silurian to find additional areas for study.

SILURIAN PALEOGEOGRAPHIC RECONSTRUCTIONS.—The accuracy of Silurian paleogeography is still very much in debate. The most recent and thorough reconstruction is by Torsvik et al. (1996), but it concentrates on Laurentia, Baltica, and neighboring continents. Many regional and a few global reconstructions conflict with this work. One of the main alternative reconstructions is by Daziel et al. (1994). The present study, however, chose to use an existing climate model. Paleogeographic maps of the Silurian world with accompanying paleoclimatic simulations by Wilde et al. (1991) are reasonably close to the reconstructions of Torsvik et al. (1996). Figures 3 and 4 are slightly modified to include some of the latest revisions of the continental configuration and data from the climate modeling of Moore et al. (1994) for the Wenlock Series.

STORM DEPOSITS IN THE LITERATURE.—A search for tempestite deposits was done with Georef. Only those studies were included in which the words “tempestite” or “storm deposits” actually appear. The results of the literature search are summarized in Table 1, with references to 63 different tempestite occurrences. Plotted on Figures 3 and 4, these sites show a distinct clustering. The majority of locations occur in the English-speaking world, as found in references to Laurentia (mainly west of the Taconic orogen), Avalonia, and Baltica.

There is a clear decrease in storm deposits reported through the Silurian System. The results show 33 tempestite deposits from the Llandovery, thirteen from the Wenlock, twelve from the Ludlow, and five from the Pridoli.

The majority of tempestites (54%) are from siliciclastic units; 41% are from carbonate-dominated units; 5% are from units with mixed carbonate and siliciclastic strata. There is little difference in tempestite

occurrence in carbonate-dominated and siliciclastic-dominated lithologies through time. Regionally, however, there are strong differences. Avalonia has fourteen siliciclastic tempestite units out of a total of fifteen units. Laurentia shows seventeen siliciclastic units out of a total of 32. In Laurentia, siliciclastic tempestites occur mainly along the Appalachian Mountains. In Baltica, siliciclastic tempestites are found in the Oslo region.

DISCUSSION OF RESULTS FROM LITERATURE SURVEY.—Absence of predicted storm beds may be due to absence or inaccessibility of study, lack of outcrops, presence of deep-water facies, fair-weather deposition, or very sheltered paleoshores. Paleogeographic and paleoclimatic models may explain most of the physical parameters, and will be considered later. Absence of studies or inaccessibility of study areas, however, is a major concern. There are three potential problems: inaccessibility of the literature, non-recognition of or little emphasis on storm-deposits, and no appropriate or detailed studies in a region. The search tool, Georef, concentrates on journals published in the English language, although other major journals, especially from Europe, are also represented. This is the major reason why plots of tempestites are mainly found clustered in English-speaking countries. In the sedimentological literature from English-speaking countries, however, tempestites traditionally have been emphasized or recognized, only during the last twenty to thirty years. Other countries may still lag behind. This is true for the extensive east European literature. In the Prague Basin, substantial carbonate deposits are found in the Upper Silurian. According to Havlicek and Štorch (1990), biotrital limestones formed under rough-water conditions from Wenlock time onwards. These limestones certainly include tempestites, but there is a difference in the use of language, and storm or tempestite deposits are not mentioned.

Differences in emphasis of studies, as well as differences in use of words to describe tempestites, contribute to the negative results. Australia, Antarctica, and some Arctic regions are still frontier lands where the focus remains on primary mapping. Detailed studies on tempestites from these regions are exceptions. Tasmania and southeastern Australia (central Victoria and central New South Wales) have ample Silurian outcrops in the Tasman fold-belt and the Melbourne Trough. Traditionally, most sedimentary rocks in the Melbourne Trough, including the distal turbidites, have been interpreted as deep-water “flysch”. Garrat (1983) regards this view as erroneous, and contends that the flyschoid sediments do not necessarily include a significant component of deep-water sediments. Dyson (1996) reinterpreted both the Devonian and Ordovician distal turbidites in Victoria,

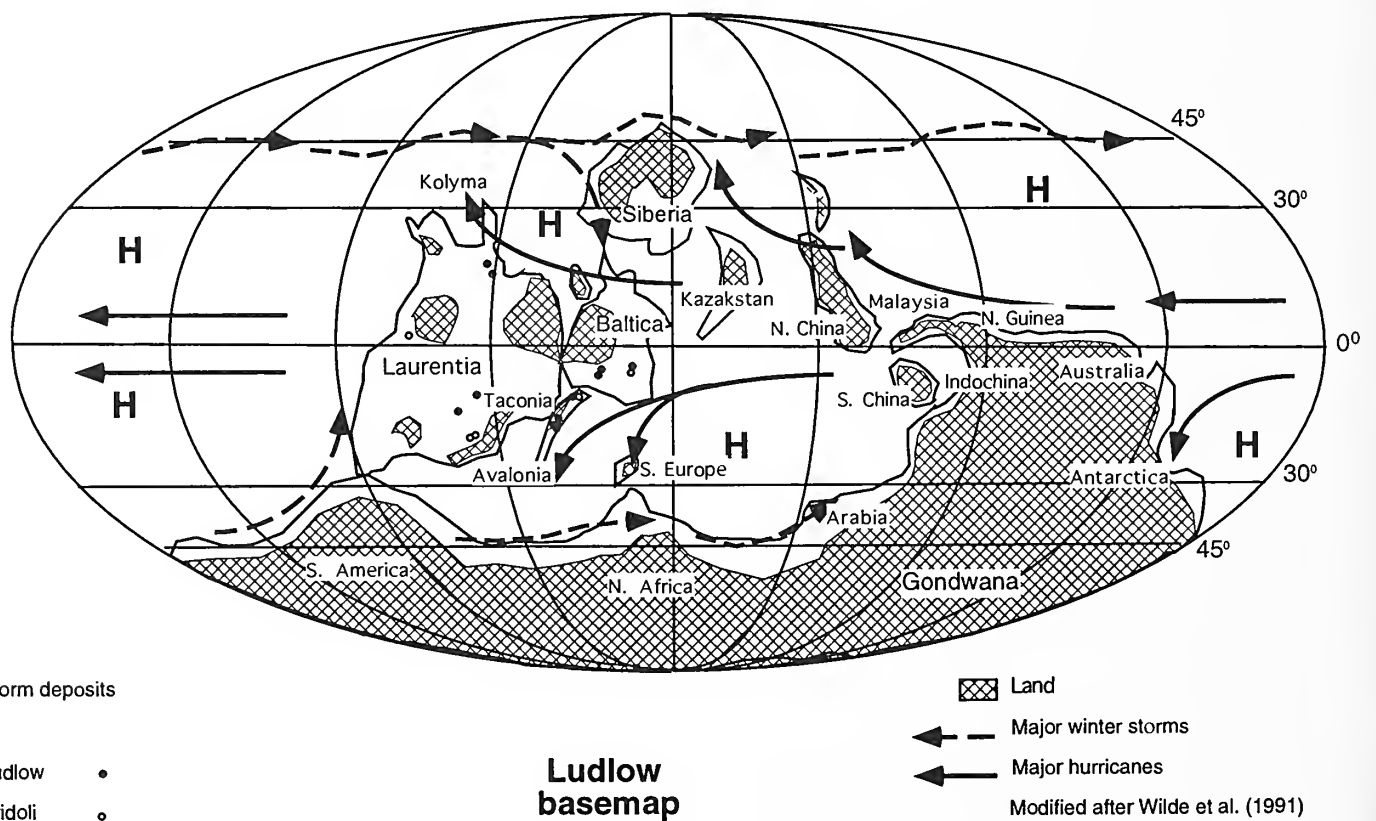
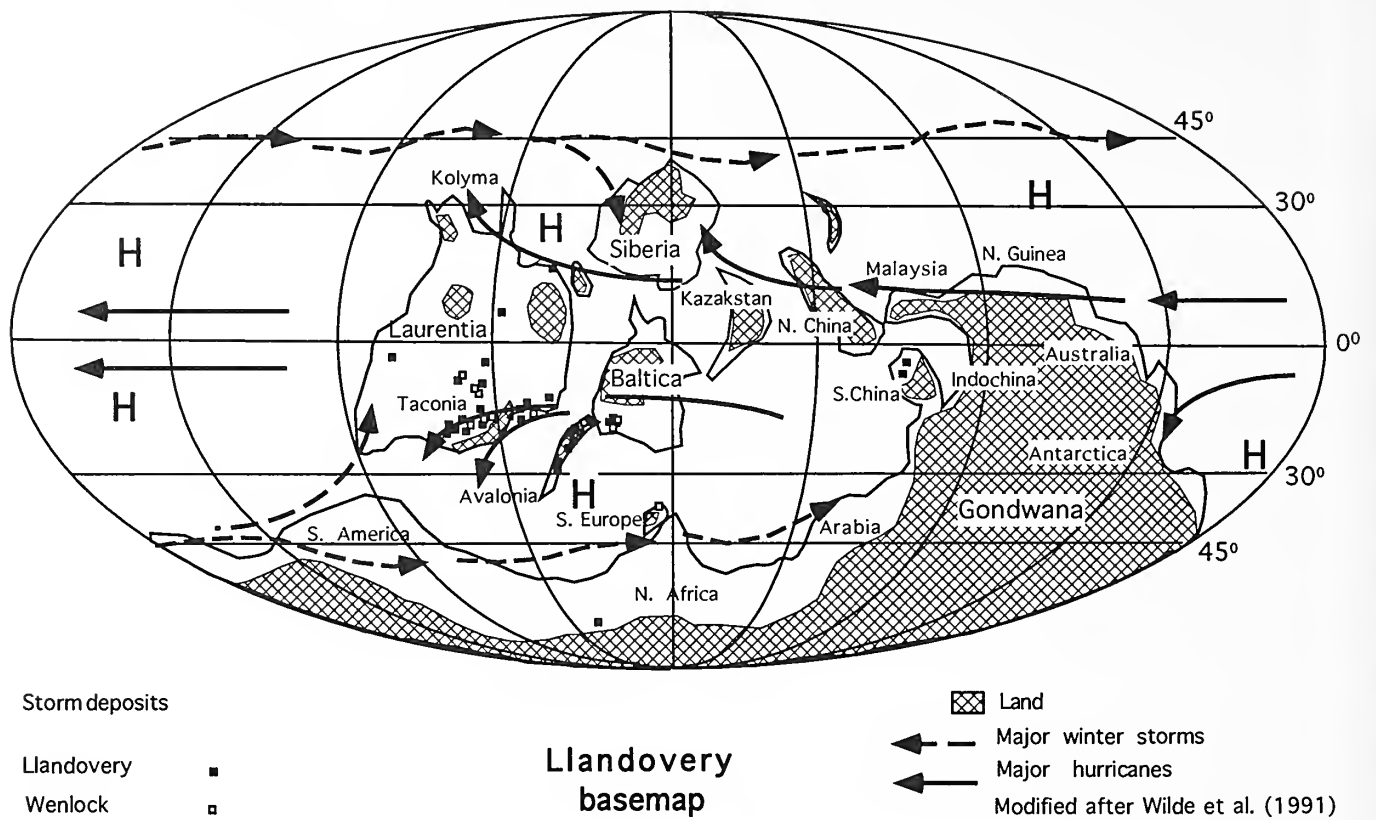


FIGURE 3—(top) Llandovery paleogeographic reconstruction that shows areas of predominantly high-pressure (H) and tracks of winter storms and hurricanes. Figure modified from Wilde et al. (1991). Storm deposits found in the literature from the Llandovery and Wenlock are marked with closed and open boxes, respectively.

FIGURE 4—(bottom) Ludlow paleogeographic reconstruction with areas of predominant high-pressure (H) and the tracks of winter storms and hurricanes. Figure modified from Wilde et al. (1991). Storm deposits found in the literature from Wenlock and Pridoli shown by closed and open circles, respectively.

Australia, as shallow storm tempestites. It is likely that some of the Silurian "flysch" of Australia also may be re-interpreted as tempestites.

For the most part, the marked decrease in tempestites through time may be explained by the duration of each series. The Digital Time Scale (Gradstein and Ogg, 1996) assigned a duration of 15 Ma for the Llandovery, 5 Ma for the Wenlock, 4 Ma for the Ludlow, and 2 Ma for the Pridoli Series. The nature of the hypsographic curve further explains some variations. This curve shows a general maximum sea-level stand in late Llandovery through early Wenlock time. There was a general draw-down in sea-level through the rest of the Silurian, until a minimum was reached at the close of the period (Johnson, 1991b; Moore et al., 1994). Thus in the later Silurian, many continents were emergent, as was the case of Gondwana, or with inland seas that displayed shallow lagoonal or evaporitic facies punctuated by smaller transgressions, as in Laurentia, Siberia, China, and Baltica. The most significant transgression occurred at the beginning of the Ludlow, when there was a pronounced deepening (Johnson et al., 1991b). This deepening may explain the similar number of tempestite localities in the Ludlow and Wenlock Series, in spite of a slightly shorter duration for the former.

Tectonic activity also may have influenced the occurrence of tempestites. A large scale collision during the Silurian led to the Caledonian orogeny, which caused uplift and resulted in a cessation of marine deposition, first in Norway at the end of the Wenlock Epoch and successively later further east in Baltica. The strong epeirogenic movement of African Gondwana was the cause of widespread emergence after Llandovery time (Wilde et al., 1991).

Table 1 shows that storm deposits are recognized in both carbonate and siliciclastic settings, with just a slight predominance of the latter. This result is somewhat surprising. Hummocky cross-stratification, as first described by Harms et al. (1975), is the most distinctive single sedimentary structure attributed to storm sedimentation. The structure tends to be best preserved in siliciclastic sediments. The paleogeographic setting seems to be most important. Tectonically active areas, such as the western part of Baltica, Avalonia, and Laurentia immediately west of the Taconic orogen, display siliciclastic tempestites. Stable platform regions have tempestites in carbonate settings.

STORMS AND CLIMATE MODELS.—Severe storms are the primary agents that cause tempestite deposition (Marsaglia and de Vries Klein, 1983; Barron, 1989). Major winter storms today are typically strongest in higher latitudes above 45°, while hurricanes have their maximum

between 20° and 30°. From 30–45°, there is a zone of mixing where both type of storms may occur. Tropical storms are also typically stronger on the east coast of continents than on the west coast. As Barron (1989) pointed out, however, a direct projection of today's climate may not be appropriate. The nature of atmospheric circulation, overall global temperature, and the arrangements of continents in the past may have led to a distinctly different distribution of storms.

EARLIER CLIMATE MODELS.—A number of studies have tried to link storm type to the sedimentary record based on latitude and paleogeography. This linkage has not, however, been accomplished so far. Marsaglia and de Vries Klein (1983) used a relatively simple model that extrapolated present-day distributions of storm systems to paleostorm models on the basis of latitude and paleogeography. They recorded 69 tempestite deposits through the geological record, with seven from the Silurian. Duke (1985) made a similar study using a slightly larger database (107 tempestites), although he noted only six Silurian examples. Marsaglia and de Vries Klein (1983) and Duke (1985) were criticized by Barron (1989) for using simplistic methods. Paleoclimate is controlled by paleogeography, paleotopography, Milankovitch-type climate fluctuations, sea-level fluctuations, and variations in the paleoatmosphere (Moore et al., 1994). Consequently, more recent climate studies have been based on increasingly intricate climate-model simulations for past geographies, where all these criteria are taken into account. There are several climate models specifically designed for the Silurian Period. An early attempt to model climate for the Silurian was made by Ziegler et al. (1977). A thorough, computerized study of the oceanic and atmospheric circulation system for the Silurian was executed by Wilde et al. (1991). They provided separate maps for Llandovery, Wenlock, and Ludlow times. Refined paleogeographic maps were used by Moore et al. (1994) for paleoclimatic modeling of the Wenlock Series.

STORM DEPOSITS PREDICTED FROM CLIMATE MODELS.—Figure 3 shows major storm tracks on a paleogeographic map for the Llandovery, modified from Wilde et al. (1991). The major hurricane track would affect southern Baltica, Avalonia, the present east side of Laurentia, and possibly the present east coast of Australia and parts of Antarctica in the southern hemisphere. In the northern hemisphere, hurricanes would impact New Guinea, parts of the North China Platform and Kazakstan, northern Laurentia (including Greenland and Kolyma), and most of northern Siberia. The northern hemisphere, with a distinct lack of land above 45°, could be expected to maintain a strong zonal circulation in all seasons. Siberia,

TABLE 1—Sources of data on Silurian cycles and proximity trends of tempestites.

Silurian continent and references	Unit	Lithology	Region	Age
AVALONIA				
Cant 1980, Bambach 1993	Arisaig Group	Silicicl.	Arisaig, Nova Scotia	L1.
"	"	Silicicl.	"	We. Lu.
"	"	Silicicl.	"	Pr.
"	"	Silicicl.	"	"
Hurst and Pickerill 1986	Ross Brook Fm.	Silicicl.	Arisaig Nova Scotia	L1.
Pickerill and Hurst 1983	Beechill Cove Fm.	Silicicl.	Arisaig, Nova Scotia	L1.
Benton and Gray 1981,	Hughley Shale	Silicicl.	Welsh Borders	L1.
Gray and Benton 1982				
Cocks et al. 1984	Bronydd Fm.	Silicicl.	South Wales	L1.
"	Crychan Fm.	Silicicl.	"	L1.
"	Trefawr Fm.	Silicicl.	"	L1.
Goldring and Bridges 1973	Wych Fm.	Silicicl.	England	L1.
Goldring and Aigner 1982	Black Cock Bed	Silicicl.	South Wales	Lu.
Richardson and Rasul 1990;	Whitcliffe Fm.	Carbon.	Welsh Borderland	Lu.
Watkins 1978				
Watkins 1978; Cherns 1988	Leintwardine Fm.	Silicicl.	Welsh Borderland	Lu.
Tyler and Woodcock 1987	Baily Hill Fm.	Silicicl.	Welsh Borderland	Lu.
LAURENTIA				
Hurst 1980	Alequatsiaq Fjord Fm.	Carbon.	Washington Land, Greenland	L1.
Graf and Dixon 1986	Duoro Fm.	Carbon.	Devon Island, N.W.T.	Lu.
Jones and Dixon 1976	Read Bay Fm.	Carbon.	Somerset Island, N.W.T.	Lu.
Larsson and Stearn 1986	Severn River Fm.	Carbon.	Hudson Bay	L1.
Sami and Desrochers 1992	Becscie Fm.	Carbon.	Anticosti Island, Que.	L1.
"	Merrimack Fm.	Carbon.	"	L1.
Pratt and Miall 1993	Amabel Fm.	Carbon.	southern Ontario	We.
Anastas and Coniglio 1993	Manitoulin Fm.	Carbon.	southern Ontario	L1.
Brett 1983	Rochester Shale	Silicicl.	New York, Ontario	We.
O'Brien et al. 1994	Lewiston Mb., Rochester Shale	Silicicl.	New York	We.
Duke 1982; Duke et al. 1991	Medina S.s.	Silicicl.	New York, Ontario	L1.
Kleussendorf and Miculic 1994;	Brandon Bridge Fm.	Carbon	Walworth Co., Wisconsin	L1.
Watkins et al. 1994				
Kuglitsch 1994	Byron Dol.	Carbon.	Waukesha Co., Wiscon.	L1.
"	Hendricks Fm.	Carbon.	"	L1.
Harris and Sheehan 1996	Laketown Dol.	Carbon.	Great Basin, USA	L1.
Kahle and Stevenson 1988	Greenfield Dol.	Carbon.	southern Ohio	Lu./Pr.
Cotter 1983	Tuscarora Fm.	Silicicl.	Pennsylvania	L1.
Cotter 1979, 1988; Cotter and Link	Rose Hill Fm.,	Silicicl.	Pennsylvania	We.
1993	Mifflington Fm.	Carbon.	"	We.
Goldring and Bridges 1973; Cotter	Keefer Mb.	Silicicl.	Pennsylvania	We.
1990				
Meyer et al. 1992	Keefer Sandstone	Silicicl.	West Virginia, Maryland	We.
Dorobek and Read 1986	Keyser Fm.	Carbon.	Maryland, Virginia	Pr.
"	Clifton Forge Ss.	Silicicl.	Virginia	Pr.
Dehler 1994	No name	Mix	Idaho	Pr.
Driese 1986	Rockwood Fm.	Silicicl.	Tennessee	L1.
Driese et al. 1991;	Clinch Sandstone	Silicicl.	Tennessee	L1.
Driese 1988	Brassfield Fm.	Carbon.	"	L1.
Phelps 1990	Louisville Fm.	Carbon.	Kentucky	Lu.
Baarli et al. 1992	Red Mountain Fm.	Silicicl.	Birmingham, Alabama	L1.
Ziegler 1989; Bourker and Holland	Red Mountain Fm.	Silicicl.	Georgia	L1.
1996				

TABLE 1 (continued)

Silurian continent and references	Unit	Lithology	Region	Age
Nealon and Williams 1988	Lough Muck Fm.	Silicicl.	Galway, Ireland	We.
Comrie and Caldwell 1993	Ripogenus Fm.	Mix	Maine	L1.
BALTICA				
Baarli 1988	Solvik Fm.	Silicicl.	Asker, Oslo	L1.
"	Solvik-Sælabonn Fm.	Silicicl.	Sylling, Norway	L1.
Braithwaite et al. 1995	Sælabonn Fm.	Silicicl.	Hadeland, Norway	L1.
Whittaker 1973; Thomsen 1982	Sælabonn Fm.	Silicicl.	Ringerike, Norway	L1.
Möller 1987; Johnson 1989	Rytteråker Fm.	Carbon.	Oslo Region, Norway	L1.
Worsley et al. 1983	Bruflat Fm.	Silicicl.	Ringerike, Hadeland,	We.
"	Malmøya Fm.	Carbon.	Holmestrand	We.
Kershaw 1993	Hemse Group	Carbon.	Gotland	Lu.
Long, 1993	Burgsvik Beds	Mix	Gotland, Sweden	Lu.
Nestor 1990	Kuresaa Fm.	Carbon.	Estonia	Lu.
"	Kaugatuma Fm.	Carbon.		Pr.
GONDWANA				
de Castro et al. 1991	Tanezzuft Fm.	Silicicl.	Murzuq Basin, Libya	L1.
"	Acacus Fm.	Silicicl.	"	Wen.
SOUTH-CENTRAL EUROPE				
Havlíček and Štorch 1990	Motol Fm.	Carbon.	Sedlec, Bohemia	We.
YANGTZE PLATFORM				
Zhang et al. 1993	Ninggiang Fm.	Carbon.	NW Sichuan	L1.
"	Shihniulan Fm.	Carbon.	SE Sichuan	L1.

Alaska, and Kolyma were within reach of winter storms. Storms in the higher latitudes in the southern hemisphere were weaker, and most dominant during the summer. They made landfall on the western margin of Gondwana at about 45° in present-day Arabia and the northern parts of India, southwest Laurentia, and possibly south-central Europe, which still remained close to Gondwana.

The Iapetus and the Rheic Oceans were closing during the Wenlock, thus changing the zonal flow in the later Silurian (Figure 4). Wilde et al. (1991) showed a model where the storm track on the west side of the Taconic orogen ceased to exist. Baltica moved north, nearer to the equator and was less affected by tropical storms. South-central Europe moved gradually further north towards the equator. By Late Silurian time, south-central Europe seems to have been adjacent to the southern parts of Baltica (Tait et al., 1994), and thus well in the hurricane belt. Parts of Australia moved further into the zone between 5° and the equator, which is a zone with low cyclonic activity due to a lack of necessary vorticity (Barron, 1989).

COMPARISON OF LITERATURE SURVEY RESULTS WITH PALEOCLIMATE MODEL.—For Llandovery time, the storm records identified in the literature occurred in areas pre-

dicted by modeling, with one exception. The exception is the occurrence of tempestites in the Yangtze Basin of South China. The climate model, however, indicates many areas where storm deposits might be expected, although none were found. These include Siberia, Kazakhstan, Australia, and North China in the northern hemisphere, and with one exception in each region, the west coast of Gondwana and south-central Europe in the southern hemisphere.

There are comparably few records of tempestites for the later Silurian. The only places where storms are known on predicted storm-battered coasts are in Avalonia and the northern parts of Laurentia. Baltica was predicted to move into the quiet equatorial zone, but tempestites continued to be deposited there. The most notable deviation between the climate model and available literature for the later Silurian is the many occurrences of tempestites that occur west of the Taconic orogen.

DISCUSSION OF THE PALEOCLIMATE MODEL.—Lack of recorded tempestites, apart from human shortcomings, are attributed to areas with fair-weather conditions, presence of deep-water facies, and lack of outcrops. The areas of

predicted fair-weather conditions are strongly dependent on correct paleogeographic maps. Here we start with the assumptions that the simulated climate model and the paleogeographic reconstruction it depends on are correct. Can we explain the lack of tempestites on storm-ridden coasts by presence of deep-water facies or lack of outcrops?

The Silurian is an interval with widespread graptolitic black shales and organic-rich source rocks mainly deposited in deeper waters, especially in the Llandovery Series. According to climate modeling for the Wenlock Series by Moore et al. (1993), the coast of Gondwana, including south-central Europe, coincided with the zone of the westerlies and experienced strong up-welling. Large areas of this shelf were flooded, and Silurian black shale is very common. Other basins with graptolitic black shale include parts of northern and eastern Baltica, the northern margin of Laurentia (including Kolyma and the island arcs off the western coast), and parts of the South China Platform and eastern Australia. Very few tempestites were found here, as expected. The occurrences in South China and in south central Europe are late Llandovery and late Wenlock, respectively, when shallow carbonate deposition resumed. The Gondwana occurrence was in the small, isolated Murzuq Basin of Libya. The black shale basins were generally not exceedingly deep, and the coasts of Gondwana and Baltica are predicted by the climate model to be in the track of major storms. Brett et al. (1993) reported that the water depth probably did not exceed 50–100 m either in the Eurafrian or South China Platform basins. In order to maintain a thermocline in such shallow basins, storm activity must have been low to moderate.

The later Silurian was marked by local uplift in African Gondwana, western Baltica, and the South China Platform. The North China Platform was an area of little or no deposition throughout the Silurian. Through the later Silurian, there was a general drop in sea-level that transformed many epicontinental shelves into areas of vast evaporite or tidal-sediment deposition, as mentioned above. The recorded lack of tempestites is thus explained by deeper water deposits and lack of outcrops, with the exceptions of Siberia, Kazakstan, Kolyma, east-central Europe, and eastern Australia.

Part of the explanation for the lack of tempestites in eastern Australia, south-central Europe, Siberia, and Kazakstan surely lies in the inaccessibility or non-emphasis of tempestites in the literature. However, there may be other explanations at least for Siberia and Kazakstan.

The Silurian paleogeographic position of Siberia and Kazakstan is still very much in question. Traditionally (e.g., McKerrow et al., 1991), Siberia is depicted in an inverted position (Figure 2), with large parts north of 30°. Episodic reef and carbonate deposition did occur there

throughout the Silurian in the Altai region (Yolkin, 1996). With Siberia in an inverted position, these reefs would be far north of any other known Silurian reefs. Rotating Siberia nearly back to its present-day position would bring the Altai region within 30°. This would also create the same problem on the main Siberian platform, which also has thick carbonate sequences throughout the Silurian. There is no room to move Siberia equatorward, so perhaps it was in another position altogether. On the basis of reef growth during the Silurian, Copper and Brunton (1991) concluded that not only was Siberia in the wrong position, but Kazakstan was placed on the wrong side of equator. In addition the northeast China, Malaysian, and Australian plates ought to be further away from the tropical belt. Some of these conclusions are controversial (Sengor et al., 1993; Dalziel, 1994; Baarli, 1995 for Kazakstan; Wang and Chen, 1991, for Asia and Australia). This situation illustrates the continuing state of uncertainty in paleogeographic reconstructions.

The literature review revealed two tempestite locations that are unanticipated by the model. The interior of Laurentia, and especially the west side of the Taconic orogen have tempestites in the Llandovery, as predicted by the model, and also through the Wenlock and even higher in the Silurian. The South China Platform also records tempestites in the latest Llandovery, in spite of its position in the lee of Gondwana.

The Taconic orogen would have to have been nearly parallel to the equator in Silurian time, but sufficiently south of it to be in the hurricane belt. In treating the Lower Silurian of East Tennessee, Driese et al. (1991) favored a zone of hurricane formation in the Iapetus Ocean that tracked southwestward along the basin axis and in the lee of the Taconic orogen, as predicted by Wilde et al. (1991). Driese et al. (1991) also mentioned the possibility of rare, mid-latitude winter storms that tracked northwestward. As Marsaglio and de Vries Klein (1983), they did not exclude formation of hurricanes on an interior, shallow, continental platform. The two last possibilities would still be valid for the later Silurian, when the Iapetus Ocean narrowed. The paleogeographic model of Dalziel et al (1994) is very different from the one used by Wilde et al. (1991). They imply a collision of Laurentia and South America during Ordovician time to create the Taconic orogen. In this model, mid-latitude storms that tracked north would probably be of little importance, because there was no ocean between Gondwana and Laurentia. The closure of the Iapetus Ocean, however, is inferred to have happened further north in Laurentia, and left open ocean to the east of the Taconic orogen, where hurricanes also may also have formed in later Silurian time.

The paleogeography of southeast Asia is very much in question. In the model of Wilde et al. (1991) there is a

possibility that intense mid-latitude storms traveled up the west coast of Gondwana and reached China. China is so close to the equator, however, that this is not very plausible. The Indochina and Malaysian platforms are positioned north of the South China Platform in the reconstruction of Wilde et al. (1991), and partly sheltered it from storms. The former two platforms are, however, positioned south of the South China Platform in a reconstruction by Wang and Chen (1991), while the South China Platform is placed north of the equator. In this position, parts of the South China platform would lie in the hurricane track.

In summary, places not recorded in this study but likely to yield Silurian tempestites are southeast Australia, south-central Europe, Kolyma, and probably Siberia and Kazakstan. This assumes these regions are placed in their correct paleogeographic position.

CONCLUSIONS

Data for the Llandovery Series illustrate a good fit of sea-level curves derived from proximity-trend analysis and the Silurian standard sea-level curve (Johnson, 1996). Proximity-trend analysis is thus a valid method for detecting sea-level cycles, if applied with caution. Caution should also be used in attempting such analyses in tectonically active areas, in situations of sediment by-pass on shallow shelves, and in situations with sediment starvation after major flooding episodes. It should preferably be combined with other bathymetric methods of interpretation. A first-order proximity curve may commonly be compared to the third-order eustatic cycles of Vail et al. (1977), while the highest order proximity curve compares to the fifth-order eustatic curve of Vail et al. (1977) or to Milankovitch sea-level cycles.

Review of the literature implies a strong decrease in the occurrence of tempestites through the Silurian. This may be explained by the decreasing durations of the individual series, and by a lower global sea-level towards the end of the Silurian. All the sites found in the literature search, with only two exceptions, occurred in places where storm deposits were predicted by the paleoclimatic model. The exceptions were Llandovery tempestites on the South China Platform and Wenlock to Upper Silurian tempestite deposits on the west side of the Taconic orogen. A different paleogeographic position may explain the former, while formation of hurricanes on the epicontinental platform or exceptionally strong mid-latitude storms may explain the latter.

The use of paleoclimatic models points out many additional coasts not identified in the literature study where tempestites may be expected to be common. Many

of these places experienced non-deposition because of exposure, or they were deeper-water areas below the normal zone of tempestite deposition. Lack of investigation of Silurian tempestites, or bias in the availability of literature on a region-by-region basis, are probably most significant in the constraints of this review. Uncertainty in paleogeographic position is another possible reason for the scarcity of findings.

ACKNOWLEDGMENTS

I am grateful to R.K. Pickerill and T.M. Chowns for constructive reviews of the manuscript. I also thank Rong J.-y. for discussions of the Chinese platforms.

REFERENCES

- AIGNER, T. 1985. Storm Depositional Systems. Springer Verlag, Berlin.
- , AND H.-E. REINECK. 1982. Proximity-trends in modern storm sands from the Helgoland Bight (North Sea) and their implications for basin analysis. *Senckenbergiana marina*, 14:183–215.
- ANASTAS, A.S., AND M. CONIGLIO. 1993. Sedimentology of an Early Silurian carbonate ramp: the Manitoulin Formation, southern Ontario. *Canadian Journal of Earth Sciences*, 30:2453–2464.
- BAARLI, B.G. 1988. Bathymetric co-ordination of proximity-trends and level-bottom communities: a case study from the Lower Silurian of Norway. *Palaio*, 3: 577–587.
- . 1990. Peripheral bulge of a foreland basin in the Oslo region during the early Silurian. *Palaeogeography, Palaeoclimatology, Palaeoecology*, 78:149–161.
- . 1995. Orthacean and strophomenid brachiopods from the Lower Silurian of the central Oslo region. *Fossils and Strata*, No. 39.
- , S. BRANDE, AND M.E. JOHNSON. 1992. Proximity-trends in the Red Mountain Formation (Lower Silurian) of Birmingham, Alabama. *Oklahoma Geological Survey Bulletin*, 145:1–17.
- BAMBACH, R.K. 1993. Bivalves and storms; tracking relative sea-level through the Silurian in a shallow shelf sea. *Geological Society of America, Abstracts with Programs*, 25:360, 361.
- BARRON, E.J. 1989. Severe storms during earth history. *Geological Society of America Bulletin*, 101:601–612.
- BENTON, M.J., AND D.J. GRAY. 1981. Lower Silurian distal shelf storm-fossils. *Journal of the Geological Society of London*, 138: 675–604.
- BOUCOT, A. J. 1975. *Evolution and Extinction Rate Control*. Elsevier, New York.
- BOURKER, P.A., AND S.M. HOLLAND. 1996. Quantifying tempestite proximity, Ringgold Gap, Georgia. *Geological Society of America, Abstracts with Programs*, 28:24.
- BRAITHWAITE, C.J.R., A.W. OWEN, AND R.A. HEATH. 1995. Sedimentological changes across the Ordovician–Silurian boundary in Hadeland and their implications for regional patterns of deposition in the Oslo region. *Norsk Geologisk Tidsskrift*, 75:181–198.
- BRENCHLEY, P.J., M. ROMANO, AND J.C. GUTIÉRREZ-MARCO. 1986. Proximal distal hummocky cross-stratified facies on a wide Ordovician shelf in Iberia, p. 241–255. *In* R.J. Knight and

- J.R. McLean (eds.), *Shelf Sands and Sandstone*. Canadian Society of Petroleum Geologists, Memoir II.
- BRETT, C.E. 1983. Sedimentology, facies, and depositional environment of the Rochester Shale (Silurian, Wenlockian) in western New York and Ontario. *Journal of Sedimentary Petrology*, 53:187-219.
- , A.J. BOUCOT, AND B. JONES. 1993. Absolute depths of Silurian benthic assemblages. *Lethaia*, 26:25-40.
- , S.E. SPEYER, AND G.C. BAIRD. 1986. Storm-generated sedimentary units: tempestite proximity and event stratification in the Middle Devonian Hamilton Group of New York, p. 129-156. In C.E. Brett (ed.), *Dynamic Stratigraphy and Depositional Environments of the Hamilton Group (Middle Devonian) in New York State, Part I*. New York State Museum Bulletin 457.
- BUSH, D.M. 1991. Storm sedimentation on the northern shelf of Puerto Rico. Unpublished Ph.D. dissertation, Duke University, 366p.
- CANT, D.J. 1980. Storm-dominated shallow marine sediments of the Arisaig Group (Silurian-Devonian) of Nova Scotia. *Canadian Journal of Earth Sciences*, 17:120-131.
- CARNEIRO DE CASTRO, J., J.C. DELLA FAVERA, AND M. EL JADI. 1991. Tempestite facies, Murzuq Basin, Great Socialist People's Libyan Arab Jamahiriya: their recognition and stratigraphic implications. Symposium on the Geology of Libya, 3:1757-1765.
- CHERNS, L. 1988. Faunal and facies dynamics in the Upper Silurian of the Anglo-Welsh Basin. *Palaeontology*, 31:451-502.
- CHOWNS, T.M. 1996. Sequence stratigraphy of the Silurian Red Mountain Formation in Alabama and Georgia, p. 31-47. In T.W. Broadhead (ed.), *Sedimentary Environments of Silurian Taconia*. University of Tennessee Studies in Geology, 26.
- , AND F.K. MCKINNEY. 1980. Depositional facies in the Middle-Upper Ordovician and Silurian rocks of Alabama and Georgia, p. 323-348. In R.W. Frey (ed.), *Excursions in South-Eastern Geology: Guidebook for Field Trip No. 16*, Geological Society of America Annual Meeting, Atlanta.
- COCKS, L.R.M., N.H. WOODCOCK, R.B. RICKARDS, J. TEMPLE, AND P.D. LANE. 1984. The Llandovery Series of the type area. *Bulletin of the British Museum (Natural History), Geology Series*, 8:131-182.
- COMRIE, T.A., AND D.W. CALDWELL. 1993. Sedimentology of the Ripogenus Formation, Maine; a Silurian carbonate-siliciclastic depositional system. *Geological Society of America, Abstracts with Programs*, 25:10.
- COPPER, P., AND F. BRUNTON. 1991. A global review of Silurian reefs, p. 223-259. In M.G. Bassett, P.D. Lane, and D. Edwards (eds.), *The Murchison Symposium. Special Papers in Palaeontology* 44.
- COTTER, E. 1979. Storm-interstorm alterations on a compositionally evolving shallow marine shelf: the Middle Silurian (Rose Hill and Mifflington) of central Pennsylvania. *Geological Society of America, Abstracts with Programs*, 11:8.
- . 1983. Shelf, paralic, and fluvial environments and eustatic sea-level [sic] fluctuations in the origin of the Tuscarora Sandstone Formation (Lower Silurian) of central Pennsylvania. *Journal of Sedimentary Petrology*, 53:25-49.
- . 1988. Hierarchy of sea-level cycles in the medial Silurian siliciclastic succession of Pennsylvania. *Geology*, 16:242-245.
- . 1990. Storm effects on siliciclastic carbonate shelf sediments in the medial Silurian succession of Pennsylvania, p. 245-258. In T. Aigner and R.H. Dott (eds.), *Processes and Patterns in Epeiric Basins*. *Sedimentary Geology*, 69.
- , AND J.E. LINK. 1993. Deposition and diagenesis of Clinton Ironstones (Silurian) in the Appalachian foreland basin of Pennsylvania. *Geological Society of America Bulletin*, 105:911, 922.
- DALZIEL, I.W.D., L.H. DALLA SALDA, AND L.M. GAHAGAN. 1994. Paleozoic Laurentia-Gondwana interaction and the origin of the Appalachian-Andean mountain system. *Geological Society of America Bulletin*, 106:243-252.
- DEHLER, C.M. 1994. Controls on cyclic sedimentation in Upper Silurian-Lower Devonian mixed siliciclastic-carbonate sequences of central-eastern Idaho. *Geological Society of America, Abstracts with Programs*, 26:241.
- DOROBK, S.L., AND J.F. READ. 1986. Sedimentology and basin evolution of the Siluro-Devonian Heldeberg Group, central Appalachians. *Journal of Sedimentary Petrology*, 56:601-613.
- DRIESE, S.G. 1986. Fairweather and storm shelf sequences, Rockwood Formation (Silurian), east Tennessee. *Geological Society of America, Abstracts with Programs*, 18:218, 219.
- . 1988. Depositional history and facies architecture of a Silurian foreland basin, eastern Tennessee. University of Tennessee, *Studies in Geology*, 19:62-96.
- , M.W. FISHER, K.A. EASTHOUSE, G.T. MARKS, A.R. GOGOLA, AND A.E. SCHONER. 1991. Model for genesis of shoreface and shelf sandstone sequences, southern Appalachians: palaeoenvironmental reconstruction of an Early Silurian shelf system, p. 309-338. In D.J.P. Swift, G.F. Oertel, R.W. Tillman, and J.A. Thorne (eds.), *Shelf Sand and Sandstone Bodies: Geometry, Facies, and Sequence Stratigraphy*. Special Publication of the International Association of Sedimentologists, 4.
- DUKE, W.L. 1982. The "type locality" of hummocky cross-stratification; the storm-dominated Silurian Medina Formation in the Niagara Gorge, New York and Ontario. *Annual Conference Ontario Petroleum Institute Inc.*, 21, 31 p.
- . 1985. Hummocky cross-stratification, tropical hurricanes, and intense winter storms. *Sedimentology*, 32:167-194.
- , P.J. FAWCETT, AND W.C. BRUSSE. 1991. Prograding shoreline deposits in the Lower Silurian Medina Group, Ontario and New York; storm- and tide-influenced sedimentation in a shallow epicontinental sea, and the origin of enigmatic shore-normal channels encapsulated by open shallow-marine deposits. *Special Publication of the International Association of Sedimentologists*, 14:339-375.
- DYSON, I.A. 1996. Significance of hummocky cross-stratification and quasi-planar lamination in the Lower Devonian Walhalla Group at Cape Liptrap, Victoria. *Australian Journal of Earth Sciences*, 43:189-199.
- EASTHOUSE, K.A., AND S.G. DRIESE. 1988. Paleobathymetry of a Silurian shelf system: application of proximity-trends and trace-fossil distribution. *Palaios*, 3:473-486.
- GARRAT, M.J. 1983. Silurian to Early Devonian facies and biofacies patterns of the Melbourne Trough, central Victoria. *Journal of the Geological Society of Australia*, 30:121-147.
- GOLDRING, R., AND T. AIGNER. 1982. Scour and fill: the significance of event separation, p. 354-362. In G. Einsele, and A. Seilacher (eds.), *Cyclic and Event Stratification*. Springer Verlag, New York.
- , AND P. BRIDGES. 1973. Sublittoral sheet sandstones. *Journal of Sedimentary Petrology*, 43:736-747.
- GRADSTEIN, F.M., AND J.G. OGG. 1996. Digital Time Scale. *Geonyst*, 23:2.
- GRAF, G.C., AND D.A. DIXON. 1986. Carbonate mudstone in an Upper Silurian ramp/shelf [sic, read -, not virgule] transition at Gascoyne Inlet, Devon Island, Arctic Canada. *Geological Association of Canada, Programs with Abstracts*, 11:75.
- GRAY, D.I., AND M.J. BENTON. 1982. Multidirectional palaeocurrents as indicators of shelf storm beds, p. 350-353. In G. Einsele, and A. Seilacher (eds.), *Cyclic and Event Stratification*. Springer Verlag, Berlin.

- HALLAM, A. 1992. Phanerozoic Sea-Level Changes. Perspectives in Paleobiology and Earth History Series, Columbia University Press, New York.
- HARMS, J.C., J.B. SOUTHARD, D.R. SPEARING, AND R.G. WALKER. 1975. Depositional Environments as Interpreted From Primary Sedimentary Structures and Stratification Sequences. Society of Economic Paleontologists and Mineralogists, Short Course Notes 2.
- HARRIS, M.T., AND P.M. SHEEHAN. 1996. Upper Ordovician–Lower Silurian depositional sequences determined from middle shelf sections, Barn Hills and Lakeside Mountains, eastern Great Basin, p. 161–176. *In* B.J. Witzke, G.A. Ludvigson, and J. Day (eds.), *Paleozoic Sequence Stratigraphy: Views from the North American Craton*. Geological Society of America, Special Paper 306.
- HAVLÍČEK, V., AND P. ŠTORCH. 1990. Silurian brachiopods and benthic communities in the Prague Basin (Czechoslovakia). *Ústřední Ústav Geologický, Rozpravy*, 48:1–275.
- HURST, J.M. 1980. Silurian Stratigraphy and Facies Distribution in Washington Land and Western Hall Land, North Greenland. *Grønlands geologiske undersøkelse Bulletin*, 138.
- , AND R.K. PICKERILL. 1986. The relationship between sedimentary facies and faunal associations in the Llandovery Doctors Brook Formation, Arisaig, Nova Scotia. *Canadian Journal of Earth Sciences*, 23:705–726.
- JOHNSON, H.D., AND C.T. BALDWIN. 1996. Shallow clastic seas, p. 232–280. *In* H.G. Reading (ed.), *Sedimentary Environments: Processes, Facies and Stratigraphy*. Blackwell Science, Oxford.
- JOHNSON, M.E. 1987. Extent and bathymetry of the North American platform seas in the Early Silurian. *Paleoceanography*, 2:185–211.
- . 1989. Tempestites and the alteration of *Pentamerus* layers in the Lower Silurian of southern Norway. *Journal of Paleontology*, 65:195–205.
- . 1996. Stable cratonic sequences and a standard for Silurian eustasy, p. 203–211. *In* B.J. Witzke, G.A. Ludvigson, and J. Day (eds.), *Paleozoic Sequence Stratigraphy: Views from the North American Craton*. Geological Society of America Special Paper, 306.
- , B.G. BAARLI, H. NESTOR, M. RUBEL, AND D. WORSLEY. 1991a. Eustatic sea-level [sic] patterns from the Lower Silurian (Llandovery Series) of southern Norway and Estonia. *Geological Society of America*, 103:315–335.
- , D. KALJO, AND RONG J.-Y. 1991b. Silurian eustasy, p. 145–163. *In* M.G. Bassett, P.D. Lane, and D. Edwards, (eds.), *The Murchinson Symposium. Proceedings of an International Conference on the Silurian System*. Special Papers in Palaeontology, 44.
- JONES, B., AND O.A. DIXON. 1976. Storm deposits in the Read Bay Formation (Upper Silurian), Somerset Island, Arctic Canada (an application of Markov Chain analysis). *Journal of Sedimentary Petrology*, 46:393–401.
- KAHLE, C.F., AND G. STEVENSON. 1988. Storm deposits in tidal flat carbonates: examples from Silurian Greenfield Dolomite, southern Ohio. Society of Economic Paleontologists and Mineralogists, Annual Midyear Meeting, Abstracts, 5:28.
- KERSHAW, S. 1993. Sedimentation control on growth of stromatoporeid reefs in the Silurian of Gotland, Sweden. *Journal of the Geological Society of London*, 150:197–205.
- KIDWELL, S. 1989. Stratigraphic condensation of marine transgressive records: origin of major shell deposits in the Miocene of Maryland. *Journal of Geology*, 97:1–24.
- KLEUSSENDORF, J., AND D.G. MICULIC. 1994. A peritidal biota in the Silurian of the central U.S. Geological Society of America, Abstracts with Programs, 26:24.
- KUGLITSCH, J.J. 1994. Nearshore and ramp conodont associations in the Byron and Hendricks Formations (Llandovery), Door and Waukesha Counties, Wisconsin. Geological Society of America, Abstracts with Programs, 26:49.
- LARSSON, S.Y., AND C.W. STEARN. 1986. Silurian stratigraphy of the Hudson Bay lowland in Quebec. *Canadian Journal of Earth Sciences*, 23:288–299.
- LECKIE, D.A., C. SINGH, F. GOODARZI, AND J.H. WALL. 1990. Organic-rich, radioactive marine shale—a case study of a shallow-water condensed section, Cretaceous Shaftsbury Formation, Alberta, Canada. *Journal of Sedimentary Petrology*, 60:101–117.
- LONG, D.G.F. 1993. The Burgsvik beds, an Upper Silurian storm generated sand ridge complex in southern Gotland, Sweden. *Geologiska Föreningen i Stockholm Förhandlingar*, 115:299–309.
- MCKERROW, W.S., R.ST.J. LAMBERT, AND L.R.M. COCKS. 1985. The Ordovician, Silurian, and Devonian Periods, p. 73–80. *In* N.J. Snelling (ed.), *The Chronology of the Geological Record*. Geological Society of London Memoir, 10.
- , J.F. DEWEY, AND C.R. SCOTSE. 1991. The Ordovician and Silurian development of the Iapetus Ocean, p. 165–178. *In* M.G. Bassett, P.D. Lane, and D. Edwards (eds.), *The Murchison Symposium. Proceedings of an International conference on the Silurian System*. Special Papers in Palaeontology, 44.
- MARSAGLIA, K.M., AND G. DE VRIES KLEIN. 1983. The paleogeography of Paleozoic and Mesozoic storm depositional systems. *Journal of Geology*, 91:117–141.
- MEYER, S.C., D.A. TEXTORIS, AND J.M. DENNISON. 1992. Lithofacies of the Silurian Keefer Sandstone, east central Appalachian Basin, USA. *Sedimentary Geology*, 76:187–206.
- MISKELL-GERHARDT, K.J. 1987. Vertical and lateral proximity-trends in the Cretaceous Mowry Shale of the Western Interior Seaway. Geological Society of America, Abstracts with Programs, 19:774.
- MÖLLER, N.K. 1987. Facies analysis and palaeogeography of the Rytteråker Formation (Lower Silurian, Oslo region, Norway). *Palaeogeography, Palaeoclimatology, Palaeoecology*, 69:167–192.
- MOORE, G.T., D.N. HAYASHIDA, AND C.A. ROSS. 1993. Late Early Silurian (Wenlockian) general circulation model-generated upwelling, graptolitic black shale, and organic-rich source rocks—an accident of plate tectonics? *Geology*, 21:17–20.
- , S.R. JACOBSON, C.A. ROSS, AND D.N. HAYASHIDA. 1994. A paleoclimate simulation of the Wenlockian (late Early Silurian) world using a general circulation model with implications for early land plant paleoecology. *Palaeogeography, Palaeoclimatology, Palaeoecology*, 110:115–144.
- MYROW, P.M. 1992. Bypass-zone, tempestite facies model, and proximity trends for an ancient muddy shoreline and shelf. *Journal of Sedimentary Petrology*, 82:99–115.
- , AND J.B. SOUTHARD. 1996. Tempestite deposition. *Journal of Sedimentary Research*, 66:875–887.
- NEALON, T., AND D. M. WILLIAMS. 1988. Storm influenced shelf deposits from the Silurian of western Ireland: a reinterpretation of deep water basin sediments. *Geological Journal*, 23:311–320.
- NESTOR, H. 1990. Locality 9: Silurian sequences at Sarghaua Field Station, p. 184. *In* Kaljo, D. and H. Nestor (eds.), *Field Meeting, Estonia 1990. An Excursion Guidebook*. Tallinn 1990.
- O'BRIEN, N.R., C.E. BRETT, AND W.L. TAYLOR. 1994. Microfabric and taphonomic analysis in determining sedimentary processes in marine mudstones: example from the Silurian of New York. *Journal of Sedimentary Research, Section A: Sedimentary Petrology and Processes*, 64:847–852.

- PALMER, A.R. 1983. The Decade of North American Geology 1983 Geological Timescale. *Geology*, 11:503–504.
- PEMBERTON, S.G., AND R.W. FREY. 1984. Ichnology of storm-influenced shallow water marine sequence: Cardium Formation (Upper Cretaceous) at Seebe, Alberta, p. 281–304. *In* D.F. Stott and D.J. Glass (eds.), *The Mesozoic of Middle North America*. Canadian Society of Petroleum Geologists Geologists, Memoir, 9.
- PHELPS, D.J. 1990. Characterization and paleoenvironment interpretation of the Louisville Limestone (Silurian), west-central and western Kentucky. Unpublished M.Sc. thesis, University of Kentucky, 211p.
- PICKERILL, R.K., AND J.M. HURST. 1983. Sedimentary facies, depositional environments, and faunal associations of the lower Llandovery (Silurian) Beechhill Cove Formation, Arisaig Nova Scotia. *Canadian Journal of Earth Sciences*, 20:1761–1779.
- PRATT, B.R., AND A.D. MIAL. 1993. Anatomy of a bioclastic megashoal (Middle Silurian, southern Ontario) revealed by ground-penetrating radar. *Geology*, 21:223–226.
- READ, J.F., AND R.K. GOLDHAMMER. 1988. Use of Fischer plots to define third-order sea-level curves in Ordovician peritidal cyclic carbonates, Appalachians. *Geology*, 16:895–899.
- REINECK, H.-E., AND I.B. SINGH. *Depositional Sedimentary Environments*. Springer Verlag, New York.
- RICHARDSON, J.B., AND S.M. RASUL. 1990. Palynofacies in a Late Silurian regressive sequence in the Welsh Borderland and Wales. *Journal of the Geological Society of London*, 147:675–686.
- ROSS, C.A., AND J.R.P. ROSS. 1996. Silurian sea-level fluctuations, p.187–192. *In* B.J. Witzke, G.A. Ludvigson, and J. Day, (eds.), *Paleozoic Sequence Stratigraphy: Views from the North American Craton*. Geological Society of America Special Paper 306.
- ROWDAN, R.D., AND R.L. BRENNER. 1985. The proximity-trends in the Spring Canyon Member of the Blackhawk Formation (Upper Cretaceous), east-central Utah. *Geological Society of America, Abstracts with Programs*, 17:324.
- RYER, T.A. 1983. Transgressive-regressive cycles and the occurrence of coal in some Upper Cretaceous strata of Utah. *Geology*, 11:207–210.
- SAMI, T., AND A. DESROCHERS. 1992. Episodic sedimentation on an Early Silurian, storm-dominated carbonate ramp, Bescie and Merrimack Formations, Anticosti Island, Canada. *Sedimentology*, 39:355–381.
- SENGÖR, A.M.C., B.A. NATAL'IN, AND V.S. BURTMAN. 1993. Evolution of the Altaid tectonic collage and Paleozoic crustal growth in Eurasia. *Nature*, 364:299–307.
- TAIT, J.A., V. BACHTADSE, AND H. SOFFEL. 1994. Silurian paleogeography of Armorica: new paleomagnetic data from central Bohemia. *Journal of Geophysical Research*, 99:2897–2907.
- THOMSEN, E. 1982. Saelabonn Formation (nedre Silur) i Ringerike, Norge. *Dansk geologisk Forening, Årsskrift for 1981*, p. 1–11.
- TORSVIK, T.H., M.A. SMETHURST, J.G. MEERT, B. VAN-DER-VOO, W.S. MCKERROW, M.D. BRASIER, B.A. STURT, AND H.J. WALDERHAUG. 1996. Continental break-up and collision in the Neoproterozoic and Paleozoic; a tale of Baltica and Laurentia. *Earth-Science Reviews*, 40:229–258.
- TYLER, J.E., AND N.H. WOODCOCK. 1987. The Bailey Hill Formation: Ludlow Series turbidites in the Welsh Borderland reinterpreted as distal storm deposits. *Geological Journal*, 22:73–86.
- VAIL, P.K., R.M. MICHUM, AND S. THOMPSON III. 1977. Seismic stratigraphy and global changes in sea-level. Part 4, Global cycles of relative changes in sea-level, p. 83–97. *In* E.D. Payton (ed.), *Seismic Stratigraphy—Applications to Hydrocarbon Exploration*. American Association of Petroleum Geology, Memoir 26.
- WANG H. AND CHEN J. 1991. Late Ordovician and Early Silurian rugose coral biogeography and world reconstruction of paleocontinents. *Paleogeography, Paleoclimatology, Paleoecology*, 86:3–21.
- WATKINS, R. 1978. Bivalve ecology in a Silurian shelf environment. *Lethaia*, 11:41–56.
- , P. E. MCGEE, AND J.J. KIEGLISCH. 1994. The Silurian (upper Llandovery) Brandon Bridge Formation, Walworth County, Wisconsin. *Geological Society of America, Abstracts with Programs*, 26:67.
- WHITTAKER, J.H.M. 1973. "Gutter casts", a new name for scour-and-fill, Malmøya, southern Norway. *Norsk Geologisk Tidsskrift*, 53:403–417.
- WILDE, P., W.B.N. BERRY, AND M.S. QUINBY-HUNT. 1991. Silurian oceanic and atmospheric circulation and chemistry, p. 123–143. *In* M.G. Bassett, P.D. Lane, and D. Edwards (eds.), *The Murchison Symposium. Proceedings of an International Symposium on the Silurian System, Special Papers in Palaeontology* 44.
- WORSLEY, D., N. AARHUS, M.G. BASSETT, P.A. HOWE, A. MØRK, AND S. OLAUSSEN. 1983. The Silurian succession of the Oslo region. *Norges Geologiske Undersøkelse*, 384:1–57.
- YOLKIN, E.A. 1996. Silurian stratigraphy and paleogeography of the Altai and Tuva. *The James Hall Symposium, Second International Symposium on the Silurian System, Program and Abstracts*, University of Rochester, p. 107.
- ZHANG T., HOU F., GAO W., AND LAN G.. 1993. The Lower Silurian tempestites in NW Sichuan and their environmental palaeoecological significance. *Acta Sedimentologica Sinica*, 11:66–75 (in Chinese).
- ZIEGLER, A.M., K.S. HANSEN, M.E. JOHNSON, M.A. KELLY, C.R. SCOTSE, AND R. VAN DER VOO. 1977. Silurian continental distributions, paleogeography, climatology, and biogeography. *Tectonophysics*, 40:13–51.
- ZIEGLER, E.L. 1989. Sequatchie and Lower Silurian Red Mountain Formations, northwestern Georgia. Unpublished M.Sc. thesis, Emory University, 288 p.

EARLY SILURIAN CONDENSED INTERVALS, IRONSTONES, AND SEQUENCE STRATIGRAPHY IN THE APPALACHIAN FORELAND BASIN

CARLTON E. BRETT¹, B. GUDVEIG BAARL², TIMOTHY CHOWNS³, EDWARD COTTER⁴, STEVEN DRIESE⁵, WILLIAM GOODMAN⁶, AND MARKES E. JOHNSON²

¹Department of Earth and Environmental Sciences, University of Rochester, Rochester, New York 14627

²Department of Geology, Williams College, Williamstown, Massachusetts 01267

³Department of Geology, West Georgia College, Carrollton, Georgia 30118

⁴Department of Geology, Bucknell University, Lewisburg, Pennsylvania 17837

⁵Department of Geological Sciences, University of Tennessee at Knoxville, Knoxville, Tennessee 37996, and

⁶The Sear-Brown Group, 85 Metro Park, Rochester, New York 14623

ABSTRACT—This report summarizes Early Silurian (Llandovery–early Wenlock) sequences, events, and biostratigraphy of the Appalachian foreland basin (AFB) in eastern North America. The four Llandovery and the early Wenlock eustatic cycles are recognized throughout the AFB. They form third-order depositional sequences that are synchronous with current biostratigraphic resolution, and display marked similarities along the northeast–southwest depositional strike. Sequence I (Rhuddanian–early Aeronian) is siliciclastic-dominated (Medina [New York, Ontario], Tuscarora [Pennsylvania, Maryland, Virginia], and Clinch [Tennessee] Formations), with a transgressive sandstone that overlies the Ordovician at the Cherokee Unconformity. Gray sandy shales that reflect tectonically induced, early Rhuddanian marine incursion generally occur in the lower third of Sequence I. Sequence II (middle–late Aeronian; lower Clinton Group [New York]; lower Rose Hill Shale [central Appalachians]; middle member of Rockwood and Red Mountain Formations [Tennessee, Alabama]) is characterized by fine-grained siliciclastics, carbonates, and ferruginous to phosphatic shell-rich beds that mark flooding surfaces. Sequence III (lower–middle Telychian) comprises green–maroon shales and ferruginous to phosphatic sandstones (Sauquoit–Otsuquo [New York], middle Rose Hill [central Appalachians], upper member of Rockwood–Red Mountain Formations, in part [Tennessee, Alabama]). The Sequence II–III boundary appears conformable in the central Appalachians, where sandstones of a lowstand wedge or shelf margin systems tract (Cabin Hill Member) occur in the Rose Hill Shale. The thin, distinctive Sequence IV (late Telychian–earliest Wenlock) overlies a prominent, regional angular unconformity that truncates parts of Sequences I–III in the northwestern part of the basin (New York, Ontario, Ohio, Kentucky). Center Member sandstones of the Rose Hill

may again record lowstand progradation in the basin center. Oolitic ironstones (e.g., Westmoreland Iron Ore [New York]) and carbonates mark the transgressive systems tract and condensed section of Sequence IV. Overlying dark gray, fossiliferous shales (Williamson–Willowvale [New York], uppermost Rose Hill [central Appalachians], and upper Rockwood–Red Mountain [southern Appalachians]) record the deepest water facies (Benthic Association 3–5) in most sections. Sequence V (early Wenlock–Sheinwooian) records renewed influx of coarser-grained siliciclastics (Herkimer–Keefer Sandstones) that possibly reflects foreland basin flexure and regression. Overlying dark gray shales (Rochester–Mifflintown) record middle Wenlock highstand.

Proximal ferruginous and distal phosphatic shell-rich beds are regional markers in the AFB Lower Silurian. An association with condensed sections indicates that they record sediment starvation during transgressions. Chamositic precursors of hematites and phosphorites formed near sediment redox boundaries, but oolitic hematites seem to occur in more agitated, better-oxygenated settings than phosphorites. Ironstone and phosphorite development was favored by tectonic quiescence. Global sea-level maxima are coeval with the major marine incursions of the transgressive or highstand systems tracts of the large-scale depositional sequences in the AFB. Sea-level maxima are marked by ferruginous or phosphatic shelly beds.

INTRODUCTION

Sedimentary cycles of various scales have long been recognized by stratigraphers. Large-scale, unconformity-bound Phanerozoic sequences were first described in

North America by Wheeler (1958) and Sloss (1963). Vail et al. (1977) noted similar unconformity-bound sequences in the sedimentary prisms of passive continental margins, and suggested a global, probably eustatic control on these cycles. However, only recently have workers attempted regional/global correlation of apparent Paleozoic cycles. In particular, Dennison and Head (1975), McKerrow (1979), Johnson et al. (1985, 1991a, 1991b), and Johnson (1987, 1996) have focused attention on the widespread, possibly global nature of sedimentary cycles attributable to relative sea-level changes in several Silurian basins of North America, Great Britain, and China. These cycles have been defined and correlated largely on the basis of paleontological evidence (Figure 1). In particular, workers have used the onshore-offshore spectrum of benthic assemblages first worked out by Ziegler (1965) and Ziegler et al. (1968) to reconstruct the relative bathymetry of stratigraphic successions. Relative highstands and lowstands have then been correlated regionally and globally on the basis of biostratigraphy. Other researchers have applied a mixture of bio-, sequence, and event stratigraphy to recognize and correlate Silurian sedimentary cycles regionally (e.g., Brett et al., 1990; Ross and Ross, 1996; Witzke et al., 1996; Chowns, 1996). Recently, Ruppel et al. (1996) have recognized a cyclic signature in Lower and middle Silurian rocks that is recorded by fluctuations of strontium isotopic ratios in conodonts. Fluctuations in $^{87}\text{Sr}/^{86}\text{Sr}$ apparently correspond to sea-level fluctuations, with relative lowstands (regressions) coinciding with increases in the ratio, and highstands with abrupt decreases (Montañez et al., 1996). In particular, there appears to be a close relationship between excursions in the $^{87}\text{Sr}/^{86}\text{Sr}$ curve and sequence boundaries (Ruppel et al., 1996).

Such lines of evidence suggest a strong allocyclic and probable eustatic control on the stratigraphic record of Silurian marine basins. However, precise identification and correlation of specific sea-level events over many coeval basins must be done before the role of eustasy in governing Silurian stratigraphic architecture can be defined unambiguously. Additional detailed work remains to be completed in many of the classic areas, such as the Appalachian foreland basin (AFB). In particular, several key issues require resolution. How well can the larger-scale cycles be recognized regionally, and how did the sedimentary response vary locally? Can smaller-scale, higher-order cyclicity be recognized and correlated regionally within a single basin? Are various previously identified lithostratigraphic units, including such marker beds as widespread shell beds, phosphatic nodules, and oolitic hematites, related to these large- and smaller-scale cycles? Finally, how is the global cyclicity recognized by

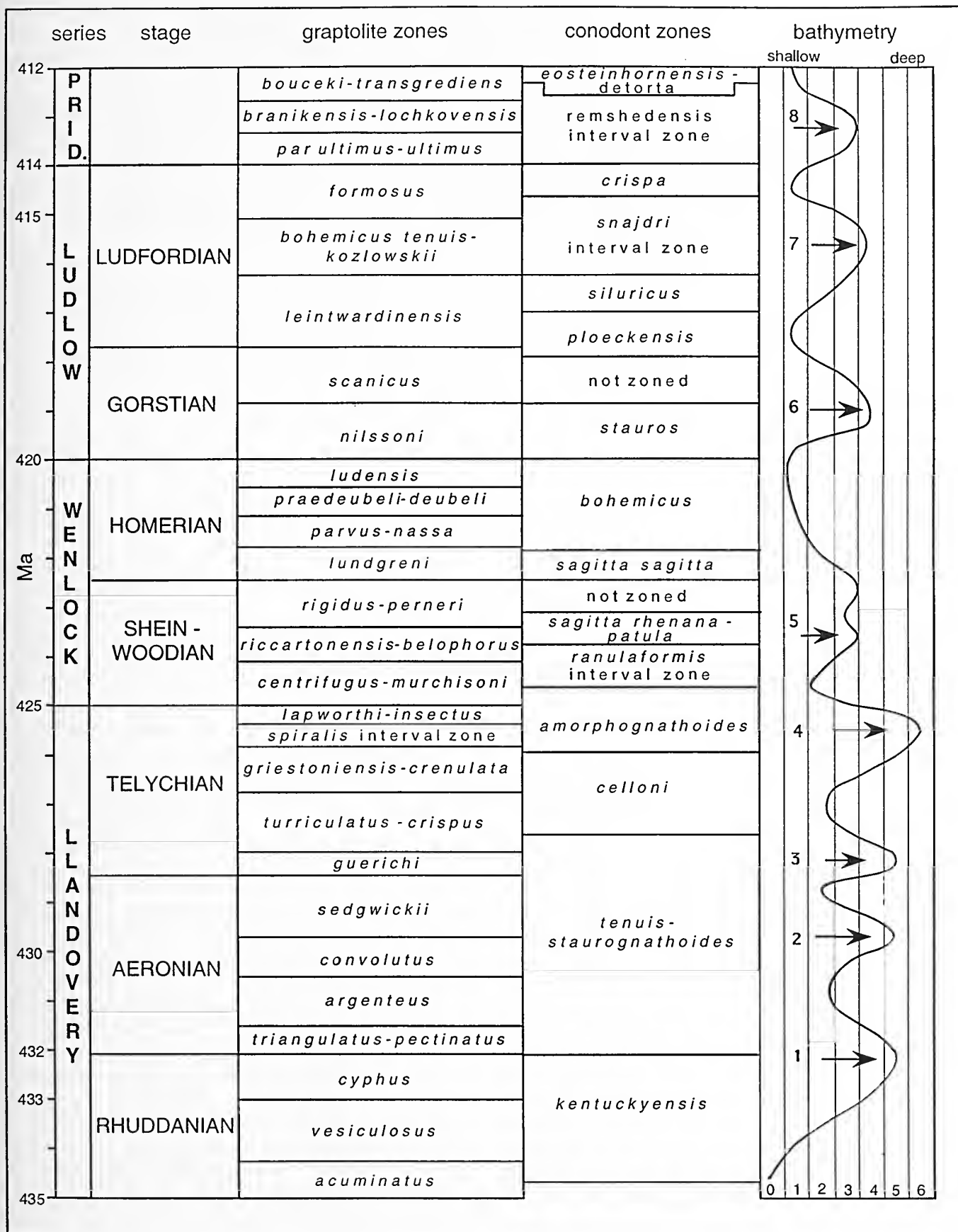
Johnson (1996; Figure 1) related to locally identified depositional sequences and their bounding surfaces?

The paradigm of sequence stratigraphy provides a process-oriented perspective for analysis of stratigraphic successions. The recognition by seismic stratigraphers of widespread seismic reflectors proved the existence of regionally extensive surfaces that cross-cut facies belts within sedimentary prisms (Vail et al., 1977). Several distinctive types of surfaces came to be recognized: a) erosion surfaces developed during sea-level lowstands; b) transgressive ravinement surfaces, which commonly merge with sequence boundaries; and c) surfaces of sediment starvation or maximum flooding surfaces that may be associated with thin condensed intervals (Vail et al., 1977, 1991; Wilgus et al., 1988; Emery and Meyers, 1996, and references therein). Thus, distinctive stratigraphic surfaces were effectively linked to synchronously and dynamically changing marine environments in response to relative sea-level change.

This concept of eustatic control on facies change contradicted the entrenched thinking that stratigraphic patterns were largely artifacts of intrinsic depositional/sedimentologic processes operating independently in specific environmental settings. Application of this facies-model approach led many sedimentary geologists to view the stratigraphic record as a mosaic of local lenticular sedimentary bodies with little lateral continuity and little or no relationship to similar-appearing beds in other sections. Earlier attempts to link marker horizons into a regional framework were viewed with suspicion and commonly castigated as antiquated "layer-cake stratigraphy", although in many cases the early attempts were based on strong empirical evidence. With its renewed emphasis on through-going discontinuities and condensed beds, the sequence approach has encouraged a broader, more regional view of stratigraphy and an appreciation of the genetic significance of particular beds and surfaces. To some degree, it vindicates the earlier "layer-cake" stratigraphic approach. Sequence stratigraphy, originally developed from remote seismic studies of passive margin sedimentary wedges, is now being applied at an outcrop scale to diverse depositional settings, including Early to Middle Paleozoic epicratonic and peripheral foreland basins (Brett et al., 1990; Witzke et al., 1996, and references therein).

Silurian strata of the north-central to northern AFB (Figure 2) provide an excellent field laboratory for appli-

FIGURE 1—(opposite) Silurian sea-level curve and graptolite and conodont biostratigraphy. Note the positions of highstands 1–5 in Llandovery and Wenlock. After Johnson (1996).



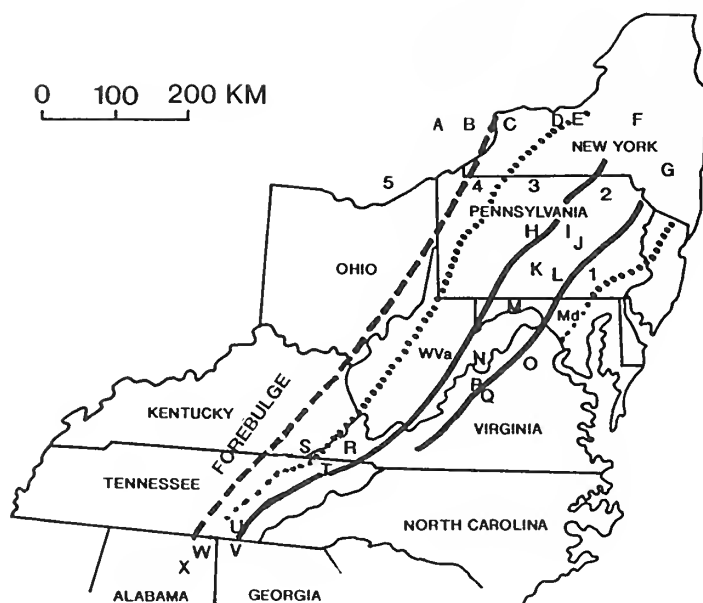


FIGURE 2—Map of Appalachian region with key localities. Lines show orientation of depositional strike and position of Appalachian Foreland Basin (without palinspastic restoration) and forebulge during the Early Silurian. Facies belts numbered: 1, marine shoreface and shelf sand complexes; 2, 3, terrigenous mud and storm sands ("Rose Hill shelf lagoon"); 4, mixed carbonate, ironstone, and mudrock; 5, carbonate shelf. Sections referred to in text indicated by letters: A, Hamilton, Ontario; B, St. Catharines, ON; C, Niagara Gorge, ON-NY; D, Rochester, NY; E, Sodus, NY; F, Clinton-Utica, NY; G, Shawangunk Mountains, NY-PA; H, Lock Haven, Mill Hall, PA; I, Allenwood, PA; J, Danville, PA; K, Millerstown, PA; L, Harrisburg, PA; M, Cumberland, MD-Keyser, WV; N, Huntersville, WV; O= Massanutten Mountain, VA; P= Clifton Forge, VA; Q, Roanoke, VA; R, Duffield, VA; S, Cumberland Gap, VA-TN-KY; T, Clinch Mountain, TN; U, Tiptonia, TN; V, Ringgold Gap, GA; W, Gadsden, AL; X, Birmingham, AL.

cation of sequence-stratigraphic models. The strata are well-exposed, and display marked vertical facies changes that are commonly associated with distinctive condensed beds and/or discontinuities. Unfortunately, truncation of the Upper Silurian (Ludlow-Pridoli) in the southern Appalachians at the Salinic and/or Wallbridge Unconformities precludes basin-wide study through this interval. However, the Llandovery and lower Wenlock are better preserved and adequately exposed in several key outcrop areas along the Appalachian trend to permit intrabasinal comparison. Preliminary study indicates that biostratigraphically dated sections from Alabama to New York (Berry and Boucot, 1970) display similarities in facies and stacking patterns that suggest regional persistence of unconformity-bounded intervals and condensed beds at least along depositional strike. Although some earlier workers recognized these fundamental similarities of beds and stacking patterns of facies (e.g., Swartz, 1923, 1934a, 1934b; Swartz and Swartz, 1931; Gillette,

1947; Hunter, 1970), there has been little attempt to make additional detailed correlations between the classic sections in upstate New York and those of the central and southern Appalachians (Figure 2).

The historic lack of emphasis on correlation within the AFB can be attributed to several factors. First, few stratigraphers have studied the sections over a broad region. As a consequence, geologists who specialize in particular regions have developed discrete provincial terminologies and approaches that render a patchwork stratigraphic nomenclature to the Silurian-age basin fill. Secondly, studies that compared strata in different regions rarely emphasized the importance of depositional strike. Thus, for example, a comparison of the Silurian of the central Appalachians with the classic Niagaran sections of western New York suggests little similarity, with the exception of the Rochester Shale. Conversely, detailed comparison of the central Appalachians with the poorly exposed, short sections of central New York (Brett et al., 1990) revealed many similarities—indeed, a bed-for-bed correlatability. This persistence of facies over several hundred kilometers along depositional strike reflects the tremendous continuity of litho- and biofacies belts in the AFB. During the Silurian, the eastern shoreline and axis of the foreland basin trough were oriented approximately northeast-southwest (Figure 2). Hence strata exposed in the Valley and Ridge Province of Pennsylvania and Maryland display facies comparable to those seen east of Syracuse, New York. Similarly, Alabama and east Tennessee facies can more readily be compared with strata in the central Appalachians than those found in intervening stretches along the main Appalachian trend in most of Virginia (Figure 2). A third reason for lack of detailed correlations along the full length of the AFB is that workers in the different areas have developed independent working methodologies and "philosophies" as to how stratigraphy should be approached. For example, because of an early emphasis on bounding marker beds, the definitions of stratigraphic units identified in New York State and Maryland were fundamentally similar to sequence stratigraphic or allostratigraphic units. Hence, the same name was commonly applied to an interval if it was bounded by similar markers over a large region, even if the lithology between the markers varied substantially over the region. In contrast, workers in Pennsylvania and parts of the southern Appalachians have tended to combine varied, thin units into larger heterolithic formations for convenience in mapping. In a very real sense, many fundamental similarities in Silurian sections with disparate nomenclatures have been overlooked because the strata have been subdivided differently and because nearly identical strata masquerade under different names in different areas.

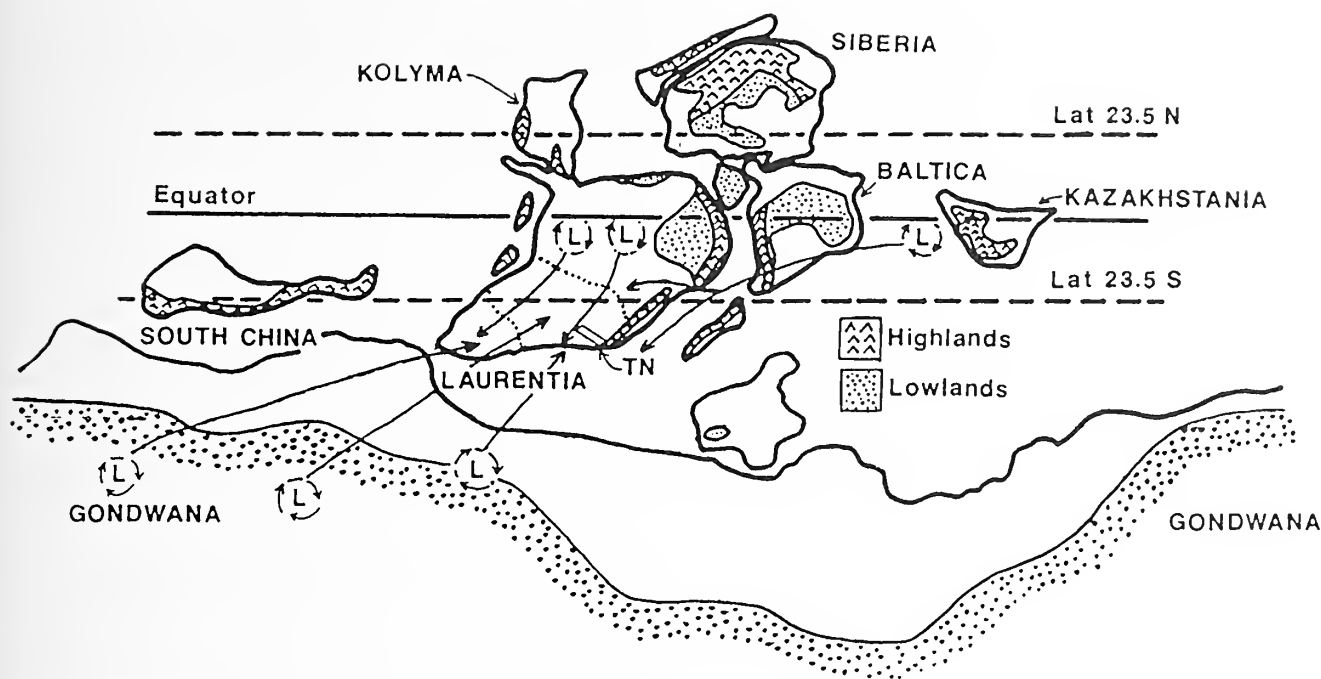


FIGURE 3—Early Silurian paleogeography of Laurentia. Note position of Appalachian Foreland Basin from about 23°S in New York (NY) to 30°S Tennessee (TN); hypothetical storm tracks are indicated (L). Modified from Driese et al. (1991).

Development of a detailed Silurian sea-level curve for the AFB is a major objective of this report. In recent years, workers in parts of the Appalachians from New York to Alabama have undertaken detailed, local to regional studies of Silurian facies and their arrangement into stratigraphic cycles. Until recently, however, relatively little effort has been expended to synthesize sequence stratigraphy of Silurian strata throughout the entire AFB. Thus, the last comprehensive synthesis is the large-scale lithostratigraphic compilation of Hunter (1970), who reviewed occurrences of ironstones in the Silurian in eastern North America and presented important cross-sections through the northern and central Appalachian basin. Dennison and Head (1975) inferred eustatic sea-level fluctuations based upon existing correlations of Silurian and Devonian strata. Building upon these reports, various workers have begun to synthesize the details of local sections in a sequence-stratigraphic context (Brett et al., 1990; Chowins and Bolton, 1993; Goodman and Brett, 1994; Chowins, 1996; Driese, 1996). Now that detailed regional studies have been published, an attempt can be made to summarize the sequence stratigraphy of the entire foreland basin.

During 1996, in conjunction with the Second International Symposium on the Silurian System, a regional field conference examined Silurian strata from Alabama to New York (Figure 2). In the resulting publication (Broadhead, 1996), local researchers documented facies

patterns attributable to sea-level changes in several regions from Alabama to New York State. Chowins (1996) and Baarli et al. (1996) presented details of sequence stratigraphy and biostratigraphy of the Red Mountain Formation in northern Alabama, northwestern Georgia, and southeastern Tennessee. Driese (1996) summarized stratigraphic relationships and facies architecture of the Rockwood and Clinch Formations from east Tennessee to southern Virginia, and Diecchio and Dennison (1996) summarized Silurian stratigraphy in central to northern Virginia. Cotter (1996) summarized the Silurian stratigraphy of Pennsylvania, and Brett and Goodman (1996) described the Llandovery–Ludlow of the northern and north-central parts of the AFB in a regional sequence-stratigraphic context. One outcome of this survey was to reinforce the concept of basin-wide, large-scale sedimentary cycles and certain event beds.

In this report, we compare the sequence stratigraphy of the various regions and emphasize the persistence of unconformities, critical marker beds, and similarities of facies-stacking patterns along depositional strike. Where possible, biostratigraphic control has been established by traditional brachiopod and ostracode zonations (Figures 3–5) established by Ulrich and Bassler (1923), Swartz and Swartz (1931), and Berry and Boucot (1970), and the recently revised conodont zonation of Kleffner (1989, 1991). The international biostratigraphic zonation for the Silurian (Johnson, 1996; Figure 1) has limited use because it is

based largely on graptolites, which are rare or absent in most of the Appalachian basin. In the second part of this report, we discuss the genesis of various types of condensed facies, especially ferruginous beds, and relate them to Silurian sequence stratigraphy. The final part of this report reviews examples of particular condensed beds, followed by a discussion of their lateral correlation between regions and their relationship to global sea-level events.

GEOLOGICAL SETTING

TECTONIC SETTING.—The Appalachian Foreland Basin was initiated by collisions between Laurentia and arc terrains in the Middle–Late Ordovician Taconic orogeny, and remained an actively subsiding northeast-trending (present-day orientation) depocenter throughout the Silurian. The foreland basin intermittently received siliciclastic sediments from source terrains throughout this period. These sediments accumulated in subtropical climates at approximately 23°–30° south latitude (see Driese et al., 1991). Tropical storms and hurricanes exerted a strong influence on shelf sedimentation (Figure 3). A final, early Llandovery pulse (tectophase) of the Taconic orogeny may have led to the deposition of coarse-grained siliciclastic wedges of the lowest Silurian Tuscarora, Clinch, Rockwood, and Medina Groups (Cotter, 1983; Goodman and Brett, 1994; Ettensohn and Brett, 1996). During the Early to Middle Silurian, the foreland basin appears to have migrated to the east or southeast, perhaps in response to a phase of tectonic quiescence and thrust-load relaxation (see Beaumont et al., 1988; Goodman and Brett, 1994).

An abrupt reversal of basin axis migration, coincident with uplift and erosional truncation of a broad forebulge, occurred in the late Llandovery (Brett et al., 1990; Ettensohn, 1992; Goodman and Brett, 1994; Ettensohn and Brett, 1996). This episode of cratonic upwarping and reversal in direction of basin axis migration also coincided with an influx of coarser-grained siliciclastics (Keefer Sandstone, Herkimer Formation, upper Shawangunk Conglomerate, Eagle Rock Sandstone). This evidence suggests that the Middle Silurian (late Llandovery–early Wenlock) featured a new pulse of tectonism, herein referred to as the “Salinic Orogeny”, along the eastern margin of Laurentia (Ettensohn and Brett, 1996).

Lithospheric flexure controlled the locus of the depocenter and the deepest portions of the AFB, and produced local erosional effects and variations in accommodation space. Coarse-grained siliciclastics accumulated far out in the basin during times of more active thrusting. Deposition of siliciclastic mudstones and carbonates in basinal areas reflected more quiescent interludes. None-

theless, despite these locally produced tectonic effects, Appalachian Basin Silurian strata display widely correlatable cycles. Within the existing, although admittedly crude, biostratigraphic resolution, these cycles appear to be synchronous, and therefore are inferred to be allocyclic and, quite possibly, eustatic in nature (Dennison and Head, 1975; Johnson, 1987; Brett et al., 1990; Johnson et al., 1991a, 1991b; Goodman and Brett, 1994).

ELEMENTS OF APPALACHIAN BASIN SEQUENCES.—The Silurian of the Appalachian foreland basin is divisible into sedimentary cycles of varying scales and motifs. At the broadest scale, the Silurian–Lower Devonian of the Appalachian Basin can be assigned to the upper, or Tutelo, holostrome of the Tippecanoe Super-sequence, a package bounded below by the latest Ordovician–earliest Silurian Cherokee Unconformity, and above by the Lower Devonian (Pragian) Wallbridge Unconformity (Sloss, 1963; Dennison and Head, 1975). Brett et al. (1990) defined a hierarchy of sedimentary packages that can be adapted to the widely used “orders” of cyclicity and their estimated recurrence intervals that are based in part on Milankovitch orbital periods (e.g., Vail et al. 1991; Meyers and Milton, 1996). Although we recognize that such classifications may be overly simplistic and may impose an artificial hierarchy on a more nearly continuous range of cycle scales, we will use this terminology to indicate the approximate magnitude of cycles. Accordingly, we consider decimeter-scale rhythmic alternations in certain Silurian facies to comprise sixth-order cycles with durations of a few tens of thousands of years. Decimeter-scale cycles may be bundled within meter-scale cycles that commonly exhibit an asymmetrical, shallowing-up motif; these fifth-order cycles probably represent auto- or allocyclic fluctuations of about 40,000–100,000 years. In the parlance of sequence stratigraphy, they may be termed parasequences.

At the next level, parasequences can be grouped into packages, or the “parasequence sets” of Van Wagoner et al. (1988). Parasequence sets display retrograding (back-stepping), prograding, or aggrading patterns, and help to define systems tracts of larger cycles that are typically several meters in thickness. In this report, we focus on these larger unconformity-bounded genetic units that correspond to third- and fourth-order depositional sequences. For this reason, some of the more generalized sea-level curves emphasize abrupt shallowing surfaces (facies dislocations) and not the minor flooding surfaces of small-scale parasequences. Following currently used durations for these scales of cycles (e.g. Meyers and Milton, 1996), we suggest that fourth-order cycles represent about 0.1–0.5 Ma, while third-order cycles span 0.5–3 Ma; this is a slight modification of the durations listed by Brett et al. (1990).

Fourth-order sequences, or "subsequences" (Brett et al., 1990), are bounded by sharp facies dislocations (i.e. surfaces at which shallower facies rest directly on deeper-water facies [Meyers and Milton, 1996]). These were termed "sea-level drop surfaces" by Brett et al. (1990). Although these surfaces may not represent major sub-aerial unconformities, their sharpness implies that transitional shallowing-up facies have been truncated. We have used the terms "relative lowstand" to indicate shallow water (lowstand to transgressive), and "relative highstand" to indicate deeper but shallowing-up parts of the subsequences. These are analogous to systems tracts of third-order sequences.

Third-order sequences are bounded by larger facies dislocations and demonstrable erosional truncation surfaces that probably passed upslope into subaerial unconformities. In some cases, such as the sequence III–IV boundary, these unconformities were enhanced by local tectonic uplift of basin margins. Although we are unable to map the complete three-dimensional geometry of these sequences, the widespread, circum-basinal nature of facies dislocations indicates that they were also produced by allocyclic sea-level fall and rise. It is clear that most Silurian third-order sequences are actually "composite sequences" (i.e., composed of two or more fourth-order sequences that typically form the systems tracts of the larger sequence).

Within the Silurian AFB, certain widespread stratigraphic markers can be related to sequence stratigraphy. These beds/intervals fall into two categories: 1) bundles of hummocky to trough cross-stratified sandstones and conglomerates in otherwise shaley successions, and 2) condensed shell and/or ferruginous–phosphatic beds. The sandstone bundles form basinward-thinning tongues. They may occur at the tops of gradationally upward-coarsening successions, or they may display sharp bases with coarse-grained erosional-lag conglomerates. The tops of the sandstone bundles are typically sharp, and may be separated from overlying shales by thin condensed beds. The sandstone wedges appear to correlate cratonward with unconformities, and both of these features may be related to relative lowering of sea-level. Depending upon the apparent degree of erosion on the upper and lower bounding surfaces, the sandstones may be interpreted either as late highstand (regressive) deposits at the top of a major cycle or lowstand deposits at the base of the overlying large-scale cycle (Goodman and Brett, 1994).

Thin, shell-rich, burrowed, and typically ferruginous and/or phosphatic beds commonly overlie the sandstone bundles or correlative unconformities, are regionally extensive, and appear to correlate with sea-level rises of a basin-wide scale. Detailed sedimentology, paleontology, and mineralogy of these beds varies gradually

on a regional scale (i.e., some beds, which in western sections are thin phosphatic lags, grade laterally into oolitic hematites to the southeast [Hunter, 1970; Brett et al., 1990; LoDuca and Brett, 1994]). However, these beds collectively display features that indicate sedimentary condensation on environmental to biostratigraphic time scales (i.e., thousands to tens of thousands of years; see Kidwell, 1991; Kidwell and Bosence, 1991, for discussion of scales). Such beds are associated with prolonged intervals of sediment starvation on basin ramps produced by relatively abrupt sea-level rise and alluviation in coastal sediment traps. As such, they typically mark marine flooding surfaces of varied scales, ranging from those of fifth-order parasequence bases to condensed sections at the base of highstand systems tracts of large-scale, third-order depositional sequences.

By integrating new data on biostratigraphy with various lithostratigraphic indicators, it is possible to reconstruct a coherent regional framework of depositional sequences and cycles. Synthesis of these data suggests that previously recognized larger cycles (Johnson, 1996; Figure 1) and higher-order (i.e., smaller-scale) cycles are recognizable basin-wide in some coastal and most marine facies belts. Moreover, various condensed beds that are recognized locally may be related to one another and used to identify widespread flooding surfaces.

SEQUENCE STRATIGRAPHY AND CONDENSED BEDS IN SILURIAN CYCLES OF APPALACHIAN FORELAND BASIN

In the following sections, we summarize the stratigraphic relationships of the Llandovery–Wenlock from New York and Ontario southward to Alabama. Similarity of cyclic stratigraphic patterns is evident in most exposures of the marine facies belts, although sometimes obscured in sections proximal to the southeastern margin due to the apparently high influx of coarse-grained siliciclastics. We also illustrate examples of widespread ferruginous and/or phosphatic shell-rich beds in sections from New York to Alabama, and point out the relationship between sequence and systems tract boundaries and the stratigraphic position of these beds. Sequence stratigraphy of Lower Silurian strata is discussed by region in the following sections.

SEQUENCES IN NEW YORK, ONTARIO, AND OHIO

EARLIER WORK.—The Silurian of New York has been studied since the mid-1800s (Vanuxem, 1839, 1840, 1842;

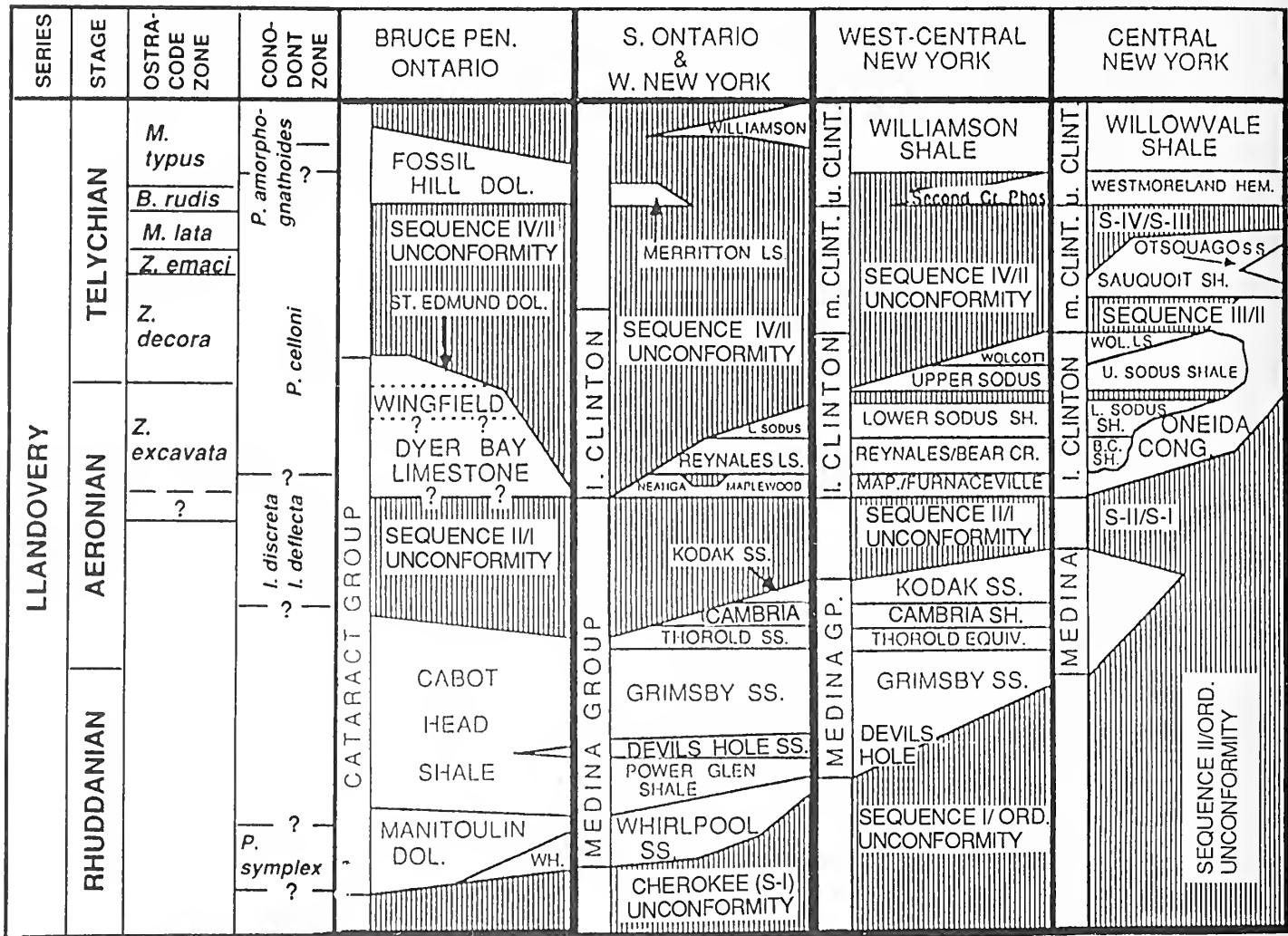


FIGURE 4—Chronostratigraphy of Lower Silurian (Llandovery) Sequences I-IV in Ontario, New York, and northeast Pennsylvania. Abbreviations in this and following figures: B., *Bonnemaia*; B.C., Bear Creek Shale; DH, Devils Hole Sandstone; DOL., dolostone; DW, Dawes Formation; F., Furnaceville Ironstone; FM., formation; I., *Icriodella*; I.O., iron ore; LS, limestone; MAP., Maplewood Shale; M., *Mastigobolbina*; Mbr., member; P., *Pterospirifer*; SH., shale; SS, sandstone; Strickl., limestone rich in *Stricklandia lens progressa*; WEN, Wenlock; WH, Whirlpool Sandstone; WOL, Wolcott Limestone and Wolcott Furnace Iron Ore; Z., *Zygobolbina*; Z. emaci, *Z. emaciata*. Modified from Brett et al. (1990).

Hall, 1839, 1840, 1843, 1852). West-central New York is the type region of the widely known "Clinton Iron Ores", which were mined for many years as a source of paint pigment. Many regional studies have contributed to understanding the Medina and Clinton Groups in New York and adjacent Ontario (Schuchert, 1914; Chadwick, 1918; Sanford, 1934, 1935; Alling, 1947; Gillette, 1947; Bolton, 1957; Rickard, 1975; Brett et al., 1995).

The Lower Silurian (Llandovery–Wenlock) in New York and Ontario has recently been subdivided by Brett et al. (1990, 1995; see Goodman and Brett, 1994) into six large-scale, third-order sequences that represent about 3–5 Ma each, and a larger number of smaller-scale, fourth-order cycles, each averaging about 1 Ma (Figure

4). Third-order sequences consist of facies that range from shallow marine to non-marine siliciclastics in the Medina Group (Sequence I, Rhuddanian), to mixed siliciclastics and carbonates of the lower Clinton Group (Sequence II, Aeronian), to dominantly marine siliciclastics in the middle–upper Clinton Group (Sequences III–V, Telychian–middle Wenlock), and, finally, to dominantly dolomitic carbonates and subordinate shales in the Lockport Group (Sequence VI, upper Wenlock–lower Ludlow) (Figure 4). Each sequence contains widespread condensed beds that mark major marine flooding surfaces. The Llandovery–lower Wenlock sequence stratigraphy and condensed beds of the New York–Ontario outcrop belt are described in some detail

below as a standard of comparison with less-well-known sections farther south.

SEQUENCE I.—The lowest Silurian depositional sequence is the revised Medina Group (see Brett et al., 1995), a succession of locally calcareous, quartz arenites, gray to maroon shales, and mottled, bioturbated, red, pink and white sublitharenites (Figures 4–6). The base of the Medina Group is a major erosion surface, the Cherokee Unconformity, which regionally bevels the Upper Ordovician (Queenston, Oswego, Lorraine Groups) in an eastward direction. This erosional episode may be associated with isostatic uplift during a time of tectonic quiescence, whereas Medina Group siliciclastics suggest renewed tectonism, possibly a late Taconic tectophase (Quinlan and Beaumont, 1984; Tankard, 1986; Goodman and Brett, 1994; Ettensohn and Brett, 1996). Biostratigraphic dating of Medina strata is imprecise, but the unit is bracketed by the Upper Ordovician and lower Aeronian. The Medina Group has generally been assigned to the Rhuddanian (Berry and Boucot, 1970; Rickard, 1975), but the upper part may be Aeronian, particularly in the subsurface of western New York where progressively younger strata are preserved beneath the upper sequence-bounding unconformity in basinal areas.

Sequence I is subdivided into five minor fourth-order subsequences that correspond to couplets of presently defined formations within the Medina Group (Figure 6; Brett et al., 1990, 1995) and that represent the component systems tracts of third-order depositional sequences. The stratigraphically lowest subsequence (IA) consists of the Whirlpool Sandstone and the overlying Power Glen Shale in New York, and the laterally equivalent Whirlpool, Manitoulin Dolostone, and lower part of the Cabot Head Shale in Ontario (Figure 6). The formations in western New York are arranged in a retrogradational succession that contains a basal non-marine sandstone of a shelf margin (or lowstand) systems tract and an overlying marine sandstone to shale of a transgressive systems tract. The basal, non-marine sandstone is not present in the most basinal sections in Ontario. A thin bed near the top of the Manitoulin Formation near Hamilton, Ontario, contains abundant, bright green glauconite grains. This horizon grades eastward into a thin, commonly bioturbated sandstone bed that is locally enriched in small phosphatic nodules and fossil steinkerns at the top of the Whirlpool Sandstone in Niagara County, New York. The glauconitic horizon and phosphate bed mark a maximum marine flooding surface on the eastern basin ramp that was produced by the rapid transgression that initiated Power Glen Shale deposition. A thin fossil hash bed may also be associated locally with this flood-

ing surface. The Power Glen Shale consists of dark gray to greenish-gray shales with thin-bedded sandstones that contain wispy to small-scale hummocky cross-lamination, basal scours, and gutter casts. To the west, the Power Glen–lower Cabot Head becomes richly fossiliferous and contains a moderately diverse fauna of bryozoans, brachiopods, bivalves, and echinoderms that suggest benthic assemblage (BA) 2–3 (see Boucot, 1975). Taken together, these features indicate deposition in a storm-dominated shallow shelf below normal wave base. The Power Glen facies of Ontario and New York represents the deepest water conditions along the Medina Group outcrop belt. Drill core studies demonstrate that the marine shales grade laterally into calcareous and/or feldspathic sandstones with ooids, fossil fragments, and authigenic K-feldspar (J. Castle, personal commun., 1997, *In press*).

The second fourth-order sequence (IB) in the Medina Group is represented by a thin (1.5–2.5 m) interval of quartz arenite (Devils Hole Sandstone), overlying shales, and fine-grained quartz arenite of the Grimsby Formation in western New York and Ontario (Fig. 6). The Devils Hole Sandstone is a planar-laminated shoreface quartz arenite with linguloid brachiopod valves near Lockport, New York. The top of these sandstones is marked by a thin spastolithic hematite horizon. East of Lockport, this spastolithic horizon grades into a red shale pebble conglomerate, while to the west this bed grades into a phosphatic dolostone, the Art Park Phosphate Bed, which contains abundant phosphatic steinkerns of small gastropod shells and bryozoans. A thin phosphatic to hematitic limestone at this horizon has been traced westward at least to Hamilton, Ontario (Duke and Fawcett, 1987). The sharp base of the Devils Hole Sandstone is interpreted as a subsequence (fourth-order) bounding erosion surface, whereas the Art Park Phosphatic Bed and its lateral equivalents are interpreted to mark the maximum flooding surface at the base of the condensed section in the lower part of the highstand systems tract. Greenish-gray to reddish shales near the base of the Grimsby Formation represent the highstand portion of Sequence IB. An abrupt facies dislocation occurs at the contact between greenish-gray or maroon fossiliferous shales of the lower Grimsby and the first major, thicker-bedded, reddish sandstones of the upper Grimsby. This contact was interpreted as another subsequence (fourth-order sequence) boundary by Brett et al. (1990). Thus, the upper part of the Grimsby was assigned to subsequence IC (Figure 6), although in some outcrops this interval might be better interpreted as a late highstand or regressive systems tract of subsequence IB. The upper part of the Grimsby Formation consists of reddish and pale gray

WEST

EAST

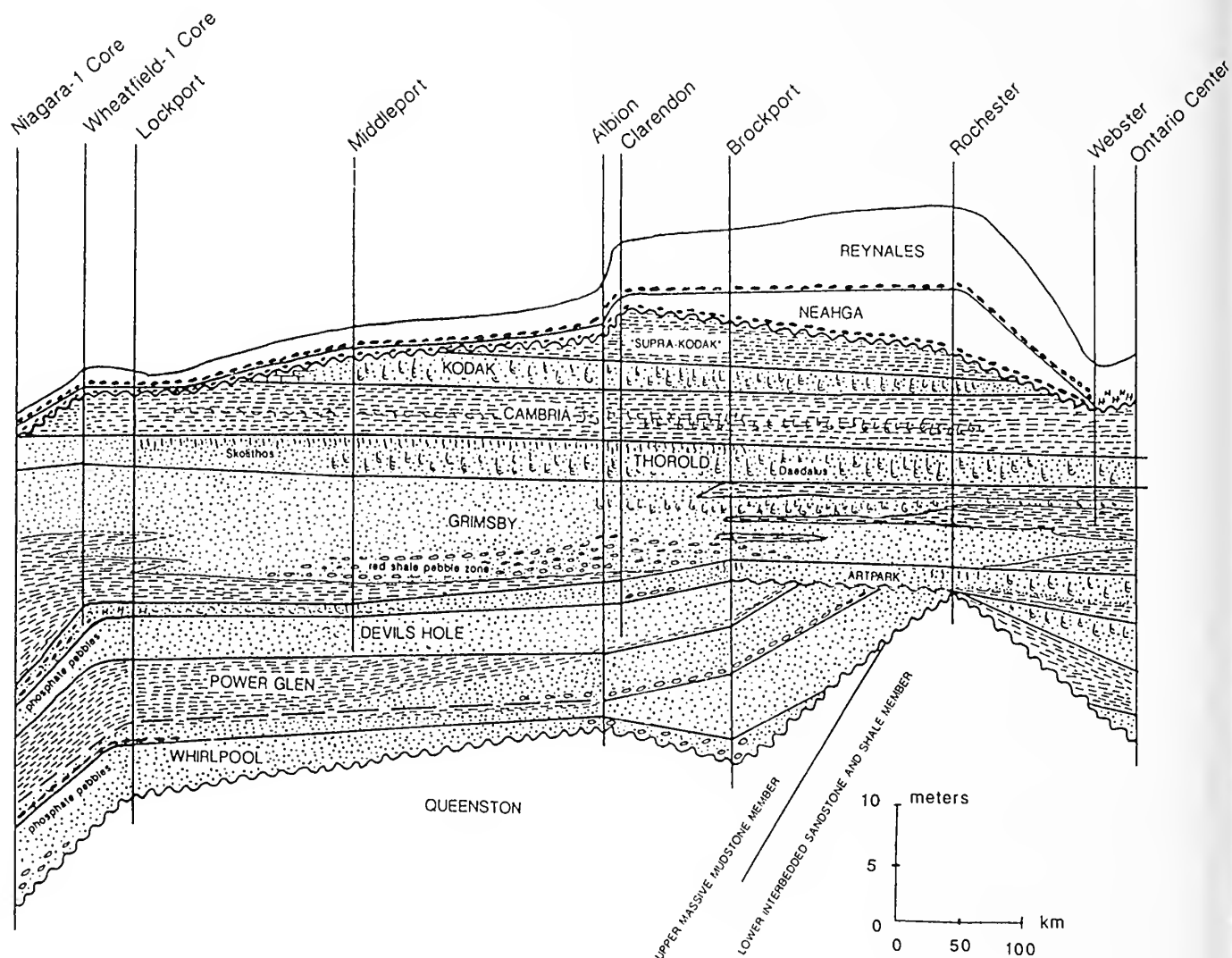


FIGURE 5—Cross-section of Medina Group (Sequence I) between Niagara Falls and Rochester, New York (see Figure 8.2 for outcrop belt map). Vertical lines show measured sections or drill cores.

mottled sandstones and maroon shales (Figures 5, 6). Thin, slightly hematitic to phosphatic shell lags occur at the tops of several small-scale (parasequence) cycles within the Grimsby Formation (see Duke and Fawcett, 1987; Duke and Brusse, 1987). This interval exhibits a marked upward-coarsening and -shallowing trend. Lower beds in western New York and Ontario are generally in a linguloid biofacies, whereas the top of the unit generally carries an *Arthrophyicus*-dominated ichnofacies and lacks body fossils (Figures 5, 6).

The base of the next subsequence (ID) is marked by the sharp lower contact of the widespread, thin (0.5 to 2.5 m) Thorold Sandstone (Figures 4–6). This formation was

earlier assigned to the Clinton Group by Gillette (1947) and Rickard (1975). The upper part of the Thorold Sandstone is a widespread interval of heavily burrowed sandstone with abundant *Arthrophyicus* trace fossils and the distinctive spreiten of *Daedalus* (which may have been produced by the same or a very similar organism to that which formed *Arthrophyicus*; A. Seilacher, personal comm., 1996). In Orleans County, vertical *Skolithos* burrows overlie the *Daedalus* traces, and to the west, near Lockport, Niagara County, the upper contact of the Thorold (*Daedalus* beds) is marked by a thin hash of linguloid brachiopod fragments and is overlain by maroon mudstones with abundant ostracodes that are

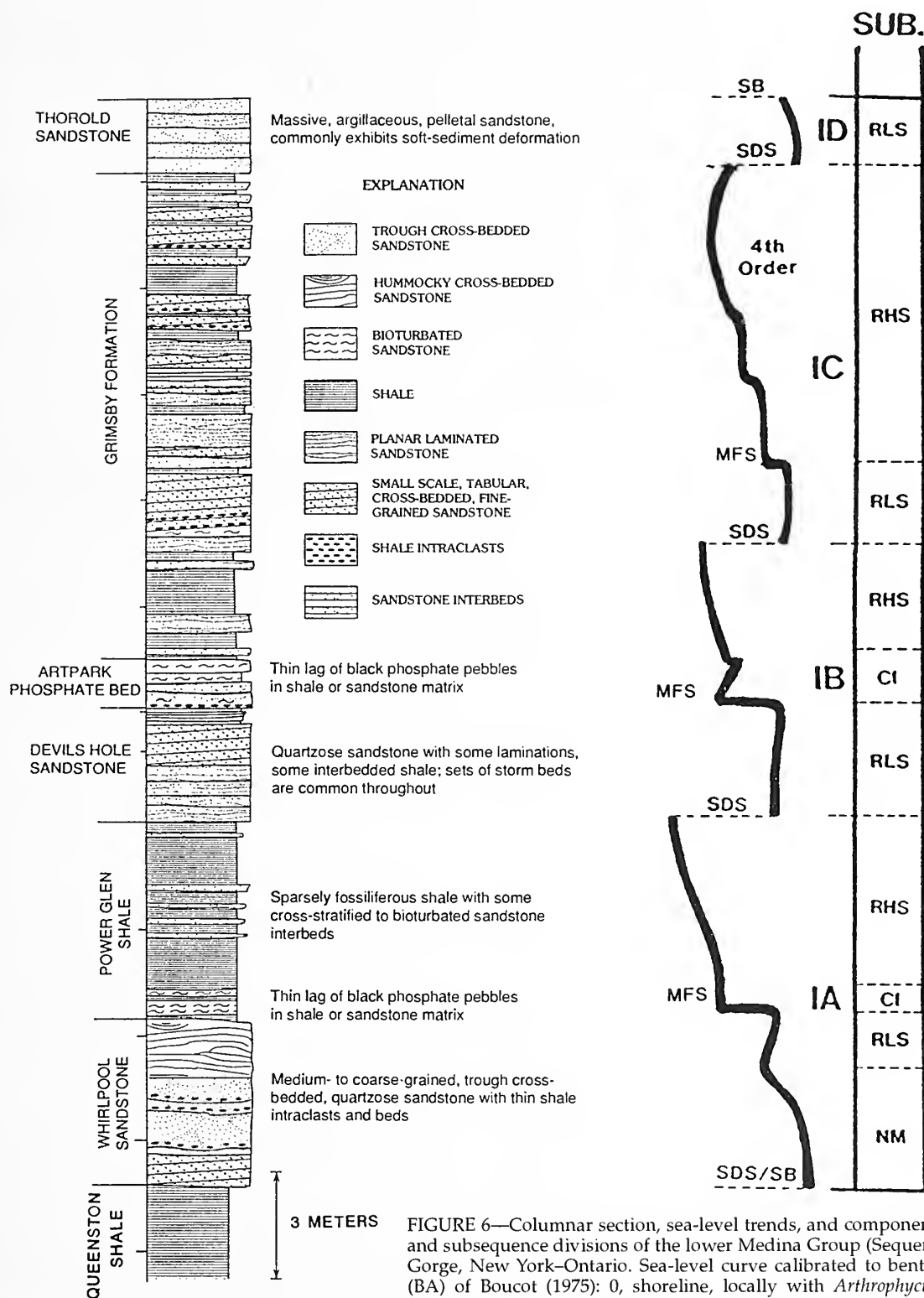


FIGURE 6—Columnar section, sea-level trends, and component systems tracts and subsequence divisions of the lower Medina Group (Sequence I) at Niagara Gorge, New York-Ontario. Sea-level curve calibrated to benthic assemblages (BA) of Boucot (1975): 0, shoreline, locally with *Arthropycus* and *Daedalus* (upper tidal flats); 1, lingulid; 2, *Eocoelia* assemblage with low-diversity, rhynchonellid brachiopod-crinoid associations; 3, *Pentamerus* assemblage with *Helopora*-diverse brachiopod associations; 4, diverse brachiopod-stricklandid biofacies; 5, monograptid-*Dicoelosia* or *Chorinda* community. Sea-level curve shows larger-scale cyclicity; deeper to left, shallower to right. Abbreviations for this and subsequent figures: Cht., chert; CI, condensed interval; CS, condensed section; EHS, early highstand; LHS, late highstand; LSST, lowstand of shelf margin systems tract; MFS, maximum flooding surface; RHS, relative highstand; RLS, relative lowstand; RLS A, relative sea-level curve based on smaller (5th-order and 6th-order cycles); RLS B, generalized sea-level curve for large-scale cyclicity; SB, major sequence boundary; SDS, surface of sea-level drop (i.e., minor sequence boundary); Sh., shale; SUB., subsequences (or 4th-order sequences) IA-ID; TST-CS, transgressive systems tract-condensed section of larger sequences. After Brett et al. (1990).

assigned to the overlying Cambria Shale (Figures 4, 5). Thus, an offshore bathymetric gradient to the west can be discerned from ichnofacies and limited skeletal biofacies of the uppermost Thorold Sandstone over a 100 km distance across western New York. The Thorold is considered to represent a transgressive sandstone comprised of laterally amalgamated, tidal channel sand bodies in which the *Daedalus* beds represent an interlude of relative sediment starvation and intense burrowing activity; the Cambria Shale represents very shallow, marginal marine muds that accumulated during highstand conditions. The Cambria Shale may locally contain body fossils and a marine ichnofacies. The unit reveals a biofacies transition from a *Daedalus* to a *Skolithos* to an ostracode-bivalve biofacies with rare *Rusophycus* and common ferruginous stromatolites.

The uppermost subsequence (IE) of the Medina Group consists of another widespread, calcareous, heavily bioturbated sandstone and overlying green to maroon, sandy shale that have collectively been assigned to the Kodak Sandstone. The Kodak lithology and succession resemble the older Thorold, and the two units have been miscorrelated in the past (see Kilgour, 1964; LoDuca and Brett, 1994). The Kodak Sandstone bundle may be a signature of the final shallowing of the Medina Group. The top shaley facies have been documented in drill cores to thicken considerably a few kilometers to the south (i.e., basinward) of the outcrop belt. Thus, these relative highstand shales of subsequence ID are truncated progressively northward by the regional angular unconformity at the Sequence I-II boundary (Figures 4, 5).

Facies that represent the deepest water conditions (maximum flooding) of Sequence I occur low in the Medina Group. Although poorly dated, the upper Whirlpool Sandstone, Power Glen, and lower Cabot Head gray shales contain the oldest diverse Silurian marine fauna in North America (probably of early-middle Rhuddanian; Kilgour and Liberty, 1981). Moreover, a comparable maximum highstand interval occurs low in the Silurian throughout much of the Appalachian region (see below). However, this deepening is too early to represent Johnson's (1996) first major eustatic sea-level highstand, which is dated as late Rhuddanian (Figure 1). Thus, this widespread deepening may reflect tectonically induced subsidence associated with a terminal pulse of the Taconic orogeny (Ettensohn and Brett, this volume). Generally upward-shallowing trends recorded in the upper part of the Medina Group in the late Rhuddanian are opposed to the global trend of eustatic sea-level rise (Johnson, 1996), and may have resulted from progradation of siliciclastics from the Taconic orogen. However, the highstand recorded by the Cambria Shale (subsequence IC) and coeval marginal to open marine

facies elsewhere (see below) may reflect transgression associated with the late Rhuddanian eustatic rise that partially countered the local progradational trend. The Cambria interval is quite widespread in the subsurface of New York, Pennsylvania, and Ohio (J. Castle, personal commun., 1997, In press).

SEQUENCE II.—The second sequence of the Silurian, the lower part of the Clinton Group (or lower Clinton sequence; Figures 7–9), is sharply demarcated from the underlying Medina by a regional angular unconformity that bevels successively older Medina units from west-central New York westward into Ontario (Brett et al., 1990; Figures 4, 5, 7). Sequence II is divided into two major subsequences—the Maplewood Shale–Wallington Limestone and lower Sodus Shale–Wolcott Limestone (Figure 9). Each of these subsequences commences with a phosphatic to hematitic basal lag, that is overlain by greenish-gray to purple clay shales. These, in turn, are abruptly overlain by hematitic limestone and skeletal pentamerid-rich limestones and shales (Figure 9).

A widespread layer of phosphatic nodules and fossil steinkerns, termed the "Densmore Creek Phosphate Bed" (LoDuca and Brett, 1994; Brett et al. 1995), sharply overlies the Sequence II basal unconformity throughout west-central New York. This bed is traceable between Rochester, New York, and St. Catharines, Ontario, a distance of about 150 km. Throughout its extent, the Densmore Creek phosphate bed is overlain by greenish-gray to dark gray, very platy shales (Maplewood–Neahga Shales; Figure 8). East of Rochester, the greenish Maplewood Shale pinches out abruptly, and the basal phosphatic bed merges with thin splayed phosphate beds that occur within the shales to form a condensed bed up to about 30 cm-thick. This unit, the Webster Bed (LoDuca and Brett, 1994), contains a mixture of quartz pebbles and sand grains; phosphatic nodules, many of them multi-generational; and hematitic-coated grains and ooids (LoDuca and Brett, 1994). In Niagara County, the Densmore Creek Bed becomes a thin (2–10 cm) sandy dolostone with abundant shells of the brachiopod *Hyattadina*. Near St. Catharines, Ontario, the bed is approximately 30 cm-thick, and contains abundant brachiopods and bryozoans in a sandy limestone. It is sharply overlain by a very thin interval of dark gray Neahga Shale. Phosphate-coated, sandy limestone clasts with abundant *Trypanites* borings occur near the base of this shale. Thus, a gradual offshore transition from an oolitic hematite lag bed to a phosphate nodule bed, to a phosphatic shelly limestone is present, as in many other condensed levels.

The hematitic Webster Bed, its lateral equivalent the Densmore Creek Phosphate Bed, and the somewhat thicker phosphatic beds at St. Catharines, Ontario, repre-

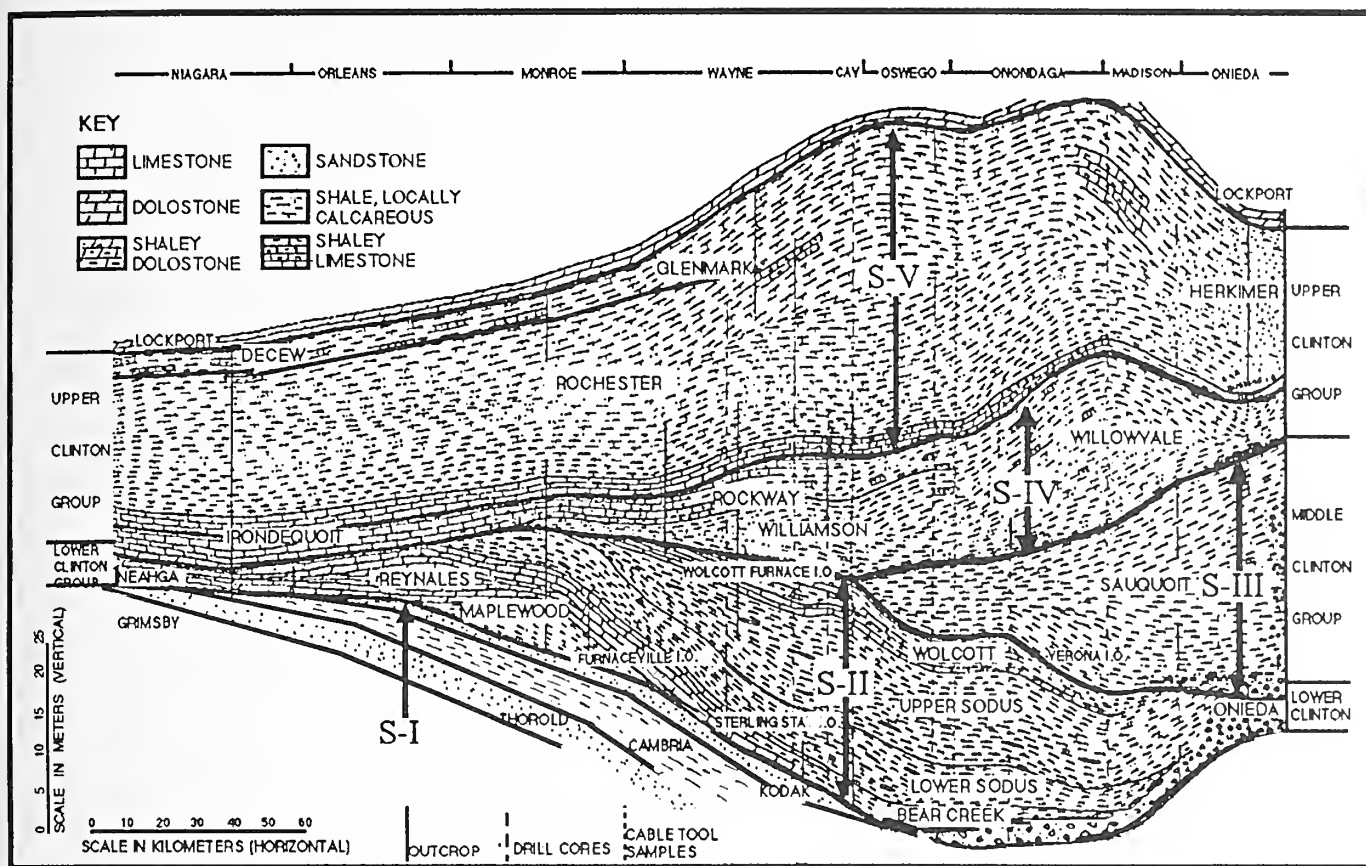


FIGURE 7—West-east cross-section of Clinton Group (Llandovery-lower Wenlock) in western to central New York (Niagara-Oneida Counties). Position of most of cross-section shown in Figure 8.2. Major depositional Sequences II-IV bounded by bold lines. Abbreviations: Cay, Cayuga County; i. o., iron ore; Sterling Sta, Sterling Station. After Gillette (1947).

sent a highly condensed, transgressive systems tract at the base of Sequence II. No evidence of deposits that comprise a shelf margin (lowstand) systems tract exists at the latitude of the outcrop belt.

Some of the most notable and persistent Silurian hematite beds occur within the lower part of the Clinton Group in subsequence IIA (Alling, 1947; Gillette, 1947; Figures 7, 8). The Furnaceville Iron Ore (Gillette, 1947) is a thin (10–30 cm), intraclast-bearing, fossil fragment, hematite-hematitic limestone (western facies) or sandy oolitic ironstone (eastern facies) near the base of the Reynales Formation (Figure 8). It passes westward near Rochester into phosphate pebble-bearing, brachiopod pack- and grainstones known as the Brewer Dock Member (Kilgour, 1964; LoDuca and Brett, 1994). It is overlain in some areas by greenish-gray shale that resembles the underlying Maplewood Shale. The Furnaceville and laterally equivalent Brewer Dock Limestone interval display some evidence of condensation (at least at an ecological scale duration) east of Rochester, and, as such, these deposits may be associated with the maximum

flooding at the base of the Sequence IIA highstand systems tract. There is an abrupt change in composition of conodont assemblages immediately above this bed. The Reynales Limestone and the underlying Maplewood Shale belong to a single ostracode zone (*Zygobolba excavata* Zone; Figure 10), and conodonts indicate assignment to the *Icriodella discreta-I. deflecta* Zone (middle-late Aeronian; Rexroad and Rickard, 1965; M.A. Kleffner, personal commun., 1996). This basal hematite and the laterally equivalent phosphatic limestone beds can be traced within New York State from the Sodus, Wayne County, area westward to Niagara County.

The upper member of the Reynales, the Wallington Limestone, is not younger than late Aeronian, as it falls into the *Icriodella discreta-I. deflecta* Zone (Brett et al., 1990; M.A. Kleffner, personal commun., 1997). The Wallington consists of mixed dolomitic, commonly cherty, wacke-, pack-, and grainstones; thin hematitic stringers; and some greenish-gray shale (Figures 8, 9). It becomes more shaley east of Sodus, New York, and grades into the Bear Creek Shale. Slightly ferruginous pack- and grainstone

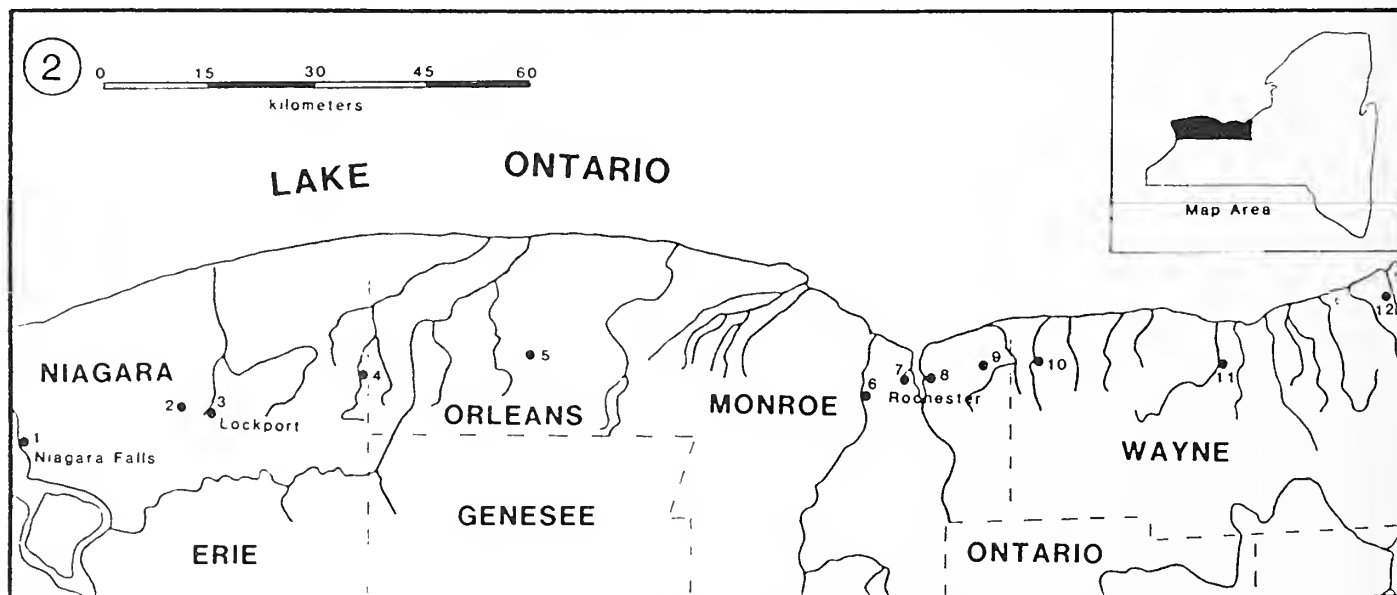
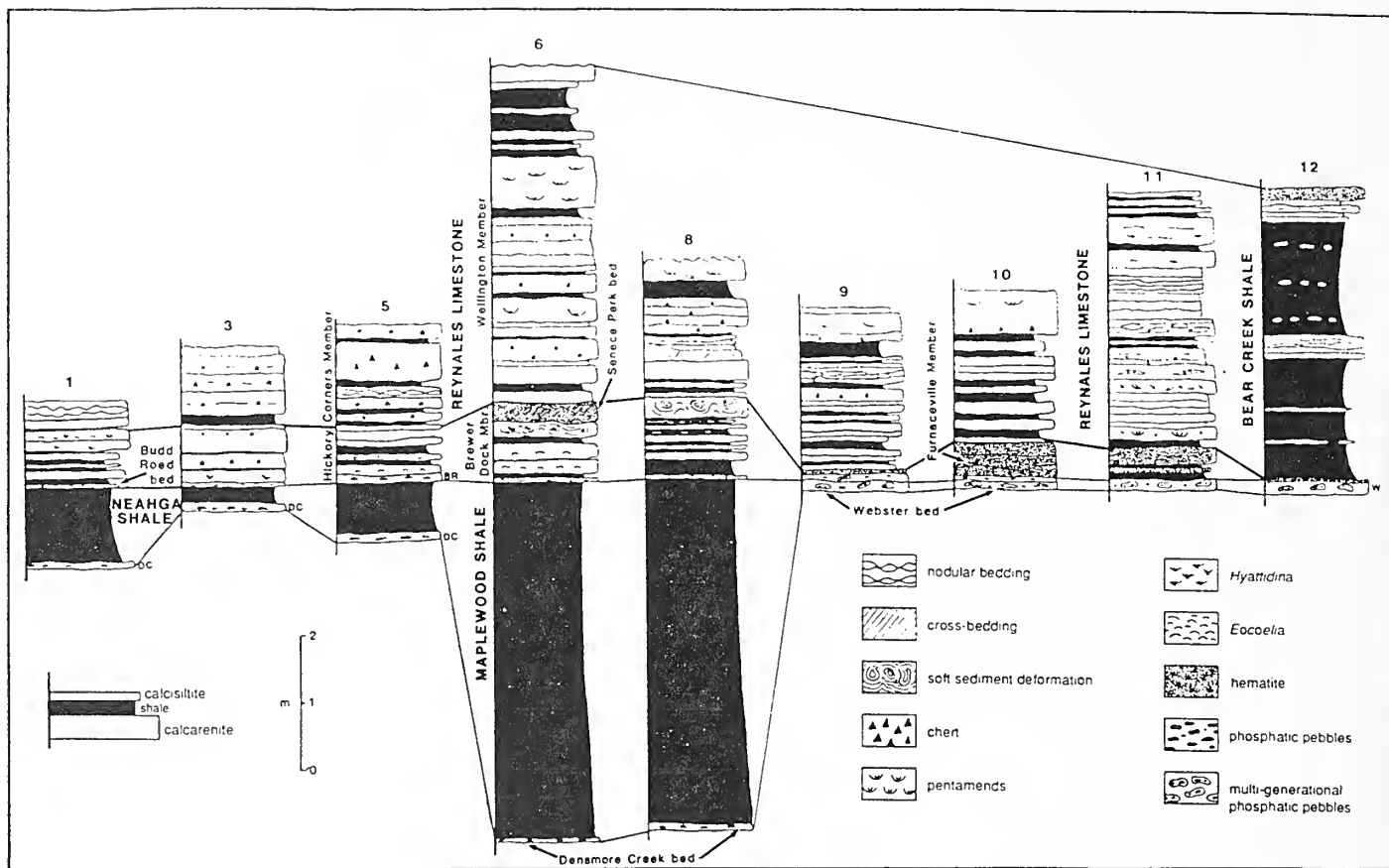


FIGURE 8—Relationships of the lower Clinton Group (Sequence IIA) in western New York. 1, Stratigraphic relationships of Maplewood–Neahga Shales, Reynales Limestone, and Bear Creek Formation; 2, Map of western New York with location of outcrops and drill cores in Figure 8.1. After LoDuca and Brett (1994, figs. 1 and 10).

beds are rich in *Pentamerus oblongus*, and have also yielded *Eocoelia* sp. cf. *E. intermedia* and the ostracode *Zygobolba excavata*. These taxa indicate assignment of the Wallington to the middle-late Aeronian (C1–C2). Thus, this unit is probably the local record of Johnson's (1996) second Silurian eustatic highstand.

Another thin hematitic bed, the Sterling Station Iron Ore of Gillette (1947), occurs near the top of the Wallington Limestone, just below its contact with the overlying purple and green lower Sodus Shale (Figure 7). Therefore, the Sterling Station hematite appears to occur within either a regressive or a progradational interval at the boundary between presumably more offshore, *Pentamerus*-rich (BA 3) limestones of the Wallington Member and *Eocoelia*-bearing (BA 2) Sodus Shale. However, a disconformity may actually intervene between the top bed of the Wallington or Sterling Station hematite and the underlying, slightly deeper water carbonates (*Pentamerus* brachiopod biofacies). The Sterling Station Iron Ore is probably correlative with a phosphatic limestone bed with an encrusted hardground on its upper surface that contains phosphate-stained, bored, and encrusted limestone cobbles in sections to the west in the Rochester area (LoDuca and Brett, 1994). Thus, there is sedimentologic evidence that the highest beds of the Wallington Limestone may be separated in time from those of most of the Reynales Formation, and that the Sterling Station bed is a part of the transgressive systems tract of subsequence IIB. Nonetheless, the lower Sodus Shale has yielded the same ostracodes of the *Zygobolba excavata* Zone and the same brachiopod (*Eocoelia* sp. cf. *E. intermedia*) as the underlying Wallington (Figures 4, 10; Gillette, 1947). Therefore, any discontinuity at this level must be relatively minor.

No major hematites appear in the lower Sodus Shale, but a slightly hematitic to phosphatic, nodule-bearing horizon occurs locally at the unconformable contact between the lower and upper divisions of the Sodus (Figures 8, 9). This slightly hematitic bed may represent a very thin transgressive lag deposit that formed after a period of erosion during a sea-level drop and subsequent rise. This lean hematite bed marks a shale-on-shale unconformity that is associated with the abrupt change from the *Zygobolba excavata* to the *Z. decora* Zones. Samples obtained from *Eocoelia*-dominated, coquinoid limestones that occur in shale tentatively identified as basal upper Sodus Shale near Rochester, New York, have also yielded *Pterospirifer celloni* Zone conodonts, and are thus assignable to the lower Telychian (probably C4; M.A. Kleffner, personal commun., 1997).

The upper Sodus Shale displays a transition into the overlying Wolcott Limestone, a second *Pentamerus*-bearing skeletal pack- and grainstone unit that is assignable to the *Z. decora* and *Eocoelia curtisi* Zones (Figures 9, 10). A thin

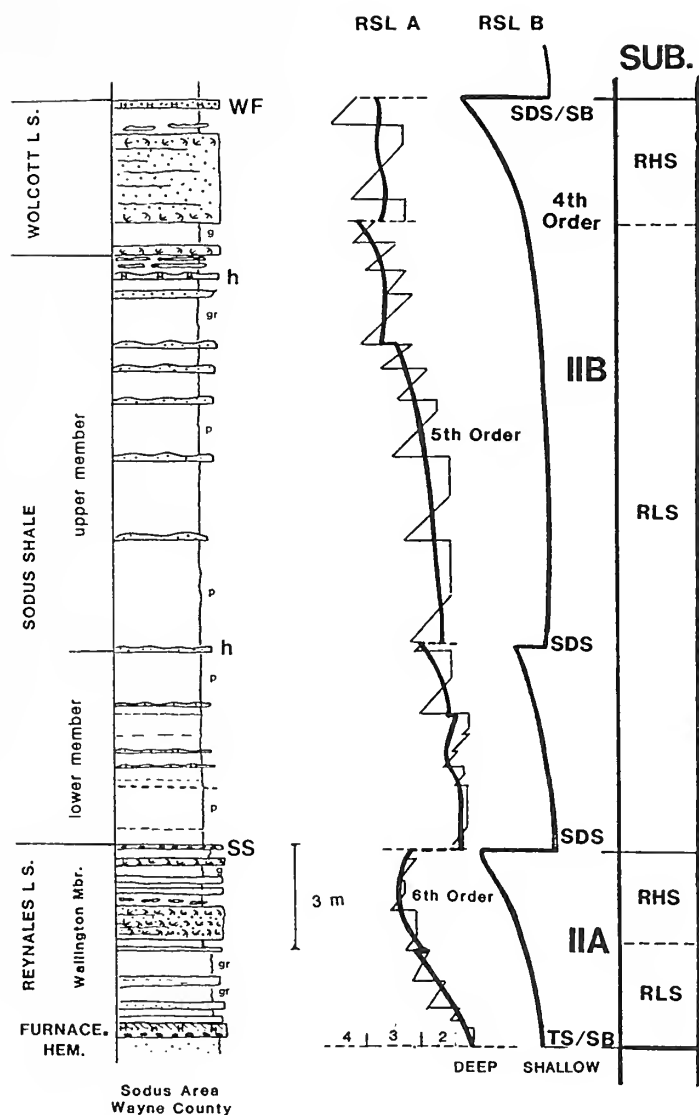


FIGURE 9—Columnar section, biostratigraphy, relative sea-levels, component systems tracts, and subsequence divisions of lower Clinton Group (Sequence II) in central New York. Sea-level curve is calibrated to benthic assemblages (BA); see Figure 6 explanation. Symbols for ironstone beds to right of stratigraphic column: h, hematitic limestone (unnamed); SS, Sterling Station Iron Ore; WF, Wolcott Furnace Iron Ore; other abbreviations in Figure 6.

hematitic limestone and shale succession occurs above the Wolcott Limestone; it was mined along Wolcott Creek and hence was named the Wolcott Furnace Iron Ore (Gillette, 1947). The Wolcott Furnace hematite occurs at a major flooding surface, as it lies between *Pentamerus*-rich limestones of the Wolcott and overlying greenish-gray shales that contain an offshore *Stricklandia* brachiopod association. Unfortunately, the upper part of these shales is removed under the unconformity at the base of Sequence III and the Sauquoit Shale of the middle Clinton Group. The Wolcott Limestone and Wolcott Furnace Ironstone, which

CLINTON OSTRACODE ZONES				
	NIAGARA COUNTY		MONROE COUNTY	
UPPER	PARAECHMINA SPINOSA ZONE ROCHESTER		PARAECHMINA SPINOSA ZONE ROCHESTER	
	MASTIGOBOLBINA TYPUS ZONE IRONDEQUOIT		MASTIGOBOLBINA TYPUS ZONE WILLIAMSON	
MIDDLE				
LOWER				
	ZYGOLBOLBA EXCAVATA ZONE REYNALES NEANGA		ZYGOLBOLBA EXCAVATA ZONE LOWER SODUS REYNALES FURNACEVILLE	
	WAYNE COUNTY		ONEIDA COUNTY	
UPPER	PARAECHMINA SPINOSA ZONE ROCHESTER		PARAECHMINA SPINOSA ZONE HERKIMER KIRKLAND	
	MASTIGOBOLBINA TYPUS ZONE IRONDEQUOIT WILLIAMSON		MASTIGOBOLBINA TYPUS ZONE WILLOWVALE WESTMOSELAND	
MIDDLE			MASTIGOBOLBINA LATA ZONE SAUQUOIT ONEIDA	
			ZYGOLBOLBA DECORA ZONE ONEIDA	
LOWER				

FIGURE 10—Ostracode zones of the Clinton Group in New York. Note unconformity between *Zygobolbina decora* and *Mastigobolbina lata* Zones, with *Z. emaciata* Zone (of the complete Rose Hill succession) missing, and between the *M. lata* and *M. typus* Zones, with *Bonnemaiia rudis* Zone missing. After Gillette (1947).

represent facies similar to those of the older Wallington, have been recognized by Johnson (1987, 1996) as the probable local signature of the third Silurian (early Telychian) sea-level highstand (Figures 1, 9). The discovery of *Pterospathodus celloni* Zone conodonts in the Wolcott and subjacent Sodus Shale (M.A. Kleffner, personal commun., 1997) is somewhat problematic, as Johnson's (1996) sea-level curve shows the third peak within the upper third of the older *Distamodus stauognathoides* Zone.

SEQUENCE III.—Near Syracuse an oolitic hematite bed about 40 cm-thick, named the Verona Station Iron Ore (Gillette, 1947), locally marks the unconformable contact between the Wolcott Furnace shales and the Sauquoit Shale (Sequence III; Figures 4, 7). This surface is considered to represent a major sequence boundary, because one ostracode zone appears to be missing at this formation boundary. The *Zygobolbina emaciata* Zone, which intervenes between the *Zygobolbina decora* and *Mastigobolbina lata* Zones in central Pennsylvania, is absent at this contact in New York (Figure 10). This boundary is only seen in a few outcrops and drill cores in central New York. The contact between a tongue of coarse sandstones and conglomerates of the Oneida Conglomerate that onlaps a major unconformity on Upper Ordovician Frankfort Shale in

central New York (e.g., in the famous roadcuts in Frankfort Gorge; Baarli and Johnson, 1996) likely represents the same sequence boundary. The Oneida Conglomerate may represent a transgressive systems tract locally preserved at the base of Sequence III in central New York.

Farther west, a thinner zone of hematitic ooids overlain by dark sandy shale with phosphate nodules occurs just below the Sauquoit Shale. A thin phosphatic ooid bed also occurs at the probable Sauquoit–Wolcott shale boundary in its westernmost outcrops. These beds appear to represent a basal transgressive lag and sediment-starved transgressive systems tract directly above the Sequence II–III boundary. Sandy phosphatic–hematitic conglomerate beds occur near the base of the Sauquoit Formation, and represent the early transgressive systems tract of Sequence III.

The overlying greenish-gray Sauquoit Shale and laterally equivalent Otsquago red sandstones and shales yield ostracodes of the *Mastigobolbina lata* Zone (Gillette, 1947; Figures 4, 10), conodonts of the *Pterospathodus celloni* Zone, and the brachiopods *Eocoelia curtisi* and *E. sulcata*. Thus, this interval clearly is early Telychian (C5). The presence of herringbone cross-beds in portions of the Otsquago suggests a tidally influenced shoreface setting. The Otsquago also includes highly ferruginous and phos-

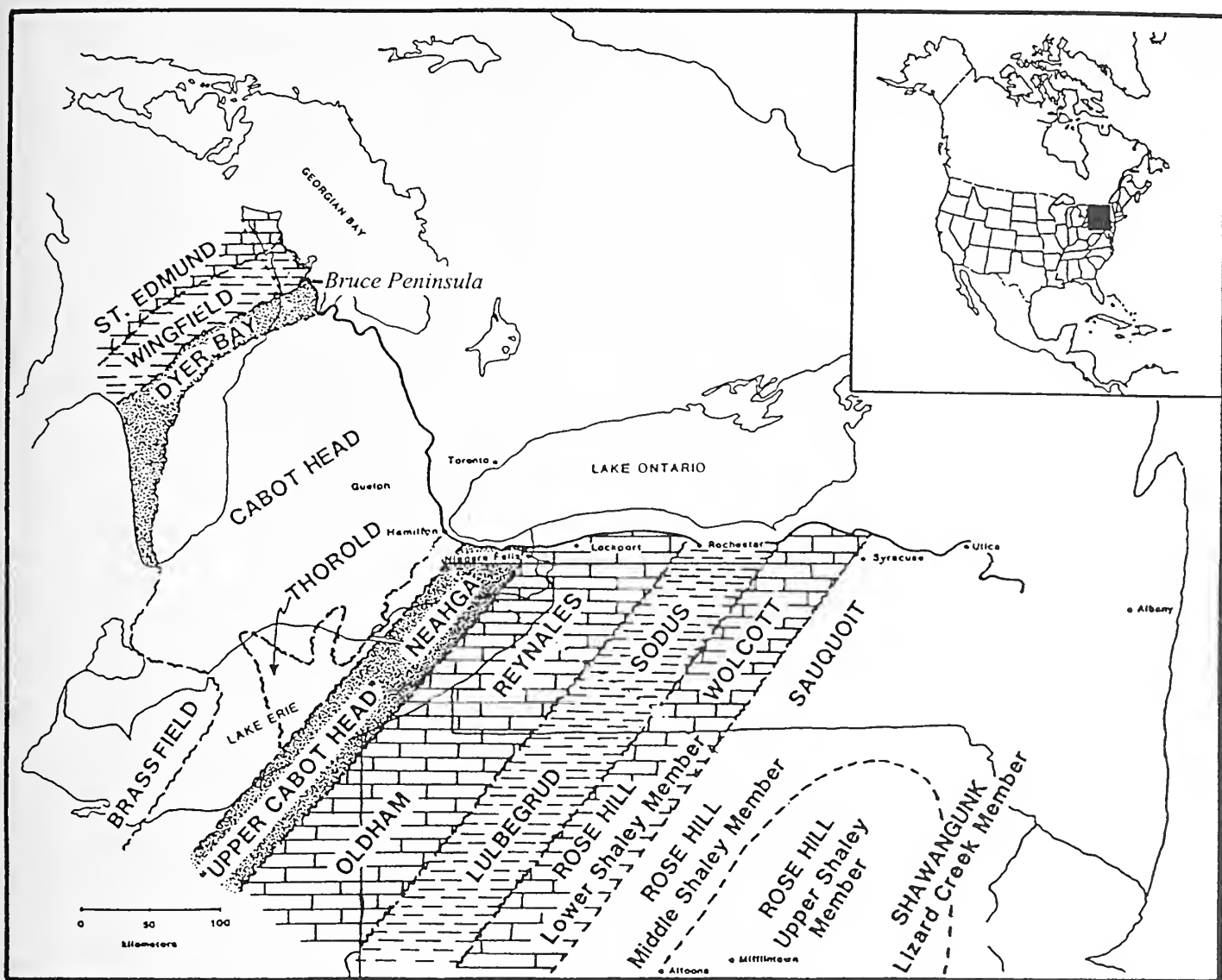


FIGURE 11—Subcrop map of strata beveled by late Llandovery Sequence IV. Note that area of maximum erosion from western New York to Bruce Peninsula, Ontario, delineates an arch-like feature. From LoDuca and Brett (1994, fig. 2).

phatic beds that may represent minor flooding surfaces (Muskatt 1969, 1972).

The western Sauquoit facies are greenish *Eocoelia*-rich (BA 2) shales with some sandstones and several beds of quartz and phosphate pebbles. These represent shallow, offshore, muddy environments. The marine transgression that created the accommodation space for the Sauquoit offshore mud facies is herein interpreted to record a minor sea-level rise in the middle Telychian that is not represented on Johnson's (1996) curve, but appears to be widespread in the Appalachian Basin (see below).

SEQUENCE IV.—A major, regional, angular unconformity forms the lower boundary of Sequence IV (Figures 4, 7). This erosion surface is probably coextensive with a re-

gional angular unconformity beneath the Dayton Limestone that has been mapped in Ohio and Kentucky on the east flank of the Cincinnati Arch (Lukasik, 1988) and a major unconformity below the Fossil Hill Formation in the Bruce Peninsula of Ontario (Lin and Brett, 1988; Brett et al., 1990; Figure 11). In New York, the Sequence III-IV boundary is the sharp basal contact of the Westmoreland Hematite on the Sauquoit Shale near Clinton and Utica, New York (Figures 12, 13). The absence of ostracodes of the *Bonnemaia rudis* Zone that occur in the upper Rose Hill Formation of Pennsylvania indicates that this contact in central New York is unconformable (Figures 4, 10). In west-central and western New York, this erosion surface completely truncates Sequence III (the Sauquoit Shale) and produces a Sequence II-IV unconformity (in Wayne

County). It then progressively bevels the Wolcott Furnace, Wolcott, upper Sodus (near Rochester), lower Sodus (west of Rochester), and Wallington and Brewer Dock (Niagara County), and finally oversteps the Neahga Shale to produce a Sequence I–IV unconformity near St. Catharines, Ontario (Lin and Brett, 1988; Figures 4, 11).

Detailed correlations have demonstrated that a major change in basin axis migration is also associated with the Sequence II–IV boundary (Goodman and Brett, 1994). Throughout deposition of the Medina Group and lower and middle Clinton Group sequences (Sequences I–III), both the eastern shoreline and the depocenter of successive subsequences shifted progressively eastward from southern Ontario to central New York State. This pattern reversed abruptly above the lower unconformity of Sequence IV. The depocenters of successively higher subsequences in the upper part of the Clinton Group (sequences IV and V) shift back westward toward western New York (Brett et al. 1990; Goodman and Brett, 1994).

The regionally angular nature of the lower unconformity of Sequence IV and reversal in the direction of basin axis migration immediately above the unconformity indicate that this surface is at least partly tectonic in origin and probably related to uplift and erosion of a peripheral bulge during the middle–late Llandovery (Brett et al., 1990; Goodman and Brett, 1994; Ettensohn and Brett, 1996, this volume). However, deposition of middle–late Telychian lowstand sandstone–conglomerate in the central Appalachians (see below) and overlying transgressive deposits indicate that the erosion surface is related to a widespread late Telychian (late C5–C6) fall and subsequent rise in sea-level (see sea-level curves of Johnson et al., 1990; Johnson, 1996; Ruppel et al., 1996; Figure 1).

The most widespread and notable oolitic hematite in the New York Silurian section is the Westmoreland iron ore, which overlies the Sequence IV basal unconformity (Figures 4, 7, 12, 13). This unit, formerly mined in the vicinity of Clinton, New York, probably gave rise to the term “Clinton hematites”, which has been used so extensively in the Appalachian region (Gillette, 1947). The Westmoreland is a complex unit that locally contains several beds up to 0.5 m-thick. It contains a series of decimeter-scale, oolitic hematite beds that alternate with dark greenish-gray shales and ferruginous dolostones, some of which consist of offshore, fossiliferous, arenaceous dolostone facies with diverse brachiopods and even monograptids. The Westmoreland is a condensed interval, not a single bed, and is the most typical example of a hematitic transgressive systems tract. Conodonts from this bed and the immediately overlying Willowvale Shale indicate to the lower *Pterospiriferus amorpho-*

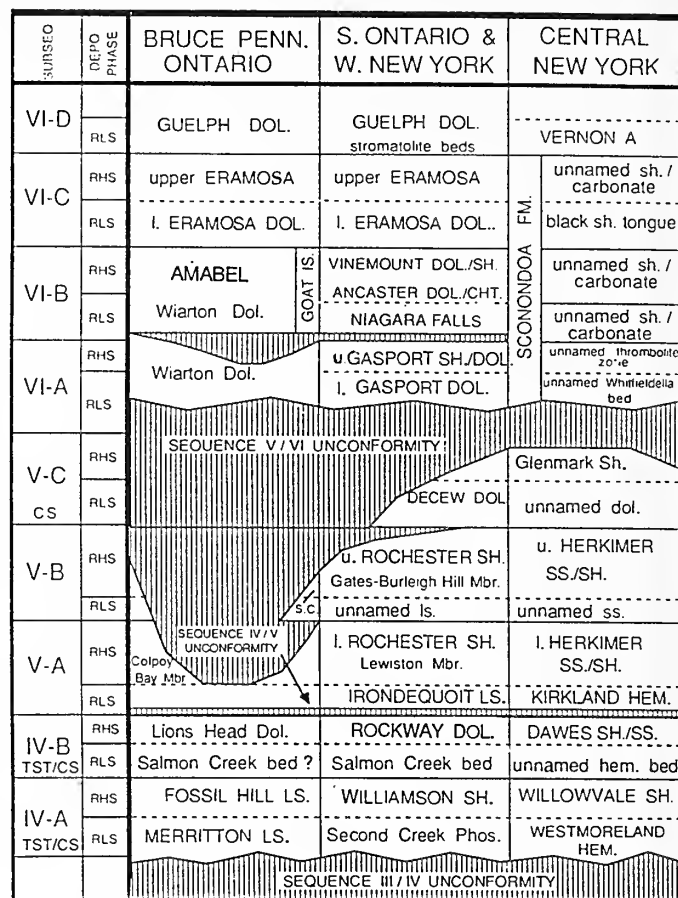


FIGURE 12—Sequence and subsequence divisions of the upper Clinton and Lockport Groups (sequences IV–VI) in Ontario and New York. Units scaled to relative time. Formation names capitalized. Abbreviations: SC, Stony Creek Member of Rochester Shale; other abbreviations in Figure 6. After Brett et al. (1990).

gnathoides Zone, with possibly some admixture of *P. celloni* Zone elements. These conodonts indicate a late Telychian (C6) age (Berry and Boucot, 1970; Rickard, 1975; Kleffner, 1988; M.A. Kleffner, personal commun., 1997; Figures 4, 12).

In more basinal sections in west-central New York, the Westmoreland grades into a very thin (2–5 cm) but persistent basal conglomerate that is rich in quartz and phosphatic pebbles. This is the Second Creek Bed (Lin and Brett, 1988; Brett et al. 1995; Figure 12). This complex bed is considered to represent an extremely condensed transgressive lag.

The Westmoreland is overlain by greenish-gray shale of the Willowvale Formation (Figures 4, 12, 13). This unit contains a diverse (BA 2–4) fauna of brachiopods with the lowest appearance of many taxa typical of the “upper Clinton–Lockport fauna” (see Gillette, 1947; Muskatt, 1972; Eckert and Brett, 1988; Brett and Baird,

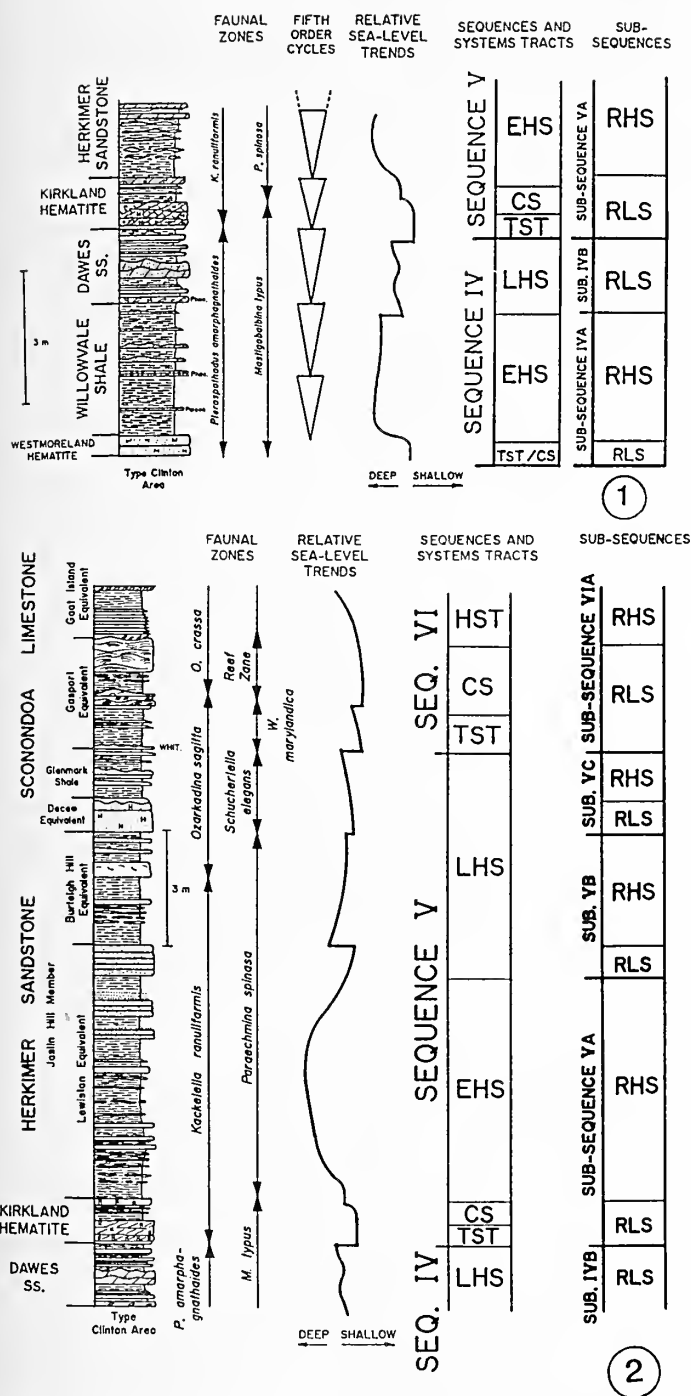


FIGURE 13—Upper Clinton Group at Clinton, central New York State. 1, Columnar section, biostratigraphy, relative sea-levels, and component systems tracts and subsequences of Sequence IV; 2, Columnar section, biostratigraphy, relative sea-levels, component systems tracts, and sub-sequence divisions of Sequences IV–VI. Abbreviations: *Palaeo.*, *Palaeocyclus* (corals); H, hematite; Phos., phosphatic pebbles; other abbreviations in Figure 6 explanation. After Goodman and Brett (1994).

1995). The Willowvale Shale contains ostracodes of the *Mastigobolbina typus* Zone, the small discoidal rugose coral *Palaeocyclus rotuloides*, and *Pterospiriferus amorphognathoides* Zone conodonts (Figures 4, 13). To the west, the Willowvale grades into green and dark gray or black, laminated Williamson Shale with the graptoloids *Monograptus clintonensis* and *Retiolites genitizianus*, all of which point to a late Telychian age (Figures 4, 12). The Willowvale–Williamson interval records the deepest water conditions in the Silurian of New York, and is evidently the local signature of the late Telychian maximum highstand, which has been identified in nearly all locations globally (Johnson et al., 1985, 1990a, 1990b; Johnson, 1996). Thin, apparently bentonitic clays near the base of the Williamson Shale (Brett et al., 1994) may also signal renewed tectonism in the Appalachian hinterland (Ettensohn and Brett, this volume). It is notable that ash beds may also occur in late Telychian strata elsewhere in the Appalachians (see section on Alabama, below).

The Williamson–Willowvale interval (subsequence IVA) has been interpreted as the early (maximum) highstand of Sequence IV (Brett et al., 1990; Figure 12). The higher parts of this depositional sequence (subsequence IVB) are recorded in rhythmically bedded, argillaceous carbonates and shales of the Rockway Formation in western New York (Figures 4, 12, 14). These beds contain *Costistricklandia* sp. cf. *C. lirata* and conodonts of the upper *Pterospiriferus amorphognathoides* Zone (Rexroad and Rickard, 1965; Kleffner, 1991). Hence the Rockway may be latest Telychian or earliest Wenlock. It generally displays a distinctive basal lag bed with phosphatic nodules and scattered quartz granules (Salmon Creek bed; Lin and Brett, 1988; Brett et al., 1995; Figure 12).

Eastward in central New York, the Rockway Formation becomes increasingly shaley. Easternmost sections contain thin- to medium-bedded intervals of hummocky cross-laminated, fine-grained dolomitic sandstone or sandy dolostone near Clinton, New York, where the interval is designated the Dawes Formation (Figures 4, 12, 13; Zenger, 1971). The basal Salmon Creek Bed becomes increasingly enriched in hematitic ooids and pebble-sized quartz grains, and it locally resembles and has been confused with the younger Kirkland Iron Ore (Figures 12, 13).

SEQUENCE V.—The upper part of the Clinton Group sharply overlies the Rockway–Dawes succession (Figures 4, 7, 12). The contact is everywhere marked by a planar to slightly wavy erosion surface (Brett et al., 1995), but there does not appear to be any major regional beveling of beds or a major biostratigraphic discontinuity at this disconformity in New York.

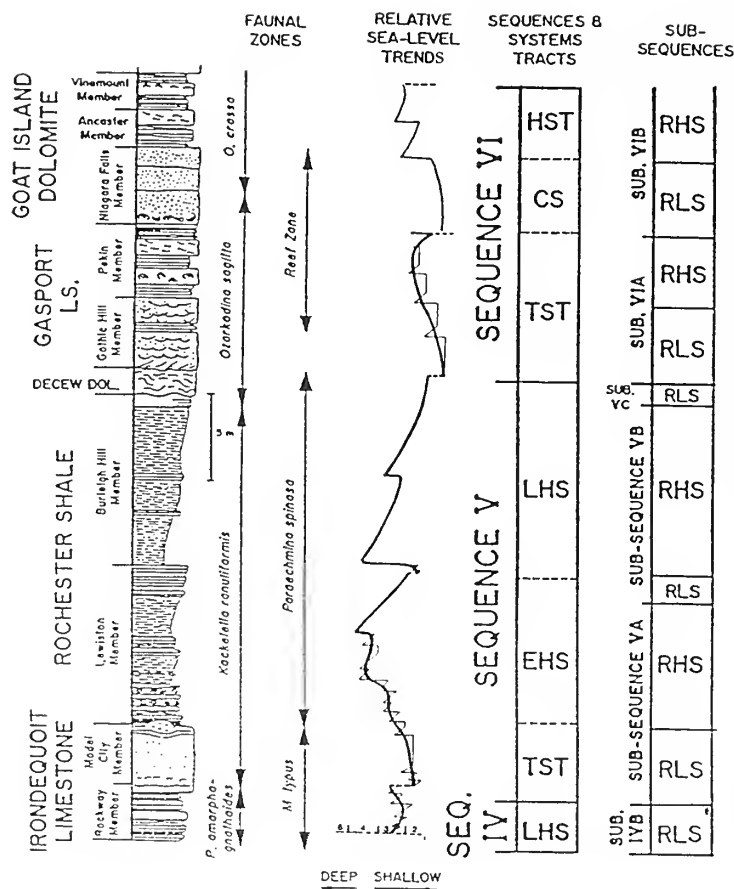


FIGURE 14—Columnar section, biostratigraphy, relative sea-levels, component systems tracts, and subsequences of Sequences IV–VI at Niagara Gorge, New York–Ontario. Abbreviations in Figure 6 explanation. Relative sea-level curve is calibrated by benthic assemblages (BA) 1–5; see Figure 9 for explanation. After Brett et al. (1990).

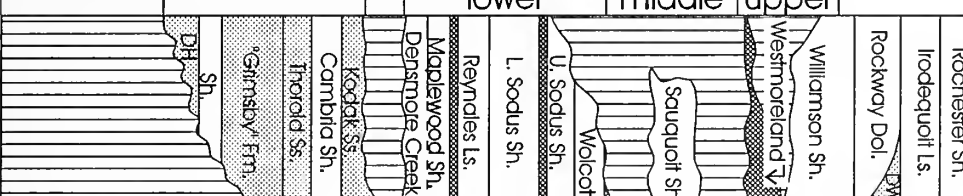
In western New York and Ontario, Sequence V comprises three formations and has been divided into three subsequences (Figures 12, 14). The Irondequoit Limestone consists of 2–3 m of crinoidal pack- or grainstone with small bryozoan–algal mud mounds. It is early Wenlock on the basis of the ostracode *Paraechmina spinosa* and *Kockellella ranuliformis* Zone conodonts near its top (Rexroad and Rickard, 1965; Kleffner, 1991; Figures 12–14). The overlying Rochester Shale ranges from less than 1 m (near Hamilton, Ontario) to over 40 m east of Rochester, and consists of medium to dark gray mudrock. The lower member, or Lewiston Member, displays bundles of fossiliferous (bryozoan- and brachiopod-rich) argillaceous limestone in the lower third and near its top (Figure 14). The contact with overlying dark, sparsely fossiliferous mudstone of the Burleigh Hill Member is sharp (Brett et al., 1995). The DeCew Formation is a thin (1–3 m), sparsely fossiliferous, argillaceous dolostone with distinctive slump folding

(Zenger, 1965) (Figures 12, 14). In west-central New York, the upper DeCew appears to grade into the medium gray, highly fossiliferous Glenmark Shale, which closely resembles the Rochester but carries a distinctive fauna with the brachiopods *Nucleospira pisiformis* and *Whitfieldella* sp. cf. *W. marylandica* (Brett et al. 1990, 1995). The *Kockellella ranuliformis*–*Ozarkodina sagitta* (s.l.) conodont zonal boundary occurs in the upper Rochester Shale slightly below the DeCew Dolostone (Rexroad and Rickard, 1969). Hence the Rochester and DeCew apparently are Sheinwoodian.

In central New York near Clinton, the Irondequoit Limestone becomes a ferruginous, crinoidal–bryozoan-rich dolostone (Zenger, 1971) and passes eastward into the fossiliferous Kirkland Iron Ore, the highest formally named ironstone bed of the Clinton Group. Near Herkimer, this bed apparently grades laterally into a *Skolithos*-bearing, coarse quartz arenite of the basal Herkimer Formation (Zenger, 1971; Brett and Goodman, 1996; Figures 12, 13). Also in the Clinton–Utica area, the Rochester Formation becomes increasingly sandy and contains lower, middle, and upper sandstone tongues of the Joslin Hill Member of the Herkimer Formation (Zenger, 1971; Brett and Goodman, 1996). Both the lower and middle sandstone tongues are capped locally by hematitic, crinoidal–bryozoan grainstones that closely resemble the older Kirkland Iron Ore. It is notable that these beds immediately underlie eastward-extending tongues of gray fossiliferous shale and thus represent flooding surfaces in the Rochester–Herkimer interval. Similarly, the DeCew–Glenmark interval persists eastward as a shaly, fossiliferous zone with very minor phosphatic–hematitic beds near its base.

The DeCew–Rochester interval is everywhere sharply overlain by crinoidal grainstones or dolomitic sandstones of the basal Lockport Group (Sequence V; Figures 12, 14). This contact is also a regional angular unconformity, with the DeCew–Rochester succession completely cut out between St. Catharines and Hamilton, Ontario. A similarly sharp but more cryptic contact separates the Glenmark Shale from overlying shales and limestones of the Sconondoa–Ilion (McKenzie) Members in central New York (Brett et al., 1990; Brett and Goodman, 1996), and a comparable contact exists in Pennsylvania and Maryland (discussed below).

FIGURE 15—(opposite) Llandovery–lower Wenlock from west-central New York to southeast Tennessee. Light gray stipple is sandstone facies; dark gray is ironstone (hematite ore) beds. Abbreviations: SH, Sheinwoodian; WEN, Wenlock; P.G., Power Glen Shale; other abbreviations in Figures 4 and 6.

LLANDOVERY											W	SERIES																																																																																																																																																																																																																																																																																																																																																																																																																																																																																																																																																																																																																																																																																																																																																																												
RHUDDANIAN				AERONIAN			TELYCHIAN				SH.	STAGES																																																																																																																																																																																																																																																																																																																																																																																																																																																																																																																																																																																																																																																																																																																																																																												
A1	A2	A3	A4	B1	B2	C1	C2	C3	C4	C5	C6	OSTRACODE ZONE																																																																																																																																																																																																																																																																																																																																																																																																																																																																																																																																																																																																																																																																																																																																																																												
				Z. erecta		Z. excavata	Z. decora	Z.	M. lata	B. rudis	M. typus																																																																																																																																																																																																																																																																																																																																																																																																																																																																																																																																																																																																																																																																																																																																																																													
simplex				l. irregulari		l. discreta	P. celloni			P. amorpho-gnathoides		CONODONT ZONE																																																																																																																																																																																																																																																																																																																																																																																																																																																																																																																																																																																																																																																																																																																																																																												
MEDINA GRP.												CLINTON																																																																																																																																																																																																																																																																																																																																																																																																																																																																																																																																																																																																																																																																																																																																																																												
lower												middle	upper																																																																																																																																																																																																																																																																																																																																																																																																																																																																																																																																																																																																																																																																																																																																																																											
												Rochester Sh.	Iroquoit Ls.	Rockway Dol.	Williamson Sh.	Westmoreland V.	Sauquoit Sh.	Wolcott	L. Sodas Sh.	Reynolds Ls.	Maplewood Sh.	Dennison Creek	Kodak Ss.	Cambria Sh.	Thorold Ss.	Glimsby Fm.	Sh.	DH																																																																																																																																																																																																																																																																																																																																																																																																																																																																																																																																																																																																																																																																																																																																																												
TUSCARORA												ROSE HILL	MIFF.																																																																																																																																																																																																																																																																																																																																																																																																																																																																																																																																																																																																																																																																																																																																																																											
lower shaley mbr.												upper shaley	middle shaley	Cabin Hill	Cresup-town	Costanaea Member	Cam	PG	Tuscarora	Ss.	lower	Tuscarora	Sh.	Rochester Sh.	Keefer ss.	Dawes - equivalent																																																																																																																																																																																																																																																																																																																																																																																																																																																																																																																																																																																																																																																																																																																																																														
TUSCARORA												ROSE HILL																																																																																																																																																																																																																																																																																																																																																																																																																																																																																																																																																																																																																																																																																																																																																																												
upper												Upper shaley	"Center"	Cabin Hill (?)	Cacapon Ss.	upper	Tuscarora	lower	Tuscarora	Ss.	lower	Tuscarora	Sh.	dark shale	Keefer ss.	UPPER																																																																																																																																																																																																																																																																																																																																																																																																																																																																																																																																																																																																																																																																																																																																																														
RUNKLES GAP												PASSAGE CREEK	UPPER																																																																																																																																																																																																																																																																																																																																																																																																																																																																																																																																																																																																																																																																																																																																																																											
MASSANUTTEN SANDSTONE																																																																																																																																																																																																																																																																																																																																																																																																																																																																																																																																																																																																																																																																																																																																																																																								
TUSCARORA												R.H.	EAGLE ROCK																																																																																																																																																																																																																																																																																																																																																																																																																																																																																																																																																																																																																																																																																																																																																																											
lower												upper	middle	lower	upper	upper	lower	upper	lower	upper	lower	upper	lower	upper	upper	upper	upper	upper	upper	upper	upper	upper	upper	upper	upper	upper	upper	upper	upper	upper	upper	upper	upper	upper	upper	upper	upper	upper	upper	upper	upper	upper	upper	upper	upper	upper	upper	upper	upper	upper	upper	upper	upper	upper	upper	upper	upper	upper	upper	upper	upper	upper	upper	upper	upper	upper	upper	upper	upper	upper	upper	upper	upper	upper	upper	upper	upper	upper	upper	upper	upper	upper	upper	upper	upper	upper	upper	upper	upper	upper	upper	upper	upper	upper	upper	upper	upper	upper	upper	upper	upper	upper	upper	upper	upper	upper	upper	upper	upper	upper	upper	upper	upper	upper	upper	upper	upper	upper	upper	upper	upper	upper	upper	upper	upper	upper	upper	upper	upper	upper	upper	upper	upper	upper	upper	upper	upper	upper	upper	upper	upper	upper	upper	upper	upper	upper	upper	upper	upper	upper	upper	upper	upper	upper	upper	upper	upper	upper	upper	upper	upper	upper	upper	upper	upper	upper	upper	upper	upper	upper	upper	upper	upper	upper	upper	upper	upper	upper	upper	upper	upper	upper	upper	upper	upper	upper	upper	upper	upper	upper	upper	upper	upper	upper	upper	upper	upper	upper	upper	upper	upper	upper	upper	upper	upper	upper	upper	upper	upper	upper	upper	upper	upper	upper	upper	upper	upper	upper	upper	upper	upper	upper	upper	upper	upper	upper	upper	upper	upper	upper	upper	upper	upper	upper	upper	upper	upper	upper	upper	upper	upper	upper	upper	upper	upper	upper	upper	upper	upper	upper	upper	upper	upper	upper	upper	upper	upper	upper	upper	upper	upper	upper	upper	upper	upper	upper	upper	upper	upper	upper	upper	upper	upper	upper	upper	upper	upper	upper	upper	upper	upper	upper	upper	upper	upper	upper	upper	upper	upper	upper	upper	upper	upper	upper	upper	upper	upper	upper	upper	upper	upper	upper	upper	upper	upper	upper	upper	upper	upper	upper	upper	upper	upper	upper	upper	upper	upper	upper	upper	upper	upper	upper	upper	upper	upper	upper	upper	upper	upper	upper	upper	upper	upper	upper	upper	upper	upper	upper	upper	upper	upper	upper	upper	upper	upper	upper	upper	upper	upper	upper	upper	upper	upper	upper	upper	upper	upper	upper	upper	upper	upper	upper	upper	upper	upper	upper	upper	upper	upper	upper	upper	upper	upper	upper	upper	upper	upper	upper	upper	upper	upper	upper	upper	upper	upper	upper	upper	upper	upper	upper	upper	upper	upper	upper	upper	upper	upper	upper	upper	upper	upper	upper	upper	upper	upper	upper	upper	upper	upper	upper	upper	upper	upper	upper	upper	upper	upper	upper	upper	upper	upper	upper	upper	upper	upper	upper	upper	upper	upper	upper	upper	upper	upper	upper	upper	upper	upper	upper	upper	upper	upper	upper	upper	upper	upper	upper	upper	upper	upper	upper	upper	upper	upper	upper	upper	upper	upper	upper	upper	upper	upper	upper	upper	upper	upper	upper	upper	upper	upper	upper	upper	upper	upper	upper	upper	upper	upper	upper	upper	upper	upper	upper	upper	upper	upper	upper	upper	upper	upper	upper	upper	upper	upper	upper	upper	upper	upper	upper	upper	upper	upper	upper	upper	upper	upper	upper	upper	upper	upper	upper	upper	upper	upper	upper	upper	upper	upper	upper	upper	upper	upper	upper	upper	upper	upper	upper	upper	upper	upper	upper	upper	upper	upper	upper	upper	upper	upper	upper	upper	upper	upper	upper	upper	upper	upper	upper	upper	upper	upper	upper	upper	upper	upper	upper	upper	upper	upper	upper	upper	upper	upper	upper	upper	upper	upper	upper	upper	upper	upper	upper	upper	upper	upper	upper	upper	upper	upper	upper	upper	upper	upper	upper	upper	upper	upper	upper	upper	upper	upper	upper	upper	upper	upper	upper	upper	upper	upper	upper	upper	upper	upper	upper	upper	upper	upper	upper	upper	upper	upper	upper	upper	upper	upper	upper	upper	upper	upper	upper	upper	upper	upper	upper	upper	upper	upper	upper	upper	upper	upper	upper	upper	upper	upper	upper	upper	upper	upper	upper	upper	upper	upper	upper	upper	upper	upper	upper	upper	upper	upper	upper	upper	upper	upper	upper	upper	upper	upper	upper	upper	upper	upper	upper	upper	upper	upper	upper	upper	upper	upper	upper	upper	upper	upper	upper	upper	upper	upper	upper	upper	upper	upper	upper	upper	upper	upper	upper	upper	upper	upper	upper	upper	upper	upper	upper	upper	upper	upper	upper	upper	upper	upper	upper	upper	upper	upper	upper	upper	upper	upper	upper	upper	upper	upper	upper	upper	upper	upper	upper	upper	upper	upper	upper	upper	upper	upper	upper	upper	upper	upper	upper	upper	upper	upper	upper	upper	upper	upper	upper	upper	upper	upper	upper	upper	upper	upper	upper	upper	upper	upper	upper

SEQUENCES IN CENTRAL PENNSYLVANIA AND WESTERN MARYLAND

EARLIER WORK.—The central Appalachian fold belt extends through central Pennsylvania and western Maryland and has excellent exposures of Silurian strata (Figures 2, 15). Indeed, most of the ridges of the Valley and Ridge Province are underlain by resistant Lower Silurian Tuscarora Sandstone. Studies of Silurian stratigraphy in Pennsylvania commenced in the 1830s with the work of H.D. Rogers. Rogers (1858) divided the Lower Silurian into the "Levant Series", roughly the Tuscarora Sandstone, and the "Surgent Series", approximately the equivalent of the Clinton Group in New York and with most of the significant iron ore beds. Subsequently, important studies of stratigraphy and biostratigraphy of the Lower Silurian of Pennsylvania and Maryland included those of Ulrich and Bassler (1923), Swartz (1923), Swartz and Swartz (1931), and Swartz (1934a, 1934b), all of whom emphasized ostracode zonation in attempts to correlate the thick Rose Hill and Mifflintown Formations into the better-known sections in New York (Figure 10). The seminal work of Hunter (1970) helped define lithofacies patterns in the subsurface of the central Appalachians. More recently, studies by Cotter (1983, 1988, 1991, this volume) and Cotter and Link (1993) have elucidated sedimentologic aspects and small-scale cyclicity of Silurian rocks, especially those of the ferruginous strata in central Pennsylvania. Brett et al. (1990) and Goodman and Brett (1994, 1996) attempted to place the Silurian strata of the central Appalachians into the framework of depositional sequences and subsequences recognized in New York and Ontario. The following sections summarize the present status of these litho- and biostratigraphic studies.

SEQUENCE I.—The Tuscarora Sandstone is a thick (200–300 m), lithologically variable siliciclastic wedge (Figures 15, 16, 29). To the northwest near the Allegheny Front, the formation consists of interbedded sandstone, siltstone, and shale with marine trace fossils that suggest fully marine to somewhat restricted (brackish water?) environments (Cotter, 1983a; Figure 16). The Tuscarora becomes an increasingly coarse-grained, massive to trough cross-stratified sandstone and conglomerate to the southeast in Pennsylvania. These facies are inferred to represent shelf sand-wave environments (Cotter, 1983a; Figure 16). These deposits pass laterally to the northeast into the basal, coarse sandstones and conglomerates of the Shawangunk Formation; the latter have been interpreted as subaerial braidplain deposits (Cotter, 1983a). Thus, a full spectrum of depositional environments from continental

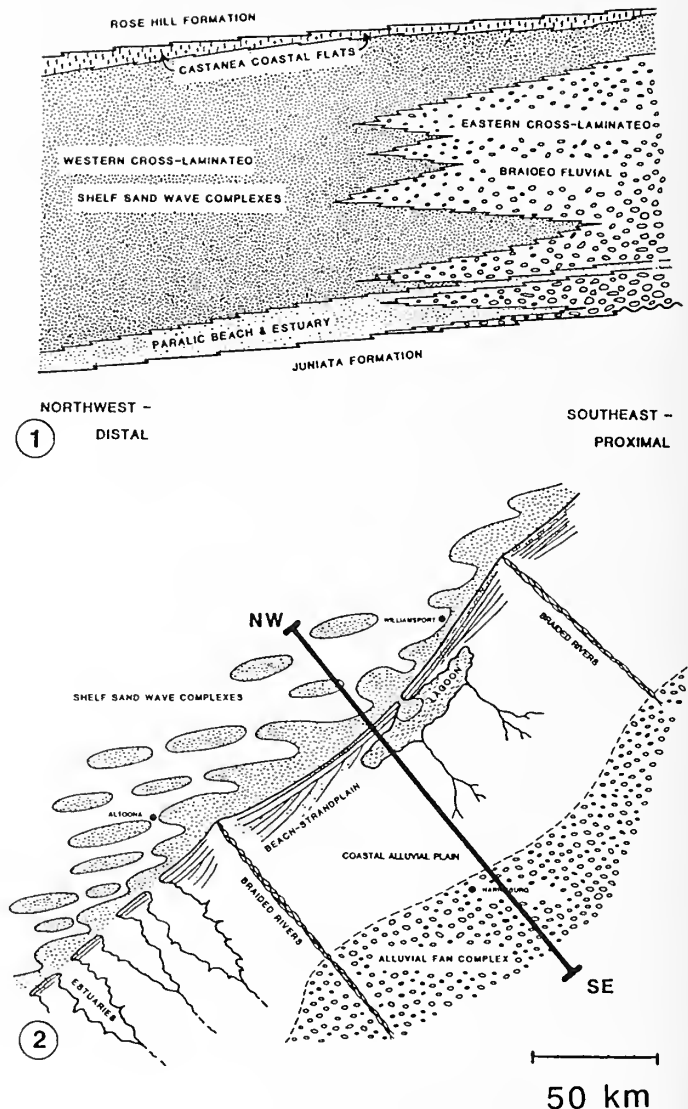


FIGURE 16—Tuscarora Formation in Pennsylvania. 1, Cross-section of Tuscarora Formation across the valley and ridge from northwest-southeast with facies interpretation. Note southeast-extending tongues of marine-influenced facies near base and top of formation; 2, Inferred paleogeography for Tuscarora Sandstone. Note line of cross-section in Figure 16.11. Adapted from Cotter (1983).

to fully subtidal marine are represented in the Tuscarora Sandstone.

Despite the much greater thickness, northwestern exposures of the Tuscarora Formation (more than 200 m-thick) display some striking similarities with the Medina Group (15–30 m) in New York. A succession somewhat comparable to that of the Medina Group occurs in the Tuscarora at Mill Hall, Pennsylvania, the most distal outcrop (Figure 17). The lower part of this succession consists of massive, trough cross-bedded quartz arenite, possibly correlative with the Whirlpool in western New

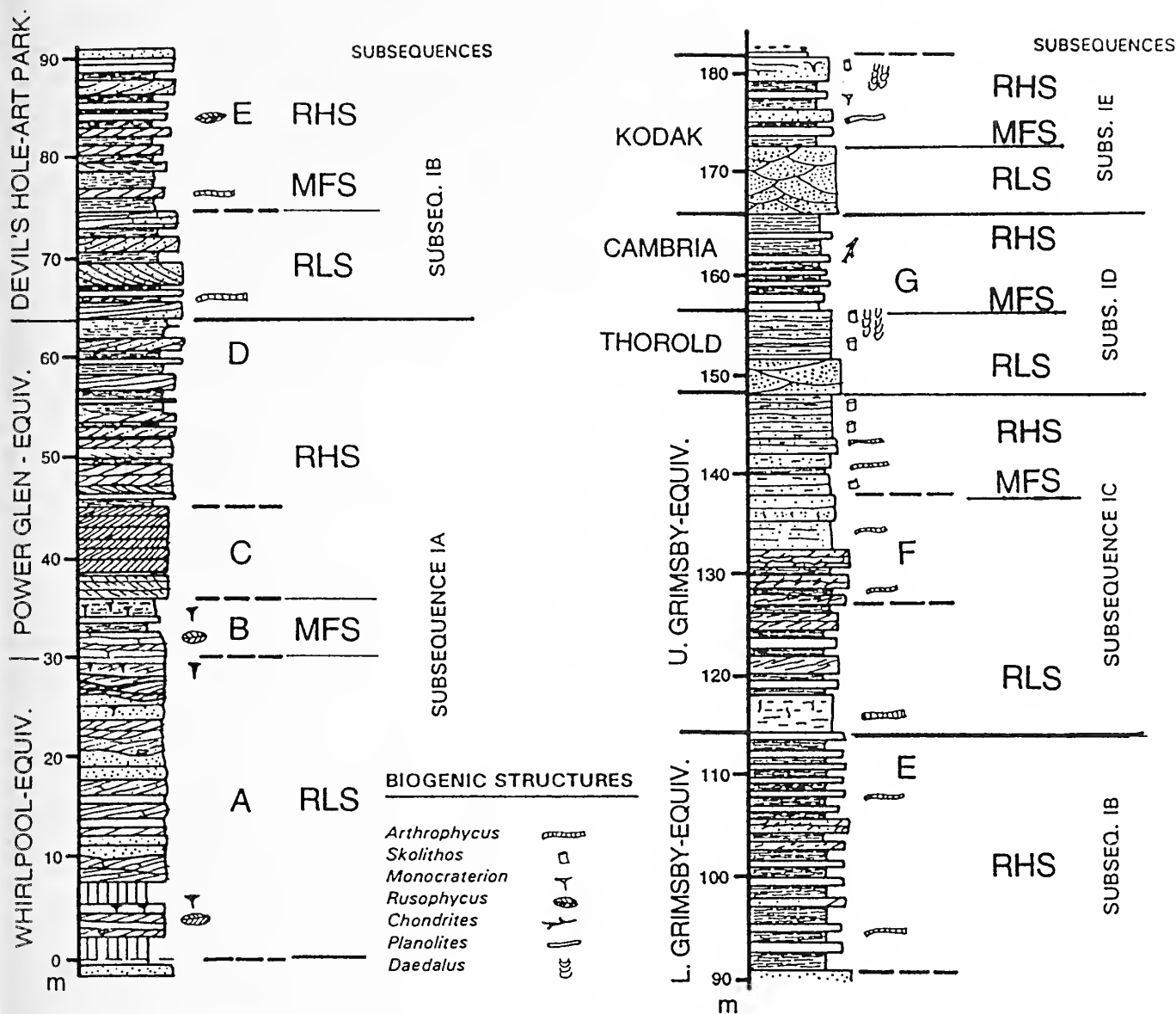


FIGURE 17—Tuscarora Sandstone at Mill Hill, Pennsylvania, with distribution of sandstones (stippled). Explanation: diagonal ruling, tabular cross-bedded; concave-up surfaces, trough cross-bedded; and mudstones (black), and various trace ichnogenera. Units A–G of Cotter (1983; see text for discussion). Probable lithostratigraphic equivalents of Medina Group in western New York indicated to left of columns; sequence stratigraphic term abbreviations explained in Figure 6. Adapted from measured section in Cotter (1983a).

York. A sharp change to a 30 m-thick interval of dark gray shales with interbedded, cross-bedded sandstones about 32 m above the base of the Tuscarora may correlate with the basal flooding surface of the Power Glen–Cabot Head Shale of New York and Ontario (Brett and Goodman, 1996). Both appear to record the first major Silurian marine transgression in the Appalachian Basin (subsequence IA). As noted above, this deepening may be due to tectonic subsidence, and does not appear to correlate with Johnson's (1996) earliest Silurian sea-level highstand.

Overlying hummocky cross-stratified quartz arenites and shales appear in the approximate position of

the Devils Hole and Grimsby Sandstones of the New York Medina Group (subsequences IB and IC; Figure 17). The upper 43 m of the Tuscarora that were assigned by Cotter (1983a) to the Castanea Member consist of red to reddish-gray, trough cross-bedded bioturbated sandstone. These beds were interpreted by Cotter (1983) as coastal-flat sandstones. At Mill Hall, a dusky, reddish-gray sandstone bed within this interval exhibits thorough bioturbation (large *Daedalus* and *Arthropycus*; identified as *Diplocraterion* by Cotter, 1983a; see Brett and Goodman, 1996). This bed may correlate with the main *Daedalus* interval in the Thorold Formation (base of subsequence ID)

in New York. This sandstone is overlain by about 8 m of reddish sandy shale and argillaceous sandstone that is perhaps equivalent to the Cambria Shale that overlies the Thorold in New York. The latter correlations are supported by subsurface correlations (J. Castle, personal communication, 1997; In press). Finally, the Castanea Member is capped by about 3 m of heavily burrowed (including small *Daedalus*), reddish-gray sandstone and sandy shales. This unit appears to correspond to the Kodak Formation, the uppermost formation in the Medina Group in west-central New York. It is further notable that a thin layer of bluish-gray-weathering, phosphatic nodules occurs at the upper contact of the Tuscarora with the Rose Hill Shale. This bed, which is probably correlative with the Densmore Creek phosphate bed of western New York, marks a major transgressive surface-sequence boundary at the top of Sequence I.

SEQUENCE II.—Much of the Lower Silurian in central Pennsylvania and western Maryland consists of a clay shale-dominated succession assigned to the Rose Hill Formation (Figures 15, 18). The Rose Hill Formation is a relatively thick (300–350 m), poorly differentiated interval of greenish-gray to maroon clay shales that is probably middle Aeronian–latest Telychian and which may range into the early Wenlock (Berry and Boucot, 1970). Rose Hill strata record a general marine transgression and a major influx of fine-grained siliciclastics, but a reduction of sand and coarser-grained sediments. Hence Rose Hill deposition may be associated with erosional lowering of relief during a tectonically quiescent interlude. Carbonate- and hematite-rich intervals are less prominent than in the New York sections of equivalent Clinton Group strata, but two major packages of thin- to medium-bedded, laminated to hummocky cross-stratified hematitic sandstone have been recognized. These units are the Cabin Hill and Center Members (see Cotter 1988, 1991, 1996) that separate the informally recognized (Cotter, 1983b, 1988) lower, middle, and upper shaly members of the Rose Hill Formation (Figures 15, 18).

The Rose Hill is particularly rich in ostracodes, and the succession of ostracodes in Maryland and Pennsylvania was detailed by Ulrich and Bassler (1923), Swartz and Swartz (1931), Swartz (1934a, 1934b). Ostracode biostratigraphy provides the primary means to correlate members of the Rose Hill with Clinton Group units in New York sections and elsewhere (Figure 10). Based upon ostracode zonation, the five lithological subdivisions of the Rose Hill can be correlated with units of the lower-middle parts of the Clinton Group in west-central New York. Contrary to Hunter's (1970) correlation of the Reynales and Wolcott Limestones with the Cabin Hill and Center Members, respectively, ostracode biostratig-

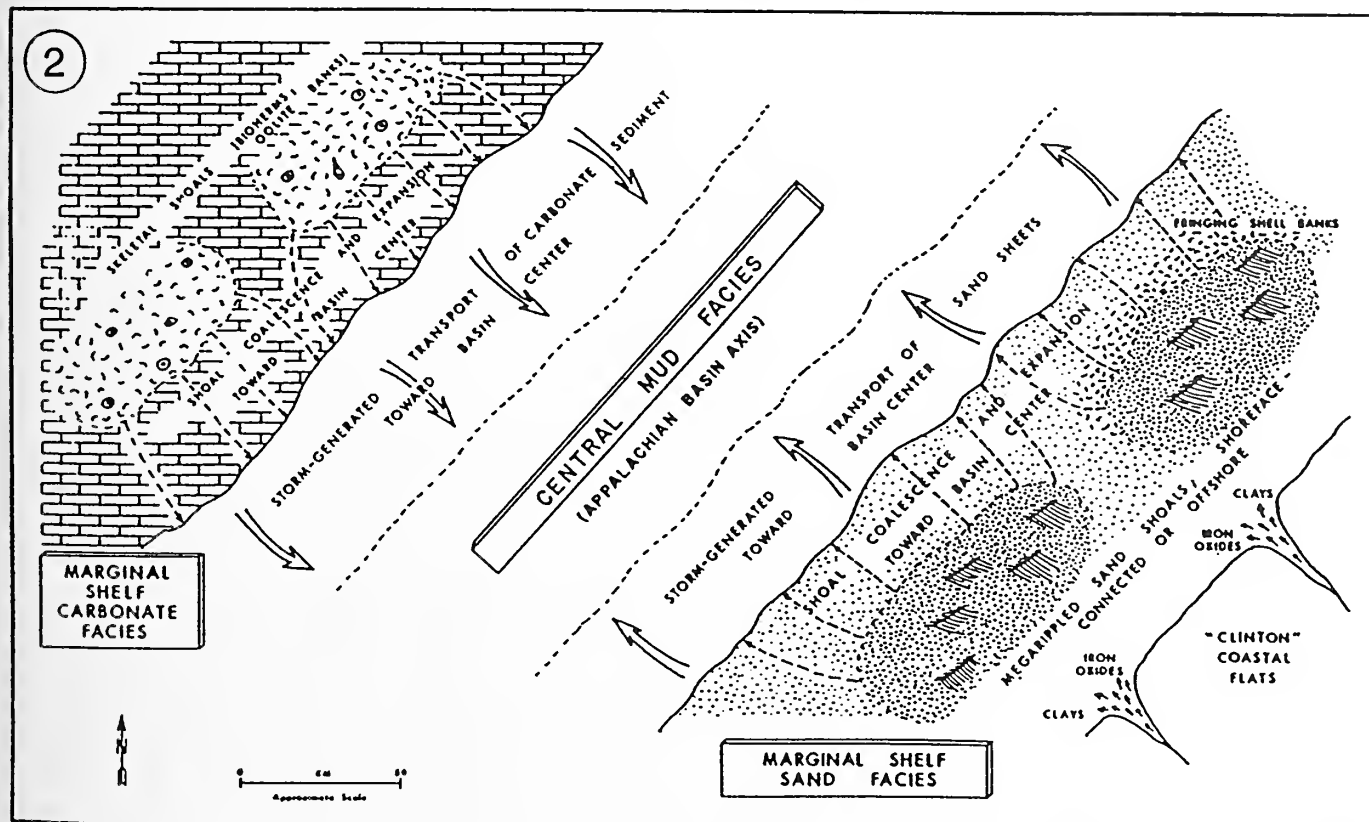
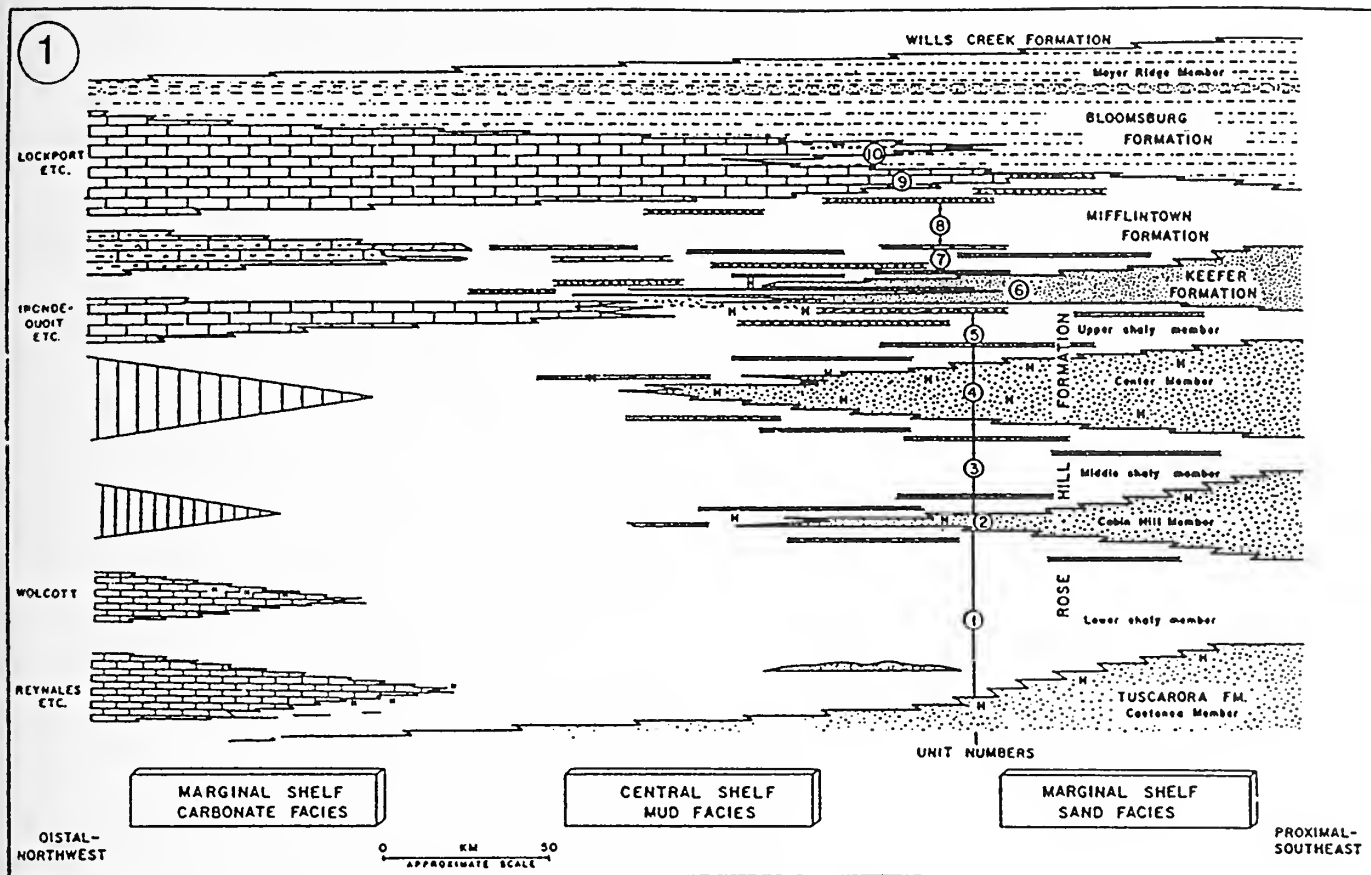
raphy indicates that the entire Maplewood–Wolcott Furnace interval (Sequence II) in New York is equivalent only to the lower shaly member of the Rose Hill (see Figures 4, 15, 18, 29). The Cabin Hill and Center Member sandstones are interpreted by Brett et al. (1990) as lowstand sandstones. These sandstones appear to divide the Rose Hill into three depositional sequences equivalent to sequences II, III, and IV and to the lower, middle, and upper Clinton intervals of New York, respectively (Brett et al., 1990).

The lower shaly member of the Rose Hill Formation (ca. 60–100 m-thick) is poorly exposed, but where seen, it is a greenish to maroon clay shale with very minor, thin, calcareous sandstones. Lithologically, much of this interval closely resembles the thinner but partially equivalent lower and upper Sodus Shale of central New York (Figures 15, 29). The lower shaly member bears a moderately diverse fauna dominated by small brachiopods, tentaculitids, and ostracodes that are suggestive of shallow water, inner-shelf environments (Benthic Assemblage 2 or *Eocoelia* biofacies of Boucot, 1975).

Three ostracode zones are recognized in this lower shale interval (Ulrich and Bassler, 1923; Swartz and Swartz, 1931). These zones are the *Zygobolbina erecta*, *Z. excavata*, and *Z. decora* Zones. The *Z. erecta* Zone has not been recognized in New York, and may be absent at the basal unconformity of Sequence II (Figures 10, 18). The *Z. excavata* Zone of the lower member is broadly equivalent to the Maplewood (Neahga) Shale–Reynales Limestone interval, which also contains *Z. excavata* (Gillette, 1947). As yet, no distinctive condensed interval that would correspond to the Furnaceville or Sterling Station Hematites is recognized in Pennsylvania. However, a ferruginous sandstone and oolitic ironstone, the Cresuptown ironstone, occurs at this approximate position in the lower Rose Hill near Cumberland, Maryland (Swartz, 1923; Berry and Boucot, 1970; Figure 20).

The *Zygobolba decora* Zone of the lower Rose Hill is the equivalent of the Sodus Shale–Wolcott interval in New York (Figure 18). Further study is required to determine whether or not any distinctive markers occur in this interval that would facilitate detailed correlations. At present,

FIGURE 18—(opposite) 1, Northwest-southeast cross-section of Aeronian–Ludlow (Clinton–Rose Hill and Lockport–Mifflintown) across central Pennsylvania. Tongues of sandstone (Cabin Hill, Center, and Keefer Members) that prograded into the basin from the southeast correspond to sequence-bounding unconformities in northwest; tongues of carbonate extending into basin from northwest are approximately equivalent to tops of coarsening-up sandstone tongues; H is hematitic beds. 2, Appalachian Foreland Basin in Pennsylvania with relationships to southeast margin shelf sand, central mud (= Rose Hill belt), and northwest carbonate facies belts. After Cotter (1983b).



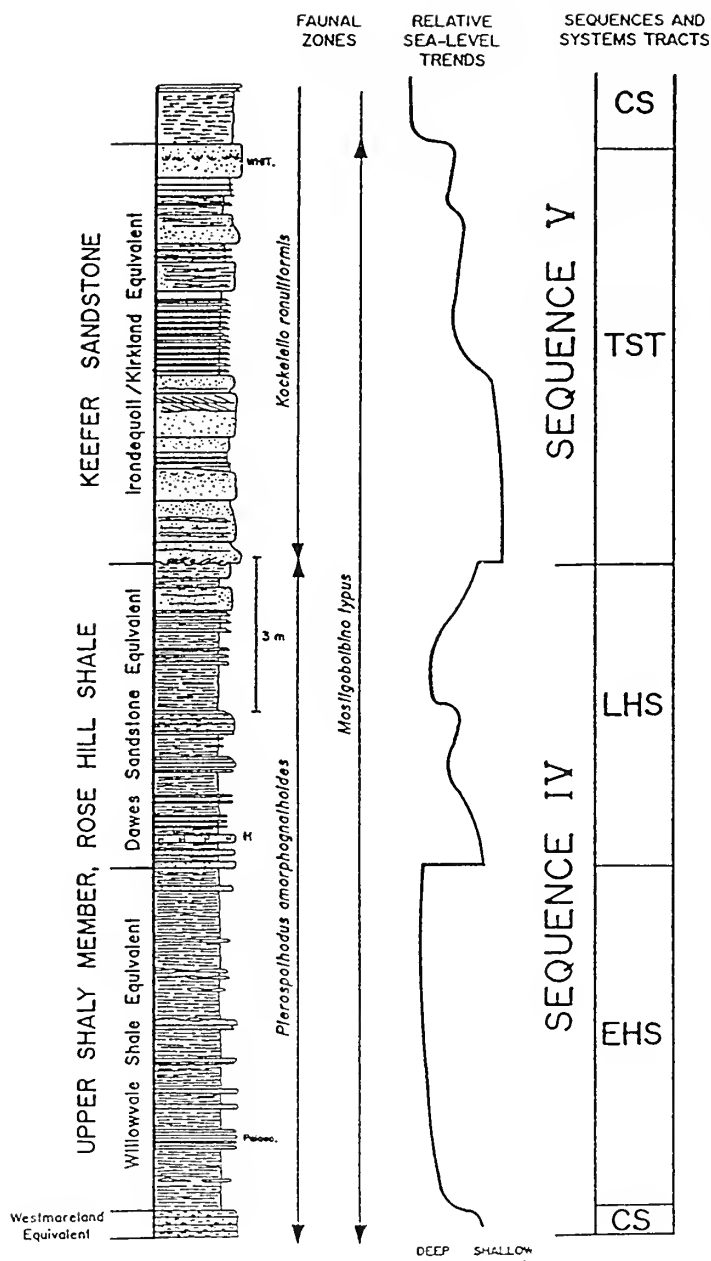


FIGURE 19—Columnar section, biostratigraphy, relative sea-levels, component systems tracts, and subsequences of Sequences IV at Allenwood, Pennsylvania. Abbreviations: *Palaeo.*, *Palaeocyclus* (corals); H, hematite; other abbreviations in Figure 6.

we can only note that the two well-defined carbonate intervals in Sequence II in New York are poorly defined in the lower Rose Hill (Figure 18). We suspect that this reflects the relatively proximal position of the Rose Hill in central Pennsylvania. During deposition of the lower Rose Hill, this region lay almost entirely within the inner-shelf mud belt. In the subsurface of western Pennsylvania and eastern Ohio, however, *Pentamerus*-rich crinoidal limestones (Packer Shell or Oldham Limestone) interfinger

with the lower Rose Hill (Crab Orchard Group) Shale (Lukasik, 1988; Figures 15, 29). Thus, the subsurface region of western Pennsylvania and Ohio probably lies along depositional strike with the lower Clinton sections near and east of Rochester, New York (i.e., northwest of the inner-shelf mud belt of the Rose Hill).

SEQUENCE III.—The Cabin Hill Member, which consists of ferruginous sandstones and sandy shales, contains ostracodes of the *Zygobolbina emaciata* Zone (Swartz and Swartz, 1931), an interval that has not been identified in the New York Clinton Group (Figures 10, 18, 29). This sandy interval probably represents deposition of coarser-grained siliciclastics with a drop in relative sea-level that produced the Sequence II–III unconformity in New York (Figure 18). The tongue of Oneida Conglomerate at Frankfort Gorge in New York (Baarli and Johnson, 1996) may signal the same lowstand–early transgressive event as the Cabin Hill Member (Figures 28, 29). This bed is possibly of *Z. emaciata* Zone age, because it underlies shales with *Mastigobolbina lata*, but has not yet yielded diagnostic ostracodes.

The relatively thick middle shaly member of the Rose Hill is referable to the *Mastigobolbina lata* Zone (Swartz and Swartz, 1931; Gillette, 1947), and is thus correlative with the Sauquoit Shale–Otsquago Sandstone in central New York (Figure 20). These shaly intervals are the highstand deposits of Sequence III.

SEQUENCE IV.—In thick sections of central Pennsylvania and Maryland, the middle shaly member of the Rose Hill Formation shows an upward increase in thin sandstone beds and appears to grade upward into the Center Member (Figures 17, 29). The latter unit, which attains thicknesses up to 30 m, consists of interbedded shales and hummocky cross-bedded sandstones that are arranged into about thirteen coarsening-up cycles (Cotter, 1988). Each of the 1–3 m-thick cycles commences with greenish-gray shale and passes upward into hummocky cross-bedded to flaser-bedded, ferruginous sandstones (Cotter, 1988, 1991, this volume). The Center Member generally appears to represent deposition during an interval of relative sea-level lowstand. Ostracodes of the *Bonnemaia rudis* Zone, a biostratigraphic interval missing in New York, have been reported from the Center Member (Swartz and Swartz, 1931; Figures 15, 18).

We infer that the Center Member reflects progradation of coarser siliciclastics in a series of small cycles during a regional lowstand in the middle–late Telychian (C5). Brett et al. (1990) inferred that this lowstand also produced the major regional unconformity at the base of Sequence IV. Hence the Center Member is interpreted as the lowstand deposits of Sequence IV, and

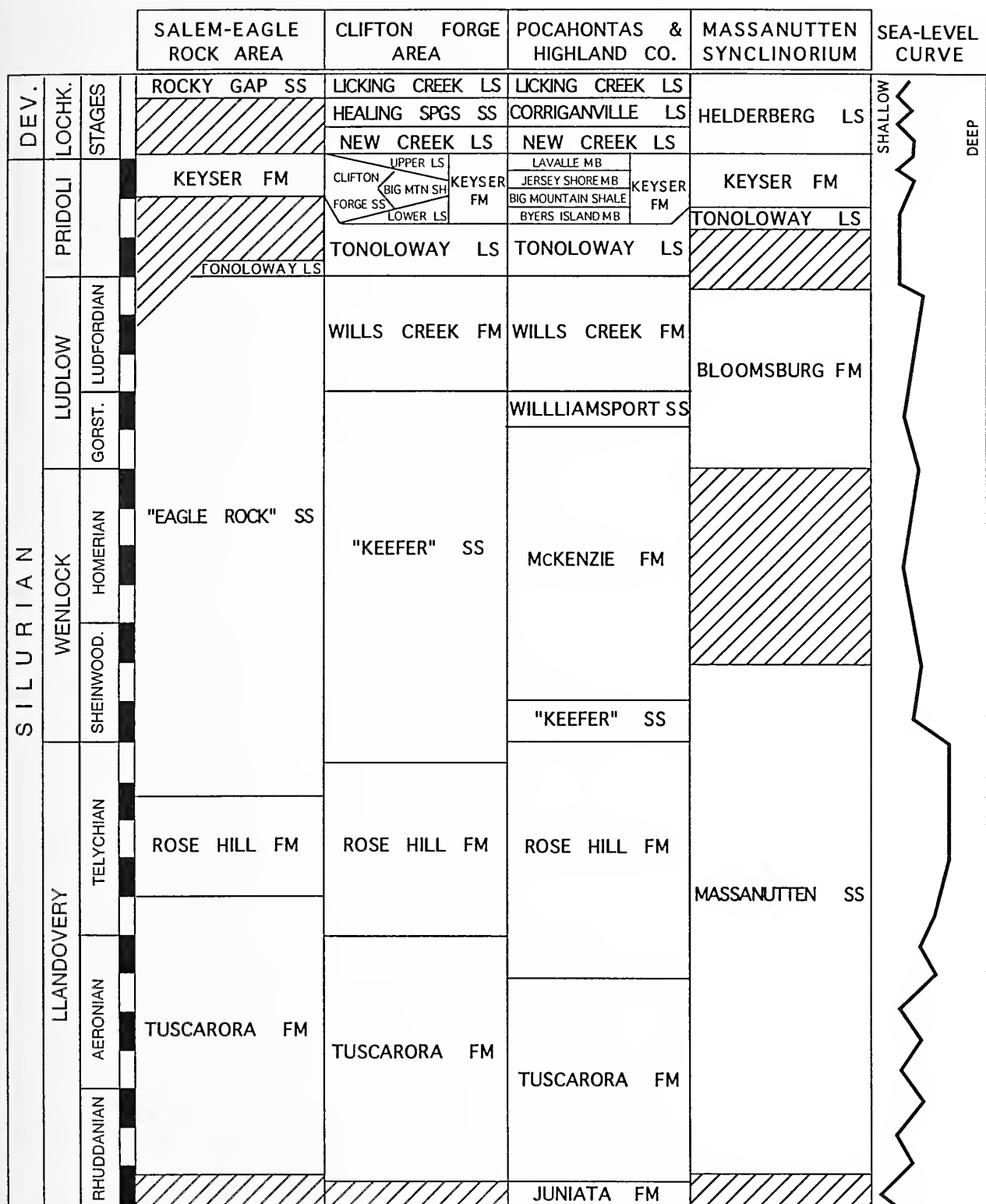


FIGURE 20—Correlation chart for northern and central Virginia. Diagonally ruled areas are hiatuses. After Diecchio and Dennison (1996).

is equivalent to an unconformity in areas that underwent lower subsidence. Locally in western parts of the Valley and Ridge belt of Pennsylvania and Maryland, the sandstone facies of the Center Member are absent, and the equivalent strata are distinguishable only as an interval of maroon shale.

The Center Member is overlain by 10–15 m of shale with thin fine-grained sandstones and limestones assigned to the upper shaly member (Cotter, 1996). This interval is divisible into two parts (Figures 15, 18, 19). The lower half consists of purplish to greenish-gray shales with widely scattered lenses of coquinooid limestones rich in *Eocoelia sulcata* and other brachiopods. Toward the top of the lower half, coquinooid limestones become increasingly abundant, and at nearly all localities, they are capped by a 0.5–1.0 m bundle of thin-bedded, ferruginous, skeletal packstones. Locally, this distinctive marker interval is rich enough in ferric oxide to be mineable as iron ore (e.g., “Fossil Ore” bed near Danville, Pennsylvania; see Cotter, 1996). The position of these ferruginous limestones within the *Mastigobolbina typus* Zone, and the occurrence of the zonally significant small rugose coral *Palaeocyclus rotuloides* within and slightly above these beds, strongly indicate that these “Fossil Ore” beds correlate with the Westmoreland oolitic hematite of New York (Figure 19). These beds are interpreted as a condensed deposit formed during sediment-starved conditions close to the maximum flooding of the major, late Telychian transgression.

The uppermost Rose Hill Formation (upper part of upper shaly member) consists of medium to dark gray fossiliferous shale with thin coquinooid limestones and typically at least one bed of hematitic limestone in the middle of the interval (Cotter, 1983b; Brett et al. 1990; Brett and Goodman 1996). These uppermost beds of the Rose Hill contain diagnostic *Mastigobolbina typus* Zone ostracodes, and have been correlated with the uppermost *Pterospirifer celloni* to lower *Pterospirifer amorphognathoides* (conodont) Zones in New York (Figures 18, 28, 29). This highest shaly interval is correlated with the Williamson–Willowvale Shale interval of New York on the basis of ostracodes (*M. typus* Zone), brachiopods (*Eocoelia sulcata*), and corals (Brett et al., 1990). The diverse fauna of this zone suggests outer BA 3 to inner BA 4 benthic assemblages. This interval records the deepest water facies of the Rose Hill Formation (Figure 19).

At most localities, a complex condensed bed with abundant quartz pebbles, phosphatic nodules, and hematized grains occurs at or near the top of the Rose Hill Formation, as traditionally defined (Cotter, 1983b, 1996). Based on its position several meters above the Westmoreland Hematite-equivalent beds and unique

lithological features, this widely correlatable bed appears to be the lateral equivalent of the Salmon Creek or basal Dawes bed, as defined in New York sections. At most localities, the condensed bed is overlain by dark gray friable shales with thin, hummocky cross-bedded sandstones. This overlying interval is traditionally assigned to the Keefer Sandstone (a member of the Mifflintown Formation; Cotter, 1996). However, it is lithologically and biostratigraphically the approximate equivalent of the Dawes Sandstone–Rockway Formation in New York (i.e., the upper subsequence or late highstand of Sequence IV; Figures 15, 19).

SEQUENCE V.—In nearly all outcrops in central Pennsylvania, Maryland, and northern West Virginia, the Dawes-equivalent shale and sandstone interval is abruptly overlain by coarser-grained and relatively massive quartz arenite or calcareous to hematitic sandy carbonate that is assigned to the upper part of the Keefer Sandstone (Figure 15, 19). The sharp basal contact of these coarser deposits is interpreted as the Sequence IV–V boundary, and as such the upper Keefer is the equivalent of the Irondequoit Limestone and equivalent basal Herkimer Sandstone in New York (Figure 12). At proximal (southeastern) localities, this major coarse-grained zone of the Keefer closely resembles the lower Herkimer Sandstone of New York, because it is a *Skolithos*-bearing quartz arenite with minor stringers of hematitic ooids and fossils. At more distal locations near the Allegheny front, the upper Keefer displays strong similarities to the Irondequoit–Kirkland succession of west-central New York (compare Figures 13 and 19). Notably, at Allenwood, Pennsylvania, this part of the Keefer has a sharp basal contact overlain by ferruginous sandy carbonates that resemble the Irondequoit of New York, and is similarly overlain by a shaly interval. The upper beds of the 5 m-thick Keefer–Kirkland interval at the Allenwood section are sandy crinoidal and bryozoan-rich pack- and grainstone. At most localities in central Pennsylvania, the top bed of the Keefer consists of ferruginous, quartz granule-sandstone with abundant *Whitfieldella* brachiopods. Locally, some hematitic stringers are also present within the unit, and near Cumberland, Maryland, a thin bed of oolitic hematite (“Rogers Ore”) occurs at the sharp upper contact of the Keefer (Swartz, 1923). These beds comprise a condensed interval that caps the early transgressive systems tract of Sequence V, which is represented by the Keefer sandstones and carbonates.

The upper Keefer is everywhere sharply overlain by medium to dark gray shales and mudstones, typically assigned to the Rochester Member of the Mifflintown Formation (Figure 19). On the basis of ostracode biostratigraphy (*Drepanellina clarkei* and *Paraechina spinosa*

Zones), this interval is largely correlated with the Rochester Shale of New York. Indeed, a bundle of shell- and bryozoan-rich limestones near the middle of the shale probably represents the boundary between the Lewiston and Burleigh Hill Members of the Rochester, although no hematites have yet been identified at this level, as they have been in central New York. The upper quarter of this shale, which typically contains argillaceous calcisiltites and brachiopod beds with *Whitfieldella marylandica*, *Nucleospira pisiformis*, and small corals, apparently correlates with the Glenmark (or DeCew) interval of New York. This distinctive "*W. marylandica* Zone" has been correlated southward through central Pennsylvania into Maryland and northern West Virginia (Swartz, 1923; Swartz and Swartz, 1931). It is also notable that internal convoluted calcisiltite beds occur near the base of this Glenmark equivalent in central Pennsylvania, and occupy a position analogous to the slump-folded DeCew of New York (compare Figures 15 and 29). This suggests that the signature of a very major seismic event may be recorded even in the central Appalachians. Complex shell beds in the *W. marylandica* Zone also appear to be correlatable from New York to Maryland, and suggest widespread condensation, but little or no phosphatic or ferruginous material is present.

This shaly lower ("Rochester") part of the Mifflintown Formation (i.e., "Rochester") clearly represents relatively deep-water deposits. Its diverse brachiopod and trilobite assemblages indicate offshore benthic assemblages (BA 3–4; Figure 19). The sharp flooding surface at the top of the Keefer and below the overlying Rochester shales thus records the major middle Sheinwoodian highstand that is now recognized very widely (Johnson et al., 1990a, 1990b; Johnson, 1996; Ross and Ross, 1996; Figure 1). Not widely recognized is the fact that a cryptic but regionally widespread disconformity occurs above the *Whitfieldella marylandica* Zone at the sharp basal contact of the McKenzie Member of the Mifflintown Formation. Detailed observations show that this surface locally truncates parts or all of the underlying *W. marylandica* Zone shales (=Glenmark–DeCew-equivalents), as in the outcrops near Millerstown (see description by Cotter, 1996). This contact is overlain at most localities by a thin (20–30 cm), orange-weathering (ankeritic), dark gray limestone bed rich in fragmentary *Whitfieldella* shells. This bed is everywhere overlain by a distinctive succession that includes black shales with intraformational breccias and stromatolitic limestone and a pair of very widespread, *Favosites*-rich thrombolitic horizons (bioherms). A virtually identical succession is traceable into central New York, where it forms the base of the Sconodoo–Ilion Shales (=McKenzie Shale) of the lower

Lockport Group (Brett and Goodman, 1996). Thus, regional correlations indicate that the base of the McKenzie is a major sequence-bounding unconformity identical with the base of Sequence VI (lower Lockport Group) in New York and Ontario. The very shallow-water, stromatolitic sediments of the basal McKenzie–Sconodoo are regarded as a transgressive systems tract (Figures 13, 19). The very widespread thrombolitic beds are believed to correlate with reefs in the upper Gasport Formation of New York (see Zenger, 1965; =Pekin Member of Brett et al., 1995). The reefs and thrombolitic buildups are considered to reflect a maximum flooding interval in which upward growth may have been triggered by deepening and clean water. The sequence boundary and initial transgression correlate with Johnson's (1996) late Wenlock (early Homerian) sea-level fall.

SEQUENCES IN NORTHERN AND CENTRAL VIRGINIA AND WEST VIRGINIA

Most units identified in Pennsylvania and Maryland persist into the western parts of the Valley and Ridge belt in northwestern Virginia and eastern West Virginia. Stratigraphic studies of the Valley and Ridge initiated by Butts (1940) have been updated by Dennison (1970), Diecchio (1973), Helfrich (1975), and Pratt et al. (1978), and are summarized by Diecchio and Dennison (1996). Unfortunately, little detailed biostratigraphy exists for this area, which makes correlation difficult. Nonetheless, depositional sequences can be recognized and tentatively traced into adjacent regions. Lithostratigraphic units in this area include a basal Tuscarora Sandstone; maroon and green Rose Hill Shale; thin, coarse, and typically hematitic Keefer Sandstone; and overlying Rochester and McKenzie Formations (Figures 20, 21).

SEQUENCE I.—The Lower Silurian Tuscarora Formation, composed of trough cross-bedded to massive quartz arenites and conglomerates, persists throughout the Virginia Valley and Ridge and merges into the Clinch Formation to the southwest (Figures 15, 20, 21). The base of the Tuscarora–Clinch Formations is generally sharp and locally unconformable on the Upper Ordovician (Dorsch et al., 1994). Near Huntersville, West Virginia, the base of the Tuscarora as earlier identified appears to be conformable with the underlying red Juniata Formation (Bambach, 1987). However, the sharp contact between lower fine-grained sandstones and the main "coarse zone" of the upper Tuscarora near Huntersville may represent the Cherokee Unconformity and the sys-

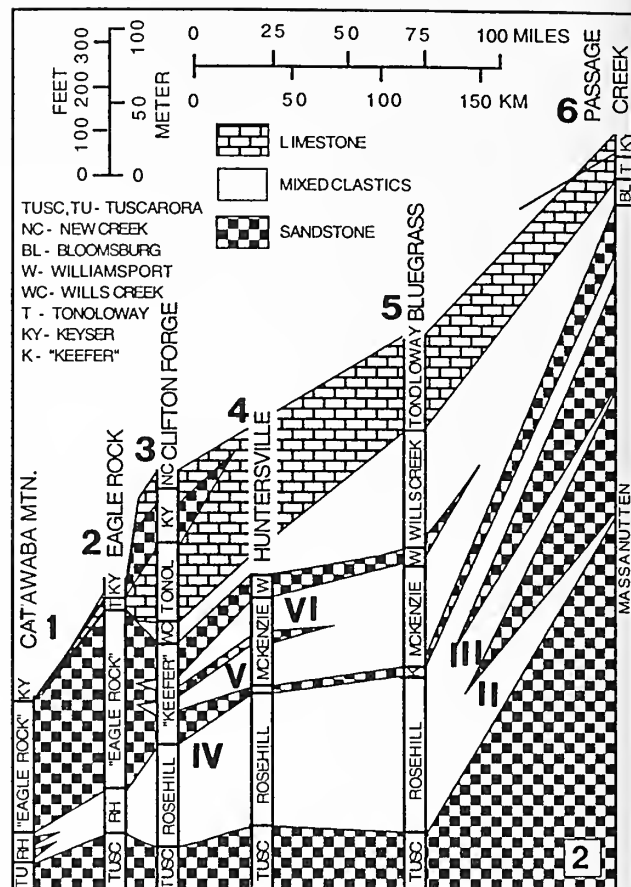
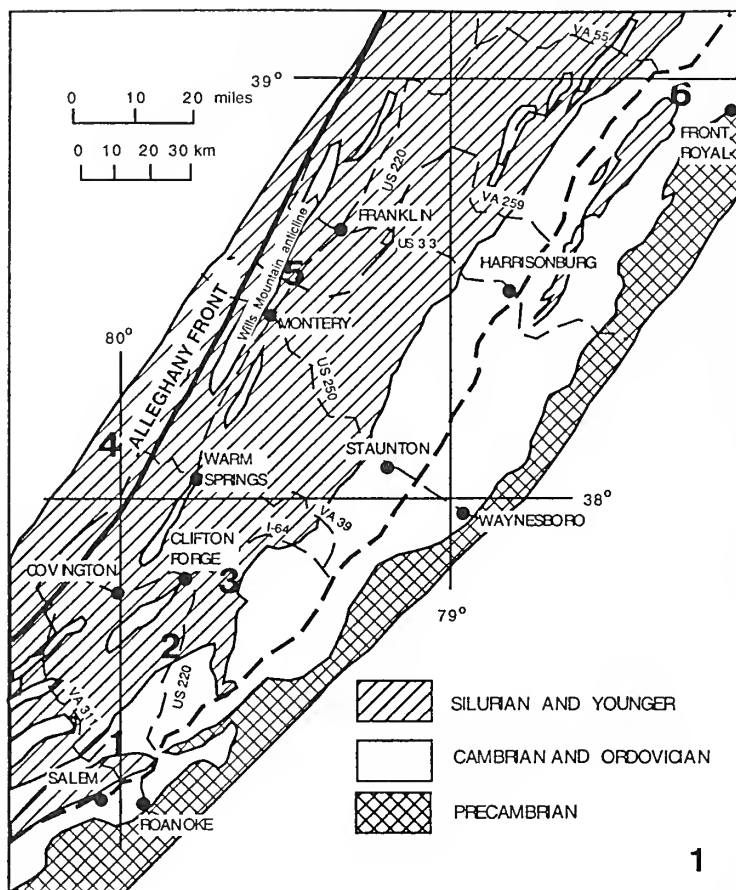


FIGURE 21—Silurian of northwest Virginia. 1, Locations of numbered columns. 2, Schematic northeast-southwest cross-section of Silurian from Massanutten Mountain to near Roanoke in northern Virginia and adjacent West Virginia. Approximate highstand intervals of sequences I-IV of Brett et al. (1990) indicated with Roman numerals. After Diecchio and Dennison (1996).

temic boundary between the Ordovician and Silurian (Dorsch et al., 1994; Driese, 1996).

SEQUENCES II-IV.—The Tuscarora Formation is overlain in western exposures by maroon sandy shales and hematitic sandstones of the Rose Hill Formation (Figures 15, 20, 21). A persistent hematitic sandstone, the Cacapon Member, in the lower part of the Rose Hill thickens southeast and probably once merged with the Massanutten Sandstone, which has been removed in southeast Virginia by post-Silurian erosion. The Cacapon may record lowstand sedimentation between Johnson's (1987, 1996) second and third Llandovery highstands (see Figure 1). This lowstand would correspond to the Sodus Shale-lower tongue of Oneida Conglomerate of central New York (Figure 15). Unfortunately, no biostratigraphic data are available for the Cacapon to test this correlation. A second and more persistent sandstone tongue probably corresponds to the Cabin Hill Member in Pennsylvania. The third and highest sand-

stone tongue in the Rose Hill, which may be equivalent to the Center Member of Pennsylvania and Maryland, records the early Telychian lowstand seen elsewhere in the basin (Figures 15, 20). As yet, no hematite equivalent to the Westmoreland condensed beds and their equivalents (base of Sequence IV) has been identified in Virginia, and the position of the late Telychian highstand has not been established biostratigraphically. However, the highest tongue of Rose Hill shale that immediately underlies the Keefer Sandstone in west-central Virginia is a reasonable correlative.

SEQUENCE V.—The Keefer Sandstone (or Keefer Member of the Mifflintown Formation) of west-central Virginia (Figures 15, 21) is a relatively thin (5–10 m) quartz arenite, typically with *Skolithos*. Its base represents the sequence boundary or lowstand of Sequence V. As in Maryland, the top of the unit is marked locally by an oolitic hematite that reflects early Wenlock condensation (Diecchio and Dennison, 1996). Locally, where the underlying sand-

stone is very thin or absent, the hematite bed persists as the main indicator of the stratigraphic position of the Keefer. The Keefer Sandstone tongue thickens both to the northeast, where it merges into the upper Massanutten Sandstone, and to the south, where it forms the basal coarse unit of the "Eagle Rock" Sandstone.

In west-central Virginia, the Keefer oolitic hematite beds are abruptly overlain by dark gray fossiliferous mudstones, siltstones, and thin limestones that are variously assigned to the Rochester Member or Cosner Gap Member (Helfrich, 1975; Diecchio and Dennison, 1996) of the Mifflintown Formation (or in some cases to the lower part of the McKenzie Formation). This relatively offshore mudrock reflects major middle Sheinwoodian transgression, and is probably equivalent, in part, to the Rochester Shale of New York and Pennsylvania. Near Huntersville, West Virginia, a coarse sandstone tongue separates this fossiliferous mudstone from the higher McKenzie shale and limestone succession. Correlations show this sandstone to be a basinward-extending tongue of the "Eagle Rock" Sandstone (Figures 15, 21). Hence this sandstone probably represents a lowstand deposit; we suggest that it may be associated with the Sequence V–VI boundary, and correlates approximately into the sub-Lockport Group (upper Wenlock, Homerian?) disconformity in the Niagara region. A higher sandstone tongue in the Clifton Forge–Huntersville area, referred to as the Williamsport Sandstone, appears to correlate into the red mudstones of the Bloomsburg Formation to the north (Berry and Boucot, 1970; Diecchio and Dennison, 1996; Figures 15, 21).

Collectively, the Keefer, lower McKenzie, and Williamsport sandstone tongues appear to merge to the south in the Roanoke, Virginia, area into a relatively thick, presently undifferentiated mass of white to red quartz arenite. This is the informally named "Eagle Rock" Formation (Figures 15, 21) that overlies the Rose Hill and probably represents much of the upper Llandovery–Ludlow. The "Eagle Rock" may represent a southwestern extension of the massive sandstones of the Massanutten Formation in the north, and as that interval, may represent non-marine-braidplain to marginal-marine environments.

SEQUENCES IN THE GREAT VALLEY OF VIRGINIA

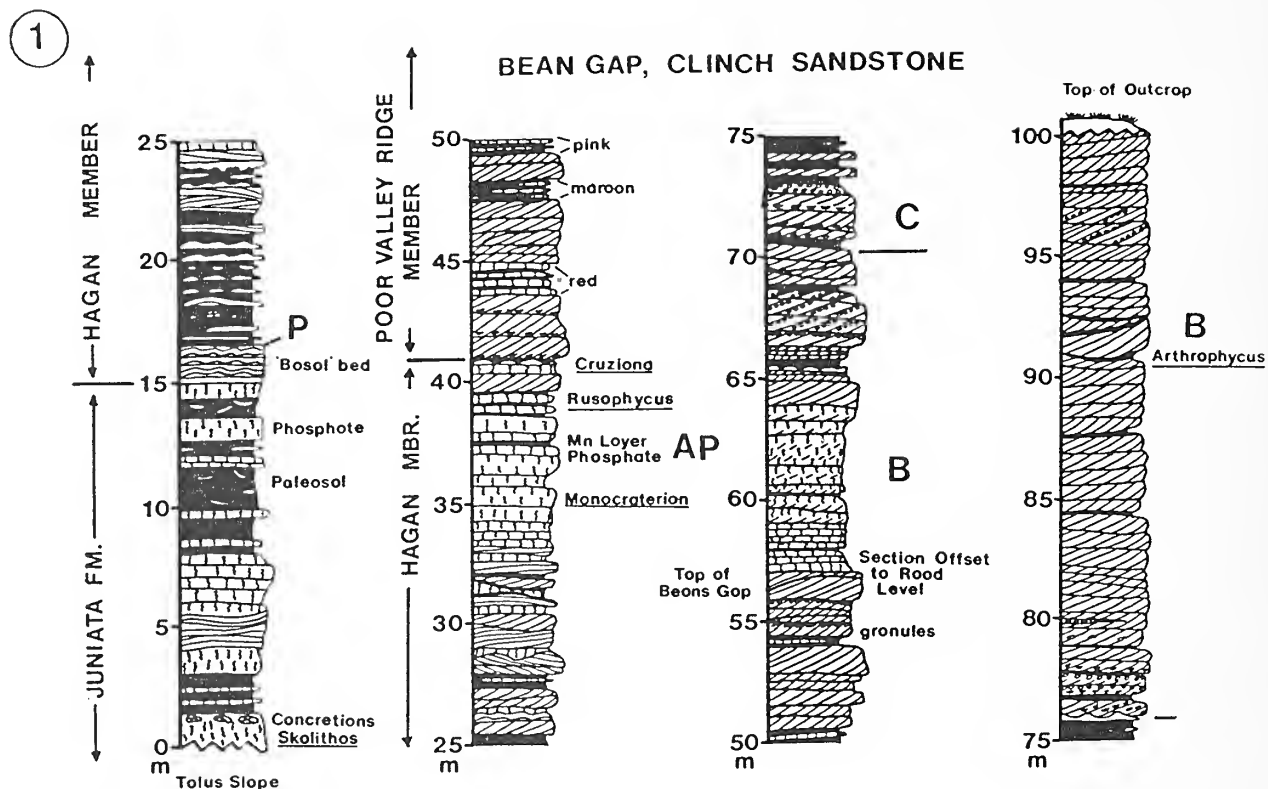
In the eastern Great Valley of Virginia, the Lower and Middle Silurian are a very thick interval (up to 500 m) of Massanutten Sandstone (Figures 15, 20, 21). Pratt et al. (1978) recognized subdivisions of this previously undivided mass of sandstone (Figure 15). The lower, or

Runkles Gap Member, comprises up to 300 m of light gray, coarse-grained quartz arenite and conglomerate that probably represent non-marine braided stream facies equivalent to the Tuscarora Formation (Sequence I) to the west (Pratt et al., 1978). A middle Passage Creek (or "Clinton") Member of pink to brown muddy sandstone is the probable lateral equivalent of the Rose Hill Shale, and apparently records marginal marine environments. In a general sense, this latter member reflects middle Llandovery transgressions (Sequences II and III) and/or reduction of siliciclastic influx. The upper part of the Massanutten displays three sandstone and shale tongues that represent marine transgressions (Figures 15, 21). The lower is represented by muddy sandstones with a sparse marine fauna; these beds may represent the late Llandovery highstand (Sequence IV; Johnson's [1996] fourth Llandovery transgression). A middle, acritarch-bearing, black shale might represent the middle Sheinwoodian ("Rochester Shale", Sequence V) sea-level rise that is recognized globally (Johnson et al., 1990a, 1990b; Johnson, 1996). The uppermost brownish shale tongue has been correlated with the McKenzie Formation (late Wenlock to early Ludlow) further west. Persistent hematite beds have not been identified within the Massanutten.

SEQUENCES IN SOUTHWEST VIRGINIA AND NORTHEAST TENNESSEE

In southwest Virginia, the Silurian is truncated by a sub-Devonian unconformity, and the Lower Silurian is represented by only two units—a lower Clinch Sandstone, laterally equivalent to the Tuscarora, and an overlying Rose Hill Shale. Near Cumberland Gap, Virginia–Tennessee–Kentucky, where the lower unit is less sandy, it has been termed the Rockwood Formation (Figures 15, 22, 23).

SEQUENCE I.—In southwest Virginia and northeast Tennessee, the Clinch Formation has been subdivided into two members, a lower Hagan Shale (15–25 m) and an upper, thicker (55–65 m) Poor Valley Ridge Sandstone (Miller, 1976). The Hagan Shale probably represents the early-middle Rhuddanian highstand recorded by the Power Glen (or lower Cabot Head) Shale of the Medina Group in New York–Ontario (sub-sequence IA, Figure 4). Condensed phosphate-, hematite-, and manganese-rich beds near the top of the Hagan Member may record the same condensed interval represented by the Art Park phosphatic beds (condensed bed in subsequence IB) in New York and Ontario. The upper, sandier Poor Valley



2

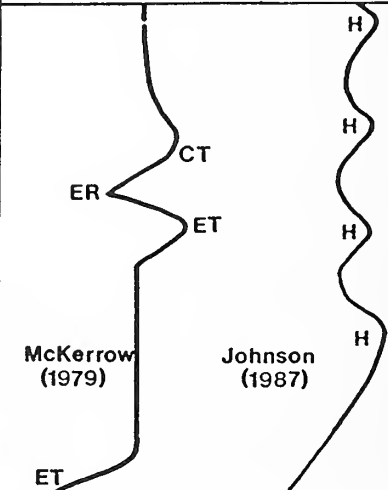
SYSTEM	SERIES	STAGE		UNIT	SEA-LEVEL (RELATIVE)										
SILURIAN	LLANDOVERY	Telychian	C ₆	CLINCH ROCKWOOD BRASSFIELD		H									
			C ₅				H								
			C ₄					H							
		Aeronian	C ₂₋₃						ER	CT	ET	H			
			C ₁												
			B ₃												
			B ₁₋₂												
		Rhuddanian	A ₄										McKerrow (1979)	Johnson (1987)	H
			A ₃												
			A ₁₋₂												
ORDOVICIAN	ASHGILL		JUNIATA/ SEQUATCHIE		ET ER										

FIGURE 22—1, Clinch Sandstone (Hagan and Poor Valley Ridge Members) at Clinch Mountain, Tennessee. Possible correlatives with Sequence I (Medina Group) in New York indicated with letters: P, major flooding surface possibly equivalent to base of Power Glen Shale in New York; AP, possible position of condensed Art Park phosphatic-hematitic beds; B, bioturbated zone with *Arthropycus*; C, possible position of Cambria Shale. 2, Approximate age relationships and relation to eustatic curves of Clinch, Rockwood, and Brassfield Formations of Tennessee. After Driese (1996).

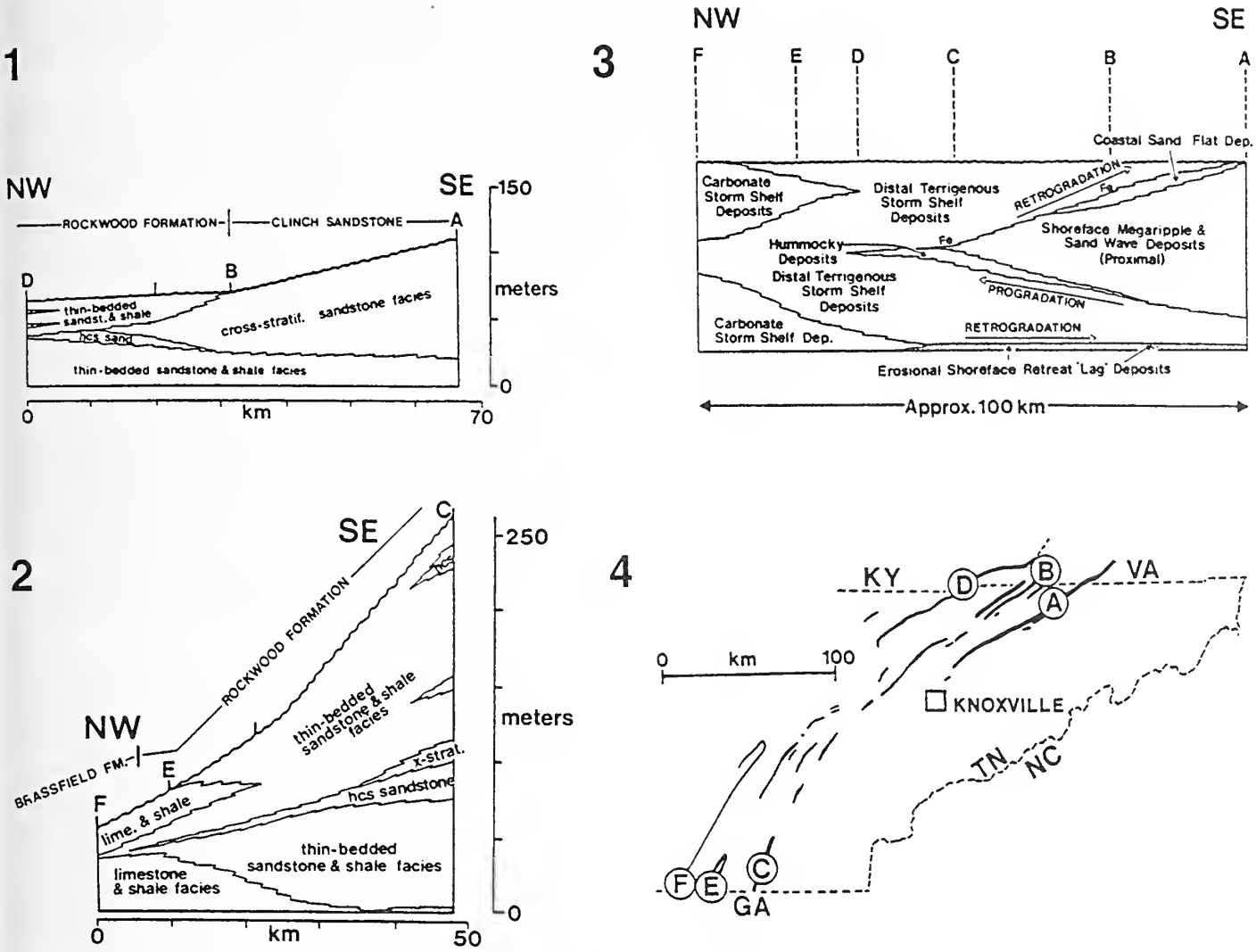


FIGURE 23—Restored cross-sections of Rockwood and equivalent Clinch Formations with regional facies relationships. 1, Northeast Tennessee. 2, Southeast Tennessee; note that outcrops E and F also appear on cross-section shown in Figure 25. 3, schematic NW-SE cross-section for eastern Tennessee with environmental interpretations. 4, Map of eastern Tennessee showing location of cross-sections in Figure 23.1-3. Abbreviations: A, Clinch Mountain; B, Powell Mountain; C, Green Gap; D, Cumberland Gap; E, Tiftonia; F, Sequatchie Valley. After Driese (1996).

Ridge Member of the Clinch and correlative upper Tuscarora is generally undifferentiated lithologically, although burrowed zones rich in *Arthropycus* may record the minor marine inundations that are reflected by the Castanea Member of the Tuscarora and upper Medina Group to the north in Pennsylvania and New York (Figures 4, 15).

The Clinch is particularly well-exposed at Beans Gap on Clinch Mountain (Driese, 1996), and this section forms the basis for most of the following discussion (Figure 16). The basal sandstone bed of the Hagan Member sharply overlies the Ordovician Juniata (or Sequatchie) Formation (Driese et al., 1991; Driese, 1996). This relatively thick bed (3 m) contains a basal lag of red shale

clasts and phosphatic nodules that are reworked from the underlying Ordovician. It is interpreted as a condensed transgressive sandstone (Driese et al., 1991; Driese, 1996). Higher parts of the Hagan Member consist of shaly siltstone and interbedded, fine-grained sandstone with small-scale, hummocky cross-stratified sandstone. Burrows and linguloid brachiopods are abundant at some levels. There is an abrupt increase in the proportion and thickness of hummocky to trough cross-bedded sandstone beds about 15 m above the base of the Hagan Member. The upper third of this sandstone bundle is extensively bioturbated and capped by a thin phosphate- and manganese-rich bed (Driese, 1996; Figure 22). This bed is overlain by thin-bedded sandstones and shales

with marine trace fossils (e.g., *Rusophycus*), which indicate a minor transgression (Driese, 1996).

It is tempting to correlate the basal sandstone, lower shale, upper sandstones, and phosphatic bed in the Hagan Shale, respectively, with the Whirlpool Sandstone, Power Glen Shale, Devils Hole Sandstone, and Art Park phosphatic beds of the lower Medina Group in western New York and Ontario, as well as with equivalent units in parts of the Tuscarora Formation (i.e., the lower two fourth-order sequences of Sequence I; compare Figures 6 and 22 and Figures 15 and 29). Unfortunately, biostratigraphic data for this interval are very limited, and the similarity of pattern is only suggestive of correlation at this time.

The upper Clinch Formation, or Poor Valley Ridge Member, is about 56 m thick at Beans Gap and consists of cross-stratified sandstones interbedded with minor pink to maroon shale. Sandstones, typically medium- to coarse-grained quartz arenite, have been divided into three facies: 1) medium to large cross-stratified; 2) medium- to large-scale, tabular cross-bedded; and 3) massive, heavily bioturbated (Figure 22). Driese (1996) reported *Skolithos* and *Diplocraterion* in these beds, which overlie sandstones rich in *Arthropycus*. These bioturbated, massive sandstone beds in the upper Clinch may correspond to the thoroughly bioturbated *Daedalus* beds of the upper Tuscarora and equivalent Thorold and Kodak Sandstones in western Pennsylvania and New York.

SEQUENCE II.—In some locations, the Clinch Formation is abruptly overlain by maroon clay shales that are assigned to the Rose Hill Formation (Marks, 1987). It is particularly notable that an oolitic ironstone bed occurs at this contact (Driese, 1996). The overlying shales have yielded *Eocoelia* sp. cf. *E. hemispherica* (R. K. Bambach, personal commun., 1989). This lag bed may thus correspond to the extensive phosphatic and hematitic conglomerates at the base of Sequence II (Densmore Creek bed of the lower Clinton Group in New York), to the corresponding phosphatic bed at the base of the Rose Hill in Pennsylvania, and to the Irondale hematitic bed at the base of the middle member of the Red Mountain Formation in Alabama (see below). Higher beds are apparently truncated by the sub-Devonian unconformity.

SEQUENCES IN SOUTHEAST KENTUCKY AND EAST TENNESSEE

Silurian strata of southeast Kentucky and most of east Tennessee have been assigned to the Rockwood Formation (also called Red Mountain Formation in Tennessee;

Chowns, 1996). This formation is laterally equivalent to the Clinch Sandstone and the overlying Rose Hill Formation of Virginia (Figures 15, 23).

SEQUENCE I.—The lower third of the Rockwood Formation, which gradationally replaces the Clinch Formation to the northwest (for example near Cumberland Gap in the Virginia-Kentucky-Tennessee tri-state area), consists of thin-bedded sandstone and shale with a middle interval of somewhat thicker-bedded, hummocky cross-bedded sandstone. Skeletal limestone and ironstone beds are more numerous in western outcrops (Driese et al., 1991; Driese, 1996; Figures 15, 23). To the northwest, the lower two-thirds of the Rockwood pass laterally into carbonates of the Brassfield Formation in Kentucky (Driese, 1996). The Rockwood and Brassfield are poorly dated, but appear to represent only the Llandovery (Rhodian-late Telychian). Higher parts of the Silurian have been removed in this region by Devonian erosion. In most areas, the Rockwood or Rose Hill Formations are overlain by Upper Devonian (Famennian) Chattanooga Shale.

Near Green Gap, Tennessee, the equivalents of the Clinch and Rose Hill Formations are assigned to the Rockwood Formation (Figures 23, 24). As with the laterally equivalent Clinch Formation, the lower part of the Rockwood Formation has a thin, basal, transgressive sandstone that is overlain by a very shale-rich interval equivalent to the Hagan Member (Figures 15, 24). Deepest water facies are represented about 60–70 m above the base of the formation; this highstand may correspond to Johnson's (1996) earliest Silurian transgression. A middle sandstone-dominated interval of the Rockwood that corresponds to the Poor Valley Ridge Member is again capped by an oolitic hematite that marks the Sequence I–II boundary, about 110 m above the base of the formation (Driese, 1996).

The upper 150 m of the Rockwood Formation are more shaly and contain a few hematitic, shell-rich sandstones. This part of the section is probably of Aeronian-late Telychian age (C1–C5) on the basis of poorly preserved *Eocoelia* brachiopods (B. G. Baarli in Driese, 1996). It thus corresponds to the Rose Hill Shale to the northeast. Detailed studies by Driese (1996) suggest that at least three sea-level maxima occur within this succession, and lie at about 130 m, 180 m, and 265 m above the base of the Rockwood (Figure 24). The two closer-spaced highstands may correspond to Johnson's second and third highstands (i.e., the Reynales and Wolcott Limestones of the New York sections). The highest one, at the top of the formation, represents the strongest deepening event, and is probably Johnson's (1996) fourth Silurian (late Telychian) highstand (compare Figures 1 and 24).

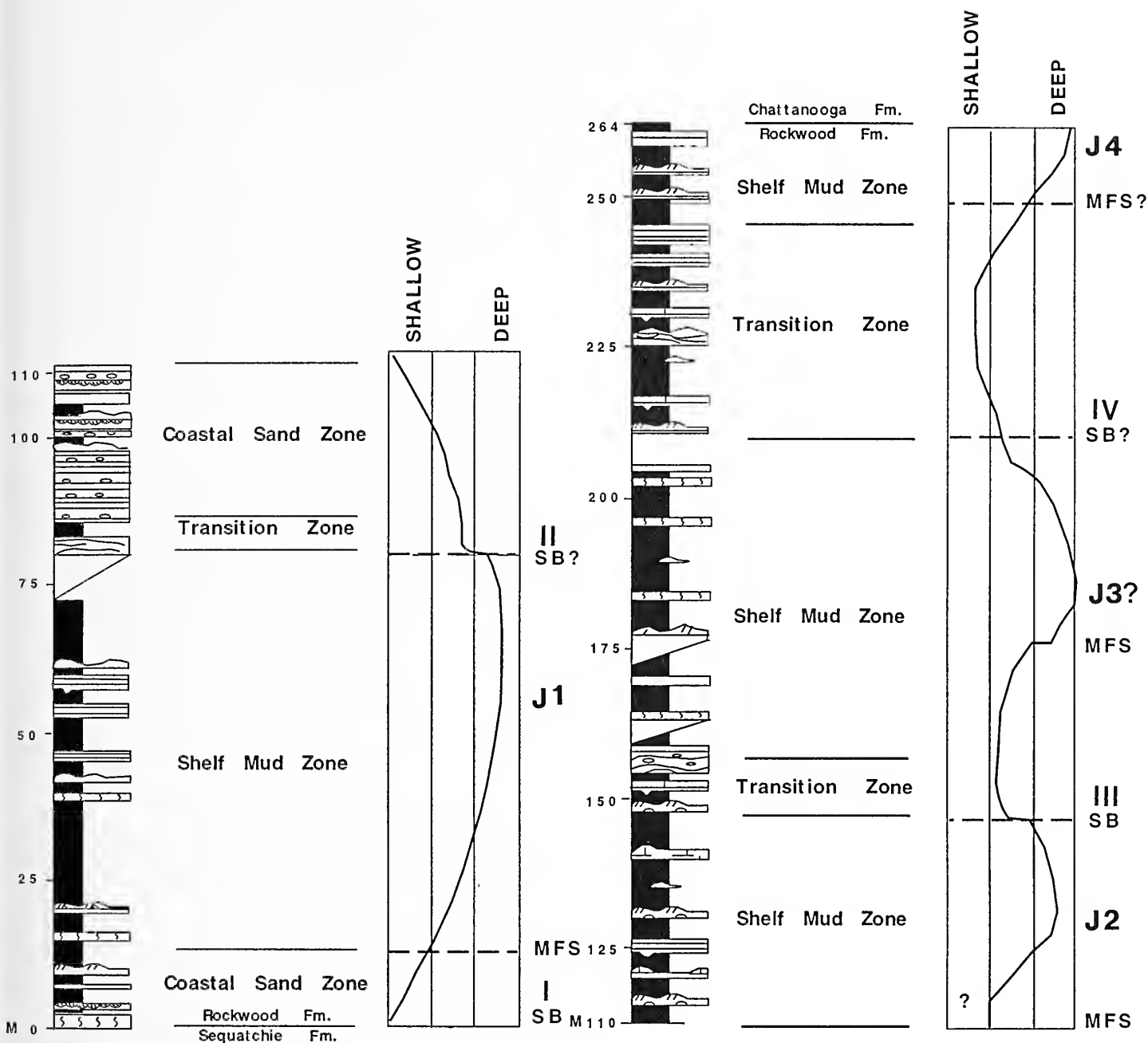


FIGURE 24—Rockwood Formation at Green Gap on Whiteoak Mountain, Tennessee, with inferred depositional environments and relative sea-level curve. Interval approximately equivalent to entire Llandovery. Johnson's (1996) sea-level highstands indicated by numbers J1–J4; boundaries of sequences I–IV of Brett et al. (1990) are shown. After Driese (1996).

SEQUENCES IN ALABAMA AND SOUTHEAST TENNESSEE

The Silurian of Alabama has been assigned to a single formation, the Red Mountain Formation, named for a ridge southeast of Birmingham (see Chowns and McKinney, 1980; Thomas and Bearce, 1986; Figures 25,

29). The Red Mountain is the source of the famous "Clinton iron ores", which were mined in the Birmingham area until 1971. The sedimentology, stratigraphy, and depositional environments of these strata have been studied recently by Chowns and McKinney (1980), Rindsberg and Chowns (1986), Driese et al. (1991), Bolton (1992), Baarli et al. (1992, 1996), Chowns and Bolton (1993), Baarli (1996), and Chowns (1996). These

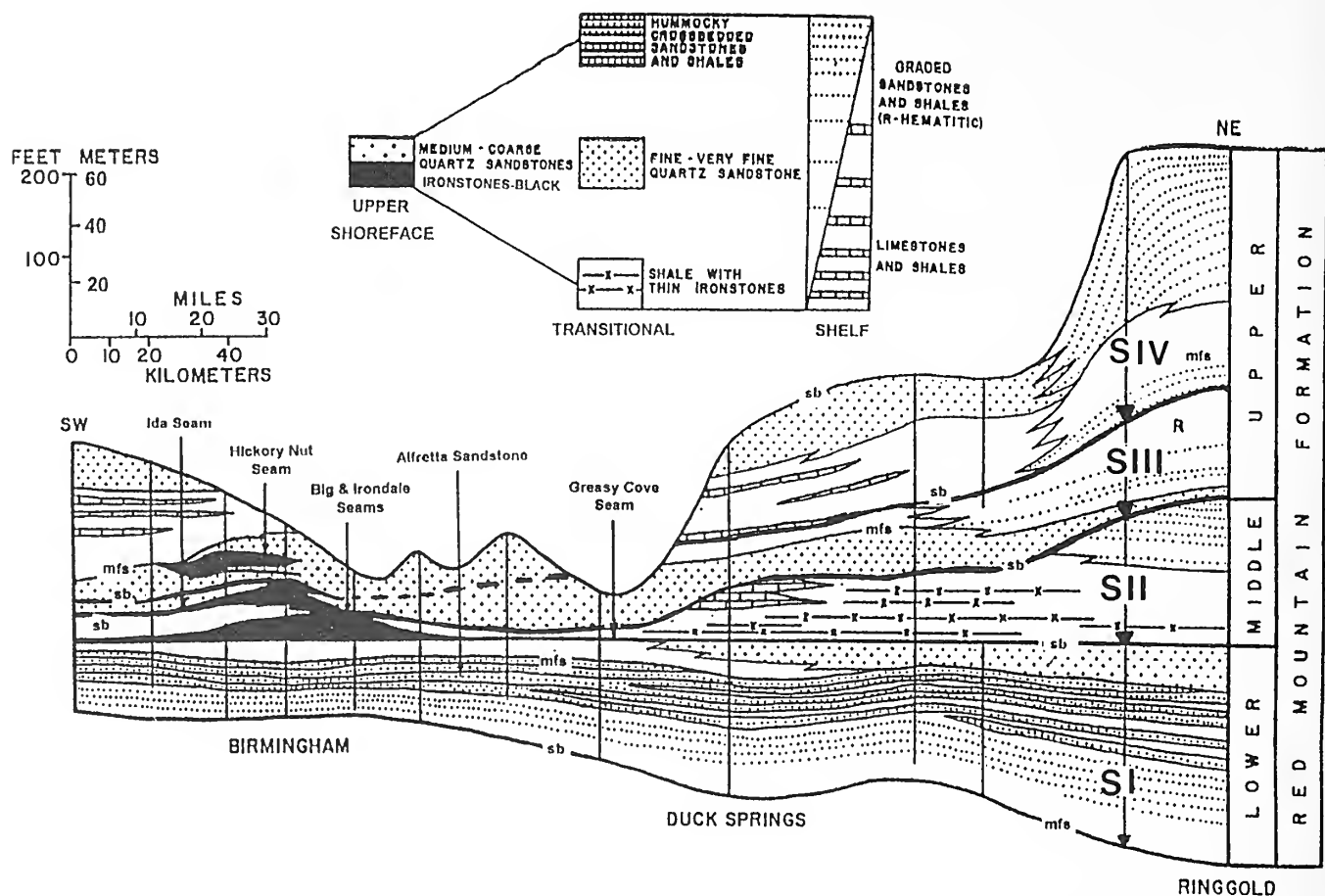


FIGURE 25—Northeast-southwest cross-section of Red Mountain Formation from northwest Georgia to Birmingham, Alabama. Abbreviations: sb, sequence boundaries; mfs, maximum flooding surfaces. Sequences recognized by Brett et al. (1990) indicated by Roman numerals. After Chowns and McKinney (1980).

publications provide the basis for this summary.

The Red Mountain Formation thickens to the northeast from about 78 m near Birmingham, where it is relatively condensed, to a maximum of over 360 m in northwest Georgia (Figure 25). This thickening is accompanied by an increase in coarse siliciclastics, especially in the upper half of the formation (Chowns and McKinney, 1980; Chowns, 1996).

Chowns (1996) subdivided the Red Mountain Formation into four informal members—a lower, middle, upper, and top member, which correspond essentially to third-order sequences (Figures 25, 26). The highest is separated from overlying beds by a substantial unconformity that is probably of Pridoli age (Berdan et al., 1986). The latter is excluded from Figure 26, because it is not considered in this paper.

A significant unconformity also exists in some areas of Alabama between the middle and upper members (Figure 26). However, in the vicinity of Birmingham, the lower three members form a relatively conformable succession of siliciclastics, thin carbonates, and ironstones

that is early Llandovery–early Wenlock, based on brachiopod, ostracode, and conodont biostratigraphic work by Berdan et al. (1986), Bolton (1990), Baarli et al. (1992), and Baarli (1996). These three members are discussed below on the basis of the type area of the Red Mountain Formation near Birmingham.

SEQUENCE I.—The lower member of the Red Mountain Formation is considered to be Rhuddanian–early Aeronian on the basis of meager biostratigraphic information, primarily the occurrence of *Stricklandia lens lens* at 27 m above the base of the formation near Gadsden (Baarli, 1996; Baarli et al., 1996). It thus occupies approximately the same position as the Rockwood, Clinch, and Tuscarora Formations and the Medina Group further north. It consists of about 40–120 m of gray to maroon shales and hummocky to trough cross-bedded sandstones. The lower member, as presently defined, should perhaps be subdivided into two submembers near Birmingham. A thin (0.2–2 m), basal, phosphatic sandstone overlies Middle to Upper Ordovician strata with a gentle

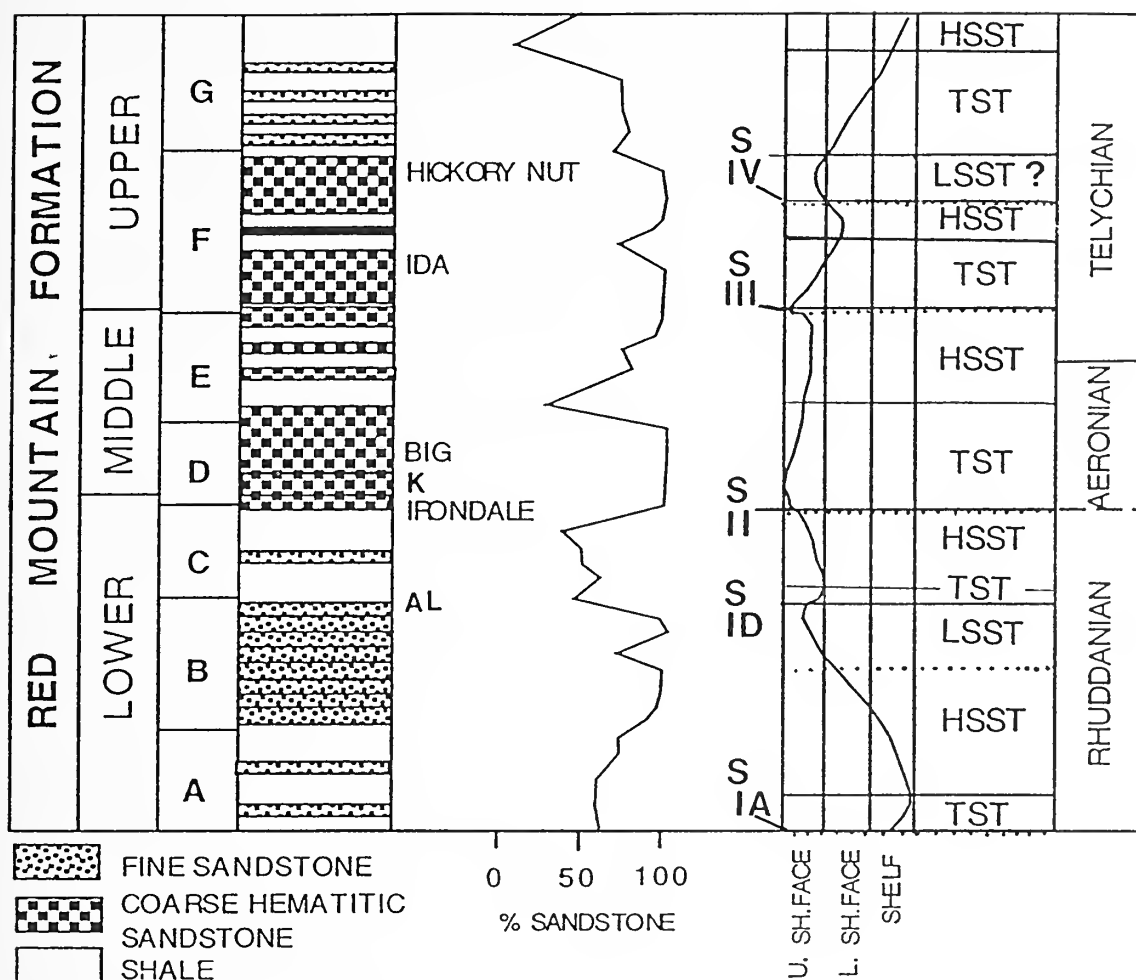


FIGURE 26—Red Mountain Formation on Red Mountain Expressway, near Birmingham, Alabama. Units A–G of Baarli et al. (1996) and variations in sandstone content, relative sea-levels, sequence interpretation, and age shown. Systems tract abbreviations in Figure 6; sequence boundaries indicated by dots below lines; one inferred subsequence (fourth-order) boundary indicated by dots. Inferred positions of boundaries of sequences of Brett et al. (1990) shown by Roman numerals I–IV. After Chowns and McKinney (1980).

angular unconformity. This is the local manifestation of the Cherokee or Taconic unconformity. The phosphatic basal beds are considered to be highly condensed by Chowns (1996), who noted that maximum flooding is close to the base of the lower member (Figure 26). We interpret the beds to be condensed lag deposits of a transgressive systems tract, and the top of the phosphatic sandstones as a maximum flooding surface. No ironstones are associated with these condensed beds, a situation generally true of the lowest Silurian sequence throughout the Appalachians.

Above the basal sandstone, the lower member displays a general coarsening-up motif (Figures 25, 26). Interbedded shales with thin-bedded sandstones to thicker, hummocky cross-stratified sandstones, to coarser, trough cross-stratified sandstones (units A and B of Baarli, 1996) are followed by a relatively finer-grained shaly inter-

val (unit C). The shaly unit A interval corresponds to the Hagan Shale and the lower Poor Valley Ridge Member of the Clinch Formation in Tennessee, and may correlate with the Whirlpool–Power Glen–Devils Hole–Grimsby succession (subsequences IA–IC) of the typical Medina Group in New York. Unit B consists of thick-bedded hematitic sandstones known as the Alfretta Sandstone (Sheldon, 1970). A thin ironstone may occur at the unit B–C contact. This indicates that the B–C contact represents a marine flooding surface. Its age is estimated to be close to the Rhuddanian–Aeronian boundary (Baarli et al., 1996). Hence the Alfretta hematitic sandstones could correspond to the thin interval of heavily burrowed sandstones near the top of the Clinch and Tuscarora (Castanea Member) Formations and Medina Group (Thorold Sandstone, *Daedalus* zone; Brett et al., 1995) further north (Figure 29). The overlying coarsening-up, shale to HCS sandstone interval (unit C) represents a

relative deepening and progradation that could be equivalent to the Cambria Shale and Kodak Sandstone high in the Medina Group (subsequence ID in New York; compare Figures 6 and 26). As noted above, this deepening may record the first major eustatic highstand of Johnson's (1996) curve. Uppermost parts of the lower member may be locally truncated by the upper sequence boundary erosion surface (Figures 26, 29).

SEQUENCE II.—The middle member (units D and E of Baarli, 1996) is highly variable in thickness because it has been truncated to a varying depth by an erosion surface (sequence boundary) at the base of the upper member. Northeast of Birmingham, the middle member may be completely missing (Chowns, 1996; Figure 25). Near Red Mountain, the middle member is dominated by highly hematitic sandstone and is comprised of four distinctive intervals (Chowns and McKinney, 1980; Chowns, 1996; Figures 25, 26). The base of this member is consistently marked by a persistent fossiliferous bed (1.5 m) rich in quartz sand and oolitic hematite known as the Irondale ore seam (Sheldon, 1970; Chowns, 1996). This ore is considered to be early Aeronian (C1–C2). Northeast of Birmingham, near Gadsden at the Duck Springs section (Figure 25), this bed is represented by a coral- and intraclast-bearing hematitic shale, which is locally mined and referred to as the "Big coral bed" (Chowns, 1996; Figure 27). The Irondale ore seam is a transgressive lag bed that may equate with the oolitic hematite bed at the base of the Rose Hill Shale to the north or the basal Densmore Creek phosphatic bed at the base of Sequence II in New York and Ontario (Figures 26, 29). This lag bed is overlain by a conglomeratic bed, termed the "Kidney seam" by miners (see Bearce, 1973), that bears hematite-coated fossils and ironstone clasts bored by *Trypanites*. Bearce (1973) and Baarli et al. (1996) interpreted this bed as a transgressive erosion lag. If so, it apparently overlies an erosion surface on the underlying Irondale ore seam. This lowstand could be correlative with the shallow water Maplewood–Neahga Shale in New York (Figure 29). It is noteworthy that reworked *Trypanites*-bored clasts also are common in the Densmore Creek lag bed of the lowest Maplewood and Neahga Shales of the basal Clinton Group (Sequence II of Brett et al., 1990) in New York and Ontario (Figure 29).

The third part of unit D in the Birmingham area is a thick (4.5 m) bed of ferruginous, fossiliferous sandstone and quartzose ironstone with a sharp base, known locally as the "Big Seam" (Sheldon, 1970; Chowns and McKinney, 1980; Chowns, 1996; Baarli et al., 1996; Figure 29). Hematite-coated large corals and pentamerid fragments are especially common in a zone near the top of this interval, and may represent a condensed bed associated with

maximum flooding that is possibly equivalent to the Furnaceville Ironstone (Brewer Dock) of the lower Reynales Formation in New York (Figure 29). The "Big Seam" becomes shaly north of Birmingham, but the equivalent 15 m interval of the middle member at Gadsden has thin, fossiliferous ironstone beds in sandy shale (Figures 25, 27).

The top of the middle member (unit E, 7 m) near Birmingham consists of thinner-bedded silty shale and coarse-grained lenticular sandstone with discontinuous stringers of hematitic ooids (Figure 26). It is capped by 1.5 m of thicker, more continuous sandstone beds, and thus apparently displays a shallowing-up pattern typical of a late highstand ("regressive") systems tract (Figures 26, 27). A correlative coarsening-up interval that exceeds 20 m in thickness is present at the top of the middle member in more proximal sections near Ringgold, Georgia (Chowns, 1996). The age of this interval appears to be constrained by the occurrence of *Stricklandia lens progressa* in overlying beds and *Pentamerus oblongus* above and below. The late Aeronian (C2–C3) age of this shallowing interval may correspond to the shallow-water Sodus Shale in the Clinton Group of New York.

Near Gadsden, Alabama, the equivalent of unit E consists of gray silty shale, and a coarsening-up sandstone interval is not present. However, a 5–7 m interval of argillaceous, very fossiliferous limestone with abundant *Stricklandia lens progressa* abruptly overlies unit E shales. The basal contact of this limestone may be an erosion surface, probably the subsequence IIB boundary, which removed much of the shallowing-up facies at this location. The carbonates are considered to represent the transgressive systems tract and early highstand of this fourth-order subsequence. The *Stricklandia*-rich limestones appear to correlate with a tongue of calcareous sandstone with abundant *Pentamerus* and *Eocoelia* that has been mapped as the base of the upper member of the Red Mountain Formation and that changes northeast into proximal reddish shale facies (Chowns, 1996). The presence of *Pentamerus oblongus* and *S. lens progressa* in these limestones and sandstones (Chowns, 1996; Baarli, 1996) suggests a late Aeronian–early Telychian age for this interval and a possible equivalency with the Wolcott Limestone (highstand portion of subsequence IIB) in New York (Figure 29). The middle member of the Red Mountain Formation thus represents much of Sequence II and Johnson's (1996) second (middle Aeronian); locally, it represents parts of the third (early Telychian) Llandovery transgressions and the intervening shallowing interval (compare Figures 1, 26, 27).

SEQUENCE III.—In the classic Red Mountain sections near Birmingham, the upper member, as presently defined, commences with a 5 m interval of ferruginous sandstone

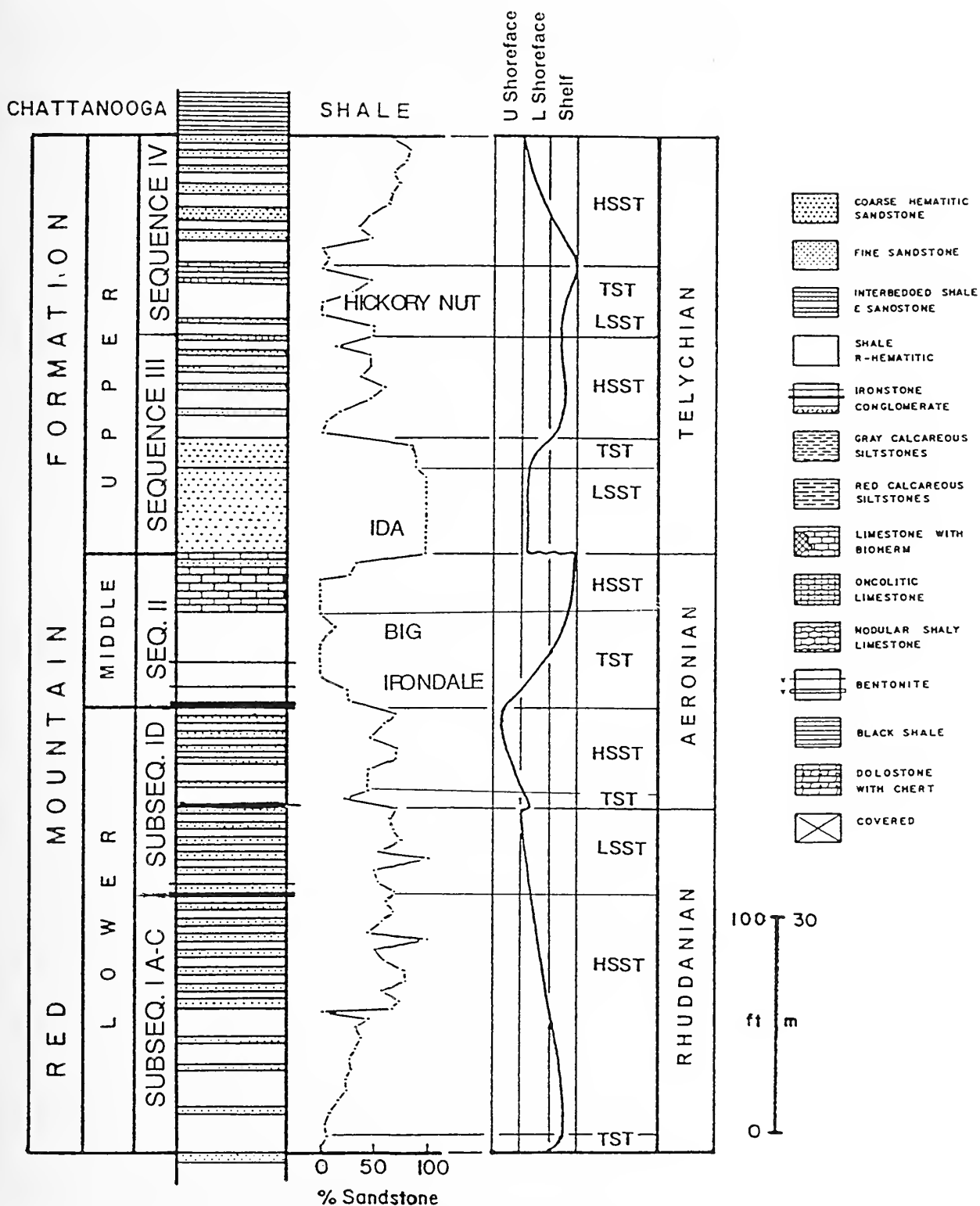


FIGURE 27—Columnar section, relative sea-levels, inferred systems tracts, and inferred sequence stratigraphy of Red Mountain Formation at Duck Springs near Gadsden, Alabama. Systems tracts abbreviations and inferred sequence boundaries are indicated as in Figures 6 and 26. After Chowins (1996).

and quartzose oolitic ironstone ore that closely resembles the older "Big Seam" (Figures 25, 26, 29). As the "Big Seam", oolitic ironstone is concentrated in the lower and upper parts of this interval, while the middle third is composed of red ferruginous sandstone. Some authors have referred just the lower 0.5 m of conglomeratic ironstone to the "Ida seam" (Baarli et al., 1996), while others (e.g., Chowns, 1996) refer the upper 3.0 m of fossiliferous, oolitic hematite to the "Ida". Because of this confusion in terminology, we refer herein to the entire 5 m interval from the basal conglomerate to the top of the oolitic ironstone as the "Ida beds".

As noted above, the base of the "Ida beds" (and the base of the upper member) is delimited in the Birmingham area by a sharply defined erosion surface that is, in turn, overlain by a 0.5 m-thick hematitic conglomerate, with clasts of quartz, laminated carbonates, and ironstone (i.e., the basal "Ida" conglomerate; Baarli et al., 1996). This bed overlies an important erosion surface (sequence boundary) that locally truncates major parts of the middle member, apparently including the *Stricklandia*-rich carbonates of the Gadsden area (see Chowns, 1996, for discussion). The basal "Ida" bed is considered to represent another transgressive lag conglomerate, analogous to the "Kidney Seam" (Baarli et al., 1996). We interpret the "Ida" interval as a transgressive systems tract, and the well-washed oolitic ironstones at the top as a maximum flooding interval.

The exact age of the "Ida beds" remains in question. Baarli et al. (1996) reported *Stricklandia lens progressa*, which indicates a late Aeronian–early Telychian age, from float samples probably derived from the lower "Ida beds" near Birmingham. Conversely, the occurrence of probable *Stricklandia laevis* in the "Ida beds" at Birmingham, and probably in correlative sandstones near Gadsden (identified by A.J. Boucot in Chowns, 1996), indicates an early Telychian (C4–C5) age for this bed (Baarli et al., 1996). The latter age is also suggested by the discovery of brachiopods transitional between *Pentamerus oblongus* and *Pentameroides suberectus* near the base of the upper Red Mountain Formation (probable "Ida beds") at Fort Payne, Alabama (M.E. Johnson, unpublished data, 1997), and probably in the "Ida" interval south of Birmingham (Baarli et al., 1992). Based on this evidence, we interpret the "Ida beds" to be early Telychian, and approximately equivalent to the middle Clinton Group (Sequence III) in New York.

The erosional sequence boundary below the "Ida beds" probably represents the Sequence II–III boundary of the northern Appalachian Basin. However, this unconformity appears to die out near Gadsden, where pentamerid-bearing HCS sandstones correlative with the

lower "Ida beds" appear to rest conformably on underlying *Stricklandia lens*-bearing limestones. These sandstones may be lowstand deposits analogous to the Cabin Hill Member sandstones in the Rose Hill Formation of Pennsylvania, or to the Oneida Conglomerate tongue and Vernon Station Iron Ore at the base of the Sauquoit Shale in New York (Figures 26, 29).

The majority of Baarli et al.'s (1996) unit F above the "Ida beds" consists of hematitic sandstones with thin stringers of hematitic ooids and shales (Figure 29). A thin (30 cm) oolitic ironstone bed has been traced within the middle of this interval near Birmingham, but its significance is uncertain. It is notable that the correlative interval in northwest Georgia consists of distinctive red shales and thin sandstones (Chowns, 1996), which are comparable to the middle shaly member of the Rose Hill Formation in Virginia, Maryland, and Pennsylvania and to upper parts of the Sauquoit–Otsquago Formations in New York (Brett and Goodman, 1996). These beds are interpreted as the highstand systems tract of Sequence III.

SEQUENCE IV.—Unit F displays an apparent coarsening-up succession. Sandstones near the top may be equivalent to the Center Member of the Rose Hill Formation in Pennsylvania, and form the lowstand sandstone bundle of Sequence IV (Brett et al., 1990; Cotter, 1996). These beds are abruptly overlain by hematitic sandstones and ferruginous limestones, earlier referred to as the "Hickory Nut seam" (Chowns and McKinney, 1980; Chowns, 1996). Near Birmingham, the Hickory Nut seam is a 5–6 m of red ferruginous sandstone capped by purer oolitic ironstones. There is some confusion as to what exactly the term "Hickory Nut Seam" refers to, and we designate the entire red ferruginous interval the "Hickory Nut beds". This interval is analogous to the "Big seam" and "Ida beds", and as them, has a sharply defined base with minor shale rip-up clasts, although no major conglomerate is present.

The ferruginous sandstone of the "Hickory Nut beds" is capped by oolitic hematite with abundant hematized *Pentamerus*, *Stricklandia* sp. cf. *S. laevis*, corals, and bryozoans (Chowns, 1996). The hematite represents a condensed maximum flooding interval analogous and probably equivalent to the Westmoreland Iron Ore beds in the type Clinton Group of New York (Figures 25, 26, 29). The probable equivalent of the top of the "Hickory Nut beds" is represented near Gadsden, Alabama, by a bundle of calcareous sandstones.

An abrupt shift to dominantly shaly facies (unit G of Baarli et al., 1996) above the "Hickory Nut seam" is interpreted herein as a maximum flooding surface. Lower unit

G shows a gradual upward transition from fossiliferous, greenish shelf mudstones to sandy shales and sandstones (Figure 26). Brachipods transitional between *Stricklandia laevis* and *Costistricklandia lirata* (Baarli, 1996; M.E. Johnson, unpublished data, 1997) date these beds as late Telychian (C5–C6). This major deepening almost certainly represents the fourth and largest transgression of the Llandovery (Johnson, 1996), and corresponds to the shales of the Williamson–Willowvale–uppermost Rose Hill interval (subsequence IVA) in the northern part of the basin (Figure 29).

It is noteworthy that Baarli et al. (1996) reported two possible bentonite beds within unit G, one near the base and another about 7 m above the base. The lower of these may correspond to the probable K-bentonites near the base of the Williamson Shale near Rochester, New York (Brett et al., 1994). Geochemical fingerprinting could help test this hypothesis.

A fourth-order subsequence boundary is inferred to occur in the upper part of Baarli et al.'s (1996) unit G. A 3 m-thick bundle of hummocky cross-stratified calcareous sandstone about 5 m above the upper oolitic hematites of the "Hickory Nut beds" at Birmingham has yielded abundant corals and *Costistricklandia*. A similar and probably correlative coral bed at Gadsden has also yielded *Costistricklandia lirata* in life position (Bolton, 1990). The bed also has diverse, relatively large rugose corals, favositids, and stromatoporoids. It is not known whether *Palaeocyclus* occurs in this bed, but the fauna of this coralliferous bed (Figure 27) may be related to that of the diverse coral beds of the late Telychian Fossil Hill Formation in Ontario (see Bolton, 1957). The coral- and *Costistricklandia*-bearing bed in Alabama exhibits a minor facies dislocation at its base, and is in turn overlain by gray silty to sandy mudstones and sandstones. This succession is interpreted as a fourth-order sequence, probably equivalent to subsequence IVB, the Rockway Dolostone–Dawes Sandstone or lower Keefer Sandstone in the north-central Appalachians. The coral–*Costistricklandia* bed may be equivalent to the minor transgressive systems tract represented by the Salmon Creek–basal Dawes bed in New York. It is noteworthy that an epibole of *Costistricklandia* sp. cf. *C. lirata* occurs immediately above the base (Salmon Creek bed) of the Rockway Formation in southern Ontario and western New York.

The coral–*Costistricklandia* bed is overlain at Birmingham and Gadsden by soft sandy shales and interbedded, thin, hummocky cross-bedded sandstones. These upper fossiliferous beds of Baarli et al.'s (1996) unit G may range into the lower Wenlock (Berdan et al., 1986); however, they are largely truncated by a major unconformity.

SEQUENCE V.—Upper unit G shales and sandstones near Birmingham are sharply overlain by an 8–9 m interval of massive, slightly ferruginous sandstone and quartzose crinoidal limestone that locally has large-scale soft sediment deformation or slump features. These strata were earlier identified as part of the Lower Devonian Frog Mountain Formation (see Ferrill, 1984; Thomas and Bearce, 1986; Chowns, 1996). However, fossils from limestones near the top of this interval include corals and *Costistricklandia*, which indicate a latest Llandovery–early Wenlock age (Ferrill, 1984). We infer that this sandstone–carbonate unit records the early Wenlock lowstand–transgressive systems tract of Sequence V (i.e., it is the southern extension of the upper Keefer Sandstone or Bisher Formation). It is important to note in this context that the possibly correlative interval in the Bisher Formation of eastern Kentucky has similar large-scale slump structures. This deformation could represent a seismite, comparable to those described above for the somewhat younger (Wenlock) DeCew Formation. At Centennial Plaza northwest of Birmingham, these sandstones are apparently conformably overlain by 1–2 m of dark gray shales. These beds have not yielded diagnostic fossils, but could represent a feather edge of the Rochester Shale (or Mifflintown Formation). Unfortunately, they are largely cut out at a major unconformity.

Where overlain by the Pridoli "top" member of the Red Mountain, this surface probably is the Salinic Unconformity of the northern Appalachian Basin. Elsewhere, the Red Mountain Formation is unconformably overlain by the Frog Mountain Formation *sensu strictu* or by the Upper Devonian–Mississippian Chattanooga Shale or Maury Formation (Chowns, 1996).

In contrast to earlier interpretations, we infer that the Red Mountain Formation comprises parts of five third-order sequences. The lower and middle members appear to correspond to Sequences I and II of the northern Appalachian region. However, the upper member, as presently defined, can be divided into three sequences, rather than one as in earlier interpretations (e.g., Chowns, 1996). The "Ida" and "Hickory Nut beds" are analogous to the "Big seam" succession of the middle member, and all three ironstones appear to represent lowstand to transgressive systems tracts of third-order Sequences II, III, and IV, respectively. Sequence V is incompletely represented by a slightly ferruginous and strongly deformed sandstone with a sharp base that is probably equivalent to the upper Keefer and the overlying dark gray shale.

Each Red Mountain Formation sequence starts with a sharp erosional base that is correlative with a sequence boundary recognized throughout the Appalachian Basin (Figures 25, 26, 29). These sequence boundaries are over-

lain by ferruginous sandstones and/or conglomerates that are inferred to represent transgressive basal lags. In each case, the sandstones are capped by oolitic hematites and/or shell- and coral-rich beds that reflect transgressive systems tracts.

SEQUENCES IN ROCKWOOD AND RED MOUNTAIN FORMATIONS, GEORGIA AND SOUTHERN TENNESSEE

The Red Mountain Formation shows an abrupt north-west-thinning from over 360 m in northeast Georgia to less than 100 m in southeast Tennessee (Bolton, 1992; Chowns, 1996; Figure 28). As noted above, the interval is commonly termed the "Rockwood Formation" in Tennessee (Driese, 1996; Chowns, 1996), and this local usage obscures its synonymy with the Red Mountain Formation. Chowns (1996; Figure 15) recognized the lower, middle, and upper members of the Red Mountain Formation in the "Rockwood Formation" in Georgia and Tennessee. As the Clinch and "Rockwood" Formations in northern Tennessee, the lower member in Georgia and southern Tennessee has a thin phosphatic basal sandstone; a lower shaly interval (roughly equivalent to the Hagan Member); and an upper hematitic sandstone (Figures 28, 29). To the west, the "Rockwood" thins and has an increasing proportion of skeletal, hematitic limestones that occur in three major tongues or bundles (Driese, 1996). Just over 20 m of equivalent limestone-rich strata crop out at Anderson Ridge in southeast Tennessee, where the term "Brassfield Formation" may be applied (Driese et al. 1991; Driese, 1996).

As in Alabama, the lower member of the "Rockwood Formation" in southeast Tennessee is unconformably overlain by the middle member. The unconformity appears to truncate successively higher beds of the lower member ("Rockwood"-Brassfield) toward the west in precisely the same manner that upper Sequence I (Medina Group) in western New York and Ontario is cut out beneath the Sequence II (lower Clinton) sequence boundary (Figure 29). This parallelism may reflect a persistent NE-SW trending high or forebulge that developed on the western rim of the foreland basin.

The base of the middle member of the "Rockwood Formation" is a thin hematitic bed that appears to be coextensive with the Irondale seam in Alabama (Chowns, 1996; Figures 28, 29). This hematitic bed is almost certainly equivalent to the oolitic hematite bed observed at several localities at the contact between the Clinch (or middle sandstones of the "Rockwood") and Rose Hill shales or equivalents to the north (Driese, 1996; discussed

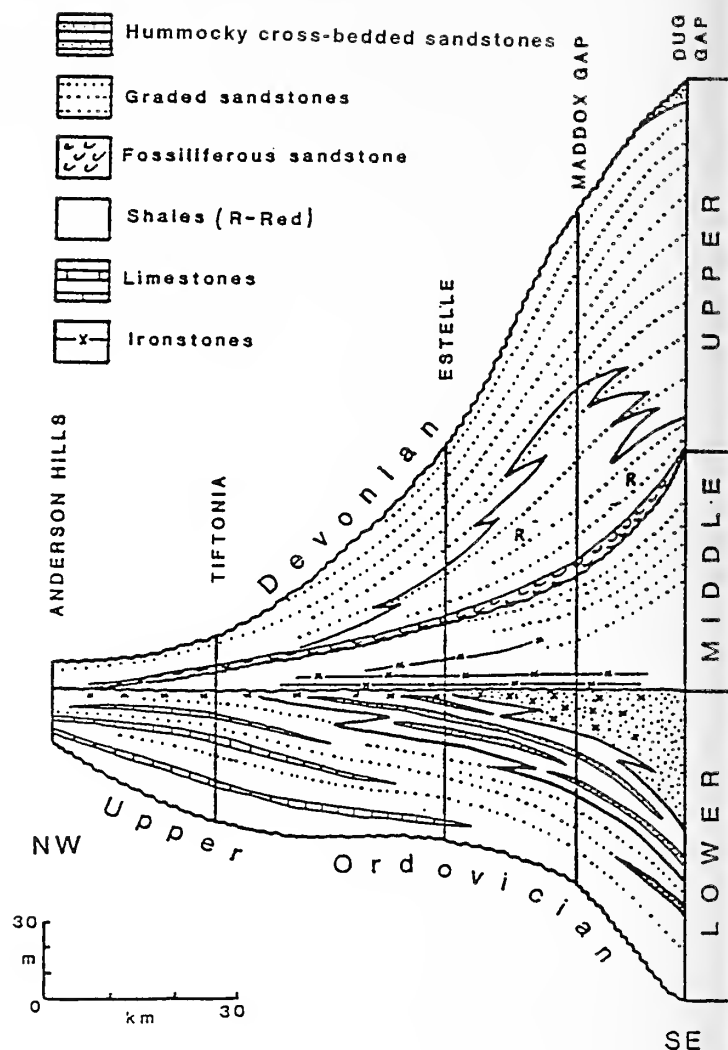


FIGURE 28—Cross-section of Rockwood-Red Mountain Formation in northwest Georgia and southeast Tennessee. From Chowns (1996).

above). Just as in the Red Mountain Formation in Alabama and the Rose Hill to the north, the middle member of the "Rockwood" in Tennessee is relatively shaly, and contains at least two persistent ironstone intervals that probably correspond to the "Kidney bed" and "Big seam" of the Birmingham area (Chowns, 1996).

The upper member of the "Rockwood Formation" has a major sequence-bounding unconformity at its base that is overlain by a shell- and phosphate-rich lag bed (Chowns, 1996), which is probably equivalent to the *Stricklandia lens progressa* limestone package at Gadsden, Alabama (discussed above) or possibly to the "Ida" seam (Figures 25–29). As in Alabama, these lower sandstones are overlain by maroon shale, and these are overlain, in turn, by more cross-bedded sandstone at Ringgold, Georgia (Chowns, 1996) and Green Gap, Tennessee (Easthouse

and Driese, 1988; Figure 29). The maroon shales are tentatively assigned to a middle Aeronian–early Telychian (C1–C5) age on the basis of a succession of poorly preserved *Eocoelia* species. These include *E. sp. cf. E. hemispherica*, *E. intermedia*, and *E. curtisi* (B.G. Baarli in Chowns, 1996; Figure 29). The occurrence of *E. hemispherica* above the pentamerid-rich sandstone at Ringgold, Georgia, is problematical, as the sandstone appears to correlate with strata to the southwest that contain *Stricklandia lens progressa*, a form that normally appears above the range of *E. hemispherica*. This problem demands further study. At present, the maroon shales and some of the overlying sandstones are tentatively correlated with the “Ida beds” and overlying greenish mudstone interval in Alabama.

The stratigraphy of the upper Rockford Formation has not been studied in detail. However, the uppermost sandstones become thinner-bedded and distinctly more shaly, and contain diverse brachiopods and even corals (Chowns, 1996). This change signals the major deepening associated with the fourth Llandovery transgression (Figures 1, 29). The overall succession probably correlates with Baarli et al.’s (1996) units F and G (including the “Hickory Nut beds”) at Birmingham (Figures 26, 29).

GENESIS OF SILURIAN CONDENSED BEDS

In this report, we have employed a broad definition of the terms “condensed facies” or “condensed beds”. These are thin intervals, typically 1–2 m or less in thickness, that represent prolonged intervals of geologic time and show evidence for a complex series of processes. The qualitative term “time-rich strata” is more or less synonymous with condensed beds. “Condensed interval” has also come to take on a more specific meaning in the context of sequence stratigraphy, and refer to thin, time-rich strata located in the transgressive to early highstand systems tract and which are typically associated with a surface of maximum sediment starvation (Loutit et al., 1988; Baum and Vail, 1988; Kidwell, 1991). Most of the widespread shelly, ferruginous, and phosphatic beds discussed in higher sections of this study occur low in depositional sequences. In some instances, they immediately overlie the sequence boundary as transgressive lags (e.g., basal phosphatic–hematitic sandstones of Sequences I and II and Westmoreland Hematite in Sequence IV). In others, they occur at or slightly above a maximum flooding (starvation) surface (e.g., Furnaceville and Wolcott Furnace hematites in Sequence II and “Rogers ore” in sequence V). Condensed beds in a particular region are typically thin relative to equivalent strata elsewhere (Fürsich, 1978; Baum and

Vail, 1988; Kidwell, 1991; Kidwell and Bosence, 1991). However, many condensed intervals reported herein in the Silurian Appalachian Basin remain rather uniformly thin over large distances, although they may have once been thicker in areas proximal to the paleoshoreline. Unfortunately, such evidence has typically been lost during post-Silurian erosion, which has removed the most proximal facies from most sequences.

Although it is impossible to ascertain the exact time interval represented by a given set of condensed strata, it is frequently possible to make an assessment of the relative magnitude of time represented by such beds through their relationship to sedimentary cycles. If it is assumed that the cycles were generated by roughly symmetrical oscillations in sea-level (which may or may not be a valid assumption; see Cotter, 1988), one may gauge the rough duration of beds by the scale of cyclicity of which they are a part. Durations of larger cycles may be estimated biostratigraphically, and those of their subdivisions by interpolation. For example, a condensed bed may represent either a major portion or nearly all of the transgressive phase of a third-order cycle (e.g. Westmoreland Hematite in Sequence IV of central New York), and may be a few million years in duration (e.g., Meyers and Milton, 1996). In such a case, the component beds would probably each represent a few hundred thousand years of accumulation. On the other hand, other condensed beds clearly lie on flooding surfaces associated with minor cycles or parasequences that are small increments of the larger-scale cycles. This is the case with a number of thin phosphatic to ferruginous beds at the tops of coarsening-up shale–sandstone cycles, such as those documented in the Medina Group in New York (Duke and Brusse, 1987) and in the Rose Hill Formation in Pennsylvania (Cotter, 1988). These beds represent, at most, an average duration of a few tens of thousands of years of accumulation and non-deposition.

The scales of sedimentary time-averaging may also provide another important clue for estimating the duration of condensed beds (Fürsich, 1978; Kidwell, 1991). Kidwell and Bosence (1991) proposed a classification scheme for time-averaging that takes into account taxonomic and ecological factors. Event beds that show evidence for very rapid deposition by turbulence depositional events include turbidites and tempestites (Aigner, 1985; Kidwell, 1991). The presence of single event beds should not be used to rule out the possibility that an interval with such beds is time-averaged. For example, very condensed intervals may consist of a stack of event deposits, each one separated widely in time from adjacent beds. This may be the case with stacked graded tempestites that occur near the base of the uppermost Rose Hill Formation in Pennsylvania.

LLANDOVERY												W	SERIES
RHUDDANIAN				AERONIAN				TELYCHIAN				SH.	STAGES
A1	A2	A3	A4	B1	B2	C1	C2	C3	C4	C5	C6		OSTRACODE ZONE
					?	Z. erecta	Z. excavata	Z. decora	Z.	M. lata	B. rudis	M. typus	
						Irregular	l. discreta		P. celloni			P. amorpho-gnathoides	
RED MOUNTAIN FORMATION													N.E. ALABAMA - N.E. GEORGIA
<div>lower</div> <div>unit A shale - sandstone</div> <div>phosphatic ss</div>													
<div>middle</div> <div>Big Seam</div> <div>unit E</div> <div>Kidney - Ironstone</div> <div>Alfreto Ss.</div> <div>unit B sandstone</div>													
<div>upper</div> <div>unit G sandstone</div> <div>Hickory Nut</div> <div>gray shale</div> <div>sandy shale</div> <div>lca</div>													
ROCKWOOD (RED MOUNTAIN) FORMATION													N.E. GEORGIA - S.E. TENNESSEE S.E. KENTUCKY
<div>lower member</div> <div>"Hagen" shale</div> <div>phos. ss</div>													
<div>middle member</div> <div>unit B</div> <div>Kidney - Ironstone</div> <div>Big Seam - equiv.</div> <div>unit E - equivalent</div>													
<div>upper member</div> <div>gray shale</div> <div>red shale</div> <div>Keokuk ss</div>													
BRASSFIELD				NOLAND		CRAB ORCHARD				NORTH-CENTRAL KENTUCKY, SOUTH OHIO			
<div>lower shale</div> <div>Belfast</div>				<div>Purn Creek Shale</div> <div>Oldham ls.</div> <div>lubegrud</div>		<div>Waco ls.</div> <div>Estill Sh.</div> <div>lower Bisher Dol.</div> <div>upper Bisher Dol.</div>							
CABOT HEAD				NOLAND						EAST-CENTRAL OHIO, WESTERN NEW YORK			
<div>"White Clinton"</div> <div>Power Glen</div> <div>Belfast</div> <div>Whitpool</div>				<div>"Red Clinton"</div> <div>"Gray Clinton"</div> <div>Rocker Shell</div> <div>Neanga Shale</div>		<div>Dayton ls.</div> <div>Estill Sh.</div> <div>Bisher Frn.</div> <div>Rochester Sh.</div>							
MEDINA GRP.				CLINTON				WEST-CENTRAL NEW YORK					
						lower		middle		upper			
<div>SH.</div> <div>"Gimbley" fm.</div> <div>Theroid ss.</div> <div>Corbica Sh.</div> <div>Keokuk ss.</div>						<div>Reynolds ls.</div> <div>Madlawood Sh. - Desmore Creek</div> <div>L. Sodas Sh.</div> <div>U. Sodas Sh.</div> <div>Wolcott</div>		<div>Sauquoit Sh.</div> <div>Williamson Sh.</div> <div>Westmoreland</div> <div>Rockway Dol.</div> <div>Ilodquoit ls.</div> <div>Rochester Sh.</div>					
SEQUENCE I				SEQ. II		SEQ. III		SEQ. IV		SEQ. V		SEQUENCE	
												SEA LEVEL CURVE	
												0 1 2 3 4 5	

Within-habitat time-averaging is common in many sedimentary beds. It is indicated by slightly different modes of preservation of fossils that represent a roughly similar habitat or community. Most intervals recognized in this report as relatively condensed contain reworked, disarticulated, and abraded shell material, with well-preserved articulated individuals of the same species on the same bedding planes. In such cases in shallow marine environments, one may estimate the durations of these beds at decades to a few thousand years at most (Parsons et al., 1988; Kidwell and Bosence, 1991). During such a time interval, the sea floor environment remained relatively uniform, as indicated by the presence of similar suites of fossils with differing modes of preservation above and below the condensed bed.

Beds with fossils that represent rather distinct depositional settings indicate long time spans of very low net accumulation and, consequently, sedimentary condensation. Such accumulations have been termed "ecologically time-averaged" (Kidwell and Bosence, 1991), and the beds containing them are time-rich and probably represent time spans of thousands to a few tens of thousands of years. Ecologically time-averaged beds might represent the transgressive systems tract of a third-order sequence. For example, certain beds in the Silurian Red Mountain Formation contain mixtures of offshore to shoal facies with *Pentamerus* (BA-3) and deeper subtidal *Stricklandia* (BA-4) biofacies. Extreme examples of ecological time-averaging might feature mixtures of fossils that represent nearshore to deep marine biofacies. For example, the 1–5 cm-thick Second Creek phosphatic bed at the base of the Williamson Formation (Sequence IV) in central New York contains mixtures of reworked *Eocoelia* (BA-2) and *Whitfieldella-Atrypa-Eoplectodonta* (BA-3–4) brachiopod associations, and is immediately overlain by black shale with monograptids and *Dicoelosia* (BA-4–5). Although precise water depths are difficult to assess, one may estimate that the BA-2–5 depth spectrum spanned tens of meters (Brett et al., 1993). However, remains of organisms that span this complete depth range are mixed in a single bed. The Second Creek bed and other similar units (e.g., Densmore Creek bed at base of sequence II) may record the entire deepening phase (TST) of a large-scale cycle. Such condensation seems clearly to require the passage of a substantial amount of time. Even

at the fastest rates of sea-level rise during deglaciation, this type of shift in relative water depths would probably require many thousands of years (see Kidwell and Bosence, 1991).

In some instances, there is direct biostratigraphic evidence for very long-term mixing within a bed. Index fossils that represent two or more distinctive biostratigraphic zones may be present in a thin stratigraphic interval or a single bed. Such accumulations, referred to as "biostratigraphically condensed", clearly represent long time intervals. One may reasonably estimate that such mixtures represent time-averaging and condensation on the scale of several hundred thousand to a few million years. Only a few possible examples of biostratigraphic condensation can be noted in the Silurian sequences considered herein. Green shales in the lower transgressive beds (Whirlpool Sandstone) of Sequence I contain reworked Late Ordovician and non-reworked Early Silurian palynomorphs (M. Miller, personal commun., 1986). Mixtures of different conodont zones have been discovered in the Furnaceville Hematite at the base of Sequence II, and conodonts attributable to the *Pterospathodus celloni* and *P. amorphognathoides* Zones have been found commingled in the Second Creek phosphatic bed and equivalent Westmoreland Hematite (M.A. Kleffner, personal commun., 1997).

Other evidence for time richness in sedimentary units comes from the taphonomy of fossils and early diagenetic mineralization features. In particular, reworked fossils that show evidence of early diagenetic alteration provide clear-cut evidence for erosional reworking and suggest long-term time-averaging. Rotated geopetal fillings and bored and encrusted steinkerns (internal molds) provide evidence for long intervals of relative sediment starvation and minor erosion of the sea floor (see Brett and Baird, 1986, 1993; Kidwell, 1991). Most of the phosphatic beds (Art Park, Densmore Creek, Second Creek, Salmon Creek) and oolitic hematite beds (e.g., Furnaceville, Westmoreland, and Kirkland in New York and Irondale, "Kidney", and "Ida" beds in Alabama) feature corroded, bored, and mineralized steinkerns and/or intraclasts.

Another important indicator of sedimentary condensation is early diagenetic mineralization within sediments, such as the fillings of fossils, particularly hematite impregnation or phosphatization of skeletal fillings. Phosphorite is common at certain horizons in the Silurian of the Appalachian Basin, and typically occurs as glossy black nodules or reworked bored pebbles. Ferruginous mineralization, in the form of chamositic or hematitic ooids or fossil impregnations, is notable in the Silurian. Both phosphorite and chamosite (but perhaps not hematite) are evidently early diagenetic, and probably both

FIGURE 29—(opposite) Llandovery–Wenlock from Birmingham, Alabama, to west-central New York. Sequence interpretations and relative sea-level curve based on strata in central New York; relative depth scale calibrated by Boucot's (1975) benthic assemblages (BA) 0–5 (see Figure 6 explanation). Abbreviations: SH, Sheinwoodian; other abbreviations in Figure 4 and 6 explanations.

formed within the upper few centimeters of sediment, as indicated by the fact that these minerals are commonly reworked into such lag deposits as storm layers and reworked, cross-bedded, skeletal hash deposits. Conditions under which these two forms of mineralization take place remain somewhat problematical. However, in recent years, some progress has been made toward understanding the genesis of phosphatic nodules and ironstones.

Ironstones appear to have formed non-randomly in earth history, and are particularly typical of times of "greenhouse climates". These include the Ordovician-Devonian and Jurassic-Early Cenozoic (Van Houten and Bhattacharya, 1982). Their formation may have been favored by increased weathering of terrigenous rocks under higher concentrations of atmospheric CO₂. They also appear to be typical of quiescent intervals between tectophases of orogenies. Hence in eastern North America, they occur in the early Middle Ordovician, very Late Ordovician, and Middle Silurian, and less commonly in the late Early and Middle Devonian (Van Houten and Bhattacharya, 1982). These are all intervals of reduced tectonic activity between orogenic pulses. This association may result from enrichment of iron in sediments during times of lowered sediment influx and/or deeper weathering due to less active erosion and lower relief of source terranes (Cotter, 1991; Cotter and Link, 1993).

Under mildly reducing conditions, the precursors of ironstone, such as the iron-rich clays berthierine or chamosite, may precipitate in the upper part of the sediment, commonly as oolitic coatings or impregnations of skeletal grains. Later diagenesis may further oxidize these precursors to hematite or goethite (Cotter, 1991). Most Clinton "fossil ores" occur near the interfaces of reduced iron-rich muds and carbonate or sandy shoal facies. This suggests that critical redox-boundary conditions existed in areas of relatively low sediment accumulation in mixed siliciclastic-carbonate sequences (Cotter, 1991; Cotter and Link, 1993). In particular, oolitic hematites are most commonly associated with evidence for at least intermittent agitation of the sea floor by currents or waves. Many oolitic hematite beds exhibit cross-stratification, ripples, sharply scoured base, and sparry cements (with winnowing of fine-grained sediment; see LoDuca and Brett, 1994; CEB, unpublished data, 1997). Hence they tended to form close to normal wave base, within a zone that was stirred frequently by storms. This is indicated by the fragmental nature of fossils, concentrically coated grains of chamositic, hematitic ooids, or spastoliths. Ironstone beds in the Silurian are typically associated with green to purplish, nearshore mudrock facies. In most cases, these sediments were not highly organic-rich.

Cotter (1991) has shown conclusively that many or most of the Silurian ferruginous ooids and iron impregnations of skeletal grains were originally chamositic clays. Thus, they derived from ferrous clays that must have formed under reducing conditions. He inferred that most of the alteration of these original iron silicates to hematite occurred during deep-burial diagenesis during the Late Pennsylvanian-Permian Alleghanian orogeny, when hot brines were flushed through older sediments. Although this may be true in many cases, there are other situations in which it appears that the hematite formed quite early. Some of this oxidation of the ooids may have occurred during reworking of the chamosite-replaced material on the sea floor within oxidizing environments (see Chowns, 1996, discussion of chamositic and hematitic ooids in the Ordovician of Alabama).

Silurian hematitic beds are commonly associated with relatively diverse, open marine fossil assemblages with pelmatozoans, bryozoans, and a variety of brachiopods. Cotter and Link (1993) argued that the shells were emplaced into "deep water" dysoxic to anoxic muds, which are typically represented by shales barren of fossils. They inferred that many of the hematitic fossil beds represent allochthonous shell accumulations. However in many cases, sparsely fossiliferous greenish-gray and purple shales interbedded with the ironstones actually contain sparse remains of the same species of brachiopods and other fossils that are found in the ferruginous beds. Similarly, Chowns (1996) reported in situ burrowing bivalves in mudstones that contain chamosite and hematite ooids. These data indicate that the muddy seafloors were not necessarily anoxic, but represent environments similar to those in which the ironstones accumulated. Shells in at least some ironstone beds (e.g., Westmoreland Iron Ore, upper Rose Hill Formation, and "Kidney" and "Ida" beds) were probably concentrated during periods of low sediment accumulation rates, rather than as influxes from adjacent oxygenated shoal environments into lifeless sea-floor settings below an oxycline. However, the chamositic cements may have formed in reducing micro-environments within sediment pores and skeletal interstices. The origin of the concentric chamositic coatings is more obscure. These apparently formed as plastic iron-rich clays, because they are flattened and deformed to form spastoliths (discoidal or "flaxseed" ooids). The precipitation of such ferrous clays in oxidizing environments may have been mediated by bacterial coatings on grains (Chowns, 1996).

LoDuca (1988) identified two main depositional settings for Clinton "iron ore" or ferruginous beds. These are shoal margins and transgressive lags. The first type occurs as localized lenses associated with inner shoal margin facies at the interface between skeletal limestones and mudrocks. Iron, which was originally concentrated

in chamositic clays, was probably derived from deeply weathered terrigenous sediments. Iron-rich clays were precipitated around such nucleation sites as sand grains and small skeletal fragments. Mixed redox conditions probably occurred at the boundaries between inner-shoal margins and "lagoonal" reducing muds. Cotter and Link (1993) proposed a somewhat similar mechanism for the concentration of ferruginous clays that were ultimately oxidized into hematites along the outer edges of shoreface sand bodies. They noted the association of ferric iron enrichment in the upper sands of many shallowing- or coarsening-up, nearshore, mud-to-sand cycles. Precipitation of hematitic cements and ooid coats on both the inner sandy and outer carbonate-bank sides of broad shelf lagoons is a consistent interpretation. This precipitation in both settings was a response to lowered sediment accumulation rates, either due to winnowing and bypass of sediments or sea-level rise, which flooded coastal and starved offshore areas.

Lenticular, hematized, fossil-debris grainstones, or "fossil ores", should be distinguished from more widespread sedimentary iron ores. The latter include oolitic and phosphate-rich ironstone beds that appear to form condensed intervals either at the tops of shallowing-up cycles or the bases of overlying sequences and subsequences. Such "transgressive lag" ironstone beds appear to cross-cut underlying facies to some degree. Skeletal grainstone or packstone bodies in the Clinton Group may be capped by fossil fragmental or oolitic hematites. Oolitic hematites, commonly with quartz sand grain nuclei, also occur on the tops of coarse-grained sandstone bodies and are overlain by and/or interbedded with greenish-gray shales (see Hallam and Bradshaw, 1974; Hallam, 1992; Cotter and Link, 1993; Driese, 1996; Chowns, 1996). The primary controls on their formation may have again been very widespread intervals of sediment starvation during maximum sea-level rise, and the reworking and concentration of iron from such older sediments as earlier-formed chamositic ooids and coated fossil or quartz sand grains. These widespread units represent major condensed beds that overlie diastems or major erosion surfaces.

Widespread complex oolitic and shelly ironstone beds tend to pass laterally offshore into thin phosphatic lag deposits. This pattern is seen, for example, in the Art Park hematitic and phosphatic beds (Sequence I), the Webster hematitic conglomerate and laterally equivalent Densmore Creek phosphatic bed (base of Sequence II), the Verona Station oolitic ore and unnamed phosphatic ooid bed (base of Sequence III), and the Westmoreland oolitic ironstone and coeval Second Creek phosphatic bed (base of Sequence IV). Both ferruginous and phosphatic enrichments record sediment-starved conditions, but

they evidently formed under somewhat different sea-floor environments.

In contrast to ferruginous sediments, phosphorites seem to have formed on genuinely dysoxic sea floors. In general, there is less evidence for bottom-water agitation in phosphorite nodule beds, although examples of concentrically coated phosphorite ooids are also known, as noted above, in both the Verona Station and Westmoreland beds (CEB, unpublished data, 1997). Unlike the typically fossiliferous ironstone beds, phosphatic nodule beds generally contain a low-diversity fauna composed largely of small gastropods, bivalves, and brachiopods, which represent more stressed, dysoxic sea-bottom conditions.

Precipitation of phosphorite was favored by an oxidizing micro-environment. Release of dissolved phosphate into a sediment's pore waters occurred under anaerobic conditions. Under oxic conditions, the phosphate can become adsorbed to ferrous hydroxides in sediment (Swirydczuk et al., 1981; Berner 1981; Allison, 1988a, 1988b; Lucas and Prévôt, 1991). As these ferrous hydroxides were buried and passed through the sediment anoxic-oxic boundary, they were reduced. This liberated phosphates to pore water (Swirydczuk et al., 1981; Lucas and Prévôt, 1991). Another probable source of phosphate is organic matter, and this may also help to explain the association of phosphatic nodule beds in relatively organic-rich, dark, offshore marine muds. Dissolved phosphate may be released back to the water column if anoxia persists to the sediment-water interface. However, if a thin oxidizing zone exists in pore water within the upper sediment column, then the phosphates may be reprecipitated, especially around such phosphatic skeletal nuclei as bones, conodont elements, linguloid brachiopod valves, or various arthropod sclerites (Berner, 1981; Swirydczuk et al. 1981; Lucas and Prévôt, 1991).

If the sediment accumulation rate was low, then the time spent at this transition from deeper anoxic to surface oxidized interface will be high. Thus, a large proportion of the dissolved phosphate compounds will be concentrated in one sediment layer. This can increase pore water levels of phosphorus so that phosphate minerals can precipitate. These minerals may impregnate muds or form concretions (Baird, 1978; Lucas and Prévôt, 1991). Thus the occurrence of phosphatic fossil molds or concretions is nearly always an indicator of low rates of sediment accumulation. Phosphorite is commonly reworked during transgressive ravinement, and most Silurian basal transgressive lags (i.e., bases of Sequences I-IV) are enriched in phosphatic pebbles. Thin and more discontinuous phosphatic pebble beds may also occur at marine flooding surfaces (including maximum flooding surfaces). Examples include the contact of the Whirlpool Sandstone

and the Power Glen or the contact of the Devils Hole Sandstone and lower Grimsby shales. Locally, these pebble beds grade into oolitic ironstones.

In summary, phosphatic nodules and ironstones are genetically related. Both tend to occur in thin lag accumulations that are laterally extensive, and may also overlie the tops of shallowing-up cycles and/or sequence-bounding erosion surfaces. Phosphatic and ferruginous deposits are commonly associated with skeletal concentrations, in which taxonomic and ecological composition suggest environmental scales of time-averaged sedimentation accumulation with prolonged sediment starvation. Phosphatic nodules and ferruginous sediments may co-occur. Hematitic beds may grade laterally (typically in an offshore direction) into non-ferruginous phosphatic nodule beds that represent distinctive types of depositional environments. Most importantly in the Silurian of the Appalachian Basin, widespread ironstones and phosphatic nodule horizons are very important indicators of sediment starvation within mudrocks, and commonly indicate major transgressions and/or marine flooding surfaces (Baird, 1978; Witzke and Bunker, 1996).

DISCUSSION

Figures 15 and 29 summarize the inferred correlations of Llandovery–early Wenlock strata from Birmingham, Alabama, to Ohio, and into central New York. Regional stratigraphy indicates the persistence of five major (third-order) depositional sequences in Lower Silurian strata throughout the Appalachian Foreland Basin. Higher sequences can be traced from New York into central Virginia, but erosional truncation of Upper Silurian strata to the south prevents extension of these correlations into the southern Appalachians. Moreover, some of the smaller-scale subsequences (or fourth-order sequences) may also be recognizable in appropriate facies from New York to Alabama. A key limitation is the lack of detailed biostratigraphic zonation in some areas, but tentative correlations can be made with existing biostratigraphic control and details of cycle and event stratigraphy. Lowstands and highstands of the depositional sequences can also be related to the global falls and rises of sea-level recognized by Johnson (1996) and others.

Sequences and subsequences are most distinct in more offshore (mid-shelf) facies throughout the study area, but tend to become obscured in thick marginal marine sandstone equivalents (Shawangunk, Massanutten, Eagle Rock, Clinch), where lowstand to transgressive sand bodies tend to become amalgamated. Nonetheless, the occurrence of shaly, slightly fossiliferous tongues within these sand bodies permits tentative recognition of

major highstands. Shell-rich and typically ferruginous to phosphatic beds mark many of the major condensed intervals associated with marine transgressions, and are among the most extensive and useful regional markers.

Sequence I is characterized throughout the Appalachian Basin by a sharp basal erosion surface overlain by a relatively thick siliciclastic-dominated succession (Medina Group and Tuscarora, Clinch, lower Rockwood–Red Mountain Formations). At most locations, Sequence I is readily differentiated into at least three internal subsequences (Figures 15, 29). Nearly all areas show a basal transgressive sandstone that is typically marked near its top by thin phosphatic deposits (Whirlpool, lower Tuscarora, basal transgressive sandstone of Clinch, Rockwood, and Red Mountain Formations). This is succeeded by shaly deposits that occur relatively low in the succession and record maximum flooding, probably during an early–middle Rhuddanian sea-level highstand.

As this highstand does not appear to correlate with Johnson's (1996) late Rhuddanian eustatic rise, it may instead record a very widespread episode of foreland basin subsidence. These shale-rich beds are abruptly overlain by a thin sandstone interval, commonly with phosphorite and/or oolitic hematite at their tops, and succeeded by a return to shale deposition (Devils Hole–Art Park phosphate beds and oolitic iron ore beds in the Clinch Formation of Virginia). This represents the lowest ironstone in the Silurian. Finally, several sections have thin, heavily bioturbated (with the apparently time-specific trace fossils *Arthropycus* and *Daedalus*), ferruginous sandstones that indicate minor condensed intervals (Thorold and Kodak Sandstones in New York; Castanea Member in Pennsylvania and Maryland; and upper Clinch and Rockwood–Red Mountain Formations in Virginia, Tennessee, Alabama, and Georgia). Evidence of condensation and a widespread shaly interval high in Sequence I (Cambria Shale; Clinch–Rockwood; upper part of lower member of Red Mountain) may be a local, subdued reflection of the earliest Silurian eustatic highstand.

Sequence II is marked nearly everywhere by an abrupt change to finer-grained, green-gray to maroon siliciclastics, carbonates, and ironstones (lower Clinton Group [New York], lower Rose Hill Formation [central Appalachians], middle member of Rockwood–Red Mountain Formation [southern Appalachians], top of Brassfield Formation [Kentucky, Ohio]) (Figures 15, 29). This change appears to coincide with an early Aeronian sea-level highstand, but the decrease in coarser-grained siliciclastics and influx of red clays may also signal a tectonically quiescent interlude, lower relief, and deeper weathering of source terranes. Overall, Sequence II is the most phosphate- and iron-rich of all of the sequences. A thin bed of phosphatic nodules and/or oolitic hematite,

the second major ironstone, immediately overlies the basal contact at most sections (Densmore Creek–Webster beds [New York and Pennsylvania], unnamed hematites [central Appalachians], Irondale bed [Alabama]). This unit represents a basal transgressive lag. Several beds or stringers of fossiliferous to oolitic hematite also occur in Sequence II in New York (Furnaceville, Sterling Station, middle Sodus, and Wolcott Furnace ironstones) and in Alabama (“Big seam” and laterally equivalent ironstone stringers in the Rockwood Formation). These hematitic beds reflect minor, probable fourth-order flooding surfaces, especially in the middle Aeronian (Reynales Limestone and associated hematites) and early Telychian (Wolcott Furnace). With the exception of the Cresuptown bed of Maryland, ironstones are not prominent within the majority of the Rose Hill Formation, but do occur in laterally equivalent carbonates (e.g., Packer Shell in the western subsurface of Pennsylvania, Ohio, and Kentucky; Figures 15, 29).

The abundance of ferruginous and phosphatic material at the beginning of Sequence II may reflect an increased supply of iron-rich clays from weathered source terranes. Two widespread carbonate intervals within an otherwise shaly succession (i.e. Reynales and Wolcott Limestones in New York) appear to correspond to Johnson’s (1996) middle Aeronian and early Telychian highstands. The signatures of these deepening events are very subtle in the central Appalachians. More detailed bio- and event-stratigraphic work is required to determine whether or not individual subsequences (e.g., Reynales and Wolcott Limestone) recognized in the classic Clinton Group of New York can be discerned within the main mass of the lower Rose Hill Formation or the middle member of the Rockwood–Red Mountain Formations. In northeast Alabama, a shaly limestone interval rich in *Stricklandia lens progressa* high in the middle member of the Red Mountain Formation may mark the position of the Wolcott. A probable fourth-order sequence-bounding disconformity appears to underlie this package.

A sand-rich interval in the Rose Hill–Rockwood Formation (Cabin Hill Member) appears to record a progradation of coarse-grained siliciclastics triggered by a middle Telychian sea-level drop. This is the lowstand systems tract of Sequence III (Figures 15, 29). In central New York, this lowstand may be recorded by a tongue of Oneida Conglomerate. However, in west-central New York, the sequence boundary is marked only by a minor erosion surface again overlain by a transgressive lag rich in phosphate and oolitic hematite (Verona Station ore in central New York). In Alabama, the approximately equivalent interval is the hematitic “Ida beds” at the base of the upper member of the Red Mountain Formation,

and the sequence boundary is a more prominent, regional angular unconformity that removed upper parts of Sequence II (middle member). Highstand deposits of Sequence III appear to represent relatively shallow, muddy-shelf conditions comparable to those in Sequence II (Sauquoit Shale of New York, middle shaly member of Rose Hill Formation [Pennsylvania, Maryland, and West Virginia], shales in the lower part of the upper member of the Red Mountain Formation [Alabama]). This was probably a relatively minor transgression, not previously recognized on global sea-level curves, and possibly due to tectonic subsidence.

The base of Sequence IV is marked in western and west-central New York by the most prominent erosion surface of the Silurian. This regional angular unconformity also extends into Ontario, Ohio, and Kentucky. It is interpreted as an erosive beveling of a regional arch or forebulge during a late Telychian sea-level lowstand. In the depocenter of the foreland basin, no prominent unconformity is observed, but a second bundle of sandstones, the Center Member, seems to reflect the same lowstand. Ferruginous sandstones in the middle of the upper member of the Red Mountain Formation (“Hickory Nut seam”) may also record this lowstand and/or the initial transgression of Sequence IV. More importantly, virtually all localities that preserve this interval have a very distinct, condensed shell-rich bed as the transgressive systems tract of Sequence IV (Dayton–Waco Limestones [Ohio, Kentucky], Merrittton–Fossil Hill Limestones [Ontario], Westmoreland Hematite–Second Creek phosphate bed [New York], “fossil ore” bed of upper Rose Hill Formation [Pennsylvania, Maryland, West Virginia], unnamed coral-rich hematites at top of “Hickory Nut seam” [Alabama]). Although the beds may be slightly diachronous, the distinctive brachiopod, coral, ostracode, conodont, and/or graptolite faunas associated with these carbonates and ironstones bracket them within the upper Telychian *Pterospiriferus amorphognathoides* Zone. This condensed interval is everywhere overlain by shales (Willowvale–Williamson [New York], Estill [Ohio, Kentucky], uppermost Rose Hill Formation [central Appalachians], and upper Red Mountain–Rockwood Formation shales [Tennessee, Georgia, Alabama]). The faunas of these shales suggest a similar age and relatively offshore (BA 3–5) biofacies that are typically the deepest water assemblages found in any section. Thus, there can be little doubt that the Westmoreland-equivalent condensed beds and overlying shales record the fourth and strongest Silurian sea-level transgression–highstand. Even minor fourth-order cycles, especially the basal condensed Rockway–Dawes Sandstone of Sequence IV, can be correlated regionally in New York and Pennsylvania.

Sequence V, although imperfectly preserved due to later erosion, shows a similar regional persistence. Nearly all localities in the northern and central parts of the basin have a dolomitic or ferruginous carbonate (Irondequoit Limestone [western New York], Kirkland Hematite [central New York], Bisher Dolostone [Ohio, Kentucky]) or calcareous sandstone (Keefer [Pennsylvania, Maryland] and unnamed uppermost Red Mountain Formation sandstones [Alabama]) that sharply overlie finer-grained sediments. This interval represents the lowstand-transgressive phase of a Sheinwoodian depositional sequence. A sharp change at the top of this interval to mudrocks with offshore biofacies (parts of Bisher Dolostone, Rochester Shale–Glenmark Shale–DeCew Dolostone in northern and central Appalachians) records a major apparent eustatic highstand.

The widespread nature of major depositional sequences and condensed beds in the Appalachian foreland basin provides strong support for generation of cycles by eustatic fluctuation (see Johnson et al., 1985; 1990a, 1990b; Johnson, 1996; Ross and Ross, 1996). Moreover, tentative correlation of several smaller-scale condensed beds suggests that even higher-order eustatic fluctuations may be recorded. Thus, despite strong tectonic overprint on the Appalachian foreland basin, we argue that many features of the stratigraphic pattern reflect allogenic cyclicity.

CONCLUSIONS

This report presents a synthesis of Early Silurian (Llandovery–early Wenlock) sequences, events, and biostratigraphy from seven areas of the Appalachian Foreland Basin from Ontario to northeastern Alabama. Higher parts of the Silurian are not considered in detail because they have been removed in southern areas at post-Wenlock erosion surfaces.

Inter-regional comparisons of successions in the various areas indicate that four or five (or more depending upon extent of erosional truncation) major third-order depositional sequences, and at least some of their component subsequences, persist throughout the Appalachian Foreland Basin. These sequences are most readily identified in offshore heterolithic facies, but tend to be more obscured in eastern siliciclastic facies. Despite major differences in local nomenclature, facies successions within sequences display similarities, at least along the northeast-trending depositional strike. These depositional sequences are approximately synchronous as judged from the rather loose constraints of the available biostratigraphy.

Sequence I is characterized by a coarse-grained, siliciclastic-dominated succession (Medina, Tuscarora,

Clinch) with a complex, basal transgressive sandstone that overlies the regional Cherokee Unconformity. It is of late Rhuddanian–early Aeronian age. The west-tapering wedge of sandstones and conglomerates suggests input with renewed tectonic uplift in the latest phase of the Taconic orogeny. Deepest water facies (typified by benthic assemblages 2–3) generally occur in the lower third of the sequence, and sandy gray shales are capped by phosphatic to hematitic beds. Upper parts of this sequence are coarser-grained, gray to red sandstones, typically quartz arenites, with minor shaly intervals and bioturbated zones (with the temporally restricted traces *Arthropycus* and *Daedalus*) that appear to record minor transgressions, possibly associated with the late Rhuddanian eustatic highstand. In general, however, coarse-grained sandstone beds occur near the top and signal regressive conditions that led up to the Sequence I–II lowstand.

Sequence II (lower Clinton Group, lower Rose Hill Formation, middle member of Rockwood–Red Mountain Formations), of middle–late Aeronian age is marked nearly everywhere by a change to finer-grained siliciclastics. The basal contact is sharp and may truncate beds in upper Sequence I. The transgressive surface is marked in most areas by a phosphatic pebble or oolitic hematite horizon. Ferruginous sandstones pass northwestward into green and maroon shales with BA 2, *Eocoelia*-dominated faunas (Rose Hill, middle Rockwood–Red Mountain Formations); and these, in turn, change northeastward into *Pentamerus*-rich carbonates (BA 3). Ferruginous to phosphatic shell-rich beds are prominent, especially in the transitions between green-maroon mudrock into overlying skeletal carbonate or ferruginous sandstone facies (i.e., on either side of the Rose Hill Formation shale belt).

Sequence III (lower–middle Telychian) is similar in lithology to Sequence II, and consists of thick, green-maroon shales and ferruginous to phosphatic sandstones (Sauquoit–Otsquago, middle Rose Hill, basal (i.e., “Ida beds”) of upper member of Rockwood–Red Mountain, in part). The lower sequence boundary is prominent and regionally angular in the southern Appalachians and sharp in New York, but appears conformable in the central Appalachians, where a lowstand sandstone bundle may be represented by the Cabin Hill Member of the Rose Hill Formation.

Sequence IV (late Telychian–earliest Wenlock) has a very prominent regionally angular unconformity at its base that truncates parts of Sequences I–III in New York, Ontario, Ohio, and Kentucky. This corresponds to a middle late Telychian lowstand, but may also be partially tectonic. The unconformity is less prominent in the central and southern Appalachians, presumably due to higher subsidence rates. Again, a bundle of sandstones,

the Center Member of the Rose Hill Formation, may record lowstand progradation. Very distinctive oolitic, hematitic, shell-rich beds (Westmoreland, Second Creek, "Hickory Nut") and carbonates mark the transgressive-condensed interval of this sequence. Overlying dark shales (Williamson-Willowvale, uppermost Rose Hill, upper Rockwood-Red Mountain) record the deepest-water facies (BA 3-5) in most sections.

Sequence V (early Wenlock, Sheinwoodian) shows a renewed influx of coarser-grained siliciclastics (Herkimer-Keefer Sandstones) that possibly reflects a new tectophase. These lowstand to early transgressive sands rest sharply on shales, and grade northwestward into ferruginous or dolomitic crinoidal grainstone (Irondequoit, Bisher) with *Whitfieldella*-dominated (BA 3) biofacies. Dark gray shales (Rochester-Mifflintown) reflect a middle Wenlock highstand. Sequence V is unconformably overlain by carbonates of Sequence V (Lockport-McKenzie). This sequence was thought to have been missing in the southern Appalachians until the discovery of late Telychian-Wenlock fossils in sandstones earlier assigned to the Devonian Frog Mountain Formation near Birmingham, Alabama.

Ferruginous or phosphatic shell-rich beds are among the most important inter-regional markers in the Lower Silurian of the Appalachian Basin. Most of these beds are condensed at ecological or even biostratigraphic time scales (10-100 Ka). Although some of these beds are local in distribution, others, especially the oolitic hematites and phosphatic nodule beds, are widespread. In general, they occur immediately above sequence boundaries or at surfaces of maximum flooding, and seem to record sediment starvation associated with inundation of coastlines and sequestering of sediment in coastal traps. As a rule, oolitic hematites occur in proximal areas; they pass basinward into ferruginous shell beds and/or thin phosphatic pebble horizons. Both the chamositic precursors of hematites and phosphorites may have formed near redox boundaries, but in general the oolitic hematites seem to occur in more agitated and better-oxygenated settings than phosphorites.

Hematitic beds are particularly prominent in heterolithic facies (typically mixed carbonates or calcareous sandstones and maroon to green shales) of Sequences II, III, and the lower part of IV. They are less prominent in thicker siliciclastic sections and are nearly absent in purer carbonate successions. This may reflect variations in the supply of ferrous iron. Input of ferruginous clays may have been greatest during initial intervals of tectonic quiescence, when source terranes experienced relatively deep weathering. Ironstone development was also favored during times of relative sediment starvation, when accretion of chamositic clays was not diluted by sedimentation.

At least three of the five major Llandovery-Wenlock sea-level cycles identified in Johnson's (1996) eustatic curve are consistently identifiable. The sea-level maxima of Johnson's (1996) curve coincide in age with maximum highstands of the second, fourth, and fifth large-scale depositional sequences, and are marked locally by ferruginous or phosphatic shelly beds. Evidence for Johnson's (1996) third (early Telychian) highstand, which coincides with the Wolcott Limestone of New York, is also widespread as transgressive to highstand deposits of a subsequence (IIB) of Sequence II. However, this subsequence is locally absent in some sections, where it has been removed by erosion at the Sequence II-III boundary.

However, it should be noted that the highstands of sequences I and III, while identifiable throughout much of the Appalachian Basin, do not appear to correlate with global highstands on Johnson's (1996) sea-level curve, and may have been produced by regional foreland basin subsidence. Other less prominent (subsequence level) highstands can be recognized regionally in the Appalachian Foreland Basin, and may be allocyclic. This evidence suggests that further refinements of the global sea-level curve may be possible.

ACKNOWLEDGMENTS

We are grateful to the participants at the James Hall Meeting for stimulating discussions on various topics covered herein. CEB and WG acknowledge support from the American Chemical Society under Petroleum Research Fund Grant 21987-AC. The efforts of many students, including J.D. Eckert, S.T. LoDuca, B.-Y. Lin, and D.K. Tetreault, have contributed to the understanding of Silurian strata and fossils. L. Abbott, K. Brett, and L. Olsen helped with final redrafting of several figures. We thank G. Ludvigson and an anonymous reviewer for critical reviews of the manuscript, and E. Landing for his efforts in editing this volume. (Editors' note: S.G. Driese contributed \$200 from National Science Foundation grant EAR94-18183 and \$200 from the Research Incentive Fund of the University of Tennessee toward publication of this report).

REFERENCES

- AIGNER, T. 1985. Storm Depositional Systems: Dynamic Stratigraphy in Modern and Ancient Shallow Marine Sequences. Lecture Notes in the Earth Sciences, Springer-Verlag, Berlin.
- ALLING, H.L. 1947. Diagenesis of the Clinton hematite ores of New York. Geological Society of America Bulletin, 58:991-1018.
- ALLISON, P.A. 1988a. The role of anoxia in decay and mineralization of proteinaceous organic macrofossils. Paleobiology, 14:139-154.

- . 1988b. Konservat-Lagerstätten. Cause and classification. *Paleobiology*, 14:331–344.
- BAARLI, B.G. 1996. Biostratigraphy of stricklandid brachiopods, p. 56–60. In T.W. Broadhead (ed.), *Sedimentary Environments of Silurian Taconia: Field Trips to the Appalachians and Southern Craton of Eastern North America*. University of Tennessee, Department of Geological Sciences, Studies in Geology 26.
- , AND M.E. JOHNSON. 1996. Lower Silurian strata at Frankfort Gorge and South Moyer Creek, New York, p. 160–167. In T.W. Broadhead (ed.), *Sedimentary Environments of Silurian Taconia: Field Trips to the Appalachians and Southern Craton of Eastern North America*. University of Tennessee, Department of Geological Sciences, Studies in Geology 26.
- , S. BRANDE, AND M.E. JOHNSON. 1992. Proximity trends in the Red Mountain Formation (Lower Silurian) of Birmingham, Alabama, p. 1–17. In J.R. Chaplin and J.E. Barrick (eds.), *Special Papers in Paleontology and Stratigraphy: A Tribute to Thomas W. Amsden*. Oklahoma Geological Survey Bulletin 145.
- , ———. 1996. Stop 2. Red Mountain Expressway, p. 47–54. In T.W. Broadhead (ed.), *Sedimentary Environments of Silurian Taconia: Field trips to the Appalachians and Southern Craton of Eastern North America*. University of Tennessee, Department of Geological Sciences, Studies in Geology 26.
- BAIRD, G.C. 1978. Pebbly phosphorite in shale: a key to recognition of a widespread submarine discontinuity. *Journal of Sedimentary Petrology*, 48:105–122.
- BAMBACH, R.K. 1987. The Ordovician–Silurian unconformity in western Virginia and adjacent West Virginia, p. 2–14. In R.S. Schumacher (ed.) *Appalachian Basin Industrial Associates*, Fall 1987, V. 13, Morgantown, West Virginia.
- BAUM, G.R., AND P.R. VAIL. 1988. Sequence stratigraphic concepts applied to Paleogene outcrops, p. 309–328. In C.K. Wilgus et al. (eds.), *Sea-Level Changes—An Integrated Approach*. Society of Economic Paleontologists and Mineralogists, Special Publication, 42.
- BEARCE, D.N. 1973. Origin of conglomerates in the Silurian Red Mountain Formation of central Alabama: their paleogeographic and tectonic significance. *American Association of Petroleum Geologists Bulletin*, 57:688–701.
- BEAUMONT, C., B. QUINLAN, AND J. HAMILTON. 1988. Orogeny and stratigraphy: numerical models of the Paleozoic in the eastern interior of North America. *Tectonics*, 7:389–416.
- BERDAN, J.M., A.J. BOUCOT, AND B.A. FERRILL. 1986. The first fossiliferous Pridolian beds from the southern Appalachians in northern Alabama, and the age of the Red Mountain Formation. *Journal of Paleontology*, 60:180–185.
- BERNER, R.A. 1981. Authigenic mineral formation resulting from organic matter decomposition. *Fortschritte der Mineralogie*, 59:117–135.
- BERRY, W.B.N., AND A.J. BOUCOT. 1970. Correlation of North American Silurian Rocks. *Geological Society of America Special Paper* 102.
- BOUCOT, A.J. 1975. *Evolution and Extinction Rate Controls*. Elsevier Press, New York.
- BOLTON, J.C. 1990. Sedimentologic data indicate greater range of water depths for *Costistricklandia lirata* in the southern Appalachians. *Palaios*, 5:371–374.
- . 1992. Depositional history of the Red Mountain Formation in northwest Georgia and northern Alabama. Unpublished Ph.D. dissertation, University of Tennessee, Knoxville, 210 p.
- BOLTON, T.E. 1957. Silurian Stratigraphy and Palaeontology of the Niagara Escarpment in Ontario. *Geological Survey of Canada, Memoir* 289.
- BRETT, C.E., AND G.C. BAIRD. 1993. Taphonomic approaches to temporal resolution in stratigraphy: examples from Paleozoic marine mudrocks, p. 250–274. In S.M. Kidwell and A.K. Behrensmeier (eds.), *Taphonomic Approaches to Time Resolution in Fossil Assemblages*. Paleontological Society, Short Courses in Paleontology, G.
- , AND ———. 1995. Coordinated stasis and evolutionary ecology of Silurian–Devonian faunas in the Appalachian Basin, p. 285–315. In D.H. Erwin and R.L. Anstey (eds.), *New Approaches to Speciation in the Fossil Record*. Columbia University Press, New York.
- , AND W.M. GOODMAN. 1996. Sequence stratigraphy of central New York and central Pennsylvania: a regional synthesis. p. 170–200. In T.W. Broadhead (ed.), *Sedimentary Environments of Silurian Taconia: Fieldtrips to the Appalachians and Southern Craton of Eastern North America*. University of Tennessee, Department of Geological Sciences, Studies in Geology 26.
- , W.M. GOODMAN, AND S.T. LODUCA. 1990. Sequences, cycles, and basin dynamics in the Silurian of the Appalachian Foreland Basin. *Sedimentary Geology*, 69:191–244.
- , ———, AND D.F. LEHMANN. 1994. Ordovician and Silurian strata in the Genesee Valley area: sequences, cycles, and facies, p. 381–442. In *New York State Geological Association Field Trip Guidebook*, 66th Annual Meeting, Rochester, NY.
- , D.H. TEPPER, W.M. GOODMAN, S.T. LODUCA, AND B.-Y. LIN. 1995. Revised Stratigraphy and Correlations of the Niagaran Provincial Series (Medina, Clinton, and Lockport Groups) in the Type Area of Western New York. *U.S. Geological Survey Bulletin* 2086.
- BROADHEAD, T.W. (ED.). 1996. *Sedimentary Environments of Silurian Taconia: Fieldtrips to the Appalachians and Southern Craton of eastern North America*. University of Tennessee, Department of Geological Sciences, Studies in Geology 26.
- BUTTS, C. 1940. *Geology of the Appalachian Valley in Virginia*. Virginia Geological Survey Bulletin 52.
- CASTLE, J. In press. Sedimentological and sequence stratigraphic framework of the Lower Silurian clastic wedge, northern Appalachian Foreland Basin. *American Association of Petroleum Geologists, Bulletin*.
- CHADWICK, G.H. 1918. Stratigraphy of the New York Clinton. *Geological Society of America Bulletin*, 29:327–368.
- CHOWNS, T.M. 1996. Sequence stratigraphy of the Silurian Red Mountain Formation in Alabama and Georgia, p. 31–42. In T.W. Broadhead (ed.), *Sedimentary Environments of Silurian Taconia: Fieldtrips to the Appalachians and Southern Craton of Eastern North America*. University of Tennessee, Department of Geological Sciences, Studies in Geology 26.
- , AND J.C. BOLTON. 1993. Sequence stratigraphy of the Red Mountain Formation (Lower Silurian) in Alabama and Georgia. *Geological Society of America, Abstracts with Programs* 25(6):362.
- , AND F.K. MCKINNEY. 1980. Depositional facies in the Middle–Upper Ordovician and Silurian rocks of Alabama and Georgia, p. 323–348. In R.W. Frey (ed.), *Excursions in Southeastern Geology—Guidebook for Field Trip No. 16*. Geological Society of America.
- COTTER, E. 1983a. Shelf, paralic and fluvial environments and eustatic sea-level fluctuations in the origin of the Tuscarora Formation (Lower Silurian) of central Pennsylvania. *Journal of Sedimentary Petrology*, 53:25–49.
- . 1983b. Silurian depositional history, p. 3–27. In R.P. Nickelson and E. Cotter (eds.), *Silurian Depositional History and*

- Alleghanian Deformation in the Pennsylvania Valley and Ridge, Danville, Pennsylvania. Guidebook, 48th Annual Field Conference of Pennsylvania Geologists.
- . 1988. Hierarchy of sea-level cycles in the medial Silurian siliciclastic of Pennsylvania. *Geology*, 16:242–245.
- . 1991. Diagenetic alteration of chamositic clay minerals to ferric oxide in oolitic ironstone. *Journal of Sedimentary Petrology*, 62:54–60.
- . 1996. Silurian of central Pennsylvania, p. 128–154. In T.W. Broadhead (ed.), *Sedimentary Environments of Silurian Taconia: Fieldtrips to the Appalachians and Southern Craton of Eastern North America*. University of Tennessee, Department of Geological Sciences, Studies in Geology 26.
- . 1998. Silurian coastal sedimentation in the Appalachian Foreland Basin of Pennsylvania and meter-scale rhythms. *New York State Museum Bulletin* 491 (this volume).
- , AND J.E. LINK. 1993. Deposition and diagenesis of Clinton ironstones (Silurian) in the Appalachian Foreland Basin of Pennsylvania. *Geological Society of America Bulletin*, 105:911–922.
- DENNISON, J.M. 1970. Silurian stratigraphy and sedimentary tectonics of southern West Virginia and adjacent Virginia. *Appalachian Geological Society, Field Conference Guidebook*, p. 2–33.
- , AND J.M. HEAD. 1975. Sea-level variations interpreted from the Appalachian Basin Silurian and Devonian. *American Journal of Science*, 275:1089–1120.
- DIECCHIO, R.J. 1973. Lower and Middle Silurian ichnofacies and their paleoenvironmental significance, central Appalachian basin. Unpublished M.Sc. thesis, Duke University, Durham, North Carolina, 100 p.
- , AND J.M. DENNISON. 1996. Silurian stratigraphy of central and northern Virginia and adjacent West Virginia, p. 107–118. In T. W. Broadhead (ed.), *Sedimentary Environments of Silurian Taconia: Fieldtrips to the Appalachians and Southern Craton of Eastern North America*. University of Tennessee, Department of Geological Sciences, Studies in Geology 26.
- DORSCH, J., R.K. BAMBACH, AND S.G. DRIESE. 1994. Basin rebound origin for the "Tuscarora Unconformity" in southwestern Virginia and its bearing on the nature of the Taconic Orogeny. *American Journal of Science* 294:237–255.
- , AND S.G. DRIESE. 1995. The Taconic foredeep as a sediment sink and sediment exporter: implications for the origin of the white quartz arenite blanket (Upper Ordovician) of the central and southern Appalachians. *American Journal of Science*, 295:201–243.
- DRIESE, S.G. 1996. Depositional history and facies architecture of a Silurian foreland basin, p. 68–106. In T.W. Broadhead (ed.), *Sedimentary Environments of Silurian Taconia: Fieldtrips to the Appalachians and Southern Craton of Eastern North America*. University of Tennessee, Department of Geological Sciences, Studies in Geology 26.
- , M.W. FISCHER, K.A. EASTHOUSE, G.T. MARKS, A.R. GOGOLA, AND A.E. SCHONER. 1991. Models for genesis of shelf sandstone sequences, southern Appalachians: paleoenvironmental reconstruction of an Early Silurian shelf system, p. 309–338. In D.J.P. Swift, G.F. Oertel, T.W. Tillman, and J.A. Thorne (eds.), *Shelf Sand and Sandstone Bodies: Geometry, Facies, and Sequence Stratigraphy*. International Association of Sedimentologists Special Publication 14.
- DUKE, W.L., AND W.C. BRUSSE. 1987. Cyclicity and channels in the upper members of the Medina Formation in the Niagara Gorge, p. 46–65. In W.L. Duke (ed.), *Sedimentology, Stratigraphy, and Ichnology of the Lower Silurian Medina Formation in New York and Ontario*. Society of Economic Paleontologists and Mineralogists, Northeast Section, Field Trip Guidebook.
- , AND P.J. FAWSETT. 1987. Depositional environments and regional sedimentation patterns in the upper members of the Medina Formation, p. 81–95. In W.L. Duke (ed.), *Sedimentology, Stratigraphy, and Ichnology of the Lower Silurian Medina Formation in New York and Ontario*. Society of Economic Paleontologists and Mineralogists, Northeast Section, Field Trip Guidebook.
- EASTHOUSE, K.A., AND S.G. DRIESE. 1988. Paleobathymetry of a Silurian shelf system: application of proximality trends and trace fossil distributions. *Palaeos*, 3:473–486.
- ECKERT, B.-Y., AND C.E. BRETT. 1989. Bathymetry and paleoecology of Silurian benthic assemblages, late Llandoveryan, New York State. *Palaogeography, Palaeoclimatology, Palaeoecology*, 74:297–326.
- EMERY, D., AND K.J. MEYERS (EDS.) 1996. *Sequence Stratigraphy*. Blackwell Science Ltd., Oxford.
- ETTENSohn, F.R., AND C.E. BRETT. 1996. Did Taconic convergence continue into Silurian time?—stratigraphic evidence from northwestern parts of the Appalachian Foreland Basin. *Geological Society of America, Abstracts with Programs*, 28:52.
- , AND ———. 1998. Identifying tectonic components in Silurian cyclicity: examples from the Appalachian Basin and their global implication. *New York State Museum Bulletin* 491 (this volume).
- FÜRSICH, F.T. 1978. The influence of faunal condensation and mixing on the preservation of fossil benthic communities. *Lethaia*, 8:151–172.
- GILLETTE, T. 1947. The Clinton of Western and Central New York. *New York State Museum Bulletin* 341.
- GOODMAN, W.M., AND C.E. BRETT. 1994. Roles of eustasy and tectonics in development of Silurian stratigraphic architecture of the Appalachian Foreland Basin, p. 147–169. In *Society for Sedimentary Geology, Studies in Sedimentology and Paleontology*, 4.
- HALL, J. 1839. Third annual report of the Fourth Geologic District of the State of New York. *New York State Geological Survey Annual Report*, 3:287–339.
- . 1840. Fourth annual report of the Fourth Geologic District of New York. *New York State Geological Survey Annual Report*, 4:389–456.
- . 1843. *Geology of New York. Part IV, Comprising the Survey of the Fourth Geologic District*. Carroll and Cook, Albany.
- . 1852. *Palaeontology of New York, II*. C. van Benthuyzen and Sons, Albany.
- HALLAM, A. 1992. *Phanerozoic Sea-Level Changes. Perspectives in Paleobiology and Earth History Series*, Columbia University Press, New York.
- , AND M.J. BRADSHAW. 1979. Bituminous shales and oolitic ironstones as indicators of transgressions and regressions. *Journal of the Geological Society of London*, 36:157–164.
- HELFRICH, C.T. 1975. Silurian Conodonts from Wills Mountain Anticline, Virginia, West Virginia, and Maryland. *Geological Society of America Special Paper* 161.
- HUNTER, R.E. 1970. Facies of iron sedimentation in the Clinton Group, p. 101–124. In G.W. Fisher, I.J. Pettijohn, and K.N. Weaver (eds.), *Studies of Appalachian Geology: Central and Southern*. Wiley Interscience, New York.
- JOHNSON, M.E. 1987. Extent and bathymetry of North American seas in the Early Silurian. *Paleoceanography* 2:185–211.
- . 1996. Stable cratonic sequences and a standard for Silurian eustasy, p. 203–211. In B.J. Witzke, G.A. Ludvigson, and J.E. Day (eds.), *Paleozoic Sequence Stratigraphy: Views from the North American Craton*. *Geological Society of America Special Paper* 306.

- , G. BAARLI, H. NESTOR, M. RUBEL, AND D. WORSLEY. 1991. Eustatic sea-level patterns from the Lower Silurian (Llandovery Series) of southern Norway and Estonia. *Geological Society of America Bulletin*, 103:315–335.
- , D. KALJO, AND RONG J.-Y. 1991. Silurian eustasy, p. 145–163. *In* M.G. Bassett, P.D. Lane, and D. Edwards (eds.), *The Murchison Symposium: Proceedings of an International Conference on the Silurian System*. Special Papers in Palaeontology 44.
- , RONG, J.-Y., AND YANG X.-C. 1985. International correlation by sea-level events in the Early Silurian of North America and China (Yangtze Platform). *Geological Society of America Bulletin*, 96:1384–1397.
- KIDWELL, S.M. 1991. The stratigraphy of shell concentrations, p. 211–290. *In* P.A. Allison and D.E.G. Briggs, (eds.), *Taphonomy: Releasing the Data Locked in the Fossil Record*. Plenum Press, New York.
- , AND D.W.J. BOSENCE. 1991. Taphonomy and time-averaging of marine shelly faunas, p. 116–211. *In* P.A. Allison and D.E.G. Briggs (eds.), *Taphonomy: Releasing the Data Locked in the Fossil Record*. Plenum Press, New York.
- KILGOUR, W.J. 1963. Lower Clinton (Silurian) relationships in western New York and Ontario. *Geological Society of America Bulletin*, 74:1127–1141.
- , AND B.A. LIBERTY. 1981. Detailed stratigraphy, p. 173–196. *In* I.H. Tesmer (ed.), *Colossal Cataract: The Geologic History of Niagara Falls*. State University of New York Press, Albany.
- KLEFFNER, M.A. 1989. A conodont-based Silurian chronostratigraphy. *Geological Society of America Bulletin*, 101:904–912.
- . 1991. Conodont biostratigraphy of the upper part of the Clinton Group and the Lockport Group (Silurian) in the Niagara Gorge region, New York and Ontario. *Journal of Paleontology*, 65:500–511.
- LIN, B.-Y., AND C.E. BRETT 1988. Stratigraphy and disconformable contacts of the Williamson–Willowvale interval: revised correlations of the late Llandoveryan (Silurian) in New York State. *Northeastern Geology*, 10:241–253.
- LODUCA, S.T. 1988. Lower Clinton hematites: implications for stratigraphic correlations. Abstracts of the Central Canada Geological Conference, London, Ontario, p. 62.
- , AND C.E. BRETT. 1994. Revised stratigraphic and facies relationships of the lower part of the Clinton Group (middle Llandoveryan) of western New York State, p. 161–182. *In* E. Landing (ed.), *Studies in Stratigraphy and Paleontology in Honor of Donald W. Fisher*. New York State Museum Bulletin 481.
- LOUTIT, T.S., J. HARDENBOL, P.R. VAIL, AND G.R. BAUM. 1988. Condensed sections: the key to age determination and correlation of continental margin sequences, p. 183–213. *In* C.K. Wilgus et al. (eds.), *Sea-Level Changes, An Integrated Approach*. Society of Economic Paleontologists and Mineralogists, Special Publication 42.
- LUCAS, J., AND L.E. PRÉVOT. 1991. Phosphate and fossil preservation, p. 389–411. *In* P.A. Allison and D.E.G. Briggs (eds.), *Taphonomy: Releasing the Data Locked in the Fossil Record*. Plenum Press, New York.
- LUKASIK, D.M. 1988. Lithostratigraphy of Silurian rocks in southern Ohio and adjacent Kentucky and West Virginia. Unpublished Ph.D. dissertation, University of Cincinnati, 313 p.
- MARKS, G.T. 1987. The lithology and paleoenvironmental interpretation of the Clinch Sandstone at Powell Mountain, southwestern Virginia. Unpublished M.Sc. thesis, University of Tennessee, Knoxville, 263 p.
- MEYERS, K.J., AND N.J. MILTON. 1996. Concepts and principles of sequence stratigraphy, p. 11–44. *In* D. Emery and K.J. Meyers (eds.), *Sequence Stratigraphy*. Blackwell Science Ltd, Oxford.
- MILLER, R.I. 1976. Silurian Nomenclature and Correlations in Southwest Virginia and Northeast Tennessee. U.S. Geological Survey Bulletin 1405-H.
- MONTAÑEZ, I.P., J.L. BANNER, D.A. OSLEGER, L.E. BORG, AND P.J. BOSSERMAN. 1996. Integrated Sr isotope variations and sea-level history of Middle to Upper Cambrian platform carbonates: implications for the evolution of Cambrian $^{87}\text{Sr}/^{86}\text{Sr}$. *Geology* 24:917–920.
- MUSKATT, H.S. 1969. Petrology and origin of the Clinton Group of east-central New York and its relationship to the Shawangunk Formation of southeastern New York. Syracuse University, Unpublished Ph.D. dissertation, 343 p.
- . 1972. The Clinton Group of east-central New York. New York State Geological Association, 44th Annual Meeting Guidebook, p. A1–A37.
- PARSONS, K.M., C.E. BRETT, AND K.B. MILLER. 1988. Taphonomy and depositional dynamics of Devonian shell-rich mudstones. *Palaeogeography, Palaeoclimatology, Palaeoecology*, 63:109–140.
- PRATT, L.M., T.L. PHILLIPS, AND J.M. DENNISON. 1978. Evidence of non-vascular land plants from the Early Silurian (Llandoveryan) of Virginia, U.S.A. *Reviews of Paleobotany and Palynology*, 25:121–149.
- REXROAD, C.B., AND L.V. RICKARD. 1965. Zonal conodonts from the Silurian of the Niagara Gorge. *Journal of Paleontology* 39:1217–1220.
- RICKARD, L.V. 1975. Correlation of the Silurian and Devonian Rocks of New York State. New York State Museum, Map and Chart Series, No. 24.
- RINDSBURG, A.K., AND T.M. CHOWNS. 1986. Ringgold Gap: progradational sequences in the Ordovician and Silurian of northwest Georgia, p. 159–162. *In* Geological Society of America, Centennial Field Guide 6.
- ROGERS, H.D. 1858. *The Geology of Pennsylvania—A Government Survey*. J.P. Lippencott & Co., Philadelphia.
- ROSS, C.A., AND J.R.P. ROSS. 1996. Silurian sea-level fluctuations, p. 187–211. *In* B.J. Witzke, G.A. Ludvigson, and J.E. Day (eds.), *Paleozoic Sequence Stratigraphy: Views from the North American Craton*. Geological Society of America, Special Paper 306.
- RUPPEL, S.C., E.W. JAMES, J.E. BARRICK, G.S. NOWLAN, AND T.T. UYENO. 1996. High resolution $^{87}\text{Sr}/^{86}\text{Sr}$ chemostratigraphy of the Silurian: implications for event correlation and strontium flux. *Geology*, 24:831–834.
- SANFORD, J.T. 1935. The “Clinton” in western New York. *Journal of Geology*, 43:167–183.
- . 1936. The Clinton in New York. *Journal of Geology*, 44:797–814.
- SCHUCHERT, C. 1914. Medina and Cataract Formation. Historical review. *Geological Society of America Bulletin*, 25:277–320.
- SHELDON, R.P. 1970. Sedimentation of iron-rich rocks of Llandovery age (Lower Silurian) in the southern Appalachian basin, p. 107–112. *In* W.B.N. Berry and A.J. Boucot (eds.), *Correlation of North American Silurian Rocks*. Geological Society of America, Special Paper 102.
- SLOSS, L.L. 1963. Sequences in the cratonic interior of North America. *Geological Society of America Bulletin*, 74:93–114.
- SWARTZ, C.K. 1923. Correlation of the Silurian formations of Maryland with those of other areas, p. 183–230. *In* Silurian. Maryland Geological Survey.
- , AND F.M. SWARTZ. 1931. Early Silurian formations of southeast Pennsylvania. *Geological Society of America Bulletin*, 42:621–662.

- SWARTZ, F.M. 1934a. Relations of the Silurian Rochester and McKenzie Formations near Cumberland, Maryland, and Lakemont, Pennsylvania. *Geological Society of America Bulletin*, 46:1165–1194.
- . 1934b. Silurian sections near Mt. Union, central Pennsylvania. *Geological Society of America Bulletin*, 45:82–134.
- SWIRYDCZUK, K., B.H. WILKINSON, AND G.R. SMITH. 1981. Synsedimentary lacustrine phosphorites from the Pliocene Glens Ferry Formation of southwestern Idaho. *Journal of Sedimentary Petrology* 51:1205–1214.
- THOMAS, W.A., AND D.N. BEARCE. 1986. Birmingham anticlinorium in the Appalachian fold belt, basement fault system, synsedimentary structure and thrust ramp, p. 191–200. *In* T.L. Neathery (ed.), *Centennial Field Guide*. Vol. 6. Geological Society of America, Southeastern Section.
- ULRICH, E.O., AND R.S. BASSLER. 1923. Paleozoic Ostracods: Their Morphology, Classification, and Occurrence. Silurian, Maryland Geological Survey.
- VAIL, P.R., F. AUDEMARD, S.A. BOWMAN, P.N. ESNER, AND C. PÉREZ-CRUZ. 1991. The stratigraphic signature of tectonics, eustasy, and sedimentology—an overview, p. 617–659. *In* G. Einsele, W. Ricken, and A. Seilacher (eds.), *Cycles and Events in Stratigraphy*. Springer-Verlag, Berlin.
- , R.M. MITCHUM, AND S. THOMPSON III. 1977. Seismic stratigraphy and global changes in sea-level, p. 83–97. *In* C. E. Payton (ed.), *Seismic Stratigraphy—Applications to Hydrocarbon Exploration*. American Association of Sedimentary Petrologists and Mineralogists, Memoir 26.
- VANUXEM, L. 1839. Third annual report of the Geological Survey of the Third District. New York State Geological Survey Annual Report, 3:241–285.
- . 1840. Fourth annual report of the Geological Survey of the Third District. New York State Geological Survey Annual Report, 4:355–383.
- . 1842. *Geology of New York, Part III. Comprising the Survey of the Third Geologic District*. Albany, 306 p.
- VAN WAGONER, J.C., H.W. POSAMENTIER, R.M. MITCHUM III, P.R. VAIL, J.F. SARG, T.S. LOUTIT, AND J. HARDENBOL. 1988. An overview of the fundamentals of sequence stratigraphy and key definitions, p. 39–45. *In* C.K. Wilgus, B.S. Hastings, C.G. Kendall, H.W. Posamentier, C.A. Ross, and J.C. Van Wagoner (eds.), *Sea-Level Changes: An Integrated Approach*. Society of Economic Paleontologists and Mineralogists, Special Publication 42.
- VAN HOUTEN, F.B., AND D.P. BHATTACHARYA. 1982. Phanerozoic oolitic ironstones—geologic record and facies model. *Annual Reviews of Earth and Planetary Science*, 10:441–457.
- WHEELER, H.E. 1958. Time stratigraphy. *American Association of Petroleum Geologists Bulletin*, 42:1047–1063.
- WILGUS, C.K., B.S. HASTINGS, C.G. KENDALL, H.W. POSAMENTIER, C.A. ROSS, AND J.C. VAN WAGONER (EDS.). 1988. *Sea-Level Changes: An Integrated Approach*. Society of Economic Paleontologists and Mineralogists, Special Publication 42.
- WITZKE, B.J. 1990. Palaeoclimatic constraints for Palaeozoic palaeolatitudes of Laurentia and Euramerica, p. 57–73. *In* Palaeogeography and Biogeography. Geological Society Memoir 12.
- , AND B.J. BUNKER. 1996. Relative sea-level changes during Middle Ordovician through Mississippian deposition in the Iowa area, North American craton, p. 307–333. *In* B.J. Witzke, G.A. Ludvigson, and J.E. Day (eds.), *Paleozoic Sequence Stratigraphy: Views from the North American Craton*. Geological Society of America, Special Paper 306.
- , G.A. LUDVIGSON, AND J.E. DAY (EDS.). 1990. *Paleozoic Sequence Stratigraphy: Views from the North American Craton*. Geological Society of America, Special Paper 306.
- ZENGER, D.H. 1965. Stratigraphy of the Lockport Formation (Middle Silurian) in New York State. *New York State Museum Bulletin* 404.
- . 1971. Uppermost Clinton (Middle Silurian) Stratigraphy and Petrology, East-Central New York. *New York State Museum Bulletin* 417.
- ZIEGLER, A.M. 1965. Silurian marine communities and their environmental significance. *Nature* 207:270–272.
- , L.R.M. COCKS, AND R.K. BAMBACH. 1968. The composition and structure of Lower Silurian marine communities. *Lethaia*, 1:1–27.

TECTONIC COMPONENTS IN THIRD-ORDER SILURIAN CYCLES: EXAMPLES FROM THE APPALACHIAN BASIN AND GLOBAL IMPLICATIONS

FRANK R. ETTENSOHN¹ AND CARLTON E. BRETT²

¹Department of Geological Sciences, University of Kentucky, Lexington, KY 40506, and

²Department of Earth and Environmental Sciences, University of Rochester, Rochester, NY 14627

ABSTRACT—Effects of supracrustal and subcrustal loading due to subduction and orogeny on the Appalachian margin in the latest Ordovician–Silurian are suggested to have had a major influence on sequences and cyclicity in the Appalachian Basin. Criteria from lithospheric flexure models for supracrustal loading (i.e., the nature and distribution of unconformities, flexural stratigraphic sequences, and distribution in time and space of dark shale-filled foreland basins) suggest the probable influence of Silurian tectonism in the Appalachian Basin. Especially important are far-field tectonic effects that lead to epeirogenic subsidence and allocyclicity and that may influence cratonic stratigraphy up to 2,000 km from an orogeny. These criteria confirm an Early Silurian phase of Taconian tectonism and two Salinic tectophases, all recently identified in the northern Appalachians from non-stratigraphic criteria. Major subsidence resulting from supracrustal and subcrustal loading during each tectophase appears to coincide with Silurian highstands. Other data, though less constrained, suggest coeval tectonic phases elsewhere on the assembling continent (Laurussia), and in some cases in orogens across the Silurian world. Subsidence with widespread coeval tectonism could have far-ranging influence on sea-level fluctuations, and suggests that orogenic, epeirogenic, and eustatic effects are closely related.

Comparison of Appalachian tectonism with Silurian sea-levels and Silurian glaciation allows inferences about the importance of tectonic versus glacio-eustatic components in regional and global highstands. An early Rhuddanian highstand largely restricted to the east-central United States and Canada and other parts of Laurussia cannot be related to deglaciation, but is ideally situated in time and space to have resulted from tectonic subsidence with an Early Silurian Taconian tectophase in the northern Appalachians. A global late Telychian highstand that was the greatest inundation of the Silurian, and one of the greatest of the Phanerozoic, probably reflects both Silurian deglaciation and global tectonic reorganization that included the Salinic and Scandian orogenies. Because of potential widespread subsidence by far-field effects, regional tectonism

during periods of nearly synchronous global tectonic reorganization may be as important as glacio-eustasy in explaining eustatic cycles. Tectonism, even in local or regional settings such as the Appalachian Basin, may point to global causes of Silurian cyclicity.

INTRODUCTION

Traditional interpretations of the Appalachian Basin during Silurian time suggest tectonic stability and eustatic variability between the Taconian and Acadian orogenies. The stratigraphic record of the period, especially in north and north-central parts of the basin, is divided into several cyclic sequences by unconformities (Rickard, 1975; Brett et al., 1990a, 1990b, 1994, 1996; Goodman and Brett, 1994), many of which have been attributed to eustatic regression accompanied by exposure and erosion of basin margins (Dennison and Head, 1975; Johnson et al., 1985; Brett et al., 1990). The apparent global nature of some interpreted sea-level fluctuations, and their general coincidence with episodes of Silurian Gondwanan glaciation (Grahn and Caputo, 1992) and with probable long-term Caledonian tectono-eustasy, has favored interpretations of eustatic control on sedimentary cycles in the Appalachian Basin and elsewhere (Johnson et al., 1985, 1991a, 1991b; Johnson, 1987, 1996).

However, evidence of apparent sea-level highstands and lowstands localized on one continent or on parts of a continent, clear coincidence of the highstands with phases of a nearby orogeny, and the nature and distribution of sedimentary sequences and their bounding unconformities in time and space have suggested that tectonic components may play an important role in development of some Silurian cycles (e.g., McKerrow, 1979; Baarli, 1990; Johnson et al., 1991a, 1991b; Goodman and

Brett, 1994; Ettensohn, 1994; Johnson, 1996). The question then arises: are there more definitive criteria for recognizing tectonic contributions to Silurian cyclicity? Based on well-known sequences in the Appalachian Basin and on the increasingly better-known tectonic history of the region, we believe that the sedimentary record is evidence of the tectonic components of relative sea-level changes. Because recognition of tectonic controls can have important implications for understanding global and regional sea-level cyclicity, we present criteria for recognition of tectonic influences, the models on which these criteria are based, and examples from the Silurian of the Appalachian Foreland Basin. Admittedly the tectonic models employed are applied to Silurian foreland basin sequences, but the fact that flexural stresses responsible for tectonic components of relative sea-level variations may be transmitted through the continental lithosphere across distances of up to 2,000 km (e.g., Karner and Watts, 1983; Ziegler, 1987; Gurnis, 1991) indicates that tectonic activity in marginal basins probably influenced Silurian epeirogenesis and cratonic sequences some distance from the foreland basin and its related craton-margin orogen.

BASIC MODELS

Relationships between waxing and waning ice sheets and eustasy have been understood, at least in a general sense, for some time. Although the influence of craton-margin tectonism on eustasy has been postulated for almost as long, the mechanisms behind the necessary epeirogenic movements, especially in anorogenic cratonic areas distant from coeval active orogens, have been poorly understood. However, work on this problem since the 1970s has shown that proximal and distal epeirogenic movements are largely controlled by subcrustal and supracrustal loading at and near active orogenic belts (e.g., Walcott, 1970; Price, 1973; Sloss and Speed, 1974; Cross and Pilger, 1978). Subcrustal loading is related to changing mantle dynamics near subduction zones, where variations in mantle temperature and viscosity and the angle of slab penetration may generate long wavelength subsidence and tilting of the crust up to 2,000 km away (Cross and Pilger, 1978; Mitrovica et al., 1989; Gurnis, 1990, 1991, 1992; Kominz and Bond, 1991; Coakley and Gurnis, 1995; Moresi and Gurnis, 1996). This means that the effects of subcrustal loading may influence relative sea-level fluctuation and cratonic sedimentary sequences across large parts of those continents with converging margins (Cross and Pilger, 1978; Kominz and Bond, 1991; Gurnis, 1993; Burgess et al., 1995). In particular, long wavelength subsidence of the continental lithosphere occurs rapidly upon initiation of slab subduction, at rates

possibly exceeding 100 m/Ma (Gurnis, 1992), and may result in maximum crustal depression of 100–300 m at distances up to 2,000 km from the subduction zone (Gurnis, 1991). Obviously the potential influence of subduction on relative sea-level variation is great, but the rate and effects of these sea-level rises increase substantially toward the convergent margins (Gurnis, 1992, 1993). As rates of subduction are related to plate velocities, models predict a general correlation between plate velocities and rates of subsidence and inundation at convergent margins (Gurnis, 1993). Because the Silurian was a time of extensive subduction zones (e.g., Scotese and Golonka, 1992) (Figure 1) and relatively high plate velocities (Gurnis and Torsvik, 1994), it is difficult to escape the conclusion that much Silurian relative sea-level variation had subcrustal tectonic underpinnings. Moreover, these underpinnings must have been especially effective across most of Laurentia, which had a high Silurian drift velocity (Gurnis and Torsvik, 1994) and was nearly surrounded by subduction zones (Ziegler, 1989; Scotese and Golonka, 1992; Figure 1).

Models involving supracrustal loads derive from the fact that surface and subsurface loading generated by the fold thrust belt during orogeny depresses the lithosphere cratonward of the orogen to form a migrating foreland basin (Price, 1973). The full implications of these models for epeirogenesis and foreland tectonic influence were largely uncertain until elucidated by the debate on elastic versus visco-elastic models of lithospheric flexure (e.g., Beaumont, 1981; Jordan, 1981; Quinlan and Beaumont, 1984). In these competing models, it was argued that lithospheric loading, induced by convergence-related deformation, generated or relaxed stresses that caused adjacent parts of the craton to rise or subside, and thereby affected relative sea-levels across broad areas. The nature of predicted lithospheric responses in these models necessarily depends on the rheology assumed for the lithosphere (Quinlan and Beaumont, 1984), but comparison of model predictions with sedimentary sequences in the Appalachian Basin seems to support the loading and unloading of a temperature-dependent, visco-elastic lithosphere as modeled by Quinlan and Beaumont (1984), Beaumont et al. (1987, 1988), and Jamieson and Beaumont (1988).

It is now clear that the effects of subcrustal and supracrustal loading may be similar and concurrent (Gurnis, 1992). Moreover, the effects of both types of loading may contribute to the long wavelength tilting, subsidence, and reactivation of basement structures in the foreland, variously called epeirogenesis or far-field tectonics. More important, however, is the fact that the orogenic, epeirogenic, and eustatic processes are closely related (e.g., Gurnis, 1992), and that the presence of likely

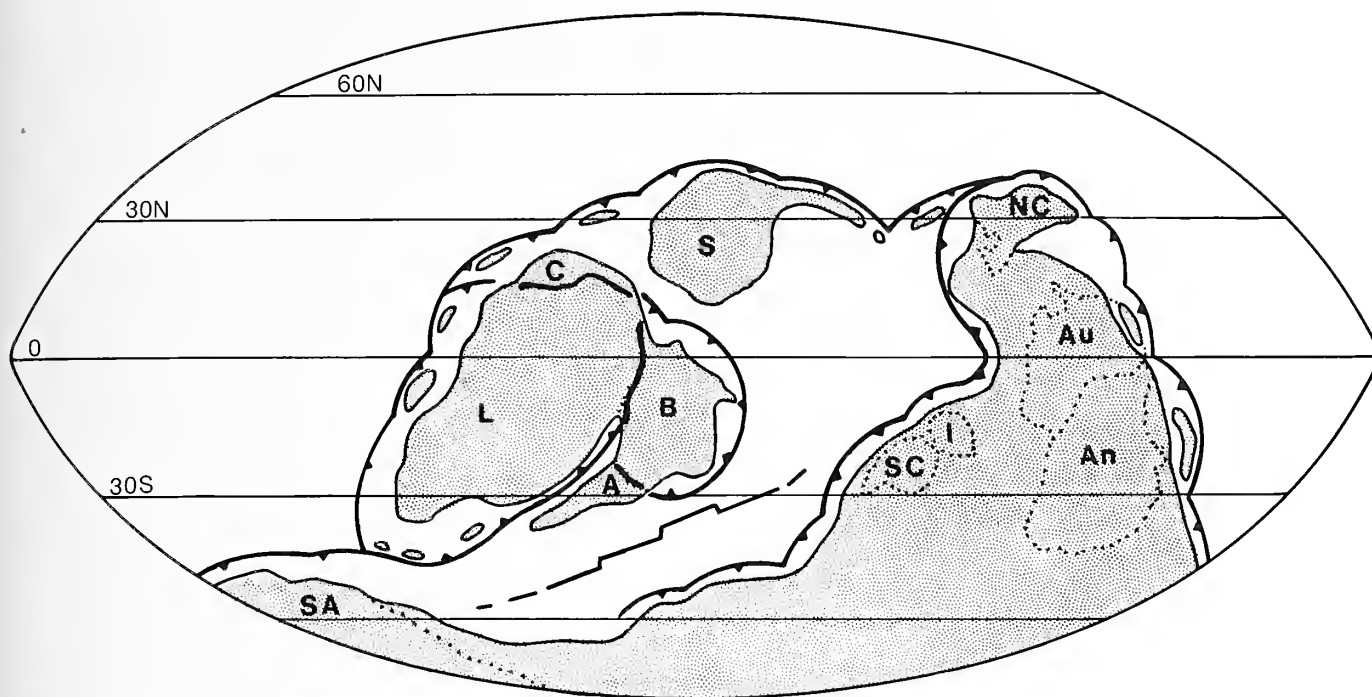


FIGURE 1—Early Silurian (Telychian) world after Scotese and Golonka (1992) showing land masses (stipple), subduction zones (barbed arcs), and spreading centers (segmented straight lines). Subduction zones after Ziegler (1989) and Scotese and Golonka (1992) continue around the south margin of Gondwana. Parts of assembling Laurussian land mass: L, Laurentia; C, Chukotka; B, Baltica; A=Avalonia. Parts of Gondwana: SA, South America; SC, South China (Yangtze craton); I, Indochina; An, Antarctica; Au, Australia; NC, North China; S is Siberia.

tectonic controls must be considered in all discussions of eustasy. Even in discussions of glacio-eustasy, there are now suggestions of interaction between tectonics and glaciation (Cloetingh and Kooi, 1992) of the sort that could influence sea-level fluctuations on glaciated continents. Nonetheless, in the following parts of this report, we try to “tease apart” the evidence for glacio-eustasy versus tectono-eustasy by using flexural models based on supracrustal loading. The use of these models does not preclude the effects of subcrustal loading, but merely reflects the fact that we are largely working in foreland basins where the relationships between sedimentation and surface orogenic loads are better understood.

The extent of relative sea-level changes and creation of new accommodation space associated with orogeny-related, cratonic flexure are best considered regional phenomena, but the related effects of continental-scale epeirogenesis and tectono-eustatic fluctuations (Hays and Pittman, 1973) may be of longer duration, and global in scale (Dickinson et al., 1994, fig. 4). Moreover, if Silurian continents were largely surrounded by subduction zones (Figure 1) as suggested by Scotese and Golonka (1992), plate reorganization initiated on one margin may have caused nearly synchronous tectonism and associated flexure on other margins as well. If the above considerations are valid, a series of nearly synchronous,

regional tectonic events could have combined to create continental- to global-scale epeirogenic movements that produced a signal of very wide extent. Evolving models that relate periods of coeval, global tectonism to rapid drift rates, accelerated subduction, and sea-level high-stands, as suggested for Early Silurian time, largely rely on explanations involving pulsatory changes in mantle convection (e.g., Sheridan, 1997).

FLEXURAL MODELS AND STRATIGRAPHIC MANIFESTATIONS.—Most flexural models indicate that surface and subsurface deformational loading by flakes, blocks, thrusts, nappes, and folds produces both a downwarped flexural or retro-arc foreland basin cratonward of the orogen and a peripheral bulge on the cratonward margin of the basin due to regional isostatic compensation by the lithosphere (Figure 2). As orogeny proceeds and thrust loads shift cratonward, the foreland basin and peripheral bulge also migrate cratonward away from the load. Most of the loading and the accompanying basin-and-bulge migration will progress cratonward in a direction perpendicular to the strike of the orogenic belt. If the orogeny is diachronous along its length, deformational loading and attendant basin-and-bulge migration will also shift parallel to the strike of the orogenic belt (Ettensohn, 1987). The initial result of the loading is bulge move-out

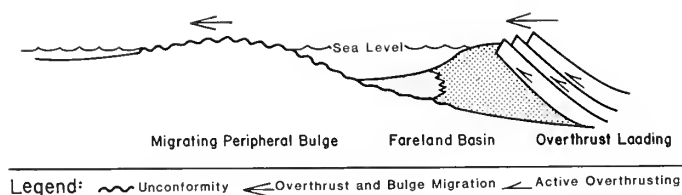


FIGURE 2—Development of a foreland basin, peripheral bulge, and bulge-related unconformity with deformational loading in orogen. Early sediments in distal foreland basin with initiation of deformation will be largely organic-rich muds (after Quinlan and Beaumont, 1984, fig. 18a).

and accompanying uplift of the foreland to generate a regional unconformity (Figure 2) (Quinlan and Beaumont, 1984). Because the unconformity advances cratonward toward areas of decreasing subsidence and deposition on or near intra-cratonic highs like the Cincinnati Arch, such unconformities typically "open up" cratonward, and the space-time value of the lacuna on the unconformity increases in the same direction. The distribution of an unconformity so generated is also generally localized to parts of the foreland basin and adjacent craton next to the locus of tectonism, and will be approximately parallel to the strike of the associated orogen (Ettensohn, 1993, 1994). Moreover, because much Appalachian tectonism was apparently localized near continental promontories that were subject to greater shortening and resulting deformation (Dewey and Burke, 1974; Dewey and Kidd, 1974; Ettensohn, 1985, 1991), the distribution of unconformities in the Appalachian Basin is commonly asymmetric toward the affected promontories, even within a foreland basin (Ettensohn, 1991, 1994). Thus unconformity distribution in time and space can be an important indication of tectonic influence.

After bulge move-out, subsidence (i.e., an isostatic response to deformational loading in the adjacent orogen) generates the foreland basin (Figure 2). Because

much of the initial loading is thought to occur in the sub-surface and in subaqueous environments that generate little subaerial relief (Karner and Watts, 1983), no major source of externally derived sediment is usually available during the early phases of orogeny. In the absence of major clastic influx, organic matter from the water column and suspended clays and silt compose most of the sediment in the early basin (Ettensohn, 1992a). Inasmuch as the foreland basin undergoes rapid subsidence and sediment accumulation cannot keep pace, the water column may become stratified, so that the organic matter is buried within dark or black muds in the resulting anoxic environments. As a result, the bulge-induced unconformity is typically overlain abruptly by dark shales, although a transgressive carbonate or siliciclastic facies that forms a condensed succession may intervene. While dark muds are being deposited in central parts of the basin, the effects of flexural subsidence, though reduced, can be expected to persist in distal parts of the foreland basin and at some distance beyond the basin itself. This results in regional transgression and an apparent rise in relative sea-level. As a result, transgressive carbonates or light-colored shales that overlie an unconformity in distal parts of the foreland basin, on the bulge, or on the craton may represent the same initial subsidence event that is represented by the dark shales in the basin center.

Dark-mud deposition will predominate in central parts of the foreland basin as long as active orogeny and deformational loading continue. However, once active thrust movement declines and tectonic quiescence ensues, the deformational load becomes static. The lithosphere responds to the now largely static load by relaxing stress, so that the foreland basin subsides and narrows as the peripheral bulge is uplifted and shifts toward the load (Figure 3.1). By this time, substantial subaerial relief has been generated by emplacement of a surface load (fold-thrust belt), and surface drainage

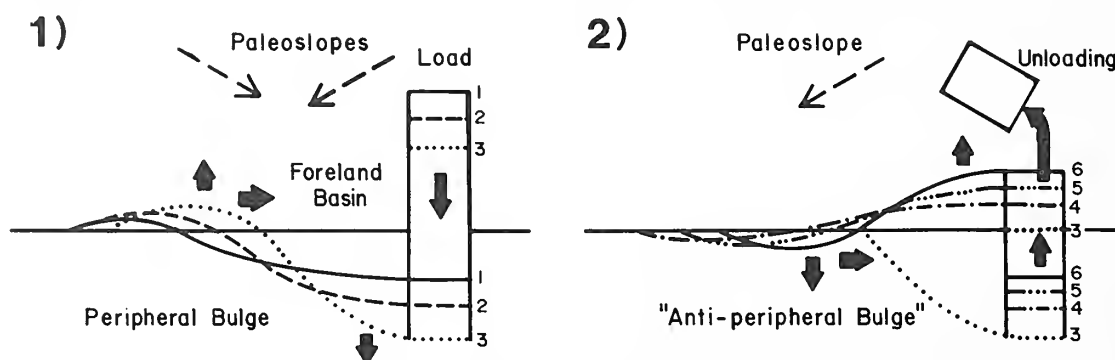


FIGURE 3—Two types of flexural response to lithospheric stress relaxation related to supracrustal loading (after Beaumont et al., 1988). 1, "loading-type" relaxation—thrust migration largely ceases; in response to a now-static load, the lithosphere relaxes as peripheral bulge migrates toward the load with a concomitant deepening of the foreland basin. 2, "unloading-type" relaxation—erosional unloading results in rebound near the unloaded area and an "anti-peripheral bulge" or peripheral sag that deepens and migrates toward the former load.

nets have had adequate time to develop. As a result, coarser-grained clastic debris is eroded and transported into the foreland basin in the form of deeper water deltaic deposits, turbidites, contourites, and debris flows. Nearshore siliciclastic sediments may also be redistributed as tempestites by storms. While these flysch-like sediments accumulate at increasing rates in the foreland basin, uplift and basinward movement of the adjacent bulge may generate a regressive carbonate sequence or another regional unconformity that truncates previously deposited flysch-like sediments, depending upon the relative disposition of sea level (Figure 3.1). The basin sequence generated during this loading-type relaxation will be regressive, and as the bulge migrates back toward the load and sediments overflow from the filled basin, adjacent cratonic sequences will also appear regressive in nature.

Eventually, as the surface load is eroded, the rate of siliciclastic influx into the basin will exceed basin subsidence rates, and the foreland basin will fill or overflow with siliciclastic sediment. The filling of the basin with siliciclastics, combined with greatly lowered source areas, may set the stage for deposition of an extensive blanket of shallow-water carbonates or mixed carbonates and shales. These carbonates or shales mark the culmination of a shallowing or regressive phase (Figure 4) that began with loading-type relaxation and the influx of coarser clastic sediment into the basin. This thin carbonate or shale blanket may be very widespread because the overflowing basin and lowered source areas briefly approach the same elevation, and the shallow seas can expand widely.

Generally, this phase of "elevational equilibrium" is short-lived, because the area of the former orogen and foreland basin begins to rebound upward in isostatic response to the lost load. During this unloading-type relaxation, a compensating "anti-peripheral bulge" (Figure 3.2), perhaps better called a peripheral sag, forms and moves toward the rebounding area (Beaumont et al., 1988). Although a short-lived transgressive sequence of shallow, open-marine carbonates or shales may be deposited in the anti-peripheral bulge or peripheral sag (Figure 4), the overall sedimentary response is a cratonward-prograding wedge of marginal marine and terrestrial sediments, which commonly contain redbeds. Because of rebound and the resulting progradation, it appears that the foreland basin has "overflowed" onto the craton. The foreland basin may experience cannibalization, and this process may result in an unconformity in proximal parts of the basin, which "opens up" toward the tectonic highlands (Goodman and Brett, 1994). Such an unconformity, however, can be easily subsumed by erosion that accompanies the bulge move-out of a succeeding tectophase or orogeny.

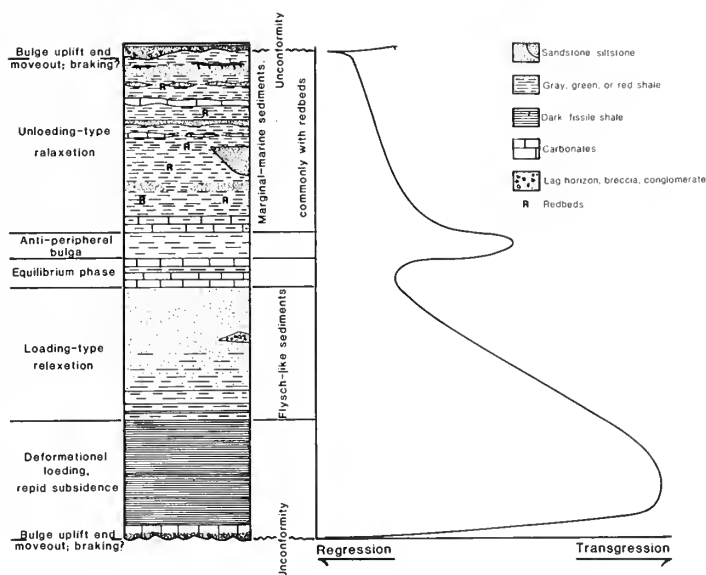


FIGURE 4—Flexural events, facies, and transgressive-regressive curve for early subduction-type orogenies on continental margin. Sequence includes: 1) unconformity formation with bulge uplift and moveout; 2) dark shale deposition with rapid subsidence during active deformational loading; 3) deposition of flysch-like clastics with loading-type relaxation; and 4) deposition of marginal marine sediments with redbeds that record unloading-type relaxation. Sequence bound by unconformities that mark onset of deformational events (from Ettensohn, 1994, fig. 3).

SUMMARY AND IMPLICATIONS.—If the above model is valid, then the presence of an unconformity followed by a stratigraphic sequence, such as in Figure 4, is a strong indication of tectonic influence and the presence of a major regional tectonic component in relative sea-level curves. Moreover, if there is any synchronicity between tectonic events on the same continent and on nearby continents, as suggested by Johnson (1971) for Devonian orogenies on Laurussia, then the effects on relative sea-level may be inter-regional or global in scale.

Each generally regressive flexural sequence begins with an unconformity that marks the inception of loading and bulge move-out. The typically asymmetric distribution of such an unconformity toward a continental promontory or angularity is a strong sign of major tectonic involvement (Ettensohn, 1994), rather than the simple sea-level drawdown that accompanies glaciation.

Overlying parts of the flexural sequence include in ascending order: 1) transgressive carbonates or shallow marine sands; 2) dark shales; 3) a flysch-like clastic sequence; and 4) a sequence of marginal marine clastic sediments with redbeds (Figure 4). Moreover, because orogenies progress in pulses or tectophases on the order of 5 Ma or less in duration (Jamieson and Beaumont, 1988), unconformities and their associated sedimentary sequences are generally cyclic during any one orogeny

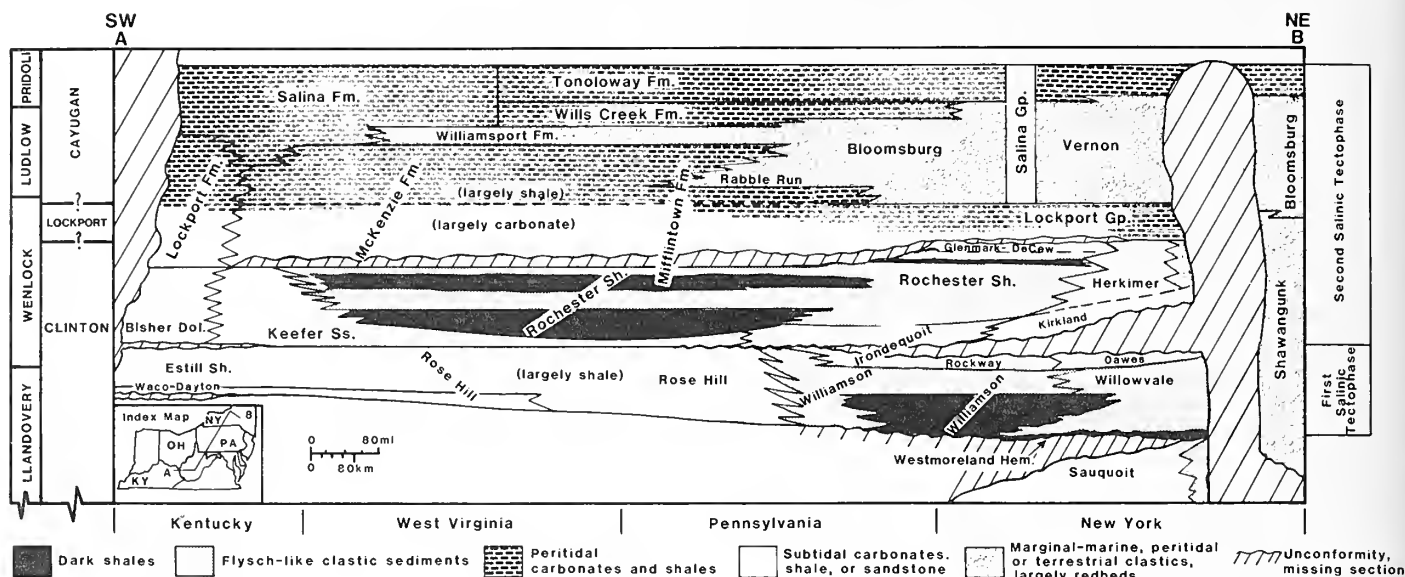


FIGURE 5—Schematic section in part parallel to Appalachian Basin strike that shows repetition and southward migration of flexural foreland basin sequences and accompanying unconformities related to Salinic disturbance. The first late Telychian tectophase never went to completion before onset of second tectophase in the Sheinwoodian, which apparently did run to completion. Missing section along unconformities shown by diagonal ruling. No vertical scale intended (after Ettensohn, 1992b, 1994).

(Ettensohn, 1994). Every cycle, however, may not exhibit the complete sequence of lithologies, because a new tectophase may begin before the sedimentary expression of the previous one is complete or because erosion that accompanies new bulge uplift and move-out destroys parts of the previous sedimentary record. One consistent feature of these cycles is that the sedimentary record of each successive tectophase cycle migrates farther cratonward than the previous one (Figures 5, 6), and reflects the continued cratonward movement of supra-crustal deformation.

Concomitant movement of successive sequences parallel to the strike of the orogen similarly indicates oblique convergence or transpression (Ettensohn, 1987). The cratonward movement of flexural sequences is best illustrated by mapping the distribution of the dark shale units, because these units are easily identified in the surface and subsurface and because they probably represent the time of most active tectonism and subsidence. These shales are thickest and best developed behind the promontory on which convergence is concentrated, and the distribution of the shales will commonly be asymmetric toward that promontory. These shales are also important, because in the standard bathymetric analysis based on recurrent benthic assemblages from Silurian rocks (e.g., Ziegler, 1965; Ziegler et al., 1968; Boucot, 1975), dark shales generally represent the greatest depths (Boucot, 1975; Kaljo, 1978) and are normally interpreted to reflect maximum highstand conditions. However, we suggest that if such shales are parts of cyclic flexural sequences

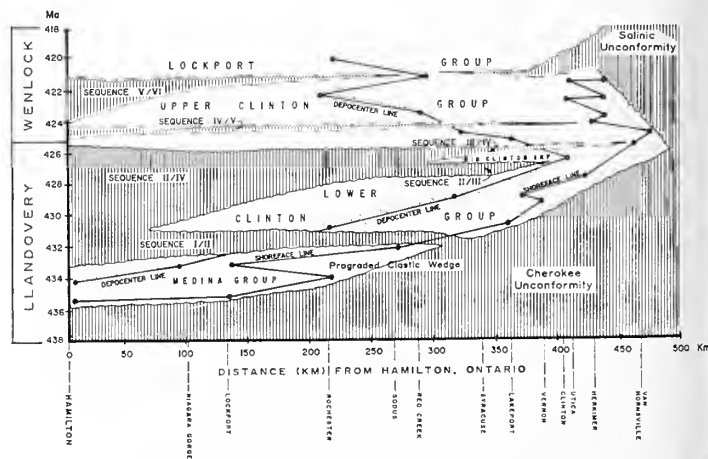


FIGURE 6—Lower-Middle Silurian along New York outcrop belt shows migration of shoreface and depocenter of major sequences and sequence-bounding unconformities. Major sequence-bounding unconformities shown with vertical ruling. Unconformity that marks late Telychian onset of Salinic disturbance is below Sequence III-IV (from Goodman and Brett, 1994, fig. 13).

(Figure 4) in which subsequent dark shale units can be shown to migrate cratonward in time (Ettensohn, 1985, 1987, 1991; Ettensohn and Brett, 1996a, 1996b) (Figure 5), then the highstands represented by the shales probably contain a substantial tectonic component. More detailed mapping of the entire foreland basin sequence in a space-time framework (Figure 6) offers even greater possibilities of discerning tectonic influence, because patterns of basin and unconformity migration are more readily

observed (Goodman and Brett, 1994). Of course, the presence of a nearby coeval orogeny makes any such interpretation even more likely.

Finally, it is important to note that although the distinctive dark shale–redbed flexural sequence and related criteria may be restricted to foreland basins where flexure was greatest, flexural stresses associated with the supracrustal deformational load may be transmitted to adjacent parts of the craton across distances in excess of 1,300 km (e.g., Karner and Watts, 1983; Ziegler, 1987), while the effects of concomitant subcrustal loading may be transmitted across distances up to 2,000 km (Gurnis, 1991). Hence cratonic sedimentation distal to the foreland basin setting may clearly reflect patterns of relative sea-level fluctuation that correspond in nature and origin to flexural events in foreland basins.

SILURIAN TECTONICS OF THE APPALACHIAN MARGIN AND GLOBAL CONNECTIONS

Traditionally, the tectonic history of the Appalachian margin has been divided into several discrete orogenic events. With the exception of a few workers who extended Taconian orogeny into Early Silurian time (e.g., Quinlan and Beaumont, 1984; Tankard, 1986; Hatcher, 1987), the Silurian of the Appalachian Basin has generally been considered anorogenic. More recent work, however, has shown that tectonism was nearly continuous in some form on the Appalachian margin from Late Cambrian through Permian time (e.g., Rast and Skehan, 1993). Of special interest to us has been the tectonic history of the Ordovician–Silurian transition and the Silurian, and the possibility of discerning tectonic influence on Silurian cyclicity. Most workers have not strongly considered the possibility of tectonic influence at this time because the Taconian orogeny is commonly interpreted to have ended with the Ordovician; whatever Silurian tectonism was present (Salinic disturbance; Boucot, 1962) was thought to have been weak and generally ineffectual. Better dating techniques, more field work, and improved models now provide results that challenge these earlier notions. Evidence in the form of volcanism, plutonism, deformation, and foreland basin stratigraphy from the northern and central Appalachians (Pickering, 1987; Laird, 1988; Thirlwall, 1988; Wones and Sinha, 1988; Bevier and Whalen, 1990; Ettensohn, 1992b, 1994; van Staal, 1994; Goodman and Brett, 1994; van Staal and de Roo, 1995; Ettensohn and Brett, 1996a, 1996b) suggests that the Silurian of the Appalachian margin was also a period of tectonism, which should be reflected in Silurian stratigraphy.

Silurian tectonism on the Appalachian margin reflects the continuing closure of the Iapetus Ocean that had already begun by Late Cambrian time. Most of the closure apparently took place in Ordovician time as island arcs and/or microcontinents of suggested Theic (Faill, 1997) or—less likely—Avalonian (e.g., Keppie et al., 1996) affinity converged diachronously from south to north with the Appalachian margin. The resulting orogeny is called Taconian, and evidence for its continuation into Early Silurian time is growing. At the same time, closure of the Iapetus between Baltica and the northern (Greenland) margin of Laurentia was also ongoing. Although the entire closure of the northern margin is called the Caledonian orogenic cycle, actual collision between Baltica and Laurentia probably began in late Llandovery time and is called the Scandian orogeny (Gee, 1975). It was succeeded at various times and places with strike slip and transpressive deformation (Gee and Roberts, 1983; Hurst et al., 1983; Ziegler, 1989; Torsvik et al., 1996). Scandian movements were probably not without effect on the Appalachian margin, because by Late Ordovician time terranes interpreted by some workers to be of Avalonian affinity collided with southern Baltica to form a southern prong-like extension that converged with the northern Appalachian margin in the New England–Maritime province area in Silurian time (McKerrow and Ziegler, 1972; Scotese and McKerrow, 1990; Torsvik et al., 1996) (Figure 7). This convergence event seems to be the same as the Salinic disturbance (Boucot, 1962; Rodgers, 1970, 1987; Fairbairn, 1971), the main focus of which was concentrated at the St. Lawrence Promontory (Rodgers, 1987).

In the northern Appalachians, evidence for Silurian tectonism is already present at the Ordovician–Silurian transition and in the Lower Silurian. Based on the mapping of tectonic terranes and on the history of deformation in the Canadian Appalachians, van Staal (1994) and van Staal and de Roo (1995) recognized a Late Ordovician–Early Silurian subduction zone and collision between Laurentia and the Gander margin of Avalon in the area of the St. Lawrence promontory. Probable flexural stratigraphic sequences that cross the Ordovician–Silurian boundary in Newfoundland (Pickering, 1987) also support the occurrence of orogeny at this time. Although not kinematically related to other phases of Taconian orogeny, the location and timing of the event, as well as the fact that it continues the general northwardly migrating trend of Taconian tectonism in time along the southeastern Laurentian margin, suggest that this event represents a continuation of Taconian convergence into the Silurian. In the Appalachian Basin, stratigraphic and sedimentologic evidence for this event have been provided by Goodman and Brett (1994), Dorsch and Driese (1995), and Ettensohn and Brett (1996a, 1996b).

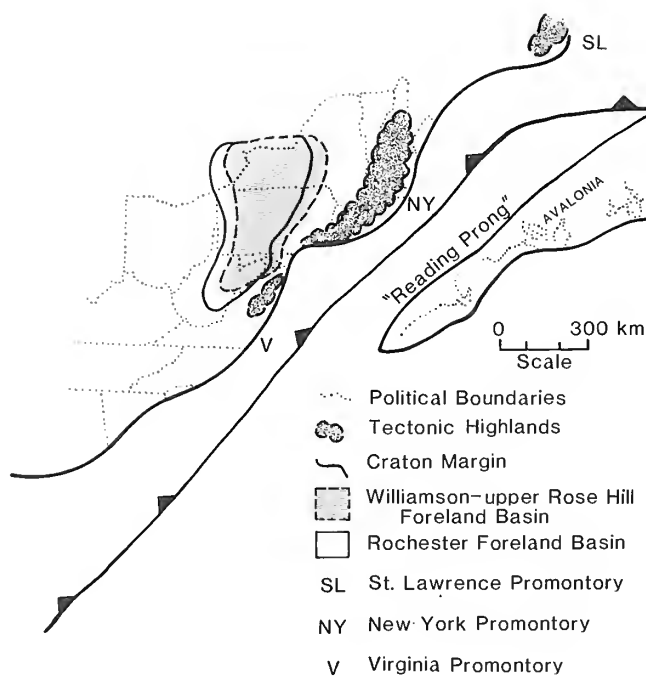


FIGURE 7—Tectonic setting of possible convergence of Avalonian terranes with northern Appalachian margin that gave rise to the Salinic disturbance in late Llandovery–Wenlock. Note southwest migration of dark shale basins through time (see Figure 5) and asymmetry of these basins toward continental promontories.

In the succeeding upper Llandovery and lower Wenlock section, structural and stratigraphic evidence indicate renewed orogeny along the Appalachian margin, probably related to transpression or oblique subduction between the Laurentian margin and the southward-extending prong of likely Avalonian terranes (Figure 7). Although most workers have indicated a later Silurian time for the Salinic disturbance, we suggest a late Llandovery inception for the event based on the stratigraphic evidence presented in the next section. The uplift and erosion that most workers have associated with the Salinic disturbance is indeed Salinic, but is more likely related to late-stage uplift that accompanied unloading-type relaxation (Goodman and Brett, 1994) (Figure 3.2).

The Silurian, especially the Early Silurian, was a time of enhanced global tectonic activity that involve the Caledonian consolidation of Laurentia, Baltica, Chukotka, and likely Avalonian terranes to form Laurussia (e.g., Trettin, 1987; Ziegler, 1989; Torsvik et al., 1996; Khain and Sesslavinsky, 1996; Figure 1). Partly coeval tectonism was also ongoing at many other locations in the Silurian world (Figure 1). These included the Sakmuri–Magnitogorsk arc of northern and eastern Baltica (Ziegler, 1989; Khain and Sesslavinsky, 1996); the Cordilleran margin of western Laurentia (Churkin and Eberlein, 1977); the Altaid belt of southern Siberia, Mongolia and

“Kazakhstan” (Şengör and Natal’in, 1996; Khain and Sesslavinsky, 1996); the Cathaysian belt on the southeastern margin of the South China (Yangtze) craton and Indochina (Institute of Geology et al., 1985; Scotese and Golonka, 1992); the north and west parts of the North China craton (Scotese and Golonka, 1992); eastern Australia; western Antarctica; and western South America (Khain and Sesslavinsky, 1996). Although not directly related to the consolidation of Laurussia, much of this tectonism is also commonly labeled “Caledonian” because of its contemporaneity with that event.

TECTONIC COMPONENT OF APPALACHIAN SILURIAN CYCLES

Silurian cyclicity in the Appalachian Basin is well established and largely attributed to eustatic or tectono-eustatic causes (e.g., Dennison and Head, 1975; Johnson et al., 1985; Johnson, 1987), but more recent work has documented significant tectonic components (e.g., Brett et al., 1990b; Goodman and Brett, 1994; Ettensohn, 1994). As the Silurian was a period of widespread tectonism that involved most major continents and the Appalachian Basin was proximal to various phases of the Caledonian consolidation of Laurussia, major tectonic influence should be expected. Moreover, because the flexural effects of an orogeny can be transmitted up to 2,000 km from an orogen, orogeny on one part of a continent may lead to flexural consequences across large parts of a newly consolidated continent such as Laurussia. Thus the stratigraphic criteria and models discussed above allow both an examination of the Appalachian Silurian sequence for indications of tectonic influence and a consideration of the likely effects of glacio-eustatic causes. A curve showing the expected relative subsidence resulting from Appalachian flexural movements is plotted for comparison in Figure 8.

TACONIAN INFLUENCE.—The earliest indication of Silurian tectonic influence in the Appalachians is at the Ordovician–Silurian boundary unconformity, which was called the Cherokee Unconformity by Dennison and Head (1975). In the central Appalachians, this is called the Tuscarora Unconformity (Dorsch and Driese, 1995). This unconformity is commonly attributed to a glacio-eustatic drawdown supported by worldwide sedimentologic and stratigraphic evidence (Dennison, 1976; McKerrrow, 1979), as well as by evidence of coeval Gondwanan glaciation (Figure 8) (e.g., Hambrey, 1985; Grahn and Caputo, 1992; Buggisch and Astini, 1993). However, in the Appalachian Basin the distribution of the unconformity shows three

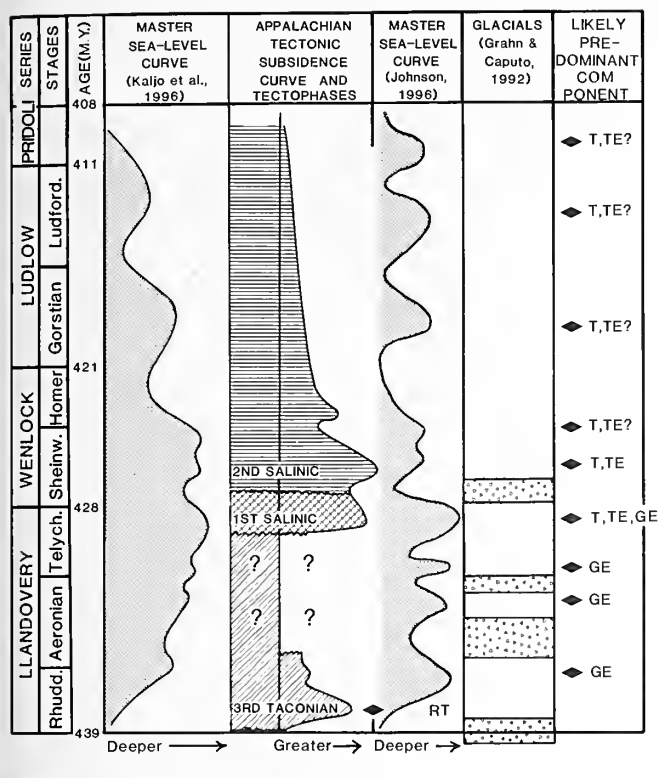


FIGURE 8—Comparison of tectonic subsidence curve and tectophases with master sea-level curves and known glacial events. Kaljo et al.'s (1996) curve adapted from Johnson et al. (1991) and attempts to combine tectono- and glacio-eustatic effects without scaling sea-level changes to the Standard Benthic Association Zones (as does Johnson's (1996) curve. Curve for possible late relaxation phases of the third Taconian tectophase not shown as it has been severely perturbed, probably by glacio-eustatic overprint. Black diamonds on right mark major highstands based on master curves and the likely predominant causal component. Abbreviations: RT, regional tectonism; GE, glacio-eustasy; T, major tectonism, possibly global in scope; TE, tectono-eustasy. Ages from Kaljo et al. (1996).

eastwardly projecting salients that correspond to continental promontories (Figure 9), and a pattern of increasing northward erosional truncation and deformation of Ordovician strata toward the New York Promontory (Ettensohn, 1994). In fact, in parts of the basin behind the New York Promontory, the unconformity is a regional angular unconformity (Brett et al., 1990b; Brett and Goodman, 1996) that becomes a very pronounced angular unconformity proximally (Rodgers, 1971; Liebling and Scherp, 1982), which indicates a tectonic influence. The fact that the unconformity occurs on the Taconic flexural sequence (Ettensohn, 1991; Figure 10) and opens in an eastward direction (Goodman and Brett, 1994; Figures 6, 10) suggests that the unconformity in this part of the basin is probably related in large part to isostatic rebound that accompanied unloading-type relaxation (Figure 3.2) at the end of the Taconic tectophase (Figure 10).

More recent evidence, however, indicates that the unconformity may also reflect uplift caused by bulge

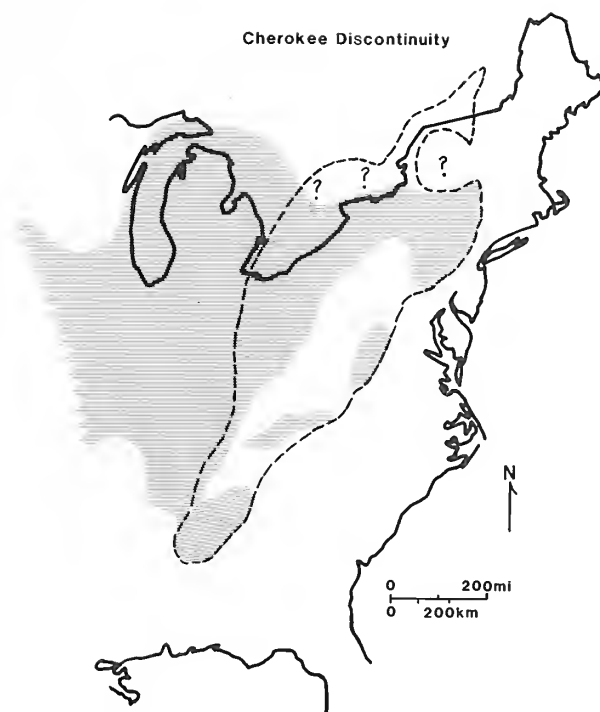


FIGURE 9—Distribution of the Cherokee (Ordovician-Silurian) Unconformity in Appalachian Basin and adjacent areas. Note asymmetry of the unconformity toward continental promontories in proximal parts of the Appalachian Foreland Basin (dashed line) (from Ettensohn, 1994).

move-out that accompanied an Early Silurian tectophase of the Taconian orogeny (van Staal, 1994; Ettensohn and Brett, 1996a, 1996b). Van Staal (1994) first recognized a Late Ordovician–Early Silurian subduction complex associated with the St. Lawrence Promontory in the Canadian Appalachians. Ettensohn and Brett (1996a, 1996b) later recognized the presence of a partial Lower Silurian flexural sequence in western New York (Figure 10), and mapped the distribution of the dark Power Glen–lower Cabot Head Shales to reveal a foreland basin that migrated farther northwest than the older Martinsburg Basin and was asymmetrical toward the St. Lawrence Promontory (Figure 11). Inasmuch as this basin reflects a continuation of the northwest-migrating trend of earlier Taconian basins (Figure 11), and its asymmetry reflects a focus of tectonism at the St. Lawrence Promontory that seems to coincide in time and space with a Taconian event reported by van Staal (1994), the evidence points to a third and final tectophase of Taconian orogeny centered on the St. Lawrence Promontory.

The Grimsby Sandstone and other siliciclastic units of the Medina Group that overlie the Power Glen Shale (Figure 10) appear to record loading-type relaxation (Figure 3.1). However, carbonate and siliciclastic units of the overlying lower and middle Clinton Group contain several smaller sequences and unconformities atypical of an

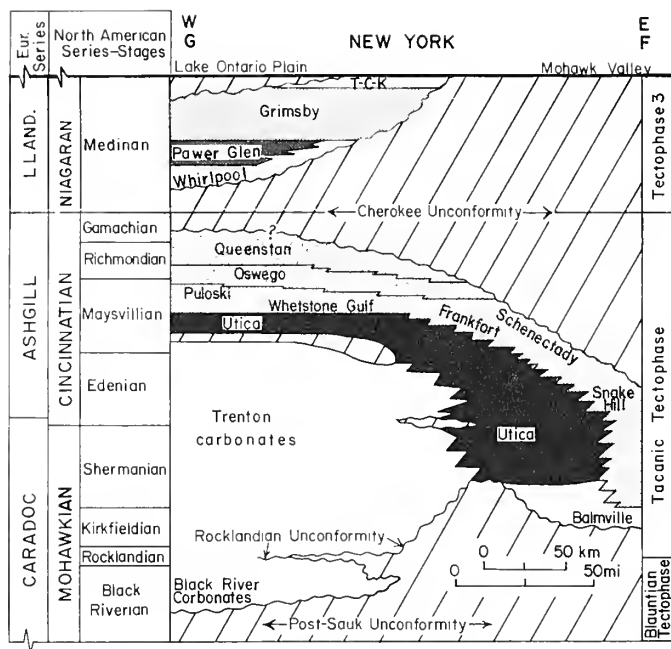


FIGURE 10—Section perpendicular to strike of northern Appalachian Basin in New York (line G–F of Figure 11), with nature and disposition of Taconian flexural sequences. Note relative westward migration of foreland basins between time of deposition of Utica and Power Glen Shales (see Figure 11). Black River Group carbonates record Blountian tectophase of Taconian orogeny, but never developed into a typical flexural sequence because of distance from the southerly locus of the tectophase. Major unconformities shown by diagonal ruling. T–C–K is Thorold, Cambria, and Kodak Formations. No vertical scale intended; legend same as that on Figure 5 (after Ettensohn, 1991, 1994).

unloading-type sequence, but do show the typical migration toward the orogen (Figure 6). These units may record an unloading-type or late-stage relaxation sequence (Goodman and Brett, 1994), but if so, it is a sequence perturbed by superimposed eustatic fluctuations and/or reactivation of local structures.

If the dark Power Glen Shale and equivalents are assumed to represent the time of maximum tectonic subsidence in this tectophase (Figure 8), it is important to compare the location and timing of the resulting deepening event with other Rhuddanian highstands to determine the likely predominance of one component over another. Although the Silurian master curve shows only a late Rhuddanian highstand (e.g., Johnson, 1996; Figure 8), curves from the Laurentian parts of Great Britain and Ireland (Leggett, 1980; Leggett et al., 1982), from the Avalonian parts of Great Britain and Ireland (McKerrow, 1979; Leggett, 1980), and from Bohemia (Johnson, 1996) suggest a highstand that endured for nearly all of the Rhuddanian. On the other hand, apparently distinct early Rhuddanian highstands are known from the eastern and east-central United States and Canada (Johnson et al., 1985; Johnson, 1987), Poland (McKerrow, 1979), Estonia

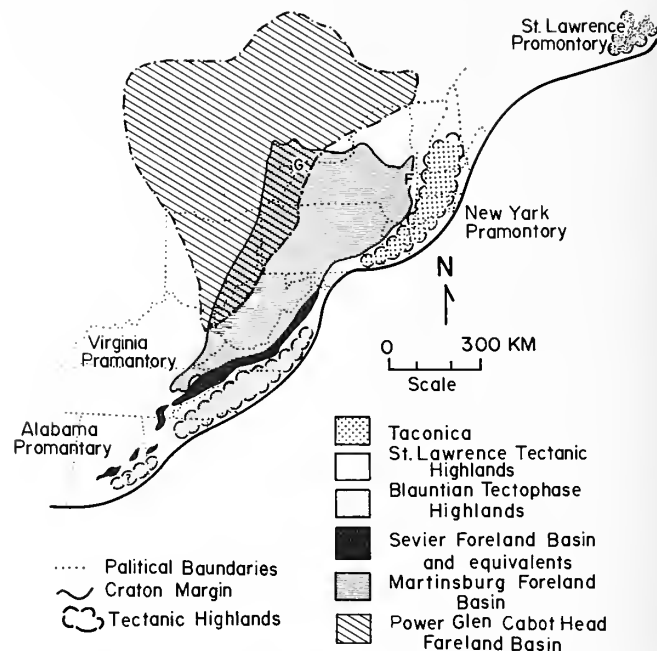


FIGURE 11—Map of central and southern Appalachians with positions of Taconian tectonic highlands and dark shale foreland basins relative to continental promontories during Middle Ordovician–Early Silurian. Note northwest shift of dark shale foreland basins in time and asymmetry of basins toward continental promontories. Power Glen–Cabot Head Shales represent time of greatest deformational loading and subsidence in the Early Silurian Taconian tectophase; basin is asymmetrical toward St. Lawrence Promontory, the likely locus of this tectophase (after Ettensohn, 1991, 1994).

(Johnson and McKerrow, 1991; Johnson et al., 1991a, Johnson, 1996), and Siberia (Tesakov et al., this volume). Clearly, imprecise dating may figure into the interpretations of two Rhuddanian highstands and the timing of possibly related Ordovician–Silurian glacial events. In fact, both highstands could represent the same event. Nonetheless, taken at face value, the fact that all early Rhuddanian highstands, except the Siberian one, are present on assembling Laurussian continents or microcontinents relatively close to the locus of subduction and tectonism (e.g., Scotese and Golonka, 1992) (Figure 1) suggests a tectono-eustatic origin for this early Rhuddanian highstand related to the ongoing assembly of Laurussia. The highstand in Siberia (Tesakov et al., this volume) may merely reflect the presence of coeval orogeny in the Altaid belt of southern Siberia, Mongolia, and “Kazakhstan” (Şengör and Natal’in, 1996; Khain and Seslavinsky, 1996).

SALINIC INFLUENCE.—The beginning of the Salinic influence is represented by a prominent regional unconformity at the base of the late Llandovery upper Clinton Group (Ettensohn, 1992b, 1994; Goodman and Brett,

1994). This late Telychian unconformity "opens" to the west (Figure 6), extends cratonward as a regional angular unconformity beyond the Algonquin and Cincinnati Arches (Rickard, 1975; Lukasik, 1988; Brett et al., 1990b; Goodman and Brett, 1994; Andrews and Ettensohn, 1996), and appears in other areas of the east-central United States as a disconformity (Ham and Wilson, 1967; Shaver, 1985; Patchen et al., 1985) (Figure 12). The angularity of the unconformity and its asymmetrical distribution toward the Virginia and New York Promontories (Figure 12) indicate a largely tectonic origin (Ettensohn, 1994). Its tectonic origin is also supported by a partial flexural sequence that overlies the unconformity (Figure 5). The sequence begins with a condensed section (Westmoreland Hematite), followed by dark Williamson Shale that represents maximum loading, and is succeeded by a very thin, greenish-gray, flysch-like sequence that records initiation of loading-type relaxation. The sequence is capped by argillaceous offshore carbonates of the Rockway Formation, which probably reflect eastward bulge movement that accompanied loading-type relaxation (Lin and Brett, 1988; Eckert and Brett, 1989; Brett et al., 1990a, 1990b, 1991; Ettensohn, 1992b, 1994; Goodman and Brett, 1994; Brett and Goodman, 1996) (Figure 5). Although prominent, this tectophase was short-lived, and the full flexural sequence never developed because it was rapidly followed by a second Salinic tectophase (Figures 5, 8).

The second tectophase began with an early Wenlock or Sheinwoodian unconformity that has a distribution pattern also asymmetrical toward the New York and Virginia Promontories, and indicates the likely influence of bulge uplift which emanated from the promontories (Ettensohn, 1994) (Figure 12). This time, however, the flexural sequence is complete (Figures 5, 8). The sequence begins with a transgressive carbonate (Irondequoit Limestone and equivalents) that grades upward into dark Rochester shales and mudstones, which are overlain by lighter colored tempestitic and calcareous sediments (Folk, 1962; Smosna and Patchen, 1978; Brett, 1983; Brett et al., 1990a, 1990b, 1991; Goodman and Brett, 1994; Brett and Goodman, 1996). This part of the flexural sequence is capped with a another carbonate unit (DeCew Dolostone and equivalents) and truncated in places by an unconformity that likely records the eastward bulge movement that accompanied the final phases of loading-type relaxation (Figures 3.1, 5, 6). The late Wenlock-early Ludlow spread of Lockport Group carbonates throughout the basin reflects complete basin infill during loading-type relaxation (Figures 3.1, 4, 5). The shallow-water marine shales in eastern parts of the partially equivalent McKenzie Formation (Figure 5) probably records development of an anti-peripheral bulge or peripheral sag and

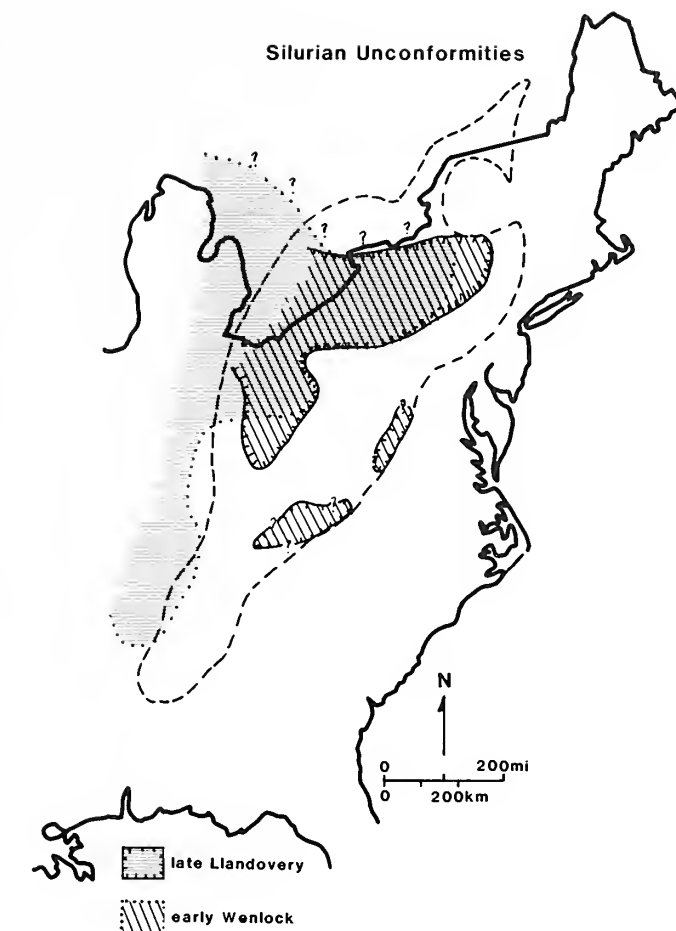


FIGURE 12—Distribution of two late Llandovery (late Telychian) and early Wenlock (Sheinwoodian) unconformities related to the Salinic disturbance in the Appalachian Basin (dashed line) and adjacent areas. Note pronounced asymmetry of unconformity distribution toward promontories (from Ettensohn, 1994, fig. 10).

the beginning of unloading-type relaxation (Figures 3.2, 4). The marginal marine redbeds, dolostones, and shales of the Vernon and Bloomsburg Formations (Figure 5) are what most workers have identified with the Salinic disturbance, but they are merely the last part of a complete flexural sequence that represents the cratonward progradation of marginal marine beds that accompanied unloading-type relaxation (Ettensohn, 1992b, 1994). Rebound associated with this relaxation was apparently substantial enough in eastern New York that parts of the Vernon Shale were uplifted and truncated on the Salinic unconformity (Brett et al., 1990).

The age of deformation, magmatism, and metamorphism defines the beginning of the Salinic disturbance in the Canadian Appalachians at about 430 Ma (Cawood et al., 1995), and this age coincides well with the late Telychian inception of the event as interpreted from the stratigraphic record (Figure 8). The angularity of the

unconformity, its distribution, and an overlying flexural stratigraphic sequence all support a major late Telychian tectonic component. Similar lines of evidence support the presence of a second Salinic tectophase that began about in the middle Sheinwoodian and continued almost to the end of the Silurian (Figures 5, 8). Regional cross-sections (Figures 5, 6) and basin maps (Figure 7) show the cratonward migration of successive dark shale basins. The overall southward migration of these basins (Figure 7) marks them as distinct from the northwestwardly migrating Taconian basins (Figure 11). Hence the evidence strongly supports a major tectonic component in the late Telychian and middle Sheinwoodian highstands in the Appalachian area, as both highstands coincided with the inception of Salinic tectophases.

Interestingly, the Scandian orogeny is also interpreted to have begun in the late Llandovery, with evidence for late Telychian nappe emplacement in Greenland (Hurst et al., 1983), coeval tectonism in Norway and Sweden (Andersen, 1981; Gee and Roberts, 1983; Dallmeyer, 1988; Roberts, 1988), late Llandovery bentonites in Scandinavia (Bruton and Harper, 1988), and possible late Llandovery–early Wenlock flexural foreland basin sequences (Bassett et al., 1982; Gee and Roberts, 1983; Bassett, 1985). The fact that the inceptions of the Scandian and Salinic orogenies were late Telychian on separate parts of the same suture suggests that convergence may have been active along the entire Caledonian suture at this time. If so, flexural subsidence may have been a major component of any late Telychian highstand recorded within at least 1,300 km of the suture, and even perhaps further away.

Late Early Silurian tectonism is also recorded on the southeast South China (Yangtze) craton (Institute of Geology et al., 1985; Khain and Soslavinsky, 1996) and Australia (Pickett, 1982; Khain and Soslavinsky, 1996), although the descriptions and timing of orogeny are less clear. Whether or not the orogenic events on separate plates are related is uncertain, but it is clear that the late Llandovery was a time of global tectonic reorganization that involved the consolidation of Laurussia along the Caledonian suture. Hence it is a time when widespread tectonic subsidence should be expected—even while some nearby areas were experiencing uplift.

The likelihood of widespread tectonic subsidence at this time is all the more important, because it apparently coincided with the late Telychian highstand (Figure 8), one of the best documented and most extensive of Silurian highstands, and one of the greatest of the Phanerozoic (Vail et al., 1977; Scotese and Golonka, 1992). In comparing the late Telychian highstand with the Silurian glacial record (Grahn and Caputo, 1992; Caputo, 1996), it is apparent that the highstand immediately preceded the

youngest known Silurian glaciation. Although Grahn and Caputo (1992) and Caputo (1996) indicated that this glaciation was latest Llandovery to earliest Wenlock, the highstand had apparently peaked before the advent of glaciation. This is supported by the carbon isotope record (Kaljo et al., this volume; Heath et al., this volume), which suggests that the glaciation was earliest Sheinwoodian (earliest Wenlock). This means that glacio-eustasy cannot be ruled out as a major contributor to the late Telychian highstand, although it does leave unexplained a middle Telychian lowstand for which no glaciation is now known (Figure 8). However, the late Llandovery also seems to have been a period of global tectonic reorganization, and the widespread flexural subsidence, far-field tilting, and tectono-eustasy that must have accompanied the nearly coeval orogenies on various Laurussian and Gondwanan subcontinents cannot be ignored in explanations of this highstand. In addition, it is likely that once the ages of some of the more loosely dated “Silurian” orogenies on other continents become more precisely known, the effects of this late Llandovery reorganization will prove to be even more widespread. Thus for the late Telychian highstand, it is difficult to assign predominance to one component over another. Indeed, it seems that tectono- and glacio-eustatic components reinforced each other in the late Telychian to produce what has been interpreted as the maximum sea-level rise of the Silurian.

The second Salinic tectophase interpreted from the Appalachian Basin is a Wenlock or middle Sheinwoodian event that also coincides with a major Silurian highstand (Figure 8) that has been recorded in Iowa, Avalonia, Estonia, Bohemia, Australia, and Siberia (Johnson, 1996; Tesakov et al., this volume). Tectonism of approximately similar age reported in Scandinavia (Roberts, 1988; Torsvik et al., 1996) and possibly in Greenland and Svalbard (Roberts, 1988) suggests that this tectophase may have occurred to some extent along the entire Caledonian suture. The more regional nature of this tectonism, in contrast to the apparently global late Telychian tectonism, may explain the fact that the middle Sheinwoodian highstand is largely restricted to the continents and terranes that were assembling to form Laurussia (Johnson and McKerrow, 1991; Johnson, 1996), where the effects of accompanying flexural subsidence would have been concentrated. The occurrence of apparently coeval highstands on parts of Australia and Siberia, however, may merely reflect concurrent episodes of tectonism that was ongoing in both areas throughout the Silurian (Şengör and Natal'in, 1996; Khain and Soslavinsky, 1996). By this time, moreover, the effects of glaciation were apparently inconsequential, and this is generally supported by Silurian conodont $^{87}\text{Sr}/^{86}\text{Sr}$ chemostratigraphy (Ruppel et al., 1996).

A similar highstand at the Sheinwoodian–Homerian transition may also reflect tectonic influence. This highstand occurs at about the time during the second Salinic tectophase when a returning antiperipheral bulge or peripheral sag (Figure 3.2) would have been likely. As does its predecessor, it reflects a smaller flooding event, and the apparent extent of the highstand is even more narrowly confined to parts of the assembling Laurussian continent near the Scandian orogen (Johnson and McKerrow, 1991; Johnson, 1996).

For the remaining parts of the Wenlock, Ludlow, and Pridoli, unloading-type relaxation (Figures 5, 11) characterized the Appalachian Basin, and with it came a slow infilling of the basin with shallow-marine to marginal marine carbonates and siliciclastics. The overall trend is one of regression, but smaller-scale transgressive and regressive excursions are present on the curve (Brett and Goodman, 1996). These excursions may reflect tectono-eustasy related to Scandian tectonism in Scandinavia (e.g., Gee and Roberts, 1983; Roberts, 1988) that had no counterparts along the Appalachian parts of the Caledonian suture.

CONCLUSIONS

The subcrustal and supracrustal loading that normally accompanies orogenic events provides diverse mechanisms for generating widespread, relatively rapid tectonic subsidence of the sort that could readily influence sea-level fluctuations on regional to possibly global scales. Of the two types of loading, it is the flexural effects of supracrustal loading that are currently best understood and that provide the most effective approach to discern the presence and nature of tectonic components in cyclicity. Although it is probably impossible to differentiate “purely” eustatic from tectonic causes, some of the results of flexural modeling make it possible to detect the tectonic component, and in some instances to suggest the relative predominance of one component over another, especially when the most important causes of “pure eustasy” at the time are well known. The Silurian time frame and the nature of the Silurian section of the Appalachian Basin provide just such an opportunity. Glaciation is now thought to have controlled much of the eustatic variation during the Early Silurian and early Late Silurian, and the nature and timing of glacial events are now reasonably well understood (e.g., Grahn and Caputo, 1992). This kind of understanding is important because it provides a background against which the relative influence of tectonic causes can be evaluated. For most of the Late Silurian, however, a glacio-eustatic component is absent, because glaciation was either inconsequential, absent, or evidence for it is not yet known.

The nature of the stratigraphic record is important in this regard. Although the Appalachian orogen has been multiply deformed, most of the foreland basin escaped severe deformation. This means that the major source of flexural evidence, the Silurian foreland basin stratigraphic sequence, is largely intact and available for analysis. Unfortunately the tectonic history of the Caledonian belt in the Appalachians is not as well understood, and for some time the presence and nature of Silurian tectonism was unrecognized or unappreciated here. New studies are now changing this state of affairs (e.g., van Staal, 1994; van Staal and de Roo, 1995; van Staal et al., 1996; Torsvik et al., 1996), but until this line of research fully matures, analyses of Silurian sequences based on flexural models (e.g., Brett et al., 1990b; Ettensohn, 1992b, 1994; Goodman and Brett, 1994) probably provide the best evidence for the timing of Silurian tectonism on the Appalachian margin. This kind of evidence is equally important because it provides a way to compare Appalachian Silurian tectonism with that of other parts of the Caledonian belt and, for that matter, with tectonism in other parts of the world.

Recent structural and flexural analyses are now beginning to show that the Appalachian margin was indeed the scene of Silurian tectonism, albeit not as intense or prolonged as tectonism recorded farther north along the Caledonian suture. Much of the earlier evidence had either gone unrecognized or has been interpreted as Taconian or Acadian, even though some of the distinctions between individual tectonic events are beginning to break down, as the Appalachian margin was the site of nearly continuous tectonism from the Late Cambrian to Permian. Nonetheless, our examination of the Appalachian Silurian for flexural evidence of tectonism, based on the nature and distribution of unconformities, flexural stratigraphic sequences, and dark shales, suggests three major tectophases, each of which must have contributed some component to the local and regional eustatic situation.

The first of these is an extension of the Taconian orogeny into the Silurian. The nature of the underlying unconformity, presence of a partial flexural sequence, and foreland basin subsidence recorded in a pattern of dark shale distribution that apparently reflects a northward extension of previous Taconian trends, all indicate a third Early Silurian tectophase of the Taconian orogeny. A coeval highstand not only occurs in the Appalachian Foreland Basin, but is largely restricted to other assembling parts of Laurussia, where the far-field effects of tectonic subsidence can be expected. Regional structural analysis (van Staal, 1994; van Staal and de Roo, 1995) also supports the proximity and timing of a coeval orogenic event. It is difficult to relate the accompanying highstand to any known glacial or tectonic event (Figure 8). This

Rhuddanian highstand appears to be a largely Laurussian event that coincides in location and timing with a newly recognized orogenic phase, and the absence of a coeval highstand on most other continents suggests the predominance of a tectonic component.

The second and third examples record two tectophases of the Salinic disturbance. Evidence similar to that used above was collected, with the exception that analysis of dark shale distribution in the foreland basins shows a sense of basin migration (Figure 7) different than that of Taconian basins (Figure 11), thus confirming the separate and distinct nature of Salinic tectonism. What is not so obvious about the initial late Telychian tectophase is that it coincided with the inception of Scandian orogeny along much of the Caledonian suture and with apparent Early Silurian tectonism around the globe. Moreover, the global tectonic reorganization that included the Salinic tectophase coincided with a late Telychian highstand that was the greatest of the Silurian flooding events (e.g., Johnson, 1996; Kaljo et al., 1996). Although this highstand was coeval with a period of deglaciation, the highstand is so much greater than other Silurian deglaciation events that it seems necessary to call on the reinforcing effects of global tectonism to explain its magnitude. A substantial part of the late Telychian highstand may reflect the extensive tectonic reorganization of the time, apparently in large part initiated by the assembly of Laurussia.

A subsequent middle Sheinwoodian highstand coincided with the second Salinic tectophase in the Appalachian Basin (Figure 8) and with apparently coeval tectonism lateral to the Caledonian suture. Both the tectonism and the highstand are more regional in scope than similar late Telychian events and are largely restricted to Laurussian subcontinents, but they suggest a relationship between tectonism, highstands, and the likely predominance of a tectonic component in the highstand. A subsequent late Sheinwoodian–early Homerian highstand was apparently even more restricted in distribution, and may be related to a minor deepening that accompanied early unloading-type relaxation in the Salinic disturbance and coeval orogeny on other continents and terranes that were assembling to form Laurussia. After the early Homerian, the flexural tectonic curve in the Appalachian Basin (Figure 8) apparently reflected slow regression and basin infilling that accompanied relaxation and the impending conclusion of Salinic tectonism. Although both regional and global eustatic curves continue to show transgressive and regressive excursions during the remainder of Silurian time (Figure 8), these fluctuations likely reflect tectonic events beyond the Appalachians in the absence of known glacial events.

Clearly the criteria developed from flexural models to discern the influence of tectonism in the sedimentary

record and the relative effects of eustasy are powerful tools in determining ultimate causes. This is especially true when information about contributions from the other most likely cause (i.e., glacio-eustasy) is also known, as is the case through much of the Silurian. This kind of information, when used with established sea-level curves, makes it possible to establish the relative predominance of tectonic versus glacio-eustatic components in some sea-level cycles; the likelihood of regional versus global tectonic causes; and the presence of destructive versus constructive interference between glacio-eustatic and tectonic components. Even though the global record of Silurian tectonism is imperfectly known, regional syntheses from such areas as the Appalachian Basin aid in our determination of ultimate causes on various scales and our understanding of the interrelationships between these causes. The implications of lithospheric flexure and far-field tectonics, even for local and regional settings like the Appalachians, may have global significance.

ACKNOWLEDGMENTS

We thank M.G. Bassett, W.S. McKerrow, and N. Rast for valuable discussions and literature references. We also thank J.M. Dennison, W.M. Goodman, M.E. Johnson, and E. Landing for their reviews and helpful comments on the manuscript. C.E. Brett's research was supported by a grant from the Petroleum Research Fund of the American Chemical Society. (Editors' note: FRE contributed \$100 from personal funds toward publication of this report.)

REFERENCES

- ANDERSEN, T.B. 1981. The structure of the Magerø nappe, Finnmark, north Norway. *Norges Geologiske Undersøkelse*, 363:1–23.
- ANDREWS, W.M., JR., AND F.R. ETTENSOHN. 1996. Regional and local structural controls on deposition of the Lower Silurian (Llandoveryan) Brassfield Formation west of the Cincinnati Arch, p. 25. *In* The James Hall Symposium: Second International Symposium on the Silurian System, Program and Abstracts. University of Rochester.
- BAARLI, B.G. 1990. Peripheral bulge of a foreland basin in the Oslo region during the Early Silurian. *Palaeogeography, Palaeoclimatology, Palaeoecology*, 78:149–162.
- BASSETT, M.G. 1985. Silurian stratigraphy and facies development in Scandinavia, p. 283–292. *In* D.G. Gee and B.A. Sturt (eds.), *The Caledonian Orogen—Scandinavia and Related Areas*, Part 1. John Wiley and Sons, Chichester.
- , L. CHERNS, AND L. KARIS. 1982. The Röde Formation, early Old Red Sandstone facies in the Silurian of Jämtland, Sweden. *Sveriges Geologiska Undersökning, Series C*, 793:1–24.
- BEAUMONT, C. 1981. Foreland basins. *Geophysical Journal of the Royal Astronomical Society*, 65:291–329. *Journal of the Royal Astronomical Society*, 65:291–329.

- , G.M. QUINLAN, AND J. HAMILTON. 1987. The Alleghanian orogeny and its relationship to the evolution of the eastern interior, North America, p. 425–445. *In* C. Beaumont and A.J. Tankard (eds.), *Sedimentary Basins and Basin-Forming Mechanisms*. Canadian Society of Petroleum Geologists, Memoir 12.
- , AND ———. 1988. Orogeny and stratigraphy: numerical models of the Paleozoic in the eastern interior of North America. *Tectonics*, 7:389–416.
- BEVIER, M.L., AND J.B. WHALEN. 1990. Tectonic significance of Silurian magmatism in the Canadian Appalachians. *Geology*, 18:411–414.
- BOUCOT, A.J. 1962. Chapter 10, Appalachian Siluro-Devonian, p. 155–163. *In* K. Coe (ed.), *Some Aspects of the Variscan Fold Belt*. Manchester University Press.
- . 1975. *Evolution and Extinction Rate Controls*. Elsevier Scientific Publishing Company, Amsterdam.
- BRETT, C.E. 1983. Sedimentology, facies, and depositional environments of the Rochester Shale (Silurian, Wenlockian) in western New York and Ontario. *Journal of Sedimentary Petrology*, 53:947–971.
- , AND W.E. GOODMAN. 1996. Silurian sequence stratigraphy of north western New York with emphasis on the type Niagaran series, p. 25–72. *In* C.E. Brett and P.E. Calkin (co-leaders), *Silurian Stratigraphy and Quaternary Geology of the Niagara Area, A Guidebook for Field Trips in Niagara County, New York*. Annual Northeast Section Meeting of the Geological Society of America, Buffalo.
- , ———, AND S.T. LODUCA. 1990a. Sequence stratigraphy of the type Niagaran Series (Silurian) of western New York and Ontario, p. C1–C71. *In* G.G. Lash (ed.), *New York State Geological Association 62nd Annual Field Trip Guidebook, Western New York and Ontario*. New York State Geological Association, Fredonia.
- , ———, AND ———. 1990b. Sequences, cycles and basin dynamics in the Silurian of the Appalachian Foreland Basin. *Sedimentary Geology*, 69:191–244.
- , ———, ———, AND D.F. LEHMANN. 1994. Ordovician and Silurian strata in the Genesee Valley area: sequences, cycles, and facies, p. 381–441. *In* C.E. Brett and J. Scatterday (eds.), *Field Trip Guidebook, New York State Geological Association, 66th Annual Meeting*.
- , ———, ———, AND ———. 1996. Upper Ordovician and Silurian strata in western New York: sequences, cycles, and depositional dynamics, p. 71–120. *In* C.E. Brett and W.M. Goodman (co-leaders), *Upper Ordovician and Silurian Sequence Stratigraphy and Depositional Environments in Western New York, A Field Guide for the James Hall Symposium*. Second International Symposium on the Silurian System, University of Rochester.
- BRUTON, D.L., AND D.A.T. HARPER. 1988. Arenig-Llandovery stratigraphy and faunas across the Scandinavian Caledonides, p. 247–268. *In* A.L. Harris and D.J. Fettes (eds.), *The Caledonian–Appalachian Orogen*. Geological Society Special Publication No. 38.
- BUGGISCH, W., AND R. ASTINI. 1993. The Late Ordovician ice age: new evidence from the Argentine Precordillera, p. 439–447. *In* R.H. Findlay, R. Unrug, M.R. Banks, and J.J. Vevers (eds.), *Gondwana Eight—Assembly, Evolution, and Dispersal*. A.A. Balkema, Rotterdam.
- BURGESS, P.-M., M. GURNIS, AND L.-N. MORESI. 1995. Geodynamical contributions to the formation of North American cratonic stratigraphic sequences. *Eos*, 76:535.
- CAPUTO, M.V. 1996. Silurian glacial paleogeography in South America, p. 40. *In* The James Hall Symposium: Second International Symposium on the Silurian System, Program and Abstracts. University of Rochester.
- CAWOOD, P.A., J.A.M. VAN GOOL, AND G.R. DUNNING. 1995. Collisional tectonics along the Laurentian margin of the Newfoundland Appalachians, p. 283–301. *In* J.P. Hibbard, C.R. van Staal, and P.A. Cawood (eds.), *Current Perspectives in the Appalachian–Caledonian Orogen*. Geological Association of Canada Special Paper 41.
- CHURKIN, M., AND G.D. EBERLEIN. 1977. Ancient borderland terranes of the North American Cordillera: correlation and microplate tectonics. *Geological Society of America Bulletin*, 88:769–786.
- CLOETINGH, S., AND H. KOOL. 1992. Tectonics and global change— inferences from Late Cenozoic subsidence and uplift patterns in the Atlantic/Mediterranean region. *Terra Nova*, 4:340–350.
- COAKLEY, B., AND M. GURNIS. 1995. Far-field tilting of Laurentia during the Ordovician and constraints on the evolution of a slab under an ancient continent. *Journal of Geophysical Research*, 100:6313–6327.
- CROSS, T.A., AND R.H. PILGER, JR. 1978. Tectonic controls of Late Cretaceous sedimentation, western interior, USA. *Nature*, 274:653–657.
- DALLMEYER, R.D. 1988. Polyphase tectonothermal evolution of the Scandinavian Caledonides, p. 365–379. *In* A.L. Harris and D.J. Fettes (eds.), *The Caledonian–Appalachian Orogen*. Geological Society Special Publication No. 38.
- DENNISON, J.M. 1976. Appalachian Queenston Delta related to eustatic sea-level drop accompanying Late Ordovician glaciation centered in Africa, p. 107–120. *In* M.G. Bassett (ed.), *The Ordovician System: Proceedings of a Palaeontological Association Symposium*. University of Wales Press and National Museum of Wales, Cardiff.
- , AND J.W. HEAD. 1975. Sea level variations interpreted from Appalachian Basin Silurian and Devonian. *American Journal of Science*, 275:1089–1120.
- DEWEY, J.F., AND K.C.A. BURKE. 1974. Hot spots and continental breakup: implications for collisional orogeny. *Geology*, 2:57–60.
- , AND W.S.F. KIDD. 1974. Continental collisions in the Appalachian–Caledonian belt: variations related to complete and incomplete suturing. *Geology*, 2:543–546.
- DICKINSON, W.R., G.S. SOREGHAN, AND K.A. GILES. 1994. Glacio-eustatic origin of Permo–Carboniferous stratigraphic cycles: evidence from the southern Cordilleran foreland region, p. 25–34. *In* J.M. Dennison and F.R. Ettensohn (eds.), *Tectonic and Eustatic Controls on Sedimentary Cycles*. SEPM Concepts in Sedimentology and Paleontology, 4.
- DORSCH, J., AND S.G. DRIESE. 1995. The Taconic foredeep as sediment sink and origin of the white quartzarenite blanket (Upper Ordovician–Lower Silurian) of the central and southern Appalachians. *American Journal of Science*, 295:201–243.
- ECKERT, B.-Y., AND C.E. BRETT. 1989. Bathymetry and paleoecology of Silurian benthic assemblages, late Llandoveryan, New York State. *Palaeogeography, Palaeoclimatology, Palaeoecology*, 74:297–326.
- ETTENSOHN, F.R. 1985. The Catskill Delta complex and the Acadian orogeny, p. 39–49. *In* D.W. Woodrow and W.D. Sevon (eds.), *The Catskill Delta*. Geological Society of America, Special Paper 201.
- . 1987. Rates of relative plate motion during the Acadian orogeny based on the spatial distribution of black shales. *Journal of Geology*, 95:572–582.
- . 1991. Flexural interpretation of relationships between Ordovician tectonism and stratigraphic sequences, central and southern Appalachians, U.S.A., p. 213–224. *In* C.A. Barnes, and S.H.

- Williams (eds.), *Advances in Ordovician Geology*. Geological Survey of Canada, Paper 90-9.
- . 1992a. Controls on the origin of the Devonian–Mississippian oil and gas shales, east-central United States. *Fuel*, 71:1487–1492.
- . 1992b. General Silurian paleogeographic and tectonic framework for Kentucky, p. 149–150. In F.R. Ettensohn (ed.), *Changing Interpretations of Kentucky Geology—Layer-Cake, Facies, Flexure, and Eustasy*. Ohio Division of Geological Survey, Miscellaneous Report No. 5.
- . 1993. Possible flexural controls on the origins of extensive ooid-rich, carbonate environments in the Mississippian of the United States, p. 13–30. In B.D. Keith and C.W. Zuppan (eds.), *Mississippian Oolites and Modern Analogs*. American Association of Petroleum Geologists, *Studies in Geology* No. 35.
- . 1994. Tectonic control on formation and cyclicity of major Appalachian unconformities and associated stratigraphic sequences, p. 217–242. In J.M. Dennison and F.R. Ettensohn (eds.), *Tectonic and Eustatic Controls on Sedimentary Cycles*. SEPM Concepts in Sedimentology and Paleontology, 4.
- , AND C.E. BRETT. 1996a. Did Taconian convergence continue into Silurian time?—stratigraphic evidence from northwestern parts of the Appalachian Foreland Basin. *Geological Society of America, Abstracts with Programs*, 28:52.
- , AND ———. 1996b. Stratigraphic manifestations of Silurian tectonism from the Appalachian Foreland Basin and adjacent craton, p. 50. In *The James Hall Symposium: Second International Symposium on the Silurian System, Program and Abstracts*. University of Rochester.
- FAILL, R.T. 1997. The geologic history of the north-central Appalachians, Part 1. Orogenesis from the Mesoproterozoic through the Taconic orogeny. *American Journal of Science*, 297:551–619.
- FAIRBAIRN, H.W. 1971. Radiometric age of mid-Paleozoic intrusives in the Appalachian–Caledonide mobile belt. *American Journal of Science*, 220:203–217.
- FOLK, R.L. 1962. Petrography and origin of the Silurian Rochester and McKenzie Shales, Morgan County, West Virginia. *Journal of Sedimentary Petrology*, 32:539–578.
- GEE, D.G. 1975. A tectonic model for the central part of the Scandinavian Caledonides. *American Journal of Science*, 275a:532–568.
- , AND D. ROBERTS. 1983. Timing and deformation in the Scandinavian Caledonides, p. 279–292. In P.E. Schenk (ed.), *Regional Trends in the Geology of the Appalachian–Caledonian–Hercynian–Mauritanide Orogen*. NATO ASI Series C: Mathematical and Physical Sciences Volume 116. D. Reidel Publishing Company, Dordrecht.
- GOODMAN, W.M., AND C.E. BRETT. 1994. Roles of eustasy and tectonics in development of Silurian stratigraphic architecture of the Appalachian Foreland Basin, p. 147–169. In J.M. Dennison and F.R. Ettensohn (eds.), *Tectonic and Eustatic Controls on Sedimentary Cycles*. SEPM Concepts in Sedimentology and Paleontology, 4.
- GRAHN, Y., AND M.V. CAPUTO. 1992. Early Silurian glaciations in Brazil. *Palaeogeography, Palaeoclimatology, Palaeoecology*, 99:9–15.
- GURNIS, M. 1990. Ridge spreading, subduction, and sea level fluctuations. *Science*, 250:970–972.
- . 1991. Depressed continental hypsometry behind oceanic trenches: a clue to mantle convection controls on sea level change. *Eos*, 72:271.
- . 1992. Rapid continental subsidence following the initiation and evolution of subduction. *Science*, 255:1556–1558.
- . 1993. Phanerozoic marine inundation of continents driven by dynamic topography above subducting slabs. *Nature*, 364:589–593.
- , AND T.H. TORSVIK. 1994. The role of lateral variations in viscosity in controlling the drift rate of continents, or why did some large continents drift so fast during the late Precambrian and Paleozoic? *Eos*, 75:326.
- HAM, W.E., AND J.L. WILSON. 1967. Paleozoic epeirogeny and orogeny in the central United States. *American Journal of Science*, 265:332–407.
- HAMBREY, M.J. 1985. The Late Ordovician–Early Silurian glacial period. *Palaeogeography, Palaeoclimatology, Palaeoecology*, 51:273–289.
- HATCHER, R.D., JR. 1987. Tectonics of the southern and central Appalachian Internides. *Annual Review of Earth and Planetary Science*, 15:337–362.
- HAYS, J.D., AND W.C. PITMAN III. 1973. Lithospheric plate motion, sea-level changes, and climate and ecological consequences. *Nature*, 246:18–22.
- HURST, J.M., W.S. MCKERROW, N.J. SOPER, AND F. SURLYK. 1983. The relationship between Caledonian nappe tectonics and Silurian turbidite deposition in north Greenland. *Journal of the Geological Society of London*, 140:123–132.
- INSTITUTE OF GEOLOGY, CHINESE ACADEMY OF GEOLOGICAL SCIENCES, AND WUHAN COLLEGE OF GEOLOGY. 1985. *Atlas of the Paleogeography of China*. Cartographic Publishing House, Beijing.
- JAMIESON, R.A., AND C. BEAUMONT. 1988. Orogeny and metamorphism: a model for deformation and pressure–temperature–time paths with applications to the central and southern Appalachians. *Tectonics*, 7:417–445.
- JOHNSON, J.G. 1971. Timing and coordination of orogenic, epeirogenic, and eustatic events. *Geological Society of America Bulletin*, 82:3263–3298.
- JOHNSON, M.E. 1987. Extent and bathymetry of North American platform seas in the Early Silurian. *Paleoceanography*, 2:185–211.
- . 1996. Stable cratonic sequences and a standard for Silurian eustasy, p. 203–211. In B.J. Witzke, G.A. Ludvigson, and J.E. Day (eds.), *Paleozoic Sequence Stratigraphy: Views from the North American Craton*. Geological Society of America Special Paper 306.
- , B.G. BAARLI, H. NESTOR, M. RUBEL, AND D. WORSLEY. 1991a. Eustatic sea-level patterns from the Lower Silurian (Llandovery Series) of southern Norway and Estonia. *Geological Society of America Bulletin*, 103:315–335.
- , D. KALJO, AND J.-Y. RONG. 1991b. Silurian eustasy, p. 145–163. In M.G. Bassett, P.D. Lane, and D. Edwards (eds.), *The Murchison Symposium, Proceedings of an International Conference on the Silurian System*. Special Papers in Paleontology No. 44.
- , AND W.S. MCKERROW. 1991. Sea level and faunal changes during the latest Llandovery and earliest Ludlow (Silurian). *Historical Biology*, 5:153–169.
- , RONG J.-Y., AND YANG X.-C. 1985. Intercontinental correlation by sea-level events in the Early Silurian of North America and China (Yangtze Platform). *Geological Society of America Bulletin*, 96:1384–1397.
- JORDAN, T.E. 1981. Thrust loads and foreland basin evolution, Cretaceous, western United States. *American Association of Petroleum Geologists Bulletin*, 65:2506–2520.
- KALJO, D. 1978. On the bathymetric distribution of graptolites. *Acta Palaeontologica Polonica*, 23:523–531.
- , A.J. BOUCOT, R.M. CORFIELD, A. LE HERISSE, T.N. KOREN', J. KRÍŽ, P. MÄNNIK, T. MÄRSS, V. NESTOR, R.H. SHAVER, D.J. SIVETER, AND V. VIIRA. 1996. Silurian bio-events, p. 173–224. In O.H. Walliser (ed.), *Global Events and Event Stratigraphy in the Phanerozoic*. Springer-Verlag, Berlin.

- KARNER, G.D., AND A.B. WATTS. 1983. Gravity anomalies and flexure of the lithosphere at mountain ranges. *Journal of Geophysical Research*, 88 (B12):10449–10477.
- KEPPIE, J.D., J. DOSTAL, J.B. MURPHY, AND R.D. NANCE. 1996. Terrane transfer between eastern Laurentia and western Gondwana in the Early Paleozoic: constraints on global reconstruction, p. 369–380. *In* R.D. Nance and M.D. Thompson (eds.), *Avalonian and Related Peri-Gondwanan Terranes of the Circum-North Atlantic*. Geological Society of America Special Paper 304.
- KHAIN, V.E., AND K.B. SESLAVINSKY. 1996. *Historical Geotectonics, Palaeozoic*. Russian Translation Series 115. A.A. Balkema, Rotterdam, 414 p.
- KOMINZ, M.A., AND G.C. BOND. 1991. Unusually large subsidence and sea-level events during Middle Paleozoic time: new evidence supporting mantle convection models for supercontinent assembly. *Geology*, 19:56–60.
- LAIRD, J., 1988. Arenig to Wenlock age metamorphism in the Appalachians, p. 311–345. *In* A.L. Harris and D.J. Fettes (eds.), *The Caledonian–Appalachian Orogen*. Geological Society Special Publication No. 38.
- LEGGETT, J.K. 1980. British Lower Palaeozoic black shales and their palaeo-oceanographic significance. *Journal of the Geological Society of London*, 137:139–156.
- , W.S. MCKERROW, AND D.M. CASEY. 1982. The anatomy of a Lower Palaeozoic accretionary forearc: the southern uplands of Scotland, p. 495–520. *In* J.K. Leggett (ed.), *Trench–Forearc Geology: Sedimentation and Tectonics on Modern and Ancient Active Plate Margins*. Geological Society Special Publication No. 10.
- LIEBLING, R.S., AND H.S. SCHERP. 1982. Late Ordovician/Early Silurian hiatus at the Ordovician–Silurian boundary in eastern Pennsylvania. *Northeastern Geology*, 4:17–19.
- LIN, B.-Y., AND C.E. BRETT. 1988. Stratigraphy and disconformable contacts of the Williamson: revised correlation of the late Llandoveryan in New York State. *Northeastern Geology*, 10:241–253.
- LUKASIK, D.M. 1988. Lithostratigraphy of Silurian rocks in southern Ohio and adjacent Kentucky and West Virginia. Unpublished Ph.D. dissertation, University of Cincinnati, 401 p.
- MCKERROW, W.S. 1979. Ordovician and Silurian changes in sea level. *Journal of the Geological Society of London*, 136:137–145.
- , AND A.M. ZIEGLER. 1972. Paleozoic oceans. *Nature*, 240:92–94.
- MITROVICA, J.X., C. BEAUMONT, AND G.T. JARVIS. 1989. Tilting of continental interiors by the dynamical effects of subduction. *Tectonics*, 8:1079–1094.
- MORESI, L., AND M. GURNIS. 1996. Constraints on the lateral strength of slabs from three-dimensional dynamic flow models. *Earth and Planetary Science Letters*, 138:15–28.
- PATCHEN, D.G., K.L. AVARY, AND R.B. ERWIN. 1985. Southern Appalachian region. *In* F.A. Lindberg (ed.), *Correlation of Stratigraphic Units of North America (COSUNA) Project*. American Association of Petroleum Geologists COSUNA Chart SAP.
- PICKERING, K.T. 1987. Deep-marine foreland basin and forearc sedimentation: a comparative study from Lower Paleozoic northern Appalachians, Quebec and Newfoundland, p. 190–211. *In* J.K. Legett and G.G. Zuffa (eds.), *Marine Clastic Sedimentation: Concepts and Case Studies*. Graham and Trotman, London.
- PICKETT, J. 1982. The Silurian System in New South Wales. *Geological Survey of New South Wales, Bulletin* 29.
- PRICE, R.A. 1973. Large-scale gravitational flow of supracrustal rocks, southern Canadian Rockies, p. 491–502. *In* K.A. deJong and R. Scholten (eds.), *Gravity and Tectonics*. John Wiley, New York.
- QUINLAN, G.M., AND C. BEAUMONT. 1988. Appalachian thrusting, lithospheric flexure, and the Paleozoic stratigraphy of the eastern interior of North America. *Canadian Journal of Earth Sciences*, 21:973–996.
- RAST, N., AND J.W. SKEHAN. 1993. Mid-Paleozoic orogenesis in the North Atlantic: the Acadian orogeny, p. 1–25. *In* D.C. Roy and J.W. Skehan (eds.), *The Acadian Orogeny: Recent Studies in New England, Maritime Canada, and the Autochthonous Foreland*. Geological Society of America, Special Paper 275.
- RICKARD, L.V. 1975. Correlation of the Silurian and Devonian rocks in New York State. New York State Museum and Science Service, Map and Chart Series No. 24.
- ROBERTS, D. 1988. Timing of Silurian to Middle Devonian deformation in the Caledonides of Scandinavia, Svalbard, and E Greenland, p. 429–435. *In* A.L. Harris and D.J. Fettes (eds.), *The Caledonian–Appalachian Orogen*. Geological Society, Special Publication No. 38.
- RODGERS, J. 1970. *The Tectonics of the Appalachians*. Wiley-Interscience, New York.
- . 1971. The Taconic orogeny. *Geological Society of America Bulletin*, 82:1141–1178.
- . 1987. The Appalachian–Ouachita orogenic belt. *Episodes*, 10:259–266.
- RUPPEL, S.C., E.W. JAMES, J.E. BARRICK, G. NOWLAN, AND T.T. UYENO. 1996. High-resolution $^{87}\text{Sr}/^{86}\text{Sr}$ chemostratigraphy of the Silurian: implications for event correlation and strontium flux. *Geology*, 24:831–834.
- SCOTese, C.R., AND J. GOLONKA. 1992. PALEOMAP Paleogeographic Atlas. PALEOMAP Progress Report #20. Department of Geology, University of Texas at Arlington.
- , AND W.S. MCKERROW. 1990. Revised world maps and introduction, p. 1–21. *In* W.S. McKerrrow and C.R. Scotese (eds.), *Paleozoic Palaeogeography and Biogeography*. Geological Society, Memoir No. 12.
- ŞENGÖR, A.M.C., AND B.A. NATAL'IN. 1996. Paleotectonics of Asia: fragments of a synthesis, p. 486–640. *In* Y. An and T.M. Harrison (eds.), *The Tectonic Evolution of Asia*. Cambridge University Press.
- SHAVER, R.H. 1985. Midwestern basins and arches region. *In* F.A. Lindberg (ed.), *Correlation of Stratigraphic Units of North America (COSUNA) Project*. American Association of Petroleum Geologists, COSUNA Chart MBA.
- SHERIDAN, R.E. 1997. Pulsation tectonics as a control on the dispersal and assembly of supercontinents. *Journal of Geodynamics*, 23:173–196.
- SLOSS, L.L., AND SPEED, R.C. 1974. Relationships of cratonic and continental-margin tectonic episodes, p. 98–119. *In* W.R. Dickinson (ed.), *Tectonics and Sedimentation*. Society of Economic Paleontologists and Mineralogists, Special Publication No. 22.
- SMOSNA, R., AND D. PATCHEN. 1978. Silurian evolution of central Appalachian Basin. *American Association of Petroleum Geologists Bulletin*, 62:2308–2328.
- TANKARD, A.J. 1986. On the depositional response to thrusting and lithospheric flexure: examples from the Appalachian and Rocky Mountain Basins, p. 369–392. *In* P.A. Allen and P. Homewood (eds.), *Foreland Basins*. International Association of Sedimentologists, Special Publication No. 8.
- THIRLWALL, M.F. 1988. Wenlock to mid-Devonian Volcanism of the Caledonian–Appalachian orogen, p. 415–428. *In* A.L. Harris and D.J. Fettes (eds.), *The Caledonian–Appalachian Orogen*. Geological Society Special Publication No. 38.
- TORSVIK, T.H., M.A. SMETHURST, J.G. MEERT, R. VAN DER VOO, W.S. MCKERROW, M.D. BRASIER, B.A. STURT, AND H.J. WALDERHAUG. 1996. Continental break-up and collision in the Neoproterozoic and Palaeozoic—a tale of Baltica and Laurentia. *Earth Science Reviews*, 40:229–258.

- TRETTIN, H.P. 1987. Pearya: a composite terrane with Caledonian affinities in northern Ellesmere Island. *Canadian Journal of Earth Sciences*, 24:224-245.
- VAIL, P.R., R.M. MITCHUM, JR., AND S. THOMPSON III. 1977. Seismic stratigraphy and global changes in sea level, part 4: global cycles of relative changes in sea level, p. 83-97. *In* C.E. Peyton (ed.), *Seismic Stratigraphy—Applications to Hydrocarbon Exploration*. American Association of Petroleum Geologists, Memoir 26.
- VAN STAAL, C.R. 1994. Brunswick subduction complex in the Canadian Appalachians: record of Late Ordovician to Late Silurian collision between Laurentia and the Gander margin of Avalon. *Tectonics*, 13:946-962.
- , AND J.A. DE ROO. 1995. Mid-Paleozoic tectonic evolution of the Appalachian central mobile belt in northern New Brunswick, Canada: collision, extensional collapse and dextral transpression, p. 367-389. *In* J.P. Hibbard, C.R. van Staal, and P.A. Cawood (eds.), *Current Perspectives in the Appalachian-Caledonian Orogen*. Geological Association of Canada, Special Paper 41.
- , R.W. SULLIVAN, AND J.B. WHALEN. 1996. Provenance and tectonic history of the Gander Zone in the Caledonian/Appalachian orogen: implications for the origin and assembly of Avalon, p. 347-367. *In* R.D. Nance and M.D. Thompson (eds.), *Avalonian and Related Peri-Gondwanan Terranes of the Circum-North Atlantic*. Geological Society of America, Special Paper 304.
- WALCOTT, R.I. 1970. Isostatic response to loading of the crust in Canada. *Canadian Journal of Earth Sciences*, 7:2-13.
- WONES, D.R. AND A.K. SINHA. 1988. A brief review of Early Ordovician to Devonian plutonism in the North American Caledonides, p. 3381-3388. *In* A.L. Harris and D.J. Fettes (eds.), *The Caledonian-Appalachian Orogen*. Geological Society Special Publication No. 38.
- ZIEGLER, A.M. 1965. Silurian marine communities and their environmental influence. *Nature*, 207:270-272.
- , L.R.M. COCKS, AND R.K. BAMBACH. 1968. The composition and structure of Lower Silurian marine communities. *Lethaia*, 1:1-27.
- ZIEGLER, P.A. 1987. Late Cretaceous and Cenozoic intra-plate compressional deformations in the Alpine foreland—a geodynamic model. *Tectonophysics*, 137:389-420.
- . 1989. *Evolution of Laurussia*. Kluwer Academic Publishers, Dordrecht.

PART II: TEMPORAL FAUNAL PATTERNS RELATED TO EUSTASY

GLOBAL DIVERSITY AND SURVIVORSHIP PATTERNS OF SILURIAN GRAPTOLIDS

MICHAEL J. MELCHIN¹, TATJANA N. KOREN², AND PETR ŠTORCH³

¹Department of Geology, St. Francis Xavier University, P.O. Box 5000, Antigonish, Nova Scotia B2G 2W5,

²All-Russian Geological Research Institute (VSEGEI), Sredny pr.74, 199026, St. Petersburg, Russia, and

³Geological Institute of the Czech Academy of Sciences, Rozvojová 135, 165 00, Prague 6, Czech Republic

ABSTRACT—This study presents a high-resolution analysis of Silurian graptoloid diversity and survivorship with data from all paleolatitudes. This permits a view of worldwide faunal dynamic patterns and the relationship of these patterns with sea-level change.

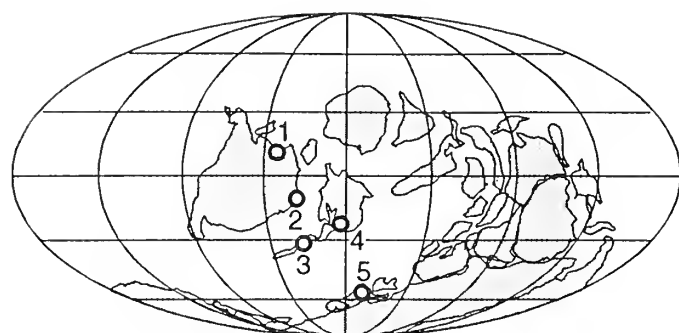
The overall diversity trend shows a stepwise increase from the Late Ordovician extinction to a peak in the early Aeronian, and an overall diversity decline from the early Telychian through the remainder of the Silurian. The most significant graptoloid extinctions are the *Monograptus transgrediens* Event (79% of taxa extinct), *Neocuculograptus kozlowskii* Event (70% extinct), late *Cyrtograptus lundgreni* Event (69% extinct), late *Parakidograptus acuminatus* Event (65% extinct), *Cyrtograptus murchisoni* Event (64% extinct), *Monograptus* (*Uncinograptus*) *spineus* (late *M. (Formosograptus) formosus*) Event (64% extinct), *Cyrtograptus lapworthi* Event (62% extinct), and early *Stimulograptus sedgwickii* Event (59% extinct). Events of regional or lesser significance include the *Stimulograptus utilis* (*Spirograptus turriculatus*) Event (52% extinct), and the late *Saetograptus leintwardinensis* Event (52% extinct). Of these, only the late *P. acuminatus* Event has not been previously described.

There is a coincidence between most of these events and reported eustatic fall. The precise way in which sea-level fall may be related to changes in oceanic temperature, circulation, and rates of upwelling and productivity, and the effect of these changes on Silurian planktic food webs, remains controversial. If the sub-photoc, dysaerobic zone that today characterizes upwelling zones was the preferred graptolite habitat, then the dramatic reduction in that habitat with regression, whatever its cause, could have resulted in widespread graptolite extinction.

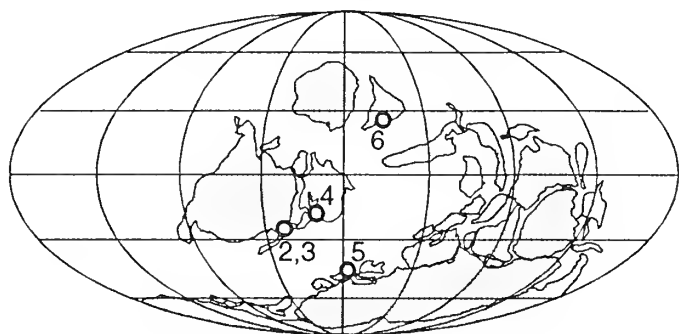
INTRODUCTION

Biodiversity and extinction patterns in the Silurian graptoloids have been the subject of analysis for several decades (e.g., Bouček, 1953; Bulman, 1964; Rickards, 1978). Koren' (1987) was the first to consider diversity dynamics and bioevents and their relation to important global physical events. Since that time, the two major Silurian graptolite bioevents that have received the most attention have been the radiation following the Late Ordovician extinction event (e.g., Koren', 1991a; Melchin and Mitchell, 1991; Štorch, 1996; Koren' and Bjerreskov, In press; Lukasik and Melchin, In press) and the Homeric extinction and subsequent radiation (e.g., Jaeger, 1991; Koren', 1991b; Lenz, 1993a; Urbanek, 1993; Legrand, 1994; Štorch, 1995a; Gutierrez-Marco et al., 1996). However, a number of other graptolite bioevents have been the focus of study (Koren', 1993; Urbanek, 1993, 1995; Loydell, 1994; Melchin, 1994; Štorch, 1995a). Overall patterns of Silurian graptolite diversity have been summarized by Kaljo et al. (1995). A prevailing theme among these studies is the apparent relationship between graptoloid diversity and extinction patterns and eustatic change. Most authors have not regarded the connection between graptoloid dynamics and sea-level change to be direct. Rather, sea-level change is often regarded as coinciding with such oceanographic events as changes in circulation, temperature, oxygenation, and/or productivity that are more likely to affect planktic communities directly.

Of the earlier studies, most have focused on a particular time interval, examined trends through the Silurian in a particular region, or plotted diversity data compiled from one or a few regions. The purpose of this report is, for the first time, to compile the most up-to-date diversity and survivorship data for the whole Silurian, at the highest resolution possible and from different paleo-



Early Silurian (Llandovery)



Late Silurian (Ludlow)

FIGURE 1—Paleogeographic maps for Early (Llandovery) and Late Silurian (Ludlow) (after Cocks and Scotese, 1991), with location of the main study regions. Locations: 1, Arctic Canada; 2, northwest Britain, with northwest Ireland and Scotland; 3, southeast Britain, with Wales, southeast Ireland, and much of England; 4, Poland and Bornholm; 5, Bohemia; 6, central Asia and Kazakhstan.

continents and paleolatitudes. The objective is to get a glimpse of the global patterns of graptoloid diversity and extinction in the Silurian with regional differences filtered out.

One of the major difficulties of undertaking such a study is the problem of inter-regional correlation and the inadequacies of the data sets from many parts of the world. Several areas have very refined graptoloid zonal subdivisions, but these zonations cannot always be recognized in other parts of the world. For this reason, the less detailed but more globally applicable zonation of Koren' et al. (1996) was used for this report. The regions and data sets chosen for this report had to be limited to those with graptoloid range data at a resolution of at least one-half of a zone, and those that presented the range data in a relatively consistent manner for a considerable portion of Silurian time. Such data sets were found to be available from the Prague Basin area of Perunica (Bohemia, Czech Republic [Příbyl, 1983; H. Jaeger in Kříž et al., 1986; Štorch, 1993, 1994a, 1994b, 1995a, 1995b, 1996, unpublished data]); the Avalon and Iapetus margins of the British Isles (Rickards, 1976), especially Wales (Loydell, 1991, 1992, 1993; Loydell and Cave, 1993, 1996; Zalasiewicz, 1994; Zalasiewicz and Tunnichliff, 1994); the

Baltic regions of Bornholm (Bjerreskov, 1975; Koren' and Bjerreskov, In press) and Poland (Teller, 1964, 1969; Urbanek, 1966, 1970, In press); the Llandovery–Wenlock of Laurentian Arctic Canada (Melchin, 1989, unpublished data; Melchin et al., 1991; Lenz and Melchin, 1991; Lenz, 1995); and the Rhuddanian and late Wenlock–Pridoli of central Asia (Kazakhstan margin [Koren', 1989, 1992, 1994; Koren' and Lytochkin, 1992; Koren' and Sujarkova, In press; Pickering et al., in press; TNK and MJM, unpublished data]). Each part of the Silurian is thus represented by relatively high, middle, and low paleolatitude localities (Figure 1). In the following sections, observations made concerning any of these regions can be assumed to be derived from the references listed above, unless otherwise specified. Note that the zonation and range data compiled by Rickards (1976) represent a composite of information compiled from throughout the British Isles, but is the only comprehensive source of graptolite ranges for much of the Silurian of this region; the zonation has been widely used as a Silurian standard. More recently published data from the Llandovery and lower Wenlock of Wales (Loydell, 1991, 1992, 1993; Loydell and Cave, 1993, 1996; Zalasiewicz, 1994; Zalasiewicz and Tunnichliff, 1994) are treated separately because they provide a more detailed zonation and range data set, but of a more limited stratigraphic interval.

FIGURE 2—(opposite) Early Silurian correlations between main study regions. Generalized zonation of Koren' et al. (1996). British Isles zonation with composite zonation of Great Britain and Ireland (Rickards, 1976); Wales zonation from Zalasiewicz (1990, 1994), Loydell (1991, 1992, 1993), Loydell and Cave (1993, 1996), Zalasiewicz and Tunnichliff (1994); Bohemia zonation from Štorch (1994a, 1994b, 1995a, 1996); Poland and Bornholm zonation from Teller (1969), Bjerreskov (1975), Koren' and Bjerreskov (In press); Arctic Canada zonation from Melchin (1989), Melchin et al. (1991), Lenz and Melchin (1991), and Lenz (1995). Asterisks show Welsh zones that are divided into subzones: 1) *Spirograptus guerichii* Zone consists in ascending order of *Paradiversograptus runcinatus*, "*Monograptus*" *gemmatus*, *Pristiograptus renaudi*, and lower *Stimulograptus utilis* Subzones; 2) *Spirograptus turriculatus* Zone includes upper *Stimulograptus utilis*, *Streptograptus johnsonae*, *Torquigraptus proteus*, and *Torquigraptus carnicus* Subzones; 3) *Monograptus crispus* Zone includes *Monoclimacis? galaensis*, *Monograptus crispus*, and *Streptograptus sartorius* Subzones. Abbreviations in Figures 2–4: Ak.=*Akidograptus*, At.=*Atavograptus*, B.=*Bohemograptus*, Cam.=*Campograptus*, Ce.=*Cephalograptus*, Co.=*Coronograptus*, Col.=*Colonograptus*, Cu.=*Cucullograptus*, Cy.=*Cyrtograptus*, Cys.=*Cystograptus*, Dm.=*Demirastrites*, F.=*Formosograptus*, G.=*Gothograptus*, H.=*Hirsutograptus*, L.=*Lobograptus*, Lg.=*Lagarograptus*, M.=*Monograptus*, Mcl.=*Monoclimacis*, N.=*Normalograptus*, Nc.=*Neocucullograptus*, Ndp.=*Neodiplograptus*, Ndv.=*Neodiversograptus*, Nl.=*Neolobograptus*, O.=*Oktavites*, P.=*Pristiograptus*, Pb.=*Pribylograptus*, Pk.=*Parakidograptus*, Pm.=*Paramonoclimacis*, Pol.=*Polonograptus*, Pp.=*Parapetalolithus*, Psm.=*Pseudomonoclimacis*, Ra.=*Rastrites*, S.=*Saetograptus*, Sp.=*Spirograptus*, St.=*Stimulograptus*, Sto.=*Stomatograptus*, Te.=*Testograptus*, To.=*Torquigraptus*, U.=*Uncinograptus*.

SERIES and Stages		Generalized zonation	British Isles		Bohemia	Poland & Bornholm	Arctic Canada
WENLOCK	Homerian	"M". ludensis	"M". ludensis		"M". ludensis		"M". ludensis
		"M". deubeli ^U	G. nassa		"M". deubeli	"P. vulgaris"	"M". deubeli
		"M". praedeubeli-L			"M". praedeubeli-		"M". praedeubeli-
		P. parvus-G. nassa			P. parvus-G. nassa	G. nassa	P. dubius-G. nassa
	Sheinwoodian	Cy. lundgreni ^U	Cy. lundgreni		Cy. lundgreni	Cy. lundgreni	Te. testis
		Cy. lundgreni-L				Cy. radians	Cy. lundgreni-
		Cy. perneri ^U	Cy. ellesae		Cy. ramosus	Cy. ellesae-	M. opimus
		Cy. rigidus-L	M. flexilis		Cy. perneri-		Cy. perneri-
			Cy. rigidus		Cy. rigidus	Cy. rigidus	
		M. belophorus ^U	M. riccartonensis	M. riccartonensis	M. belophorus	M. riccartonensis	Cy. kolobus
		M. riccartonensis-L		M. firmus	P. dubius		M. instrenuus-
					M. riccartonensis		
		Cy. murchisoni ^U	Cy. murchisoni	Cy. murchisoni	Cy. murchisoni	Cy. murchisoni	Cy. centrifugus
		Cy. centrifugus-L	Cy. centrifugus	Cy. centrifugus	Cy. centrifugus	Cy. centrifugus	
LLANDOVERY	Telychian	Cy. insectus ^U		Cy. insectus	Cy. insectus	Cy. lapworthi	Cy. insectus
		Cy. lapworthi-L		Cy. lapworthi	Sto. grandis		Cy. sakmaricus
		O. spiralis		O. spiralis	O. spiralis	O. spiralis	
		Mcl. crenulata ^U	Mcl. crenulata	Mcl. crenulata	To. tullbergi	Mcl. griestoniensis	Mcl. ^U
		Mcl. griestoniensis-L	Mcl. griestoniensis	Mcl. griestoniensis	Mcl. griestoniensis		griestoniensis ^M
		M. crispus ^U	M. crispus	M. crispus*	M. crispus	M. crispus	M. crispus
	Aeronian	Sp. turriculatus-L	Sp. turriculatus	Sp. turriculatus*	Sp. turriculatus	Sp. turriculatus	Sp. turriculatus
		Sp. guerichi ^U	Ra. maximus	Sp. guerichi*	Pp. hispanicus		Sp. guerichi ^U
		Sp. guerichi-L			Ra. linnaei		
					Pp. palmeus		
		St. sedgwickii ^U	St. sedgwickii	St. halli	St. sedgwickii	?	?
		St. sedgwickii-L		St. sedgwickii			
	Rhuddanian	Dm. convolutus ^U	Dm. convolutus	Dm. convolutus	Dm. convolutus	Ce. cometa	
		Dm. convolutus-L				Dm. convolutus	Dm. convolutus
		M. argenteus	Pb. leptotheca	Pb. leptotheca	Dm. simulans	?	Ra. orbitus
		Dm. pectinatus ^U	Ndp. magnus	Ndp. magnus	Dm. pectinatus	Dm. pectinatus	Dem. ^U
		Dm. triangulatus-L	Dm. triangulatus	Dm. triangulatus	Dm. triangulatus-	Co. Dm. triangulatus	Cam. pectinatus-L
		Co. cyphus ^U	Co. cyphus	Co. cyphus	Co. cyphus	M. revolutus	Co. cyphus
		Co. cyphus-L	"Lg." acinaces	"Lg." acinaces			
		Cys. vesiculosus ^U	At. atavus	At. atavus	Cys. vesiculosus	Cys. vesiculosus	"Lg." acinaces
		Cys. vesiculosus-L					At. atavus
		Pk. acuminatus ^U	Pk. acuminatus	Pk. acuminatus	Pk. acuminatus	Pk. acuminatus	H. sinizini
		Pk. acuminatus-L			Ak. ascensus-	Ak. ascensus-	N. mademii-
							N. lubricus

CORRELATION

The first step in compiling the composite range data for Silurian graptoloids was to establish a correlation between the zonations of each of the regions and the generalized, global zonation of Koren' et al. (1996) (Figures 2

and 3). The general principle employed in most cases was that the base of each zone was recognized in each region by the first appearance of the eponymous taxon. In those cases where the eponymous taxon was missing in a particular region, a temporally associated assemblage of taxa was used. Among the four regions (Britain, Bohemia,

SERIES/Stages		Generalized biozonation	British Isles	Poland	Bohemia	Central Asia & Kazakhstan
PRIDOLI		<i>M. trangrediens</i> U		<i>M. trangrediens</i> <i>M. perneri</i>	<i>M. trangrediens</i>	<i>M. microdon aksajensis</i> <i>M. perneri kasachstanensis</i>
		<i>M. bouceki</i> - L		<i>M. bouceki</i>	<i>M. bouceki</i>	<i>Psm. bandaletovi</i> <i>M. bouceki</i> -
		<i>M. lochkovens</i> U		<i>M. lochkovens</i>	<i>M. lochkovens</i>	<i>M. beatus</i> <i>M. lochkovens</i>
		<i>M. branikensis</i> - L			<i>M. pridoliensis</i>	<i>M. branikensis</i>
		<i>Pm. ultimus</i> U		<i>Pm. ultimus</i>	<i>Pm. ultimus</i>	<i>Pm. ultimus</i>
		<i>Pm. parultimus</i> - L		<i>Pm. parultimus</i>	<i>Pm. parultimus</i> -	<i>Pm. parultimus</i>
LUDLOW	Ludfordian	<i>M. (F.) formosus</i> U	<i>Bohemograptus</i>	<i>M. (U.) spineus</i> <i>M. (U.) acer</i> <i>M. balticus</i> <i>M. hamulosus</i> <i>M. latilobus</i>	<i>P. fragmentalis</i>	<i>P. fragmentalis</i> <i>M. (U.) spineus</i> ---
		<i>M. (F.) formosus</i> - L				<i>M. (F.) formosus</i> - <i>M. latilobus</i>
		<i>Nc. kozlowskii</i> U		<i>Nc. kozlowskii</i> <i>Nc. inexpectatus</i> <i>Nl. auriculatus</i> <i>B. cornutus</i> <i>B. bohemicus</i>	<i>Nc. kozlowskii</i>	<i>Pol. podoliensis</i>
	<i>B. bohemicus tenuis</i> - L	<i>Nc. inexpectatus</i> <i>B. bohemicus</i>	<i>B. cornutus</i> -			
	<i>S.</i> U	<i>S.</i>	<i>S.</i>	<i>S. linearis</i>	<i>S.</i>	
	<i>leintwardinensis</i> L					<i>leintwardinensis</i>
	Gorstian	<i>L. scanicus</i> U	<i>S. incipiens</i> <i>P. tumiscens</i> -	<i>Cu. hemiaversus</i> <i>L. invertus</i> <i>L. parascanicus</i>	<i>L. scanicus</i>	<i>L. scanicus</i> <i>S. chimaera</i> -
		<i>L. scanicus</i> L	<i>L. scanicus</i>			
<i>Ndv. nilssoni</i> U		<i>Ndv. nilssoni</i>	<i>L. progenitor</i>	<i>L. progenitor</i>		
<i>Ndv. nilssoni</i> L	<i>Ndv. nilssoni</i>		<i>Ndv. nilssoni</i>	<i>Col. colonus</i> <i>Ndv. nilssoni</i> -		

FIGURE 3—Late Silurian zonation of the main study regions: Generalized zonation of Koren' et al. (1996), British zonation of Rickards (1976), Bohemian zones of Štorch (1995a, 1995b), Polish zones of Teller (1964, 1969) and Urbanek (1966, 1970, In press), central Asia and Kazakhstan zonates of Koren' (1989, 1992, 1994), Koren' and Lytochkin (1992), Koren' and Sujarkova (In press), and Pickering et al. (In press). Abbreviations as Figure 2.

Bornholm and Poland, and Arctic Canada for the Llandovery–Wenlock; Britain, Poland, Bohemia, and central Asia and Kazakhstan for the Ludlow–Pridoli), most of the zones could be correlated at the precision of a lower and upper subzone.

The basal Silurian *Parakidograptus acuminatus* Zone, which is effectively a composite of the *Akidograptus ascensus* and *P. acuminatus* Zones, is marked by the lowest local appearance of *A. ascensus* in all of the studied regions except Arctic Canada and central Asia. In these areas, the base of the Silurian is identified by the appearance of *Normalograptus madernii* and/or *N. lubricus*, which are only known to occur elsewhere in association with *A. ascensus* (Melchin et al., 1991; MJM and TNK, unpublished data, 1996). The upper half of the *P. acuminatus* Zone is recognized by either the lowest occurrence or the acme of *P. acuminatus*.

The base of the *Cystograptus vesiculosus* Zone is a matter of some difficulty. In Bornholm and Bohemia, the ranges of *C. vesiculosus* and species of *Atavograptus* and *Huttagraptus* do not overlap that of *Parakidograptus acuminatus*. In Arctic Canada, *C. vesiculosus* has not been

reported, and the base of the *C. vesiculosus* Zone is indicated by the appearance of *Atavograptus atavus*. However, in Britain, particularly at Dob's Linn (Toghill, 1968), the ranges of *P. acuminatus* and *C. vesiculosus* are reported to overlap considerably. It is not clear whether this is the result of the later occurrence of *P. acuminatus* or the earlier appearance of *C. vesiculosus* in that region relative to others. However, examination of recently collected specimens of *Cystograptus* from the *P. acuminatus* Zone of Dob's Linn (MJM and PŠ, unpublished data, 1996) suggests that most of those forms are actually *Cystograptus ancestralis* rather than *C. vesiculosus*. With the high degree of deformation typical of the Dob's Linn specimens, the two taxa may be easily mistaken, and Toghill's (1968) work at Dob's Linn was done before *C. ancestralis* was described as a distinct species. Hutt (1974–1975) also illustrated a specimen of *C. vesiculosus* from the *P. acuminatus* Zone of the English Lake District that shows the relatively narrow width, closer thecal spacing, shorted sicula, long th_1 , and slender virgula characteristic of *C. ancestralis* (Štorch, 1985). Only the highest levels of co-occurrence of *P. acuminatus* and *Cystograptus* at

Dob's Linn contain *C. vesiculosus*, with an otherwise generalized early Rhuddanian fauna. This same pattern was noted by Štorch (1996) in peri-Gondwanan Europe. Therefore, for this study, the base of the *C. vesiculosus* Zone is considered to be marked by the lowest appearance of *C. vesiculosus*, and *P. acuminatus* is regarded as persisting into the lowest part of that zone. Most other taxa usually regarded as being restricted to the *P. acuminatus* Zone have not been observed to extend into this interval of overlap between *P. acuminatus* and *C. vesiculosus*. The upper half of the *C. vesiculosus* Zone is indicated by the first appearance of "*Lagarograptus*" *acinaces*.

The base of the *Coronograptus cyphus* Zone is defined by the lowest appearance of the eponymous species. This zone encompasses the "*Lagarograptus*" *acinaces* and *Coronograptus cyphus* Zones of Rickards (1976) and the *Monograptus revolutus* Zone in Bornholm (Bjerreskov, 1975). In the different study regions, the upper half of the *C. cyphus* Zone is marked by the appearance of somewhat different taxa, but in all cases, it shows a marked increase in diversity.

The base of the Aeronian *Demirastrites triangulatus*-*D. pectinatus* Zone is marked by another sharp increase in diversity and the lowest appearance of triangulate monograptids and species of *Petalolithus*. The upper half of this zone is marked by the appearance of *Neodiplograptus magnus*, *N. thuringiacus*, and *Pseudorthograptus insectiformis*. The base of the *Monograptus argenteus* Zone in Britain [= *Pribylograptus leptotheca* Zone of Rickards (1976)] can be identified by the lowest appearance of the eponymous species, as well as by *Monograptus limatulus* and *M. lobiferus*, which commonly have their lowest occurrence together with *M. argenteus*. Based on the lowest occurrences of *M. limatulus* and *M. lobiferus*, it appears that the base of the *M. argenteus* Zone occurs within the *Demirastrites simulans* Zone of Štorch (Štorch, 1994a).

New biostratigraphic data from Arctic Canada permit a finer subdivision of the lower Aeronian than was possible at the time of publication of Melchin's (1989) report. The *Campograptus curtus* Zone can now be subdivided into three subzones that can be correlated directly with the lower and upper *Demirastrites triangulatus*-*D. pectinatus* and *Monograptus argenteus* Zones, respectively, based on lowest appearances of some of the taxa listed above. Based on the data available from the four regions, it was not possible to subdivide the *M. argenteus* Zone reliably into lower and upper subzones.

In all study regions, the base of the *Demirastrites convolutus* Zone can be defined by the lowest occurrence of *D. convolutus*, as well as by assemblages of other taxa. An upper subzone can be clearly distinguished in each of the regions except the British Isles, but the base of this

subzone is marked by the lowest occurrences of different taxa in each of the other areas.

In most regions, the lowest occurrence of *Stimulograptus sedgwickii* does not overlap the range of *Demirastrites convolutus* and many of its associates. In the English Lake District (Hutt, 1974–1975), however, *D. convolutus* and *S. sedgwickii* co-occur at two localities. These occurrences must, by the definition used herein, be assigned to the lower *S. sedgwickii* Zone, and the ranges of the typical *D. convolutus* Zone forms found at those localities must be extended accordingly upward. *Demirastrites convolutus* and *S. sedgwickii* have also been observed to co-occur in the Polar Urals (TNK, unpublished data, 1996). This has had the result of shifting the peak of the upper *D. convolutus* Zone extinction event (Štorch, 1995a) into the overlying *S. sedgwickii* Zone. This discrepancy may well be due to diachroneity in the timing of the lowest appearance of *S. sedgwickii*, rather than in the timing of the extinctions.

In Wales and southern Scotland, the interval between the top of the *Demirastrites convolutus* Zone and the base of the Telychian *Spirograptus guerichi* Zone can be divided into the *Stimulograptus sedgwickii* and *Stimulograptus halli* Zones, and these are regarded as comprising the lower and upper subzones of the *S. sedgwickii* Zone, respectively, of the generalized zonation (Figure 2). The *S. sedgwickii* Zone cannot be recognized in Arctic Canada or Bornholm, although the *Cephalograptus cometa* Band of the latter region may be at least partly correlative with the lower *S. sedgwickii* Zone. In Bohemia, only the lower *S. sedgwickii* Zone is clearly distinguishable, whereas the upper part of this zone is incomplete and is separated from the lower *S. guerichi* Zone by non-graptolitic beds deposited under well-oxygenated conditions.

The base of the *Spirograptus guerichi* Zone is marked by the lowest appearance of the eponymous species, which is synonymous with *Monograptus turriculatus minor* (*sensu* Melchin [1989] and many earlier authors). The lowest specimens of *S. turriculatus* reported in Bornholm may be assignable to *S. guerichi* as well, although the *S. turriculatus* Zone in Bornholm is of low diversity and cannot be readily subdivided. The upper *S. guerichi* Zone can be only be identified by the appearance of regionally significant taxa in each of the four study areas.

The lower part of the *Spirograptus turriculatus*-*Monograptus crispus* Zone is defined by the first occurrence of *S. turriculatus*, and the upper half by the appearance of *M. crispus*. Similarly, the lower and upper parts of the *Monoclimacis griestoniensis*-*M. crenulata* Zone are marked by the appearances of *M. griestoniensis* and *M. crenulata*, respectively.

The *Oktavites spiralis* Zone is defined by the appearance of *O. spiralis* in Wales and Bornholm and the acme of

that species in Bohemia. This biostratigraphic interval and the overlying zone were not recognized in the rest of the British Isles by Rickards (1976), although the range of *O. spiralis* was reported to extend into several underlying zones, as is the case in Arctic Canada. The co-occurrence of *O. spiralis* with an assemblage that is otherwise typical of the *Spirograptus turriculatus*-*Monograptus crispus* and *Monoclimacis griestoniensis*-*M. crenulata* Zones (Rickards, 1976; Lenz, 1982; Melchin, 1989) suggests that the range of *O. spiralis* is more restricted in Wales, Bornholm, and Bohemia than in other parts of the British Isles and northern Canada. The lower, middle, and upper subzones of the *Monoclimacis griestoniensis* Zone of Arctic Canada coincide approximately with the lower and upper *M. griestoniensis*-*M. crenulata* and *O. spiralis* Zones, respectively, based on the ranges of taxa in the Arctic sections that also occur elsewhere.

The base of the *Cyrtograptus lapworthi*-*C. insectus* Zone is marked by the appearance of species of *Cyrtograptus*, especially *C. lapworthi* subsp., although in some Canadian Arctic sections, *C. polyrameus* or *C. solaris* appear slightly below the eponymous species. A distinct *Cyrtograptus insectus* Zone has hitherto only been documented in Bohemia and Wales, not in Baltica or Arctic Canada, although its recent recognition in Spain (PŠ, unpublished data, 1996) suggests that it may be distinguishable throughout much of peri-Gondwanan Europe. In addition, recent, detailed recollecting of the type section of the Cape Phillips Formation in Arctic Canada by MJM and TNK (unpublished data, 1996) has revealed a stratigraphic interval with *C. insectus* below the lowest appearance of *C. centrifugus*, the eponymous species of the overlying zone and index to the base of the Wenlock Series. Besides *C. insectus*, this interval contains a depauperate fauna otherwise typical of the lower *C. centrifugus*-*C. insectus* Zone as described by Lenz and Melchin (1991). This fauna can tentatively be used to distinguish a *C. insectus* Zone in Arctic Canada. In addition, several new occurrences of species of *Cyrtograptus* were found in the uppermost *C. sakmaricus* Zone (= upper part of lower *C. lapworthi*-*C. insectus* Zone). These include *C. laqueus*, *C. malgusaricus*, *C. n. sp. aff. C. bohemicus* (= *C. sp. aff. C. murchisoni bohemicus?* of Lenz, 1978) and *C. falcatus*. The last of these is now known to span the interval from the uppermost *C. sakmaricus* through *C. centrifugus* Zones.

In the British Isles and Bohemia, distinct *Cyrtograptus centrifugus*, *C. murchisoni*, *Monograptus riccartonensis*, *M. belophorus*, *C. rigidus*, *C. perneri*, and *C. lundgreni* zones can be recognized based on the eponymous taxa, although the regional zonations through this interval (Figure 2) are often based on other locally common species. In Poland, all of these but the *M. belophorus* inter-

val can be distinguished. In Arctic Canada, *Cyrtograptus murchisoni*, although previously unreported, has recently been found (A.C. Lenz, personal commun., 1997). The *Monograptus instrenuus*-*C. kolobus* Zone appears to encompass the *M. riccartonensis*-*M. belophorus* and *C. rigidus* intervals of the generalized zonation. An upper *C. lundgreni* Zone can be recognized in each of the regions, but the nature of the faunal changes that distinguish this level are somewhat different in each region.

The upper Homerian faunas of Britain and Poland are relatively depauperate and difficult to subdivide. The Arctic Canadian and Bohemian successions can, however, be subdivided based on the occurrences of "*Monograptus*" *praedeubeli*, "*M. deubeli*", and "*M. ludensis*". The most detailed biostratigraphic subdivision of this interval has been achieved in south Kirghizstan (Koren', 1992, 1994).

The basal Ludlow *Neodiversograptus nilssoni* Zone is readily recognized by the first appearance of the eponymous species, as well as *Colonograptus colonus* and *Bohemograptus bohemicus*. The upper half of this zone is marked, in most areas, by the appearance of *Lobograptus progenitor*, although in Arctic Canada this species occurs immediately above uppermost Homerian faunas (A.C. Lenz, personal commun., 1997). The base of the *Lobograptus scanicus* Zone can be distinguished by the lowest occurrence of *Lobograptus scanicus*, but the upper half of this zone is marked by different species in different regions. The lowest appearances of *Saetograptus leintwardinensis* and *S. linearis* mark the base of the *S. leintwardinensis* Zone. The upper half of that zone can be recognized by the lowest occurrences of *Neolobograptus auriculatus* in central Asia and Poland and *Pristiograptus longus* in Bohemia. Neither this interval, nor any of the higher Silurian graptolite zones used here, can be confidently recognized in Britain (Rickards, 1976; Figure 3).

The base of the *Bohemograptus bohemicus tenuis*-*Neocucullograptus kozlowskii* Zone is commonly marked by an acme of *B. bohemicus tenuis*, although in central Asia it is more reliably identified by the lowest appearance of *Bohemograptus cornutus* and *Polonograptus podoliensis*. The upper half of this zone is distinguished by the appearance of *N. kozlowskii* and *Monograptus abhorrens*. The lower and upper halves of the interval encompassed by the *M. (Formosograptus) formosus* Zone are quite variable between the study regions in terms of the order of appearance of the key taxa (i.e., *M. (F.) formosus*, *M. latilobus*, *M. (Uncinograptus) spineus*, *M. (U.) acer*, and *Pristiograptus fragmentalis*), and this makes precise inter-regional correlation particularly difficult in this interval.

The lower and upper halves of the *Pseudomonoclimacis parultimus*-*P. ultimus* and *Monograptus branikensis*-

M. lochkovens Zones can be recognized by the lowest occurrences of each of the four eponymous taxa, respectively, although the range of overlap of *M. branikensis* and *M. lochkovens* seems to be greater in Bohemia than in Poland. The base of the *Monograptus bouceki*-*M. transgrediens* Zone is marked by the lowest appearance of *M. bouceki*, and the upper half of the zone is commonly recognized by the acme of *M. transgrediens*, although the appearance of *M. perneri* subsp. is used to define it herein.

DIVERSITY TRENDS

In order to maintain consistency in calculation of taxonomic numbers in each zonal interval, the following guidelines were employed: 1) Each species and named subspecies was recognized as a separate taxon; 2) No attempts were made to synonymize different taxa between regions, except in well-known cases (e.g., *Monograptus discus*=*M. veles*); 3) Taxa reported in the original sources in open nomenclature (i.e., identified with cf., aff., ?, or sp.) were not included in the counts or ranges, except in those cases where the taxa were specifically identified as new (undescribed) species or subspecies; 4) Owing to the difficulty in relating zonal intervals to specific temporal durations, no attempt was made to normalize the diversity data for the time length of each zone or subzone. Whereas this is likely to have an impact on many of the smaller-scale fluctuations seen in the diversity and survivorship curves, we do not believe that this factor would be significant enough to influence the major trends and events discussed below.

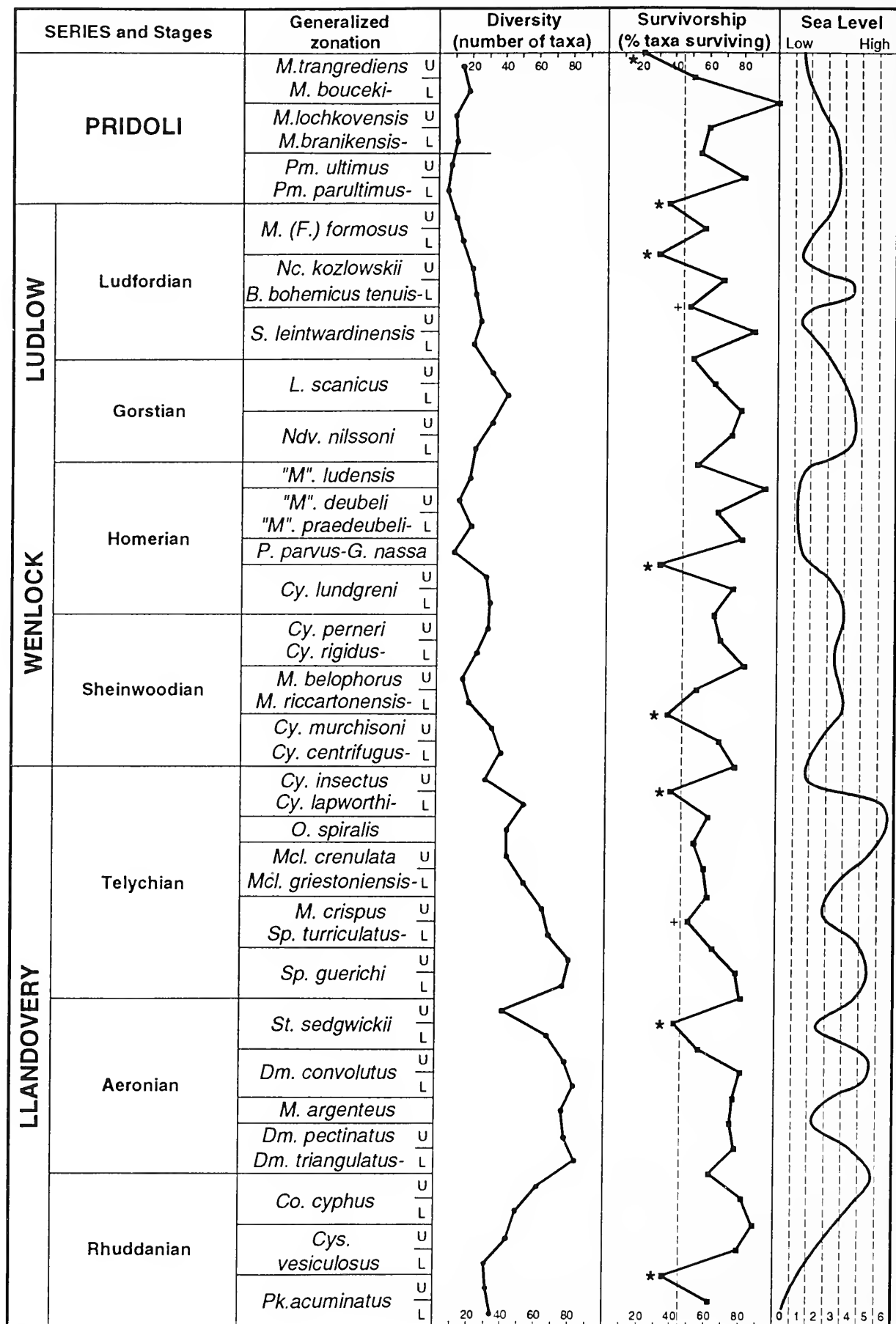
The available data, compiled from the most up-to-date data available from diverse regions of the Silurian world, show that the overall pattern of graptoloid diversity matches the one known since the 1960s and 1970s. This pattern includes a dramatic radiation of taxa in the Rhuddanian (beginning in the Hirnantian) to a diversity peak in the early Aeronian and an overall decline from the early Telychian through the rest of the Silurian, with lowest diversity in the late Homerian and early Pridoli (Figure 4). In detail, however, this curve shows some features not revealed by previous analyses. The Hirnantian-early Aeronian radiation event occurs in two marked phases of diversity increase. The first (not shown in Figure 4) is the rise from three or four taxa that have been shown to survive the end-Rawtheyan (Late Ordovician) extinction event (Melchin and Mitchell, 1991) to 38 taxa now known in the lower *Parakidograptus acuminatus* Zone. This phase is truncated by the late *P. acuminatus* Event, but the diversification quickly resumes to reach a peak of 83 taxa now recorded from the

study regions in the lower *Demirastrites triangulatus*-*D. pectinatus* Zone.

The diversity high of the early Aeronian of 75–83 taxa per subzone, with the exception of a conspicuous drop in the *Stimulograptus sedgwickii* Zone (the early *S. sedgwickii* Event), is maintained through the early Telychian *Spirograptus guerichi* Zone. The high numbers of taxa now known in the *Demirastrites convolutus* and *S. guerichi* Zones are the result of recent comprehensive studies in Bohemia (Štorch, 1994a) and Wales (Loydell, 1992, 1993). The fact that the Llandovery diversity peak is reached in different zones in different regions is a reflection of different ecological conditions in the various basins and their changes through the Aeronian and early Telychian.

Newly available data from Wales (Loydell and Cave, 1996) and Bohemia (Štorch, 1994b) also permit a much improved correlation of the Llandovery–Wenlock boundary interval, particularly between Arctic Canada and Europe, than was possible at the time of publication of Melchin's (1994) report. This interval is still a time of overall diversity decline, but the small diversity peak of the *Cyrtograptus lapworthi* Zone, the low point in the *C. insectus* Zone, and the subsequent rise and fall through the *C. centrifugus*-*C. munchisoni* and *Monograptus riccartonensis*-*M. belophorus* Zones are features not noted by Melchin (1994) or Kaljo et al. (1995). These patterns are much closer to those reported by Štorch (1995a), although in that study the low point in diversity through this interval is in the *Stomatograptus grandis* (=upper *C. lapworthi*) Zone. This is the result of a very depauperate *S. grandis* Zone fauna in Bohemia. The pattern for the remainder of the Wenlock is the familiar one reported by Kaljo et al. (1995) and Štorch (1995a) of a gradual increase in diversity through the *Cyrtograptus lundgreni* Zone, a very pronounced extinction event, and erratic recovery through the rest of the Homerian. The apparent magnitude of the diversity drop in the *Pristiograptus parvus*-*Gothograptus nassa* Zone is somewhat weakened by recent findings of several plectograpine species that span this interval (e.g., Lenz, 1993a, 1995; TNK, unpublished data, 1996) with a very few species of *Pristiograptus*. Otherwise, the late *C. lundgreni* Event is as severe as has been previously described (see below).

For the Upper Silurian, the diversity pattern matches well with the one described by Kaljo et al. (1995), with a large diversity drop in the upper Ludlow *Monograptus* (*Formosograptus*) *formosus* Zone. The small diversity peak seen in the upper Pridoli *Monograptus bouceki*-*M. transgrediens* Zone is largely the result of unusually diverse faunas of this age in Kazakhstan (Koren', 1989).



GLOBAL EXTINCTION EVENTS

In order to distinguish events that represent significant episodes of extinction from background extinction rates, some criteria must be employed to make the distinction. Štorch (1996) regarded a survivorship of less than 50% as a reasonable cutoff point. This level was difficult to employ in this study because seven levels showed survivorship rates between 48% and 53%, and it seemed unreasonable to divide these arbitrarily into events and "non-events" based on a difference of 1%–5% survivorship.

Survivorship and diversity data were collected from 50 distinct levels through the Silurian in the selected study regions. From these, the mean survivorship rate was found to be 63.0% of taxa surviving from one subzone to the next. The standard deviation was 17.4%. Those events with survivorship rates that fall below the standard deviation from the mean (45.6%) can be regarded as having extinction rates above normal, and can be considered significant extinction events. There is a gap in the distribution of survivorship rates, with eight intervals showing rates of 41% or lower and the remainder with rates of 48% or higher (Figure 4). These eight events are here considered to be the globally significant graptoloid extinctions of the Silurian, although two other events of lesser magnitude are also discussed below.

The graptoloid extinction events of the Silurian are, in order of decreasing magnitude: the *Monograptus transgrediens* Event (21% survivorship, 11 of 14 taxa extinct), the *Neocuculograptus kozlowskii* (= *Polonograptus podoliensis*) Event (30% survivorship, 14 of 20 taxa extinct), the late *Cyrtograptus lundgreni* Event (31% survivorship, 20 of 29 taxa extinct), the late *Parakidograptus acuminatus* Event (35% survivorship, 20 of 31 taxa extinct), the *Cyrtograptus murchisoni* Event (36% survivorship, 21 of 33 taxa extinct), the *Monograptus* (*Uncinograptus*) *spineus* (=late *M. (Formosograptus) formosus*) Event (36% survivorship, 7 of 11 taxa extinct), the *Cyrtograptus lapworthi* Event (38% survivorship, 32 of 52 taxa

extinct), and the early *Stimulograptus sedgwickii* Event (41% survivorship, 39 of 66 taxa extinct). Events of lesser or regional significance include the *Stimulograptus utilis* (= *Spirograptus turriculatus*) Event (48% survivorship, 33 of 67 taxa) and the late *Saetograptus leintwardinensis* Event (48% survivorship, 12 of 25 taxa extinct).

The extinctions of the *Demirastrites convolutus* Event described by Štorch (1995a) appear in this report as early *Stimulograptus sedgwickii* extinctions, because of the greater overlap of some *D. convolutus* and *S. sedgwickii* Zone taxa and the higher overall diversity of the lower *S. sedgwickii* Zone fauna in Britain as compared with Bohemia. The *Stimulograptus utilis* Event of Loydell (1994) and Štorch (1995a), which spans the *Spirograptus guerichi*–*S. turriculatus* zonal boundary, is partly blurred in this study by the 'lower biostratigraphic resolution used herein, as compared with the reports cited above, and appears as an event at the end of the *S. turriculatus* Chron. It is also weakened by the much higher rates of survivorship seen through this interval in Arctic Canada. The extinctions of the *Oktavites spiralis* Event of Štorch (1995a) and the Llandovery–Wenlock boundary Event reported by Melchin (1994) appear to be the same event recorded herein in the *Cyrtograptus lapworthi* Zone. This is partly the result of the recognition that the top of the *Cyrtograptus sakmaricus* Zone of Melchin (1989, 1994) does not coincide with the Llandovery–Wenlock boundary (see discussion above). In addition in Bohemia, the top of the *O. spiralis* Zone overlaps the lower *C. lapworthi* (= *C. sakmaricus*) Zone of other regions, and the overlying *Stomatograptus grandis* Zone has an unusually depauperate fauna as compared with Britain and, especially, Arctic Canada.

LATE PARAKIDOGAPTUS ACUMINATUS EVENT.—It is remarkable that this event, which is second-highest in percentage magnitude of all the Early Silurian extinction events and discernible in all four study regions, has been hitherto completely unrecognized. There seem to be two reasons for this. First, it is only very recently that the relatively diverse *P. acuminatus* and *Cystograptus vesiculosus* Zone faunas of Bohemia (Štorch, 1994a), Bornholm (Koren' and Bjerreskov, in press), and Arctic Canada (Melchin et al., 1991; MJM, unpublished data, 1996) have been fully documented. Second, the high rate of extinction in the late *P. acuminatus* Chron is not manifested by low diversity in the overlying lower *C. vesiculosus* Zone because of high speciation rates throughout this interval. These high speciation rates may result from the fact that this event took place within the background of the more profound Rhuddanian radiation event that followed the Late Ordovician extinction. Because extinction events

FIGURE 4—(opposite) Diversity (in number of taxa) and survivorship (percentage of taxa surviving from one zone or subzone to the next) plotted against global graptolite zonation of Koren' et al. (1996) and eustatic change in units of benthic assemblages 0–6 (Johnson, 1996). Data on diversity and survivorship derived mainly from sources for Figures 2 and 3 and supplemented by sources in text and authors' unpublished data. Asterisks show main graptolite extinction events; crosses are events of lesser or regional significance discussed in the text. Abbreviations as in Figure 2.

have been traditionally recognized by episodes of low diversity rather than by plots of extinction or survivorship rates, it is not surprising that this event went unnoticed.

Akidograptus, *Parakidograptus*, and *Hirsutograptus* become extinct at or near the *Parakidograptus acuminatus*–*Cystograptus vesiculosus* zonal boundary, along with species of *Normalograptus*, *Neodiplograptus*, *Cystograptus*, and *Atavograptus*. The subsequent radiation includes a dramatic diversification, particularly in monograptid and dimorphograptid taxa.

The late *Parakidograptus acuminatus* Event is not linked with any known episodes of major, global sea-level change, but it seems to be in the middle of the overall Rhuddanian transgression. However, the global sea-level curve (Johnson, 1996) is based on cratonic successions. The occurrence and dating of early Rhuddanian strata in most cratonic regions is very poor, and a late *P. acuminatus* Chron regression could well be unrecognizable or indistinguishable from the Hirnantian regression at many shallow-shelf localities. Facies changes from graptolitic shales to sandy-silty laminites have been observed in Bohemia (Štorch, 1986), the Yangtze Platform of China, and the Carnic Alps (Pš, unpublished data, 1990, 1995). In the southern part of the Cape Phillips Basin in Arctic Canada, which was a distal-ramp environment in the early Rhuddanian (Melchin, 1987, 1989), the graptolitic, calcareous mudstones of the *Normalograptus persculptus* and *P. acuminatus* Zones are interrupted by an interval of massive dolostones at the *P. acuminatus*–*Atavograptus atavus* zonal boundary (MJM, unpublished data, 1992, 1996). These observations suggest that widespread changes in sea-level and/or oceanic circulation may have occurred at this time. Grahn and Caputo (1992) indicated that the earliest of four intervals of Silurian glacial sedimentation documented in South America is most likely early Llandovery (Rhuddanian). However, imprecision in the dating of these deposits and current scarcity of documented evidence for regression coincident with the late *P. acuminatus* Event make a link between the glaciation and extinctions, as suggested for the late Ashgill and later Llandovery events, a tenuous one at best for this extinction episode. Recognition of this event and its timing should lead to future research into possible physical, chemical or other biotic changes that might be associated with it.

EARLY STIMULOGRAPTUS SEDGWICKII EVENT.—The early *S. sedgwickii* Event, unlike the late *Parakidograptus acuminatus* Event, is marked by high extinction rates in the upper *Demirastrites convolutus* and lower *S. sedgwickii* Zones and by dramatically reduced diversity, especially in the upper *S. sedgwickii* (= *S. halli*) Zone. This may be, to

some extent, due to the fact that in the four study regions the *S. halli* Zone is only recognized in Britain, although it is most likely represented in the uppermost *S. sedgwickii* Zone of Bohemia as well. Within Britain, however, the diversity of the *S. halli* Zone is significantly lower than that of the preceding *S. sedgwickii* and succeeding *Spirograptus guerichi* Zones (Rickards, 1976; Loydell, 1991, 1993), and it does appear to be an interval of overall low diversity. In addition, the lack of graptolite occurrences in the other study regions could be a real reflection of restricted graptolite distributions and diversity in this time interval.

Štorch (1995a) described the taxonomic patterns of this extinction and subsequent radiation, and these patterns generally hold elsewhere. Many early and middle Llandovery lineages, namely pseudorthograptids and normalograptids, were terminated; specialized monograptids (*Campograptus*, *Coronograptus*, *Rastrites*, *Demirastrites*) were severely reduced, and some disappeared. In the *Stimulograptus sedgwickii* Zone of Bohemia, Arctic Canada, Bornholm, Spain, Poland, areas in Scandinavia, and some parts of China (Ni Yunan, personal commun., 1990), better-oxygenated, graptolite-free beds or interbeds often appear. This graptolite crisis corresponds in time with the significant regression suggested by Johnson (1996), as well as with the Sandvika Event, an oceanic event and conodont mass extinction recorded by Jeppsson (1990) and Aldridge et al. (1993).

STIMULOGRAPTUS UTILIS (=SPIROGRAPTUS TURRICULATUS) EVENT.—This event and its taxonomic patterns of extinction and recovery were described by Loydell (1994) and Štorch (1995a), and the event was also recorded from Spain (Gutierrez-Marco and Štorch, In press). It is not recognized as a significant event in Arctic Canada (Melchin, 1994) or Bornholm (Bjerreskov, 1975), and this, combined with its relatively low global extinction rate (52%), suggests that its importance is more regional than global in nature. Extinction rates were found to be highest among taxa with restricted geographic distributions (Loydell, 1994).

The lowermost Telychian is marked by a large eustatic rise (Johnson, 1996), accompanied by a considerable radiation among graptolite stocks. The radiation terminated during the succeeding drop in sea-level at about the top of the *Spirograptus guerichi* Zone. The extinction event was first described by Loydell (1994) from the *Stimulograptus utilis* Subzone, which corresponds with the boundary beds between the *S. guerichi* and *S. turriculatus* Zones. Loydell (1994) explained the graptolite crisis by a brief glacio-eustatic fall related to the second horizon of the Silurian glacio-marine diamictites in Brazil (Grahn and Caputo, 1992). In Bohemia, the immediate

extinction level is masked by a widespread oxygenated, graptolite-free horizon between the pre-extinction *Rastrites linnaei* Zone and post-extinction *S. turriculatus* Zone. The *S. utilis* Event resulted in a near extinction of biserial graptolites, with the exception of the Retiolitidae and a few survivors among the petalograptids, metaclimacograptids, glyptograptids, and rastritids. Jeppsson (1996) considered this extinction to coincide with an unnamed event of transition between oceanic states ("Secundo" to "Primo" episodes - see discussion below).

CYRTOGRAPTUS LAPWORTHII EVENT.—As noted above, this event has been described by Štorch (1995a) as the *Oktavites spiralis* Event and by Melchin (1994) as a Llandovery–Wenlock boundary event. Improved biostratigraphic data from Arctic Canada, Wales, and Bohemia now show that these are the same event, and it occurs within the *C. lapworthii* Zone. Both Melchin (1994) and Štorch (1995a) described the taxonomic patterns seen in the extinctions. This event features a termination of such genera as *Oktavites* and *Torquigraptus* and near extinction of *Streptograptus*, *Diversograptus*, and *Cyrtograptus*. The new Bohemian and Welsh data show that a somewhat larger number of taxa span this event than was evident in Melchin's (1994) analysis. In addition, it is now known that ten species of *Cyrtograptus* occur in the *C. lapworthii* Zone among the four regions, with nine in Arctic Canada and only *C. lapworthii lapworthii* in the other study areas. Only two of these ten cyrtograptid taxa, *C. lapworthii lapworthii* and *C. falcatus*, are now known to span the *C. lapworthii*–*C. insectus* zonal boundary, and only *C. falcatus* and *C. insectus* are reported to survive the Llandovery–Wenlock boundary.

As noted by Melchin (1994), this event corresponds with the largest eustatic regression of the entire Silurian, as identified by Johnson (1996). In addition, it also seems to coincide, at least approximately, with reported widespread glaciogenic deposits in Brazil (Grahni and Caputo, 1992), and it was presumably that glaciation which was responsible for the regression. This extinction also matches well with the beginning of the Ireviken Oceanic Event (Jeppsson et al., 1995).

CYRTOGRAPTUS MURCHISONI EVENT.—This extinction, which terminated many lineages (e.g., *Barrandeograptus*, *Mediograptus*, and the *C. murchisoni* group), was also recorded by Koren' (1987), Štorch (1995a), and Kaljo et al. (1995). It may be correlated with the latest phase of the Ireviken Oceanic Event (Jeppsson et al., 1995) and a conodont extinction analyzed by Jeppsson (In press). Unlike preceding events, this extinction occurs during an early

Sheinwoodian rise in sea-level (Johnson, 1996), and is not followed by a strong diversification of graptolites. The low rates of speciation and relatively low survivorship seen in this event and in the lower *Monograptus riccartonensis*–*M. belophorus* Zone result in very low overall diversities through the latter zone.

LATE CYRTOGRAPTUS LUNDGRENII EVENT.—In terms of percentage of species that went extinct, termination of lineages, and the succeeding low diversity, this is the most severe extinction event of the Early Silurian. Only the plectograptines and species of the *Pristiograptus dubius* group are known to have survived the *C. lundgreni* to *Pristiograptus parvus*–*Gothograptus nassa* zonal boundary, although species of *Monograptus* that appear later in the Ludlow may represent survivors of the event that are unrepresented in any known successions in the extinction interval (i.e., "Lazarus taxa"). As noted above, this event has been widely studied and characterized around the world (e.g., Jaeger, 1991; Koren', 1991b; Lenz, 1993a; Urbanek, 1993; Koren' and Urbanek, 1994; Legrand, 1994; Štorch, 1995a; Gutierrez-Marco et al., 1996). It occurred during a prolonged, Homeric eustatic regressive phase (Johnson, 1996). The graptolite recovery following the late *C. lundgreni* Event led to the evolution of new monograptids of the "*Monograptus*" *ludensis* and *Lobograptus?* *sherrardae* groups, as well as varied plectograptids. However, the radiation that brought new morphotypes into the fauna began with the subsequent transgression in the earliest Ludlow *Neodiversograptus nilssoni* Chron (Koren', 1992; Koren' and Urbanek, 1994). This extinction episode coincides with the start of the Mulde Event of Jeppsson et al. (1995).

LATE SAETOGRAPTUS LEINTWARDINENSIS EVENT.—Although the magnitude of this event seems to fall within the range of "normal" extinction rates, it was described as an event by Koren' (1993), Urbanek (1993, 1995), and Kaljo et al. (1995), and was noted by Štorch (1995a). It coincides with a peak eustatic regression (Johnson, 1996). This event terminated the plectograptines and a number of diverse and specialized monograptid lineages.

NEOCUCULLOGRAPTUS KOZLOWSKII (=POLONOGRAPTUS PODOLIENSIS) EVENT.—With an extinction of 70% of the taxa in the late *Bohemograptus bohemicus tenuis*–*Neocucullograptus kozlowskii* Chron, this event has the second-highest extinction rate of any event in the Silurian. This event has been well-characterized by Koren' (1993), Urbanek (1993, 1995), Kaljo et al. (1995), and Štorch (1995a). Several specialized genera, including *Neocucullograptus*, *Bohemograptus*, and *Polonograptus*, became extinct, along

with other forms. This event was shown by Johnson (1996) to correspond to the penultimate regressive episode of the Silurian.

MONOGRAPTUS (UNCINATOGRAPTUS) SPINEUS (LATE M. (FORMOSOGRAPTUS) FORMOSUS) EVENT.—Koren' (1993), Urbanek (1993), and Kaljo et al. (1995) recorded the *M. (U.) spineus* Event as a time of diversity reduction. This event saw the termination of only seven species, primarily specialized monograptids, from a total diversity of eleven species known within this subzone. This event does not correspond with a known eustatic regression, but occurs within the latest Ludlow–early Pridoli transgression of Johnson (1996).

MONOGRAPTUS TRANSGREDIENS EVENT.—The last graptolite extinction event of the Silurian, which marks the end of Silurian time, is also the most significant in terms of the percentage of extinctions (79%). Of the fourteen taxa known from the upper *Monograptus bouceki*-*M. transgrediens* Zone, only three are known to have survived into the Early Devonian; these are *Monograptus microdon*, *M. birchensis*, and *Linograptus posthumus*. The genera *Pseudomonoclimacis* and *Pristiograptus*, as well as all other species of *Monograptus s.l.*, became extinct within the *M. transgrediens* zonal interval. This event was extensively discussed by Koren' and Rickards (1979), Koren' (1993), Urbanek (1993, 1995), and Kaljo et al. (1995), and was noted by Štorch (1995a). It corresponds to the late Pridoli regression noted by Johnson (1996).

DISCUSSION

For much of the Silurian, the link between sea-level fall and high extinction rates is fairly clear (Figure 4), as noted by many authors. Three exceptions to this, however, are the late *Parakidograptus acuminatus* Event (although see discussion above), the *Cyrtograptus murchisoni* Event, and the *Monograptus (Uncinograptus) spineus* (=late *M. (Formosograptus) formosus*) Event, which featured significant extinctions and no identified eustatic fall. A fourth exception is the earliest Aeronian, which is marked by eustatic fall (Johnson, 1996), but no significant rise in extinction rates. With the database that is now available, it seems unlikely that further research will bring a higher-magnitude extinction event to light in the early Aeronian.

Grahn and Caputo (1992) reported evidence for several glacial episodes in the Early Silurian of South America. Johnson (1996) suggested that if the cycles of sea-level lows and highs in the Llandovery represent glacial and non-glacial periods, respectively, the duration of

each glaciation is on the order of 1 Ma. Whereas these intervals are approximately an order of magnitude longer than the glacial–interglacial cycles of the Pleistocene, the area glaciated is also much larger, which may have resulted in longer cycles (Johnson, 1996). It is also possible that each of the currently known cycles consists of two or more smaller, unresolved glacial–interglacial fluctuations. Johnson (1996) suggested that sea-level cycles of post-Llandovery times, which are of somewhat longer duration, may be related to tectonic cycles.

As noted in the introduction to this report, the link between sea-level change and planktic graptolite diversity is not considered to be a direct one by most authors. However, Kirk (1991), who considered that planktic graptoloids had a benthic early growth stage that lived in deeper waters, suggested that sea-level fall would reduce the habitat for the benthic stage, and would result in the observed extinctions. No field evidence has been presented in favor of a benthic sicular stage for graptoloids, and Melchin et al. (1995) have presented preliminary taphonomic evidence, based on relative abundances and orientations of numerous uncompressed specimens in concretions, that the sicular stages shared the same planktic habitat as the mature rhabdosomes. On the other hand, eustatic fall would certainly reduce the area of deep-shelf habitat over the cratonic and craton margin regions, a cause widely cited for extinctions of benthic organisms (e.g., Brenchley, 1984). Although the deep-shelf graptolite biofacies is generally not as diverse as the more pelagic assemblages, the drastic reduction or elimination of many deep-shelf settings would account for at least some graptolite extinctions.

Rather than sea-level fall as the main cause of extinction in these events, it is more commonly regarded as associated with other changes in oceanic conditions that may have affected pelagic faunas. As noted by Loydell (1994), the relationship between graptolite diversity and other environmental changes does not match well with the predictions of the model of changing oceanic states put forward by Jeppsson (1990, 1996), Aldridge et al. (1993), and Jeppsson et al. (1995). For the Llandovery, their "Secundo (S) episodes", which are predicted to be times of low planktic diversity, span the two intervals of highest graptolite diversity in the Silurian, the early Aeronian and earliest Telychian. Conversely, the lower diversity of the middle Telychian is considered to be within a "Primo (P) episode," which their model predicts to show high planktic diversities. A similar lack of correspondence occurs in the Wenlock, where times of highest diversity occur within the Ireviken Event (*Cyrtograptus centrifugus* Chron) and the Hellvi S episode (*Cyrtograptus lundgreni* Chron). Some of the changes between episodes in the Llandovery, as identified by Aldridge et al. (1993)

and Jeppsson (1996), do correspond in timing with the early *Stimulograptus sedgwickii*, *Spirograptus turriculatus*, and *Cyrtograptus lapworthi* Events identified herein, although, as noted by Loydell (1994), the magnitudes of the extinctions do not always correspond with those predicted by the model. The Jeppsson (1990) model predicts that planktic extinctions should be highest during times of transition from P to S episodes. During the Wenlock, P-S transitions are recorded by Jeppsson et al. (1995) to occur within the late *Monograptus riccartonensis*-*M. belophorus* Chron, the *Cyrtograptus rigidus*-*C. perneri* Chron, and near the beginning of the *Cyrtograptus lundgreni* Chron, none of which is a period with a high extinction rate. The most significant graptolite extinction in the Wenlock, the late *C. lundgreni* Event, corresponds to a time of transition between two S episodes. In contrast, Jeppsson (1996) suggested that transition events between S-P and S-S episodes should be even more severe than P-S events, although the reason why this should be the case was not clearly explained. In addition, Jeppsson (1996) did not explain why no extinction events have yet been described for the S-P transitions of the Early Silurian (e.g., early-middle Aeronian, early-middle and late-middle Sheinwoodian), except for the relatively weak early Telychian *Stimulograptus utilis* (= *Spirograptus turriculatus*) Event. The second most severe extinction of the Early Silurian, the late *Parakidograptus acuminatus* Event, occurs within an S episode, although it is possible that this represents a hitherto unrecognized S-S event, similar to that which corresponds to the late *C. lundgreni* Event.

Quinby-Hunt and Berry (1991) examined the possible causes of the late *Cyrtograptus lundgreni* Event. They suggested that the Silurian was a time of widespread anoxia below the surface-mixed layer of the oceans, and that the subphotic dysaerobic zone immediately overlying the anaerobic waters was the habitat of the most diverse graptoloid communities (Berry et al., 1987). They attributed the extinction primarily to a global rise in temperature and a decrease in O₂ concentrations in the oceans and atmosphere that resulted in a shoaling of the anoxic waters into the surface-mixed layer and a compression or elimination of the intervening suboxic habitat. They noted that the survivors of the extinction were primarily surface-water dwellers. As a secondary factor, they cited the tectonic uplift of many cratonic regions and an associated loss of deep-shelf environments. However, Jaeger (1976), Koren' (1987), Kemp (1991), and Štorch (1995a) have all noted, based on lithologic evidence, that the latest Wenlock and other phases of regression were times of retreat, rather than a spread, of the anoxic black shale facies that resulted primarily from eustatic fall. As proposed by Štorch (1995a), global reduction in the

regional distribution of the oceanic anoxic and suboxic zones that accompanies sea-level falls would also result in a loss of preferred graptolite habitat, except for those taxa that lived in surface, well-oxygenated waters.

Loydell (1994) suggested for the early Telychian *Stimulograptus utilis* (= *Spirograptus turriculatus*) Event that glacio-eustatic fall would be accompanied by an increase in rates of deep ocean circulation and upwelling. Similar suggestions have also been made for other Paleozoic events of sea-level fall (e.g., Landing et al., 1992). The regressive episode would also be a time of higher rates of continental erosion and increased rates of input of nutrients to the ocean. The higher rates of upwelling and terrestrial nutrient input would result in overall higher rates of oceanic productivity. In modern oceans, regions of high oceanic productivity are generally characterized by high abundance but low overall diversity in plankton communities (e.g., Hallock, 1987). Loydell (1994) proposed, therefore, that the Telychian *Stimulograptus utilis* (= *Spirograptus turriculatus*) Event of graptolite diversity fall was caused by a phase of a glacio-eustatically induced increase in productivity. Martin (1996) developed an overall model of changing productivity and diversity through time that supports these suggestions, and provided faunal, lithologic, and isotopic evidence in support of it. He, as Branchley et al. (1995) and Wenzel and Joachimski (1996), explained the positive shift in $\delta^{13}\text{C}$ values that are associated with the Late Ordovician and Silurian regressions as the result of enhanced primary productivity and/or organic carbon burial rate associated with increased rates of upwelling and nutrient runoff from land.

In contrast, Pederson and Calvert (1990) documented an oceanic circulation model that predicts that rates of deep oceanic circulation, upwelling, and productivity should be higher in non-glacial intervals of geologic time than during glaciations. They suggested that times of widespread black shales (generally non-glacial times) are the result of the anoxia produced by the high rates of upwelling and productivity, and led to high biological oxygen demand in deeper waters rather than to deep-ocean stagnation, as suggested by Martin (1996) and others. In addition, Van Cappellen and Ingál (1994) proposed a model for carbon and phosphorus cycling that suggests that times of oceanic anoxia-dysoxia should be times of high primary productivity. The suggested cause is differences in the chemical state of phosphorus and the resulting changes in burial rate under oxic versus anoxic conditions. Reduced rates of phosphorus burial under anoxic conditions result in a higher rate of recycling and higher overall productivity.

Studies of modern upwelling systems and their variability show that their occurrence and intensity are

primarily the result of surface wind stress fields that result in surface current divergence (Summerhayes et al., 1995). Upwelling patterns are not a function of deep-ocean circulation rates, although both are climatically controlled. In addition, most upwelling systems do not involve deep-ocean waters, but only the intermediate waters immediately below the surface-mixed layer where nutrient levels are commonly highest. Through the Quaternary, there is not a consistent relationship between rates of upwelling in particular regions and glacial advance and retreat (Anderson, 1995; Summerhayes et al., 1995). Landing et al. (1992) and Landing and Bartowski (1996) provided evidence for episodic anoxia on the outer shelf and slope during the Cambrian and Ordovician, when the deep-ocean was oxygenated. This indicates that widespread black shale deposition is not necessarily indicative of sluggish deep ocean circulation.

Too many uncertainties exist in our current models of upwelling, our understanding of past ocean and atmospheric systems, and how variations in these are reflected in the sedimentary record to generate meaningful reconstructions of the dynamics of ancient oceanic states and upwelling patterns in response to climate (Jahnke and Shimmiel, 1995; Peterson et al., 1995).

Nigrini and Caulet (1992) and Peterson et al. (1995) noted that some groups of organisms that reach their maximum abundance in upwelling waters (e.g., Radiolaria) also reach their maximum diversity there. The general inverse relationship between productivity and diversity noted above does not necessarily apply to those particular groups of organisms with a preferred habitat in nutrient-rich waters.

In summary, it seems clear that the association between eustatic fall, temporary termination of "graptolitic shale" (anoxic-suboxic facies) deposition, and graptolite extinction is relatively consistent through the Silurian in many regions of the world (with some notable exceptions), whether or not there exists evidence for glaciation. Beyond this, however, considerable uncertainty exists concerning the following points: 1) the relative importance of rates of deep ocean circulation versus primary productivity in producing the widespread oceanic anoxia-dysoxia that characterizes much of the Early-Middle Paleozoic; 2) the physical relationship between changing climate, deep ocean circulation, and rates of upwelling; 3) the probable relationship between the diversity dynamics of a zooplankton group such as the graptoloids and changes in rates of upwelling or primary productivity; and 4) the forcing mechanism of the eustatic cycles seen throughout the Silurian System. Although cycles in the Llandovery can be temporally linked to reported glacial deposits in South America (Grahn and Caputo, 1992), the documentation of the glacial origin of

those deposits and their precise temporal correlation with sea-level changes are not as well-demonstrated as in the case of the Ashgill glaciation. The post-Llandovery cycles cannot be linked to any known glacial events. However, if the sub-photic, dysaerobic zone that today characterizes upwelling zones was indeed the preferred graptolite habitat as suggested by Berry et al. (1987), then the loss of that habitat in many regions with regression, whatever its cause, could have resulted in widespread graptolite extinction.

ACKNOWLEDGMENTS

The authors thank D.K. Loydell and S.H. Williams for access to material from Dob's Linn, and M.E. Johnson, A.C. Lenz, D.K. Loydell, and A. Urbanek for helping us to incorporate the most up-to-date graptolite range and sea-level data. E. Landing, M.E. Johnson, A.C. Lenz, and B.S. Norford provided helpful comments on the manuscript. Financial support to MJM from the Natural Sciences and Engineering Research Council and the Polar Continental Shelf Project; to TNK from the Russian Foundation for Fundamental Investigations (Grant No. 96 05 65 758) and from a James Chair Visiting Professorship at St. Francis Xavier University; and to PŠ from the Grant Agency of the Czech Republic (Grant No. 205/95/1516) are gratefully acknowledged. (Editors' note: M. Melchin contributed \$400 toward publication of this article from his Natural Sciences and Engineering Research Council [NSERC] grant.)

REFERENCES

- ALDRIDGE, R.J., L. JEPSSON, AND K.J. DORNING. 1993. Early Silurian oceanic episodes and events. *Journal of the Geological Society of London*, 150:501-513.
- ANDERSON, D.M. 1995. Sensitivity of ocean upwelling to climate forcing on millennial time scales, p. 259-272. *In* C.P. Summerhayes, K.-C. Emeis, M.V. Angel, R.L. Smith, and B. Zeitshel (eds.), *Upwelling in the Ocean: Modern Processes and Ancient Records*. J. Wiley and Sons, New York.
- BERRY, W.B.N., P. WILDE, AND M.S. QUINBY-HUNT. 1987. The graptolite habitat: an oceanic non-sulfide low oxygen zone? *Bulletin of the Geological Society of Denmark*, 35:103-113.
- BJERRESKOV, M. 1975. Llandoveryan and Wenlockian Graptolites from Bornholm. *Fossils and Strata*, 8.
- BOUČEK, B. 1953. Biostratigraphy, development and correlation of the Zerkovice and Motol Beds of the Silurian of Bohemia. *Sbornik Ustredniho ustavu Geologickeho*, 20:421-484.
- BRENCHLEY, P.J. 1984. Late Ordovician extinctions and their relationship to the Gondwana glaciation, p. 291-315. *In* P.J. Brenchley (ed.), *Fossils and Climate*. J. Wiley and Sons, New York.
- , G.A.F. CARDEN, AND J.D. MARSHALL. 1995. Environmental changes associated with the "first spike" of the late Ordovician mass extinction. *Modern Geology*, 20:69-82.

- BULMAN, O.M.B. 1964. Lower Palaeozoic plankton. *Quarterly Journal of the Geological Society of London*, 120:455–476.
- COCKS, L.R.M., AND C.R. SCOTSE. 1991. The global biogeography of the Silurian, p. 109–122. *In* M.G. Bassett, P.D. Lane, and D. Edwards (eds.), *The Murchison Symposium. Proceedings of an International Conference on the Silurian System. Special Papers in Palaeontology*, No. 44.
- GRAHN, Y., AND M.V. CAPUTO. 1992. Early Silurian glaciations in Brazil. *Palaeogeography, Palaeoclimatology, Palaeoecology*, 99:9–15.
- GUTIERREZ-MARCO, J.C., A.C. LENZ, M. ROBARDET, AND J.M. PICARRA. 1996. Wenlock–Ludlow graptolite biostratigraphy and extinction: a reassessment from the southwestern Iberian Peninsula (Spain and Portugal). *Canadian Journal of Earth Sciences*, 33:656–663.
- , AND P. ŠTORCH. In press. Graptolite biostratigraphy of the Lower Silurian (Llandovery) shelf deposits of the Western Iberian Cordillera, Spain. *Geological Magazine*.
- HALLOCK, P. 1987. Fluctuations in the trophic resource continuum: a factor in global diversity cycles? *Paleoceanography*, 2:457–471.
- HUTT, J.E. 1974–1975. The Llandovery Graptolites of the English Lake District. *Palaeontographical Society Monograph*, Parts 1–2.
- JAEGER, H. 1976. Das Silur und Unterdevon vom thuringischen Typ im Sardinien und seine regionalgeologische Bedeutung. *Nova Acta Leopoldina*, 45:263–299.
- . 1991. Neue Standard-Graptolithenzonenfolge nach der "Grossen Krise" an der Wenlock/Ludlow Grenze (Silurs). *Neues Jahrbuch für Geologie und Paläontologie, Abhandlungen*, 182:303–354.
- JANKE, R.A., AND G.B. SHIMMELD. 1995. Particle flux and its conversion to the sediment record: coastal ocean upwelling systems, p. 83–100. *In* C.P. Summerhayes, K.-C. Emeis, M.V. Angel, R.L. Smith, and B. Zeitshel (eds.), *Upwelling in the Ocean: Modern Processes and Ancient Records*. J. Wiley and Sons, New York.
- JEPPSSON, L. 1990. An oceanic model for lithological and faunal changes tested on the Silurian record. *Journal of the Geological Society of London*, 147:663–674.
- . 1996. Recognition of a probable secundo–primo event in the Early Silurian. *Lethaia*, 29:311–315.
- . In press. The anatomy of the mid–Early Silurian Ireviken Event. *In* C.E. Brett (ed.), *Paleontological Event Horizons, Ecological and Evolutionary Implications*. Columbia University Press, New York.
- , R.J. ALDRIDGE, AND D.K. DORNING. 1995. Wenlock (Silurian) oceanic episodes and events. *Journal of the Geological Society of London*, 152:487–498.
- JOHNSON, M.E. 1996. Stable cratonic sequences and a standard for Silurian eustasy, p. 203–211. *In* B.J. Witzke, G.A. Ludvigson, and J.E. Day (eds.), *Paleozoic Sequence Stratigraphy: Views from the North American Craton*. Geological Society of America, Special Paper 306.
- KALJO, D., A.J. BOUCOT, R.M. CORFIELD, A. LE HERISSE, T.N. KOREN', J. KRÍŽ, P. MÄNNIK, T. MÄRSS, V. NESTOR, R.H. SHAVER, D.J. SIVETER, and V. VIIRA. 1995. Silurian bio-events, p. 173–224. *In* O.H. Walliser (ed.), *Global Events and Event Stratigraphy in the Phanerozoic*. Springer-Verlag, Berlin.
- KEMP, A.E.S. 1991. Mid Silurian pelagic and hemipelagic sedimentation and palaeoceanography, p. 261–299. *In* M.G. Bassett, P.D. Lane, and D. Edwards (eds.), *The Murchison Symposium. Proceedings of an International Conference on the Silurian System. Special Papers in Palaeontology*, 44.
- KIRK, N.H. 1991. Construction, form and function in the Graptolithina: a review. *Modern Geology*, 15:287–311.
- KOREN', T.N. 1987. Graptolite dynamics in Silurian and Devonian time. *Bulletin of the Geological Society of Denmark*, 35:149–159.
- . 1989. The graptolitic Ludlow and Pridoli series in Kazakhstan, p. 149–158. *In* C.H. Holland, and M.G. Bassett (eds.), *A Global Standard for the Silurian System*. National Museum of Wales, Geological Series, 9.
- . 1991a. Evolutionary crisis of the Ashgill graptolites, p. 157–164. *In* C.R. Barnes, and S.H. Williams (eds.), *Advances in Ordovician Geology*. Geological Survey of Canada Paper 90-9.
- . 1991b. The *lundgreni* extinction event in central Asia and its bearing on graptolite biochronology within the Homerian. *Proceedings of the Estonian Academy of Science, Geology*, 40:74–78.
- . 1992. New late Wenlock monograptids of the Alai Range. *Paleontologicheskij Zhurnal*, 2:21–33 (In Russian).
- . 1993. Main event levels in the evolution of the Ludlow graptolites. *Stratigraphy. Geological Correlation*, 1:44–52 (In Russian).
- . 1994. The Homerian monograptid fauna of Central Asia: zonation, morphology and phylogeny, p. 140–148. *In* Chen X., B.-D. Erdtmann, and Ni Y.-n. (eds.), *Graptolite Research Today*. Nanjing University Press, Nanjing.
- , AND M. BJERRESKOV. In press. Early Llandovery monograptids from Bornholm and south Urals. *Bulletin of the Geological Society of Denmark*, 44.
- , A.C. LENZ, D.K. LOYDELL, M.J. MELCHIN, P. STORCH, AND L. TELLER. 1996. Generalized graptolite zonal sequence defining Silurian time intervals for paleogeographic studies. *Lethaia*, 29:59–60.
- , AND V.V. LYTOCHKIN. 1992. Upper Silurian graptolite biozonation of the Turkestan–Alai Mountains. *Sovetskaja Geologia*, 11:37–43 (In Russian).
- , AND R.B. RICKARDS. 1979. Extinction of the graptolites, p. 457–466. *In* A.L. Harris, C.H. Holland, and B.E. Leake (eds.), *The Caledonides of the British Isles—Reviewed*. Geological Society of London.
- , AND A.A. SUJARKOVA. In press. Late Ludlow and Pridoli monograptids from the Turkestan–Alai Mountains. *Palaeontographica*.
- , AND A. URBANEK. 1994. Adaptive radiation of monograptids after the late Wenlock crisis. *Acta Palaeontologica Polonica*, 39:137–167.
- KRÍŽ, J., H. JAEGER, F. PARIS, AND H.P. SCHÖNLAUB. 1986. Pridoli—the fourth subdivision of the Silurian. *Jahrbuch der geologischen Bundesanstalt, Wein*, 129:291–360.
- LANDING, E., AND K.E. BARTOWSKI. 1996. Oldest shelly fossils from the Taconic Allochthon and late Early Cambrian sea-levels in eastern Laurentia. *Journal of Paleontology*, 70:741–761.
- , A.P. BENUS, AND P.R. WHITNEY. 1992. Early and early Middle Ordovician Continental Slope Deposition: Shale Cycles and Sandstones in the New York Promontory and Quebec Reentrant Region. *New York State Museum Bulletin* 474.
- LEGRAND, P. 1994. Sea-level and fauna change during the late Wenlock and earliest Ludlow (Silurian): a point of view from the Algerian Sahara. *Historical Biology*, 7:271–290.
- LENZ, A.C. 1978. Llandoveryan and Wenlockian *Cyrtograptus* and some other Wenlockian graptolites from northern and Arctic Canada. *Geobios*, 11:623–653.
- . 1982. Llandoveryan Graptolites of the Northern Canadian Cordillera: *Petalograptus*, *Cephalograptus*, *Rhaphidograptus*, *Dimorphograptus*, *Retiolitidae*, and *Monograptidae*. *Life Sciences Contributions*, Royal Ontario Museum, 130.
- . 1993a. Late Wenlock–Ludlow (Silurian) graptolite extinction, evolution, and biostratigraphy: perspectives from Arctic Canada. *Canadian Journal of Earth Sciences*, 30:491–498.

- . 1993b. Late Wenlock and Ludlow (Silurian) Plectograptinae (Retiolitid Graptolites), Cape Phillips Formation, Arctic Canada. *Bulletins of American Paleontology*, 104.
- . 1995. Upper Homerian (Wenlock, Silurian) graptolites and graptolite biostratigraphy, Arctic Archipelago, Canada. *Canadian Journal of Earth Sciences*, 32:1378–1392.
- , AND M.J. MELCHIN. 1991. Wenlock (Silurian) graptolites, Cape Phillips Formation, Canadian Arctic Islands. *Transactions of the Royal Society of Edinburgh: Earth Sciences*, 82:211–237.
- LOYDELL, D.K. 1991. Dob's Linn—the type locality of the Telychian (upper Llandovery) *Rastrites maximus* Biozone? *Newsletters on Stratigraphy*, 25:155–161.
- . 1992. Upper Aeronian and lower Telychian (Llandovery) graptolites from western mid-Wales. Part 1. *Palaeontological Society Monograph*, p. 1–55.
- . 1993. Upper Aeronian and lower Telychian (Llandovery) graptolites from western mid-Wales. Part 2. *Palaeontological Society Monograph*, p. 56–180.
- . 1994. Early Telychian changes in graptoloid diversity and sea level. *Geological Journal*, 29:355–368.
- , AND R. CAVE. 1993. The Telychian (upper Llandovery) stratigraphy of Buttington Brick Pit, Wales. *Newsletters on Stratigraphy*, 29:91–103.
- , AND ———. 1996. The Llandovery–Wenlock boundary and related stratigraphy in eastern mid-Wales with special reference to the Banwy River section. *Newsletters on Stratigraphy*, 34:39–64.
- LUKASIK, J.J., AND M.J. MELCHIN. In press. Morphology and classification of some Early Silurian monograptids (Graptoloidea) from the Cape Phillips Formation, Canadian Arctic Islands. *Canadian Journal of Earth Sciences*, 34.
- MARTIN, R.E. 1996. Secular increase in nutrient levels through the Phanerozoic: implications for productivity, biomass and diversity of the marine biosphere. *Palaos*, 11:209–219.
- MELCHIN, M.J. 1987. Upper Ordovician graptolites from the Cape Phillips Formation, Canadian Arctic Islands. *Bulletin of the Geological Society of Denmark*, 35:191–202.
- . 1989. Llandovery graptolite biostratigraphy and paleobiogeography, Cape Phillips Formation, Canadian Arctic Islands. *Canadian Journal of Earth Sciences*, 26:1726–1746.
- . 1994. Graptolite extinction at the Llandovery–Wenlock boundary. *Lethaia*, 27:285–290.
- , M. BESON, AND J.J. LUKASIK. 1995. A new technique for taphonomic study of graptolites in concretionary or bedded limestones. *Graptolite News*, 8:50–51.
- , A.D. MCCracken, AND F.J. OLIFF. 1991. The Ordovician–Silurian boundary on Cornwallis and Truro islands, Arctic Canada: preliminary data. *Canadian Journal of Earth Sciences*, 28:1854–1862.
- , AND C.E. MITCHELL. 1991. Late Ordovician extinction in the Graptoloidea, p. 143–156. In C.R. Barnes, and S.H. Williams (eds.), *Advances in Ordovician Geology*. Geological Survey of Canada, Paper 90-9.
- NIGRINI, C., AND J.-P. CAULET. 1992. Late Neogene radiolarian assemblages characteristic of Indo-Pacific areas of upwelling. *Micro-paleontology*, 38:139–164.
- PEDERSEN, T.F., AND S.E. CALVERT. 1990. Anoxia vs. productivity: what controls the formation of organic carbon-rich sedimentary rocks? *American Association of Petroleum Geologists Bulletin*, 74:454–466.
- PETERSON, L.C., M.R. ABBOTT, D.M. ANDERSON, J.-P. CAULET, J.-P. CONTE, K.-C. EMEIS, A.E.S. KEMP, and C.P. SUMMERHAYES. 1995. Group report: how do upwelling systems vary through time?, p. 285–311. In C.P. Summerhayes, K.-C. Emeis, M.V. Angel, R.L. Smith, and B. Zeitzschel (eds.), *Upwelling in the Ocean: Modern Processes and Ancient Records*. J. Wiley and Sons, New York.
- PICKERING, K.T., T.N. KOREN', V.N. LYTOCHKIN, AND D.J. SIVETER. In press. Siluro–Devonian deep-marine depositional systems, southern Tien Shan, Central Asia. *Journal of the Geological Society of London*.
- PŘIBYL, A. 1983. Graptolite zones of the Kopanina and Pridoli formations in the Upper Silurian of central Bohemia. *Casopis pro Mineralogii a Geologii*, 28:149–167.
- QUINBY-HUNT, M.S., AND W.B.N. BERRY. 1991. Late Wenlock (Middle Silurian) global bioevent: possible chemical cause for mass graptolite mortalities. *Historical Biology*, 5:171–181.
- RICKARDS, R.B. 1976. The sequence of Silurian graptolite zones in the British Isles. *Geological Journal*, 11:153–188.
- . 1978. Major aspects of evolution of the graptolites. *Acta Palaeontologica Polonica*, 23:585–594.
- ŠTORCH, P. 1985. *Orthograptus* s.l. and *Cystograptus* (Graptolithina) from the Bohemian lower Silurian. *Vestník Ustředního Ústavu Geologického*, 60:87–100.
- . 1986. Ordovician–Silurian boundary in the Prague Basin (Barrandian area, Bohemia). *Sborník geologických věd, Geologie*, 41:69–103.
- . 1993. The Wenlock/Ludlow [sic, read n-dash, not virgule] boundary in the Prague Basin (Bohemia): *Jahrbuch der geologischen Bundesanstalt*, Wein, 136:809–839.
- . 1994a. Graptolite biostratigraphy of the Lower Silurian (Llandovery and Wenlock) of Bohemia. *Geological Journal*, 29:137–165.
- . 1994b. Llandovery–Wenlock boundary beds in the graptolite-rich sequence of the Barrandian area (Bohemia). *Journal of the Czech Geological Society*, 39:163–182.
- . 1995a. Biotic crises and post-crisis recoveries recorded by graptolite faunas of the Barrandian area (Czech Republic). *Geolines*, 3:59–70.
- . 1995b. Upper Silurian (upper Ludlow) graptolites of the *N. inexpectatus* and *N. kozłowski* Zones from Kosov Quarry near Beroun (Barrandian area, Bohemia). *Vestník Ceskeho Geologického Ústavu*, 70:65–89.
- . 1996. The basal Silurian *Akidograptus ascensus*–*Parakidograptus acuminatus* Biozone in peri-Gondwanan Europe: graptolite assemblages, stratigraphical ranges and palaeobiogeography. *Vestník Ceskeho Geologického Ústavu*, 71:177–188.
- SUMMERHAYES, C.P., K.-C. EMEIS, M.V. ANGEL, R.L. SMITH, AND B. ZEITSCHSEL. 1995. Upwelling in the ocean: modern processes and ancient records, p. 1–37. In C.P. Summerhayes, K.-C. Emeis, M.V. Angel, R.L. Smith, and B. Zeitzschel (eds.), *Upwelling in the Ocean: Modern Processes and Ancient Records*. J. Wiley and Sons, New York.
- TELLER, L. 1964. Graptolite Fauna and Stratigraphy of the Ludlowian Deposits of the Chelm Borehole, Eastern Poland. *Studia Geologica Polonica*, 13.
- . 1969. The Silurian biostratigraphy of Poland based on graptolites. *Acta Geologica Polonica*, 19:393–501.
- TOGHILL, P. 1968. The graptolite assemblages and zones of the Birkhill Shales (Lower Silurian) at Dob's Linn. *Palaeontology*, 11:654–668.
- URBANÉK, A. 1966. On the morphology and evolution of the Cucullograptinae (Monograptidae, Graptolithina). *Acta Palaeontologica Polonica*, 15:291–554.
- . 1970. Neocucullograptinae n. subfam. (Graptolithina)—their evolutionary and stratigraphic bearing. *Acta Palaeontologica Polonica*, 11:163–388.

- . 1993. Biotic crisis in the history of Upper Silurian graptoloids: a palaeobiological model. *Historical Biology*, 7:29–50.
- . 1995. Phyletic evolution of the latest Ludlow spinose monograptids. *Acta Palaeontologica Polonica*, 40:1–17.
- . In press. Late Ludfordian and early Pridoli monograptids from the Polish Lowland. *Palaeontologia Polonica*, 56.
- VAN CAPPELEN, P., AND E.D. INGALL. 1994. Benthic phosphorus regeneration, net primary productivity, and ocean anoxia: a model of the coupled marine biogeochemical cycles of carbon and phosphorus. *Paleoceanography*, 9:677–692.
- WENZEL, B., AND M.M. JOACHIMSKI. 1996. Carbon and oxygen isotopic composition of Silurian brachiopods (Gotland/Sweden [sic, read comma not virgule]: palaeoceanographic implications. *Palaeogeography, Palaeoclimatology, Palaeoecology*, 122:143–166.
- ZALASIEWICZ, J. 1990. Silurian graptolite biostratigraphy in the Welsh Basin. *Journal of the Geological Society of London*, 147:619–622.
- . 1994. Middle to late Telychian (Silurian: Llandovery) graptolite assemblages of central Wales. *Palaeontology*, 37:375–396.
- , AND S. TUNNICLIFF. 1994. Uppermost Ordovician to Lower Silurian graptolite biostratigraphy of the Wye Valley, Central Wales. *Palaeontology*, 37:695–720.

APPENDIX 1—LIST OF SPECIES AND SUBSPECIES NAMES CITED IN THE TEXT WITH AUTHORSHIP

- Akidograptus ascensus* Davies, 1929
- Atavograptus atavus* (Jones, 1909)
- Bohemograptus bohemicus* (Barrande, 1850)
- B. bohemicus tenuis* (Bouček, 1936)
- B. cornutus* Urbanek, 1970
- Campograptus curtus* Obut and Sobolevskaya, 1968
- Cephalograptus cometa* (Geintitz, 1852)
- Colonograptus colonus* (Barrande, 1850)
- Coronograptus cyphus* (Lapworth, 1876)
- Cucullograptus hemiaversus* Urbanek, 1960
- Cyrtograptus bohemicus* Bouček, 1931
- C. centrifugus* Bouček, 1931
- C. ellesae* Gortani, 1922
- C. falcatus* Lenz and Melchin, 1991
- C. insectus* Bouček, 1931
- C. kolobus* Lenz and Melchin, 1991
- C. laqueus* Jackson and Etherington, 1969
- C. lapworthi* Tullberg, 1883
- C. lundgreni* Tullberg, 1883
- C. malgusaricus* Golikov, 1974
- C. murchisoni* Carruthers, 1867
- C. perneri* Bouček, 1933
- C. polyrameus* Fu and Song, 1985
- C. radians* Törnquist, 1887
- C. ramosus* Bouček, 1931
- C. rigidus* Tullberg, 1883
- C. sakmaricus* Koren', 1968
- C. solaris* Bouček, 1931
- Cystograptus ancestralis* Storch, 1985
- C. vesiculosus* (Nicholson, 1868)
- Demirastrites convolutus* (Hisinger, 1837)
- D. pectinatus* (Richter, 1853)
- D. simulans* (Pedersen, 1922)
- D. triangulatus* (Harkness, 1851)
- Gothograptus nassa* (Holm, 1890)
- Hirsutograptus sinizini* (Chaletzkaya, 1960)
- "Lagarograptus" acinaces* (Törnquist, 1899)
- Linograptus posthumus* (R. Richter, 1875)
- Lobograptus invertus* Urbanek, 1966
- L. parascanicus* (Kühne, 1955)
- L. progenitor* Urbanek, 1966
- L. scanicus* (Tullberg, 1883)
- L? sherrardae* (Sherwin, 1975)
- Monoclimacis crenulata* (Elles and Wood, 1911)
- M? galaensis* (Lapworth, 1876)
- M. griestoniensis* (Nicol, 1850)
- "Monograptus" abhorrens* Přibyl, 1983
- M. argenteus* (Nicholson, 1869)
- M. balticus* Teller, 1964
- M. beatus* Koren', 1983
- M. belophorus* (Meneghini, 1857)
- M. birchensis* Berry and Murphy, 1975
- M. bouceki* Přibyl, 1940
- M. branikensis* Jaeger, 1986
- M. crispus* Lapworth, 1876
- "M". deubeli* Jaeger, 1959
- M. discus* Törnquist, 1883
- M. firmus* Bouček, 1931
- M. flexilis* Elles, 1900
- "M". gemmatus* (Barrande, 1850)
- M. hamulosus* (Tsegelnyuk, 1976)
- M. instrenuus* Lenz and Melchin, 1991
- M. latilobus* (Tsegelnyuk, 1976)
- M. limatulus* Törnquist, 1892
- M. lobiferus* M'Coy, 1850
- M. lochkovenski* Přibyl, 1940
- "M". ludensis* (Murchison, 1839 [=Pristiograptus vulgaris Wood, 1990])
- M. microdon* R. Richter, 1875
- M. microdon aksajensis* Koren', 1983
- M. opimus* Lenz and Melchin, 1991
- M. parultimus* Jaeger, 1975
- M. perneri* Bouček, 1931
- M. perneri kasachstanensis* Mikhaylova, 1975
- "M". praedeubeli* Jaeger, 1990
- M. pridoliensis* Přibyl, 1981
- M. revolutus* Kurck, 1882
- M. riccartonensis* Lapworth, 1876
- M. transgrediens* Perner, 1899
- M. ultimus* Perner, 1899

- M. (Formiosograptus) formosus* (Bouček, 1931)
M. (Uncinograptus) acer (Tsegelnyuk, 1976)
M. (Uncinograptus) spineus (Tsegelnyuk, 1976)
Neocucullograptus inexpectatus (Bouček, 1932)
N. kozlowskii Urbanek, 1970
Neodiplograptus magnus (Lapworth, 1900)
N. thuringiacus (Eisel, 1919)
Neodiversograptus nilssoni (Lapworth, 1876)
Neolobograptus auriculatus Urbanek, 1970
Normalograptus lubricus (Chen and Lin, 1978)
N. nadernii (Koren' and Mikhaylova, 1980)
Oktavites spiralis (Geinitz, 1842)
Paradiversograptus runcinatus (Lapworth, 1876)
Parakidograptus acuminatus (Nicholson, 1867)
Persculptograptus persculptus (Elles and Wood, 1907)
Parapetalolithus hispanicus (Habermelner, 1931)
P. palmeus (Barrande, 1850)
Polonograptus podoliensis Přibyl, 1983
Pribylograptus leptotheca (Lapworth, 1876)
Pristiograptus dubius (Suess, 1851)
P. fragmentalis (Bouček, 1936)
P. longus (Bouček, 1936)
P. parvus Ulst, 1974
P. renaudi (Philippot, 1950)
P. tumescens (Wood, 1900)
Pseudomonoclimacis bandaletovi Mikhaylova, 1975
Pseudorthograptus insectiformis (Nicholson, 1969)
Rastrites linnaei Barrande, 1850
R. maximus Carruthers, 1867
R. orbitus Churkin and Carter, 1970
Saetograptus chimaera (Barrande, 1850)
S. incipiens (Wood, 1900)
S. leintwardinensis (Hopkinson, 1880)
S. linearis (Bouček, 1936)
Spirograptus guerichi Loydell, Štorch and Melchin, 1993
S. turriculatus (Barrande, 1850)
Stimulograptus halli (Barrande, 1850)
S. sedgwickii (Portlock, 1843)
S. utilis Loydell, 1991
Stomatograptus grandis (Suess, 1851)
Streptograptus johnsonae Loydell, 1991
S. sartorius (Törnquist, 1881)
Testograptus testis (Barrande, 1950)
Torquigraptus carnicus (Gortani, 1923)
T. proteus (Barrande, 1850)
T. tullbergi (Bouček, 1931)

RECURRENT SILURIAN–LOWEST DEVONIAN CEPHALOPOD LIMESTONES OF GONDWANAN EUROPE AND PERUNICA

JIRÍ KRÍŽ

Division of Regional Geology of Sedimentary Formations

Czech Geological Survey, P.O.B. 85, Praha 011, 118 21, Czech Republic

ABSTRACT—*Silurian–lowest Devonian cephalopod limestones of Gondwana and Perunica developed on the sea floor below wave base, but were ventilated by surface currents. These limestones are cyclic and indicate sea-level lowstands. This biofacies is represented by thirteen stratigraphic horizons. Comparison of the cephalopod limestone occurrences in different Gondwanan and Perunican basins in Europe makes it possible to distinguish between lowstands caused by syndimentary tectonic uplift and those that resulted from eustatic oscillations. In the Testograptus testis, Colonograptus colonus, upper Saetograptus chimaera, lower S. linearis, Monograptus fragmentalis, M. ultimus, upper M. transgrediens, and lower M. uniformis Zones, cephalopod limestones indicate early transgressive phases of cycles. The oldest cephalopod limestones are in the Cyrtograptus rigidus Zone in the Carnic Alps. Wenlock and Ludlow cephalopod limestones are associated with recurrent bivalve-dominated communities of the Cardiola Community Group, which is composed mostly of epibyssate forms. The upper Přidoli cephalopod limestones have the bivalve-dominated, largely infaunal Joachymia-Cardiolinka-Pygolfia Community of the Snoopyia Community Group. Lowest Devonian cephalopod limestones have the bivalve-dominated Antipleura bohemia Community of the Antipleura-Hercynella Community Group and include mostly infaunal, reclining, and epibyssate forms.*

INTRODUCTION

Silurian and lowest Devonian cephalopod limestones are characterized by abundant cephalopods and bivalves. Gastropods and other mollusks are less common; trilobites and brachiopods are absent or very rare. Cephalopod limestones typically form massive beds about 1 m-thick in the middle and uppermost Ludlow, and occur within shales as isolated nodules, lenses, and thin layers (Wenlock and lower Ludlow). They occasionally form massive layers up to several meters thick (upper Ludlow and upper Přidoli of the Prague Basin), and they may

also occur in sequences dominated by brachiopod and crinoid limestones (upper Ludlow and Přidoli).

Silurian and lowest Devonian cephalopod limestones are known from North Gondwana in Morocco, Algeria, Spain, the Montagne Noire and Massif Armorica in France, Sardinia, the Carnic Alps in Italy and Austria, eastern Serbia, Macedonia, and Turkey (Figure 1). They occur on the Perunica microcontinent (Havlíček et al., 1994) in the Prague Basin of Bohemia.

The Bohemian Massif is assumed to be a composite unit with Gondwanan, Perunican, and Baltic elements (Havlíček et al., 1994). The Perunica microcontinent extends from the south margin of the Bohemian Massif northwards to the mid-European suture that originated with closure of the Rheic Sea, and is now the boundary between the Saxothuringicum and Rhenohercynicum in the Variscan orogen (Burrett-Griffiths, 1977). The tectonic contact between Perunica and the Brunovistulicum is associated with significant overthrusts and nappes with a pronounced eastern vergence, which was first recognized by Suess (1912). The Perunica microcontinent drifted from high latitudes in the southern hemisphere across the paleoequator to the low northern latitudes in the latest Paleozoic. Data for this supposition are presented from Bohemia by Krs et al. (1986, 1987). The independent development of Perunica may be deduced from its probable rotation, as shown by changes in paleomagnetic directions from about 65° in the Middle Cambrian, through 90° in the Upper Cambrian, to 127°–132° in the Lower Ordovician (Krs et al., 1986). These data support Burrett (1983), who reinterpreted the apparent polar wander path to suggest that the Bohemian Massif moved independently of Armorica during the Early Paleozoic.

Cephalopod limestones were recognized by early collectors as rocks with a high concentration of fossils, and have been quarried for those fossils since the eighteenth century. Samples from the Prague Basin in Bohemia with the bivalve *Cardiolinka bohemia* and cephalopods were described and figured by Zeno (1770, p. 397, figs. 2 and 3) almost 230 years ago (Figure 2).

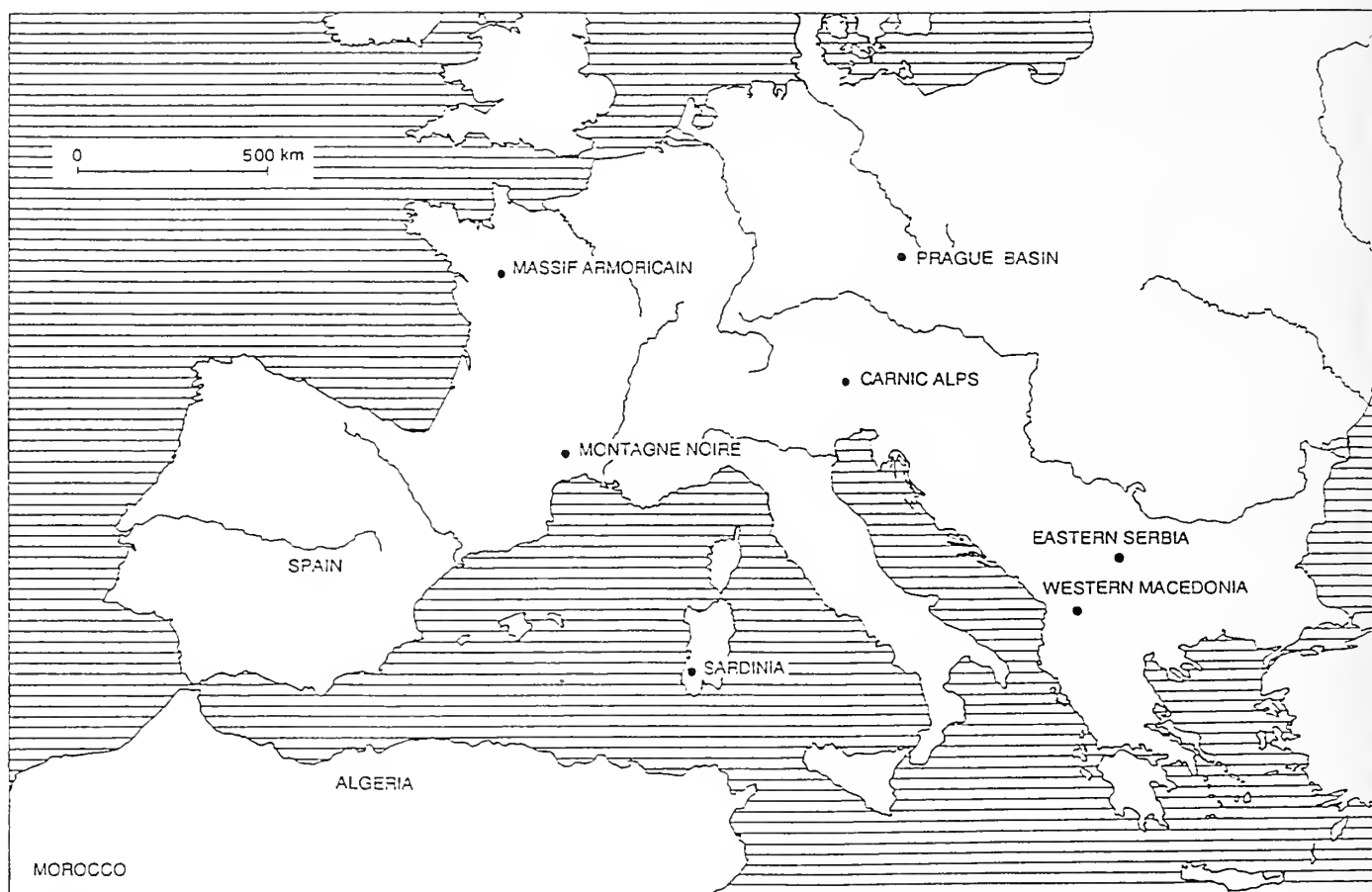


FIGURE 1—Principal localities of cephalopod limestones in Europe and North Africa marked by bold dots.

The cephalopod limestone biofacies in the Prague Basin was first studied by Petránek and Komárková (1953). They measured orientations on current-oriented cephalopod shells in the field, and most of their results are still useful. Detailed interpretation of the biostratigraphy of the biofacies of the Prague Basin is in Ferretti and Kříž (1995). Two facies types were recognized. One was the product of surface currents (i.e., Braník type—named for Braník in the Prague Basin, Figure 3) and the other (Kosov type—named for Kosov in the Prague Basin, Figure 4) resulted from local storm-wave redeposition within a surface current in a shallow environment. The Braník type is more common, and was interpreted (Ferretti and Kříž, 1995) as the “normal” depositional facies (Figure 3). Cephalopod shells are abundant in the limestone and have a uniform orientation.

CEPHALOPOD LIMESTONE BIOFACIES

Cephalopod limestones usually mark a significant change in sedimentation in a generally low-energy envi-

ronment in sequences dominated by shale with micritic limestone intercalations. Deposition of the cephalopod limestone facies (Kříž, 1992, 1997, In press) took place in the upper photic zone below wave base, where surface currents reached the bottom and aligned the shells of nekto-benthic cephalopods. Thick beds of fossil-hash limestones (wacke- to packstones), which represent relatively short periods of high-energy sediment accumulation, alternate with thin micritic limestone intercalations that probably represent long periods of quiet sediment accumulation (Kříž, 1991, 1992).

Microfacies analysis (Ferretti and Kříž, 1995) supports episodic higher-energy deposition of cephalopod wacke- to packstones in sequences characterized by low-energy, finer-grained micritic sediment with small ostracodes, juvenile bivalves, gastropods, crinoids, graptolites, cephalopods, and muellerisphaerids. Small pelagic forms seem to be dominant in the finer-grained sediment. Dissolution effects (stylolites) occur at the lower contact of the wackestones–packstones with the fossiliferous mudstones.

Surface currents ventilated the anoxic bottom below wave base, and periodically lowered the sediment accu-

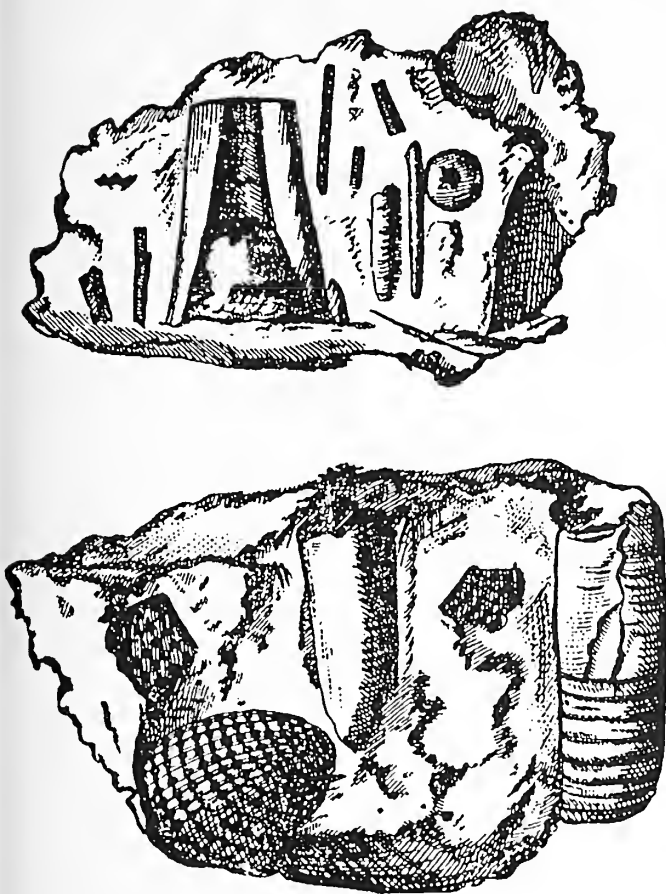


FIGURE 2—Cephalopod limestone samples from quarries in the vicinity of Prague, Bohemia, figured by Zeno (1770).

mulation rate by carrying away the fine-grained, micritic fraction (Kříž, 1997, In press). Large quantities of empty, mostly current-oriented cephalopod shells were deposited. They were probably carried there, at least in part, by the current as empty, floating orthocone shells. Many of the shells came from cephalopods that lived locally in the cephalopod limestone biofacies. This is substantiated by the variable composition of the cephalopod assemblages within a basin (e.g., Prague Basin) and between localities of the same age. Larvae and juvenile forms of trilobites, bivalves, gastropods, cephalopods, and brachiopods, which occupied favorable bottom conditions of at least partially oxic facies, were quickly distributed by surface currents over North Gondwana and Perunica. Longer periods without oxygen or with very low oxygen content are indicated by the limited occurrence of brachiopods, trilobites, and other groups dependent on oxygenated conditions. Some bivalves became specialized for the cephalopod limestone biofacies. Low oxygen content caused periodic mass mortality of the early ontogenetic stages of bivalves, gastropods, and cephalopods at the sediment–water interface, yet the adults survived

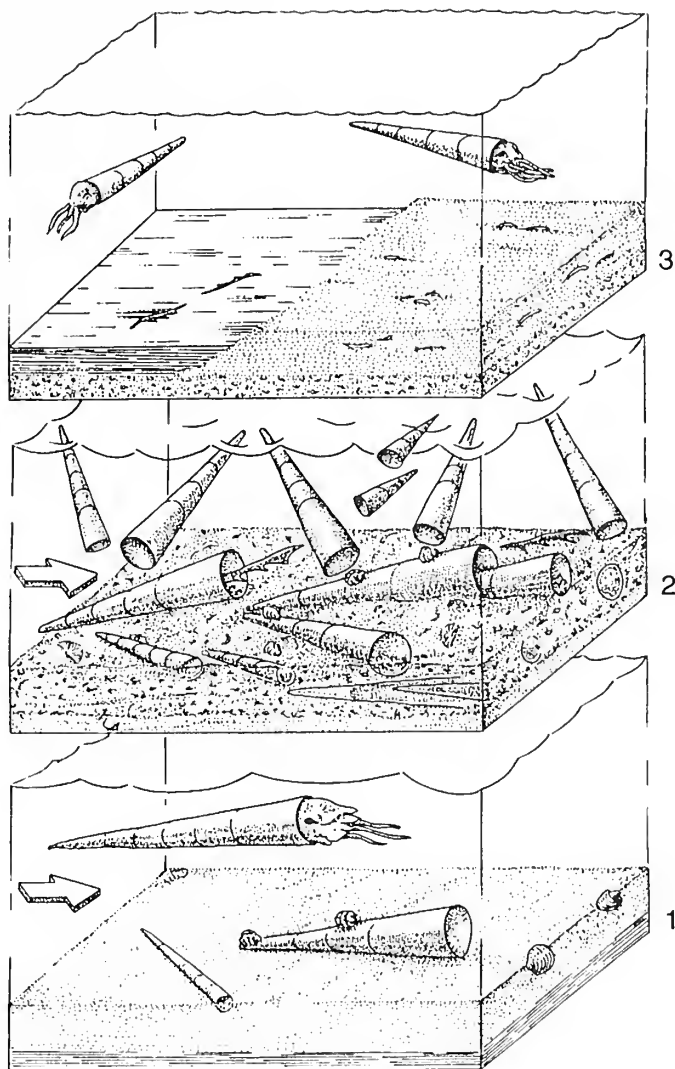


FIGURE 3—Cephalopod limestone biofacies of Braník Type, Prague Basin, Bohemia. 1, quiet area with dark micrite sedimentation and bivalve-dominated *Cheiropteria glabra* Community; 2, deposition of current-oriented cephalopod conchs in cephalopod limestone biofacies; 3, micritic cover is locally developed, or the shell hash limestone is covered by shale. After Ferretti and Kříž (1995).

(Ferretti and Kříž, 1995). The successful and rapid colonization of this unstable environment, which was characterized by fluctuating oxygen content and temperature was often undertaken by cardioid bivalves that shortened their generation times by undergoing early sexual maturity and were thus able to survive (Kříž and Bogolepova, 1995).

A cephalopod limestone facies, in which the sea floor was covered by empty, dead cephalopod conchs, appeared at a number of horizons from the middle Wenlock to the uppermost Přidoli. It was colonized by the Bohemian-type, bivalve-dominated *Cardiola* Community Group (Kříž and Serpagli, 1993; Kříž, 1997, In press),



FIGURE 4—Distribution of Silurian rocks (in black) in the Prague Basin.

which is characterized by dominant epibyssate *Cardiolo-*acea specimens accompanied by *Lunulacardiidae* and *Antipleuridae*. During the Llandovery and early Wenlock, the first representatives of these groups appeared in North Gondwana and Perunica (Havlíček et al., 1994). Their small, pelagic progenetic stages (Gould, 1977; Kříž, 1984) occur in the "shelf pelecypod-graptolite bearing shales" of Berry and Boucot (1967). These bivalves played an important role in colonization of the cephalopod limestone biofacies when conditions were temporarily much more favorable.

The *Cardiola* Community Group includes ten recurring communities (Kříž and Serpagli, 1993; Kříž, 1996, 1997, In press), which mainly reflect the Wenlockian and Ludlovian evolutionary history of epibyssate *Cardiolo-*acea (*Carnalpia*, *Cardiola*, *Slavinka*), *Butovicellidae* (*Butovicella*), and *Lunulacardiidae* (*Mila*, *Spanila*, *Patrocardia*). In this community group, epibyssate forms are dominant (39%–98%) and characteristic. Diversity and population densi-

ties are usually high. Semi-infaunal byssate bivalves are quite common (*Cardiopsis*, *Cardiola*); infaunal bivalves (*Slava*, *Isiola*, *Praecardium*, *Cardiolinka*, *Cardiola*) are generally not dominant, and reclining bivalves are generally very rare (*Maminka*, *Slavinka*, *Dualina*, *Procarinaria*, *Praeostrea*). At each higher stratigraphic level, adaptation to the depositional conditions became better. Kříž (1979) documented the gradual adaptation of the *Cardiolidae* to attachment to the cylindrical surface of dead cephalopod shells.

The *Cardiola* Community Group is very important for stratigraphic purposes. Each cephalopod limestone biofacies level corresponds in the Prague Basin (Kříž,

FIGURE 5—(opposite) Distribution of cephalopod limestones in the Silurian–Lower Devonian of Gondwana and Perunica. Dotted areas represent continuous interval of cephalopod limestones in Prague Basin, Sardinia, and Montagne Noire sequences.

CHRONO - STRATIGRAPHY			BIOSTRATIGRAPHY					
DEVONIAN	LOWER DEVONIAN	LOCHKOVIAN						
			<i>M. uniformis</i> Zone					
SILURIAN	PŘÍDOLÍ		<i>M. transgrediens</i> Zone					
			<i>M. perneri</i> Zone					
			<i>M. bouceki</i> Zone					
			<i>M. lochkovenski</i> Zone					
			<i>M. ultimus</i> Zone					
			<i>M. parullimus</i> Zone					
	LUDLOW	LUDFORDIAN	<i>M. fragmentalis</i> Zone					
			<i>M. latilobus</i> Zone					
			<i>N. kozlowskii</i> Zone					
			<i>N. Inexpectatus</i> Zone					
			<i>B. bohemicus tenuis</i> Zone					
			<i>S. linearis</i> Zone					
	GORSTIAN		<i>S. chimaera</i> Zone					
			<i>C. colonus</i> Zone					
	HOMERIAN		<i>P. ludensis</i> Zone					
			<i>P. praedeubeli</i> - <i>P. deubeli</i> Z.					
			<i>G. nassa</i> Zone					
			<i>P. parvus</i> Zone					
			<i>C. lundgreni</i> Z.	<i>T. testis</i> Subz. <i>C. radians</i> Subz.				
	SHEINWOODIAN		<i>C. perneri</i> / <i>C. ramosus</i> Z.					
			<i>C. rigidus</i> Zone					
			<i>M. belophorus</i> Zone					
			<i>P. dubius</i> Zone					
			<i>M. riccartonensis</i> Zone					
			PRAGUE BASIN					
			NORTHERN SEGMENT	WESTERN SEGMENT	W.-CENTRAL SEGMENT	E.-CENTRAL SEGMENT	PANKRÁC SEGMENT	SOUTHERN SEGMENT

1979) and also in other regions (Sardinia [Kříž and Serpagli, 1993]; France [Kříž, 1996]; Carnic Alps in Austria and Italy [Schönlaub, 1980]) to established graptolite and conodont zones, and may be recognized and correlated solely on the basis of the bivalve community composition despite the fact that graptolites or conodonts are usually rare or missing. Most of these levels occur close to the series boundaries (Wenlock–Ludlow, Ludlow–Přidoli, and Přidoli–Lochkov; Figure 5).

During the late Přidoli, the *Cardiola* Community Group was replaced by communities of the *Snoopyia* Community Group. The later is represented in the cephalopod limestone biofacies by the *Joachymia-Cardiolinka-Pygolfia* Community. The base of the Lochkov (Lower Devonian) has the later *Antipleura-Hercynella* Community Group, which is represented in the cephalopod limestone biofacies by the *Antipleura bohémica* Community (Kříž, 1997, In press). The number of epibyssate forms decreases in the upper Přidoli (26%) and in the Lochkov (16–18%), and reclining and infaunal forms become dominant (Přidoli with 69.5%, and Lochkov with 81%).

CYRTOGRAPTUS RIGIDUS ZONE LIMESTONE

GEOGRAPHIC DISTRIBUTION.—Carnic Alps of Austria and Italy (North Gondwana).

TYPE LOCALITY, LITHOLOGY, AND AGE.—Mount Cellon in the Carnic Alps, Austria (Kříž, 1979). Lenses of dark biomicrite to shell-hash limestone with juvenile cephalopods in dark graptolitic shales of Kok Formation, middle Wenlock (Sheinwoodian Stage). Horizon is part of the ferruginous limestone interval. Age from Jaeger (1975), who found *Cyrtograptus rigidus* in the shales (layer 12 C) just above lenses of cephalopod limestone (layer 12 B), and from Schönlaub (1980), who identified the *Kockella patula* Zone in layers 12 B and 12 C.

FOSSIL COMMUNITY DESCRIPTION.—*Carnalpia nivosa* Community of the *Cardiola* Community Group (Kříž, 1997, In press). Mostly disarticulated bivalves. Population densities reasonably high. All bivalves filter feeders; 58.5% epibyssate, 22% semi-infaunal, 6% reclining. Epibyssate bivalves show adaptations to life on bottom sediment. Bivalvia: *Cardiola bifasciata*, *Cardiola* sp. aff. *C. agna*, *Cardiolopsis alpina*, *Carnalpia nivosa*, *C. rostrata*, "*Hemicardium*" sp., *Maminka* sp. cf. *M. comata*, *Patrocardia* sp., *Slavinka* sp., rare disarticulated trilobites (*Aulacopleura*, Cheiruridae, Encrinuridae, Odontopleuridae, Proetidae), common juvenile stages of bivalves and gastropods, cephalopod fragments, and very rare disarticulated bra-

chiopods. Cephalopods (Š. Manda, personal commun., 1997) mostly juvenile forms; most common are *Hemicosmorthoceras* sp., *Michelinoceras* n. sp., *Orthocycloceras* sp. aff. *O. pedum*, *Parasphaerorthoceras*? sp., and *Protobactrites* sp.

LOCALITIES.—Austria—Carnic Alps, Mount Cellon (Schönlaub, 1980); Italy—Carnic Alps, Mt. Cocco (Heritsch, 1929; von Gaertner, 1931).

TESTOGRAPTUS TESTIS SUBZONE LIMESTONE

GEOGRAPHIC DISTRIBUTION.—Prague Basin, Bohemia (Perunica); Carnic Alps, Austria (North Gondwana).

TYPE LOCALITY, LITHOLOGY, AND AGE.—Arethusina Gorge, Praha-Řeporyje, Prague Basin, Bohemia. Lenticular fossil-hash limestone with cephalopods form a thin bed (up to 10 cm) in graptolitic shales of Motol Formation, upper Wenlock (Homerian Stage). Age determined by *Testograptus testis* in the shales below and above the cephalopod limestone (Kříž et al., 1993). At this level, the conodont *Ozarkodina sagitta sagitta* occurs with early representatives of *Ozarkodina bohémica* and indicates the *Ozarkodina sagitta sagitta* Zone (H.P. Schönlaub in Kříž et al., 1993).

FOSSIL COMMUNITY DESCRIPTION.—*Cardiola agna agna* Community of the *Cardiola* Community Group (Kříž, 1997, In press). Population densities high. Very common fragments and complete shells of cephalopods, mostly orthocones, covered most of the sea floor and formed a substrate for abundant epibyssate bivalves (39.2%). Some genera (*Cardiola*, *Patrocardia*, and *Spanila*) show adaptations to firm byssate attachment on the surface of cylindrical cephalopod shells (Kříž, 1979, 1984). Shell-hash sediment also suitable for infaunal bivalves (37.7% *Slava*, *Isiola*, "*Modiolopsis*"). Articulated infaunal shells are very commonly preserved in life position at the type locality (Kříž, 1985). Mostly disarticulated but common articulated infaunal bivalves preserved mostly in life position (5.4%). Bivalvia: *Butovicella migrans*, *Cardiola agna*, "*Cypricardina*", *Dualina*, *Isiola lyra*, *Maminka comata*, "*Modiolopsis*" sp., *Patrocardia*, *Praeostrea bohémica*, *Procarinata zephyrina*, *Slava pelerina*, *S. discrepans*, and *Spanila*. Trilobite *Aulacopleura konincki* disarticulated and very rare. Tabulate corals (*Favosites*) and brachiopods (*Bleshidium papalas*) rare. Very abundant fragments of non-vascular plants (*Pachytheca* and *Prototaxites*) and graptolite rhabdosomes (*Monograptus priodon flemingii*). Local accumulations of juvenile bivalves, gastropods, and cephalopods. Cephalopods: assemblage with *Aptychopsis*,

Arionoceras valens, *Harrisoceras*, *Kopaninoceras*, *Michelinoceras*, *Octameroceras*, *Oonoceras*, *Orthocycloceras pedum*, *Pseudocycloceras* sp. cf. *P. transiens*, *Sphooceras truncatum*, and *S. disjunctum* (Š. Manda, personal commun., 1997).

LOCALITIES.—Austria—Carnic Alps, Rauchkofel Boden Section (Schönlaub and Bogolepova, 1994). Bohemia—Prague Basin (Figure 4), Praha-Řeporyje, Arethusina Gorge (Kříž et al., 1993; Kříž, 1997, In press); Praha-Pankrác, Mládežnická and Motokov sections (Kříž et al., 1993); Praha-Podolí, Hláška locality; Praha-Smíchov, Konvářka Section (Kříž et al., 1993).

REMARKS.—The upper Wenlock–lowermost Ludlow cephalopod limestones in Sardinia and France represent a long stratigraphic interval from the *Cyrtograptus lundgreni* to the *Colonograptus colonus* Zones. The limestones are lenses and nodules of dark micritic limestone within shales (Kříž and Serpagli, 1993). The uppermost Wenlock *Pristiograptus parvus* to *P. ludensis* Zones are not recorded here, and sediment accumulation through this interval was most probably minimal.

The type locality for the Sardinia and France cephalopod limestones is the Xea S'Antonio, Fluminimaggiore, Sardinia. Dark micrite to biomicritic limestones (Ferretti, 1989) with cephalopods form lenses in the black shales. The Fluminimaggiore Formation is upper Wenlock and lower Ludlow. The age was determined by H. Jaeger in 1987 (Kříž and Serpagli, 1993), who identified *Monograptus priodon flemingii* from block 1/11 (which indicates the *Cyrtograptus lundgreni* Zone, Wenlock) and *Colonograptus colonus* from block 1/17 (which indicates the *C. colonus* Zone, Ludlow). From the second block, conodonts of the *Ozarkodina bohémica* and *Ancoradella ploeckensis* Zones were identified by E. Serpagli (Kříž and Serpagli, 1993). The same age in the Montagne Noire is based on the occurrence of *Monograptus priodon flemingii*, which indicates the *Cyrtograptus lundgreni* Zone for the *Cardiola agna figusi* Community.

FOSSIL COMMUNITY DESCRIPTION.—*Cardiola agna figusi* Community of the *Cardiola* Community Group (Kříž and Serpagli, 1993; Kříž, 1996). Population densities high. Abundant cephalopod shells provided a substrate for the abundant epibyssate bivalves (59.4%). Micritic sediment was suitable for infaunal bivalves (18%). The *Cardiola agna figusi* Community shows a close relationship to the *Cardiola agna* Community in Bohemia and the Carnic Alps; differences at the species and subspecies level most probably resulted from adaptation to micritic sediment in Sardinia and the Montagne Noire. Mostly disarticulated (81%) bivalves: *Butovicella migrans*, *Cardiola agna figusi*, *Isiola lyra*, *Maminka comata*, *Mytilarca* sp., *Patrocardia*

alifera, *Slava discrepans*, *S. fibrosa*, *S. pelerina*, *Spanila aspirans*, *S. cardiopsis*, *Stolidotus cactus*, *S. elongatus*, *S. siluricus*, and *S. trimerus*. Cephalopods: mostly fragmented and subinvariant to bivalves include *Aptychopsis prima*, *Arionoceras affine*, *A. submoniliforme*, *Columenoceras grande*, *Phragmoceras* sp. aff. *P. broderipi*, *Pseudocycloceras transiens*, and *P. gruenewaldti*. Very rare, smooth, articulate brachiopods relatively common, with well-preserved graptolites (*Monograptus priodon flemingii* and *Colonograptus colonus*). Cephalopods described by Gnoli and Serpagli (1991) as an assemblage with *Pseudocycloceras transiens* and *Columenoceras grande*, but because of lack of stratigraphic control, these authors mixed species from Wenlock and Ludlow.

LOCALITIES.—Italy—Sardinia, Xea S'Antonio, Fluminimaggiore (Kříž and Serpagli, 1993); France—Montagne Noire, Roquemaillière, Combe d'Yzarne, and Vigne de M. Sorgnes near Félines-Termenés (Kříž, 1996).

COLONOGRAPTUS COLONUS ZONE LIMESTONE

GEOGRAPHIC DISTRIBUTION.—Prague Basin, Bohemia (Perunica).

TYPE LOCALITY, LITHOLOGY, AND AGE.—Na Břekvici hillside, Praha-Butovice, Prague Basin, Bohemia (Kříž, 1961, 1992). Fine- to coarse-grained cephalopod limestone as lenses in tuffaceous shales and tuff, Kopanina Formation, Ludlow. Age determined in 1961 by H. Jaeger, who identified *Bohemograptus bohemicus bohemicus*, *Colonograptus colonus*, *C. roemeri*, *Monograptus uncinatus*, *Neodiversograptus nilssoni*, *Plectograptus macilentus*, and other graptolites from the cephalopod limestone (Kříž et al., 1993). Conodonts identified by H.P. Schönlaub represent the *Ozarkodina bohémica* Zone (Kříž et al., 1993). The same conodont zone was identified from cephalopod limestone blocks 1/1 and 1/3 from the Xea S'Antonio locality, Fluminimaggiore, Sardinia by E. Serpagli (Kříž and Serpagli, 1993).

FOSSIL COMMUNITY DESCRIPTION.—*Cardiola gibbosa* Community of the *Cardiola* Community Group (Kříž and Serpagli, 1993; Kříž, 1997, In press). Population density and diversity high. Post-mortem accumulations of fragments and complete shells of mostly nekto-benthic cephalopods provided a substrate for very common epibyssate bivalves (76%). Some genera (*Cardiola*, *Mila*, *Patrocardia*, *Slavinka*, and *Spanila*) adapted to life on the cylindrical shells of cephalopods (Kříž, 1979, 1984). Shell-hash sediment suitable for infaunal forms (15.2% *Isiola*, *Slava*, and

"*Modiolopsis*"), semi-infaunal forms (1% *Modiolopsis senilis*), and reclining byssate forms (6.4% *Dualina*, *Maminka*, and *Procarinaria*). Local accumulations of articulated juveniles of bivalves and brachiopods. Orthocones strongly oriented by current activity. Mostly disarticulated (96%) bivalves: *Actinopteria*, *Butovicella migrans*, *Cardiola contrastans*, *C. gibbosa*, *Dualina*, *Isiola ampliata*, *Maminka comata*, *Manulicula manulia*, *Mila*, *Modiolopsis senilis*, "M." sp., *Patrocardia*, *Procarinaria zephyrina*, *Praeostrea bohémica*, *Slava bohémica*, *S. decurtata*, *S. pelerina*, and *Slavinka*. Cephalopods: an assemblage with *Caliceras capillosum* and *Pseudocycloceras transiens* (Š. Manda, personal commun., 1997) with "*Anaspyroceras*" sp. aff. "*A.*" *pseudocalamiteum*, *Aptychopsis*, *Arionoceras*, *Caliceras spinari*, *Columenoceras*, *Jonesoceras jonesi*, *Kionoceras electum*, *Mariaceras pragense*, *Ophioceras*, *Peismoceras*, *Phragmoceras*, *Plagiostomoceras*, *Protobactrites*, *Rizosceras*, and *Sphooceras*. Gastropods distinctly subdominant to bivalves. Graptolites relatively common. Non-vascular plants (*Pachytheca* and *Prototaxites*) locally abundant. Monoplacophorids (*Drahomira* and *Undicoruu*) rare; trilobites very rare and mostly disarticulated (*Bumastus*, *Odontopleura*, and *Kosovopeltis*).

LOCALITIES.—Bohemia—Prague Basin (Figure 4), Praha-Butovice, Na Břekvici, Velká Chuchle railroad station at "colonie" Krejčí and upper part of the Kavčí Hory section (Kříž et al., 1993).

UPPER SAETOGRAPTUS CHIMAERA ZONE LIMESTONE

GEOGRAPHIC DISTRIBUTION.—Sardinia, Italy; Montagne Noire, France (North Gondwana); Prague Basin, Bohemia (Perunica).

TYPE LOCALITY, LITHOLOGY, AND AGE.—S'Antonio Donigala, Sardinia. Micritic to biomicritic, dark gray limestone, Fluminimaggiore Formation, Ludlow. E. Serpagli identified the long-ranging conodont *Ozarkodina excavata excavata* from block 6/7 (Kříž and Serpagli, 1993). In the Prague Basin, Bohemia, relatively thin layers, lenses, and nodules of cephalopod limestone occur just below the *Saetograptus linearis* Zone (Vonoklasy, Loděnice-Sedlec).

FOSSIL COMMUNITY DESCRIPTION.—*Cardiola donigala* Community and *Slava cubicula-Cardiola donigala* Community (originally published as *Slava cubicula-Cardiola docens* Community by Kříž, 1997, In press) of the *Cardiola* Community Group (Kříž and Serpagli, 1993; Kříž, 1996). *Cardiola donigala* Community (Kříž and Serpagli, 1993) has relatively low population density and diversity. Com-

mon nekto-benthic cephalopods provided a substrate for such epibyssate bivalves as *Cardiola consanguis*, *C. donigala*, *C. sp. cf. C. aff. docens*, *C. sp. cf. signata*, *Maminka comata*, *Patrocardia* sp. aff. *P. calva*, *P. sp.*, and *Slavinka amarygma*. Abundant unrevised orthocone cephalopods present. *Slava cubicula-Cardiola donigala* Community (Kříž, 1997, In press) has disarticulated shells in micritic to fossil-hash limestone, which forms a 25–30 cm-thick bed in tuffaceous shales at the Lodnice-Sedlec locality near Beroun (Kříž, 1970). Bivalves: *Cardiola donigala*, *Maminka comata*, *Mila*, *Slava cubicula*, *Slavinka damona*, and *S. iduna*. Cephalopods: mostly unrevised assemblage (Š. Manda, personal commun., 1997) with *Arionoceras*, *Cyrtocycloceras*, *Geisonoceras*, *Kopaninoceras*, *Michelino-ceras*, *Octameroceras*, *Oonoceras*, *Ophioceras simplex*, *Orthocycloceras*, *Peismoceras asperum*, *Pseudocycloceras*, and *Tetrameroceras*. Non-vascular plant (*Prototaxites*) and rare articulated brachiopod (*Septatrypa*) present.

LOCALITIES.—Italy—Sardinia, S'Antonio Donigala; France—Montagne Noire, Roquemaillère, Combe d'Yzarne; Bohemia—Prague Basin (Figure 4), Barrande's (1881) Loděnice (Lodenitz-e2) locality between the villages of Sedlec and Lodnice near Beroun (Kříž, 1970), and fields west of Vonoklasy near Praha.

LOWER SAETOGRAPTUS LINEARIS ZONE LIMESTONE

GEOGRAPHIC DISTRIBUTION.—Morocco, Spain, France, Sardinia, Austria (North Gondwana); Prague Basin, Bohemia (Perunica).

TYPE LOCALITY, LITHOLOGY, AND AGE.—Barrande's (1881) test pit near the road from Koledník hamlet to Konprusy village near Beroun, Prague Basin, Bohemia (Kodym et al., 1931, locality no. 17). Shell-hash limestone in Kopanina Formation, Ludlow. Shales above the limestone bed yield *Bohemograptus bohemicus tenuis*. At the Mušlovka no. 687 section (Kříž, 1992) near Praha-Řeporyje, the zonal species *Saetograptus linearis* occurs in the cephalopod limestone. Conodonts of the *Polygnathoides siluricus* Zone were identified in cephalopod limestones at the Mušlovka section by Schönlaub (1980). Very characteristic is the occurrence of the pelagic ostracode *Entomis migrans* in this limestone at almost all known localities in North Gondwana and Perunica (Kříž, 1991, 1997, In press).

FOSSIL COMMUNITY DESCRIPTION.—*Cardiola docens* Community of the *Cardiola* Community Group (Kříž and Serpagli, 1993; Kříž, 1996, 1997, In press). Population density and diversity very high. Post-mortem accumulations

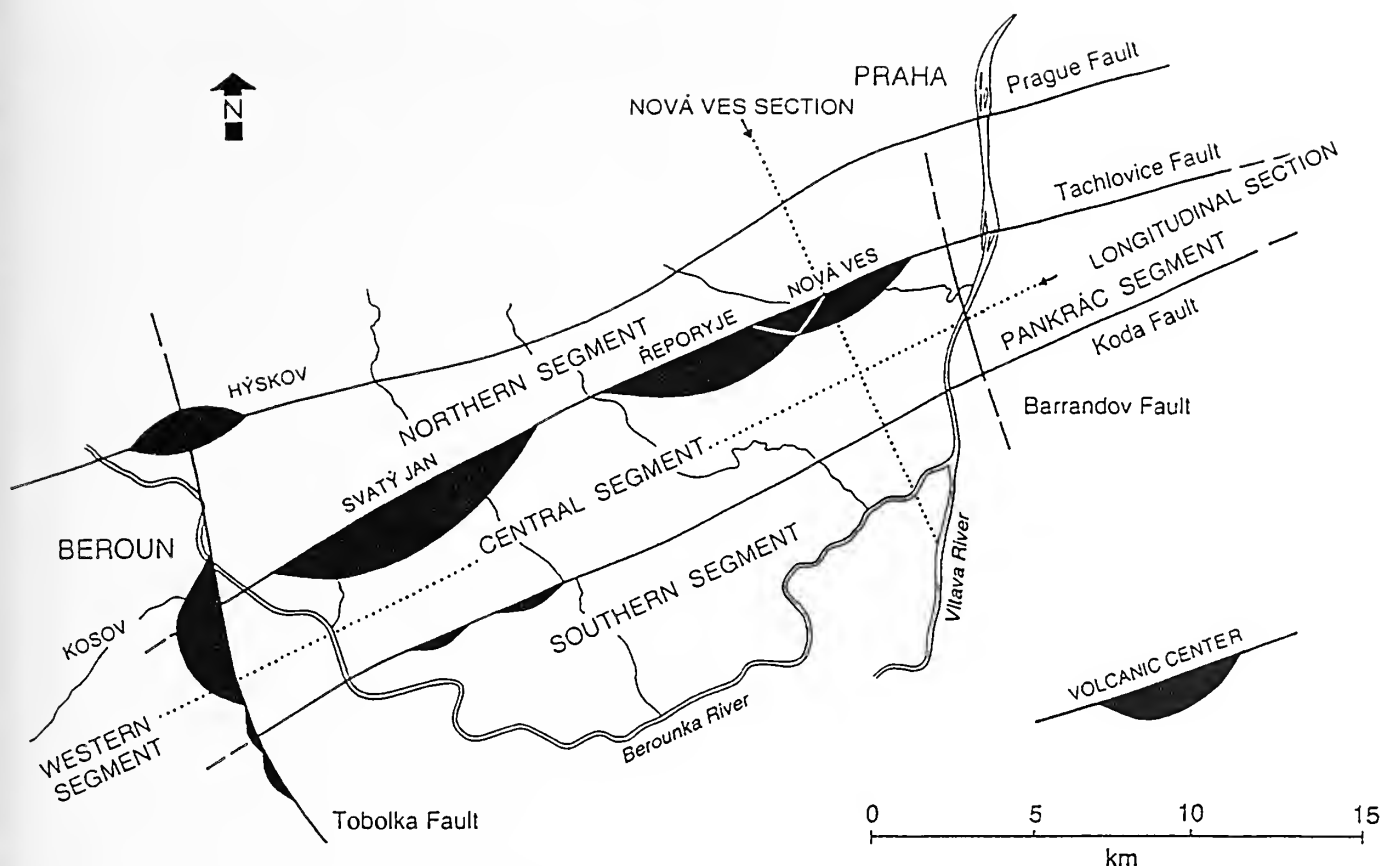


FIGURE 6—Prague Basin, Bohemia. Silurian synsedimentary tectonics, volcanic centers, and fault-bounded segments (dotted lines indicate sections in Figure 7; after Kříž, 1991).

of mostly nekto-benthic cephalopod conchs provided a substrate for very common epibyssate bivalves (95–99%). Some genera (*Cardiola*, *Mila*, *Patrocardia*, *Slavinka*, and *Spanila*) especially adapted to life on cylindrical cephalopod shells (Kříž, 1979, 1984). Shell-hash on bottom also suitable for reclining forms (*Dualina longiuscula*, *D. spp.*). Local accumulations of articulated juveniles of bivalves and brachiopods. Bivalvia: *Butovicella migrans*, *Cardiola consanguis*, *C. docens*, *C. signata*, *C. spurius*, *C. tix*, *Dualina longiuscula*, *D. sp.*, *Mila*, *Patrocardia simplex*, *Praecardium*, *Pygolfia seladon*, *Slavinka imperficiens*, *S. distincta*, and *Spanila*. Cephalopods: assemblage with *Sphooceras truncatum* (Š. Manda, personal commun., 1997) with *Kionoceras bacchus*, *Kopaninoceras*, *Michelinoceras*, *Octamero-ceras*, *Oonoceras*, *Ophioceras simplex*, and *Rizosceras*.

LOCALITIES.—Italy—Sardinia, Galemmu locality, Fontanamare, (Kříž and Serpagli, 1993); Austria—Carnic Alps, Rauchkofel Boden section, bed no. 3 (Schönlaub and Bogolepova, 1994), Mount Cellon section, *Cardiola* Formation (Schönlaub, 1980); France—Montagne Noire, Combe d'Yzarne (Kříž, 1996); Spain; Morocco; Bohemia—Prague

Basin (Figure 4), Koledník near Beroun, Lištice (Kříž, 1992); Praha-Butovice, Kovářovic mez (Kříž, 1992), oldest part exposed in the Mušlovka Quarry (Kříž, 1992) and Velký vrch u Koněprus (Kříž, 1979).

REMARKS.—General uplift of the eastern Central Segment of the Prague Basin (Kříž, 1991) during the late Ludlow and locally in the early Přidoli resulted in favorable conditions for development of cephalopod limestone biofacies (Figure 6). Cephalopod limestones in the *Saetograptus linearis*–*Monograptus fragmentalis* Zones, and even up to the *Monograptus lochkovens* Zone at the Hvíždalka locality (Kříž et al., 1986). Almost continuous cephalopod limestone sequences occur in sections through this interval in such Prague Basin localities as Praha-Vyskočilka, Praha-Velká Chuchle, Praha-Lochkov (Marble Quarry), Praha-Hvíždalka and Kosoř. Similar uplift occurred in the eastern part of the Western Segment of the Prague Basin during the early and middle Ludfordian, and led to continuous accumulation of the cephalopod limestone facies in the *Saetograptus linearis* and *Bohemograptus bohemicus tenuis* Zones at Velký vrch u Koněprus.

UPPER SAETOGRAPTUS LINEARIS ZONE LIMESTONE

GEOGRAPHIC DISTRIBUTION.—Prague Basin, Bohemia (Perunica).

TYPE LOCALITY, LITHOLOGY, AND AGE.—Mušlovka Quarry section, Praha-Řeporyje, Prague Basin, Bohemia (Kříž, 1992), a fossil-hash limestone with abundant cephalopods, beds no. 1–2 (Bouček, 1937, p. 11, layer no. 3). Kopanina Formation, upper part of *Saetograptus linearis* Zone, Ludlow (lower Ludfordian). Abundant occurrence of trilobite *Metacalymene baylei* characteristic of this cephalopod limestone at all Prague Basin localities.

FOSSIL COMMUNITY DESCRIPTION.—Population density and diversity high. Mostly nektobenthic cephalopods, which are less common than in lower *Saetograptus linearis* Zone. Common epibyssate bivalves (95–99%). Shell-hash-rich sea floor better oxygenated, with brachiopods (*Bleshidium*, *Septatrypa*) and trilobites (*Diacanthaspis* (*Acanthalomina*) *Encrinuraspis*, *Metacalymene*, *Otarion*, *Prantlia*, *Prionopeltis*, etc.). Bivalves: *Butovicella migrans*, *Cardiola docens*, *C. signata*, *Patrocardia*. Cephalopods: assemblage with *Phragmoceras* and *Protophragmoceras* (Š. Manda, personal commun., 1997) with *Octameroceras*, *Oonoceras*, *Oxygonioceras*, *Rizosceras*, and *Trimeroceras*. Brachiopods: common *Bleshidium*, rare *Septatrypa sapho*. Trilobites relatively abundant (Chlupáč, 1987): *Diacanthaspis* (*Acanthalomina*) *minuta*, *Encrinuraspis beaumonti*, *Metacalymene baylei*, *Otarion diffractum*, *Prantlialongula*, and *Prionopeltis praecedens*. Unrevised gastropods present.

LOCALITIES.—Bohemia—Prague Basin (Figure 4), Mušlovka Quarry section (Kříž, 1992); Požáry section (Kříž, 1992); Kosov Quarry section no. 777 (bed no. 29) and no. 778 (bed no. 1) (Kříž, 1992); Dlouhá Hora, south of the Kosov Quarry and Velký Vrch u Koněprus (Kříž, 1992).

BOHEMOGRAPTUS BOHEMICUS TENUIS ZONE LIMESTONE

GEOGRAPHIC DISTRIBUTION.—Prague Basin, Bohemia (Perunica).

TYPE LOCALITY, LITHOLOGY, AND AGE.—Kosov Quarry section no. 782, layer no. 10 (Kříž, 1992), Kopanina Formation, Ludlow. Shell-hash limestone developed below layers with mass occurrence of *Atrypoides linguata*.

FOSSIL COMMUNITY DESCRIPTION.—Population density and diversity of cephalopods high. Bivalves quite rare, with *Cardiola* sp. *C. aff. eximia*, *Mila*. Cephalopods: an assemblage with *Cyrtocycloceras peccatum* (Š. Manda, personal commun. 1997) and *Geisonoceras*, *Harrisoceras*, *Michelinoceras*, *Octameroceras*, *Oonoceras*, *Ophioceras*, *Parakionoceras* sp. cf. *P. originale*, and *Sphooceras truncatum*. This horizon represents the Kosov-type cephalopod limestone described by Ferretti and Kříž (1995), which is most probably the result of redeposition by the surface current in a shallow environment during storm events.

In the eastern part of the Western Segment of the Prague Basin (Velký Vrch u Koněprus locality) on a bedding surface of a thick cephalopod bed, there is a coeval cephalopod assemblage with *Murchisoniceras murchisoni* (Š. Manda, personal commun., 1997). The assemblage with *Cyrtocycloceras peccatum* lived on the gentle slope of the Kosov Volcano, while the assemblage with *Murchisoniceras murchisoni* lived on the sea floor some distance from the Kosov volcanic center. There are transitions between these assemblages.

LOCALITIES.—Bohemia—Prague Basin (Figure 4), Kosov Quarry section no. 782 and no. 418 B (Kříž, 1992), Amerika quarries near Karlštejn, and Liščí Quarry (Kříž, 1992).

NEOCUCULLOGRAPTUS KOZLOWSKII ZONE LIMESTONE

GEOGRAPHIC DISTRIBUTION.—Suva Planina Mountains, eastern Serbia (North Gondwana); Prague Basin, Bohemia (Perunica).

TYPE LOCALITY, LITHOLOGY, AND AGE.—Požáry section, Praha-Řeporyje, Prague Basin, Bohemia (Kříž et al., 1986), layers no. 33–34, Kopanina Formation, Ludlow. Fossil-hash limestone developed above layers with mass occurrence of *Atrypoides linguata*, and just below horizon with *Ananaspis fecunda*. The *Neocucullograptus kozlowskii* Zone (Štorch, 1995) occurs in the Kosov Quarry near Beroun at the same level. Conodonts of the *Polygnathoides siluricus* Zone (rich fauna with *P. emarginatus* and *P. siluricus*) was identified by Schönlaub (1980) from this level at Mušlovka Quarry.

FOSSIL COMMUNITY DESCRIPTION.—*Cardiola alata* Community of the *Cardiola* Community Group (Kříž, 1997, In press). Population density and diversity very high. Sea floor covered with shell fragments; post-mortem accumulations of fragments and complete shells of mostly nektobenthic cephalopods provided substrate for

byssate, semi-infaunal cardioids (47%). Reclining bivalves common (35.5% *Dualina*). Some genera (*Mila*, *Patrocardia*, *Spanila*, *Tenka*) epibyssate (17.5%). Local accumulations of articulated juveniles of bivalves and brachiopods. Orthocones strongly oriented by current activity. Bivalves: *Cardiola alata*, *C. eximia*, *C. pectinata*, *Dualina longiuscula*, *Mila*, *Patrocardia*, *Praecardium*, *Spanila*, and *Tenka*. Cephalopods: assemblage with *Parakionoceras* and "*Cyrtoceras*" *parvulum* (Š. Manda, personal commun., 1997). In the vicinity of the Nová Ves volcanic center, a cephalopod fauna includes *Arionoceras*, "*Cyrtoceras*" *parvulum*, *Cyrtocycloceras*, *Geisonoceras*, *Glossoceras*, *Michelinoceras*, *Octameroceras*, *Oonoceras*, *Ophioceras*, *Parakionoceras* sp. aff. *P. originale*, *Pentameroceras mirum*, *Protophragmoceras beaumonti*, and *Sphooceras*.

LOCALITIES.—Bohemia—Prague Basin (Figure 4), Praha-Vyskočilka and Praha-Slivenec (Kříž, 1961); Praha-Velká Chuchle Praha-Lochkov (Marble Quarry), Praha-Hvízdalka, and Kosoř (Kříž et al., 1986); Mušlovka Quarry section, bed no. 6 (Bouček, 1937, p. 13; Kříž, 1992, beds no. 13–15); Požáry Section, beds no. 33–34 (Kříž, 1992); Praha-Butovice and Pod Hradištěm.

LOWEST MONOGRAPTUS LATILOBUS ZONE LIMESTONE

GEOGRAPHIC DISTRIBUTION.—Prague Basin, Bohemia (Perunica).

TYPE LOCALITY, LITHOLOGY, AND AGE.—Barrande's (1881) locality in the upper Kopanina Formation between the U Topolů (Chlupáč, 1972) and the Marble Quarry section (Kříž, 1992) near Lochkov, Prague Basin, Bohemia (Kříž et al., 1986; Kříž, 1992); fossil-hash limestone with abundant cephalopods, horizon with *Ananaspis fecunda*, Ludlow (Ludfordian).

FOSSIL COMMUNITY DESCRIPTION.—Bivalves relatively rare: *Cardiola signata* and *Patrocardia* spp. Cephalopods include *Cummingsoceras sacheri*, *Glossoceras*, *Lechritrochoceras placidum*, *L. simulans*, *L. trochoides*, *Mandaloceras*, *Oocerina*, *Ophioceras*, and *Trimeroceras cylindricum* (Š. Manda, personal commun., 1997). Relatively abundant but unrevised gastropods.

LOCALITIES.—Bohemia—Prague Basin (Figure 4), localities at Butovice and tectonic blocks southwest of Kovářovic mez (Kříž, 1992); Praha-Vyskočilka, Praha-Velká Chuchle, Praha-Lochkov (Marble Quarry), Praha-Hvízdalka and Kosoř (Kříž et al., 1986; Kříž, 1992).

LIMESTONE IN MONOGRAPTUS FRAGMENTALIS–M. PARULTIMUS ZONES

GEOGRAPHIC DISTRIBUTION.—Carnic Alps, Austria; Suva Planina Mountains, eastern Serbia (North Gondwana); Prague Basin, Bohemia (Perunica).

TYPE LOCALITY, LITHOLOGY, AND AGE.—Cephalopod quarry, Praha-Lochkov, Prague Basin, Bohemia (Kříž, 1992). Fossil-hash cephalopod limestones in more than 1 m-thick bed, in *Monograptus fragmentalis* Zone to top of *M. parultimus* Zone, Kopanina Formation. At Hvíždalka section near Praha-Radotín, Prague Basin, Bohemia (Kříž et al., 1986), cephalopod limestones up to *Monograptus lochkovens* Zone (shales just above the cephalopod limestone correspond to *M. pridoliensis* Zone). Conodonts from upper part of *Ozarkodina snajdri* Zone through *O. crispa* and up to lowermost *O. remscheidensis eostein-hornensis* Zones (Schönlaub in Kříž et al., 1986).

FOSSIL COMMUNITY DESCRIPTION.—*Cardiola conformis* Community in uppermost Ludlow and *Cardiolinka bohémica* Community in lowermost Přidoli, *Cardiola* Community Group (Kříž, 1997, in press).

The *Cardiola conformis* Community features mostly disarticulated (86%–90%) shells in shell-hash limestones with abundant nektobenthic cephalopods. Epibyssate bivalves dominant (60–69%), reclining forms relatively common (23–38%), infaunal forms only at some horizons (7%). Orthoconic cephalopod conchs strongly oriented by SSW–NNE currents. Very condensed, slow sediment accumulation rate with some breaks. Population density and diversity very high. Bivalves: *Butovicella medea*, *Cardiola conformis*, *C. cornucopiae*, *C. navicula*, *Cardiolinka bohémica*, *Dualina longiuscula*, *Patrocardia*, *Spanila*, and *Tetinka*. Cephalopods include "*Cyrtoceras*" *quasirectum*, *Dawsonoceras caelebs*, *Geisonoceras nobile*, *G. rivale*, *G. severum*, *G. socium*, *Glossoceras*, *Hexameroceras*, *Kionoceras neptunicum*, *Kosovoceras nodosum*, *K. sandbergeri*, *Lechritrochoceras degener*, *Michelinoceras* sp. cf. *M. michelini*, *Oocerina lentigradum*, *Oonoceras acinaces*, *O. sociale*, *Ophioceras simplex*, *Sactoceras pellucidum*, and *Tetrameroceras* (Turek, 1992; Š. Manda, personal commun., 1997). Gastropod and bivalve juveniles abundant, trilobites generally very rare: *Cerauroides*, *Cromus*, and *Denckmannites*. Unrevised gastropods, very rare brachiopods (*Jarovathyris canaliculata*, *Lissatrypa postfumida*, *Orthostrophia mulus*, and *Stenorhynchia infelix*), and rare graptolites.

The *Cardiolinka bohémica* Community features mostly disarticulated bivalves in shell-hash limestone with relatively common nektobenthic cephalopods. Cephalopod limestone just above limestone with *Cardiola*

conformis Community. *Cardiolinka bohémica* Community differs by having 60–69% epibyssate forms and by much higher density of monospecific populations of infaunal *C. bohémica*, which is rarely associated with the dominantly epibyssate forms in older rocks. This community represents a functional change in the community group, with abrupt change in environmental conditions (Kříž, 1997, In press). Current activity somewhat lower than in older rocks with *Cardiola conformis* Community. Depth change negligible; however, bottom composition is a comparable fossil-hash, so change probably limited to conditions related to water circulation, food supply, and temperature (Kříž, 1997, In press). In Bohemia, the interval with the *C. bohémica* Community is the stratigraphically highest shell-hash limestone with cephalopods before the accumulation of micrites and calcareous shales began in the earliest Přidoli (Kříž et al., 1986; Kříž, 1991). Bivalves: *Cardiolinka bohémica*, *Dualina longiuscula*, *Patrocardia*, *Praeostrea bohémica*, and *Spanila*. Cephalopods (Š. Manda, personal commun., 1997): *Cumingsoceras*, *Dawsonocerina caelebs*, *Geisonoceras*, *Hexameroceras panderi*, *Kopaninoceras*, *Mandaloceras*, *Michelinoceras*, *Octameroceras rimosum*, *Oocerina*, *Oonoceras*, *Ophioceras simplex*, *Oocerina*, *Parakionoceras originale*, *P. striatopunctatum*, *Peismoceras*, *Plagiostomoceras protobactritids*, *Rizosceras*, *Temperoceras*, and *Umbeloceras*. Abundant juvenile bivalves and gastropods; locally very common *Monograptus parultimus*; rare trilobites (*Prionopeltis striata*, *Scharyia nympha*).

LOCALITIES.—Eastern Serbia—Suva Planina Mountains, upper Ludlow (Kříž and Veselinovic, 1975); Austria—Carnic Alps, Rauchkofel Boden section, base of bed no. 4, lower Přidoli (Schönlaub and Bogolepova, 1994); Bohemia—Prague Basin (Figure 4), Kosov Quarry, upper Ludlow (Kříž, 1992); Praha-Lochkov, cephalopod quarry, upper Ludlow and lowermost Přidoli (Kříž, 1992); Praha-Pankrác, Praha-Kavčí Hory, Praha-Braník (Kříž, 1992), Praha-Konvářka, Praha-Velká Chuchle, upper Ludlow; Praha-Lochkov, Marble Quarry (Kříž et al., 1986), upper Ludlow; Praha-Hvízdalka (Kříž et al., 1986) and Kosoř, upper Ludlow and lower Přidoli.

UPPER MONOGRAPTUS TRANSGREDIENS ZONE LIMESTONE

GEOGRAPHIC DISTRIBUTION.—Prague Basin, Bohemia (Perunica).

TYPE LOCALITY, LITHOLOGY, AND AGE.—Požáry section, Praha-Řeporyje, Prague Basin, Bohemia (Kříž et al., 1986), lower part of fossil-hash limestone bed no. 136 of Požáry

Formation, upper *Monograptus transgrediens* Zone, Přidoli. Bed recorded only in vicinity of the Nová Ves volcanic center (Kříž, 1991), just below common occurrences of brachiopod *Dubaria latisinuata*.

FOSSIL COMMUNITY DESCRIPTION.—Bivalves: *Cardiolinka* sp. cf. *C. concubina* and *Dualina* sp. Cephalopods (Š. Manda, personal commun., 1997): *Corbuloceras corbulatum*, *Dawsonocerina omega*, *Kopaninoceras*, *Michelinoceras*, *Oonoceras*, *Ophioceras simplex*, and *Orthocycloceras? fluminese*. Stems and stem plates of *Scyphocrinites* and bryozoans.

LOCALITIES.—Bohemia—Prague Basin (Figure 4), localities in Daleje Valley near Řeporyje that include the Požáry section, bed no. 136 (Kříž et al., 1986); the Mušlovka-Černý lom section, bed no. 20 (Bouček, 1937, p. 17); and Na Bříči section near Srbsko (Kříž, 1992).

REMARKS.—Continuing uplift of the eastern Central Segment of the Prague Basin (Kříž, 1991) during the Přidoli resulted in favorable conditions for almost uninterrupted development of cephalopod limestones in the *Monograptus transgrediens* Zone. Almost continuous cephalopod limestones are found in sections through this interval in the Nová Ves volcanic center and Řeporyje volcanic center regions (Kříž, 1991) at localities at Praha-Nová Ves, Hradiště, Praha-Zadní Kopanina and Praha-Přidolí. At the Praha-Zadní Kopanina locality, almost the entire Přidoli is represented by the *Monograptus transgrediens* Zone in a very condensed sequence (only up to about 6 m). Increased thickness (i.e., almost 60 m) in the western Central Segment and in the Western Segment of the Prague Basin (Kříž, 1991) corresponds to a shallow environment on an elevation related to the Wenlock Nová Ves volcanic center and the Řeporyje volcanic center (Kříž, 1991). This elevation was separated from sediment sources by surrounding deeper parts of the basin. The sequence developed as lenticular, cephalopod limestone horizons within beds of micrite. The cephalopod shells are strongly current-oriented and mixed with *Scyphocrinites* stems, relatively common gastropods, and rare specimens of the brachiopod *Hebetoechia hebe*. The environment was probably very oxic and featured bryozoans, crinoids and brachiopods.

UPPERMOST MONOGRAPTUS TRANSGREDIENS ZONE LIMESTONE

GEOGRAPHIC DISTRIBUTION.—Carnic Alps, Austria, and Suva Planina Mountains, eastern Serbia (North Gondwana); Prague Basin, Bohemia (Perunica).

TYPE LOCALITY, LITHOLOGY, AND AGE.—Budňany Rock section, beds no. 40–41, Karlštejn, Prague Basin, Bohemia (Chlupáč et al., 1972). Bed of fossil-hash limestone with abundant and mostly fragmentary cephalopods, Požáry Formation, Přidoli. *Monograptus transgrediens* in uppermost level of bed no. 40. *Monograptus uniformis uniformis* just above bed no. 41 and in the shale intercalation no. 41/42. Conodonts of *Ozarkodina remscheidensis eostein-hornensis* Zone (H.P. Schönlaub in Kříž et al., 1986).

FOSSIL COMMUNITY DESCRIPTION.—*Joachymia-Cardiolinka-Pygolfia* Community of the *Snoopyia* Community Group (Kříž, 1997, In press). Disarticulated bivalves: *Cardiolinka concubina*, *C. fortis*, *Dualina inexplicata*, *Dualina* sp. cf. *D. longiuscula*, *Joachymia falcata*, *J. impatiens*, *Leptodesma*, *Praecardium*, *Praeostrea bohemica*, *Pterinopecten* (P.) *cybele cybele*, *Pygolfia nina*, *P. radiata*, *Snoopyia insolita*, and *S. veronika*. Infaunal bivalves dominant (66.7% *Cardiolinka*, *Pygolfia*, *Dualina*, *Snoopyia*, and *Praecardium*); epibyssate bivalves relatively abundant (26% *Joachymia*, *Pterinopecten*, and *Spanila*); semi-infaunal *Leptodesma* 4.4%; reclining *Dualina* and *Praeostrea* 2.8 %. Cephalopods (Š. Manda, personal commun., 1997): actinoceratids, *Arionoceras*, *Columenoceras* sp. cf. *C. subannulare*, *Corbuloceras corbulatum*, *Cumingsoceras*, *Dawsonoceras omega*, *Hexameroceras*, *Kopaninoceras*, *Mandaloceras*, *Michelinoceras*, *Ophioceras simplex*, *Orthocycloceras? fluminese*, *Peismoceras*, *Rhizosceras mundum*, “*R.*” *intermedium*, *Sactoceras*, and *Umbeloceras*. According to Gnoli and Serpagli (1991), the cephalopod assemblage has *Kopaninoceras? thyrus* and *Orthocycloceras? fluminese*. Cephalopods mostly strongly current-oriented SSW–NNE. Population densities relatively high. Phyllocarid crustaceans (*Ceratiocaris bohemica*), juvenile bivalves, and gastropods.

LOCALITIES.—Austria—Carnic Alps, Rauchkofel Boden section, bed no. 6 (Schönlaub and Bogolepova, 1994); Italy—Sardinia, Mason Porcus (Gnoli and Serpagli, 1991, Kříž and Serpagli, 1993); eastern Serbia—Suva Planina Mountains, Rebrina locality (Kříž and Veselinovic, 1974); Bohemia—Prague Basin (Figure 4), localities at Karlštejn, Budňany Rock section; Karlštejn, beds no. 40–41 (Chlupáč et al., 1972); southern slopes of Plešivec and Hlášná Třeban and Lejškov Hill near Beroun (Kříž, 1992).

LOWER *MONOGRAPTUS UNIFORMIS* *UNIFORMIS* ZONE LIMESTONE

GEOGRAPHIC DISTRIBUTION.—Massif Armorica, la Meignanne, France; Sardinia, Mason Porcus; Morocco; Algeria (North Gondwana); Prague Basin, Bohemia (Perunica).

TYPE LOCALITY, LITHOLOGY, AND AGE.—Antipleura Gorge near Praha-Radotín, Prague Basin, Bohemia, bed 13 (Chlupáč et al., 1972). Bed of biomicrite and cephalopod limestone with graptolite *Monograptus uniformis uniformis* and trilobite *Warburgella rugulosa rugosa*, lowermost Lochkovian, Lower Devonian.

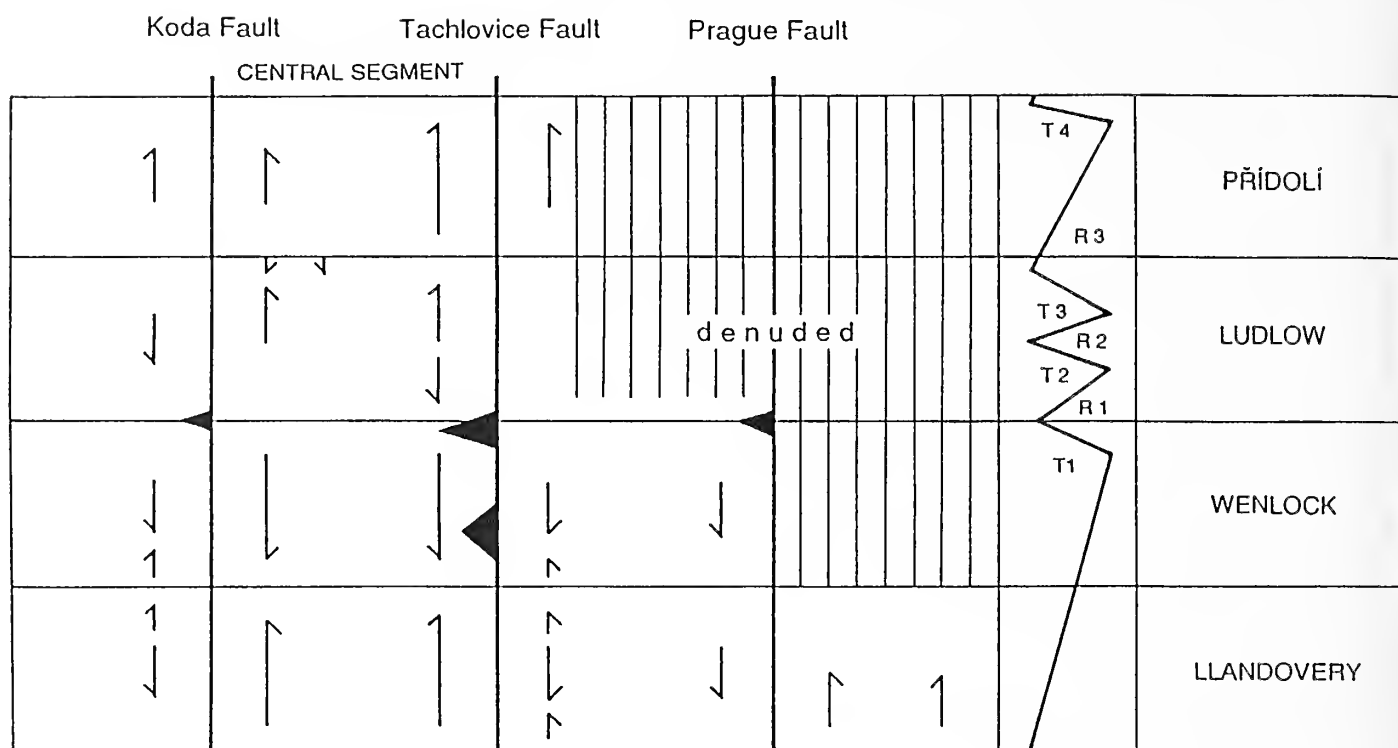
FOSSIL COMMUNITY DESCRIPTION.—In general, very high diversity and high population density. *Antipleura bohemica* Community of the *Antipleura-Hercynella* Community Group (Kříž, 1997, In press). Bivalves: common articulated *Antipleura bohemica* (40.2%), *Actinopteria*, *Dualina major*, *Jahnia*, *Leptodesma*, *Neklania*, *Mytilarca*, *Panenska*, *Paracyclas*, *Patrocardia bohemica*, *P. evolvens*, *Praelucina*, *Praeostrea*, *Pterinopecten* (P.), *Silurina*, *Spanila*, *Vevoda*, and *Vlasta*. Infaunal bivalves more than 40% (*Dualina major*, *Panenska*, *Praelucina*, *Vlasta*, etc.); reclining bivalves (*Antipleura*, *Dualina*, and *Silurina*) about 41%; epibyssate forms (*Mytilarca*, *Patrocardia*, *Pterinopecten*, and *Spanila*) relatively common (16–18%); semi-infaunal *Leptodesma* (0.8%) relatively rare. Cephalopods (Š. Manda, personal commun., 1997): *Endoplectoceras*, *Hemicosmorthoceras* sp. cf. *H. semimbricatum*, *Jovellania*, *Kopaninoceras floweri*, *Michelinoceras*, *Mimogeisonoceras*, *Oonoceras*, *Orthocycloceras pseudoextensum*, *Parakionoceras*, *Plagiostomoceras*, *Sphaerorthoceras*, and *Sthenoceras*. Cephalopods strongly current-oriented. Trilobites rare (*Otarion* and *Warburgella rugulosa rugosa*), rare graptolites (*Monograptus uniformis uniformis*), local accumulations of juvenile bivalves and gastropods.

LOCALITIES.—Austria—Carnic Alps, Rauchkofel Boden section, bed no. 8 (Schönlaub and Bogolepova, 1994); France—Massif Armorica, la Meignanne locality (Kříž and Paris, 1982); Italy—Sardinia, Mason Porcus locality, bed no. MP 6 (Kříž and Serpagli, 1993) and Corti Baccas 3rd section (Gnoli, 1984); western Macedonia (Bouček et al., 1968); Algeria—Erg Dzemel section southwest of Beni-Abbes, El-Kseib locality (Horný, 1975); Bohemia—Prague Basin (Figure 4), localities Antipleura Gorge, bed no. 13 (Chlupáč et al., 1972); Praha-Podolí locality, bed no. 10 (Chlupáč et al., 1972); Praha-Malá Chuchle, Barrandé's Rocks section.

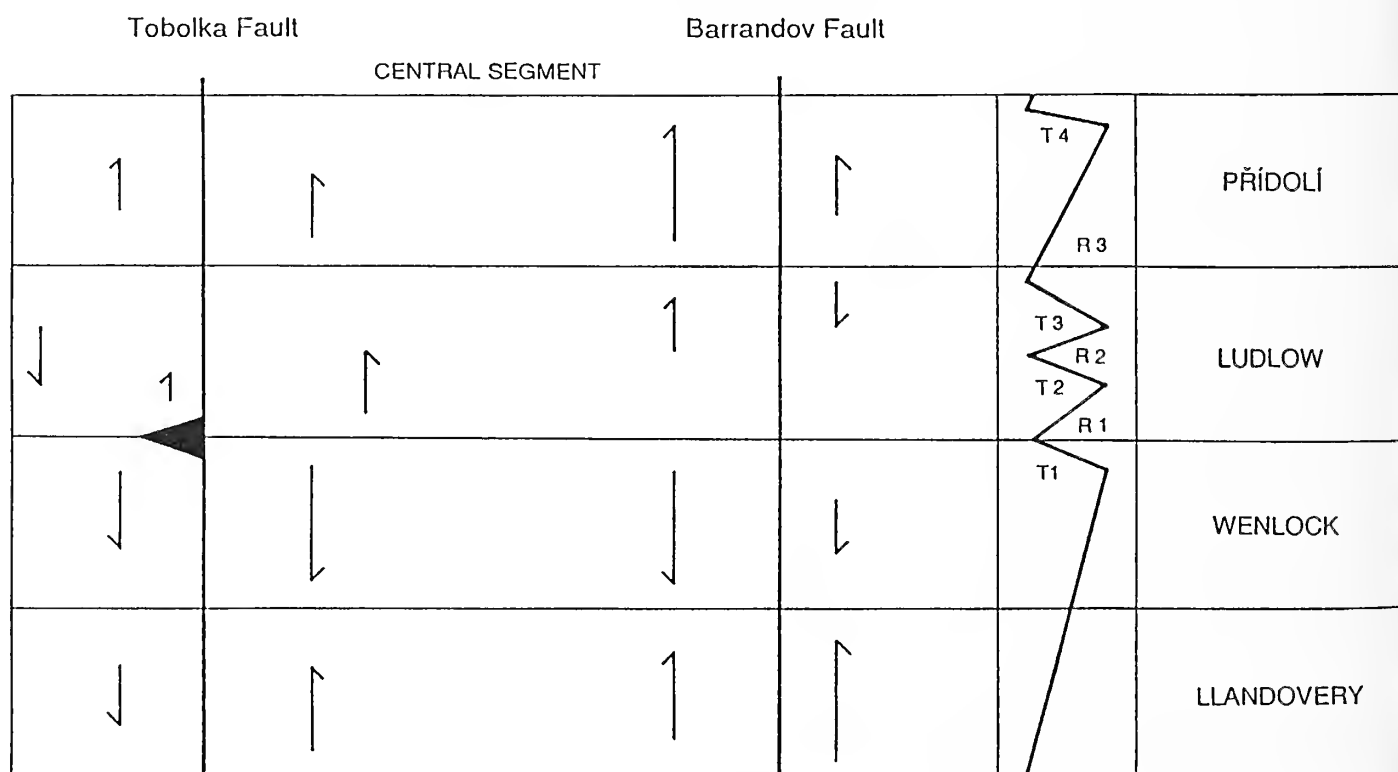
INTERPRETATION OF CEPHALOPOD LIMESTONES

The stratigraphic context of cephalopod limestones in the Silurian is best known from the Prague Basin, Bohemia (Kříž, 1991, 1992; Ferretti and Kříž, 1995). As discussed above, cephalopod limestones developed on the sea bottom when surface currents oxygenated the sea

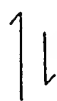
NOVÁ VES SECTION



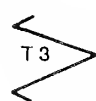
LONGITUDINAL SECTION (AXIS OF THE BASIN)



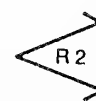
volcanism



relative uplift
and subsidence
of basin bottom



high stand



low stand

bottom below wave base. This situation prevailed during two different sorts of events: lowstands with eustatic oscillations, and uplift of the basin with synsedimentary tectonics (Kříž, 1991). It is difficult to distinguish between these two mechanisms, except by comparing the stratigraphic positions of the cephalopod limestones in different basins of North Gondwana and Perunica.

We assume that synsedimentary tectonics varied between different basins. This means that lowstands caused by uplift of basin segments will not be contemporaneous in different basins or even within one basin, and that cephalopod limestones will occur at different stratigraphic levels. Lowstands caused by eustatic oscillation will be contemporaneous in different basins, and cephalopod limestones will occur at the same stratigraphic levels.

Occurrences of cephalopod limestones in the Gondwana and Perunica basins are shown in Figure 5. Cephalopod limestones in the *Testograptus testis*, *Colono-graptus colonus*, upper *Saetograptus chimaera*, lower *S. linearis*, *Monograptus fragmentalis* and *M. ultimus*, upper *M. transgrediens*, and lower *M. uniformis uniformis* Zones occur in several basins. This may indicate eustatic lowstands, of which most are in agreement with the standard Silurian sea-level curve (Johnson, 1996) and with the representative sea-level curve for Bohemia (J. Kříž in Johnson, 1996, fig. 2d). Other occurrences may be interpreted as lowstands caused by synsedimentary tectonics.

An example from Austria that illustrates eustatic control is the cephalopod limestone in the *Testograptus testis* Zone in the Carnic Alps (Rauchkofel Boden section of Schönlaub and Bogolepova, 1994). This limestone is the lowest Silurian transgressive deposit above the shallow water, Upper Ordovician, cystoid-bearing, massive Wolayer Limestone. An example from the Prague Basin, Bohemia, documents uplift of the eastern Central Segment of the basin (Kříž, 1991) by synsedimentary tectonics (Figures 6 and 7) during the late Ludlow and Přidoli (*Saetograptus linearis* through *Monograptus transgrediens* Zones; Figure 5). As a result of this epeirogenic activity and because of almost continuous surface currents in the area, the cephalopod limestone biofacies is locally an almost continuous deposit.

It is interesting that surface currents also affected basins during highstands in the Silurian. In the Prague Basin, cephalopod limestones are developed almost con-

tinuously in the eastern Central Segment from the lower *Saetograptus linearis* through the *Monograptus lochkovens* and into the *M. transgrediens* Zones, while in other parts of the basin cephalopod limestones appear at the same levels as in North African Gondwana regions (Figure 5). A similar continuous development of the lithofacies is found in the Montagne Noire and in Sardinia between the *Testograptus testis* and *Colono-graptus colonus* Zones (Figure 5).

It is necessary to explain the absence of cephalopod limestones from some basins at levels where they should appear based on the correlations of eustatic changes. This is likely due to the specific synsedimentary tectonics of particular basins, where lowstands corresponded to subsidence of the basinal floor.

ACKNOWLEDGMENTS

The author thanks Š. Manda of the Czech Geological Survey for information on cephalopod distributions. Helpful discussions took place with A. Ferretti. The author is also indebted to those who helped in the study of cephalopod limestones in the Gondwana Basins, especially C. Babin, R. Feist, M. Gnoli, F. Paris, H.-P. Schönlaub, and E. Serpagli. A.J. Boucot, L. Cherns, R. Crick, and E. Landing are acknowledged for critical readings of the manuscript and for language corrections. A special thanks is given R. Horčíková for assistance in the graphic work.

REFERENCES

- BARRANDE, J. 1881. Systeme Silurien du Centre de la Boheme, Iere partie: Recherches paléontologiques, VI. Acéphales. Paris.
- BERRY, W.B.N., AND A.J. BOUCOT. 1967. Pelecypod-graptolite association in the Old World Silurian. Geological Society of America Bulletin, 78:1515-1522.
- BOUČEK, B. 1937. Stratigrafie siluru v dalejském údolí u Prahy a v jeho nejbližším okolí. Rozpravy II. Třída České Akademie, 46(27):1-20.
- , J. KRÍŽ, AND S. STOJANOVIC-KUZENKO. 1968. O fosilonosnom lochkovienu u Zapadnoj Makedoniji. Trudovi na geološkiot zavod na socialistička republika Makedonija, 1967-1968 (13):31-39.
- BURRETT, C. F. 1983. Palaeomagnetism and the mid-European ocean—an alternative interpretation of Lower Palaeozoic apparent polar wander. Geophysical Journal of the Royal Astronomical Society, 72:523-534.
- , AND J. GRIFFITHS. 1977. A case for mid-European ocean, p. 523-534. In La chaine varisque d'Europe moyenne et occidentale. Colloquium internationale CNRS, 243.
- CHLUPÁČ, I. 1987. Ecostratigraphy of Silurian trilobite assemblages of the Barrandian area, Czechoslovakia. Newsletter on Stratigraphy, 17(3):169-186.

FIGURE 7—(opposite) Relationships between Silurian synsedimentary movements, volcanic activity, and main sea-level changes in the Prague Basin. Location of growth faults and sections in Figure 6 (after Kříž, 1991).

- , H. JAEGER, AND J. ZIKMUNDOVÁ. 1972. The Silurian-Devonian boundary in the Barrandian. *Bulletin of Canadian Petroleum Geology*, 20:104-174.
- FERRETTI, A. 1989. Microbiofacies and constituent analysis of Upper Silurian-Lower Devonian limestones from southwestern Sardinia. *Bolletino della Società Paleontologica Italiana*, 28:87-100.
- , AND J. KRÍŽ. 1995. Cephalopod limestone biofacies in the Silurian of the Prague Basin, Bohemia. *Palaios*, 10:240-253.
- GAERTNER, H.R. 1931. *Geologie der Zentralkarnischen Alpen*. Denkschriften der Akademie der Wissenschaften in Wien, mathematisch-naturwissenschaftliche Klasse, 102(5):115-199.
- GNOLI, M. 1984. Paleontological content, constituent analysis and microbiofacies of Early Devonian pelagic limestones from the Fluminimaggiore area (SW Sardinia). *Bolletino della Società Paleontologica Italiana*, 23:221-238.
- , AND E. SERPAGLI. 1991. Nautiloid assemblages from Middle-Late Silurian of southwestern Sardinia: a proposal. *Bolletino della Società Paleontologica Italiana*, 30:187-195.
- GOULD, S.J. 1977. *Ontogeny and Phylogeny*. The Belknap Press, Harvard University.
- HAVLÍČEK, V., J. VANĚK, AND O. FATKA. 1994. Perunica microcontinent in the Ordovician (its position within the Mediterranean Province, series division, benthic and pelagic associations). *Sborník geologických Věd, Geology*, 46:23-56.
- HERITSCH, F. 1929. Faunen aus dem Silur der Ostalpen. *Abhandlungen der Geologische Bundesanstalt*, 23(2):1-183.
- HORNÝ, R. 1975. Paleontologická expedice "Maghreb 1974". *Časopis Národního Muzea, Oddíl Přírodovědný*, 144(1/4):33-43.
- JAEGER, H. 1975. Die Graptolithenführung im Silur/Devon des Cellon-Profiles (Karnische Alpen). *Carinthia II*, 165(85):111-126.
- JOHNSON, M. E. 1996. Stable cratonic sequences and a standard for Silurian eustasy, p. 203-211. In B.J. Witzke, G.A. Ludvigsen, and J.E. Day (eds.), *Paleozoic Sequence Stratigraphy: Views from the North American Craton*. Geological Society of America Special Paper 306.
- KODYM, O., B. BOUČEK, AND J. ŠULC. 1931. Guide to the geological excursion to the neighbourhood of Beroun, Koněprusy and Budňany. *Knihovna Státního geologického Ústavu Československé Republiky*, 15:43-83.
- KRÍŽ, J. 1961. Průzkum zaniklé paleontologické lokality Joachima Barranda, označované jím jako "Butowitz". *Časopis pro Mineralogii a Geologii*, 6:173-178.
- . 1970. Stratigraphy of some of Barrande's paleontological localities of Silurian age, central Bohemia. *Věstník Ústředního Ústavu geologického*, 45:295-298.
- . 1979. Silurian *Cardiolidae* (Bivalvia). *Sborník geologických Věd, Paleontology*, 22:5-157.
- . 1984. Autecology and ecogeny of Silurian Bivalvia. *Special Papers in Palaeontology*, 32:183-195.
- . 1985. Silurian *Slavidae* (Bivalvia). *Sborník geologických Věd, Paleontology*, 27:47-111.
- . 1991. The Silurian of the Prague Basin (Bohemia). Tectonic, eustatic, and volcanic controls on facies and faunal development. *Special Papers in Palaeontology*, 44:179-203.
- . 1992. Silurian Field Excursions: Prague Basin (Barrandian), Bohemia. National Museum of Wales, Geological Series, 13.
- . 1996. Silurian Bivalvia of the Bohemian type from the Montagne Noire and Mouthoumet Massif, France. *Palaeontographica, Abteilung A*, 240:29-63.
- . In press. Bivalvia-dominated communities of Bohemian type from the Silurian and Lower Devonian carbonate facies. In A.J. Boucot and J.D. Lawson (eds.), *Final Report, Project Ecostratigraphy*. Cambridge University Press.
- , AND O.K. BOGOLEPOVA. 1995. *Cardiola signata* Community (Bivalvia) in cephalopod limestones from Tajmyr (Gorstian, Silurian, Russia). *Geobios*, 28:573-583.
- , AND F. PARIS. 1982. Ludlovian, Pridolian, and Lochkovian in la Meignanne (Massif Amoricain). Biostratigraphy and correlations based on Bivalvia and Chitinozoa. *Geobios*, 15:391-421.
- , AND E. SERPAGLI. 1993. Upper Silurian and lowermost Devonian Bivalvia of Bohemian type from south-west Sardinia. *Bolletino della Società Paleontologica Italiana*, 32:289-347.
- , AND M. VESELINOVIC. 1975. Ludlovian, Pridolian, and Lochkovian bivalves from the Suva Planina Mountains (eastern Serbia, Yugoslavia). *Vestnik Ustredniho Ustavu geologickeho*, 50:365-369.
- , H. JAEGER, F. PARIS, AND H.-P. SCHÖNLAUB. 1986. Pridoli—the fourth subdivision of the Silurian. *Jahrbuch der geologischen Bundesanstalt, Wein*, 129:291-360.
- , P. DUFKA, H. JAEGER, AND H.-P. SCHÖNLAUB. 1993. The Wenlock/Ludlow [sic, n-dash, not virgule] boundary in the Prague Basin (Bohemia). *Jahrbuch der Geologischen Bundesanstalt, Wien*, 136:809-839.
- KRS, M., M. KRISOVÁ, P. PRUNER, AND V. HAVLÍČEK. 1986. Paleomagnetism, paleogeography, and multi-component analysis of magnetization of Ordovician rocks from the Barrandian area of the Bohemian massif. *Sborník geologických Věd, užita Geofyzika*, 20:9-45.
- , ———, ———, R. CHVOJKA, AND V. HAVLÍČEK. 1987. Palaeomagnetism, palaeogeography, and the multi-component analysis of Middle and Upper Cambrian rocks of the Barrandian in the Bohemian massif. *Tectonophysics*, 139:1-20.
- PETRANEK, J., AND E. KOMARKOVA. 1953. Orientace hlavonožcůve vápencích Barrandienu a její paleogeografický význam. *Sborník Ústředního Ústavu geologického*, 20:129-148.
- SCHÖNLAUB, H.-P. 1980. Field trip A: Carnic Alps, p. 5-57. In H.-P. Schönlaub (ed.), *Second European Conodont Symposium (ECOS II), Guidebook and Abstracts*. *Abhandlungen der Geologischen Bundesanstalt*, 35.
- , AND O. BOGOLEPOVA. 1994. Section 6, Rauchkofel Boden section, p. 103-110. In H.-P. Schönlaub and L.H. Kreutzer (eds.), *I.U.G.S. Subcommittee on Silurian Stratigraphy, Field Meeting, Eastern + Southern Alps, Austria 1994*. In *Memorium of H. Jaeger. Berichte Geologische Bundesanstalt*, 30.
- ŠTORCH, P. 1995. Upper Silurian (upper Ludlow) graptolites of the *N. inexpectatus* and *N. kozlowskii* Biozones from Kosov Quarry near Beroun (Barrandian area, Bohemia). *Věstník Českého geologického Ústavu*, 70(4):65-89.
- SUESS, E.F. 1912. Die moravischen Fenster und ihre Beziehung zum Grundebirge deh Hohen Gesenkes. *Denkschriften Österreichische Akademie der Wissenschaften, mathematisch-naturwissenschaftliche Klasse*, 88:541-629.
- TUREK, V. 1992. Ortocerové vápence a hlavonožci hraničních poloh kopaninského a přídolského souvrství v činném lomu na Kosově u Berouna. *Časopis Národního Muzea v Praze, Řada přírodovědecká*, 158(1989) 1-4:108.
- ZENO, F. 1770. Beschreibung des bei Prag von dem Wissehrader Tore gelegenen Kalksteinbruches, mit seinem Seeeversteinerungen und anderen Fossilien. *Neue physicalische Belustigungen*, 2:362-420.

SILURIAN CEPHALOPOD BEDS FROM NORTH ASIA

OLGA K. BOGOLEPOVA

Department of Historical Geology & Palaeontology, Institute of Earth Sciences,
Uppsala University, Norbyvägen 22, S-752 36, Uppsala, Sweden

ABSTRACT—Deposition of Silurian cephalopod limestone beds from north Asia was related to eustatic changes. Three depositional settings are recognized. Accumulation of black cephalopod limestones in the East Siberian Basin was initiated by the Early Silurian transgression. Rapid sea-level rise led to formation of an upwelling zone at the margins of the basin, where the cephalopod facies formed. Cephalopod-rich Upper Silurian limestones of Taimir, Novaya Zemlya, and Tien-Shan are in many ways similar to the east Siberian sedimentary rocks, but eustatic fall took place during their deposition. A relatively shallow-water cephalopod limestone facies occurs in the upper Llandovery–lower Wenlock of the Altai-Sayan and in the lower Ludlow of the south Urals, and is probably the result of redeposition.

INTRODUCTION

Cephalopod limestones occur at many stratigraphic levels in the Silurian, and in most cases are globally distributed. They have been examined from the viewpoint of their sedimentology, lithology, microfacies, taxonomy, paleoecology, and paleocurrents (Miagkova, 1967; Khvorova and Grigoriev, 1974; Kříž, 1979, 1992; Gnoli et al., 1979; Bourrouilh, 1981; Gnoli, 1984; Wendt and Aigner, 1985; Ferretti, 1989; Holland et al., 1994; Ferretti and Kříž, 1995; Bogolepova and Holland, 1995). Although there are still controversies regarding interpretations of some cephalopod limestones, the available information suggests some essential and shared conditions for their formation. The objective of this report is to relate the Silurian cephalopod limestone beds from North Asia to eustatic changes.

MATERIAL

EASTERN SIBERIA.—Silurian (Mojerokan Formation, Llandovery) cephalopod limestones in eastern Siberia are known from sections along the Mojerokan, Letnyaya, Levaya Tanda, and Kurejka rivers, from boreholes on the

Fat'yanikha River, and from the Norilsk region (Miagkova, 1967; Bogolepova and Kříž, 1995; Bogolepova, 1995, 1996a) (Figure 1). They are represented by black bituminous limestones of different thicknesses (from 15 cm to 5 m) with numerous cephalopod conchs and conodont elements and rare remains of brachiopods, gastropods, trilobites, and bivalves.

The most striking example is from the Mojerokan River section (Bogolepova and Holland, 1995). The 30 cm-thick bed contains abundant cephalopods, conodonts, rare brachiopods, and trilobites. The cephalopod limestone is assigned to the *Distomodus kentuckyensis* (conodont) Zone. Graptolites collected from the overlying shales narrow this interval to the *Parakidograptus acuminatus* Zone (Bogolepova, 1996a).

The basal beds in the Fat'yanikha borehole are dolomitic marls that are overlapped unconformably by black Silurian shales with small lenses and interbeds of black cephalopod limestones. Graptolites suggest that the enclosing rocks belong to the *Coronograptus cyphus* Zone (Bogolepova and Kříž, 1995).

TAIMIR.—In Taimir, in the northern facial zone, the Nizhnyaya Taimira River section (Figure 1) has been studied by Zlobin (1962, 1965). The Wenlock–Pridoli age of this succession was established by Berger et al. (1991). The Middendorf Formation (145 m-thick) consists of black graptolitic shales with interbeds (from 20 cm to 2 m) and small nodules of clayey micritic limestones with accumulations of oriented orthoconic cephalopods with bivalves (Cardiolidae), ostracodes (Entomozoidae), and rare trilobites, gastropods, and brachiopods (Kříž and Bogolepova, 1995). Four cephalopod levels can be recognized in this sequence. They are developed in the middle Ludlow (uppermost Gorstian–Ludfordian), upper Ludlow, lowermost Pridoli, and uppermost Pridoli (Figure 2). Although the sequences from north Taimir are characterized by abundant graptolites (Obut et al., 1965), correlation of the cephalopod beds with regard into the standard graptolite zonation is still uncertain. More taxonomic work needs to be done with these collections.

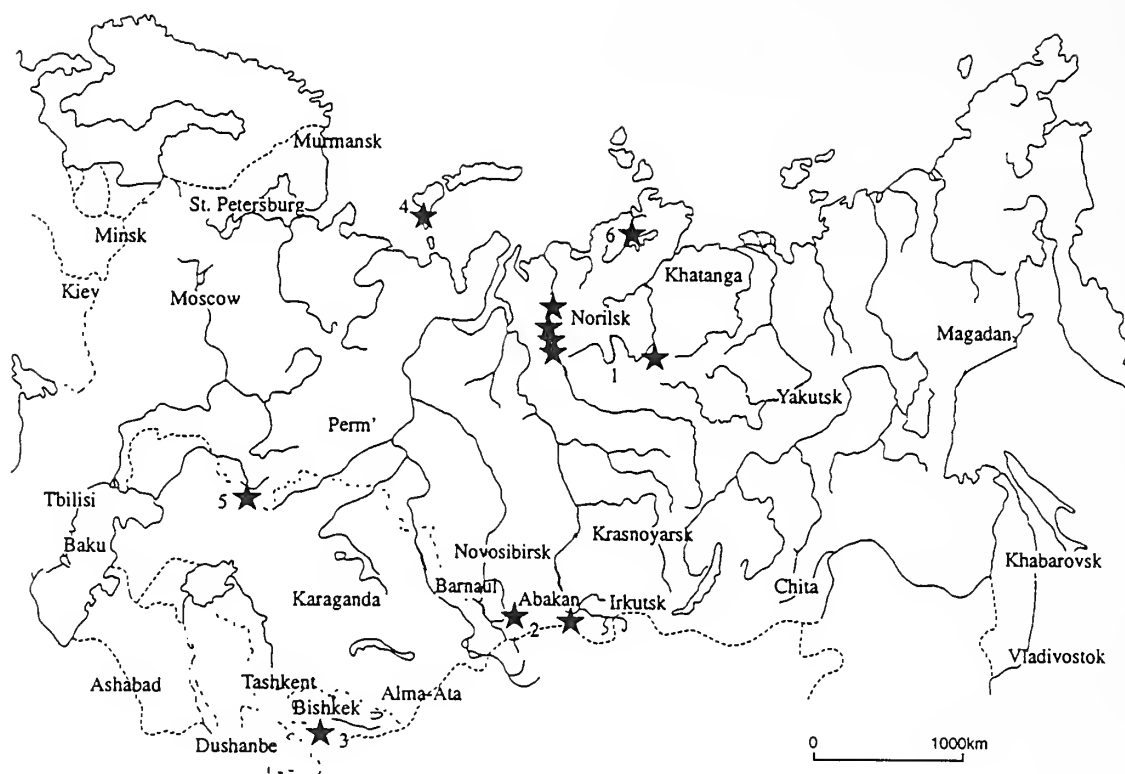


FIGURE 1—Distribution of Silurian cephalopod limestones in north Asia. 1, eastern Siberia (Bogolepova, 1995; Bogolepova and Holland, 1995). 2, Altay-Sayan region (data from Kulkov, 1967; Vladimirskaia, 1978; and Kulkov et al., 1985). 3, Tien-Shan (data from Nikiforova and Obut, 1965; Kim and Larin, 1968; Obut et al., 1968). 4, Novaya Zemlya (data from Nekhorosheva, 1981). 5, south Urals (data from Leonenok, 1955; Khvorova and Grigoriev, 1974). 6, Taimir (Zlobin, 1962, 1965; Berger et al., 1991; Kříž and Bogolepova, 1995; Bogolepova, 1996b).

NOVAYA ZEMLYA.—The Nekhvato Formation (Ludlow) in the Kuznetsova River section (Figure 1) is 1,500 m-thick and consists largely of shales (Nekhorosheva, 1981). The lower 200 m is characterized by black mudstones with small lenses, concretions (diameter 10 cm), and thin interbeds (3–5 cm) of grey to black limestone. The concretions contain small orthoconic cephalopods. In the thin interbeds, there are accumulations of long, slender, oriented cephalopods with bivalves (Cardiolidae), ostracodes, and gastropods (Bogolepova and Holland, 1995).

TIEN-SHAN.—On the eastern slope of the Alai mountain region in the Koxu River basin, dark grey limestones with abundant orthoconic cephalopods and cardiolids have been described on Ak-Bogus Creek (Figure 1). The age of beds has been determined as late Wenlock?–early Ludlow? (Nikiforova and Obut, 1965). No additional information is available.

The Kurgan Formation (Ludlow) in the section on the southern slope of Mount Merishkor in northern Nura-Tau largely consists of shales (Kim and Larin, 1968). The lower 90 m is characterized by black mudstones with interbeds of grey to black limestones that have abundant

orthoconic cephalopods, ostracodes, and rare brachiopods. Graptolites (*Pristiograptus dubius* and *Bohemograptus bohemicus*) have been found in the black shales. The cephalopod beds are referred to the *Neodiversograptus nilssoni* Zone (Obut et al., 1968).

ALTAI-SAYAN.—The lower part of the Chagyr Formation crops out on the east side of the Yavorka River (Figure 1) at Rossypnaya Hill. Light grey to red massive limestones occur at the base of the formation near Talyi village in the Gornyi Altai (Altai-Sayan region) (N.P. Kulkov, 1994, personal commun.). The beds are referred to the *Pterospirifer amorphognathoides* (conodont) Zone. The fauna includes brachiopods, trilobites, gastropods, crinoids, and corals that indicate a Wenlock age (Kulkov, 1967; Krasnov et al., 1983).

In western Tuva (Figure 1) on the west side of the River Alash near the Akdovurak–Abaza bridge, the Alash beds (Llandovery) are exposed along the road. Their basal part consists of thick, red and pink, crinoidal and stromatoporoid–coral limestones. These include interbeds of cephalopod limestone with numerous oriented orthocones. Conodonts indicate that the beds belong to the *Spathognathodus celloni* Zone (Bogolepova and

series	stages	graptolite zones	conodont zones	Eastern Siberia	Tuva	Gornyi Altai	Tian-Shan	South Urals	Novaya Zemlya	Taimir
412	P R I D.	<i>bouceki-transgrediens</i>	<i>eosteinhornensis - delorta</i>							
		<i>branikensis-lochkovenski</i>	remshedensis interval zone							
		<i>par ultimus-ultimus</i>								
414	L U D F L O W	<i>formosus</i>	<i>crispa</i>							
415		<i>bohemicus tenuis - kozlowski</i>	<i>snajdri</i> interval zone							
		<i>leintwardinensis</i>	<i>siluricus</i>							
			<i>ploeckensis</i>							
		<i>scanicus</i>	not zoned							
		<i>nilssoni</i>	<i>stauros</i>							
420	W E N L O C K	<i>ludensis</i>	<i>bohemicus</i>							
		<i>praedeubell-deubell</i>								
		<i>parvus-nassa</i>								
		<i>lundgreni</i>	<i>sagitta sagitta</i>							
		<i>rigidus-perneri</i>	not zoned							
		<i>riccartonensis-belophorus</i>	<i>sagitta rhenana - patula</i>							
		<i>centrifugus-murchisoni</i>	<i>ranulaformis</i> interval zone							
425		<i>lapworthi-insectus</i>	<i>amorphognathoides</i>							
	L L A N D O V E R Y	<i>spiralis</i> interval zone								
		<i>griestoniensis-crenulata</i>	<i>celloni</i>							
		<i>turriculatus - crispus</i>								
		<i>guerichi</i>	<i>tenuis-staurogathoides</i>							
		<i>sedgwickii</i>								
		<i>convolutus</i>								
130		<i>argenteus</i>								
	R H U D D A N I A N	<i>triangulatus-pectinatus</i>								
432		<i>cyphus</i>	<i>kentuckyensis</i>							
133		<i>vesiculosus</i>								
135		<i>acuminatus</i>								

FIGURE 2—Stratigraphic position of cephalopod limestones (in black) from north Asia.

Holland, 1995; see references to Vladimirskaia, 1978, and Kulkov et al., 1985).

SOUTH URALS.—On the western slope of the south Urals (Figure 1) in the Sakmaro-Ilek facies zone (Puchkov, 1979; Ivanov and Puchkov, 1984), Leonenok (1955) assigned the Ludlow rocks of the Kos-Istek area in Mugodzhar to the Karabutak Formation. It consists of feldspathic sandstones, conglomerates, clay slates with chert nodules, limestones, and volcanic rocks. Its age is early Ludlow on the basis of the rich faunas that occur in limestone lenses and interbeds. There are cephalopods, bivalves, gastropods, trilobites, crinoids, and rare brachiopods (Bogolepova and Holland, 1995).

DISCUSSION

Silurian cephalopod beds are known from north Asia in the lower Llandovery of eastern Siberia, the upper Llandovery of Tuva, and the lower Wenlock of Gornyi Altai. Lower Ludlow cephalopod limestone biofacies are developed in Novaya Zemlya, the south Urals, and Tien-Shan, and are recognized in the Ludlow-Pridoli of Taimir (Figure 2). They are represented by either grey to black bituminous limestones with abundant orthoconic cephalopods, bivalves (*Cardiolidae*), conodonts, pelagic ostracodes, rare brachiopods, gastropods, and trilobites, or red to pink limestones with cephalopods, crinoids, corals, stromatoporoids, gastropods, trilobites, bivalves, and rare brachiopods.

The data listed above show that Silurian cephalopod limestones vary in their character. Three depositional settings characterized by different depth and hydrodynamic regime can be recognized. Two of them may have resulted from the eustatic character of such sea-level changes as the Early Silurian transgression and the shallowing of the basins during the Late Silurian.

Accumulation of black cephalopod limestones in the East Siberian Basin began with the Early Silurian transgression. Rapid sea-level rise led to the formation of an upwelling zone at the margins of the basin, where the cephalopod facies formed.

The following model (Figure 3) for the accumulation of cephalopod limestone has been proposed (Bogolepova and Gubanov, *In press*). The accumulation of black, bituminous limestones was connected with the transgression that began in the East Siberian Basin in the Early Silurian. The global lowstand in sea-level during the Late Ordovician (McKerrow, 1979; Sislavinskii, 1987, 1988, 1991; Brenchley, 1988; Scotese and McKerrow, 1990) led to erosion of the Upper Ordovician and, to some degree, of the Middle Ordovician in Siberia. During the

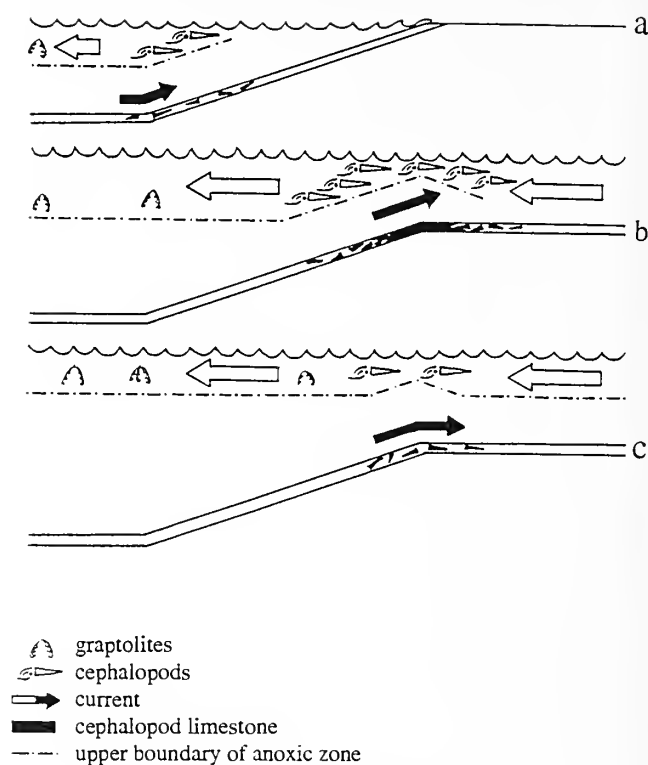
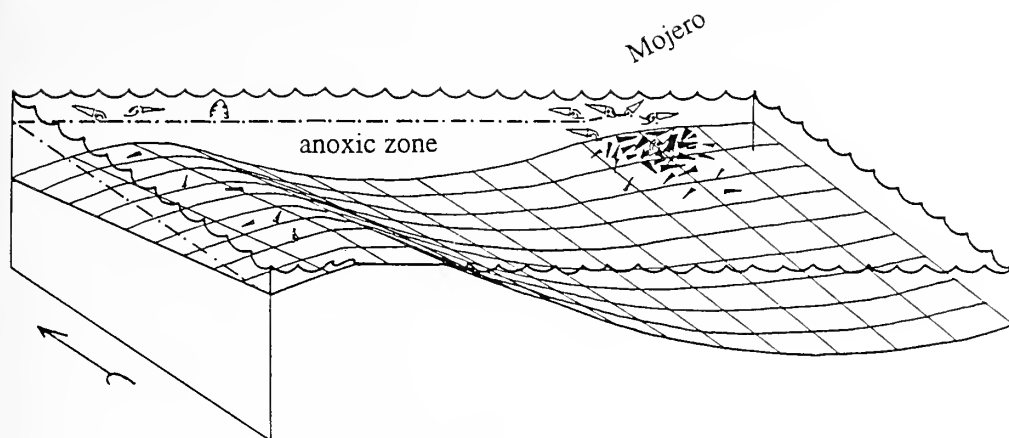


FIGURE 3—Model for the formation of cephalopod limestones. (a) Nektic cephalopods live offshore of zones of upwelling during regressive intervals; (b, c) with sea-level rise, abundant cephalopod faunas occur above zones of upwelling over shelf margin, and conchs accumulate in dysaerobic facies (labeled "anoxic zone").

Early Silurian, a rapid rise in global sea-level occurred (Figure 3a) (Berry and Boucot, 1973; McKerrow, 1979; Ziegler, 1981; Ronov et al., 1984; Sislavinskii, 1987, 1988, 1991; Brenchley, 1988; Scotese and McKerrow, 1990; Boucot, 1990; Johnson et al., 1991) that flooded the East Siberian Basin and led to the formation of an upwelling zone at its outer margins. Mixing of bottom waters rich in organic matter with the oxygen-saturated surface waters led to a burst of biological productivity and vigorous growth of nekctic cephalopods. There is a very high concentration of cephalopod remains in a narrow, elongate belt along the margin of the East Siberian Basin. Nutrient-rich, anoxic waters upwelled on the edge of the basin with a resultant strong increase in the nekctic fauna (Figure 3b). The overlying beds are black graptolitic shales. With further transgression (Figure 3c) and better circulation, non-bituminous clay shales with a different fauna began to accumulate. Cephalopods can still be found in small limestone lenses in these deposits, but their concentration is not as high as that in the earlier period of active upwelling.

Silurian deposition on the western margin of the East Siberian Basin began somewhat later than on the eastern margin (Sokolov, 1967, 1992; Sennikov, 1979;

Parakidograptus acuminatus time



Cystograptus vesiculosus - Climacograptus cyphus time

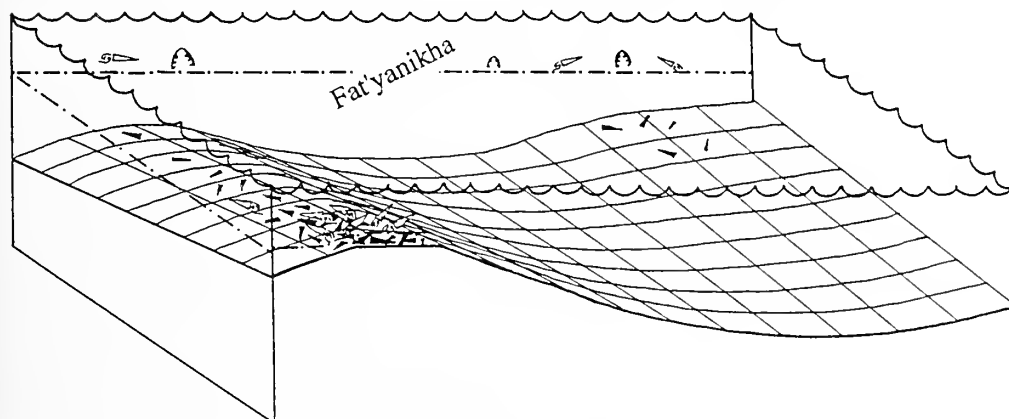


FIGURE 4—Depositional environments of cephalopod limestone biofacies across the East Siberian Basin during the Early Silurian.

Bogolepova, 1996a). Therefore, the cephalopod facies were not formed synchronously. This is explained by the fact that the western part of the platform underwent stronger vertical movement than the eastern part, as seen by the deeper erosion of Ordovician deposits to the west. Upwelling influenced the deposition of the cephalopod facies and overlying graptolite facies in the east (Mojero River) before subsequent transgression submerged the western territory and initiated the same facies changes there (Fat'yanikha River) (Figure 4).

Cephalopod limestones of the Taimir Basin occur within a black graptolitic shale facies. Cephalopods are abundant; epibyssate bivalves are represented, and are associated with abundant conodonts, pelagic ostracodes, and rare brachiopods, trilobites, and gastropods. Several transgressions and regressions can be recognized in this region during the Ludlow–Pridoli interval. These include

the early Ludlow transgression, middle Ludlow regression and transgression, late Ludlow regression, and early and late Pridoli highstands in sea-level. The sea-level curve reconstructed for the Taimir Basin shows minor sea-level falls, and the cephalopod beds indicate a shallowing of the basin (Figure 5). It can be concluded that these deposits were formed in outer-shelf environments during a regressive period in sea-level. The accumulation of recurrent cephalopod limestones in the Taimir Basin was initiated by the regressions that took place in the Late Silurian. A short-term eustatic fall led to the formation of an upwelling zone and consequent deposition of cephalopod facies in the deeper parts of the basin. Hence the situation which existed in the Taimir Basin may be interpreted as similar to that of the East Siberian Basin in terms of depth, but occurred in a period of general sea-level drop, rather than rise. There were

Taimir
Middendorf Cave

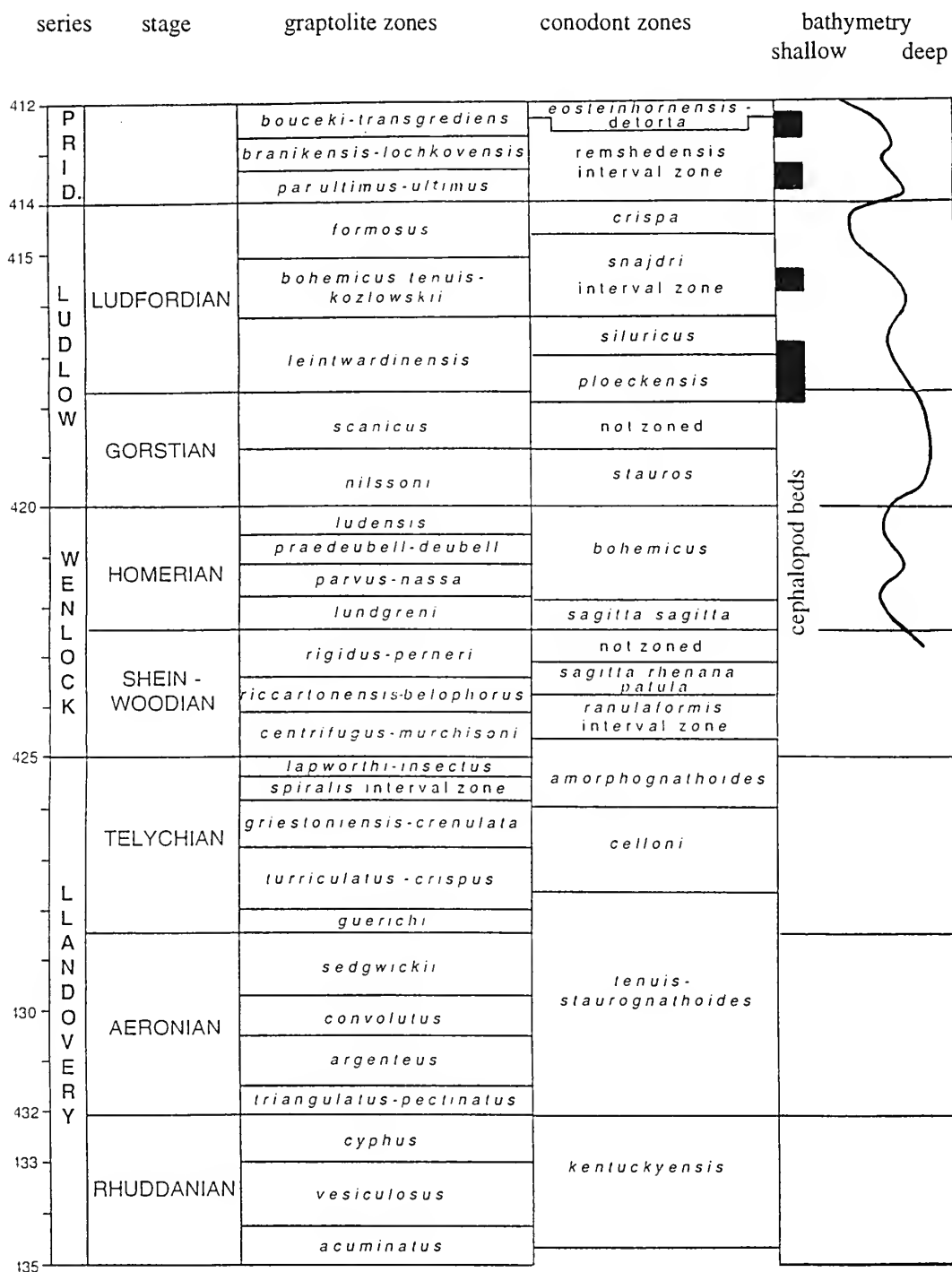


FIGURE 5—Distribution of Ludlow-Pridoli cephalopod limestones (in black) at Middendorf Cave, Taimir. Sea-level curve based on data from Berger et al. (1991).

	series	stages	graptolite zones	conodont zones	Rauchkofel	Boden	Cellon		
412	P R I D.		<i>bouceki-transgrediens</i>	<i>eosteinhornensis</i> - <i>deloria</i>					
			<i>branikensis-lochkovens</i>	<i>remshedensis</i>					
			<i>par ultimus-ultimus</i>	interval zone					
414	L U D L O W	LUDFORDIAN	<i>formosus</i>	<i>crispa</i>					
415			<i>bohemicus tenuis</i> - <i>kozlowski</i>	<i>snajdri</i>				interval zone	
			<i>leintwardinensis</i>	<i>siluricus</i>					
		GORSTIAN		<i>ploeckensis</i>					
			<i>scanicus</i>	not zoned					
			<i>nilssoni</i>	<i>stauros</i>					
420	W E N L O C K	HOMERIAN	<i>ludensis</i>	<i>bohemicus</i>					
			<i>praedeubell-deubell</i>						
			<i>parvus-nassa</i>						
			<i>lundgreni</i>					<i>sagitta sagitta</i>	
		SHEIN - WOODIAN	<i>rigidus-perneri</i>	not zoned					
			<i>riccartonensis-belophorus</i>	<i>sagitta rhenana</i> <i>palula</i>					
			<i>centrifugus-murchisoni</i>	<i>ranuliformis</i> interval zone					
425			TELYCHIAN	<i>lapworthi-insectus</i>				<i>amorphognathoides</i>	
	<i>spiralis</i> interval zone	<i>celloni</i>							
	<i>griestoniensis-crenulata</i>								
	<i>turriculatus-crispus</i>								
	<i>guerichi</i>								
	AERONIAN	<i>sedgwickii</i>	<i>tenuis</i> - <i>staurognathoides</i>						
130		<i>convolutus</i>							
		<i>argenteus</i>							
		<i>triangulatus-pectinatus</i>							
432	RHUDDANIAN	<i>cyphus</i>	<i>kentuckyensis</i>						
133		<i>vesiculosus</i>							
		<i>acuminatus</i>							
135									

FIGURE 6—Distribution of cephalopod limestones (in black) in the Silurian of the Carnic Alps. Based on data from Schönlaub et al. (1994; Cellon section), Schönlaub and Bogolepova (1994; Rauchkofel Boden section), and author's unpublished data.

other similar short-term lowstands documented by cephalopod limestone biofacies in the early Ludlow (*Neodiversograptus nilssoni* Zone) of the Tien-Shan and Novaya Zemlya Basins, as well as an influx of new graptolite and bivalve taxa.

In the Taimir Basin, cephalopod limestones are developed in the middle Ludlow (uppermost Gorstian-Ludfordian), upper Ludlow, lowermost Pridoli, and uppermost Pridoli. Comparison of the Late Silurian sea-level fluctuations in the Taimir Basin (Figure 5) and correlation of the levels with cephalopod levels in the Taimir Basin and the Carnic Alps (Figure 6) (based on data from Schönlaub et al., 1994 and Schönlaub and Bogolepova, 1994) suggest synchronous developments in the sedimentary sequences of these basins (Bogolepova, 1996b). These types of cephalopod limestones occur at many levels in the Silurian, and are, in most cases, globally distributed (Bogolepova, 1995; Ferretti and Kříž, 1995). The distribution of the cephalopod facies in the late Wenlock?–Pridoli in the marginal basins of Siberia, Kazakhstan, and Baltica and in the Wenlock–Pridoli of the North Gondwanan and Perunian (Bohemia) basins may have resulted from the eustatic character of these changes.

Relatively shallow-water cephalopod facies formed in conditions of oxygen-rich water and increased wave and current activity. This facies occurs in the upper Llandovery–lower Wenlock of the Altai-Sayan and in the lower Ludlow of the south Urals.

The distribution of Silurian cephalopod limestones in space and time requires an explanation based on further studies. Examples of further problems include: why was there no development of cephalopod biofacies in north Asian Wenlock basins? Does this indicate our lack of knowledge, or a primary paleogeographic reason? The present contribution is to be taken as a preliminary account, and a more comprehensive study of the Silurian cephalopod limestones is in progress.

ACKNOWLEDGMENTS

A travel grant from the Swedish Natural Science Research Council (NFR) allowed me to attend the James Hall Meeting in Rochester, N.Y. I am grateful to A. Ferretti, M.E. Johnson, J. Kříž, H.P. Schönlaub, and D.J. Siveter for discussions on this topic. My special thanks are given to J.S. Peel, who provided work facilities in Uppsala, and to G.E. Budd for his advice and language correction. The manuscript was reviewed by E. Landing, R.E. Crick, and D.M. Rohr. I appreciate their constructive comments and helpful suggestions.

REFERENCES

- BERGER, A.Y., N.N. PREDTECHENSKII, Y.I. TESAOKOV, E.O. KOVALEVSKAYA, L.N. MINAEVA, V.G. KHROMYKH, A.P. GUBANOV, ET AL. 1991. To Develop and Introduce a Correlation of the Lithologic–Biostratigraphic Charts for the Cambrian and Silurian of the Siberian Platform and Taimir. *Trudy VSEGEI*, Leningrad (in Russian).
- BERRY, W.B.N., AND A.J. BOUCOT. 1973. Correlation of the African Silurian Rocks. Geological Society of America, Special Paper 147.
- BOGOLEPOVA, O.K. 1995. Cephalopod limestones from Mojero River section (eastern Siberia) and their paleogeographical implications. *Jahrbuch der geologischen Bundesanstalt*, 138:155–160.
- . 1996a. The basal Silurian of eastern Siberia. *Newsletters in Stratigraphy*, 33:63–75.
- . 1996b. Silurian cephalopod limestone biofacies: Taimir–the Carnic Alps— stratigraphy. *Geological Correlation*, 4:105–109 (in Russian).
- , AND A.P. GUBANOV. In press. Silurian cephalopod limestone biofacies from Eastern Siberia—fauna, age, and environments. In F. Oloriz and F.J. Tovar (eds.), IV International Symposium on Cephalopods—Present and Past.
- , AND C. HOLLAND. 1995. Concentrations of Silurian nautiloid cephalopods from Russia and Kazakhstan. *Acta Palaeontologica Polonica*, 40:429–436.
- , AND J. KŘÍŽ. 1995. Ancestral forms of Bohemian-type Bivalvia from the Lower Silurian of Siberia (Tungusskaya syncline, Russia). *Geobios*, 28:691–699.
- BOUCOT, A.J. 1990. Silurian biogeography, p. 191–196. In W.S. McKerrow and C.R. Scotese (eds.), *Palaeozoic Palaeogeography and Biogeography*. Geological Society of London, Memoir 12.
- BOURROUILH, R. 1981. "Orthoceratitico-Rosso" et "Goniaticitico-Rosso": facies marqueurs de la naissance et de l'évolution de paleomarges au Paléozoïque, p. 39–59. In E. Farinacci and M. Elmi (eds.), *Rosso Ammonitico Symposium Programma*. Tecnoscienza, Roma.
- BRENCHLEY, P. 1988. Environmental changes close to the Ordovician–Silurian boundary. *Bulletin of the British Museum (Natural History)*, 43:486–491.
- FERRETTI, A. 1989. Microbiofacies and constituent analysis of Upper Silurian–lowermost Devonian limestones from southwestern Sardinia. *Bollettino della Società Paleontologica Italiana*, 28:87–100.
- , AND J. KŘÍŽ. 1995. Cephalopod limestone biofacies in the Silurian of the Prague Basin, Bohemia. *Palaios*, 10:240–254.
- GNOLI, M. 1984. Paleontological content, constituent analysis and microbiofacies of Early Devonian pelagic limestones from the Fluminimaggiore area (SW Sardinia). *Bollettino della Società Paleontologica Italiana*, 23:221–238.
- , G.C. PAREA, F. RUSSO, AND E. SERPAGLI. 1979. Paleoeological remarks on the "Orthoceras Limestone" of southwestern Sardinia (Middle–Upper Silurian). *Memoire Società Geologica Italiana*, 20:405–423.
- HOLLAND, C.H., M. GNOLI, AND K. HISTON. 1994. Concentrations of Paleozoic nautiloid cephalopods. *Bollettino della Società Paleontologica Italiana*, 33:83–99.
- JOHNSON, M.E., G. BAARLI, R. NESTOR, AND D. WORSLEY. 1991. Eustatic sea-level [sic] patterns from the Lower Silurian (Llandovery Series) of southern Norway and Estonia. *Geological Society of America Bulletin*, 103:315–335.

- IVANOV, S.N., AND V.N. PUCHKOV. 1984. Geology of Sakmar Zone of the Urals. Sverdlovsk, 126 p. (in Russian).
- KHVOROVA, I.V., AND V.N. GRIGORIEV. 1974. Probable homolog of limestones like the Ammonitico Rosso in the Silurian of the south Urals. *Doklady Akademii Nauk SSSR*, 214:669–672 (in Russian).
- KIM, A.I., AND N.M. LARIN. 1968. On the Silurian/Devonian [sic, read n-dash, not virgule] boundary in southern Tian-Shan, p. 86–101. In B.S. Sokolov and A.B. Ivanovskii (eds.), *Biostratigraphy of Silurian/Devonian [sic, as above] Boundary Deposits*. Nauka, Moscow (in Russian).
- KRASNOV, V.I., V.E. SAVITSKII, Y.I. TESAKOV, AND V.V. KHOMENTOVSKII (eds.). 1983. Decisions of All-Union Meeting on the Precambrian, Paleozoic, and Quaternary Stratigraphy of Middle Siberia. Novosibirsk, 202 p. (in Russian).
- KŘÍŽ, J. 1979. Silurian Cardiolidae (Bivalvia). *Sbornik Geologických Ved. Paleontologie*, 22:1–157.
- . 1992. Silurian Field Excursion—Prague Basin (Barrandian), Bohemia. *Natural Museum of Wales, Geological Series* 13.
- , AND O.K. BOGOLEPOVA. 1995. *Cardiola signata* community (Bivalvia) in cephalopod limestones from Taimir (Gorstian, Silurian, Russia). *Geobios*, 28:573–583.
- KULKOV, N.P. 1967. Brachiopods and Stratigraphy of the Silurian of Gornyi Altai. Nauka, Moscow, 143 p. (in Russian).
- , E.V. VLADIMIRSKAYA, AND N.L. RYBKINA. 1985. Brachiopods and Biostratigraphy of the Ordovician and Silurian of Tuva. Nauka, Moscow (in Russian).
- LEONENOK, N.I. 1955. Silurian deposits of Kos-Istek region (northern Mugodzhary). *Trudy Laboratorii Uglya AN SSSR, Moscow-Leningrad*, 3:116–225 (in Russian).
- McKERRROW W. 1979. Ordovician and Silurian changes in sea level. *Journal of the Geological Society of London*, 136:137–145.
- MIAGKOVA, E.I. 1967. Silurian Nautiloids of the Siberian Platform. Nauka, Moscow, 47 p. (in Russian).
- NEKHOROSHEVA, L.V. 1981. Comment on a Stratigraphic Scheme of Silurian Deposits of the Vajgachsko-Novozemel'skij Region. *VNIIOkeangeologiya Press, Leningrad* (in Russian).
- NIKIFOROVA, O.I., AND A.M. OBUT (eds.). 1965. *Silurian System. Stratigraphy of the USSR*. Nedra, Moscow (in Russian).
- OBUT A.M., Z.M. ABDUAZIMOVA, A.N. GOLIKOV, AND R.E. RINENBERG. 1968. Graptolite zonal divisions and correlation of the Silurian deposits of Middle Asia, p. 75–86. In B.S. Sokolov and A.B. Ivanovskii (eds.), *Biostratigraphy of Silurian/Devonian [sic, n-dash, not virgule] Boundary Deposits*. Nauka, Moscow (in Russian).
- , R.F. SOBOLEVSKAYA, AND V.I. BONDAREV. 1965. *Silurian Graptolites of Taimir*. Nauka, Moscow (in Russian).
- PUCHKOV, V.N. 1979. Batial Complexes of Passive Margins of Geosynclinal Regions. Nauka, Moscow (in Russian).
- RONOV, A., V. KHAIN, AND K. SESLAVINSKIJ. 1984. *Atlas of Lithologic-Paleogeographic Maps of the World, Late Precambrian and Paleozoic of Continents*. USSR Academy of Sciences, Leningrad (in Russian).
- SCHÖNLAUB, H.P., AND O.K. BOGOLEPOVA. 1994. Rauchkofel Boden section, p. 103–110. In H.P. Schönlaub and L.H. Kreutzer (eds.), *IUGS, Subcommission on Silurian Stratigraphy. Field Meeting, Eastern + Southern Alps, Austria 1994. Bibliotheka geologische Bundesanstalt, Wien*, 30.
- , L.H. KREUTZER, AND H. PRIEWALDER. 1994. Cellon section, p. 83–93. In H.P. Schönlaub and L.H. Kreutzer (eds.), *IUGS, Subcommission on Silurian Stratigraphy. Field Meeting, Eastern + Southern Alps, Austria 1994. Bibliotheka geologische Bundesanstalt, Wien*, 30.
- SCOTSE, C.R., AND W.S. McKERRROW. 1990. Revised world maps and introduction, p. 1–21. In W.S. McKerrrow and C.R. Scotese (eds.), *Palaeozoic Palaeogeography and Biogeography. Geological Society of London Memoir* 12.
- SENNIKOV, N.V. 1979. Graptolite assemblages in the Upper Ordovician and the Lower Silurian of eastern Siberia, p. 45–56. In B.S. Sokolov (ed.), *Problems of Stratigraphy and Tectonics in Siberia*. IGIG Press, Novosibirsk (in Russian).
- SESLAVINSKII, K.B. 1987. *Caledonian Sedimentation and Volcanism in Earth History*. Nedra, Moscow, 192 p. (in Russian).
- . 1988. Sedimentation and volcanism in Early and Middle Paleozoic geosynclines. *Soviet Geology*, 3:43–52 (in Russian; English version in *International Geology Review*, 1988, 30:136–145).
- . 1991. Global transgressions and regressions during the Paleozoic. *Izvestiya AN SSSR, Geology Series*, 1:71–79 (in Russian; English version in *International Geology Review*, 1991, 33:107–114).
- SOKOLOV, B.S. 1967. Basic problems of Ordovician and Silurian stratigraphy of middle Siberia, p. 19–43. In B.S. Sokolov (ed.), *Paleozoic Stratigraphy of Middle Siberia*. Nauka, Novosibirsk (in Russian).
- (ed.). 1992. *Silurian Sequences and Fauna in the North of Tunguskaya Syncline*. Nauka, Novosibirsk, 191 p. (in Russian).
- VLADIMIRSKAYA, E.V. 1978. Biostratigraphy of the Chergak Formation of Tuva, p. 10–22. In E.V. Vladimirskaia (ed.), *Stratigraphy and Paleontology of the Urals and Asian Part of the USSR*, 73 (2), Leningrad (in Russian).
- WENDT, J., AND T. AIGNER. 1985. Facies patterns and depositional environments of Paleozoic limestones. *Sedimentary Geology*, 44:263–300.
- ZIEGLER, A.M. 1981. Paleozoic paleogeography, p. 31–37. In *Paleoreconstruction of the Continents. American Geophysical Union, Geodynamical Series* 2.
- ZLOBIN, M.N. 1962. *Silurian and Devonian of eastern Taimir*. *Trudy NIIGA*, 130:27–36, (in Russian).
- . 1965. Eastern Taimir, p. 364–370. In O.I. Nikiforova and A.M. Obut (eds.), *Silurian System. Stratigraphy of the USSR*. Nedra, Moscow (in Russian).

SPECIES DIVERSITY OF SILURIAN GASTROPODS RELATED TO ABIOTIC EVENTS

ALEXANDER P. GUBANOV

*Department of Historical Geology & Palaeontology, Institute of Earth Sciences,
Uppsala University, Norbyvägen 22, S-752 36, Uppsala, Sweden
Current address: Institute of Geology, Novosibirsk 630090, Russia*

ABSTRACT—Species diversity dynamics of Silurian gastropods reveal an intimate relationship to sea-level fluctuation. In turn, sea-level fluctuation during the Silurian was associated with glacio-eustatic change in the Early Silurian and gradual shoaling of most Silurian basins as a final stage of Caledonian tectonism. This picture was complicated by other minor fluctuations of sea-level, the specific reasons for which are not always clear. Sea-level fluctuations and resultant changes of gastropod species diversity were cyclic. Four important cycles are recognized in the Silurian, and correspond to the Llandovery, Wenlock, Ludlow, and Pridoli Series. The Llandovery cycle has four subcycles. The most important changes in species diversity occurred at the boundaries between major cycles. It is assumed that species diversity was related to the total area occupied by shallow seas. A decrease this area resulted in higher interspecific competition and produced a fall in diversity, while increase in the area of shallow marine shelves caused a reduction in competition and a corresponding rise in speciation.

INTRODUCTION

Paleozoic gastropods, especially those from the Silurian, have been little studied, though they played an important role in paleoecosystems and are of interest in evaluation of abiotic environmental factors on the benthos. It has been established (Gubanov, 1985) that gastropod intraspecific variation during the Silurian was associated with basin hydrodynamics. Changes in species diversity also depended strongly on sea-level fluctuation and water depth of basins.

DATA

The stratigraphic range of Silurian gastropods in Avalonian Britain (Murchison, 1839; Donald, 1899, 1902, 1905, 1906; Longstaff, 1909; Reed, 1920–1921; Pitcher,

1939), Nova Scotia (Peel, 1977, 1978), eastern Siberia (Gubanov, 1985, 1988, 1992, 1994 a, 1994b; Gubanov and Yochelson, 1994), Estonia (Isakar et al., 1990), Gotland (Lindström, 1899; Peel and Wängberg-Eriksson, 1979), and Podolia, western Ukraine (Mironova, 1987) provides the basis for the study of their diversity through this geological period. It also provides data on the possible relationship between species diversity and abiotic events, including sea-level fluctuation and water depths. Preliminary work for this study placed all available data into a modern stratigraphical framework. Great difficulties still remain for the Barrandian in the Prague Basin and some regions of North America, where Silurian gastropods are well studied but refinement of the stratigraphic range of gastropods in individual sections remains to be done.

RESULTS

Comparison of species diversity curves of gastropods from different regions based on their stratigraphic range has shown that periods of diversity variation coincide with boundaries between major chronostratigraphic units (Figure 1). The most significant changes in gastropod phylogeny took place at the Ordovician–Silurian boundary. The Late Ordovician biotic crisis, one of the most important in earth history (Raup and Sepkoski, 1982), resulted in a nearly complete change of gastropods at the species level. Unfortunately, poor knowledge of gastropods from the boundary beds, the relative dominance of Ordovician–Silurian boundary sections from deep-water deposits where gastropods are usually absent, and a significant lack of Upper Ordovician shallow-water facies make it impossible to evaluate the number of surviving species.

The Late Ordovician glaciation resulted in a marked lowering in sea-level and narrowing of shelf areas that induced a biotic crisis. Subsequent increase in tempera-

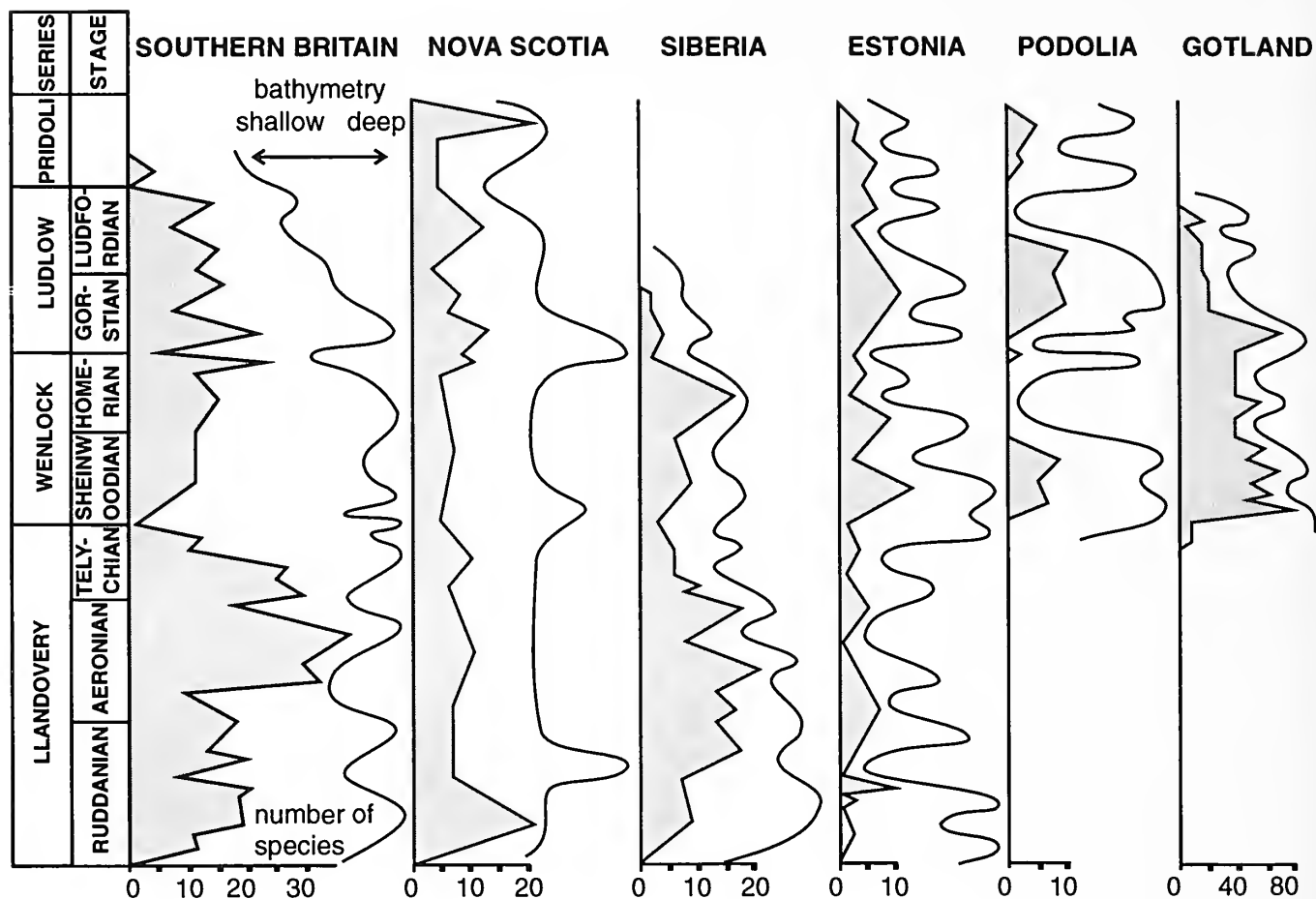


FIGURE 1—Change in gastropod species diversity and relative water depth in the Silurian of southern Britain, Nova Scotia, Gotland (after McKerrow, 1979), Estonia (after Kyrts et al., 1991), Podolia (after Gritsenko et al., 1986), and Siberia (author's unpublished data).

ture and deglaciation caused a dramatic sea-level rise at the beginning of the Early Silurian (Berry and Boucot, 1973; McKerrow, 1979; Brenchley, 1988). This event is associated with an important "anoxic event" that brought about the widespread deposition of thick black limestones and graptolite shales at the base of the Silurian (Berry and Wilde, 1978; Jeppsson, 1990).

Another important change in gastropod diversity occurred at the Llandovery–Wenlock boundary, but this change is expressed differently in different regions. In southern Britain and eastern Siberia, gastropod assemblages decrease in diversity through the upper Llandovery, and there is wide variation in the diversity of gastropods in the lower Wenlock (Figure 1). In Estonia, Gotland, and Podolia, the early Wenlock rise in diversity was explosive in character and far exceeded that of the Llandovery (Peel and Wängberg-Eriksson, 1979; Mironova, 1987; Isakar et al., 1990). A change in species composition also took place in Nova Scotia (Peel, 1977, 1978).

A major extinction of gastropods accompanied by a sharp decrease in species diversity occurred at the boundary between the Wenlock and Ludlow in southern Britain and eastern Siberia (Figure 1). In Nova Scotia and Estonia, the extinction was less profound (Peel and Wängberg-Eriksson, 1979; Isakar et al., 1990). In Podolia, gastropods disappeared from the record somewhat earlier in the middle Wenlock (Mironova, 1987). On Gotland, the diversity did not diminish in the late Wenlock. However, in the early Ludlow, the number of species increased almost twofold during a short interval (Figure 1). A significant increase in diversity at this point is observed in southern Britain, Nova Scotia, and Estonia (Peel, 1977, 1978; Isakar et al., 1990). Only *Catazone* sp. appeared in the earliest Ludlow of Podolia, but the sharp increase in the number of species occurred somewhat later there (Mironova, 1987). On the Siberian platform only *Prosolarium cirrosa* joined several species (*Murchisonia cingulata* and *Straparollus alacer*) known after the late Wenlock extinction, but by the end of the

Gorstian they also became extinct (Gubanov, 1988). Somewhat later, at the end of the early Ludfordian, the gastropods disappeared from the Podolian record, but their diversity decreased considerably for a short time in Estonia and on Gotland (Mironova, 1987).

After the late Ludfordian, the gastropods of southern Britain underwent a considerable decrease in diversity followed by an insignificant increase before they disappeared by the middle early Pridoli (Figure 1). In Nova Scotia after a 50% reduction in the number of species in the late Ludlow, the number of gastropod species was stable until the middle Pridoli, when diversity more than doubled (Peel, 1977, 1978). At the boundary between the Ludlow and Pridoli in Estonia, the number of gastropod species was reduced, but to a lesser extent than during the event at the Gorstian–Ludfordian boundary; in early Pridoli times the diversity increased for a short period (Isakar et al., 1990). In Podolia, gastropods are absent in the upper Ludfordian, but reappear in the early Pridoli and progressively increase in diversity (Mironova, 1987). Unfortunately, where gastropods are recorded up to the end of the Silurian, Devonian examples are very poorly known, and nothing is known about the change of the species composition at the Silurian–Devonian boundary.

The variations in species composition described above were closely related to fluctuations of sea-level and increase in basin depth. Such a relationship is evident when the curves for species diversity, sea-level fluctuation, and basin depth are compared for different regions (Figure 1). The data on sea-level and basin water depth changes in the Silurian of southern Britain, Nova Scotia, and Gotland are taken from McKerrow (1979). The curves for Estonia were constructed by the author using the data of Kyrts et al. (1991), and for Podolia with data from Gritsenko et al. (1986). Data for the Siberian Platform are based on the author's research. Increases in gastropod diversity are associated with transgression, and diversity decreases with regressions and changes in basin water depth. The relationship between cyclic changes of species composition, sea-level changes, and basin water depth is easily seen. The general nature of sea-level changes in the Silurian includes a sharp rise in the early Llandovery and a slow lowering through the latest Silurian. The general lowering of sea-level was affected by cyclic changes of higher-order magnitude. Four cycles are recognized in the Silurian, and correspond to the Llandovery, Wenlock, Ludlow, and Pridoli. Each cycle started with major sea-level rise. The same periodicity is noted in the species diversity of gastropods.

In well-studied Llandovery sequences in Britain, four more minor cycles of gastropod species diversity

changes can be established. The first cycle involves the lowermost Rhuddanian (A2–A4 of British standard) and ends with a 52% decrease in species diversity. Comparatively greater changes took place at this point in Estonia (100%) and Nova Scotia (65%). The lowest decrease in diversity occurred in Siberia (10%).

The second cycle comprises the upper Rhuddanian and lowermost Aeronian (B1–B3). It began with the complete replacement of gastropod species in Estonia. In Siberia, the number of species doubled. In southern Britain, the species diversity remained stable, but with an almost 50% change in species composition. In Nova Scotia, the diversity remained unchanged. The cycle ended with a considerable decrease in diversity in Britain (43%) and eastern Siberia (22%), but in Nova Scotia and Estonia, this event is not recognized.

The third cycle (middle Aeronian, C1–C3) begins with a threefold increase in diversity of gastropod species in southern Britain, and with an increase of 50% in Siberia; it ends with diversity dropping to almost half (49%) in southern Britain. In other regions, this level of change is not seen. A more significant change occurred in the gastropod composition in Estonia, with a complete disappearance of earlier species and appearance of five new ones (*Boiotremus longitudinalis*, *Kjalromphalus* new sp., *Murchisonia* sp., *Stenoloron aequilatera*, and a new pleurotomariacean). In eastern Siberia, 57% of the species disappeared before the diversity again increased by half. This happened somewhat earlier than in the British Isles. In Nova Scotia, the diversity decreases are 33% and 40%, respectively, and occurred somewhat later than in the British Isles.

The fourth Llandovery cycle is only easily recognized in British sections, and is characterized by an increase of gastropod species diversity by 30% at the beginning and by a nearly complete disappearance of Llandovery species at the end. The upper boundary of the cycle, which coincides with a boundary between cycles of a higher order, is clearly defined in all of the regions discussed.

The change in sea-level and basin water depth had a similarly cyclic recurrence in the Llandovery of southern Britain, eastern Siberia, and Estonia, and was apparently characteristic of many other regions worldwide (Johnson et al., 1991; Johnson and McKerrow, 1991; Johnson, 1996). A somewhat different situation occurred in Nova Scotia, where the cyclic changes in gastropod species diversity were minor and cyclic changes in sea-level and basin water depth are not well defined. The basin water depth remained the same throughout the Silurian. Short periods of deepening of the basin in the middle Rhuddanian and at the Llandovery–Wenlock, Wenlock–Ludlow, and

Ludlow–Pridoli boundaries were quickly compensated for by sedimentation and aggradation.

For the Wenlock, only one cycle of gastropod diversity change exists, although species composition changed diachronously in different regions. In southern Britain during the Homerian, diversity was reduced by 25% before doubling. Wenlock variation is recorded through the upper Sheinwoodian of Estonia, with a drop and rise in diversity of 75% and 300% respectively. On Gotland, this variation occurred to a somewhat lower degree than in Estonia, with a 34% and 25% change, respectively. In eastern Siberia and Podolia, the change took place at the Sheinwoodian–Homerian boundary, with diversity first dropping by 22% and then increasing by 100% in Siberia, and a complete extinction in Podolia. This level also is definable in southern Britain and on Gotland, but is rather inconspicuous. During the Ludlow and Pridoli, these smaller cycles are difficult to define. Nevertheless, a relationship between the change in species diversity of gastropods and the fluctuation of sea-level and basin water depth is clearly seen.

A special feature should be noted. In the British Isles and on the Siberian Platform, the highest species diversity occurs during the late stages of important cycles that correspond to the epochs. In the southwest and northwest Russian Platform (Podolia, Estonia, and Gotland), this high diversity coincides with the initial stages of cycles. The close match between the species diversity of Silurian gastropods and fluctuation of sea-level and basin water depth in different regions indicates a close relationship between species diversity and the events that effected the change in sea-level and water depth.

DISCUSSION

Fluctuations of sea-level and water depth were probably associated with changes in climate and tectonic regimes. A general regressive trend in sea-level change is associated with the final stage of the Caledonian cycle (Seslavinskij, 1987, 1991), and early Llandovery transgression followed Late Ordovician glacio-eustatic events (McKerrow, 1979). The subsequent Early Silurian glaciation, which is known in South America (Grahn and Caputo, 1992), apparently was considerably less important than the Late Ordovician glaciation, and the consequence for changes of sea-level and gastropod diversity were not as severe. Although the general relationship between major changes in gastropod species diversity and these events is evident, the mechanism behind it remains unclear. One possibility is MacArthur and Wilson's "theory of balance" (R.H. MacArthur and E.O. Wilson *in* Hallam, 1983). By this model, sea-level lowering reduced

the area of shallow seas. The basins on the platforms were reduced in size, and the size of the biotopes decreased simultaneously. This resulted in increased K-selection that brought about a decrease in taxonomic diversity. Conversely, an increase in sea area favored the appearance of new biotopes and extension of previous ones. The result of radiation of biotopes produced a burst of speciation.

CONCLUSIONS

Four global cycles of species diversity changes among gastropods are defined for the Silurian. The boundaries of diversity cycles coincide with those of the series. Four lower-magnitude diversity cycles are established in the Llandovery. The reasons behind these changes are as yet unclear. The change in the area of shallow seas probably had a direct influence on species diversity. Decreases in shallow-sea area led to decreases in biotopes (because of increased biological competition) and species diversity. Conversely, increased shallow-sea area resulted in radiation of new biotopes, a decrease in competition, and intense speciation.

There existed a close relationship between the change in species diversity of gastropods and sea-level changes. The most important events which caused global sea-level fluctuations were glacio-eustasy in the early Llandovery and the final stage of Caledonian tectonism. The latter was responsible for regression in the Silurian.

ACKNOWLEDGMENTS

I am indebted to J.S. Peel for helpful discussion and critical reading of the initial manuscript and for providing the opportunity to complete this study; to M.E. Johnson for encouragement and advice; and to E. Landing for careful and critical reading of the manuscript and for linguistic corrections. I thank J.A. Harper and an anonymous reader for reviews and for the opportunity of seeing the study in two different lights.

REFERENCES

- BERRY, W.B.N., AND P. WILDE. 1978. Progressive ventilation of the oceans—an explanation for the distribution of the Lower Paleozoic black shales. *American Journal of Science*, 278:257–275.
- , AND A.J. BOUCOT. 1973. Glacio-eustatic control of Late Ordovician–Early Silurian platform sedimentation and faunal changes. *Geological Society of America Bulletin*, 147:275–284.
- BRENCHLEY, P.J. 1988. Environmental changes close to the Ordovician–Silurian boundary. *Bulletin of the British Museum (Natural History)*, 43:377–385.

- DONALD, J. 1899. Remarks on the genera *Ectomaria* Koken and *Hormotoma* Salter, with descriptions of British species. Quarterly Journal of the Geological Society of London, 55:251-272.
- . 1902. Proterozoic Murchisoniidae, Pleurotomariidae and Turritelliidae. Quarterly Journal of the Geological Society of London, 58:313-339.
- . 1905. On some gastropods from the Silurian rocks of Llangadock. Quarterly Journal of the Geological Society of London, 61:567-577.
- . 1906. Notes on the genera *Omospira*, *Lophospira* and *Turritoma*; with descriptions of new Paleozoic species. Quarterly Journal of the Geological Society of London, 62:552-572.
- GRAHN, H., AND M.V. CAPUTO. 1992. Early Silurian glaciation in Brazil. Palaeogeography, Palaeoclimatology, Palaeoecology, 99:9-15.
- GRITSENKO, V. P., A.A. ISCHENKO, AND L.I. KONSTANTINENKO. 1986. Opyt rekonstruktsii yarugskikh i malinovetskh (silur Podolii) donnykh soobshestv (Reconstructions of bottom communities of Yarug and Malinovets Beds (Silurian of Podolia), p. 73-79. In D. Kaljo and E. Klamann (eds.), Theory and Practice of Ecostratigraphy. Valgus, Tallinn (In Russian with English abstract).
- GUBANOV, A.P. 1985. Izmenchivost' gastropod i ee zavisimost' ot gidrodinamiki bassejna (Gastropod variations and their dependence on basin hydrodynamics), p. 70-74. In O.A. Betekhtina and I.T. Zhuravleva (eds.), Sreda i Zhizn' v Geologicheskome Proshlom. Paleobassejny i ikh Obitateli (Environment and Life in the Geological Past. Palaeobasins and Their Habitants). Nauka, Novosibirsk.
- . 1988. Gastropody Silura Sibirskoy Platformy. Taksonomicheskii, Paleoekologicheskii i Biostratigraficheskii Analiz (Silurian Gastropoda of Siberian Platform. Taxonomic, Palaeoecologic, and Biostratigraphic Analysis). Avtoreferat na soiskanie Stepni Kandidata Geologo-Mineralogicheskikh Nauk. Institut Geologii i Geofiziki SO AN SSSR, Novosibirsk.
- . 1992. Gastropody silura opornogo razreza reki Nizhney Bol'shoy Kuondy (Silurian Gastropoda of the Nizhnyaya Bolshaya Kuonda River section), p. 128-146. In B.S. Sokolov (ed.), Razrezy i Fauna Silura Severa Tungusskoy Sineklizy (Silurian Sequences and Fauna of the North of the Tunguska Syncline). Izdatel'stvo Nauka, Novosibirsk.
- . 1994a. Dinamika izmeneniya struktury soobshchestv siluriiskikh gastropod na Sibirskoy platforme (The changing dynamics in composition of Silurian gastropod communities on the Siberian Platform), p. 11-13. In N.V. Kruchina (ed.), Dinamika Raznoobraziya Organicheskogo Mira vo Vremeni i Prostranstve (The Time-Space Diversity Dynamics of the Organic World). XL session of the All-Russian Palaeontological Society, St. Petersburg.
- . 1994b. The dynamics of change in composition of Silurian gastropod communities in the Siberian basin, p. 129-130. In H.P. Schönlaub and L.H. Kreutzer, IUGS Subcommittee on Silurian Stratigraphy—Field Meeting Eastern + Southern Alps, Austria 1994. Bibliothek Geologische Bundesanstalt, 30.
- , AND E.A. YOCHELSON. 1994. Wenlockian (Silurian) gastropod shell and operculum from Siberia. Journal of Paleontology, 68:486-491.
- HALLAM, H. 1983. Facies Interpretation and the Stratigraphic Record. Mir, Moscow.
- ISAKAR, M.A., M.G. MIRONOVA, AND V.Yu. SALADZHYUS. 1990. Klass Gastropoda-Bryukhonogie molluski (Class Gastropoda), p. 5-15. In G.N. Kiselev, I.N. Sinitsyna, M.A. Isakar, M.G. Mironova, and V.Yu. Saladzhyus, Atlas Mollyuskov Verkhnego Ordovika i Silura Severo-Zapada Vostochno Evropeiskoy Platformy (Atlas of Upper Ordovician and Silurian Molluscs of East-European Platform). Izdatel'stvo LGU, Leningrad.
- JEPPSSON, L. 1990. An oceanic model for lithological and faunal changes tested on the Silurian record. Journal of the Geological Society of London, 147:663-674.
- JOHNSON, M.E. 1996. Stable cratonic sequences and a standard for Silurian eustasy, p. 203-211. In B.J. Witzke, G.A. Ludvigson, and J.E. Day (eds.), Paleozoic Sequence Stratigraphy: Views from the North American Craton. Geological Society of America, Special Paper 306.
- , AND W.S. MCKERROW. 1991. Sea level and faunal changes during latest Llandovery and earliest Ludlow (Silurian). Historical Biology, 5:153-169.
- , B.G. BAARLI, H. NESTOR, M. RUBEL, AND D. WORSLEY. 1991. Eustatic sea-level patterns from the Lower Silurian (Llandovery Series) of southern Norway and Estonia. Geological Society of America Bulletin, 103:315-335.
- KYRTS, A.L., R.M. MYANNIL', L.Ya. PYLMA, AND R.E. EINASTO. 1991. Etapy i obstanovki nakopleniya kukersitovoy (vodoroslevoj) organiki v ordovike i silure Estonii (Time and cycles of sedimentation of Kukersits (Algae) in the Ordovician and Silurian of Estonia), p. 87-94. In D. Kaljo, T. Modzalevskaya, and T. Bogdanova (eds.), Vazhnejshie Bioticheskie Sobytiya v Istorii Zemli (Major Biological Events in Earth History). Institut Geologii AN Estonii, Tallinn.
- LINDSTRÖM, G. 1889. On the Silurian Gastropoda and Pteropoda of Gotland. Kongliga Svenska Vetenskaps Akademiens Handlingars, 19.
- LONGSTAFF, J. 1909. The genus *Loxonema*. Quarterly Journal of the Geological Society of London, 65:210-228.
- MCKERROW, W. S. 1979. Ordovician and Silurian changes in sea level. Journal of the Geological Society of London, 136:137-145.
- MIRONOVA, M.G. 1987. Klass Gastropoda-Bryukhonogie mollyuski (Class Gastropoda), p. 8-21. In Atlas Siluriiskikh Mollyuskov Podolii (Atlas of Silurian Molluscs of Podolia). Izdatel'stvo LGU, Leningrad.
- MURCHISON, R. 1839. The Silurian System. Geological Society of London.
- PEEL, J.S. 1977. Systematics and palaeontology of the Silurian gastropods of the Arisaig Group, Nova Scotia. Det Kongelige Danske Videnskabernes Selskab Biologiske Skrifter, 21:1-89.
- . 1978. Faunal succession and mode of life of Silurian gastropods in the Arisaig Group, Nova Scotia. Palaeontology, 21:285-306.
- , AND K. WÄNGBERG-ERIKSSON. 1979. Gastropods, p. 105-108. In V. Jaanusson, S. Laufeld, and R. Skoglund (eds.), Lower Wenlock Faunal and Floral Dynamics—Vatenfallet Section, Gotland. Sveriges Geoliska Undersökning, C 762.
- PITCHER, B. 1939. The Upper Valentian gastropod fauna of Shropshire. Annals and Magazine of Natural History, 11:82-132.
- RAUP, D.M., AND J.J. SEPKOSKI, JR. 1982. Mass extinction in the marine fossil record. Science, 215:1501-1503.
- REED, F. 1920-1921. British Ordovician and Silurian Bellerophonacea. Palaeontographica Society, London.
- SESLAVINSKIY, K. B. 1987. Kaledonskoe Osadkonakoplenie i Vulkanizm v Istorii Zemli (Caledonian Sedimentation and Volcanism in Earth History). Nedra, Moscow.
- . 1991. Global'nye transgressii i regressii v paleozoe (Global transgressions and regressions during the Paleozoic). Izvestiya AN SSSR, Seriya Geologicheskaya, 1: 71-79.

SILURIAN–DEVONIAN TRILOBITE EVOLUTION AND DEPOSITIONAL CYCLICITY IN THE ALTAI-SALAIR REGION, WESTERN SIBERIA

EVGENY A. YOLKIN

United Institute of Geology, Geophysics and Mineralogy, Russian Academy of Sciences,
Siberian Branch, 630090 Novosibirsk-90, Russia

ABSTRACT—Data on evolutionary lineages and transgressive–regressive (T–R) cycles allow recognition of patterns in evolutionary and depositional processes in the Silurian–Devonian Altai-Salair marginal sea. A transition from a passive into an active continental margin is recorded in this area in the earliest Emsian by a change in the magnitude of T–R cycles that did not affect iterative trilobite evolution. Repetitive patterns of dechenellid morphology are expressed by three levels of evolutionary change. Higher ranks of evolutionary stages are represented by combinations of elementary (first-rank) evolutionary changes. These patterns calibrate the western Siberia T–R succession. T–R cycles are symmetrical or asymmetrical. Reef limestones represent the second of three (transgressive, stillstand, regressive) sea-level stages.

Cycle orders in the Silurian–Devonian of western Siberia correlate with dechenellid evolutionary stages. In the Altai-Salair Silurian, only third-order T–R cycles are known. One of them is bounded by the bases of the *Glyptograptus persculptus* and *Monograptus triangulatus* Zones. The bases of the *Monograptus sedgwickii*, *Cyrtograptus lapworthi*-*C. insectus*, and *Bohemograptus bohemicus* Zones in Altai-Salair sections record the onset of sedimentary cycles comparable to second-rank dechenellid evolutionary stages (alpha and beta). Pairs of asymmetrical and symmetrical cycles within the Altaian succession are separated by the base of the *C. lapworthi*-*C. insectus* Zone, and are represented by depositional phases A and B that correspond to third-rank evolutionary stages. In Altai-Salair sections, as in other areas, the Silurian and Devonian record initial abrupt transgression and terminal strong regression. They include two- and three-fold depositional phases (A–B; A–B–C) that correspond to the structure of asymmetrical and symmetrical cycles. This arrangement suggests a higher-level, second-order cyclicity. The local sea-level curve agrees with the Silurian and Devonian curves proposed for different continents, and particularly with the Euroamerican standard.

INTRODUCTION

Long-lived lineages of dechenellid trilobites demonstrate repetitive patterns of evolutionary change (Yolkin, 1983). These patterns show up against a background of Middle Paleozoic cyclic sedimentation in the Altai-Salair basin (Yolkin, 1968; Yolkin and Zheltonogova, 1974; see Figure 1). Similar iterative patterns of trilobite evolution were described by Kaufmann (1933) from olenid trilobite lineages from the Upper Cambrian of Sweden. Comparison of the dechenellid evolutionary stages and sedimentary cycles, however, does not show a precise agreement. Furthermore, the ranges of most species in these lineages cross all facies boundaries in mixed siliciclastic and carbonate sequences. These observations lead to the conclusion that dechenellid evolutionary stages are independent of regional tectonic or depositional processes, but are influenced by outside (global) factors.

Another explanation for the recurrent morphological evolution of dechenellids may be found in applying

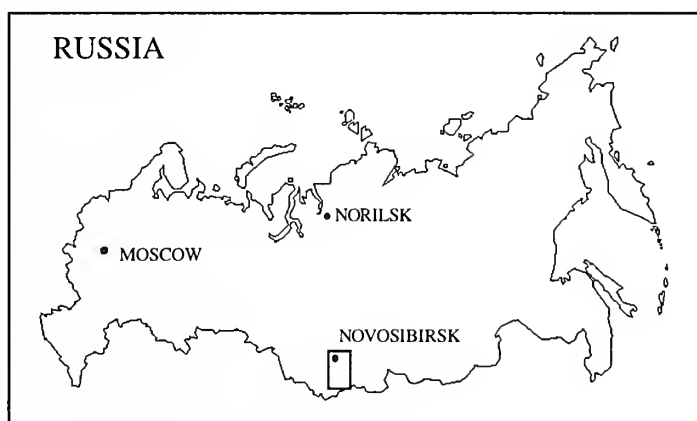


FIGURE 1—Index map of Russia with location of the Altai-Salair region southwest of Novosibirsk.

the theory of nomogenesis (Berg, 1977), or the supposed ability of organisms to evolve by regular patterns. After testing, this possibility was rejected because the long-term changes of dechenellid morphology were too complicated and regular to be accounted for by this theory. The conclusion was that these changes were forced by factors of a telluric (global) and/or cosmic origin (Yolkin, 1979).

Revitalization of Devonian eustatic studies in the 1980s (House, 1983, 1985; Johnson et al., 1985) stimulated a reconsideration of data on the cyclicity of the Devonian in western Siberian. It was found that this cyclicity has a eustatic origin (Talent and Yolkin, 1987). Recently, the same was done for the Altai-Salair Silurian sequences (Yolkin et al., 1997). The results led to an effort to calibrate the Silurian-Devonian eustatic cycles in western Siberia by means of different ranks of dechenellid evolutionary stages, with the ultimate aim of ordering the sedimentary cycles in which these trilobites occur. This goal was attractive because data on evolutionary and depositional processes can be related to a single sedimentary basin, and its tectonic environments had already been reconstructed (Yolkin et al., 1994). There are also reliable standard zonal scales for the Silurian and Devonian Systems, which offer a high level of temporal resolution, as well as exhaustive surveys on eustatic, sedimentary, and biological events (Johnson, 1996; Kaljo et al., 1996; Walliser, 1996). In this study, the entire Silurian-Devonian succession is analyzed, but primary attention is paid to the Silurian.

TERMINOLOGY

Eustasy, sedimentary cyclicity, and biotic changes have been described by numerous terms. Many have similar definitions and are applied in specific situations. For our purposes, it is important to clearly distinguish between phenomena, which are related to long-term processes (intervals) and short-term events. It is useful also to keep in mind their relationships to one another. Such a clustering of related terms for events includes: "deepening", "eustatic rise", "transgressive" stage (or phase), and "highstand". Short-term global events usually are correlated, as a rule, into the standard zones or subdivisions (Walliser, 1984, 1985, 1996; House, 1985; Johnson, 1996; Kaljo et al., 1996). Most of the T-R cycles documented in this report correspond to the third-order cycles defined by Vail et al. (1977). Although the Russian literature on Silurian-Devonian cycles in the Altai-Salair region also utilizes a numerical hierarchy, it is more-or-less the reverse of the scale proposed by Vail et al. (1997). For the sake of clarity, all references to T-R orders in this paper are transcribed to the scale of Vail et al. (1997).

In the Devonian, there are two parallel event scales (House, 1989). The first consists of the local (or standard) stratigraphic names for events. In most cases, these are related to sedimentary anoxia. Another scale represents events that are correlated by selected fossils of pelagic groups. We have combined these correlation schemes into a single event name (Yolkin et al., 1994). It should mean that, for example, the Syrovatiy (*Monograptus sedgwickii* Zone) Event has a type locality in the Altai area of the Altai-Salair region with a point in an actual stratigraphic section, and is situated at or near the lowest appearance of index species of the graptolite *Monograptus sedgwickii* Zone. In combining the potential of biostratigraphy and eustatic sedimentary markers, we attempt to improve both inter- and intraregional correlations.

It is known also that the cycles of siliciclastic and carbonate successions can be expressed another way. In general, siliciclastic cycles are composed of transgressive and regressive stages. At the same time, cyclic carbonates representative of the tropical realm with reefal accumulations typically form symmetrical (or asymmetrical) cycles with transgressive, stillstand, and regressive stages (Einsele, 1992). Cyclic carbonate sediments of both types characterized the shelf environments of the Altai-Salair region during Silurian-Devonian times.

METHOD OF ANALYSIS

The comparative analysis of dechenellid evolutionary stages and transgressive-regressive (T-R) cyclicity forms only a small part of larger-scale studies on the Middle Paleozoic Altai-Salair basin. The wider view is the so-called "basinal approach" to stratigraphical research that embraces the detailed examination of sections for a synthesis of stratigraphic, biostratigraphic, paleontologic, paleogeographic, and other features. In such cases, all of the data are tightly connected. For the area under study, much of the data is published (Yolkin, 1968; Yolkin and Zheltonogova, 1974; Sennikov, 1976).

These resources were used in the phylogenetic analysis of dechenellid lineages and led to the documentation of iterative patterns of evolutionary stages of this trilobite group and their relationship to control by global factors (Yolkin, 1979, 1983, p. 70). The data also provided the basis for paleogeographic reconstructions through narrow time slices from the Ordovician to the Devonian, with subsequent tectonic conclusions (Yolkin et al., 1994b). The results of the last noted study were especially important for an understanding of eustatic changes on the southwestern shelf of the Siberian continent in Silurian-Devonian time. They are expressed by two regional T-R cycle scales for the Devonian and Silurian

(Yolkin et al., 1994a; Yolkin et al., 1997; Yolkin et al., In press). Newly available data also allow determination of the relationship of sedimentary cyclicity to the different tectonic regimes of passive and active continental margins. This change from a passive to an active margin occurred in the Altai-Salair region at the beginning of Emsian (Early Devonian) time (Yolkin et al., 1994b).

In addition, it should be noted that global anoxic sedimentary events also coincide with eustatic events, as well as with the initiation of regional T-R cycles. They are good markers for an alignment of the local T-R cycle scales. By using the same approach for the Devonian System, we have recognized anoxic events in the Devonian (Yolkin et al., 1994b) and Silurian (Yolkin et al., 1997) of the Altai-Salair and Tian Shan regions.

SUCCESSION OF T-R CYCLES

Silurian and Devonian deposits are widely distributed in the Altai-Sayan Folded Area (ASFA). These marine facies lie on the southwestern margin of the Paleozoic Siberian continent along a narrow shelf belt (Yolkin et al., 1994b). This belt was a passive continental margin from the Ordovician to Early Devonian. It is distinctly subdivided throughout the Kuznetsk Basin and Altai-Salair region into outer and inner zones (Figure 2). The best Silurian sections are situated in the Altai area (Figure 2, locations 1 and 2), but Devonian sections occur in the Salair area of the Altai-Salair region and northwestern Kuznetsk Basin (Figure 2, locations 3 and 4).

This shelf belt was characterized by accumulation of terrigenous-carbonate deposits with local reef limestones on the outer shelf. Large-scale buildup structures developed periodically as barrier reefs on the carbonate platform.

The characteristic depositional motif in the ASFA during the Silurian and Devonian is seen in the cyclicity of the sections (Yolkin, 1968; Yolkin and Zheltonogova, 1974). Symmetrical and asymmetrical cycles can be easily distinguished from one another. Symmetrical cycles are represented by three sedimentary stages: transgressive, stillstand and regressive. In asymmetrical cycles, only the first two stages are expressed. Cycles of both types have sharp boundaries. In one situation, more often developed on the outer shelf, they are associated with sharp transitions from shallow- to deep-water deposits. In inner-shelf sections, they are associated with unconformities, which are frequently associated with basal conglomerates. On the basis of Silurian-Devonian sequences in the Kuznetsk Basin and Altai-Salair region where the T-R cycle scale is well developed, a T-R curve was constructed (Yolkin et al., 1997; Yolkin et al., in press). This scale (Figure 3)

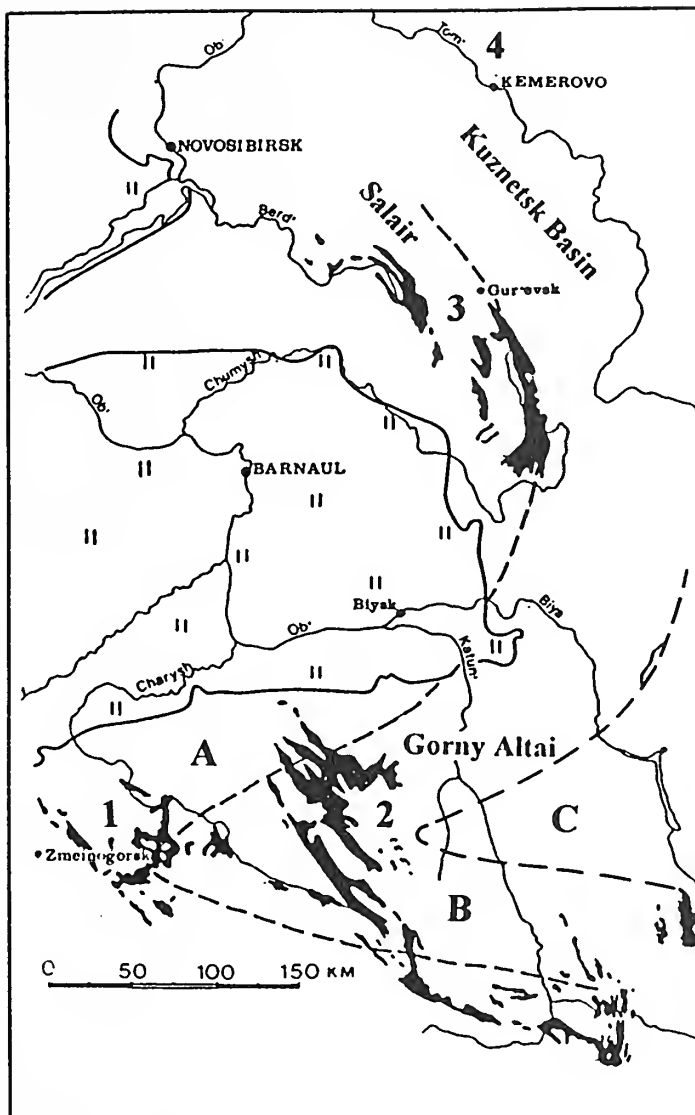
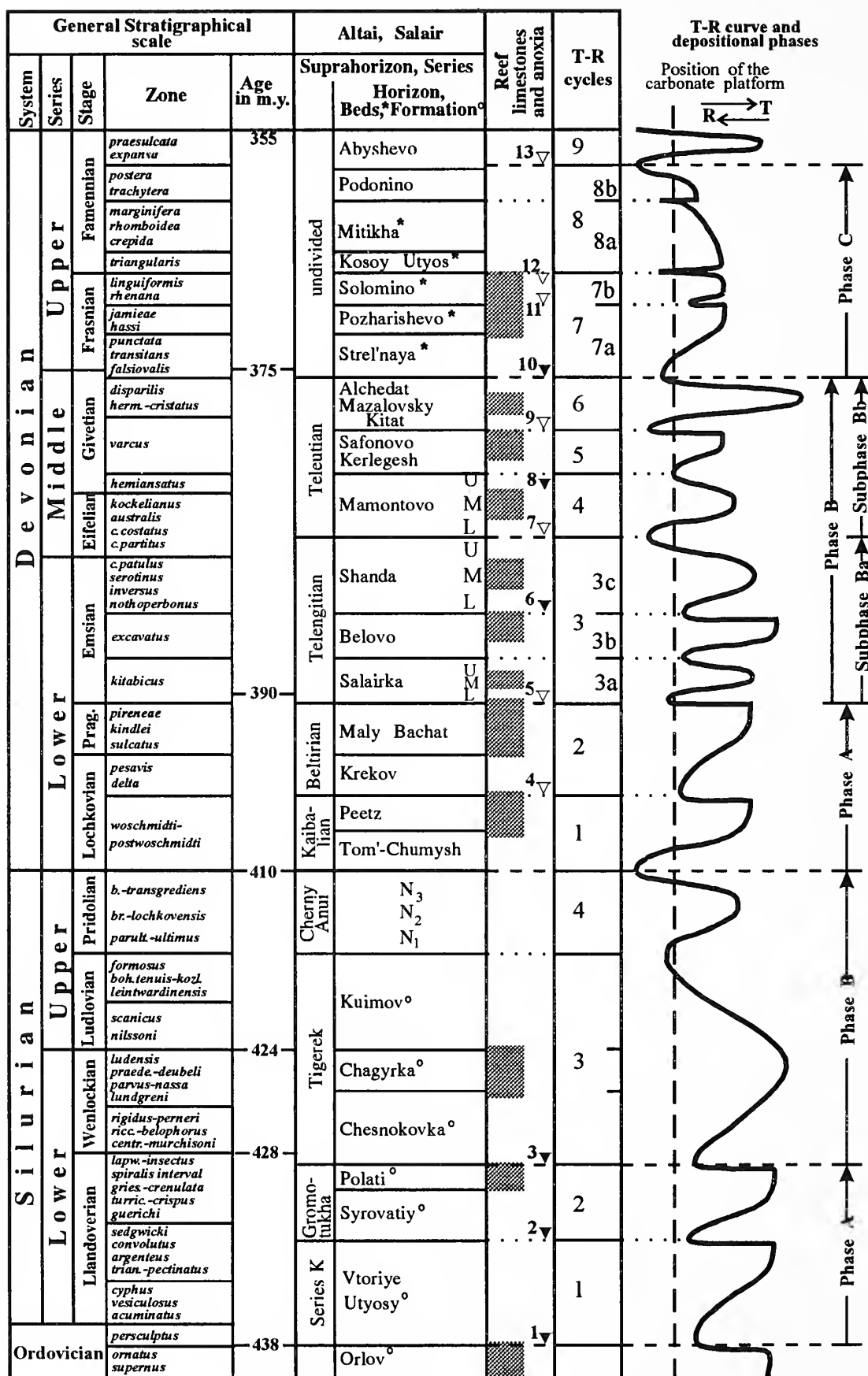


FIGURE 2—Distribution of Silurian outcrops (in black) in western part of the Altai-Sayan folded area, a shelf belt of the Siberian paleocontinent (A, outer shelf; B, inner shelf; C, land); with location of reference sections of Silurian (1, 2) and Devonian (3, 4). 1, watershed of the Inya River; 2, watershed of the Anuy River; 3, vicinity of the town of Gur'evsk; and 4, Tom' River downstream of the Kemerovo.

includes four Silurian and nine Devonian cycles. The majority of established cycles have reef limestone members, which correspond to stillstands (i.e., to the middle parts of symmetrical and the tops of asymmetrical cycles). The eustatic nature of these Devonian cycles is demonstrated by comparison with eustatic cycles of the Euramerica scale (Talent and Yolkin, 1987).

A recognition of the simple structure of the Siberian Middle Paleozoic cycles and their obvious repetitive character and relationship to eustasy appears to support the proposal of regular patterns of cyclic sedimentation



and eustatic fluctuations. As will be demonstrated below, however, a periodicity in the succession of cycles can be observed in both the Silurian and Devonian.

SILURIAN CYCLES

The first two sedimentary cycles of this system are approximately correlative with the Llandovery Series, and are bounded by three event levels (Figure 3). The lower limit of the first cycle is represented by a sharp transition from Upper Ordovician reef limestones into black shales that are characterized by *Glyptograptus persculptus* (Salter) (Yolkin et al., 1988). The initiation of this cycle and of Silurian transgression appears to be the anoxic Chineta (*G. persculptus* Zone) Event (Yolkin et al., 1997). Initiation of the second cycle also coincides with a deepening event. It is designated the Syrovatiy (*Monograptus sedgwickii* Zone) Event. It also features a sharp transition from extremely shallow-water deposits (moderately coarse-grained siliciclastics with cross-bedding) to dark shales. The beginning of the third cycle is represented by another deepening event that is shown as a shift from reef limestones to black shales. It is named the Chesnokovka (*Cyrtograptus lapworthi*-*C. insectus* Zone) Event. Thus, the former two cycles have structures characterized by asymmetrical deposition, and their boundaries are well correlated by graptolites.

Cycles 3 and 4 certainly should be regarded as symmetrical in structure. The first of them represents a typical marine sequence with siliciclastics succeeded by reef limestones and overlain by argillaceous limestones. Quite continuous transitions occur between all of these lithologies (Yolkin and Zheltonogova, 1974). At the same time, the second cycle, number 4, is composed mostly of non-marine sediments with a bedded limestone member in its middle.

In some inner-shelf sections of the Chesnokovka Formation, a transgressive stage of cycle 3 exhibits all three stages of a symmetrical cycle. A deepening event at

the base of the Kuimov Formation that includes a Ludlovian benthic faunal association can be recognized (Yolkin and Zheltonogova, 1974).

On a regional scale, the boundary between cycles 3 and 4 is very sharp, and formed by interformational conglomerates (but without significant hiatuses). This boundary has been correlated provisionally with the base of the Pridoli on the basis of benthic fossils that belong to the Cherny Anui Formation (Yolkin and Zheltonogova, 1974; Yolkin, 1983).

DEVONIAN CYCLES

Siberian Devonian cycles have been described in detail (Yolkin et al., 1994; Yolkin et al., in press). Figure 3 displays their complete succession. Many Devonian cycles are separated by unconformities. The largest one, which is angular, is correlated with the Silurian-Devonian boundary.

The first two of the Devonian cycles are Lochkovian and Pragian. They form asymmetrical cycles that are comparable to the two lowest Silurian cycles. Both these Devonian cycles, however, are transgressive sequences that start with non-marine deposits and end with reef limestones (Yolkin, 1968; Talent and Yolkin, 1987).

Along the shelf belt, the overlying Emsian-Givetian is represented by two groups of cycles. Each includes three clear-cut, T-R cycles with the same repetition of cycle types in their succession. The pattern follows from a symmetrical cycle through an asymmetrical cycle and back to a symmetrical cycle (Figure 2). Within a coastal-plain setting with mostly non-marine sedimentation, three well-developed Emsian cycles form a single cycle that is referred to cycle number 3 (Yolkin et al., 1997; in press). It lithologically resembles Silurian cycle 4.

Two Upper Devonian cycles, numbers 7 and 8 (Figure 3), show a general regressive trend. Both may be subdivided in some areas into two separate cycles (7a, 7b, 8a, 8b) by very sharp T-R transitions. Cycle 8b represents a predominantly non-marine environment. This corresponds to the real maximum of the general Devonian regression. The lower part of overlying cycle 9 is Devonian. The rest of the cycle continues into the Carboniferous.

CORRELATION OF T-R CYCLES WITH TRILOBITE EVOLUTION

Progressive evolutionary lineages are not ordinarily preserved in the paleontological record, while binary and triple phylogenetic species clusters are common. The

FIGURE 3—(opposite) Silurian-Devonian transgressive-regressive (T-R) cycles and depositional phases and western Siberian eustatic curve. Sequences show reef limestones and event levels (black triangles=anoxic events, open triangles=local T-R events). Radiometric age in m.y. after Cowie and Bassett (1989). Silurian cycles: 1) Chineta (*Glyptograptus persculptus* Zone) event, 2) Syrovatiy (*Monograptus sedgwickii* Zone) event, 3) Chesnokovka (*Cyrtograptus* Zone) event, 4) Kyk (*Monograptus prehercynicus* Zone) event. Devonian cycles: 1) Zinzilban (*Polygnathus kitabicus* Zone) event, 2) Daleye (*P. nothoperbonus* Zone) event, 3) Chotec (*P. costatus costatus* Zone) event, 4) Kacak (*Nowakia otomari*) event, 5) Taghanic event, 6) Igaroldy (*Mesotaxis falciovalis/norissi* Zone) event, 7) lower Kellwasser event, 8) upper Kellwasser event, 9) Hungenberg event.

latter are the results of a real evolutionary process that provides for a diversity of biota and its fluctuation in time.

Silurian–Devonian dechenellid lineages from the western Siberian sedimentary basin (Yolkin, 1983) provide a good opportunity to observe morphological changes from an initial stage (archetype) through a long interval of geological time. It turns out that later changes are accompanied by iterative transformations of some morphologic features, which demonstrate a periodicity of the evolutionary process.

Temporal analysis of these morphologies and the trends of some cephalon and pygidium features (with complications assigned a positive (+) value; simplifications with a negative (-) value), reveal a periodicity in dechenellid evolution (Yolkin, 1983). It consists of regular combination of the elementary evolutionary stages (I–XVII), or first-rank stages, into two types of second-rank stages (alpha and beta) and then into the third-rank stages (A and B). As a result, there are regular patterns in a successive set of different evolutionary stages. There is also a clear relationship between the higher morphological changes and the boundary levels of higher rank stages. As earlier shown (Yolkin, 1979, 1983), the characteristic rank of dechenellid evolutionary stages is independent of regional factors. Thus, it can be used to correlate such local periodic phenomena as T–R cyclicity.

Figure 4 shows a long cyclic succession through two geologic systems. It is possible to recognize some regularities in certain repetitions and excursions of this T–R curve. The first pair of Silurian cycles is identical in their asymmetrical structure to the first Devonian pair. Between them is a pair of symmetrical cycles that embrace the Wenlock–Pridoli interval. These binary cycle clusters are designated as depositional phases A and B.

Cycles of the subsequent Emsian–Famnenian interval clearly have a different frequency (Figures 3, 5), but are represented by the same symmetrical and asymmetrical cycle types. This is certainly connected with the changeover in tectonic regime on this margin of the Siberian continent from a passive to an active continental margin took place.

Devonian cycle 3, as noted above, shares features with the subsequent Devonian cycles 4–6 and with Silurian cycle 3. This leads to the conclusion that two Devonian cycle groups (namely, 3a–3c and 4–6), which are well expressed on the shelf belt, are the equivalents of two Silurian cycles 3 and 4, but have a smaller magnitude. They can be integrated into a single Devonian depositional phase B.

The same argument may be applied to interpretations of Upper Devonian cycles 7a, 7b, 8a, and 8b. If paired, they represent two asymmetrical cycles (7 and 8) that are comparable to the Lower Devonian cycles 1 and 2, but

with a general regressive trend. So a combination of these two cycles form a single, regressive sedimentary package that can be distinguished as depositional phase C.

Thus, the Silurian–Devonian succession of T–R cycles, as well as successive trilobite evolutionary stages, have a periodic style of repetition that belongs to two types, which can be related to depositional cycles of three orders. The peculiarities of these cycles are well differentiated only in intervals that exceed one geological system.

Correlation of the Devonian T–R cycles with dechenellid evolutionary stages was done mainly to check for their mutual accord. It is most important to do this for the Silurian cycles, all of which coincide with the second-rank evolutionary stages designated alpha and beta (Figure 3). If cycle 1 is correlated with the third-order cycles according to the ranges of *Warburgella calvata* Yolkin and *W. altaica* Yolkin, the transition between elementary evolutionary stages I and II is restricted to the base of the *Demirastrites triangulatus* Zone. This horizon can be used as a boundary between the two fourth-order cycles within the third-order cycle 1. It also agrees with sedimentological data. In the Ust'-Chagyrka section (Yolkin and Zheltonogova, 1974; Yolkin et al., 1988), a clear shallowing takes place within the *Coronograptus cyphus* Zone. It is represented by sparitic limestone interbeds and lenses with trilobites, brachiopods, and ostracodes. A subsequent deepening occurs near the base of the *D. triangulatus* Zone. Lithologically, it consists of black, fine-grained siliciclastics with abundant graptolites. Thus, the third-order cycle 1 may be subdivided into two fourth-order cycles, with a boundary between them at the base of the *D. triangulatus* Zone.

Another example is the Kuimov Formation (Figure 3). Its lower boundary, as noted above, coincides with a minor deepening event. This entire formation represents a shallowing-up sequence. It may be correlated by benthic fauna with the Elton, Bringewood, and Leintwardine beds of the British Isles (Cocks et al., 1971). This interval is bounded by two deepening events (Kaljo et al., 1996). It could be considered as a first-order ranking of cycle 3c in the Silurian succession.

Third-order Silurian cycles include depositional phases A and B. They are well-defined, particularly by excursions of the T–R curve (Figure 3). It is necessary to add that complete Silurian and Devonian intervals could

FIGURE 4—(opposite) Relationship of Silurian and Devonian T–R cycles, depositional phases, reef limestones, and eustatic curves. Open rectangles in reef limestone column = cross-bedded siliciclastics at top of cycle 1 and argillaceous limestones between red rocks of the Cherny Anui Formation.

General Stratigraphical scale		Altai, Salair		Evolutionary stages of dechenellids									
System	Series	Stage	Suprahorizon (Series)	Horizon (Form.)	Reef limestones and anoxia	T-R cycles	Depositional phases	KHALFINELLA		GANINELLA			
Devonian	Lower	Emsian	Telengitian	Shanda	6	3c	Phase B	B	XVII				
				Belovo	3 3b	3 3b		β	XVII				
	Pragian	Telengitian	Salaika	5	3a	Phase A	4	XV	<i>carinata</i>				
			Maly Bachat	4			7	XV	<i>elegantula</i>				
	Lochkovian	Beltirian	Krekov	4	2	Phase B	6	XIII	<i>attenuata</i>				
			Peetiz	1	1		α	XII	<i>prima</i>				
		Kaibalian	Tom'-Chumysh	1	1	Phase A	3	XI	<i>gratsiamovae</i>				
							5	XI	<i>gratsiamovae</i>				
	Silurian	Upper	Pridolian	Cherny Anui	N ₃	4	4	Phase B	3	X	<i>volkovyana</i>		
					N ₂				β	IX	<i>waigatschensis</i>		
Ludlowian		Cherny Anui	N ₁	3	3	Phase A	4	VIII	<i>tcherkesovae</i>				
							4	VIII	<i>tcherkesovae</i>				
Wenlockian		Tigerek	Kuimov	3	3	Phase B	2	VII	<i>stokesii</i>				
			Chagyrka				β	VI	<i>verecunda</i>				
Llandoveryan		Tigerek	Chesnokovka	3	3	Phase A	2	V	<i>obscura</i>				
			Polati				α	IV	<i>insperata</i>				
		Gromotukha	Syrovaty	2	2	Phase B	α	III	<i>kolobovae</i>				
			Vtoroye Utyosy	1	1		α	II	<i>altata</i>				
Ordovician			Series K		1	1	Phase A	1	I	<i>calvata</i>			

be considered as separate fourth-order cycles or depositional periods (Figure 5). The examples from the Silurian Period are asymmetrical, while the Devonian examples are symmetrical cycles.

DISCUSSION

The following discussion will be concerned mainly the Silurian part of the cycle succession. Two recent comprehensive surveys (Johnson, 1996; Kaljo et al., 1996) simplify the task of correlating the western Siberian T-R cycles globally.

The primary focus for discussion is a precise biostratigraphic correlation of the initial Silurian transgression. According to the Ordovician-Silurian Boundary Working Group decision (Williams, 1988), the base of the Silurian System is defined at the base of the *Parakidograptus acuminatus* Zone. This stratigraphic level is sometimes defined as the beginning of the initial Silurian transgression (Apollonov et al., 1988). In the Altai-Salair region (Yolkin et al., 1988) and other regions (Cuerda et al., 1988; Mu, 1988), however, the guide species of this zone appears at the bottom of black shales that embrace a large portion of the Llandovery. In the Altai-Salair sections, these shales are characterized by graptolite associations that successively change in abundance, and they conformably overlie Upper Ordovician reef limestones. Kaljo et al. (1996) noted the beginning of an innovative stepwise event in graptolite evolution with the *Glyptograptus persculptus* Zone. This event, designated by a local name, the Chineta (*G. persculptus* Zone) Event (Yolkin et al., 1997), is important. It corresponds to the start of the first Silurian T-R cycle (i.e., cycle 1), and certainly can be correlated with the beginning of the first large-scale Silurian transgression.

Deepening events at the bases of the next two T-R cycles, designated as the Syrovatiy (*Monograptus sedgwickii* Zone) and the Chesnokovka (*Cyrtograptus* Zone) Events, are in complete agreement with two highstands (2 and 4) of the Silurian sea-level standard (Johnson, 1996). Unfortunately, there are no direct data available for a precise location of the fourth cycle base. In the Altai-Salair section, it coincides with the strong regression that is considered to be Ludlovian (Figure 3). This event is followed by strata with a non-marine red color. In some aspects, this level could be correlated with the upper boundary of the *Saetograptus leintwardinensis* Zone (Kaljo et al., 1996). It is interesting to compare two versions of the post-*S. leintwardinensis* sea-level curve. Kaljo et al. (1996, fig. 6) showed it as a symmetrical T-R cycle similar to our cycle 4 (Figure 5). Another version of this curve (Johnson, 1996, fig. 1) showed two highstands

and one lowstand between them. Such a picture is normal for symmetrical T-R cycles of shallow-water continental shelves with carbonate reef buildups (see Figures 3 and 6). Thus, these three depositional stages could be considered as three of the first-order T-R cycles. In this case, their onset could be tentatively aligned with the bases of the *Bohemograptus bohemicus*, *Neocucullograptus kozlowskii*, and *Monograptus parultimus* Zones. If such a conclusion is correct, we should shift the base of the Cherny Anui Formation in the Altai sections well down into the Ludlow Series, and locate the Pridoli base at the base of the upper member of that formation (Figure 5).

As shown above, fourth-order cycles appear within the Altai-Salairian third-order cycle 3 (Figure 3). Their lower limits can be correlated with the bases of the *Neodiversograptus nilssoni* and, possibly, the *Gothograptus nassa* Zones. The first boundary is clearly expressed by a deepening in the Altai-Salair sections, but there is no evidence for the second deepening event. The best location for the second level is certainly the base of the *G. nassa* Zone, which coincides with a T-R event and biotic innovations (Kaljo et al., 1996).

There is a clear basis for distinguishing between the two fourth-order cycles within the Altai-Salairian second-order cycle 1. This is the base of the *Demirastrites triangulatus* Zone (see above). Its position is slightly offset from the eustatic curve (Johnson, 1996, fig. 1). However, this fixes the highstand (or deepening) at the level of the *Coronograptus cyphus* Zone, instead of the distinctive shallowing in Altaian sections of the Altai-Salair region where graptolite documentation is complete.

The level for recognizing two of the fourth-order cycles within the Altai-Salairian third-order cycle 2 could be the base of the *Monoclimacis griestoniensis* Zone. This marks the start of reef limestone accumulation in the Altai-Salair region, as documented by graptolites, but with no further continuation of a deepening event here. This horizon, however, coincides with the onset of transgression on both versions of the Silurian eustatic curve (Johnson, 1996, fig. 1; Kaljo et al., 1996, fig. 6).

SUMMARY AND CONCLUSIONS

In this report, the author has focused on the relationship between iterative patterns of morphological changes in dechenellid trilobites and sedimentary cycles and their regional succession in order to correlate these patterns globally. It is very important to avoid mistakes in the use of such terms as "highstand" and "deepening event". Usually they are correctly considered as coeval, but also they can be tied to different chronostratigraphic levels in specific environments, particularly in inner-shelf sec-

	Series	Stage	Graptolite zones	Formations	Bathymetry						
					0	1	2	3	4	5	6
412	PRID.		<i>bouceki-transgrediens</i>	<i>Cherny Anui</i>	N ₃						
			<i>branikensis-lochkovens</i>								
			<i>parultimus-ultimus</i>								
414	LUDLOW	Ludfordian	<i>formosus</i>		N ₂						
415			<i>bohemicus tenuis-kozlowskii</i>								
			<i>leintwardinensis</i>		N ₁						
		Gorstian	<i>scanicus</i>	<i>Kuimov</i>							
			<i>nilssoni</i>								
420	WENLOCK	Homerian	<i>ludensis</i>	<i>Chagyrka</i>							
			<i>praedeubeli-deubeli</i>								
			<i>parvus-nassa</i>								
			<i>lundgreni</i>								
		Sheinwoodian	<i>rigidus-perneri</i>	<i>Chesnokovka</i>							
			<i>riccartonensis-belophorus</i>								
			<i>centrifugus-murchisoni</i>								
425	LLANDOVERY	Telychian	<i>lapworthi-insectus</i>	<i>Polati</i>							
			<i>spiralis</i> interval zone								
			<i>griestoniensis-crenulata</i>								
			<i>turriculatus-crispus</i>	<i>Syrovatyi</i>							
			<i>guerichi</i>								
		Aeronian	<i>sedgwickii</i>								
430			<i>convolutus</i>								
			<i>argenteus</i>								
			<i>triangulatus-pectinatus</i>								
432	Ruddanian		<i>cyphus</i>	<i>Vtoriye Utyosy</i>							
433			<i>vesiculosus</i>								
			<i>acuminatus</i>								
435											

tions. Thus, the more important results of this study may be formulated as follows:

As determined earlier (Yolkin, 1983, p. 70), morphological changes in time within dechenellid lineages demonstrate iterative patterns. The appearance of each species defines its elementary evolutionary stage. Species are combined into two-fold or three-fold lineage splits by trends in the complication or simplification of glabellar and pygidial morphology. Such fragments are repeated, in their turn, by pairs. These represent three ranks of dechenellid evolutionary stages (Figure 5).

The rank of dechenellid evolution is aligned with the local Silurian–Devonian succession of T–R cycles. This process involves a sorting out of T–R initiations (or eustatic deepenings) by evolutionary stage limits for a definition of T–R cycle orders. It was found that regular patterns of cyclic deposition (or sedimentary cycles) coincide with events in trilobite evolution. They are related to regular repetitions of symmetrical and asymmetrical sedimentary cycles (Figures 4, 5). Preliminary testing reveals their agreement with the Silurian eustatic curve. After more testing of data from different tectonic environments, particularly from the North American craton (the type area for many aspects of the Silurian sea-level standard; see Brett et al., 1990; Sheehan and Boucot, 1991; Johnson, 1996), these regularities will improve the accuracy of global correlations.

The Altai–Salair Silurian succession includes four clearly expressed T–R cycles (Figures 2 and 4). They are bounded by the following event levels: Chineta (*Glyptograptus persculptus* Zone), Syrovatiy (*Monograptus sedgwickii* Zone), Chesnokovka (*Cyrtograptus lapworthi*–*C. insectus* Zone), middle Ludfordian (*Bohemograptus bohemicus* Zone) and basal Lochkovian (*Monograptus uniformis* Zone) events. Cycles 1 and 2 demonstrate third-order asymmetrical cycles. The second cyclical pair (3 and 4) belong to the same third-order cycle, but is symmetrical. Both these pairs form two depositional phases (A and B), or second-order cycles.

The Silurian succession of fourth-order cycles was reconstructed by calibration of ranks according to dechenellid evolutionary stages, and further tested by global data. Symmetrical cycles, in concordance with their three depositional stages, can be subdivided into three subcycles, but the asymmetrical ones are divisible into two subcycles or first-order cycles. Their defining horizons are the bases of the *Demirastrites triangulatus*,

Monograptus griestoniensis, *Gothograptus nassa*, *Neodiversograptus nilssoni*, and possibly the *Neocucullograptus kozlowskii* and *Monograptus parultimus* Zones.

Coincidence of regular patterns associated with dechenellid evolution and depositional cycles does not leave much room for an explanation by exotic phenomena or for a very local influence. The traditional explanation for iterative evolution in trilobites (Kaufmann, 1933) is that lineages evolved in succession from a conservative parental stock that was geographically restricted much of the time. The parental stock managed to expand periodically to wider territories under conditions where evolutionary trends repeated themselves. A possible interpretation links iterative patterns to relatively shallow-marine shelves, where sea-level fluctuations had a more profound effect. A more slowly evolving parental stock may have been restricted to much deeper, off-shelf environments, where the same sea-level fluctuations had less effect. Such assumptions, however, are not in accord with actual shallow-water environments of the Silurian–Devonian Altai–Salair region where dechenellid trilobites evolved. Available data support the idea that the main factors of iterative evolution and cyclic deposition might be connected to natural periodic processes similar to Milankovitch cycles that acted on a somewhat longer time scale than normally associated with those particular solar cycles.

ACKNOWLEDGMENTS

This report is a contribution to the activities of the Subcommission on Silurian Stratigraphy (IUGS) and IGCP Project 335. The research was supported by Grant N 96-05-66071 from the Russian Foundation for Basic Research. Travel funds from the International Science Foundation permitted the author to attend the Second International Symposium on the Silurian System. I am grateful to M.E. Johnson and V.N. Yolkina for discussions and help in preparation of this paper. Technical assistance was provided by N.G. Izokh, T.P. Kipriyanova, O.A. Rodina and E.N. Shemyakina. The manuscript was reviewed by S.R. Westrop (Brock University) and an anonymous reviewer.

REFERENCES

- APOLLONOV M.K., T.N. KOREN', I.F. NIKITIN, L.M. PALETZ, AND D.T. TZAI. 1988. Nature of the Ordovician–Silurian boundary in south Kazakhstan, USSR, p. 145–154. In L.R.M. Cocks and R.B. Rickards (eds.), *A Global Analysis of the Ordovician–Silurian Boundary*. Bulletin of the British Museum (Natural History), Geology, 43.

FIGURE 6—(opposite) Sea-level curve for the Altai Silurian from sedimentological and faunal evidence, based on absolute depth of benthic assemblages (see Brett et al., 1993).

- BERG, L.S. 1977. Trudy po Teorii Evolutsii. Nauka, Leningrad, 387 p.
- BRETT, C.E., A.J. BOUCOT, AND B. JONES. 1993. Absolute depth of Silurian benthic assemblages. *Lethaia*, 26:25–40.
- COCKS, L.R.M., C.H. HOLLAND, R.B. RICKARDS, AND I. STRACHAN. 1971. A correlation of Silurian rocks in the British Isles. *Journal of the Geological Society of London*, 127:103–136.
- COWIE, J.W., AND M.G. BASSETT. 1989. Global stratigraphic chart with geochronometric and magnetostratigraphic. Supplement to Episodes, 2.
- CUERDA, A., R.B. RICKARDS, AND C. CINGOLANI. 1988. The Ordovician–Silurian boundary in Bolivia and Argentina, p. 291–294. In L.R.M. Cocks and R.B. Rickards (eds.), *A Global Analysis of the Ordovician–Silurian Boundary*, Bulletin of the British Museum (Natural History), Geology, 43.
- EINSELE, G. 1992. Sedimentary Basins: Evolution, Facies, and Sediment Budget. Springer-Verlag, New York.
- HOUSE, M.R. 1983. Devonian eustatic events. *Proceedings of the Ussher Society*, 5:396–405.
- . 1985. Correlation of mid-Palaeozoic ammonoid evolutionary events with global sedimentary perturbations. *Nature*, 313:17–22.
- . 1989. Analysis of mid-Palaeozoic extinctions. *Bulletin de la Societe belge de Geologie*, 98:99–107.
- JOHNSON, J.G., G. KLAPPER, AND C.A. SANDBERG. 1985. Devonian eustatic fluctuations in Euramerica. *Geological Society of America Bulletin*, 96:567–587.
- JOHNSON, M.E. 1996. Stable cratonic sequences and a standard for Silurian eustasy, p. 203–211. In B.J. Witzke, G.A. Ludvigson, and J. Day (eds.), *Paleozoic Sequence Stratigraphy: Views from the American Craton*. Geological Society of America, Special Paper 306.
- KALJO D., A.J. BOUCOT, R.M. CORFIELD, A. LE HERISSE, T.N. KOREN', J. KRÍŽ, P. MANNIK, T. MERSS, V. NESTOR, R.H. SHAVER, D.J. SIVETER, AND V. VIIRA. 1996. Silurian bio-events, p. 173–224. In O. Walliser (ed.), *Global Events and Event Stratigraphy in the Paleozoic*. Springer-Verlag, New York.
- KAUFMANN, R. 1933. Variationsstatistische Untersuchungen ueber die "Artabwandlung" und "Artumbildung" an der oberkambrischen Trilobitengattung *Olenus* Dalm. Abhandlung der Geologisch- und Palaeontologisches Institut der Universitat Greifswald, 10:1–54.
- MU E.-Z. 1988. The Ordovician–Silurian Boundary in China, p. 117–131. In L.R.M. Cocks and R.B. Rickards (eds.), *A global analysis of the Ordovician–Silurian Boundary*, Bulletin of the British Museum (Natural History), Geology, 43.
- SENNIKOV, N.V. 1976. Graptolity i Stratigrafiya Nizhnego Silura Gornogo Altaya. Nauka, Moskva.
- TALENT, J.A., AND E.A. YOLKIN. 1987. Transgression–regression patterns for the Devonian of Australia and southwest Siberia. *Courier Forschungs-Institut Senckenberg*, 92:235–249.
- VAIL, P.T., R.M. MITCHUM, JR., AND S. THOMPSON III. 1977. Seismic stratigraphy and global changes of sea level. Part 4, Global cycles or relative changes of sea level, p. 83–97. In C.E. Payton (ed.), *Stratigraphic Interpretation of Seismic Data*. American Association of Petroleum Geologists Memoir 26.
- WALLISER, O.H. 1984. Geologic processes and global events. *Terracognita*, 4:17–20.
- . 1985. Natural boundaries and Commission boundaries in the Devonian. *Courier Forschungs-Institut Senckenberg*, 75:401–407.
- . 1996. Global events in the Devonian and Carboniferous, p. 225–250. In O.H. Walliser (ed.), *Global Events and Event Stratigraphy in the Paleozoic*. Springer-Verlag, New York.
- WILLIAMS, S.H. 1988. Dob's Linn—the Ordovician–Silurian boundary stratotype, p. 17–30. In L.R.M. Cocks and R.B. Rickards (eds.), *A Global Analysis of the Ordovician–Silurian Boundary*. Bulletin of the British Museum (Natural History), Geology Series, 43.
- YOLKIN, E.A. 1968. Trilobity (Dekhenellidy) i Stratigrafiya Nizhnego i Srednego Devona Yuga Zapadnoi Sibiri. Nauka, Moskva.
- . 1979. Nomogenez, paleontologiya, biokhronologiya, p. 221–254. In A.A. Trofimuk (ed.) *Metodologicheskie i Filosofskie Problemy v Geologii*. Nauka, Novosibirsk.
- . 1983. Zakonomernosti Evolutsii Dekhenellid i Biokhronologiya Silura i Devona. Nauka, Moskva.
- , R.T. GRATSIZNOVA, N.K. BAKHAREV, N.G. IZOKH, AND A.YU. YAZIKOV. 1994a. Kolebaniya Urovnya Mirovogo Okeana v Devone na Yugo-Zapadnoi Okraine Sibirskogo Kontinenta. Symposium "Devonian eustatic changes of the World Ocean Level", July 9–22, 1994, Moscow - Ukhta. Abstracts.
- , ———, N.G. IZOKH, A.YU. YAZIKOV, AND N.K. BAKHAREV. In press. Devonian sea-level fluctuations on the south-western margin of the Siberian continent. *Courier Forschungs-Institut Senckenberg*.
- , N.G. IZOKH, N.V. SENNIKOV, A.YU. YAZIKOV, A.I. KIM, AND M.V. ERINA. 1994b. Vazhneishie Global'nye Sedimentologicheskie i Biologicheskie Sobytiya Devona Yuzhnogo Tyan' Shanya i Yuga Zapadnoi Sibiri. *Stratigrafiya. Geologicheskaya Korrelyatsiya*, 2(3):24–31 Moskva.
- , A.M. OBUT, AND N.V. SENNIKOV. 1988. The Ordovician–Silurian boundary in the Altai Mountains, U.S.S.R., p. 139–143. In L.R.M. Cocks and R.B. Rickards (eds.), *A Global Analysis of the Ordovician–Silurian Boundary*. Bulletin of the British Museum (Natural History), Geology Series, 43.
- , N.V. SENNIKOV, N.K. BAKHAREV, N.G. IZOKH, AND A.YU. YAZIKOV. 1997. Periodichnost' osadkonakoplniya v silure i sootnosheniya global'nykh geologicheskikh sobytiy v srednem paleozoe na yugo-zapadnoi okraine sibirskogo kontinenta. *Geologiya i Geofizika*, 38(3):18–29.
- , ———, M.M. BUSLOV, A.YU. YAZIKOV, R.T. GRATSANOVA, AND N.K. BAKHAREV. 1994. Paleogeographic reconstructions of a western part of the Altai-Sayan area through the Ordovician, Silurian, and Devonian and their geodynamic interpretations. *Russian Geology and Geophysics*, 35:7, 8.
- , AND V.A. ZHELTONOGOVA. 1974. Drevneyshiye Dekhenellidy (trilobity) i Stratigrafiya Silura Gornogo Altaya. Nauka, Novosibirsk.

PART III: SHORT-TERM CYCLES

SILURIAN COASTAL SEDIMENTATION AND METER-SCALE RHYTHMS IN THE APPALACHIAN FORELAND BASIN OF PENNSYLVANIA

EDWARD COTTER

Department of Geology, Bucknell University, Lewisburg, PA 17837

ABSTRACT—Silurian strata on the eastern flank of the central Appalachian Foreland Basin in Pennsylvania preserve the signal of small-scale changes of relative sea-level in many coastal-margin facies. At about the same position on the southeastern flank of the basin, 1–10 m (most 1–3 m) shallowing-up sequences are superimposed on larger scale facies architectural patterns in Llandovery–Pridoli strata. Shallow-marine/coastal-margin facies in siliciclastic (Rose Hill, Keefer, Mifflintown Formations) and carbonate (Wills Creek and Tonoloway Formations) strata demonstrate repeated aggradation of the sediment–water interface to wave-base after rises of relative sea-level. Red, siliciclastic paralic strata (Castanea Member of Tuscarora Formation and Bloomsburg Formation) record repeated alternations of shallow subtidal and coastal-mudflat conditions.

These relationships demonstrate that strata through most of the Silurian in central Pennsylvania continuously experienced an equilibrium between sedimentation and basin-flank accommodation. Persistent low-energy coastal-margin conditions helped to limit transgressive truncation of the paralic depositional record. A persistently shallow pycnocline limited burrow homogenization of shallow-marine deposits. The low-energy, low-gradient coastal margin underwent repeated and extensive lateral shifts of position as a result of small-scale fluctuations of relative sea-level. Similarities of scale, facies sequence, and vertical rhythm of the sea-level cycles in so many disparate siliciclastic and carbonate depositional systems, and their development at times of minor orogenesis and tectonic quiescence, suggest that the rhythm was driven by eustasy.

INTRODUCTION

We typically see patterns in physical phenomena only after someone provides a conceptual framework in which those phenomena can be understood (Kuhn, 1962;

Walker, 1973). After a small number of insightful sedimentary geologists showed how meter-scale cyclical patterns in sedimentary strata could be related to fluctuations of relative sea-level, others began to find similar patterns. It was not long until meter-scale shallowing-up cycles were recognized in the Silurian succession of the Pennsylvanian part of the Appalachian Foreland Basin (Gwinn and Bain, 1964). Investigations of Silurian cycles at first focused on demonstrating their presence within one or two closely related stratigraphic units (Tourek, 1970; Cotter, 1983, 1988), but more recently attention has shifted to an attempt at lateral, basin-wide correlation of some of the patterns (Goodman and Brett, 1994). The approach in this report is to look at many different stratigraphic units from a variety of environments that were deposited at approximately the same position on the southeastern flank of the Appalachian Foreland Basin. The objective is to demonstrate that numerous small-scale shallowing-up cycles of similar magnitude are present in many different coastal-margin facies that range through most of the Silurian (Figure 1).

Silurian strata crop out in the Valley and Ridge Province ("Folded Appalachians") of central Pennsylvania as a series of curvilinear bands (Figure 2) that are aligned approximately parallel to the depositional strike of the flank of the foreland basin. Silurian units are adequately exposed in outcrop to allow confident interpretations of depositional conditions for each stratigraphic unit and for regional assessment of their proximal–distal stratigraphic relationships.

PALEOENVIRONMENTAL FRAMEWORK

GENERAL SETTING.—During the Silurian, Pennsylvania lay near the southern margin of Laurentia, between 20° and 30° south latitude (Van der Voo, 1988; Kent and Miller, 1988). Along the southern edge of the continent

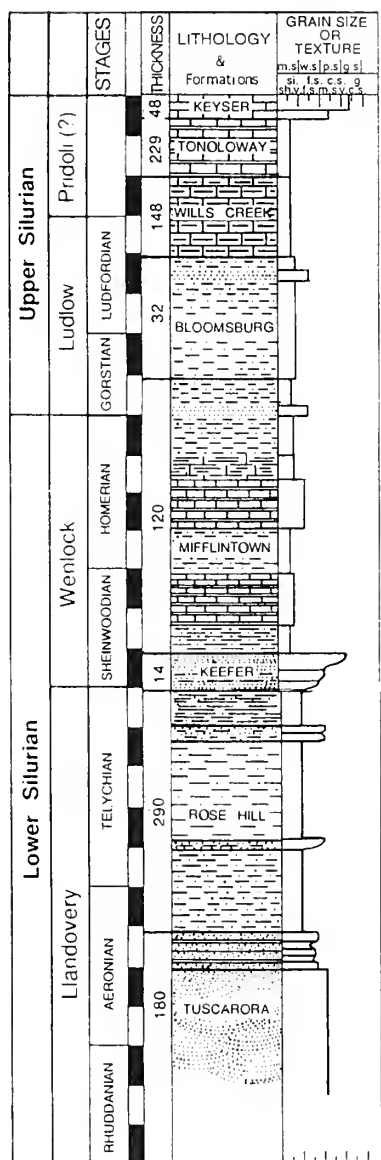


FIGURE 1—Graphic column of Silurian succession in central Pennsylvania. Tuscarora Formation extends down to the base of the Rhuddanian. Thickness in meters; grain-size scale indicated at top of column.

was the Taconic orogen that separated the Iapetus ocean from a shallow epeiric sea on the cratonward side (Ziegler et al., 1977). Between these mountains and the continent interior was a foredeep, referred to as the Appalachian Foreland Basin. From the sedimentary and low-grade metamorphic rocks exposed in the Taconic orogen, siliciclastic detritus was transported northward (present-day northwestward) into the foreland basin, where it accumulated on a low-gradient depositional ramp that was generally covered by the shallow epeiric sea (Cotter, 1990).

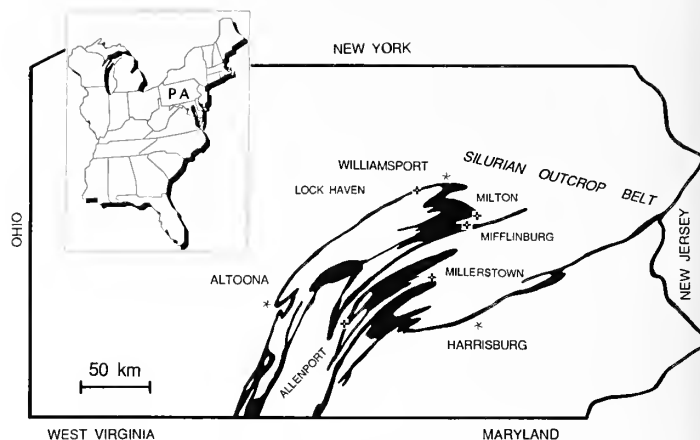


FIGURE 2—Silurian outcrop (in black) within Pennsylvania. Striped bands largely delineate the Valley and Ridge Province (Folded Appalachians) of central Pennsylvania. Inset shows location of Pennsylvania (PA) in eastern United States.

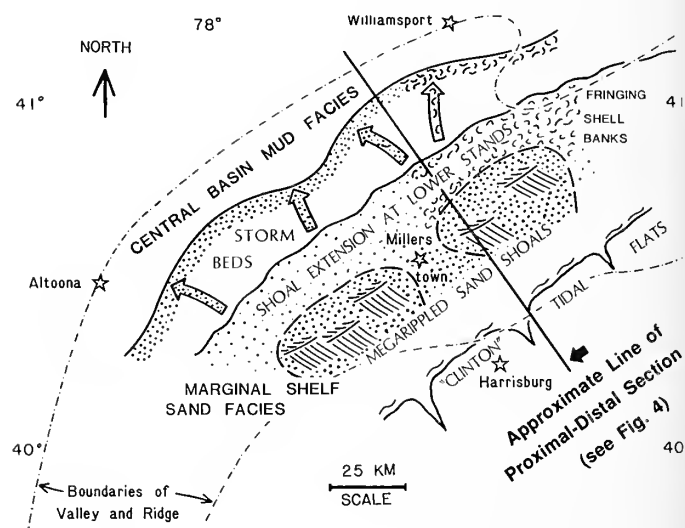


FIGURE 3—Generalized reconstruction of paleoenvironments, southeast flank of the Appalachian Foreland Basin in Pennsylvania during the medial part of the Silurian. See Figure 2 for approximate location of line of section. Modified from Cotter (1988).

PALEOENVIRONMENTS AND LITHOFACIES ARCHITECTURE.—A persistent tract of depositional facies characterized this depositional ramp through much of the Silurian. From a low-energy shoreline, typically located close to what is now the southeastern border of the Valley and Ridge structural province, the ramp deepened gradually toward a muddy, anoxic basin center in the vicinity of the northwestern margin of the Valley and Ridge (Figure 3). Between the shoreline and the basin center, a series of sandy and shelly shoals was situated on an otherwise muddy shallow shelf.

The regional architecture, on the scale of formations and members, of Silurian lithofacies across the central Pennsylvania outcrop belt was largely determined by lateral shifts of this basic facies tract. Southeasternmost (proximal) exposures in Pennsylvania have a high proportion of coastal and inner-shelf, coarser-grained lithofacies, while northwesternmost (distal) units consist largely of basin-center fissile mudrock. Between these end members, units of basin-center mudrock taper toward the southeast, while units of coarser-grained marginal facies wedge out toward the northwest (Figure 4). Later in the Silurian, the influx of siliciclastic detritus waned, and owing to the tropical location of the depositional ramp, the composition of the accumulating sediment evolved from siliciclastic to carbonate (Figures 1, 4).

DEPOSITIONAL SETTINGS, PROCESSES, AND CONTROLS.—The axial part of the foreland depositional basin had a maximum water depth of little more than 50 m (Johnson, 1987; Eckert and Brett, 1989; Cotter, 1990; Brett et al., 1993). Much of the sea floor experienced anaerobic to dysaerobic conditions through most of the Silurian. The pycnocline was very shallow, probably much less than 20 m (Cotter and Link, 1993), and reflected the generally oxygen-limited nature of Paleozoic seas (Berry et al., 1989) and the existence of “greenhouse” conditions at a time of high atmospheric CO₂ (Fischer, 1981; Berner, 1994). As a result, most Silurian shelf mudrock is unburrowed or only slightly burrowed by *Chondrites*, the ichnotaxon most tolerant of oxygen deficiency (Bromley and Ekdale, 1984). The anaerobic conditions also made most of the muddy sea floor barren of indigenous macrofauna.

Exposures of Silurian coastal facies in Pennsylvania demonstrate that depositional conditions were low-energy and mud-dominated through most of the Silurian. Such coastal facies can be seen in the Castanea Member (Llandovery, Rhuddanian) at the top of the Tuscarora Formation; this member was deposited on a low-energy shoreline with weak tidal activity (Cotter, 1983). Younger Llandovery (Telychian) coastal-zone strata have the characteristics of low- to moderate-energy tidal-flat deposits (Smith, 1968; Klein, 1977; Cotter, 1988). Shoreline deposits in the Bloomsburg Formation (Upper Silurian, Ludfordian) indicate deposition along a non-tidal, low-energy muddy coast (Driese et al., 1992). And finally, toward the close of the Silurian, Tonoloway Formation (Ludlow–Pridoli) limestones formed in association with a low-energy sabkha coast (Tourek, 1970; Seidell et al., 1987).

Between the coastal margin and the basin center, the gentle depositional ramp contained a series of mid-shelf shoal complexes on which coarser sediment (sand,

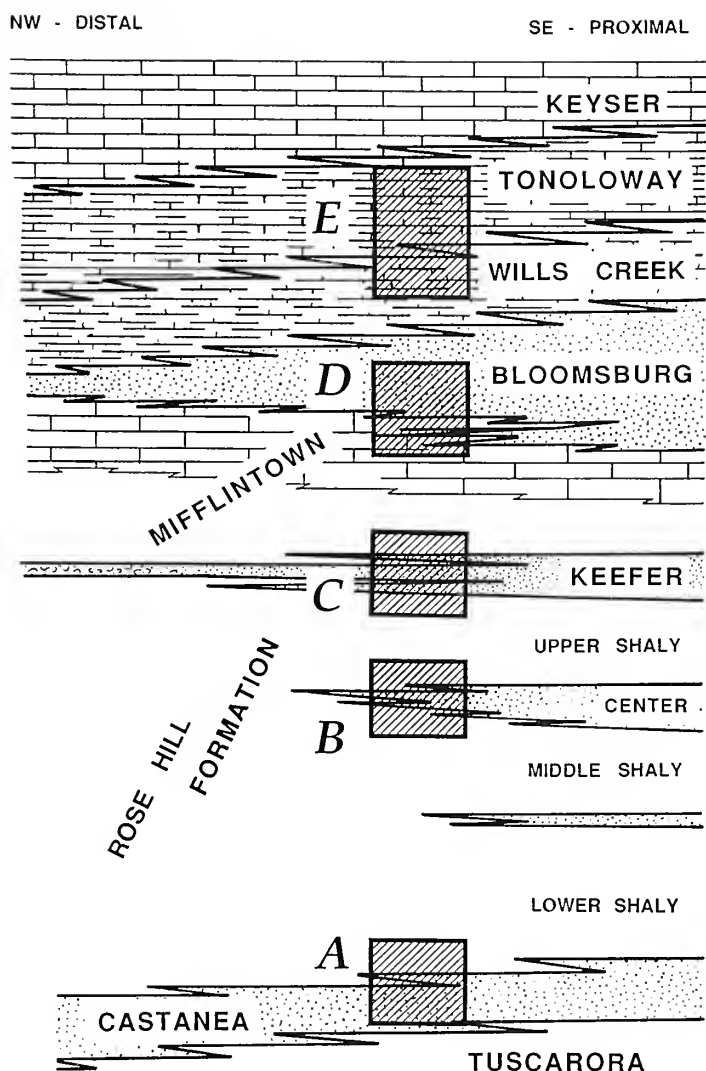


FIGURE 4—Proximal–distal lithofacies architecture along section in Figure 3. Diagonally striped boxes A–E indicate positions of units with small-scale shallowing-upward cycles. For A, see Figure 5; B, see Figure 7; C, see Figure 8; D, see Figures 9, 10; E, see Figure 12. Modified from Cotter (1988).

gravel, skeletal debris) accumulated (Cotter, 1983, 1988, 1990; Cotter and Link, 1993). The tops of these shoals were above the pycnocline, and at times hosted an indigenous benthic macrofauna. Episodically, storms interrupted the calm of the well-stratified sea and winnowed and lowered the shoal tops; this resulted in the redistribution of sand and shell hash to deeper settings as storm beds (Cotter, 1990). Such storm redistribution of sediment from shallow to deeper parts of the basin was much more effective during the repeated episodes of lowered relative sea-level (Cotter, 1990) (see below).

Changes in climate-sensitive features of the Silurian succession illustrate the effects of Laurentia's migration through different climatic zones (Kent and Miller, 1988).

Gray colors of terrestrial mudrocks in the Tuscarora Formation (lower Llandovery) suggest that environmental conditions were moister than the semi-aridity that characterized the later part of the Ordovician (Driese and Foreman, 1992; Retallack, 1993; Brogly et al., 1996). By Ludlow time, in the middle of the Silurian, conditions again became semi-arid, with a distinct alternation between wet and dry seasons (Driese et al., 1992). In the later part of the Silurian, Pennsylvania experienced more pronounced aridity, as indicated by the presence of evaporite basins (Rickard, 1969) surrounded by sabkha flats (Tourek, 1970; Seidell et al., 1987).

SMALL-SCALE SHALLOWING-UPWARD SEQUENCES

This part of the report will briefly detail the principal characteristics of small-scale, shallowing-upward sequences in six different formations of the Silurian succession in central Pennsylvania. The stratigraphic positions of these formations, with ages that range from early Llandovery to Pridoli, are shown in Figures 1 and 4.

CASTANEA MEMBER OF TUSCARORA FORMATION.—The Castanea Member (Llandovery, Aeronian) caps the Tuscarora Formation over much of the central Pennsylvania outcrop belt. Characteristically, the member consists of red siltstones and very fine-grained sandstones that are thoroughly riddled by *Skolithos* burrows and locally exhibit desiccation cracks. These features indicate deposition on low-energy coastal flats (Cotter, 1983). Better exposures demonstrate that these red parts alternate with units of drab greenish-gray, shallow subtidal shale that is partly burrowed by *Chondrites*. The Mill Hall locality, for example, exhibits three shallowing-up sequences, between 5–10 m-thick, in which shallow subtidal shale alternates with red, *Skolithos*-burrowed, coastal-margin sandstone (Figure 5).

CENTER MEMBER OF ROSE HILL FORMATION.—The Center Member of the Rose Hill Formation (upper Llandovery, Telychian) (Figures 1, 4), a coarser-grained, shallow-marine clastic unit that formed during a fall in relative sea-level (Cotter, 1988), displays numerous small-scale, shallowing-up cycles. A typical cycle progresses upward from fissile greenish-gray shale, deposited under low-energy, low-oxygen, deeper conditions, through heterolithic and symmetrically rippled beds, to thicker sandstones that are hummocky cross-stratified and commonly capped by a lag conglomerate (Figure 6).

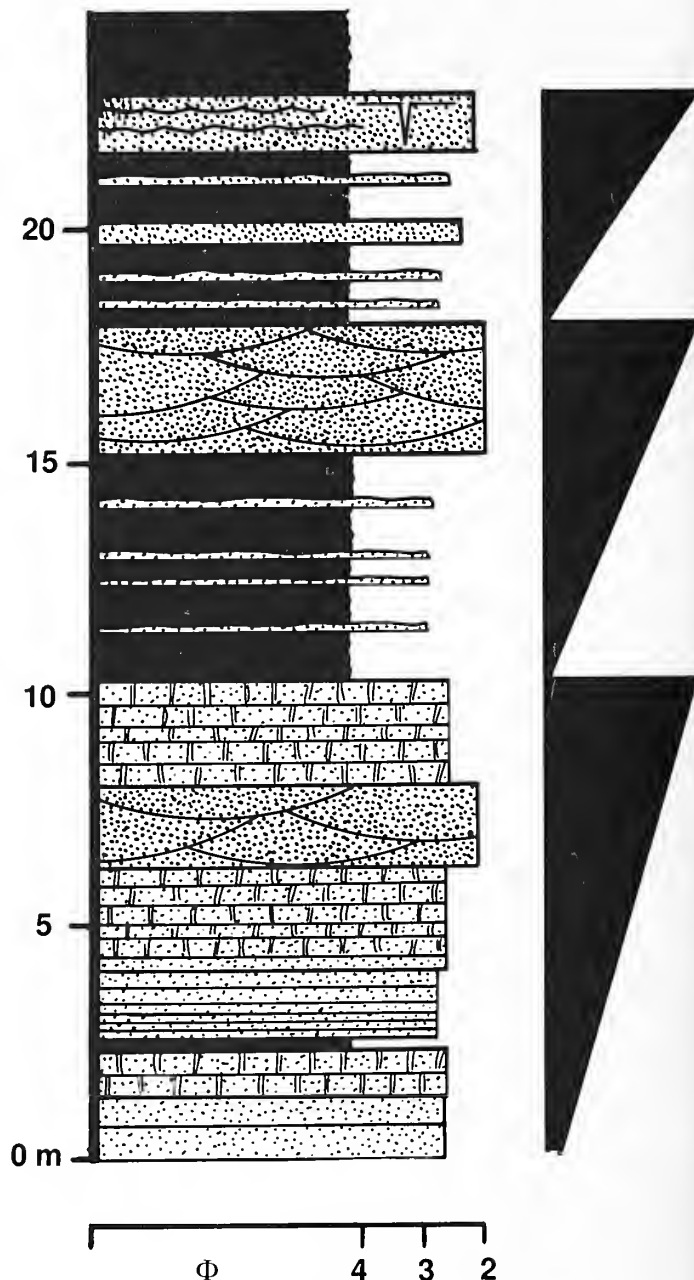


FIGURE 5—Three shallowing-up cycles in Castanea Member at top of the Tuscarora Formation. Mill Hall locality near Lock Haven, Pennsylvania.

Cycles such as these represent an alternation of relative deepening followed by shallowing of the mid-shelf shoal complexes. A representative outcrop of the Center Member along U.S. Highways 22-322 north of Millers-town, Pennsylvania, has thirteen shallowing-up cycles that range from 1–4 m-thick (Figure 7). Contemporaneous proximal strata at the southeastern edge of the outcrop belt were deposited on a tidal flat coastline; these exhibit numerous small-scale (1–5 m) fining- and shallowing-up cycles (Cotter, 1988).

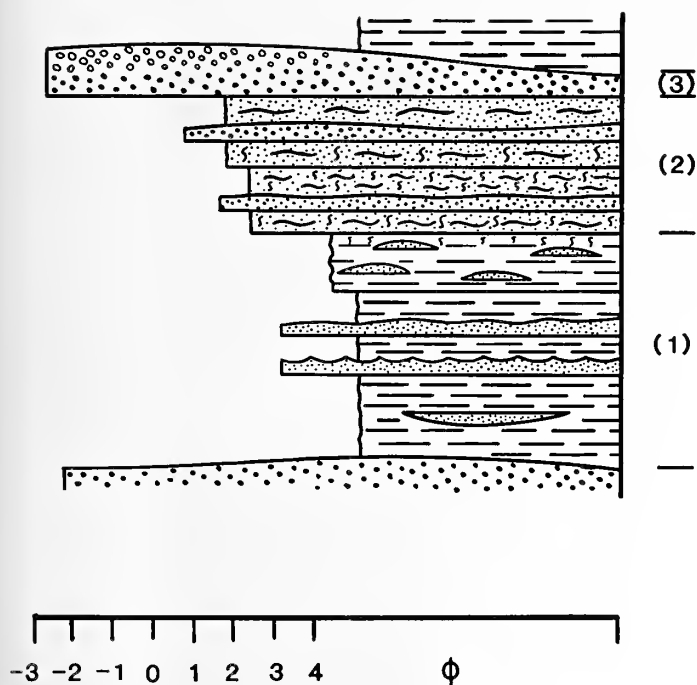


FIGURE 6—Idealized shallowing-up cycle in Center Member of the Rose Hill Formation (Figures 1, 4). Vertical scale ranges from 1–4 m (see Figure 7). From Cotter (1988).

KEEFER FORMATION.—The Keefer Formation (lower Wenlock, Sheinwoodian; Figures 1, 4) characteristically consists of three or more small-scale cycles, in which gray, fissile, subtidal mudrock grades up into medium- to coarse-grained quartz arenite that commonly contains hummocky cross-stratification. These cycles indicate that the depositional setting shallowed up from anaerobic, low-energy, deeper conditions to high-energy, storm-dominated conditions during which shelf shoals were condensed and winnowed. This situation is well-exhibited at the outcrop north of Millerstown (Figure 8).

MIFFLINTOWN FORMATION.—Above the Keefer, carbonate lithologies in the Mifflintown Formation (Wenlock) illustrate the waning influx of siliciclastic detritus from the Taconic source terrain. Much of the Mifflintown consists of heterolithic mixtures of limestone and fissile, siliciclastic mudrock. These lithologies commonly are arranged as repetitive small-scale sequences of gray fissile mudrock overlain by hummocky, intraclast-bearing limestones (Figure 9). These sequences were formed by the shallowing-up of depositional conditions from calm anoxia to episodic storm agitation (Cotter and Inners, 1986).

BLOOMSBURG FORMATION.—In Ludlow time, the south-easterly source terrain was re-elevated by an unloading type of relaxation (Ettensohn, 1994), and sluggish streams

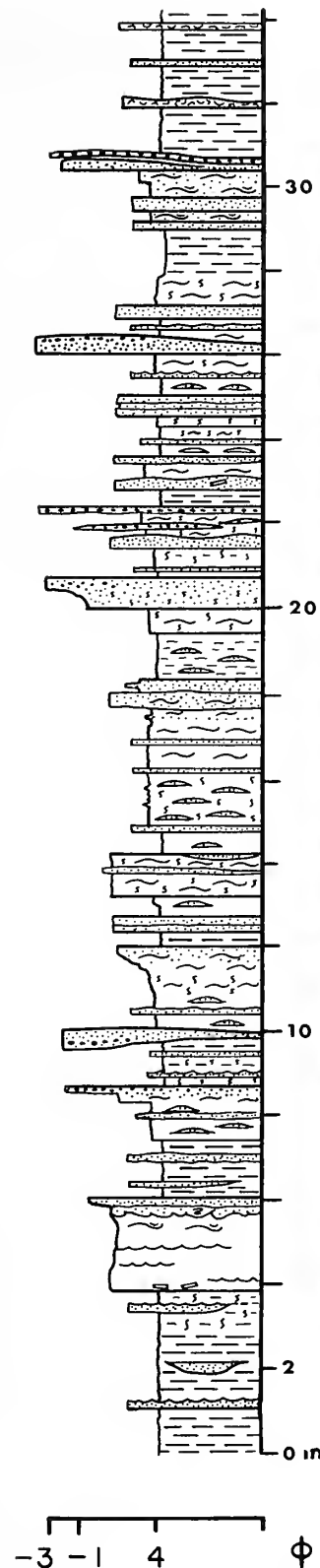


FIGURE 7—Center Member of Rose Hill Formation on east side of U.S. Highway 22-322, about 4 km N of Millerstown, Pennsylvania. Toothed bar along right edge indicates positions of thirteen shallowing-up cycles. From Cotter (1988).

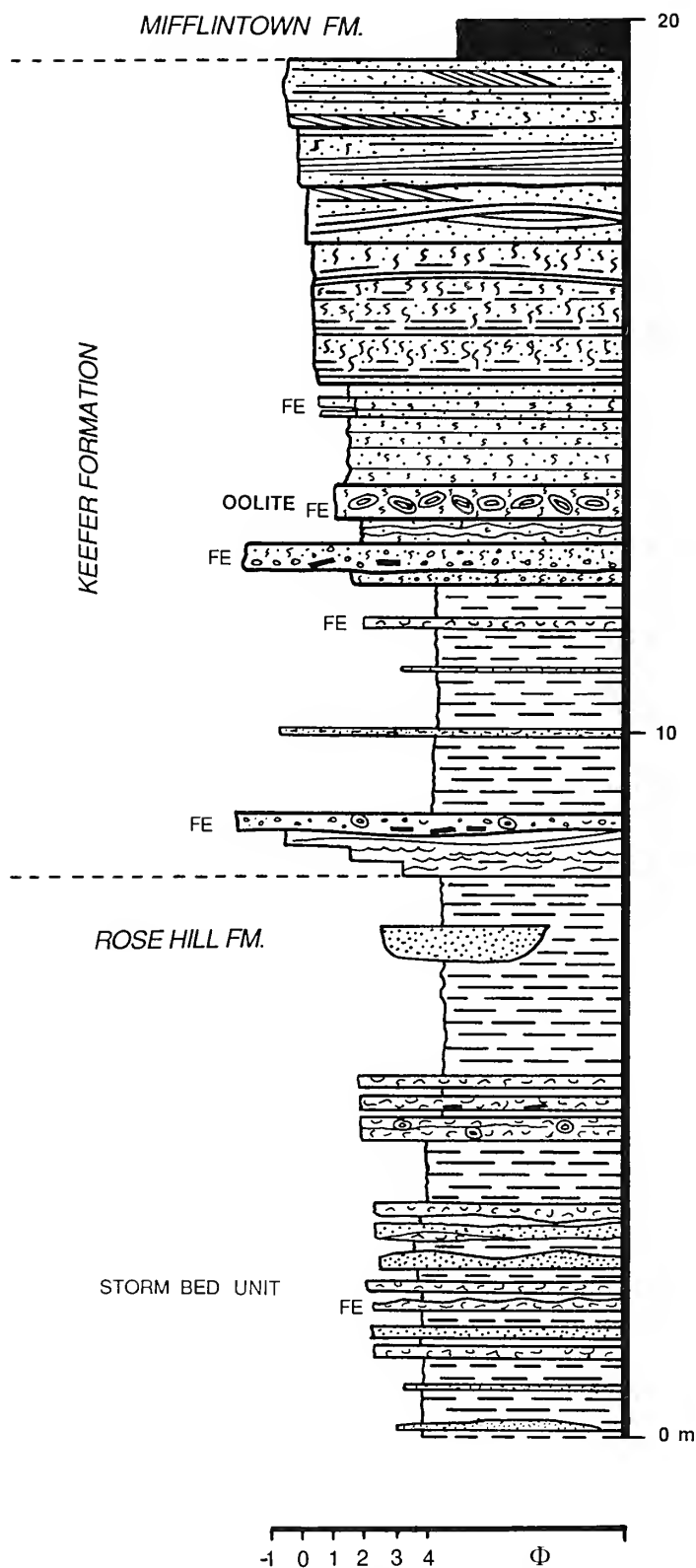


FIGURE 8—Keefer Formation, between uppermost Rose Hill and lowermost Mifflintown Formations on east side of U.S. Highway 22-322, about 4 km N of Millerstown, Pennsylvania. Coarse-grained units (at 8, 13, and 19 m) are tops of coarsening-up (shallowing-up) cycles. From Cotter and Link (1993).

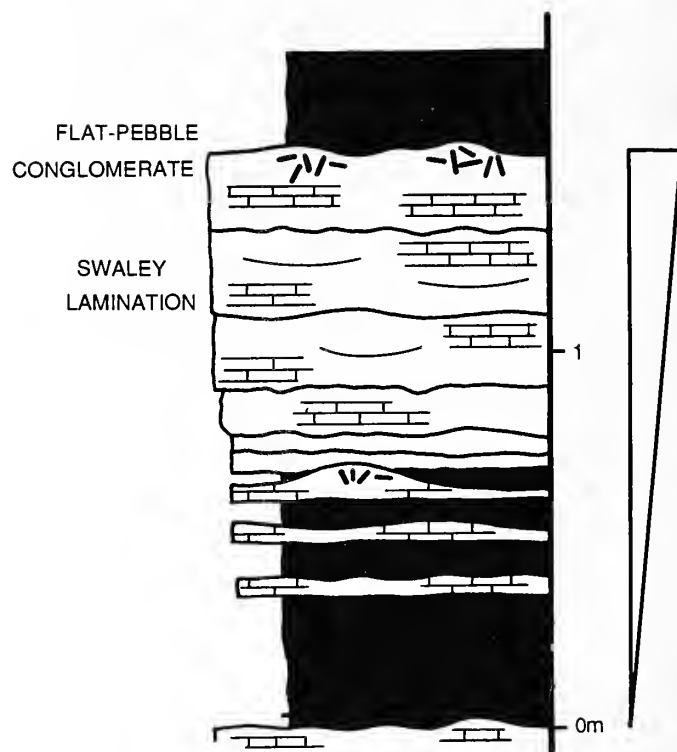


FIGURE 9—Generalized small-scale shallowing-up cycle in carbonate-dominated part of the Mifflintown Formation on Pennsylvania Highway 103 east of Allenport, Pennsylvania. Horizontal scale is weathering resistance. From Cotter (1990), with details in Cotter and Inners (1986).

contributed enough sediment to the coast that a low-energy shoreline prograded northwestward across part of central Pennsylvania (Hoskins, 1961). The resulting red mudrocks and thin red sandstones are the Bloomsburg Formation (Figures 1, 4). This formation also exhibits patterns of repeated shallowing-upward cycles (Figure 10). They are best shown in lower parts of the formation, where they occur as distinct, 1–5 m-thick intercalations of greenish marine mudrock and red, paleosol-bearing terrestrial mudrock (Driese et al., 1992). Thin transgressive lags mark transgressive flooding surfaces by low-energy marine waters over the coastal-margin flats.

TONOLWAY FORMATION.—Silurian time closed with carbonate sediment being deposited on the southeastern flank of the Appalachian Foreland Basin. As the source terrain that had provided the sediment of the Bloomsburg Formation was lowered, progressively less siliciclastic sediment of increasing fineness entered the basin, and carbonate deposition gradually took over (Figures 1, 4). The transition to carbonates is marked first by argillaceous limestone of the Wills Creek Formation (Ludlow), and then by the limestone and dolostone of the overlying Tonoloway Formation (upper Ludlow–lower

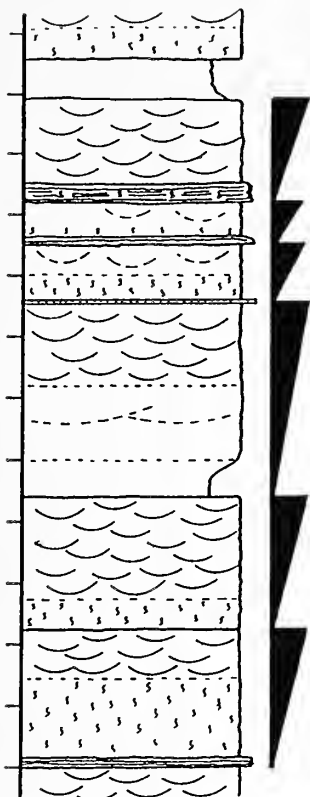


FIGURE 10—Six small-scale shallowing-up cycles in lower part of Bloomsburg Formation along railroad tracks about 6 km N of Milton, Pennsylvania. Cycles typically begin with thin transgressive sandstone lag, which is overlain by bioturbated marine mudrock, and is capped by terrestrial paleosol with desiccation cracks and pedogenic slickensided surfaces. Bars on vertical scale are 2 m apart, horizontal scale is principally weathering resistance.

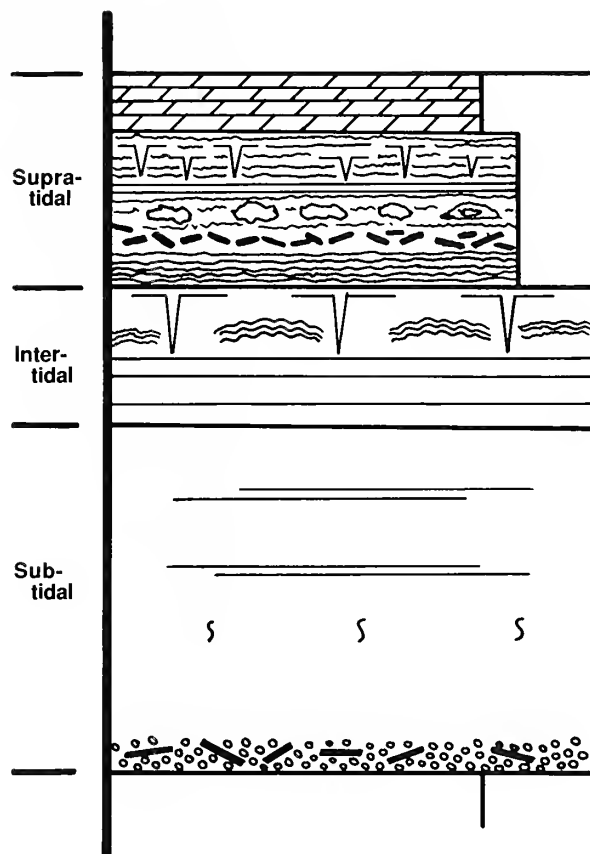


FIGURE 11—Generalized small-scale, shallowing-up cycle in Tonoloway Formation of central Pennsylvania. Vertical scale of cycles 1–3 m. Horizontal scale represents weathering resistance.

Pridoli). Both of these units accumulated in association with coastal sabkhas along the margin of a subtidal evaporite basin (Alling and Briggs, 1961; Fergusson and Prather, 1968; Rickard, 1969; Tourek, 1970; Seidell et al., 1987).

The Wills Creek and Tonoloway Formations are characterized by small-scale shallowing-up cycles. These were first documented in detail by Tourek (1970), and have more recently been described by Cotter and Inners (1986) and Goodmann (1988). Most of the cycles are between 1–3 m-thick. An idealized composite cycle (Figure 11) begins with a thin, basal transgressive lag, and progresses upward through blocky, poorly fossiliferous subtidal limestone and laminated, desiccation-cracked intertidal limestone to vuggy supratidal dolostone. Stacks of cycles with variations on this pattern are found at nearly every exposure of the Tonoloway Formation (Figure 12). Near Allenport, Pennsylvania, J. Inners (Cotter and Inners, 1986) determined that the Wills Creek and Tonoloway Formations contain 62 shallowing-up cycles, most of which are between 2–10 m-thick.

SUMMARY AND DISCUSSION

For much of Silurian time, the southeastern flank of the Appalachian Foreland Basin experienced shallow-marine shelf and coastal-margin conditions. A long-term equilibrium must have existed between sediment supply and accommodation space to keep the shelf ramp gradient very low and depths of the sea very shallow. On this ramp, accumulating sediment was segregated by grain size, and this resulted in a series of coarser-grained mid-shelf shoal complexes that formed between a low-energy, muddy coastal margin and a placid, anaerobic, deeper basin axis. Hydrographic processes were typically of low intensity in such a protected leeside location, with weak waves and little evidence of tides. Owing to a well-stratified water column and a shallow pycnocline (probably less than 10 m), many fine details of the depositional record were saved from bioturbation.

Two factors combined to keep the ramp at this equilibrium low-gradient configuration. First, episodic storms entrained coarser-grained sand and skeletal

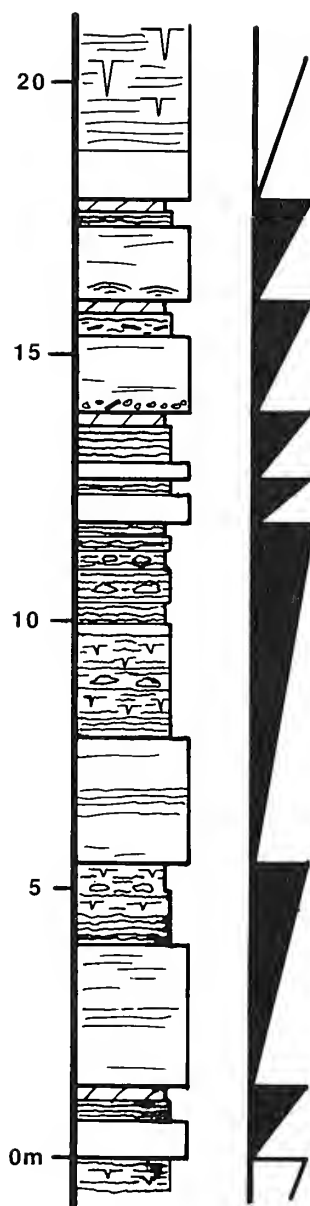


FIGURE 12—Small-scale, shallowing-up cycles in Tonoloway Formation in Iddings Quarry, 4 km W of Mifflinburg, Pennsylvania. See Figure 11 for generalized cycle. Horizontal scale is weathering resistance.

debris from the shoal complexes and other shallow areas, and redistributed these grains to deeper water locations. Secondly, frequent changes in relative sea level resulted in major shifts of shoreline location. The resulting erosional truncation (ravinement) during lowstands and subsequent transgressions also served to redistribute sediment from proximal to more distal parts of the basin. Because of the low wave and tidal energy of the Silurian coastal zone, these erosional truncations did not remove significant thicknesses of the earlier-deposited sedimentary record. With such a low ramp gradient, even small-

scale fluctuations of relative sea-level would have resulted in significant shifts of the shoreline and in distinct changes in the character of the facies that accumulated at a given location on the depositional ramp.

Persistent throughout the Silurian succession in central Pennsylvania are cyclically repeating, small-scale, shoaling-up sequences. Thicknesses of individual cycles range from 1–10 m, with most 1–5 m. Estimates of the periodicity of these cycles (Cotter and Inners, 1986; Cotter, 1988; Goodmann, 1988; Goodman and Brett, 1994) are in the range of 100 Ka or less.

The pervasiveness of small-scale cycles in this part of the Appalachian Foreland Basin is demonstrated by their presence in strata that 1) range in age from Early Silurian (Llandovery, Aeronian) to Late Silurian (Pridoli) (Figures. 1, 4); 2) have a variety of different lithologic compositions, both siliciclastic and carbonate; 3) formed at times of either tectonic quiescence or slight tectonic rejuvenation; and 4) accumulated in a great variety of depositional systems, including low-energy muddy coasts and more distal-shelf locations. It appears that whenever and wherever the low-energy, low-gradient depositional surface was poised near sea-level, the accumulating sedimentary record could resonate with whatever factor(s) forced the fluctuation of relative sea-level.

What was the cause of the meter-scale rhythm that modulated coastal and shallow-marine deposition throughout so much of the Silurian in central Pennsylvania? Arguing against their localized, autogenic origin is the persistent development of shoaling-up cycles of similar magnitude through such a temporal range and in so many disparate depositional settings and compositions. Identification of the particular extrabasinal cause or causes, however, is still a matter of conjecture, and we should be cautious about accepting either estimated periodicities (Algeo and Wilkinson, 1988) or stacking patterns (Drummond and Wilkinson, 1993) as definitive proof of Milankovitch orbital forcing.

ACKNOWLEDGMENTS

The paper was improved by the reviews of T. J. Algeo and S. G. Driese, and by editing by E. Landing. (Editors' note: the author contributed \$50 toward publication of this report from personal sources.)

REFERENCES

- ALGEO, T.J., AND B.H. WILKINSON. 1988. Periodicity of mesoscale Phanerozoic sedimentary cycles and the role of Milankovitch orbital modulation. *Journal of Geology*, 96:313–322.

- ALLING, H.L., AND L.I. BRIGGS. 1961. Stratigraphy of Upper Silurian Cayugan evaporites. *American Association of Petroleum Geologists Bulletin*, 45:515-547.
- BERNER, R.A. 1994. Geocarb II: a revised model of atmospheric CO₂ over Phanerozoic time. *American Journal of Science*, 294:56-91.
- BERRY, W.B.N., P. WILDE, AND M.S. QUINBY-HUNT. 1989. Paleozoic (Cambrian through Devonian) anoxitropic biotopes. *Palaeogeography, Palaeoclimatology, Palaeoecology*, 74:3-13.
- BRETT, C.E., A.J. BOUCOT, AND B. JONES. 1993. Absolute depths of Silurian benthic assemblages. *Lethaia*, 26:25-40.
- BROGLY, P.J., I.P. MARTINI, AND G.V. MIDDLETON. 1996. The Queenston Formation: shale-dominated, mixed terrigenous-carbonate deposits of Late Ordovician, semiarid, muddy shores in Ontario, Canada. *Geological Society of America, Abstracts with Programs*, 28(3):42.
- BROMLEY, R.G., AND A.A. EKDALE. 1984. *Chondrites*: fossil indicator of anoxia in sediments. *Science*, 224:872-874.
- COTTER, E. 1983. Shelf, paralic, and fluvial environments and eustatic sea-level [sic] fluctuations in the origin of the Tuscarora Formation (Lower Silurian) of central Pennsylvania. *Journal of Sedimentary Petrology*, 53:25-49.
- . 1988. Hierarchy of sea-level cycles in the medial Silurian succession of Pennsylvania. *Geology*, 16:242-245.
- . 1990. Storm effects on siliciclastic and carbonate shelf sediments in the medial Silurian succession of Pennsylvania. *Sedimentary Geology*, 69:245-258.
- , AND J.D. INNERS. 1986. Silurian stratigraphy and sedimentology in the Huntingdon County area. 51st Annual Field Conference of Pennsylvania Geologists, Selected Geology of Bedford and Huntingdon Counties, Guidebook, p. 27-39, 154-170.
- , AND J.E. LINK. 1993. Deposition and diagenesis of Clinton ironstones (Silurian) in the Appalachian Foreland Basin of Pennsylvania. *Geological Society of America Bulletin*, 105:911-922.
- DRIESE, S.G., AND J.L. FOREMAN. 1992. Paleopedology and paleoclimatic implications of Late Ordovician vertic paleosols, Juniata Formation, southern Appalachians. *Journal of Sedimentary Petrology*, 62:71-83.
- , C.I. MORA, E. COTTER, AND J.L. FOREMAN. 1992. Paleopedology and stable isotope chemistry of Late Silurian vertic paleosols, Bloomsburg Formation, central Pennsylvania. *Journal of Sedimentary Petrology*, 62:825-841.
- DRUMMOND, C.N., AND B.H. WILKINSON. 1993. Carbonate cycle stacking patterns and hierarchies of orbitally forced eustatic sea level change. *Journal of Sedimentary Petrology*, 63:369-377.
- ECKERT, B.-Y., AND C.E. BRETT. 1989. Bathymetry and paleoecology of Silurian benthic assemblages, late Llandoveryan, New York State. *Palaeogeography, Palaeoclimatology, Palaeoecology*, 74:297-326.
- ETTENSOHN, F.R. 1994. Tectonic control on formation and cyclicity of major Appalachian unconformities and associated stratigraphic sequences, p. 217-242. *In* J.M. Dennison and F.R. Ettensohn (eds.), *Tectonic and Eustatic Controls on Sedimentary Cycles*. SEPM (Society for Sedimentary Geology), Concepts in Sedimentology and Paleontology, Volume 4.
- FERGUSON, W.B., AND B.A. PRATHER. 1968. Salt Deposits in the Salina Group in Pennsylvania. *Pennsylvania Geological Survey, 4th Series, Mineral Resources Report* 58.
- FISCHER, A.G. 1981. Climatic oscillations in the biosphere, p. 103-131. *In* M. H. Nitecki, (ed.), *Biotic Crises in Ecological and Evolutionary Time*. Academic Press, New York.
- GOODMAN, W.M., AND C.E. BRETT. 1994. Roles of eustasy and tectonics in development of Silurian stratigraphic architecture of the Appalachian Foreland Basin, p. 147-169. *In* J.M. Dennison, and F.R. Ettensohn, (eds.), *Tectonic and Eustatic Controls on Sedimentary Cycles*. SEPM (Society for Sedimentary Geology), Concepts in Sedimentology and Paleontology, Volume 4.
- GOODMANN, P.T. 1988. Stratigraphy and basin dynamics, upper Tonoloway and Keyser Formation, (Upper Silurian-Lower Devonian) central Pennsylvania: an episodic perspective. *North-eastern Geology*, 10:231-240.
- GWINN, V.E., AND D.M. BAIN. 1964. Penecontemporaneous dolomite in Upper Silurian cyclothem, south-central Pennsylvania. *American Association of Petroleum Geologists Bulletin*, 48:528.
- HOSKINS, D.M. 1961. Stratigraphy and Paleontology of the Bloomsburg Formation of Pennsylvania and Adjacent States. *Pennsylvania Geological Survey, 4th Series, General Geology Report* 36.
- JOHNSON, M.E. 1987. Extent and bathymetry of North American platform seas in the Early Silurian. *Paleoceanography*, 2:185-211.
- KENT, D.V., AND J.D. MILLER. 1988. New perspectives from paleomagnetism: Paleozoic drift and Appalachian tectonics, p. 12-17. *In* Lamont-Doherty Geological Observatory of Columbia University, Yearbook, p. 12-17.
- KLEIN, G. DE VRIES. 1977. *Clastic Tidal Facies*. Continuing Education Publishing Co, Champaign, Illinois.
- KUHN, T.S. 1962. *The Structure of Scientific Revolutions*. University of Chicago Press, Chicago, revised edition, 1970.
- RETAILLACK, G.J. 1993. Late Ordovician paleosols of the Juniata Formation near Potters Mills, PA, p. 33-50. *In* S.G. Driese, (ed.), *Paleosols, Paleoclimate, and Paleatmospheric CO₂: Paleozoic Paleosols of Central Pennsylvania*. University of Tennessee, Department of Geological Sciences, Studies in Geology 22.
- RICKARD, L.V. 1969. Stratigraphy of the Upper Silurian Salina Group, New York, Pennsylvania, Ohio, Ontario. New York State Museum and Science Service, Map and Chart Series Number 12.
- SEIDELL, B.C., T.J. TOUREK, AND L.A. HARDIE. 1987. The Upper Silurian Wills Creek and Tonoloway Formations of the central Appalachians reevaluated; comparisons with a modern siliciclastic sabkha complex. SEPM Annual Midyear Meeting, 4:76.
- SMITH, N. D. 1968. Cyclic sedimentation in a Silurian intertidal sequence in eastern Pennsylvania. *Journal of Sedimentary Petrology*, 38:1301-1304.
- TOUREK, T.J. 1970. The depositional environments and sediment accumulation models for the Upper Silurian Wills Creek Shale and Tonoloway Limestone, central Appalachians. Unpublished Ph.D. thesis, The Johns Hopkins University, Baltimore, 282 p.
- VAN DER VOO, R. 1988. Paleozoic paleogeography of North America, Gondwana and intervening displaced terranes: comparisons of paleo-magnetism with paleoclimatology and biogeographical patterns. *Geological Society of America Bulletin*, 100:311-324.
- WALKER, R.G. 1973. Mopping up the turbidite mess, p. 1-37. *In* R.N. Ginsburg (ed.), *Evolving Concepts in Sedimentology*. The Johns Hopkins University Press, Baltimore.
- ZIEGLER, A.M., K.S. HANSEN, M.E. JOHNSON, M.A. KELLY, C.R. SCOTSE, AND R. VAN DER VOO. 1977. Silurian continental distributions, paleogeography, climatology, and biogeography. *Tectonophysics*, 40:13-51.

SILURIAN OCEANIC EVENTS: SUMMARY OF GENERAL CHARACTERISTICS

LENNART JEPPSSON

*Department of Geology, Division of Historical Geology and Palaeontology,
University of Lund, Sölvegatan 13, S-223 62 Lund, Sweden*

ABSTRACT—A model of oceanic cyclicity published in 1990 synthesized changes in biotas, lithologies, and isotopes. The oceanic model is herein developed further in order to understand and describe major differences in the characteristics of different oceanic events. Both *primo* and *secundo* events influenced the nature of succeeding events. There are four different kinds of oceanic events with variable characteristics. Milankovitch cyclicity also gave each event unique characteristics. A scale to describe the maximum severity of an event, and the effects of each datum point, is based on comparisons with the late Llandovery–early Wenlock Ireviken Event. Ten Silurian oceanic events are summarized, and other possible oceanic events are suggested. These events are interpreted to have been responsible for most Silurian extinctions.

INTRODUCTION

The oceanic model (Jeppsson 1990a, 1996, 1997) developed through efforts to understand data that suggested a cyclic pattern in global Silurian conodont diversity and in the lithologies in which conodont elements are found. Six features of the oceanic model are important to note.

First and most important, the model provides testable explanations for discoveries made after it was developed, as well as testable predictions. Thus in recent years, the most fruitful parts of my collecting on Gotland have been governed by such predictions. With thousands of unstudied localities, hundreds of meters of sections, and yields so low that 20–100 kg samples or more were needed to produce an adequate collection, early sampling was reconnaissance and based on standard intervals (e.g., every 2 m). The model led to the selection of sections where sampling on a centimeter–decimeter scale was fruitful, and suggested which additional localities should be sampled for evidence of as-yet undetected events. Instead of only describing faunas, ranges, and gaps, it has been possible to provide a coherent interpretation of the conodont succession.

Second, changes in humidity on adjacent lands are proposed to be the main cause of variation in the amount of carbonate and terrigenous material in local sections. A humid climate promotes weathering and erosion of terrigenous material. Other effects of such a climate are the freshening and nutrient enrichment of coastal water masses, which are detrimental to production and preservation of carbonates (Hallock, 1988). A dry, warm climate creates conditions suitable for extensive carbonate production, such as in reefs, and preservation of such sediments. Clear waters result in a seaward translation of many habitat boundaries, including those of the dysphotic zone and community boundaries influenced by their place in that zone.

Third, the model suggests that the main causes of mass extinctions in the marine realm are sudden brief declines (a few hundred years in duration?) in primary planktic production. This causes extinctions among holoplanktic taxa. Furthermore, benthic taxa will be affected by such a decline, because many have planktic larvae that feed on planktic organisms. Other benthic taxa are affected, because they are part of the food web. Brief drops in planktic production are due to a decrease in the mineral nutrients for planktic algae. These nutrients derive from runoff and recycling of nutrients from the deeper ocean by upwelling (Tappan, 1986). Changes in either of these sources affect primary production.

Fourth, the model suggests that changes in oceanic states were geologically fast, because they were shorter than oceanic mixing time (ca. 1 Ka in the modern ocean). As a result, oceanic changes may be recorded across a single bedding plane or over an interval of several centimeters.

Fifth, the frequency of changes in the Silurian is higher than that described by any other model used for the Paleozoic. The average duration of an episode (see below) may be 2 Ma, and the duration of an event may be perhaps 100 Ka. In many parts of the stratigraphic column, this means that identification of the oceanic state will require a higher resolution than that calibrated by existing zonations for shelly sequences.

Sixth, oceanic model suggests that sea-level changes are a consequence of changes in oceanic conditions, but are not a major force for changes in sediments and faunas. High-resolution data show that faunal and sedimentary changes precede sea-level changes.

The purpose of this report is therefore to develop further the part of the oceanic model that describes events. A summary is provided of the model's chief principles, of the Silurian record of known events, and of the literature in which the model has been cited.

SUMMARY OF THE OCEANIC MODEL

The oceanic model describes two stable and four unstable oceanic states. It details how the former two stable states are stabilized initially and then gradually destabilized until they end, and how the four unstable states develop until oceanic conditions trigger a return to a stable state. As a result of these changes, each state lasts for a limited interval of time. Such an interval is called an "episode" if it is a stable state, and an "event" if it is unstable (Figures 1, 2). The two stable states are referred to as "primo" (P) and "secundo" (S). These terms were chosen so that they do not carry any association with earlier terms for more or less similar concepts (e.g., greenhouse and ice-house states). Strong causal connections exist between the characteristics of an event and its preceding and succeeding episodes; hence the four kinds of events are indicated by their sequence (e.g., a primo-secundo event or P-S event, etc). Furthermore, each chronostratigraphic interval is named from an appropriate, geographic place name, not after a particular fossil, because the latter tends to be understood by specialists in a particular taxonomic group, thus limiting the term's effectiveness.

In many ways, conditions during a primo episode resemble the modern oceanic circulation pattern, with low atmospheric CO₂ concentration and cold high latitudes. High-latitude surface water is close to the freezing point (ca. -1.8 C), and sinks to form deep oceanic water. The rate of production of dense water is high, as are the rates of deep-water replacement and upwelling, both of which provide a stable source of nutrients for primary planktic production. Solubility of gases is highest in cold water. This factor, coupled with the high replacement rate, result in oxic deep water. Cold high latitudes may result in glaciations that reinforce the lowering of sea-level by thermal contraction of deep water.

During a secundo episode, atmospheric CO₂ concentration is high, and high latitudes are too warm to produce very dense surface waters. Instead, saline waters at intermediate latitudes are densest and form deep

oceanic waters. This deep water contains less oxygen, and the rate of deep-water production and upwelling is less than a tenth of what it is today (Bralowier and Thierstein, 1984); this results in anoxic deep waters. With reduced upwelling and dry low latitudes, planktic production is low but stable.

Global temperature is partly regulated by the oceanic storage capacity of carbon dioxide. At the onset of an episode, the change in the deep-water temperature and its storage capacity results in a drawdown of CO₂ at the beginning of a primo episode, and a release at the beginning of a secundo episode. By the icehouse-greenhouse effect, these atmospheric changes stabilize each type of episode. Another major greenhouse-icehouse effect may be related to the storage of methane hydrates in deep-water sediments when their temperature is below 7 C (MacDonald, 1997). Indeed, deep-water temperatures will pass this critical stage during every change between primo and secundo conditions. An enormous amount of methane is released when a secundo episode is initiated.

Rapid carbonate deposition and black shale formation during secundo episodes gradually decrease the greenhouse effect and the stability of a secundo episode. Similarly, the strongly reduced carbonate deposition and the oxygenated deep-water sediments during primo episodes results in a slow increase in CO₂ concentration in the atmosphere. Thus during both kinds of episodes, the climate changes slowly until the two alternative sources of deep water produce waters of the same density. Regular minor changes in global temperature caused by Milankovitch cyclicity are then enough to trigger an end to the episode.

Two alternative terminations are possible. Without strong Milankovitch perturbations, the end of a secundo episode is caused by production of denser surface water as the new deep-water source. In this way, a secundo episode is succeeded by a primo episode, and upwelling continues uninterrupted, although at the slower rate characteristic of secundo episodes. The end of a primo episode is due to Milankovitch-caused amelioration of high-latitude climate. The existing deep water is denser than either high-latitude deep water or highly saline deep water formed at low latitudes. As a result, deep-water renewal is interrupted, deep upwelling ceases, and the primo episode is terminated. A drop in nutrient supply causes extinctions that result in a "datum"—the first interval of unstable oceanic conditions during the event. Several factors contribute to a quick resumption of cold, dense, deep-water production (Jeppsson 1997), but the next similar climatic amelioration (ca. 31 Ka later in the Silurian, for example) causes a second datum. With each datum, the system comes closer to the threshold of similar densities for both high-latitude, cold-dense waters and low-latitude, dense saline waters.

Chronostratigraphy		Oceanic Regime	Standard Conodont Zonation	Graptolite Zonation	Sea-level Curve Low High
W E N L O C K	GLEEDON	Klinte Secundo Episode	<i>O. bohémica</i> Zone — — — — — —	<i>C. ? gerhardi</i> / <i>C. ? ludensis</i> <i>C. ? deubeli</i> <i>C. ? praedeubeli</i> <i>G. nassa</i> <i>P. d. parvus</i>	
		Mulde Secundo Secundo Event			
	WHITWELL	Hellvi Secundo Episode		<i>C. lundgreni</i>	
		Valleviken Ev.	<i>O. s. sagitta</i> Zone		
	SHEINWOODIAN	Allekvia Primo Episode	<i>K. o. ortus</i> Zone	<i>C. perneri</i>	
		Lansa Secundo Episode	post <i>K. walliseri</i> interregnum		
		Boge Event	uppermost <i>K. w.</i> range		
		Sanda Primo Episode	<i>K. patula</i> Zone	<i>C. rigidus</i>	
		Vattenfallet Secundo Episode	Middle <i>K. walliseri</i> Zone	<i>M. belophorus</i>	
			Lower <i>K. walliseri</i> Zone		
			<i>O. s. rhenana</i> Z. — — —	<i>M. antennularius</i>	
			Upper <i>K. ranuliformis</i> Z.	<i>M. riccartonensis</i>	
		Ireviken Event	5 Zones — — — — —	3 Zones	
	TELYCHIAN	Snipklint Primo Episode	<i>P. amorphognathoides</i> Z.	<i>C. lapworthi</i> <i>M. spiralis</i> <i>M. crenulata</i> <i>Mcl. griestonien.</i> <i>M. crispus</i> <i>St. turriculatus</i> <i>St. guerichi</i>	
		Sec.-Pri. Event	<i>P. celloni</i> Zone		
		Malmøykalven Secundo Episode	<i>Distomodus staurognathoides</i> Zone	<i>St. sedgwickii</i>	
		Sandvika Event			
		Jong Primo Ep.		<i>Dem. convolutus</i> 3 Zones	
	RUDDANIAN	Spirodden Secundo Episode	<i>Distomodus kentuckyensis</i> Zone	<i>C. cyphus</i> <i>Cyst. vesiculosus</i> <i>Par. acuminatus</i>	
		?-Sec. Event		<i>G. persculptus</i>	

FIGURE 1—Early Silurian oceanic changes. Oceanic episodes and events after Jeppsson (1990a, 1993, 1996), Aldridge et al. (1993), and Jeppsson et al. (1995). Graptolite zonation after Jaeger (1991) and Koren' et al. (1996); conodont zonation and the correlation between the two zonations after Aldridge et al. (1993) and Jeppsson (In press).

Chrono- strati- graphy	Oceanic Regime	Conodont Faunal Sequence	Graptolite Zonation	Sea-level Curve Low High
DEVONIAN	Klonk Event	<i>Oul. elegans detorta</i> Z.	<i>M. uniformis</i> Zone post <i>M. transg.</i> Z. C ₄	
P R I D O L I	late Pridoli secundo episode	<i>Ozarkodina</i> <i>r. remscheidensis</i> Zone	<i>Monograptus</i> <i>transgrediens</i> Zone	
	mid-Pridoli P-S event			
	mid-Pridoli primo episode?	<i>Oz. eosteinhorrensis</i> s. str. Zone		
	mid-Pridoli sec. episode?			
	early Pridoli event?		<i>M. perneri</i> Zone	
	early Pridoli primo episode	<i>Oz. remscheidensis</i> n. ssp. N	<i>M. bouceki</i> Zone <i>M. lochkovenski</i> Zone <i>P. ultimus</i> Zone <i>P. parultimus</i> Zone <i>M. spineus</i> Event	
L U D L O W	Klev Event			
	Hoburgen Secundo Episode	<i>Oz. crispa</i> Zone <i>Oz. scanica</i>	<i>M. formosus</i> Zone <i>N. koz- lowskii</i> <i>B. b. te- nuis</i> Zone	
	Lau Event	<i>P. equicostatus</i>	C ₃	
	Havdhem Primo Episode	<i>P. siluricus</i> Zone u m	<i>N. koz- lowskii</i> Zone	
	Etelhem Secundo Episode	<i>Oul. siluricus</i> acme	<i>B. b. tenuis</i> Zone	
	Linde Event	<i>A. ploeckensis</i> Zone	C ₂	
	Sproge	<i>Oz. excavata</i> n. ssp. A ? I?	<i>S. leintw.</i> Zone	
	Primo	Post- <i>Oz. ex.</i> n. ssp. S	<i>L. scanicus</i> Zone	
	Episode	<i>Oz. excavata</i> n. ssp. S	<i>L. progenitor</i> Zone	
		<i>K. stauros</i> <i>Oz. crassa</i> n. ssp. Zone	<i>N. nilssoni</i> Zone	
WENLOCK	Klinte Secundo Episode	<i>Erika</i>		

Oceanic events are often discovered by a multi-step process. The first step is recognition of "faunal assemblages" or "assemblage zones". Interest in the boundary interval may initially focus on the lowest appearances of taxa, perhaps with debate as to whether the zonal boundary should be based on the appearance of one taxon or presence of the "typical assemblage". By focusing on the recovery after the event, however, such an event's beginning and early development are left within the preceding zone, and the cause of the event is not examined. For example, the major part of the late Wenlock Mulde Event was long included in the *Cyrtograptus lundgreni* Zone. Even today, when the top of this zone is defined at a graptolite extinction horizon, this has left the initial 30 Ka or 100 Ka of the event unstudied. Work on boundary intervals, however, will hopefully reveal both the beginning and the end of these brief extinction events.

Efforts to identify causes of these correlated changes led to development of an empirical oceanic model (Jeppsson, 1990a). The focus shifted back to extinction events when I assembled a high-resolution record of extinctions and other changes for the Ireviken Event across the Llandovery–Wenlock boundary. This record revealed many details of the event, including the existence of a series of extinctions (datum points) and their timing and strength. The search for a cause of this event was fruitful when the effects of Milankovitch cyclicity were included in the oceanic model (Jeppsson, 1997). One result was a general model for the sequence and timing of the changes during primo–secundo events. This report thus develops another aspect of the oceanic model that results when Milankovitch perturbations, and explains why different oceanic events can have such variable characters and effects.

DEVELOPMENT AND USE OF THE OCEANIC MODEL

The oceanic model (Jeppsson, 1988a, 1989, 1990a) addressed a large number of observations on anomalies in the conodont succession (Jeppsson, 1975, 1983) and fluctuations in the frequency of certain lithologies (Jeppsson, 1984, 1985, 1987b). Further developments of the model have involved the inclusion of Milankovitch effects (Jeppsson, 1997), discovery of the possibility of different kinds of events (Jeppsson, 1990b, 1996, 1997, discussion below), a theory for primo–secundo events (Jeppsson,

1997), developments in terminology (Aldridge et al., 1993), isotope data for quantification of the degree of changes (Samtleben et al., 1996), and a calibration scale for the severity of events (Jeppsson, 1996).

Carbon and oxygen isotope changes caused by oceanic changes were predicted (Jeppsson, 1990a), and have now been found (Talent et al., 1993; Brenchley et al., 1994; Samtleben et al., 1996; Wenzel and Joachimski, 1996). These changes are too large to be explained only by a temperature change, but they fit well with the salinity changes included in the model (Samtleben et al., 1996). Calculations of the size of the salinity changes are an important contribution toward making the oceanic model more quantitative.

Carbon and oxygen isotope trends during the late Wenlock Mulde Event have been published from British sections (Corfield et al., 1992; Corfield and Siveter, 1992; D.J. Siveter in Kaljo et al., 1995). The Lau Primo–Secundo Event has been sampled in Australia and on Gotland (Talent et al., 1993). These detailed studies may be extremely important in the description of events and may determine how and when the new deep-water sources replaced the old: at the end of the event (Jeppsson, 1997)? Did the event involve a three-layered ocean? If so, when and what kind of changes took place, and in what order?

Empirical data on the global cyclicity of reef formation has been related to oceanic cyclicity (Jeppsson, 1990a; Kershaw, 1993; Kershaw and Keeling, 1994; Brunton and Copper, 1994; Brunton et al., In press). Local and regional responses to global cyclicity have been widely studied (Jeppsson, 1990a, 1997; Aldridge et al., 1993; Jeppsson et al., 1994, 1995; Wang and Jeppsson, 1994; García-López et al., 1994; Kaljo et al., 1995; Kleffner et al., 1995; Kluessendorf and Mikulic, 1996; Berry, 1996, this volume; Radcliffe, 1996; Männik and Malkowski, 1996; Snigireva and Bikbaev, 1996). The role of nutrient supply and ocean chemistry has been reviewed by Brasier (1992, 1995a, 1995b).

Late Ordovician extinctions were studied by Brenchley et al. (1994, 1995) and Armstrong (1995, 1996). Silurian extinctions caused by the primo and secundo events are now widely known (Jeppsson, 1990a, 1993, 1996, 1997, In press; Boucot, 1991; Aldridge et al., 1993; Urbanek, 1993; Melchin, 1994; Jeppsson et al., 1995; Štorch, 1995; Kaljo et al., 1995; Nestor, 1996). Documentation of range ends and extinctions within single taxonomic groups are available for the Silurian (e.g., Koren', 1991; Urbanek, 1993, 1995). Effects on fish faunas were analyzed by Fredholm (1989), chitinozoans by Sutherland (1994) and Nestor (1996), acritarchs by Le Hérisé and Gourvenec (1995) and Eriksson and Hagenfeldt (1997). A possible effect on conodont evolution was suggested by Corradini et al. (1995).

FIGURE 2—(opposite) Late Silurian oceanic changes. Oceanic sequence from L. Jeppsson and R.J. Aldridge (unpub. data). Sources of graptolite zones in Figure 1 explanation.

KINDS OF EVENTS

Extinction events may be very different from one another. In the past, studies of extinctions have often invoked hypothetical, group-specific changes, or secular changes (e.g., a late Wenlock regression or transgression) that did not explain how such presumed gradual change could trigger an extinction across a single bedding plane. Separate causes for each event were proposed, or single effects of each event were hypothesized. More than one cause of an event is certainly possible (e.g., the effects of a bolide on an extinction), although the oceanic model reveals two factors which result in a difference in the characters of the events. First, there are four kinds of oceanic events. Second, Milankovitch perturbations not only began many of the events, but also shaped their development. The pattern of Milankovitch perturbations led to the interference of several cycles with different periods. The brevity of an event and the much longer periodicity of the Milankovitch pattern give each event a unique pattern and character. Each datum probably differs, however, mainly in one variable (severity), and extinctions are triggered in the same way. The oceanic model correctly analyzes documented effects and predicts other effects.

A third cause of differences between weak and severe events may be related to the type of layered ocean that developed during each part of the event. If a three-layered ocean developed, consisting of a lower layer of aging isolated water, a middle layer, and new surface water formed from the middle layer, then most nutrients lost from the surface layer would drop down to the lower layer with very little brought up by upwelling from the middle layer. The heat flow from the newly formed ocean bottom at mid-oceanic ridges would reduce density enough to produce new surface water from the middle layer. At the end of such an interval with a three-layered ocean, heating of the bottom layer (Worthington, 1968) would proceed until it too participated in the upwelling. Primary planktic production would reflect this change, and very low production would be followed by a slight increase. A disaster fauna (i.e., 6.2 on the severity scale) may indicate a three-layered ocean. The best known Silurian disaster faunas (during the Ireviken, Mulde, and Lau Events) are strongly dominated (up to 98%) by *Panderodus equicostatus*. The rest of the fauna is often formed by *Pseudoneothodus*, *Decoriconus*, *Dapsilodus*, *Oulodus* sp., and a species of the *Ozarkodina bohémica* group. Blooms of more or less dwarfed forms of the *Pristiograptus dubius* lineage seem to be a characteristic of relatively severe intervals (Jaeger, 1991), while a graptoloid-free gap may indicate the most severe interval late in the history of the event.

DATUM POINTS

The range in duration of a datum is not yet known. At Datum 2 of the late Llandovery–early Wenlock Ireviken Event on Gotland, one subspecies of *Panderodus panderi* became extinct, but another subspecies invaded the area so quickly that it is present in the next sample. Sampling was continuous within only one bed (a few centimeters) in each sample. It follows that the maximum interval of absence of the species is only a few centimeters. The rate of sediment accumulation (Jeppsson, 1987a, 1990a) indicates that this may correspond to a few hundred years. Considering the probable maximum life span of taxa that perished (e.g., Jeppsson 1976), this would be more than enough to cause extinctions through elevated larval mortality, with decreased primary planktic productivity. The invading subspecies might have survived in refugia, may have been tolerant of the conditions during the datum, and hence may have appeared before its end, when competitive exclusion ceased.

I described a kind of intermittent (Lazarus) distribution connected with improved conditions after Datum 3 of the Ireviken Event (Jeppsson, 1997). In addition to these reappearances, the closely spaced (1–5 cm), abundant (typically several thousands of elements each) collections from Lusklint 1 have revealed a previously unknown pattern of intermittent distribution. Several taxa reappear very briefly near one or more datum points and are especially noteworthy during Datum 2, the horizon associated with the largest number of extinctions and disappearances, but are also found near other datum points (Figure 3). A probable explanation is that their intermittent appearance was due to competitive exclusion, and that this competition relaxed when physical stress increased and lowered the number of individuals. A strong decrease in conodont element frequency agrees with such an interpretation. Further analyses of the Lusklint collections are likely to reveal more such intermittent appearances. With more widely spaced collections, these sporadic appearances would easily be mistaken for a continuous range, and would therefore interfere with efforts to identify datum points and their effects. For example, in the best-known section through the early part of the Lau Event (Figure 4), the distance between the samples is about 0.1 m or more. Even though several thousand conodont elements were recovered in most collections, this was not enough to include an average of five specimens of the rarest and most interesting taxon (this was due to the very high frequency of the four dominant taxa). Further analyses, including those of frequency changes, may reveal datum points based on experience gained from the Ireviken Event.

PRIMO-SECUNDO EVENTS

Both a theoretical understanding of P-S events and the empirical knowledge of the best-known event (Jeppsson, 1997) are now better established. Several datum points indicate a stepwise deterioration through the event (Figures 3 and 4). Closely spaced collections permit identification of at least three phases of the event. During the first phase, only the Milankovitch cycle with the strongest effect at higher latitudes, or the obliquity cycle (today 41 Ka but only ca. 31 Ka in the Early Silurian [Berger et al., 1989]) caused datum points. In the second phase, the threshold was lowered so much that one or more of the other Milankovitch cycles may have triggered a halt in deep-water production that led to more closely spaced datum points. The final phase consisted of a long stop in the upward transport of nutrients.

A combination of data on the spacing of P-S events, their relative severity, the degree of recovery after each datum, and lithologic changes permits a detailed analysis of the cause and effects of and allows predictions on other undocumented effects (Jeppsson, 1997). The major problem in such an analysis is the high (local) precision required to identify the range ends (a precision of a few Ka is required) and the number of affected taxa for which data are needed. The latter requirement means that progress requires the combined efforts of many specialists.

SECUNDO-SECUNDO EVENTS

Under conditions of fluctuating salinity during a secundo episode, deep-water production is expected to be episodic. Deep-water transfer to the surface is limited by heat flow from the ocean bottom. Thus a certain degree of fluctuating salinity would not affect upwelling, but it probably would be compensated for by changes in the volume of the deep-water reservoir through small vertical changes in the position of the boundary layer (i.e., the halocline). If production of unusually salty water continued until a considerable part of the deep-water reservoir consisted of such water, a cascade of effects would take place. The surface water would be freshened by loss of salt to the deep-water reservoir. Upwelling of deep water to form surface water would also require increased energy, because it would be denser. At a certain point, deep upwelling may cease. The cutoff of one of the most important nutrient sources for planktic production (especially important during a secundo episode when the runoff from land was low) would cause a decrease in primary production and lead to extinctions among taxa that depended on it. The biologic and chemical extraction of

calcium carbonate in shallow areas would continue, and the atmosphere would lose CO₂. Because humidity and temperature are coupled, weathering would increase. Increased availability of nutrients in coastal waters would decrease the rate of calcium carbonate deposition (Hallock, 1988) and lead to more predominant argillaceous sediments. Furthermore, this change would contribute to a return of surface waters to normal densities. Meanwhile, the heat flow would steadily lower the density of the deep-water reservoir. These processes would continue until vertical circulation started again. At that time, atmospheric CO₂ content would increase, and normal secundo-episode conditions would return.

Some of the characteristics of a secundo-secundo event are similar to those of a primo episode (e.g., more argillaceous sediments and the presence of some hardy primo-state taxa during the recovery interval). Initially, some taxa may become extinct, and at the end of the event, primo-state taxa would disappear from the record. During primo-secundo and primo-primo events, however, weathering continues more or less unchanged, at least through the initial part of the event. As a result, one of the sources of nutrients for the planktic community remains. In contrast, before a secundo-secundo event (and a secundo-primo event), humidity and weathering are very low. Therefore when recycling stops at the beginning of the event, the result is a deep but brief initial drop in planktic production. It follows that the initial extinction event will be more severe than for a P-S event, and its effect on different taxonomic groups may differ.

The datum points during a primo-secundo event are linked to changes in high-latitude climate that controls the temperature at which the formation of deep water ceases. During a secundo-secundo episode, however, humidity and temperature at low latitudes control whether any water becomes dense enough to form new bottom water. The time scale of a secundo-secundo event requires identification of coeval Milankovitch cycles (for more discussion and data, see Jeppsson [1996] and description of the Mulde Event below).

SECUNDO-PRIMO EVENTS

The initial phase of a secundo-primo event should resemble a secundo-secundo event, as the characteristics of both reflect the starting conditions and the preceding secundo episode. A severe first datum is therefore expected. The final phase may deviate in some ways, and its characteristics will determine the nature of the subsequent interval (that is, whether it will be a primo or a secundo episode).

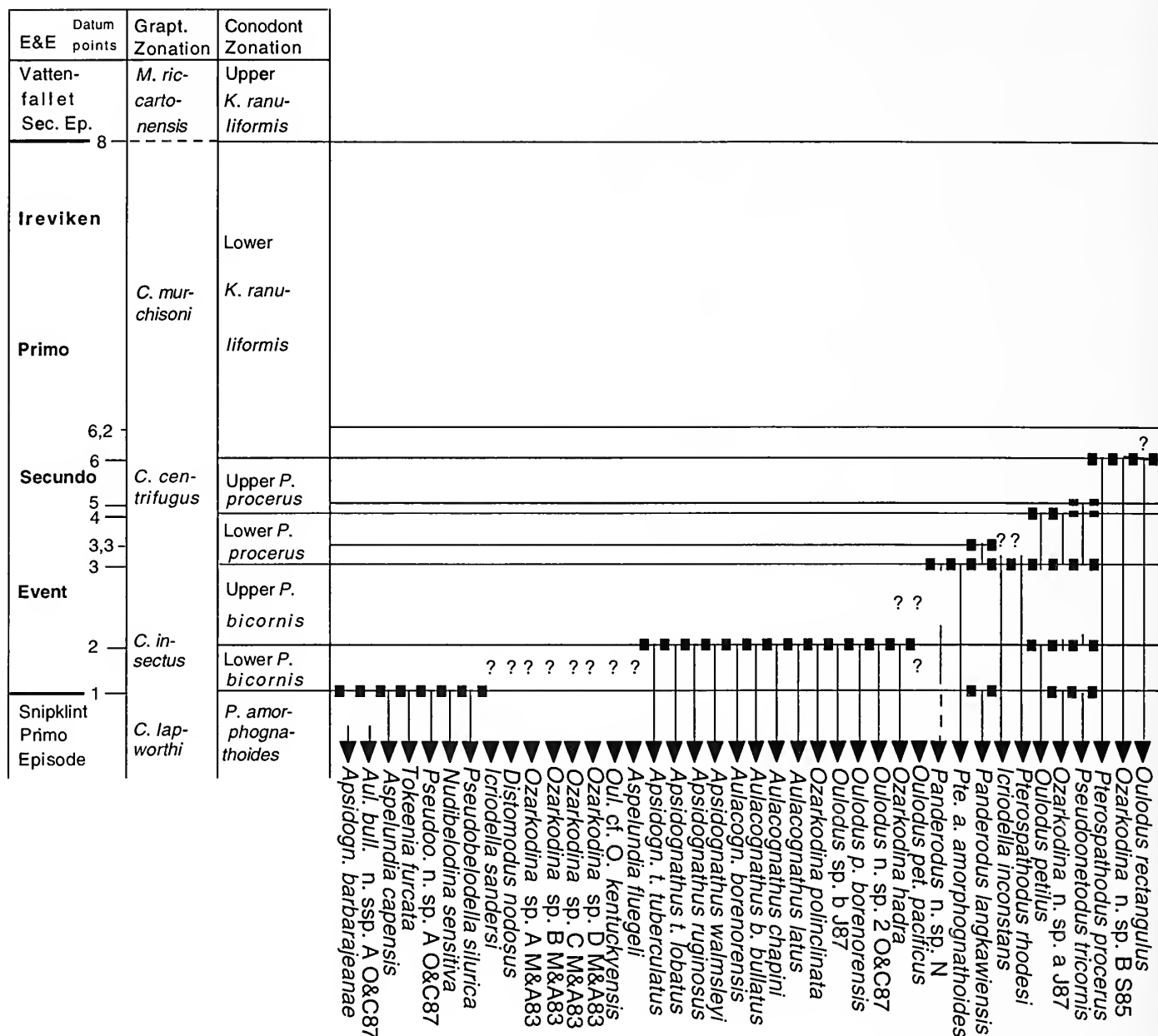
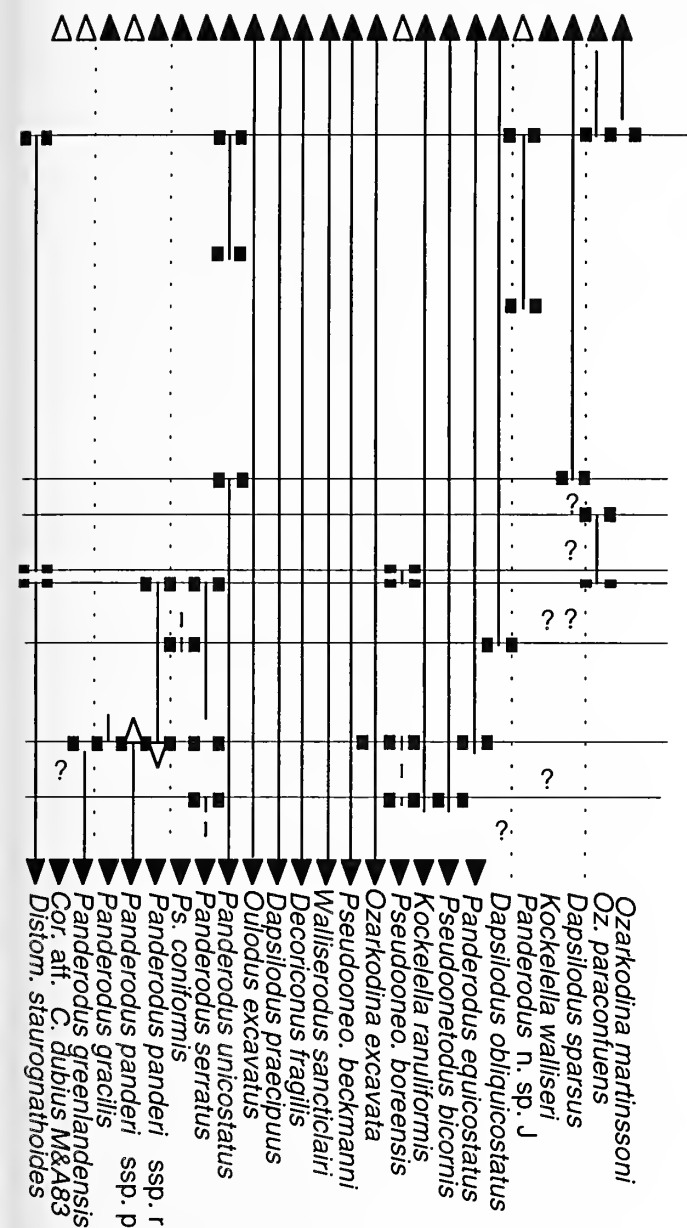


FIGURE 3—Ireviken Primo–Secundo Event and global conodont record. Zonation and ranges based on Luskint 1 and Lickershamn 2 sections on Gotland (L. Jeppsson, unpub. data) and other localities (Jeppsson, 1997b, and references therein). Arrows show ranges extend into older and younger intervals. Open arrows show taxonomically deviating segments. Squares mark FAD, LAD, Lazarus end points, and other important changes.

Two secundo–primo events are known (Jeppsson, 1996). Both had the expected strong effects (Loydell, 1994; Jeppsson, 1996). Several other effects are also known (Loydell, 1994; Jeppsson, 1996), but no data on the sequence of changes are yet available. Efforts to develop a more detailed theoretical description are best postponed until we have detailed data to test.

PRIMO–PRIMO EVENTS

A primo–primo event is similarly caused by a fluctuation in the density of the source of the deep water. The temperature of high-latitude surface water varies with time. When the water is cooler, its density increases, and deep-water production increases. Thus, upwelling con-



taxa that depend on nutrients supplied through upwelling occur, but other taxa are less affected because of the steady supply of nutrients by terrestrial weathering. The aging deep water becomes anoxic, and the deep-water sediments change correspondingly. The gradual increase in dissolved calcium carbonate characteristic of a primo episode (Jeppsson, 1990a) continues, and no cascade effect on the global temperature is expected from the event. A counter-effect may even be expected, because dissolved CO_2 remains in the surface water and causes a faster-than-average increase in atmospheric CO_2 .

In summary, primo-primo events are probably brief, have relatively low severity, cause no or few extinctions, and cause limited lithological deviations. Detection of a P-P event is therefore more difficult than other events. Events that cause an extinction will sooner or later be detected by repeated sampling below and above the exact level of extinction. Similarly, a visible lithological change that reflects oceanic cyclicity suggests an interval where an event could be sampled for and may, at least, feature Lazarus gaps. Based on available data, the first hint of the existence of a brief event, which is characterized only by Lazarus gaps, can only be detected with close sampling and sample sizes adjusted to give adequate (large) collections. This is probably the reason that no P-P event has yet been found.

PRECISION IN SILURIAN CORRELATIONS

Recognition of events and study of their details require a high level of stratigraphic precision. Hence the existing precision in Silurian correlations should be considered. Until thirty years ago, Silurian correlations had such a low resolution that a correlation error of several Ma was discovered, and resulted in recognition of a new epoch, the Pridoli. Modern application of a more detailed conodont zonation sometimes reveals local and regional correlation errors far above 100 Ka, even in very well-studied areas (e.g., Jeppsson, 1988b, In press; Jeppsson and Männik, 1993; Jeppsson et al., 1994). Recent progress in regional and global correlations has revealed at least one error as large as several Ma even in a very well-studied sequence, and several other errors of that magnitude in less well-studied areas (Jeppsson, In press). Simply stated, the errors may be larger than one episode. With frequent errors, it is understandable that our picture of the stratigraphic record looks as if background extinction was the typical or even the only factor. The situation today is that extinctions due to oceanic events are known to have been extremely important, and only subsequent, very detailed studies can show whether there was any

continues unchanged, or increases temporarily if the chilly period is long and cool enough. If a cool period is followed by a strong and rapid increase in high-latitude water temperature, then those waters are not dense enough to replace the existing deep water. As a result, downwelling and upwelling cease, and an event occurs.

The effects of the event would include a drop in planktic productivity with loss of upwelling as a source of nutrients. No initial change in humidity and weathering is expected, however, and in areas where terrestrial weathering was the main nutrient source, the effects on planktic productivity are small. Extinctions in oceanic

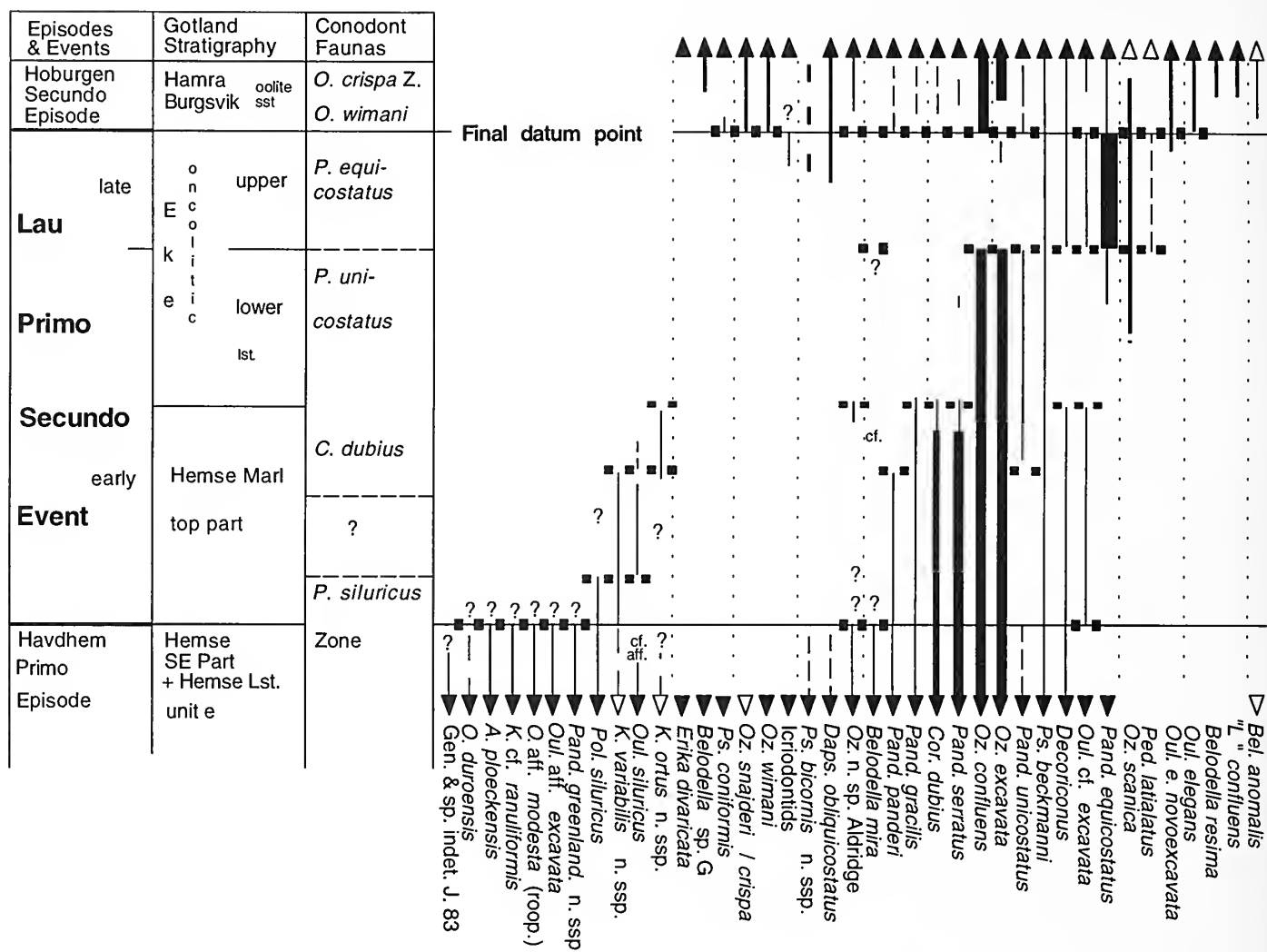


FIGURE 4—Lau Event. Stratigraphic column for Gotland; marls or limestones below the event are succeeded by the upper Hemse Marl (i.e., “flaggy” interbedded limestone, mudstone, and marl with acmes of *Daya navicula* or *Shaliera* sp.), Eke beds (oncolitic and range from crinoid limestone to marls), and Burgsvik beds (clay and sandstone capped by oolites). Conodonts of uppermost Hemse and lowermost Eke beds at Botvide 1 and Nyan 2 listed in Laufeld (1974). Apart from Gotland, few data on changes during the event are known, but approximate ranges for some taxa not found in this interval on Gotland are included. Five possible data points marked with horizontal lines.

significant background extinction in the Silurian marine realm.

The graptolite zonation has a higher precision than any other Silurian zonation scheme. Over the years, its precision has improved to the point where it has reached the necessary threshold for the detection of events. As a result, several of the strongest Silurian extinction events were first detected by studies on graptolite ranges. These have been described and discussed, however, as exclusively affecting graptolites, since most other taxa are limited to sequences that lack a good graptolite record and are therefore correlated at a much lower precision. Evidence from conodonts is now changing that situation in the Silurian. This increased precision has been important

in many papers (Jeppsson, 1988b, 1994, 1997; Jeppsson and Männik, 1993; Aldridge et al., 1993; Jeppsson et al., 1994, 1995).

The evidence shows that, first, in correlations of the conodont and graptolite zonations, the same events affected both groups. Second, the threshold of precision for discovering events in shelly sequences has been reached. Third, improved correlations of limestone sequences have revealed effects in most groups of shelly fossils and have opened for examination the effects of the events on them. Fourth, study of these faunal events in marginal carbonate ramp settings with rapidly changing lithologies has revealed a correlated faunal and lithological pattern. This has permitted analysis of the oceanic and

atmospheric changes responsible for the cyclicity that caused the events. Fifth, knowledge of physical (i.e., chiefly lithological) changes permits identification of events that include only Lazarus gaps. Such events would otherwise not have been detected, because preceding and succeeding faunas are similar and thus do not reveal the intervening event. Only a directed search with the collection of large samples will reveal Lazarus gaps to be real and not due to inadequate sampling. The faunal effects, for example, of the Valleviken Event were discovered in this way; over thirty samples totaling more than 1,000 kg yielded about 20,000 conodont elements and revealed many faunal changes.

LIST OF KNOWN SILURIAN OCEANIC EVENTS

In the following list, data on known Silurian events are summarized. Future work will probably extend the list of affected taxa to include most major taxa.

The severity scale is based on the conodont response, especially those taxa which survived several events but which were confined to refugia during more severe parts of events. The scale compares each fauna during an event with the succession of faunas during the Ireviken Event (Figure 3), using presence/absence, frequency changes, and other characteristics (e.g., effects on coniform, ramiform, and platform genera as ecologic groups). For example, during the Ireviken Event, *Panderodus serratus* abundance increased strongly after Datum 2. It became the most common species of *Panderodus*, but disappeared with *P. recurvatus* at Datum 4 when *P. equicostatus* increased strongly and became dominant. The response of these and other taxa were similar enough during other events to give a consistent picture that permits calibration of the effects.

The beginnings and ends of episodes are points when the oceanic circulation pattern changed. Therefore they are identified as precisely as possible. It follows that no area has priority as a type area, but a reference area has been given for all named events. Future discoveries may show that the beginning and/or end points were somewhat earlier or later than now known (e.g., the beginning of the Mulde Event is assumed to be slightly older than when it was first named).

SANDVIKA PRIMO-SECUNDO EVENT

History.—Described by Aldridge et al. (1993).

Position.—In *Stimulograptus sedgwicki* Zone.

Precision.—No datum points yet described.

Severity.—Not identified, but important extinctions indicate that it was relatively severe.

Taxa affected.—Conodonts, graptolites, trilobites, brachiopods, acritarchs.

Reference area.—Oslo area, Norway.

Other areas.—Britain; Severnaya Zemlya; Anticosti Island, Quebec; Mackenzie Mountains, northwest Canada (Aldridge et al., 1993); China (Wang and Jeppsson, 1994).

"UTILIS SUBZONE" SECUNDO-PRIMO EVENT

History.—Described as graptolite extinction event by Loydell (1994) and discussed as oceanic event by Jeppsson (1996).

Position.—In *Stimulograptus utilis* Subzone.

Precision.—No details for the event; in shelly sequences the position of the event remains to be identified.

Severity.—Probably rather severe, based on effects on graptolites.

Affected taxa.—Major graptolite extinctions.

Areas.—Britain and Bohemia (based on Loydell, 1994).

IREVIKEN PRIMO-SECUNDO EVENT

History.—Noted on some range charts since 1964 (e.g., Walliser, 1964); mentioned as a worldwide crisis for conodonts by Aldridge and Jeppsson (1984) and as an oceanic event by Jeppsson (1990a, 1993, 1997) and Aldridge et al. (1993).

Position.—Spans the Llandovery-Wenlock boundary.

Precision.—Ten datum points (1, 2, 3, 3.3, 4, 5, 6, 6.2, 7, 8) identified in carbonate facies from Alaska to New South Wales. The datum points allow a Milankovitch-based time scale for the early and main part of the event (Jeppsson, 1997).

Severity.—The severity scale (1–6.2) is based on this event. For conodonts, the result was community collapse.

Taxa affected.—Conodonts (80% of species extinct or disappear), trilobites (locally over 50% at Datum 2), corals (Datum 4), brachiopods (Datum 4), ostracodes (Datum 4), graptolites, chitinozoans, polychaetes, acritarchs.

Reference area.—Gotland, Sweden. Lithologies below Datum 4 are interbedded fossiliferous marls and argillaceous limestones. Datum 4 is marked by a thin pyrite layer (less-prominent pyrite layers are found just below and above this one), which has

been traced for 35 km. Shortly afterwards, the large solitary coral *Phaulactis* covered the sea bottom for over 57 km (the extent of outcrops above modern sea-level). Strata between Datum 4 and the end of the event, the upper Visby beds, differ from lower Visby beds by presence of thicker layers of argillaceous limestone, thinner interbedded marls, and development of tabulate reefs. After the event, crinoid limestone formed along entire outcrop belt. The seaward expansion of crinoidal limestone facies took time to reach some areas. For example, dense sampling at Lickershamn 2 indicates that the lithological boundary may be 1.5–2 m above beds that mark the end of the event, whereas they may coincide at Vattenfallsprofilen 1.

Other areas.—The Ireviken Event can be identified wherever any of the three graptolite zones or the five conodont zones in Figure 3 are identified. Conodont markers of event known in Britain (Aldridge et al., 1993), Australia (Aldridge et al., 1993, based on Bischoff, 1986), Alaska (Aldridge et al., 1993, based on Savage, 1985), Estonia (Jeppsson and Männik, 1993), Poland (Männik and Malkowski, 1996), Illinois and Wisconsin (Kluessendorf and Mikulic, 1996), the middle Urals (Snigireva and Bikbaev, 1996), and Nevada (Berry, this volume).

BOGE PRIMO–SECUNDO EVENT

History.—Termed an event by Jeppsson (1993) and described by Jeppsson et al. (1995).

Position.—At or just below the top of the *Kockella patula* and *Cyrtograptus rigidus* Zones.

Precision.—*Kockella walliseri* became extinct perhaps 30 Ka after *Kockella patula* and provides a second datum point.

Severity.—Unknown, probably not too severe.

Affected taxa.—Conodonts.

Reference area.—Gotland, Sweden. Only studied at Slitebrottet 2, where argillaceous limestone alternates with marls before and early in the event. Clay content considerably decreased later in the event, and the frequency of discontinuity surfaces increases. This locality was distal to the area where purer carbonates formed during the succeeding secundo episode.

Other areas.—Perhaps in Britain (Jeppsson et al., (1995).

VALLEVIKEN PRIMO–SECUNDO EVENT

History.—Termed an event by Jeppsson (1993) and described in Jeppsson et al. (1995).

Position.—Probably spans bases of Homerian and *Cyrtograptus lundgreni* Zone. Spans base of *Ozarkodina sagitta sagitta* Zone.

Precision.—Details of possible biostratigraphic importance are described below from two best-studied sections.

Severity.—Probably not more than 2.

Known effects.—Frequency changes in conodonts, temporary absence of *Kockella ortus ortus* in later part of event. Appearance of *Ozarkodina sagitta sagitta*.

Reference area.—Gotland, Sweden. Studied at Slitebrottet 1 and 5 and Lännaberget 2. Lithologic sequence and changes are similar to those for the Ireviken Event on Gotland.

Other areas.—Britain (Jeppsson et al., 1995), Nevada (Berry, this volume).

MULDE SECUNDO–SECUNDO EVENT

History.—Long evident as a faunal change at the base of the Ludlow in graptolite facies (e.g., Elles, 1900; Wood, 1900) and as a graptolite extinction event (Jaeger, 1959, 1991; Koren', 1991; Urbanek, 1995). Described as an oceanic secundo–secundo event that affected most or all taxonomic groups (Jeppsson, 1993, 1996; Jeppsson et al., 1995).

Position.—Started ca. 30 Ka (to 100 Ka?) before end of *Cyrtograptus lundgreni* Chron, at or shortly after the end of the *Ozarkodina sagitta sagitta* Zone. Ended at the top (or base) of *Colonograptus? praedeubeli* Zone.

Precision.—Two datum points and a succeeding recovery phase with two or more graptolite zone boundaries (the number depends on the position of the end and whether or not the worst conditions resulted in a graptolite-free interval (Figure 5).

Severity.—Conodont fauna after Datum 2 indicates a severity of 6.2, at least some communities collapsed.

Taxa affected.—Extinctions and disappearances among graptolites, conodonts, chitinozoans, and shelly fossils at Datum 1. Extinctions among graptolites and changes in conodonts at Datum 2.

Reference area.—Gotland, Sweden. On west Gotland, the sequence changes from interbedded marls and argillaceous limestones before the event into mudstone (locally rich in graptolites), siltstone, oolite, and brick-clay with limestone intercalations during event. At end of event, interbedded marls and argillaceous limestones reappear (at Djupvik 1–4), which laterally grade into crinoid limestones (at Loggarve 2 and Hunninge 1).

Other areas.—In graptolite facies, this event is identifiable wherever the top *Cyrtograptus lundgreni* Zone or the

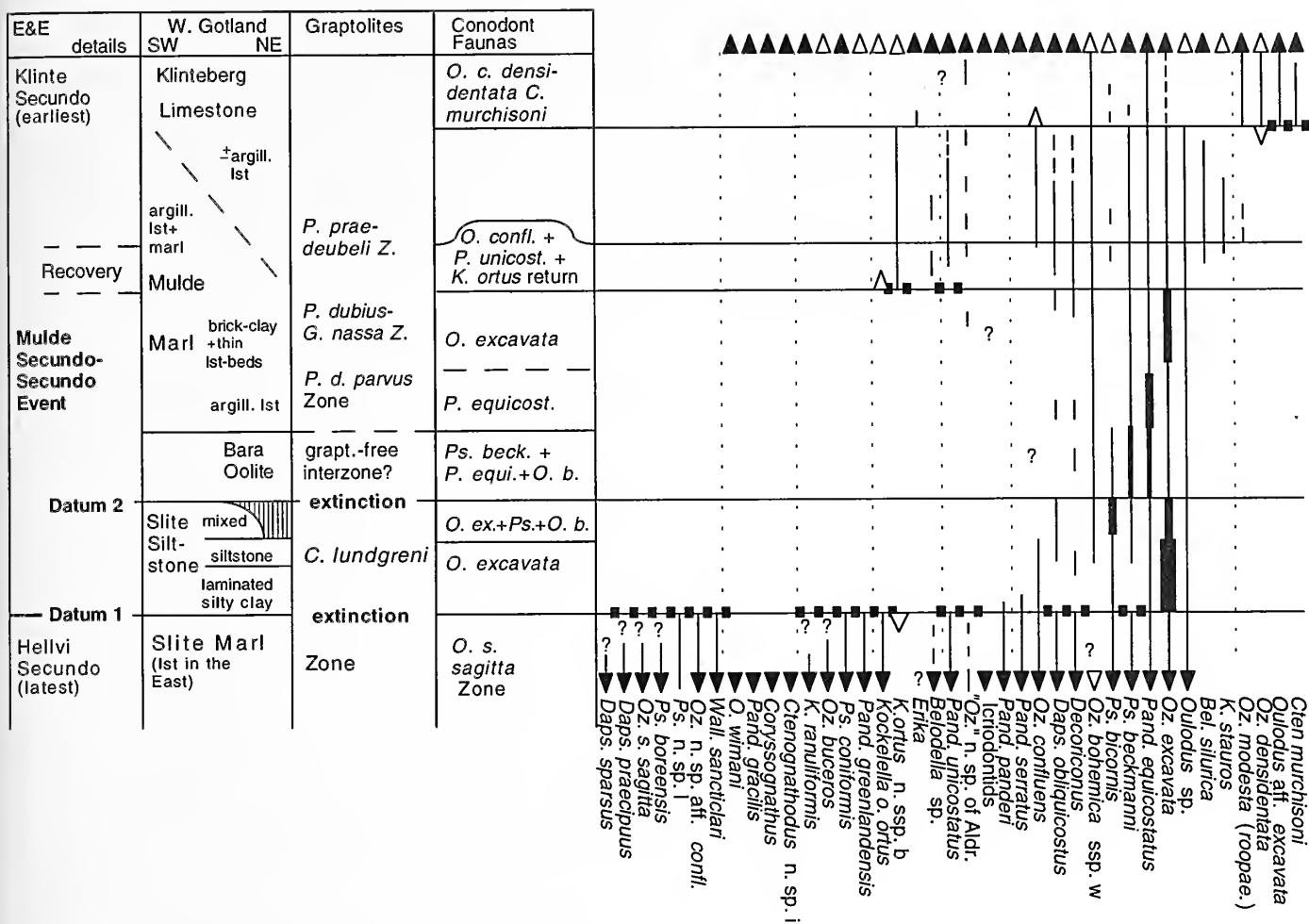


FIGURE 5—Mulde Secundo-Secundo Event. Lithologic changes of this event shown for west Gotland, where lithologies of the Slite Marl, the upper Mulde, and the Klinteberg Limestone represent the characteristic sedimentary rocks for this area during Wenlock-Ludlow. Conodont ranges chiefly based on Gotland record, where they can be tied to the graptolite zonation (Jaeger, 1991, based on data in Hede [1942] and Jaeger [1981]). The author's graptolites were identified by H. Jaeger. Uncertainty involves the *P. equicostatus*-dominated fauna, which may be older than the Bara Oolite or may occur below and above the oolite. The second- to sixth-oldest conodont faunas are indicated with the name(s) of the dominant taxon or taxa.

Pristiograptus dubius parvus, *Gothograptus nassa*-*Pristiograptus dubius*, or *Colonograptus? prae-deubeli* Zones are present (for areas and references, Koren', 1984, 1991, and Jaeger, 1991). In shelly facies, it is known in Bohemia, Britain (Jeppsson et al., 1995), and Nevada (Berry, 1996, this volume).

LINDE PRIMO-SECUNDO EVENT

History.—Termed an event by Jeppsson (1983). Correlations indicate the Linde Event caused the graptolite extinctions termed the "C₂" or the "*Saetograptus leintwardinensis* Event" by Urbanek (1993); for conflicting evidence see Lau Event, below.

Position.—High in *Ancoradella ploekensis* Zone sensu

Walliser (1964), spans the top of the faunal interval with *Kockelella variabilis variabilis* and *Ozarkodina excavata* n. ssp A.

Precision.—No details yet.

Maximum severity.—At least 3.

Affected taxa.—Conodonts, graptolites.

Reference area.—Gotland, Sweden. In Linde area, lithological changes feature interbedded marls and argillaceous limestones before and early in the event, and limestones late and after the event.

LAU PRIMO-SECUNDO EVENT

History.—Termed an event by Jeppsson (1990a, 1993), but evident in older range charts (e.g., Walliser, 1964).

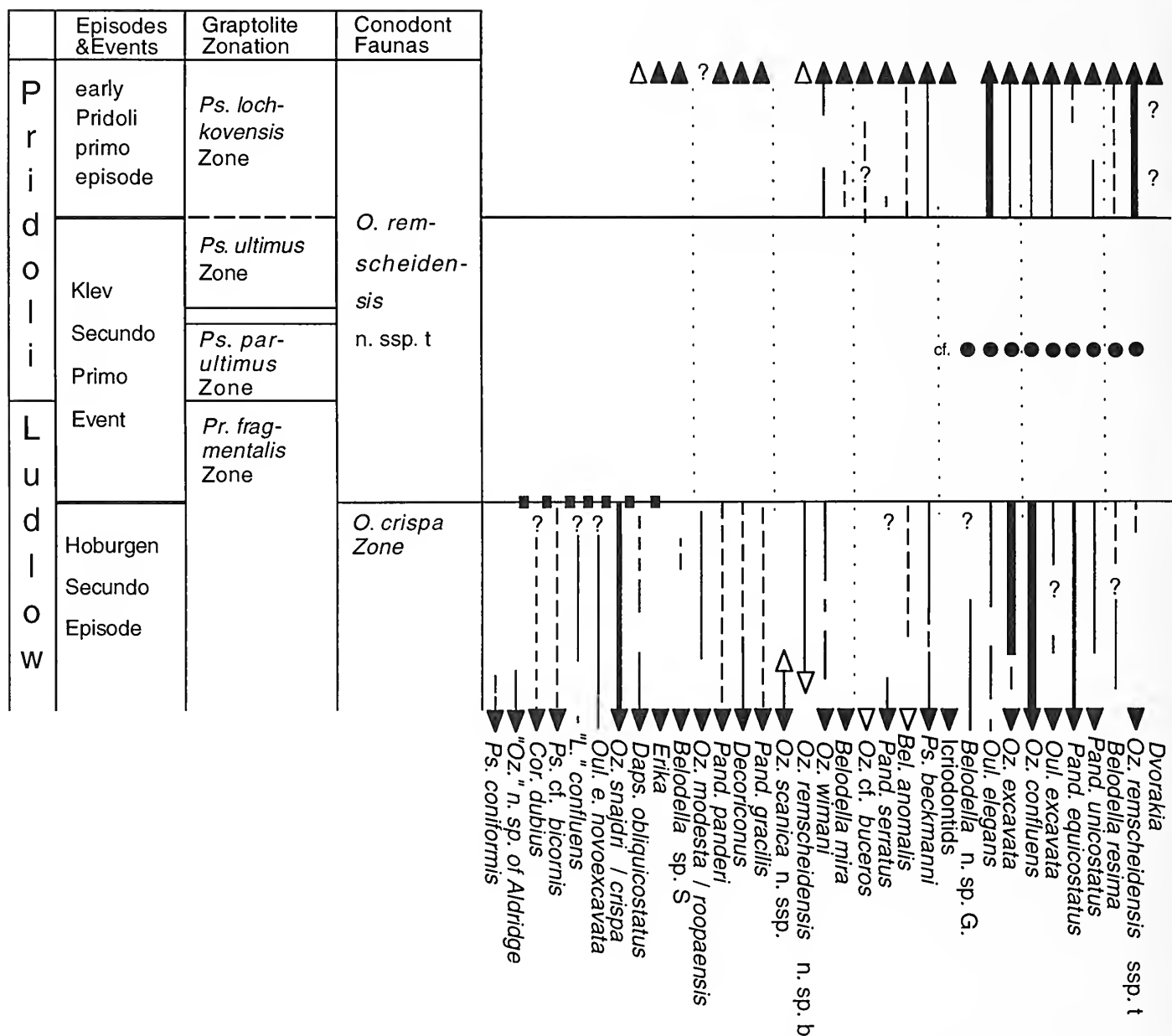


FIGURE 6—Klev Secundo-Primo Event. Correlation of graptolite and conodont sequences based on H. Jaeger and H.P. Schönlaub's data in Kříž et al. (1986). Details on order of changes during event unknown, but conodonts present before or during the event are marked. Figure mostly based on Gotland collections. Records after the event are based on restudy of published collections (e.g., H.P. Schönlaub in Kříž et al., 1986; Brazauskas, 1989) and author's collections.

Some range data (conodonts, graptolites, chitinozoans and ostracodes) indicate Lau Event caused graptolite extinctions termed the "C₂" event by Urbanek (1993). Other data point to the "C₃" or "Neocucullograptus kozlowskii Event" of Urbanek (1995). The conflicting interpretations may be due to problems in graptolite identifications.

Position.—Spans end of *Polygnathoides siluricus* Zone.

Precision.—Ranges now known (Figure 5) indicate ca. five datum points. Additional ones may be distinguished.

Severity.—Successive conodont faunas may have resulted from datum points with severities of about 1, 2, 4, and 6.2. The maximum severities of the Lau, Ireviken, and Mulde Events were comparable.

Affected taxa.—Conodonts, graptolites, chitinozoans, some fish, brachiopods.

Reference area.—Gotland, Sweden. At all sections across the island from Bodudd 1 to Botvide 1, the lithologies change from interbedded marls and argillaceous limestones before and early in the event,

through a thin, more resistant "flagstone" unit, into an oncolitic unit. Overlying sandstones and oolites appear after the event before marls and argillaceous limestones reappear.

Other areas.—The Lau Event is identifiable everywhere the extinction of *Polygnathoides siluricus* is recorded. For example, Austria (Walliser, 1964) and the middle Urals (Snigireva and Bikbaev, 1996).

KLEV SECUNDO-PRIMO EVENT

History.—Graptolite extinctions were described by Urbanek (1995). The "*Monograptus spineus* Event" of Urbanek (1993) was partly included in his "*C₃*" or "*Neocucullograptus kozlowski* Event". This event is described herein as an oceanic event. (Figure 6).

Position.—Straddles Ludlow-Pridoli boundary; started at (or possibly before) the extinction of the conodont *Ozarkodina crista* and probably ended at the appearance of the graptolite *Pseudomonoclimacis lochkovenssis*, eponymous species of the *P. lochkovenssis* Zone.

Precision.—Given the probable duration, there are two graptolite zone boundaries (base and top of the *Pseudomonoclimacis parultimus* Zone) during the event, as well as those at the beginning and end.

Severity.—Unknown, but may have been comparatively severe.

Affected taxa.—Conodonts, graptolites, chitinozoans.

Reference area.—Named for an area on Gotland where the richest pre-event conodont faunas are known, but a better reference area should probably be found.

Other areas.—Identifiable where the extinction of *Ozarkodina crista* or the presence of *Pseudomonoclimacis parultimus* has been recorded (Lithuania, based on data in Brazauskas [1989], and Czech Republic, based on data in Kříž et al. [1986]).

KLONK SECUNDO-UNNAMED EVENT

History.—Data available in Jaeger (1978) and Koren' (1979). The "*C₄*" or "*Pseudoneocolonograptus transgrediens* Event" of Urbanek (1995) involved graptolites. Attributed herein to an oceanic event. Work on the base of the Devonian generated many papers (e.g., Chlupáč et al., 1972), whose data can be reinterpreted by the oceanic model.

Position.—Spans end of the Silurian. Started at or possibly before the extinction of "*Pseudoneocolonograptus*" *transgrediens*, at or near the replacement of *Oulodus elegans elegans* by *O. elegans detorta*.

Precision.—No resolution yet possible in the Silurian part of the event.

Severity.—Record of graptoloids disappears temporarily during the early part of the event. Dominance of the conodont *Ozarkodina excavata* just before the end of the Silurian at Klonk (Jeppsson, 1988b) may be compared with its dominance in the first Devonian fauna and in the last one before recovery during the severe Mulde Event.

Affected taxa.—Graptolites, conodonts, chitinozoans, trilobites, ostracodes, cephalopods, bivalves, brachiopods.

Reference area.—Not yet selected, but Bohemia is the best-known area (data in Jeppsson, 1988b).

Other areas.—Oklahoma, based on data in Barrick and Klapper (1992).

IDENTIFICATION OF OCEANIC EVENTS

In order to identify and study aspects of oceanic extinction events and their datum points, two concerns must be addressed: 1) the precision of the local range terminations of taxa; and 2) the requirements of what we want to study. These two concerns are discussed below.

RELIABILITY OF RANGE ENDS.—Once problems in identification, contamination, and redeposition are ruled out, a single identified specimen establishes the presence of a taxon. Hence survival beyond an event or a datum point can easily be proven with small collections, if correlations are reliable. The probability that the next event caused the extinction can then be analyzed further.

Identification of a range end (FAD or LAD) or a range gap (Lazarus gap) requires much more work, because we need to establish not only species' presence but also distinguish species' absence from non-representation in an inadequate collection. It has too often been said that we can never find the last specimen of a taxon. Although this may theoretically be true, it is irrelevant and wrong when allowed to curtail a scientific quest or discussion. In the study of range ends, the relevant questions are those pertinent to analysis of data (e.g., questions on confidence intervals need to be addressed; see review by Sepkoski and Koch [1995] and Marshall [1995] for an example of the technique). With such knowledge, we can identify a range end with the precision and reliability required. Several samples from both sides of the range end must be analyzed. With closely spaced samples and sample sizes adjusted to yield adequate collections, the levels of the lowest and highest specimens can be determined with precision, if reworking is accounted for. My experience has been that a few adequate collections are better than many inadequate collections, because of the

increase in the number of specimens per man-hour (see Jeppsson, 1987a).

In my work with the Ireviken Event at Luskint 1, the emphasis was on obtaining high-quality data that reduced statistical uncertainty as much as possible. Thus, sampling was continuous near the datum planes, and sample size was calculated to yield at least five specimens of the rarest taxon in every collection. In this way, most taxa were represented by many more specimens in every sample from its FAD to its LAD, and many Lazarus gaps were documented. Separation of reworked specimens was based on the following combination of factors: presence of an atypical mixture of growth stages, atypical frequencies of the different elements of an apparatus, and elements of a color not comparable to others in that sample. Reworked specimens can be markedly darker or stained and worn (compare Kleffner, 1987). Furthermore, only rare mature specimens or fragments of the most robust elements from those taxa with the most massive elements are found among the reworked elements. In most cases, reworking was noted in only one or two samples at Luskint 1. The only exception was one fragment of the very robust platform element of *Pterospiriferus amorphognathoides* in the third sample, which occurred 10–14 cm above a sample with the latest unworked specimens. The lithologies at Luskint are highly argillaceous limestones and limestone nodules interbedded with soft marl, which facilitates such close sampling.

After the range ends are established at a locality, the next step is to evaluate how wide an area such a record represents. A benthic taxon may be more or less facies-restricted, and any difference in lithofacies at the level of a range end must be contrasted with the known habitat tolerance of that taxon. High-resolution correlations based on conodont or graptolite zonations can then be used to establish whether or not the local and regional FADs and LADs are coeval (within the precision limits set by the sampling).

NECESSARY PRECISION.—The precision needed in future work depends on the problems examined. Some examples are given below that cover the more frequent effects of oceanic changes.

Oceanic cyclicity was a global phenomenon. Accordingly, once the oceanic sequence is established and the points of change or datum points are dated by existing zonations, then identification of this sequence of episodes and events in a local stratigraphic column is a matter of ordinary correlation. The precision required is limited by the fact that some episodes are as short as 1 Ma. Recognition of the position of known events requires identification of the extinction horizon of one or several taxa. Recognition of a sequence of datum planes spaced a

few Ka to ca. 30 Ka apart requires a corresponding precision to identify the end-points of ranges.

Studies of oceanic effects on other biotic groups requires high precision in determination of range ends. If such work is undertaken in an area where the oceanic record has not been identified, the record must be established or the local effects on the studied taxon need to be correlated into an area where the oceanic sequence is known.

Establishing, correcting, and adding to the known sequence of oceanic episodes and events require high precision in correlation. Adding unknown effects of the oceanic cyclicity (e.g., whether crinoid limestone form preferentially at the beginning of a secundo episode) can be done either theoretically or empirically. Any theoretical result, however, needs to be tested. Furthermore, any empirical result needs to be extended to other areas, epochs, and facies. In such tests, precision needs to be high.

OTHER POSSIBLE EPISODES AND EVENTS

During the 1990s, the main features of the Silurian sequence of oceanic episodes and events were proposed (Jeppsson, 1990a, 1993, 1996, 1997; Aldridge et al., 1993; Jeppsson et al., 1995). In addition, extinction events described in other ways (Jaeger, 1959, 1991; Koren', 1991; Urbanek, 1993, 1995; Loydell, 1994) have been included in this sequence.

There are probably more Silurian episodes and events to be found. For example, there are intervals where the record is not well studied (e.g., middle Sheinwoodian and middle Pridoli). Furthermore, some of the longest intervals now interpreted as a single episode may include more than one episode. What is now interpreted as a long primo episode may be two strong primo episodes separated by a primo–primo event or even by a weak primo–secundo event and a weak, brief secundo episode. For example, distinct faunal changes during the Snipklint and Sproge Primo Episodes may have such a cause. Four cycles of transgressions and regressions have been identified during the Llandovery (Johnson, 1996), but only two oceanic cycles are known from that interval. We may expect that the Llandovery oceanic record was more complicated than now known.

Erosion tends to create good exposures where secundo episode limestones cap primo–secundo event marls. As a result, a distinct, protracted event at the change from primo to secundo conditions can often be established by samples large enough to yield adequate collections. In contrast, the change from secundo to primo conditions is more difficult to study for two reasons. First, the drop in sea-level at the onset of a primo

episode with thermal contraction of deep oceanic water, sometimes augmented by glaciation, will lead to erosion of the sediments from earlier events and a resultant seaward translation of the facies belt where oceanic influence was strongest. Second, more argillaceous and easily eroded strata that overlie resistant limestones are unlikely to form a good outcrop. As a result, good sections are infrequent. Our knowledge of secundo-primo episode changes (secundo-primo event or single datum?) was developed from many localities. The relative precision in the correlation of two succeeding samples between localities is thus less than ± 1 m, and an interval of several meters may easily be missed. Because of this, several secundo-primo events may remain to be discovered in the Silurian. One example where a detailed study may give such a result is the contact between the Klinte Secundo and the Sproge Primo Episode.

The total number of Silurian episodes and events may thus be over thirty-five. As shown in Figures 1 and 2, twenty-four are so well known that they have been named (Aldridge et al., 1993; Jeppsson et al., 1995); six more are indicated, and an additional three have been discussed (Jeppsson et al., 1995). A few of the latter ones will probably soon be so well known that they can be named. Wider interest in intervals of change and high-resolution identification of range ends will lead to rapidly increasing knowledge about known events and identification of as-yet undetected ones. Studies of Silurian sequences may therefore continue to yield results of general importance for study of the Phanerozoic. Oceanic events affected lithologies, stable isotopes, and most or all major taxonomic groups. Data from all specialists are thus important for future work both with known and unknown events.

ACKNOWLEDGMENTS

The range charts benefited from comparisons of my collections with those of my colleagues. A.-S. Jeppsson typed the manuscript. A. Jeppsson completed the drawings. Early drafts of the manuscript were reviewed by W.B.M. Berry, J. Kluessendorf, and an anonymous reviewer. The manuscript was written during the tenure of a grant from the Swedish Research Council.

REFERENCES

ALDRIDGE, R.J. In press. Wenlock-Pridoli conodont associations. In A.J. Boucot and J.D. Lawson (eds.), *Paleocommunities—A Case Study from the Silurian and Lower Devonian*. Project Ecostratigraphy Final Report. Cambridge University Press.

———, AND L. JEPSSON. 1984. Ecological specialists among Silurian conodonts, p. 141–149. In M.G. Bassett and J.D. Lawson (eds.), *Autecology of Silurian Organisms*. Palaeontological Association, Special Papers in Palaeontology, 32.

———, ———, AND K.J. DORNING. 1993. Early Silurian oceanic episodes and events. *Journal of the Geological Society of London*, 150:501–513.

ARMSTRONG, H.A. 1995. High-resolution biostratigraphy (conodonts and graptolites) of the Upper Ordovician and Lower Silurian—evaluation of the Late Ordovician mass extinction. *Modern Geology*, 20:41–68.

———. 1996. Biotic recovery after mass extinction: the role of climate and ocean-state in the post-glacial (Late Ordovician–Early Silurian) recovery of the conodonts, p. 105–117. In M.B. Hart (ed.), *Biotic Recovery from Mass Extinction Events*. Geological Society of London, Special Publication 102.

BARRICK, J.E., AND G. KLAPPER. 1992. Late Silurian–Early Devonian conodonts from the Hunton Group (upper Henryhouse, Haragan, and Bois d'Arc Formations), south-central Oklahoma. *Oklahoma Geological Survey Bulletin*, 145:19–65.

BERGER, A., M.F. LOUTRE, AND V. DEHANT. 1989. Influence of the changing lunar orbit on the astronomical frequencies of Pre-Quaternary insolation patterns. *Paleo-oceanography*, 4:555–564.

BERRY, W.B.N. 1996. Graptolite recovery after the mid-Wenlock Lundgreni Event: links to nutrient availability and paleo-oceanography, p. 32. In J.E. Repetski (ed.), *Sixth North American Paleontological Convention, Abstracts of Papers*. Paleontological Society, Special Publication 8.

BISCHOFF, G.C.O. 1986. Early and Middle Silurian conodonts from midwestern New South Wales. *Courier Forschungsinstitut Senckenberg*, 89:1–337.

BOUCOT, A.J. 1991. Developments in Silurian studies since 1839, p. 91–107. In M.G. Bassett, P.D. Lane and D. Edwards (eds.), *The Murchison Symposium. Proceedings of an International Conference on the Silurian System*. Special Papers in Palaeontology, 44.

BRALOWIER, T.J., AND H.R. THIERSTEIN. 1984. Low productivity and slow deep-water circulation in mid-Cretaceous oceans. *Geology*, 12:614–618.

BRASIER, M.D. 1992. Nutrient-enriched waters and the early skeletal fossil record. *Journal of the Geological Society of London*, 149:621–629.

———. 1995a. Fossil indicators of nutrient levels. 1: Eutrophication and climate change, p. 113–132. In D.W.J. Bosence and P.A. Allison (eds.), *Marine Palaeoenvironmental Analysis from Fossils*. Geological Society, Special Publications, 83.

———. 1995b. Fossil indicators of nutrient levels. 2: Evolution and extinction in relation to oligotrophy, p. 133–150. In D.W.J. Bosence and P.A. Allison (eds.), *Marine Palaeoenvironmental Analysis from Fossils*. Geological Society, Special Publications, 83.

BRAZAUSKAS, A. 1989. About the Ludlovian and Pridolian boundary according to conodonts in Lithuanian sections. *Nauchnye Trudi Vysshchikh Zavadenit Litovskoj SSR Geologiju*, 10:72–78 (In Russian).

BRENCHLEY, P.J., G.A.F. CARDEN, AND J.D. MARSHALL. 1995. Environmental changes associated with the “first strike” of the Late Ordovician mass extinction. *Modern Geology*, 20:69–82.

———, J.D. MARSHALL, G.A.F. CARDEN, D.B.R. ROBERTSON, D.G.F. LONG, T. MEIDLA, L. HINTS, AND T.F. ANDERSON. 1994. Bathymetric and isotopic evidence for a short-lived late Ordovician glaciation in a greenhouse period. *Geology*, 22:295–298.

BRUNTON, F.R., AND P. COPPER. 1994. Paleocologic, temporal, and spatial analysis of Early Silurian reefs of the Chicotte Formation, Anticosti Island, Quebec, Canada. *Facies*, 31:57–80.

- , ———, AND O.A. DIXON. In press. Silurian reef building episodes. Eighth International Coral Reef Symposium, Panama City, Panama.
- CHLUPAC, I., H. JAEGER, AND J. ZIKMUNDOVA. 1972. The Silurian-Devonian boundary in the Barrandian. *Bulletin of Canadian Petroleum Geology*, 20:104-174.
- CORFIELD, R.M., AND D.J. SIVETER. 1992. Carbon isotope change as an indicator of biomass flux and an aid to correlation during *ludensis-nilssoni* (Silurian) time. *Proceedings of the Estonian Academy of Sciences*, 41:173-181.
- , D.J. SIVETER, J.E. CARTLIDGE, AND W.S. MCKERROW. 1992. Carbon isotope excursion near the Wenlock-Ludlow (Silurian) boundary in the Anglo-Welsh area. *Geology*, 20:371-374.
- CORRADINI, C., R. OLIVIERI, AND E. SERPAGLI. 1995. Possible relationships between anomalous conodonts and Silurian oceanic episodes. *Neues Jahrbuch für Geologie und Paläontologie, Monatshefte* 1995 (12):737-746.
- ELLES, G. 1900. The zonal classification of the Wenlock shales of the Welsh Borderland. *Quarterly Journal of the Geological Society of London*, 56:370-414.
- ERIKSSON, K., AND S.E. HAGENFELDT. 1997. Acritarch assemblages from the Lower Silurian (Llandovery-Wenlock) in the Grötling-boborningen 1 core, Gotland, Sweden. *Geologiska Foreningens i Stockholm Forhandlingar*, 119:13-16.
- FREDHOLM, D. 1989. Silurian vertebrates of Gotland, Sweden. *Lund Publications in Geology*, 76:1-47.
- GARCIA-LOPEZ, S., R. RODRIGUEZ-CANERO, J. SANZ-LOPEZ, G.N. SARMIENTO, AND J.J. VALENZUELA-RIOS. 1994. Conodonts siluricos de Europa meridional y Africa septentrional, p. 84-88. In *Comunicaciones de las X Jornadas de Paleontología*, Madrid.
- HALLOCK, P. 1988. The role of nutrient availability in bioerosion: consequences to carbonate buildings. *Palaeogeography, Palaeoclimatology, Palaeoecology*, 63:275-291.
- HEDE, J.E. 1942. On the correlation of the Silurian of Gotland, p. 205-229. In *Lunds Geologiska Fältklubb, 1892-1942* (also in *Meddelanden från Lunds Geologisk-Mineralogiska Institution*, 101).
- JAEGER, H. 1959. Graptolithen und Stratigraphie des jüngsten Thüringer Silurs. *Abhandlungen der deutschen Akademie der Wissenschaften zu Berlin Klasse für Chemie, Geologie und Biologie*, 2:227.
- . 1978. Late graptoloid faunas and the problem of graptoloid extinction. *Acta Palaeontologica Polonica*, 23:497-521.
- . 1981. Comments on the graptolite chronology of Gotland, p. 22. In S. Laufeld (ed.), *Proceedings of Project Ecostratigraphy Plenary Meeting, Gotland, 1981*. Sveriges Geologiska Undersökning. Rapport och Meddelanden, 25.
- . 1991. Neue Standard-Graptolithen Zonenfolge nach der "Grossen Krise" an der Wenlock/Ludlow-Grenze [sic, e-dash, not virgule] (Silur). *Neues Jahrbuch für Geologie und Paläontologie. Abhandlung*, 182:303-354.
- JEPPSSON, L. 1975. Autecology of selected Silurian conodonts. *Geological Society of America, Abstracts with Programs*, 7:791, 792.
- . 1976. Autecology of Late Silurian conodonts, p. 105-118. In C.R. Barnes (ed.), *Conodont Paleocology*. Geological Association of Canada, Special Paper 15.
- . 1983. Facies dependence and guest stars in Silurian conodonts from Gotland. *Geological Society of America, Abstracts with Programs*, 15:220.
- . 1984. Sudden appearances of Silurian conodont lineages—provincialism or special biofacies?, p. 103-112. In D.L. Clark (ed.), *Conodont Biofacies and Provincialism*. Geological Society of America, Special Paper 196.
- . 1985. Greenhouse conditions and conodont distribution, p. 14. In R.J. Aldridge, R.L. Austin and M.P. Smith (eds), *Fourth European Conodont Symposium (ECOS IV)*, Abstracts.
- . 1987a. Some thoughts about future improvements in conodont extraction methods, p. 45-53. In R.L. Austin (ed.), *Conodonts: Investigative Techniques and Applications*. Ellis Horwood Ltd., Chichester.
- . 1987b. Lithological and conodont distributional evidence for episodes of anomalous oceanic conditions during the Silurian, p. 129-145. In R.J. Aldridge (ed.), *Palaeobiology of Conodonts*. Ellis Horwood Ltd., Chichester.
- . 1988a. Towards an oceanic model for Silurian lithologic and faunistic changes. *Courier Forschungsinstitut Senckenberg*, 102:242.
- . 1988b. Conodont biostratigraphy of the Silurian-Devonian boundary stratotype at Klonk, Czechoslovakia. *Geologica et Palaeontologica*, 22:21-31.
- . 1989. Correlated cyclicity in faunas and lithologies—a causal connection, p. 14. In F. Jerre (ed.), *Lundadagarna*, Abstracts. Lund Publications in Geology, 74.
- . 1990a. An oceanic model for lithological and faunal changes tested on the Silurian record. *Journal of the Geological Society, London* 147:663-674.
- . 1990b. A climatic and oceanic model for events, p. 91. In *Global Biological Events, Precambrian-Cambrian Event Stratigraphy*, 25-27 September, 1990. Oxford University.
- . 1993. Silurian events: the theory and the conodonts. *Proceedings of the Estonian Academy of Sciences*, 42:23-27.
- . 1994. A new standard Wenlock conodont zonation, p. 133. In H.P. Schönlaub and L.H. Kreutzer (eds.), *IUGS Subcommittee on Silurian Stratigraphy—Field Meeting Eastern + Southern Alps, Austria. Berichte Geologische Bundes-Anstalt* 30/1994.
- . 1996. Recognition of a probable secundo-primo event in the Early Silurian. *Lethaia* 29:311-315.
- . 1997. The anatomy of the mid-Early Silurian Ireviken Event, p. 451-492. In C.E. Brett and G. Baird (eds.), *Paleontological Event Horizons—Ecological and Evolutionary Implications*. Columbia University Press.
- . In press. A new early and middle Wenlock standard conodont zonation. *Transactions of the Royal Society of Edinburgh*.
- , AND P. MÄNNIK. 1993. High resolution correlations between Gotland and Estonia near the base of the Wenlock. *Terra Nova*, 5:348-358.
- , V. VIIRA, AND P. MÄNNIK. 1994. Silurian conodont-based correlations between Gotland (Sweden) and Saaremaa (Estonia). *Geological Magazine*, 131:201-218.
- , R.J. ALDRIDGE, AND K.J. DORNING. 1995. Wenlock (Silurian) oceanic episodes and events. *Journal of the Geological Society of London*, 152:487-498.
- JOHNSON, M.E. 1996. Stable cratonic sequences and a standard for Silurian eustasy, p. 203-211. In B.J. Witzke, G.A. Ludvigsson, and J.E. Day (eds.), *Paleozoic Sequence Stratigraphy: Views from the North American Craton*. Geological Society of America, Special Paper 30.
- KALJO, D., A.J. BOUCOT, R.M. CORFIELD, A. Le HÉRISSE, T.N. KOREN', J. KRÍŽ, P. MÄNNIK, T. MÄRSS, V. NESTOR, R.H. SAVER, D. SIVETER, AND V. VIIRA. 1995. Silurian bioevents, p. 173-224. In O.H. Walliser (ed.), *Global Events and Event Stratigraphy in the Phanerozoic: Results of International Interdisciplinary Cooperation in the IGCP Project 216 "Global Biological Events in Earth History"*.
- KERSHAW, S. 1993. Sedimentation control on growth of stromatoporoid reefs in the Silurian of Gotland, Sweden. *Journal of the Geological Society, London*, 150:197-205.

- , AND M. KEELING. 1994. Factors controlling the growth of stromatoporoid biostromes in the Ludlow of Gotland, Sweden. *Sedimentary Geology*, 89:325–335.
- KLEFFNER, M.A. 1987. Conodonts of the Estill Shale and Bisher Formation (Silurian, southern Ohio): biostratigraphy and distribution. *Ohio Journal of Science*, 87:78–89.
- , R. D. NORBY, J. KLUESSENDORF, AND D.G. MIKULIC. 1995. Conodont distribution and preliminary conodont chronostratigraphy of Lower Silurian strata in southeastern Wisconsin. *Geological Society of America, Abstracts with Programs*, 27(5):25.
- KLUESSENDORF, J., AND D.G. MIKULIC. 1996. An Early Silurian sequence boundary in Illinois and Wisconsin, p. 177–185. *In* B.J. Witzke, G.A. Ludvigsson, and J.E. Day (eds.), *Paleozoic Sequence Stratigraphy: Views from the North American Craton*. Geological Society of America, Special Paper 306.
- KOREN', T.N. 1979. Late monograptid faunas and the problem of graptolite extinction. *Acta Palaeontologica Polonica*, 24:78–106.
- . 1991. The Lundgreni extinction event in central Asia and its bearing on graptolite biochronology within the Homerian. *Proceedings of the Estonian Academy of Sciences (Eesti Teaduste Akadeemia Toimetised)*, 40:74–78.
- . 1984. Graptolite zones and standard stratigraphic scale of Silurian, p. 46, 47. *In* *Proceedings of the 27th International Geological Congress, Moscow, 4–14 August, 1984*. VNU Science Press, Utrecht.
- , A.C. LENZ, D.K. LOYDELL, M.J. MELCHIN, P. ŠTORCH, AND L. TELLER. 1996. Generalized graptolite zonal sequence defining Silurian time intervals for global paleogeographic studies. *Lethaia*, 29:59–60.
- KŘÍŽ, J., H. JAEGER, F. PARIS, AND H.P. SCHÖNLAUB. 1986. Pridoli—the fourth subdivision of the Silurian. *Jahrbuch Geologische Bundesanstalt*, 129:291–360.
- LAUFELD, S. 1974. Reference Localities for Palaeontology and Geology in the Silurian of Gotland. *Sveriges Geologiska Undersökning C*, No. 705.
- Le HÉRISSÉ, A., AND R. GOURVENNEC. 1995. Biogeography of upper Llandovery and Wenlock acritarchs. *Review of Palaeobotany and Palynology*, 86:111–133.
- LOYDELL, D.K. 1994. Early Telychian changes in graptoloid diversity and sea level changes. *Geological Journal*, 29:355–368.
- MACDONALD, I. R. 1997. Bottom line for hydrocarbons. *Nature*, 385:389, 390.
- MÄNNIK, P., AND K. MALKOWSKI. 1996. Silurian conodonts from the Goldap core, Poland, p. 36. *In* *Sixth European Conodont Symposium (ECOS VI) Abstracts*. Institut Paleobiologii PAN, Warsaw.
- MARSHALL, C.R. 1995. Distinguishing between sudden and gradual extinctions in the fossil record: predicting the position of the Cretaceous–Tertiary iridium anomaly using the ammonite fossil record on Seymour Island, Antarctica. *Geology*, 23:731–734.
- MELCHIN, M.J. 1994. Graptolite extinction at the Llandovery–Wenlock boundary. *Lethaia*, 17:285–290.
- NESTOR, V. 1996. Wenlock oceanic episodes and events in the succession of chitinozoans in Estonia, p. 45, 46. *In* T. Meidla, J. Puura, J. Nemliher, A. Raukas and L. Saarse (eds.), *The Third Baltic Stratigraphical Conference. Abstracts Field Guide*. Tartu.
- RADCLIFFE, G. 1996. Silurian oceanic episodes and events in the Iapetus Ocean, p. 81. *In* *The James Hall Symposium: Second International Symposium on the Silurian System. Program and Abstracts*. University of Rochester.
- RAMSKÖLD, L. 1985. Studies on Silurian trilobites from Gotland, Sweden. Unpublished Ph.D. dissertation, University of Stockholm.
- SAMTLEBEN, C., A. MUNNECKE, T. BICKERT, AND J. PÄTZOLD. 1996. The Silurian of Gotland (Sweden): facies interpretation based on stable isotopes in brachiopod shells. *Geologische Rundschau*, 85:278–292.
- SAVAGE, N.M. 1985. Silurian (Llandovery–Wenlock) conodonts from the base of the Heceta Limestone, southeastern Alaska. *Canadian Journal of Earth Sciences*, 22:711–727.
- SEPKOSKI, J.J., JR., AND C.F. KOCH. 1995. Evaluating paleontologic data relating to bio-events, p. 21–34. *In* O.H. Walliser (ed.), *Global Events and Event Stratigraphy*. Elsevier, New York.
- SNIGIREVA, M.P., AND A.Z. BIKBAEV. 1996. Analogues of Ireviken and Lau Events in the western slope of the middle Urals, p. 55. *In* *Sixth European Conodont Symposium (ECOS VI), Abstracts*. Institut Paleobiologii PAN, Warsaw.
- ŠTORCH, P. 1995. Biotic crises and post-crisis recoveries recorded by Silurian planktonic graptolite faunas of the Barrandian area (Czech Republic). *Geolines*, 3:59–70.
- SUTHERLAND, S.J. 1994. Ludlow Chitinozoans from the Type Area and Adjacent Regions. *Palaeontographical Society Monograph*, 148.
- TALENT, J.A., R. MAWSON, A.S. ANDREW, P.J. HAMILTON, AND D.J. WHITFORD. 1993. Middle Palaeozoic extinction events: faunal and isotopic data. *Palaeogeography, Palaeoclimatology, Palaeoecology*, 104:139–152.
- TAPPAN, H. 1986. Phytoplankton: below the salt at the global table. *Journal of Paleontology*, 60:545–554.
- URBANEK, A. 1966. On the morphology and evolution of the *Cucullograptinae* (Monograptidae, Graptolithina). *Acta Palaeontologica Polonica*, 2:291–547.
- . 1970. *Neocucullograptinae* n. subfam. (Graptolithina)—their [sic, its] evolutionary and stratigraphic bearing. *Acta Palaeontologica Polonica*, 15:163–393.
- . 1993. Biotic crisis in the history of Upper Silurian graptoloids: a palaeobiological model. *Historical Biology*, 7:29–50.
- . 1995. Phyletic evolution of the latest Ludlow spinose monograptids. *Acta Palaeontologica Polonica*, 40:1–17.
- WALLISER, O.H. 1964. Conodonten des Silurs. *Abhandlungen des Hessischen Landesamtes für Bodenforschung zu Wiesbaden*, No. 41.
- WANG C.-Y., AND L. JEPSSON. 1994. Jeppsson's ocean model and its application to Early Silurian (Llandovery) of South China Platform. *Acta Micropalaeontologia Sinica*, 11:71–85.
- WENZEL, B., AND M.M. JOACHIMSKI. 1996. Carbon and oxygen isotopic composition of Silurian brachiopods (Gotland/Sweden [sic, en-dash, not virgule]); palaeoceanographic implications. *Palaeogeography, Palaeoclimatology, Palaeoecology*, 122:143–166.
- WOOD, E.M.R. 1900. The lower Ludlow Formation and its graptolite fauna. *Quarterly Journal of the Geological Society of London*, 56:415–492.
- WORTHINGTON, L.V. 1968. Genesis and evolution of water masses. *Meteorological Monographs*, 5:63–67.

SILURIAN OCEANIC EPISODES: THE EVIDENCE FROM CENTRAL NEVADA

WILLIAM B.N. BERRY

Department of Geology and Geophysics, University of California, Berkeley, CA 94720

ABSTRACT—Marked changes in conodont and graptolite faunas and in the lithology of British and Scandinavian Silurian successions have been related to major changes in sites of origination of deep-ocean water. Central Nevada Silurian (principally late Llandovery–early Ludlow) graptolite faunas were re-examined to see if the oceanic events recognized in Britain and Scandinavia had an impact on graptolites in central Nevada. Restudy of graptolites in stratigraphic successions in the Roberts Mountains, Simpson Park Range, and Copenhagen Canyon in the Monitor Range suggests that most of the oceanic events recognized in Scandinavia and Britain that took place during the late Llandovery, Wenlock and early Ludlow had an impact on graptolites in central Nevada. This review suggests a correlation between sudden appearances of many new graptolite taxa and origination of deep water at high latitudes. Significant upwelling near platform margins may have been a consequence of high-latitude deep water origination. Disappearances of graptolites in central Nevada appear to be linked to times of change in origination of deep-ocean waters from high to middle latitudes.

INTRODUCTION

Graptolite radiations and near-extinctions have been linked with changes in oceanic upwelling along continental shelf margins (Berry and Finney, 1996; Finney and Berry, 1996) and in sea-level (Melchin, 1996). Wilde and Berry (1984, 1986) proposed mechanisms by which deep-ocean circulation changes that resulted from sites of origination of ocean deep waters could influence graptolite radiations and extinctions. Wilde and Berry (1984, 1986) noted that in modern oceans, deep and most intermediate-depth water originates by the sinking of cold, dense water in high latitudes. They further suggested that when cold polar regions similar to those of today existed in the geologic past, origination of deep and intermediate-depth circulation was similar to that in modern oceans. During certain prolonged intervals in the geologic record of ice-free high latitudes, intermediate depth and even deep-ocean water

could have originated by the sinking of relatively highly saline, dense waters at the cool edge of mid-latitude sites where rates of evaporation were high (Wilde and Berry, 1984, 1986). Intervals during which origination sites of intermediate-depth and deep ocean waters changed were those in which significant oceanic changes took place. Such changes could have led either to extinctions or to radiations of graptolites and other ocean plankton (Wilde and Berry, 1984, 1986).

Aldridge et al. (1993), Jeppsson et al. (1995), and Jeppsson (1996, 1997) incorporated and expanded the Wilde-Berry proposals into a comprehensive model for organismal changes linked to ocean circulation changes. Aldridge et al. (1993) and Jeppsson et al. (1995) based many aspects of their model on observations of conodonts and graptolites from Silurian sequences in Scandinavia and Britain. Their model (Aldridge et al., 1993; Jeppsson et al., 1995; Jeppsson, 1997) recognized two fundamental oceanic conditions. Under primo conditions, deep-ocean circulation is driven by sinking of cold, dense water at high latitudes, and upwelling is enhanced (Aldridge et al., 1993; Jeppsson et al., 1995; Jeppsson, 1997). Oceanic intermediate-depth and deep waters originate at the cool margins of mid-latitude sites with high rates of evaporation in secundo conditions. Relatively dense, saline waters form most deep-ocean waters during secundo conditions. Secundo episodes have markedly reduced upwelling and are accompanied by significantly reduced oceanic productivity. Jeppsson (1996, p. 59) stated, "As now known, the Silurian oceanic cyclicity includes ten precisely dated oceanic events and a couple of candidates. Each of these events caused extinctions, range gaps and lithologic changes. Six of the ten events are primo-secundo (p-s) events, and four are secundo-primo (s-p) and secundo-secundo (s-s) events." Jeppsson's (1996) discussion suggests that many, if not all, of these events could have had global impacts on faunas.

The intent herein is to follow up on Jeppsson's (1996) suggestion by reviewing the Silurian graptolite faunas in central Nevada that were documented by Berry and Murphy (1975), Berry (1986), Murphy (1989), and in

field studies in the summer of 1996, which sought local evidence in graptolite faunas for any of the proposed primo and secundo events. Present-day Nevada was on an essentially northern margin of Laurentia during the Silurian. This plate was in the tropics, at some distance latitudinally and longitudinally from the British and Scandinavian successions in which the primo and secundo episodes and events were recognized. In addition, that Laurentian margin had its own unique tectonic history during the Silurian (Sheehan and Boucot, 1991). If, as Jeppsson (1996) indicated, changes in ocean circulation did have an impact on faunas globally, then such changes may be reflected in graptolite faunas in central Nevada.

THE NEVADA SUCCESSION

Study of Silurian graptolite-bearing strata in Nevada by the author and M. A. Murphy (Berry and Boucot, 1970; Berry and Murphy, 1975; Murphy et al., 1979; Berry, 1986; and W.B.N. Berry in Finney et al., 1995) indicates two principal graptolite-bearing successions. Study of one of them led to recognition of a sequence of late Llandovery–Early Devonian zones based on successions in the Roberts Mountains and the Simpson Park Range (Berry and Murphy, 1975; Murphy, 1989) where graptolites occur in the Roberts Mountains Formation. The second sequence is the latest Ordovician–Llandovery succession in the Monitor Range recognized by M.A. Murphy and his students. Graptolites and conodonts from that sequence have been discussed by Murphy et al. (1979), Berry (1986), and Murphy (1989). Late Ordovician–early Llandovery faunas occur in the upper part of the Hanson Creek Formation. Late Llandovery and younger graptolites found in that succession are in the Roberts Mountains Formation (Berry, 1986; Sheehan and Boucot, 1991).

The Silurian graptolite faunal succession in the Roberts Mountains Formation in the Roberts Mountains and Simpson Park Range has a likely correspondence with certain primo and secundo events and episodes of Aldridge et al. (1993) and Jeppsson et al. (1995) (see Figure 1). Hurst and Sheehan (1985) and Sheehan and Boucot (1991) pointed out that the Roberts Mountains Formation in these areas accumulated on the upper part of a slope that lay adjacent to a carbonate platform with a spectrum of shallow-marine environments. The slope upon which the Roberts Mountains Formation accumulated formed in the late Llandovery by collapse of part of the platform margin (Sheehan and Boucot, 1991, p. 60). Early and middle Llandovery strata have not been found on that part of the platform that collapsed to become a slope in the late Llandovery. Graptolite-bearing, non-bioturbated, thinly bedded, silty carbonates and calcareous siltstones

and mudstones comprise the major part of the Roberts Mountains Formation. Debris flows derived from shallow-marine environments on the platform occur as interbeds in the graptolite-bearing strata. The debris flows are thicker higher in the succession, and they appear to be thicker in more eastern sequences in the area (see Berry and Murphy, 1975; Hurst and Sheehan, 1985). These debris flows bear conodonts (Klapper and Murphy, 1974), brachiopods (Johnson et al., 1973, 1976), and corals (Johnson and Oliver, 1977).

Faunas in the basal beds of the Roberts Mountains Formation include *Oktavites spiralis* Zone graptolites and *Pterospirifer celloni* Zone conodonts (see Murphy, 1989). These faunas occur as interbeds within, as well as stratigraphically above, a distinctive black chert. *Cyrtograptus sakmaricus* Zone graptolites are superjacent to those of the *O. spiralis* Zone. Appearance of a rich profusion of *O. spiralis* Zone graptolites and *P. celloni* Zone conodonts is consistent with the development of significant upwelling along the platform margin. That upwelling could reflect oceanic conditions consistent with the late Llandovery Snipklint Primo Episode.

Beds superjacent to those bearing *Cyrtograptus sakmaricus* Zone faunas are barren of graptolites and conodonts (Klapper and Murphy, 1974; Berry and Murphy, 1975; Murphy, 1989). The relatively sudden disappearance of graptolites and conodonts in the sequence coincides with a marked decline in rate of sediment accumulation. Approximately 0.3 m of strata are present between the latest Llandovery graptolites and conodonts and the appearance of the middle Wenlock *Cyrtograptus rigidus* Zone graptolites. The abrupt disappearance of conodonts and graptolites coincides and is consistent with the Ireviken Event of Aldridge et al. (1993) and Jeppsson (1997). The absence of early Wenlock conodont and graptolite faunas is consistent with development of secundo conditions during the Vattenfallet Secundo Episode (see Jeppsson et al. 1995). The marked thinness of the presumed lower Wenlock suggests low rates of production and accumulation of carbonate sediment, which are consistent with Jeppsson's (1997) observations of Ireviken Event developments elsewhere.

Renewed carbonate sediment production and accumulation on the upper part of the slope accompanied appearance of numerous specimens indicative of *Cyrtograptus rigidus* Zone faunas in the Roberts Mountains Formation. These developments are consistent with renewed upwelling along the platform margin that accompanied the Sanda Primo Episode of Jeppsson et al. (1995).

Graptolites are relatively sparse in strata between the *Cyrtograptus rigidus* and *Cyrtograptus perneri* Zones (Berry and Murphy, 1975). This sparseness may reflect low oceanic productivity conditions consistent with those

OCEANIC EVENTS AND EPISODES RECOGNIZED IN SWEDEN AND BRITAIN	SUGGESTED CORRESPONDING EVENTS IN NEVADA GRAPTOLITE FAUNAS
SECUNDO CONDITIONS	graptolites suddenly become sparse
SPROGE PRIMO EPISODE	<i>Colonog. colonus</i> - <i>Neodiversog. ludensis</i> Zone fauna appears
KLINTE SECUNDO EPISODE	<i>Pristiogr. deubeli</i> - <i>P. ludensis</i> Zone
MULDE SECUNDO EPISODE	<i>Cyrtog. lundgreni</i> Event: graptolite near extinctions
HELLVI SECUNDO EPISODE	<i>Cyrtog. lundgreni</i> - <i>Monog. testis</i> Zone
VALLEVIKEN EVENT	onset of <i>Cyrtog. lundgreni</i> - <i>Monog. testis</i> fauna
ALLEKVIA PRIMO EPISODE	<i>Monograptus perneri</i> Zone
LANSA SECUNDO EPISODE	sparse fauna
BOGE PRIMO-SECUNDO EVENT	graptolites rare
SANDA PRIMO EPISODE	<i>Cyrtograptus rigidus</i> Zone fauna appears
VATTENFALLET SECUNDO EPISODE	no fauna and thin stratigraphic interval
IREVIKEN EVENT	conodonts & graptolites disappear
SNIPKLINT PRIMO EPISODE	<i>Cyrtograptus sakmaricus</i> Zone <i>Oktavites spiralis</i> Zone <i>Pterospathodus celloni</i> Zone conodonts

FIGURE 1—Late Llandovery (Snipklint Episode), Wenlock, and early Ludlow (Sproge Episode and younger) oceanic events and episodes in Sweden and Britain. Corresponding developments, primarily in graptolites, in central Nevada in right column.

of the Lansa Secundo Episode of Jeppsson et al. (1995). Allekvia Primo conditions (Jeppsson et al. 1995) may coincide with appearance of graptolites of the *C. perneri* Zone (Berry and Murphy, 1975).

Strata above the *Cyrtograptus perneri* Zone are characterized by the relatively sudden incursion of a number of new cyrtograptid species and the appearance of numerous specimens of *Testograptus testis* (Berry and Murphy, 1975). These new appearances may reflect oceanic conditions related to the Valleviken Primo-Secundo Event of Jeppsson et al. (1995).

No evidence for the Hellvi Secundo Episode has been found in analysis of the Roberts Mountains Formation faunas. Most of the species that characterize the central Nevada *Cyrtograptus lundgreni* Zone appear to range throughout the zone.

Nearly all taxa in the relatively species-rich *Testograptus testis*-*Cyrtograptus lundgreni* Zone disappear within a thin stratigraphic interval (Berry and Murphy, 1975; Murphy, 1989). Only relatively small specimens similar to *Gothograptus nassa* and slender *Pristiograptus dubius* remain (Berry and Murphy, 1975; Murphy, 1989). This major disappearance of most graptolite taxa coincides with the

Mulde Secundo-Secundo Event of Jeppsson et al., 1995) and with the Lundgreni Event of Koren' (1991; Lenz, 1993, 1994, 1995; Koren' and Urbanek, 1994).

Corfield et al. (1992) conducted carbon isotope analyses of British strata across the interval of the Lundgreni Event. They recognized a carbon-13 isotope excursion in the interval that is consistent with markedly reduced surface water productivity at the time. Subsequently, R.M. Corfield (personal commun., 1996) analyzed Roberts Mountains Formation graptolite-bearing samples from the *Testograptus testis*-*Cyrtograptus lundgreni*, *Pristiograptus dubius*-*Gothograptus nassa*, *Colonograptus? praedeubeli*, and *Colonograptus? ludensis* Zones. The geochemical analyses of these samples yielded results generally consistent with carbon isotope studies conducted on coeval strata in Britain (R.M. Corfield, written and oral commun., 1996).

Graptolites in the Roberts Mountains Formation above the *Cyrtograptus lundgreni*-*Testograptus testis* Zone are referred to three zones, which are, in ascending order: *Gothograptus nassa*-*Pristiograptus dubius*, *Colonograptus? praedeubeli*, and *Colonograptus? deubeli* (W.B.N. Berry in Finney et al., 1995, fig. 4). A paucity of graptolites in these

zones is consistent with continued secundo conditions. Jeppsson et al. (1995, p. 495) stated that the lower three of these zones are within their Mulde Secundo-Secundo Event. The Nevada *Colonograptus? deubeli* Zone seems to be coeval with Jeppsson et al.'s (1995, p. 496) Klinte Secundo Episode.

Roberts Mountains Formation Silurian strata superjacent to the *Colonograptus? deubeli* Zone contain a profusion of new graptolite taxa. These taxa include numbers of specimens of *Colonograptus colonus*, *Neodiversograptus nilsoni*, and *Bohemigraptus bohemicus* (Berry and Murphy, 1975). This sudden incursion of many individuals of a number of new taxa is consistent with onset of the Spröge Primo Episode. The abundance of individuals of the many newly appearing taxa continues through several meters (Berry and Murphy, 1975; Murphy, 1989). This abundance of individuals and taxa disappears relatively suddenly at a level that may be about middle Ludlow (Berry and Murphy, 1975; Murphy, 1989). That stratigraphic position may coincide with the change from primo to secundo conditions noted by Jeppsson (1996) at about the middle Ludlow. Higher Roberts Mountains Formation graptolite faunas are sparse (Berry and Murphy, 1975; Murphy, 1989).

LOWER LLANDOVERY GRAPTOLITES IN THE MONITOR RANGE

Mapping by M.A. Murphy and students in the Monitor Range revealed a succession of Late Ordovician-Silurian graptolites in the Copenhagen Canyon area (see Murphy et al., 1979; Finney et al., 1995). Berry (1986) described latest Ordovician and Llandovery graptolites from the upper part of the Hanson Creek Formation in the Copenhagen Canyon succession. The lower part of the Hanson Creek Formation in that area accumulated in moderate-depth subtidal conditions (Hurst and Sheehan, 1985). Sea-level fall related to late Ordovician Gondwanan glaciation is represented in the upper part of the Hanson Creek Formation at Copenhagen Canyon by prominent medium-bedded dolostones and a quartz sandstone interval (Murphy et al., 1979; Berry, 1986; Finney et al., 1995). Subsequent sea-level rise with deglaciation is recorded in dolostones superjacent to the quartz sandstone. These dolostones accumulated in shallow-subtidal environments. They are overlain by dark gray, medium-bedded limestones and interbedded cherts that accumulated in relatively deeper subtidal environments (J.D. Cooper, personal commun., 1996). Finney et al. (1995) recorded Late Ordovician graptolite faunas below the quartz sandstone interval, and illustrated a geologic map of the area.

The Roberts Mountains Formation in the Copenhagen Canyon area bears fewer and markedly thinner debris flows than in the Roberts Mountains. As well, graptolite-bearing layers are significantly less common in Copenhagen Canyon exposures of the Roberts Mountains Formation than they are in the Roberts Mountains. Hurst and Sheehan (1985) indicated that latest Ordovician and Silurian strata in the Copenhagen Canyon area accumulated under relatively deeper shelf waters than coeval strata in the Roberts Mountains.

The latest Ordovician and Llandovery graptolites recovered from the Copenhagen Canyon section show relatively little evidence for the Llandovery oceanic events indicated by Aldridge et al. (1993), except for the earliest Llandovery Spirodden and the latest Llandovery Snipklint Episodes. The Spirodden Secundo Episode of Aldridge et al. (1993) is represented in Copenhagen Canyon by dolostones and interbedded cherts (Berry, 1986; Finney et al., 1995). A few graptolites indicative of a *Normalograptus persculptus* Zone fauna and *Dimorphograptus swanstoni* occur in strata deposited during the Spirodden Secundo Episode. The paucity of graptolites is consistent with secundo conditions. The next higher graptolite fauna found in the Copenhagen Canyon succession is indicative of the *Rastrites maximus* Subzone of the *Spirograptus turriculatus* Zone (Berry, 1986). The appearance of these graptolites may reflect onset of the Snipklint Primo Episode.

Strata superjacent to those with *Dimorphograptus swanstoni* display cut-and-fill structures. Highly contorted strata occur above these horizons. A prominent phosphatic horizon occurs above the contorted beds and below the *Rastrites maximus* Subzone (Berry, 1986; Murphy, 1989). Hurst and Sheehan (1985, p. 158) suggested that the phosphatic horizon was indicative of a relatively slow rate of sediment accumulation accompanied by relatively rapid deepening. Cut-and-fill features and the highly contorted aspect of certain strata suggest the possibility that strong currents episodically swept the sea floor. If they did, then potential faunas were removed. Such faunas would have been the evidence for the oceanic events described by Aldridge et al. (1993).

The latest Ordovician-Silurian stratigraphic and faunal record at Copenhagen Canyon indicates that some sediment did accumulate in relatively deep-shelf environments during the Llandovery, but none accumulated in the relatively shallow slope and shelf environments in the Roberts Mountains. The record also suggests that strong ocean currents and very slow rates of sediment accumulation precluded preservation of most of the Llandovery faunas that could be analyzed for possible relationships with the Aldridge et al. (1993) oceanic events seen in British and Scandinavian successions.

CONCLUSIONS

Silurian graptolite faunas and stratigraphy indicate that most of the late Llandovery–middle Ludlow oceanic episodes and events recognized by Aldridge et al. (1993), Jeppsson et al. (1995), and Jeppsson (1996, 1997) in Britain and Scandinavia influenced central Nevada graptolite faunas. Late Llandovery–Ludlow strata with graptolites were seemingly influenced by oceanic events on the upper part of the slope. The central Nevada slope was adjacent to the Laurentian continental shelf. Appearances of new graptolite faunas coincide with the onset of primo conditions, during which upwelling along the platform margin was relatively pronounced. This relationship is consistent with the model proposed by Finney and Berry (1996) for environmental conditions in which graptolites flourished and diversified. Most declines in graptolite diversity occurred during secundo conditions.

Relatively deeper-slope environments in central Nevada had a different depositional history than those of the upper slope during most of the Silurian. Local tectonism, strong oceanic currents, and lack of widespread habitats in which graptolites could flourish above the deep slope resulted in poor preservation of many graptolites.

Central Nevada Silurian graptolite faunas occur in strata that accumulated on a margin of Laurentia that was within the tropics during the Silurian. The Avalonian plate upon which the British sequence developed and the Baltoscanian plate were a significant distance from the site of modern Nevada. Nevertheless, most late Llandovery–Ludlow oceanic events and episodes recognized in Britain and Scandinavia appear to have had an impact on central Nevada graptolite faunas.

As Wilde and Berry (1984, 1986) noted, a number of different mechanisms may be responsible for the decline or radiation of graptolites during times of change in the sites where deep ocean water circulation originated. The impacts of changes at sites of origination of ocean deep waters seem to be global. Precise dating of the events and episodes discussed by Jeppsson (1996) is needed to determine cyclicity of the events.

ACKNOWLEDGMENTS

The author is indebted to P.M. Sheehan for reviewing the manuscript and for directing attention to depositional conditions in central Nevada. An anonymous reviewer provided many useful suggestions. The author thanks R.M. Corfield for carbon isotope analyses of late Wenlock graptolite-bearing samples, and thanks J.D. Cooper for discussion of deposition in Copenhagen Canyon.

REFERENCES

- ALDRIDGE, R.J., L. JEPSSON, AND K.J. DORNING. 1993. Early Silurian oceanic episodes and events. *Journal of the Geological Society of London*, 150:501–513.
- BERRY, W.B.N. 1986. Stratigraphic significance of *Glyptograptus persculptus* group graptolites in central Nevada, U.S.A., p. 135–143. In C.P. Hughes and R.B. Rickards (eds.), *Palaeoecology and Biostratigraphy of Graptolites*. Geological Society Special Publication 20. Blackwell Scientific Publications, Oxford.
- , AND A. J. BOUCOT. 1970. Correlation of the North American Silurian Rocks. Geological Society of America Special Paper 102.
- , AND S. FINNEY. 1996. Major features of Ordovician graptolite radiations and extinctions, p. 33. In J.E. Repetski (ed.), *Sixth North American Paleontological Convention, Abstracts of Papers*, The Paleontological Society Special Publication 8.
- , AND M.A. MURPHY. 1975. Silurian and Devonian graptolites of central Nevada. University of California Publications in Geological Sciences, 110.
- CORFIELD, R.M., D.J. SIVETER, J.E. CORTLIDGE, AND W.S. MCKERROW. 1992. Carbon isotope excursion near Wenlock–Ludlow boundary in Anglo-Welsh area. *Geology*, 20:371–374.
- FINNEY, S.C., AND W.B.N. BERRY. 1996. A new model of graptolite ecology. Geological Society of America, Abstracts with Programs, 28:A366.
- , ———, AND M.A. MURPHY. 1995. Post-meeting trip—Great Basin graptolites. In J.D. Cooper (ed.), *Ordovician of the Great Basin: Fieldtrip Guidebook and Volume for the Seventh International Symposium on the Ordovician System*. The Pacific Section Society for Sedimentary Geology (SEPM), Fullerton, California.
- HURST, J.M., AND P.M. SHEEHAN. 1985. Depositional environments along a carbonate shelf to basin transect in the Silurian of Nevada, U.S.A. *Sedimentary Geology*, 45:143–171.
- JEPSSON, L. 1996. Silurian events—a review of the knowledge in 1996, p.59. The James Hall Symposium. Second International Symposium on the Silurian System, Program and Abstracts, University of Rochester Press.
- . 1997. The anatomy of the mid-Early Silurian Ireviken Event and a scenario for p–s events, p. 451–491. In C.E. Brett (ed.), *Paleontological Events: Stratigraphic, Ecological and Evolutionary implications*. Columbia University Press.
- , R.J. ALDRIDGE, AND K.J. DORNING. 1995. Wenlock (Silurian) oceanic episodes and events. *Journal of the Geological Society of London*, 152:487–498.
- JOHNSON, J.G., AND W.A. OLIVER, JR. 1977. Silurian and Devonian coral zones in the Great Basin, Nevada and California. Geological Society of America Bulletin, 88:1462–1468.
- , A.J. BOUCOT, AND M.A. MURPHY. 1973. Pridolian and Gedinnian Age brachiopods from the Roberts Mountains Formation of central Nevada. University of California Publications in the Geological Sciences, 100.
- , ———, AND ———. 1976. Wenlockian and Ludlovian age brachiopods from the Roberts Mountains Formation of central Nevada. University of California Publications in the Geological Sciences, 115.
- KLAPPER, G., AND M.A. MURPHY. 1974. Silurian–Lower Devonian conodont sequence in the Roberts Mountains Formation of central Nevada. University of California Publications in Geological Sciences, 111.
- KOREN, T.N. 1991. The *lundgreni* extinction event in central Asia and its bearing on graptolite biochronology within the Homerian. *Proceedings of the Estonian Academy of Science, Geology*, 74–78.

- , AND A. URBANEK. 1994. Adaptive radiation of monograptids after the late Wenlock crisis. *Acta Palaeontologica Polonica*, 39:137–167.
- LENZ, A.C. 1993. Late Wenlock–Ludlow (Silurian) graptolite extinctions, evolution and biostratigraphy: perspectives from Arctic Canada. *Canadian Journal of Earth Sciences*, 30:491–498.
- . 1994. Extinction and opportunistic evolution among late Wenlock graptolites. *Lethaia*, 27:111–117.
- . 1995. Upper Homerian (Wenlock, Silurian) graptolites and graptolite biostratigraphy, Arctic Archipelago, Canada. *Canadian Journal of Earth Sciences*, 32:1378–1392.
- MELCHIN, M.J. 1996. Graptolite diversity, survivorship and sea level change through the late Ashgill, Llandovery and Wenlock in Arctic Canada, p. 75. *In* The James Hall Symposium: Second International Symposium on the Silurian System, Program and Abstracts, University of Rochester.
- MURPHY, M.A. 1989. Central Nevada, p. 171–177. *In* C.H. Holland and M.G. Bassett (eds.), A Global Standard for the Silurian System. National Museum of Wales Geological Series Number 9.
- , J.B. DUNHAM, W.B.N. BERRY, AND J.C. MATTE. 1979. Late Llandovery unconformity in central Nevada. *Brigham Young University Studies in Geology*, 26:21–36.
- SHEEHAN, P.M., AND A.J. BOUCOT. 1991. Silurian paleogeography of the western United States, p. 51–82. *In* J.D. Cooper and C. A. Stevens (eds.), *Paleozoic Paleogeography of the Western United States II. Volume 1*.
- WILDE, P., AND W.B.N. BERRY. 1984. Destabilization of the oceanic density structure and its significance to marine “extinction” events. *Palaeogeography, Palaeoclimatology, and Palaeoecology*, 48:143–162.
- , AND ———. 1986. The role of oceanographic factors in the generation of global bio-events, p. 75–91. *In* O.H. Walliser (ed.), *Global Bio-Events: Lecture Notes in Earth Sciences*, Number 8. Springer-Verlag, Berlin.

SILURIAN REEF EPISODES, CHANGING SEASCAPES, AND PALEOBIOGEOGRAPHY

FRANK R. BRUNTON¹, LEIGH SMITH¹, OWEN A. DIXON², PAUL COPPER³,
HELDUR NESTOR⁴, AND STEVE KERSHAW⁵

¹Department of Geological Sciences, Queen's University, Kingston, Ontario K7L 3N6.

Current address: Department of Earth Sciences, Laurentian University, Sudbury, Ontario P3A 2C6

²Department of Geology, University of Ottawa, and Ottawa Carleton Geoscience Centre, Ottawa, Ontario K1N 6N5

³Department of Earth Sciences, Laurentian University, Sudbury, Ontario P3A 2C6

⁴Institute of Geology, Estonia pst. 7, Tallinn EE 0001, Estonia, and

⁵Department of Geography and Earth Sciences, Brunel University, Borough Road, Isleworth, Middlesex TW7 5DU, UK

ABSTRACT—Eight global Silurian reef-building episodes coincide with climatic and oceanic conditions characterized by inferred, warmer, high-latitude climates; salinity-dense bottom waters; and accompanying low-diversity, planktic and nekctic faunas. Periodic removal of reef and level-bottom community habitats by tectophases and relative sea-level falls appears to have stimulated reorganization and evolution of invertebrate communities during subsequent transgressive intervals.

Latest Ordovician and early-middle Llandovery metazoans—parazoans gradually re-established shallow- and deeper-water reef ecosystems. Evolutionary radiations of coral and stromatoporoid faunas are evident in the upper Llandovery and lower Wenlock. Although corals and stromatoporoids reached their Silurian acmes in the Wenlock, stromatoporoids maintained similar diversities in the Ludlow. Numerous coral species disappeared by the early Ludlow, in part coinciding with end-Wenlock extinctions of different planktic and benthic faunas. Calcimicrobial communities and calcareous algae were important constructors in many early-middle Llandovery reefs, are less conspicuous in many late Llandovery-early Wenlock reefs, and were volumetrically important reef constructors in many Late Silurian reefs. Morphological innovations of selected Ludlow benthos and associated lithofacies show a "Devonian carbonate bank archetype", with distinguishable forereef, reef, backreef, and lagoonal facies.

Partially reef-rimmed, late Ludlow, distally-steepened, carbonate banks reflect a change in reef patterns from the patchiness that characterized most Early Silurian flat-topped carbonate bank seascapes. Wenlock and late Ludlow reef tracts were larger in areal extent than modern reef tracts and were concentrated in subtropical and equatorial climatic belts.

INTRODUCTION

The first attempt at a global analysis of Silurian reefs (bioherms and biostromes) over a span of up to 35 million years, was presented in the Murchison Symposium volume (Copper and Brunton, 1991). Silurian reefs were shown to display a full spectrum of geometries and to have been built by a variety of metazoans capable of living in different shallow- and deeper-marine environments. These carbonate buildups were also shown to have developed in a variety of tectonic settings, from regionally extensive cratonic epeiric seas to pericratonic shelves and island arcs.

The purpose of this analysis is to outline the paleogeographic, -climatic, and -biologic significance of the invertebrates, calcareous algae, and calcimicrobes involved in reef development and to discuss their collective influence on carbonate bank geometry and their response to tectophases, associated regional changes in relative sea-level, and oceanographic changes. This report elaborates: 1) the major factors that influenced reef growth; 2) the evolutionary changes recognized in reef-building and -dwelling biota and the resultant changes in reef morphology through the Silurian; 3) the changes in environmental preference of reef-building metazoans; and 4) the delineation of extensive Early and Late Silurian reef tracts.

Biostratigraphic correlation of Silurian reefs from different parts of the world has enabled the delineation of eight global reef-building episodes for the Silurian (Figures 1, 2). These reef-building episodes largely coincide with particular oceanic and climatic conditions (Figures 2, 3; Jeppsson, 1987, 1990, 1996). This climate model recognizes alternations between intervals when the climate

is wetter at low latitudes and colder at high latitudes, and intervals when the climate is drier at low latitudes and warmer at high latitudes. Jeppsson distinguished two end-member oceanic states: 1) Primo episodes (P-States) characterized by cool, high-latitude climates, cold oceanic bottom waters, and high nutrient supplies (high-diversity planktic faunas); and 2) Secundo episodes (S-States) with warmer, high-latitude climates, salinity-dense bottom waters, low-diversity planktic faunas, and carbonate deposition and associated reef development in shallow epeiric seas. Also recognized were events of step-wise extinction of significant numbers of conodont species over perceived short durations (Figure 2; Jeppsson, 1990, 1996; Aldridge et al., 1993; Männik and Viira, 1993; Jeppsson et al., 1994). S-state oceanic conditions appear to have promoted of extensive "carbonate factories" in shallow epeiric seas, and facilitated development of rich heterotroph-based and photoautotroph-dominated epibenthic associations. We have found that episodes of extensive reef development largely coincide with S-State oceans (Figures 2, 3).

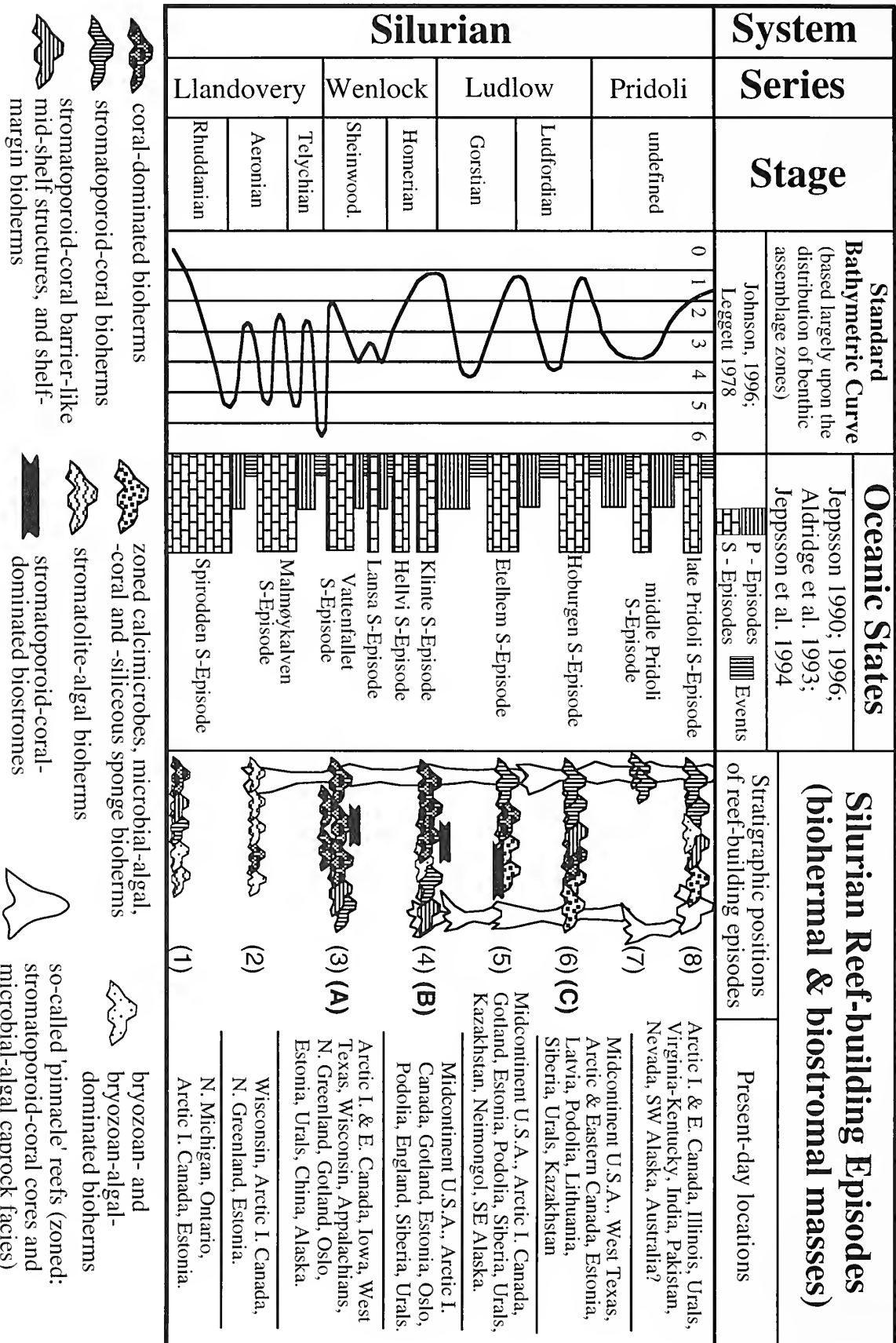
Existence and duration of S- and P-States in the Llandovery–Pridoli have been inferred from conodont faunal turnovers, data from other fossil groups, and sedimentological observations. Although the duration of the Silurian is still imprecise because of discrepancies in the ages assigned to each of the series (i.e., estimates for the Silurian range from 23–35 Ma; Figure 3), it is possible to show that the durations of S- and P-States through the Silurian differ greatly (Figures 2, 3). S-State oceans appear to have had the longest durations in the Llandovery (ca. 10 Ma; two S-State oceans) and Ludlow (ca. 7–14 Ma; two S-State oceans). The duration of the Pridoli, which has two S-State oceans, is the most poorly constrained, and estimates range from 2–10 Ma (Figure 3). The Wenlock shows the greatest number of oceanic state reversals with four S- and P-State couplets in a time span of ca. 5 Ma (Figure 3). The more persistent S-State oceanic conditions during the Wenlock (ca. 1 Ma durations) are perhaps the result of a combination of oceanic-climate stability (optimal climatic

amelioration) and relative tectonic quiescence (between Salinic disturbance 1 and 2; Figure 3). The Wenlock coincides with the acme of Silurian reef development.

Silurian reef epibenthic invertebrates, calcareous algae, and calcimicrobes also show temporal and spatial variations on different scales (Figures 1, 2). Although some metazoans, such as rugose corals, show great diversification in the early–middle Llandovery, most reef-associated metazoans and parazoans show their greatest faunal diversification during the extensive late Telychian transgressions that followed the Salinic-1 disturbance. Throughout the Early Silurian (Llandovery–Wenlock), tabulate corals outnumber stromatoporoids in reefs. Following the end-Wenlock extinctions (evolutionary replacements) of numerous epibenthic and planktic and nektic faunas, stromatoporoids (calcified sponges) became volumetrically more important than tabulate corals in most Late Silurian reefs. Calcimicrobes, calcareous algae, and enigmatic microbial components played a relatively important role in the development of many early–middle Llandovery patch reefs, a lesser role in late Llandovery–Wenlock buildups, and a substantial role in many of larger bank-margin, slope, and basinal Late Silurian reef complexes (Figures 1, 2). Lithistid sponges are important constituents in Ludlow deeper-water bank and slope reefs (Brunton and Dixon, 1994).

Equatorial reef tracts with numerous patch-reef clusters were present by the latest Telychian and early Wenlock. These reef tracts became established subsequent to late Llandovery transgressions that followed a major erosional episode (Salinic-1 disturbance in Figure 3; see also Ettensohn, 1994). Shallow-marine reef and level-bottom communities show the greatest faunal diversification of the Silurian after this major tectophase. Silurian reef tracts include: 1) subtropical reef tracts located both north and south of the paleoequator, and which flourished within the Uralian–Cordilleran and North Atlantic regions of Boucot (1990); and 2) tropical reef tracts located mostly in the Uralian–Cordilleran region. Llandovery–middle Ludlow seascapes changed from continent-wide, flat-topped carbonate banks with patchy lithofacies distributions to partially reef-rimmed in the late Ludlow and early Pridoli, with a more pronounced shelf–slope break and laterally extensive, back-reef lagoonal facies. Thick late Ludlow bank-margin reef complexes are evident along the preserved margins of Laurentia and Baltica (Figures 1, 2). The more pronounced differentiation of litho- and biofacies in middle and upper Ludlow successions of Laurentia and parts of Baltica is believed to be a biotic and sedimentologic response to increased tectonism associated with a second significant phase of the Salinic disturbance (i.e.,

FIGURE 1—(opposite) Temporal and spatial distributions and chief skeletalized animals of Silurian reefs (bioherms and biostromes). Stippled intervals (1–8) show durations of eight global reef-building episodes. Reef symbols do not accurately reflect reef shapes; numbers and sizes of symbols reflect the abundance and sizes of major reef types in each reef-building interval. Calcimicrobial communities and algae were important constructors in many early–middle Llandovery reefs; are less conspicuous constructors in late Llandovery–Wenlock reefs, and are important reef constructors the Late Silurian reef. I.Sh = inner shelf or bank, M.Sh. = middle shelf or bank, O.Sh.-P. = outer shelf and periplatform (shelf–slope break) region.



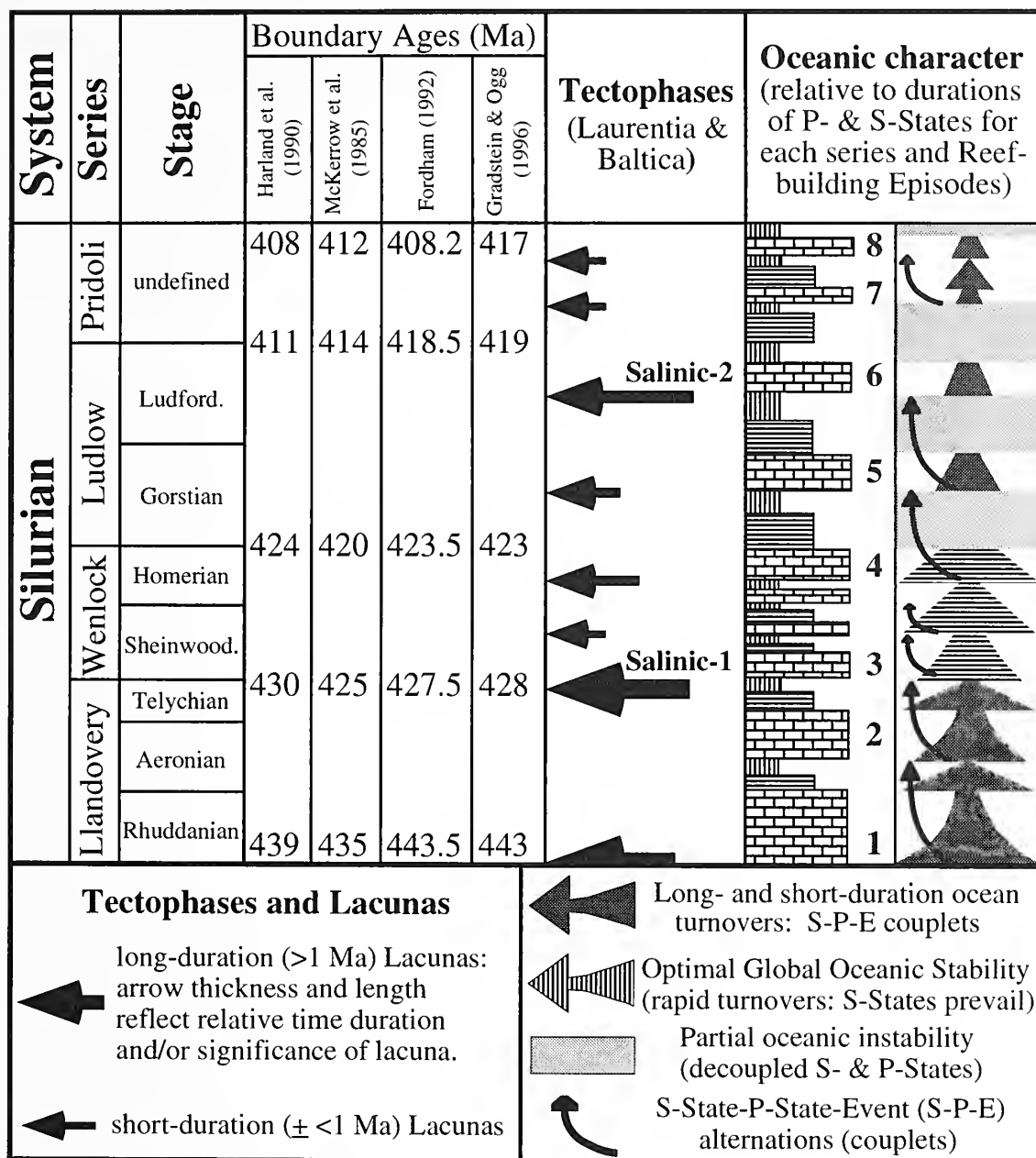


FIGURE 2—(opposite) Temporal distributions and chief biotic components of Silurian reefs related to: 1) general bathymetric curve (based on brachiopod-based “level-bottom” communities), and 2) oceanic states for Silurian. Stratigraphic positions of eight reef-building episodes (including three (A–C) major episodes) bracket initiation and climax stages of patch-reef and reef-complex development. Available data suggest some “pinnacle” reef growth may have been virtually continuous through the Silurian in some basins, and spanned more than one oceanic episode. Numbers and sizes of reef symbols reflect the abundance and sizes of the various reef types (except for “pinnacle” structures). Reef symbols do not accurately reflect true reef shapes.

FIGURE 3—(above) Ages of Silurian Series, tectophases for Laurentia and Baltica, and nature of oceans during the Silurian (see references in Figure 2). Duration of Silurian ranges from 23 Ma (McKerrow et al., 1985) to 35 Ma (Fordham, 1992). Tectophases (Jamieson and Beaumont, 1988; Ettensohn, 1994) are tectonic pulses or plate readjustments with durations ca. 5 Ma or less with short-lived regional-scale uplifts and erosional-depositional episodes in northeast (Canadian Arctic Islands–Greenland) and central (Michigan, southwest Ontario, and Appalachian regions) Laurentia and parts of Baltica (Gotland, Estonia).

Salinic-2—a reflection of increased orogenic activity along the margins of Laurentia and Baltica; Figure 3). These short-lived episodes of increased tectonism appear to have greatly affected both the style and lateral extent of sedimentation and the biotic evolution of Silurian reef and level-bottom marine faunas.

TERMINOLOGY

The term “reef” is used in a broad sense to define any biologically-constructed carbonate mass raised above the seafloor regardless of water depth and nature of the biotic components. We use the terms “patch reef”, “bioherm”, “biostrome”, “reef complex”, “reef cluster”, and “carbonate buildup” in the sense of James and Geldsetzer (1989). Included in the definition of “bioherms” (Cumings, 1932) are relatively small structures (up to tens of meters across by a few meters high) known from Llandovery and Wenlock successions of Laurentia and Baltica that show little or no evidence of auto-succession and commonly little or no reef-derived or shoal complex-derived flank lithofacies. Biostromes are tabular reef bodies from a few tens of centimeters up to 5 m-thick (usually composed of stacked accumulations of invertebrate communities), some of which extend laterally for many kilometers (e.g., Midcontinent region, U.S.A. [Shaver et al., 1978]; Canadian Arctic Islands [Brunton and Dixon, 1991a]; Hemse biostromes, Gotland [Riding, 1981; Kershaw, 1994; Kershaw and Keeling, 1994]). We do not concur with Schuhmacher and Zibrowius’ (1985) concept that “reefs, by definition, are confined to shallow water”, as Silurian reefs include shallow- and deeper-water bank and slope occurrences. “Tectophases” (Jamieson and Beaumont, 1988; Ettensohn, 1994) represent tectonic pulses or plate readjustments with time durations on the order of 5 Ma or less.

REEF-GROWTH EPISODES

Flooding of the paleocontinents and amelioration of global climates in the earliest Llandovery (Rhuddanian) after Late Ordovician glaciations allowed the gradual re-establishment of both shallow- and deeper-water reef growth. Early Llandovery reefs were constructed on areally extensive carbonate banks of Laurentia, Baltica, and China (Yangtze region) by a consortium of calcimicrobes and calcareous algae. Associated metazoans include some Late Ordovician coral and stromatoporoid stocks, but are mainly the increasingly diverse Silurian corals and fewer stromatoporoids and bryozoans (Figures 1, 2;

see Nestor, 1984; Copper and Brunton, 1991; Brunton and Copper, 1994; Copper, 1994).

The first major episode of reef growth (A in Figure 2) was latest Telychian. These reefs, which show evidence of autosuccession, contain a diverse faunal consortium of tabulate corals, stromatoporoids, bryozoans, crinozoans, calcimicrobes, and calcareous red algae. Initiation of this reef-building episode was during P-State oceanic conditions. The majority of latest Telychian reef complexes in Laurentia were spatially and temporally associated with extensive crinoidal shoal complexes. Widespread coral-stromatoporoid-bryozoan-crinozoan-calcimicrobial reef communities did not appear on a global scale in open, shallow-marine settings until the early Wenlock (Sheinwoodian). Wenlock reefs represent the acme of Silurian reef growth and coincide with S-State oceanic conditions.

EARLY AND MIDDLE LLANDOVERY REEF-BUILDING EPISODES.—Both of these reef-building episodes occurred during large-scale transgressive pulses and S-State oceanic conditions (Figure 2). Llandovery sea-level fluctuations included four major rises and falls of about 50 m (Johnson, 1996; Figure 2) over approximately 10 Ma. These fluctuations match only with three reef-building transgressive episodes in the middle Rhuddanian, middle Aeronian, and Telychian. Llandovery sea-level highstands correspond remarkably well with the four interglacial episodes dated from South America by Grahn and Caputo (1992). This temporal relationship appears to corroborate a glacio-eustatic model for the first part of the Llandovery.

These reefs developed largely on intracratonic banks and, to a lesser extent, on pericratonic shelves of northern Europe, North America, and Greenland (Laurentia and Baltica; Brunton and Copper, 1994). A shallow-marine, barrier-like reef and a reef cluster made up of over 300 small, locally coral-dominated, stromatoporoid-dominated, or bryozoan-dominated patch reefs extended for at least 50 km in central Laurentia during the Rhuddanian (Manitoulin Island, Ontario: Fay and Copper, 1982; Figure 1). Corals were most prolific in the central part of the complex, the stromatoporoids in somewhat restricted marine settings, and bryozoan reefs in marginal-marine lithofacies.

Aeronian algal- and/or microbial-dominated patch reefs, numbering in the hundreds, developed in shallow-marine, restricted-lagoonal waters (increased salinities) on carbonate banks of central (Soderman and Carozzi, 1963; Shaver et al., 1978) and northern (Brunton and Copper, 1994) Laurentia (Figure 1). Aeronian reefs in Baltica (Estonia) comprise coral-stromatoporoid tabular biostromes or banks (Nestor, 1984, 1995). Middle

Llandovery "pinnacle" reefs are present in basinal (deeper water) calcareous mudrocks of the Cape Phillips Formation, Canadian Arctic Islands (de Freitas et al., 1993a; Figures 1, 2). These structures began growth during a transgressive pulse that is recognizable in the subsurface and in exposures on several islands in the Canadian Arctic Archipelago (de Freitas, 1991). Early and middle Llandovery reefs represent early attempts at reef growth by calcimicrobes, calcareous algae, and low-diversity associations of tabulate corals, rugose corals, and a few stromatoporoids. For the brachiopods, reef associations first appear in the middle Llandovery.

LATEST LLANDOVERY-WENLOCK REEF-BUILDING EPISODES.—Reef development expanded during the late Llandovery (latest Telychian), and biotic diversity of skeletal invertebrates in reef and inter-reef ("level-bottom") communities increased dramatically (Boucot, 1990; Nestor, 1990, 1994, 1995; Kaljo and Märss, 1991; Wang and Chen, 1991; Watkins, 1993; Kaljo et al., 1995). Several new phylogenetic stocks of stromatoporoids appeared in the late Llandovery (Nestor, 1990), along with at least 84 new genera of corals (Kaljo and Märss, 1991). Clathrodictyid- and ecclimadictyid-dominated stromatoporoid faunas, spatially associated crinoid meadows (shoal complexes), and pentamerid brachiopods have been identified from central and east Laurentia (latest Telychian-Wenlock; Hudson Bay and Midcontinent region to Anticosti Island) and central and eastern Baltica (earliest Sheinwoodian; Baltic region and Severnaya Zemlya). A major late Llandovery dispersal of "level-bottom" community taxa from the Uralian-Cordilleran region into the North Atlantic region has also been documented (Boucot, 1990).

Extensive crinoid-shoal complexes and associated small patch-reef clusters became established earlier in Laurentia (latest Telychian) during the final stages of P-State oceanic conditions (Figure 2). These vast crinoid thickets, which grew mostly in mid-bank settings and may have restricted water circulation to some degree (Kaljo et al., 1991; Brunton and Copper, 1994), produced abundant sand and gravel substrates that facilitated the establishment of reef communities (Lane, 1971; Brett, 1984, 1991). By the earliest Sheinwoodian, extensive reef clusters and crinoidal shoal complexes were established in Laurentia, Baltica, and China (Yangtze platform) (Figure 1). This episode of reef growth coincides with the onset of S-State oceanic conditions. Latest Telychian to middle Sheinwoodian patch-reef cluster development represents the first major Silurian reef-building episode (A in Figure 2).

The second major Silurian reef-building episode (B in Figure 2) was late Homerian and coincided with S-State oceanic conditions. Homerian reefs are extensive in the eastern Midcontinent region (Lockport-equivalent patch reefs and so-called "pinnacle" reefs of the Michigan, Appalachian, and Illinois Basins; Shaver, 1991), Canadian Arctic Islands, Greenland, Siberia, southern Britain, Norway, Podolia, Urals, Yangtze region, and New South Wales. Patch reef clusters are absent in upper Wenlock strata of Estonia and of only minor importance in Podolia. Small patch reefs in the Halla, Mulde(?), and larger reefs in the Klinteberg Beds of Gotland possess peculiar but diverse coral and stromatoporoid species (see Klaamann and Einasto, 1982). Riding (1981) has reported coral-stromatoporoid-algal-dominated patch reefs from Shropshire, and small coral-dominated and bryozoan-dominated reefs from Norway.

LUDLOW REEF-BUILDING EPISODES.—Variety and diversity of reef-constructing metazoans declined in the early Ludlow. However, the relative skeletal volume of stromatoporoids increased in Ludlow reefs, despite their greater taxonomic diversity in the Wenlock (Nestor, 1990). The relative increase in stromatoporoid skeletal volume in many Late Silurian reefs may be the result of a drastic decline in coral diversity after the terminal-Wenlock extinctions (evolutionary replacements), and/or may reflect a change in oceanographic-sedimentologic conditions that favored stromatoporoids over other epibenthos.

The first of two Ludlow reef-building episodes was late Gorstian (middle Ludlow; Figures 1, 2). Both reef-building episodes coincide with S-State oceans (Figure 2). Middle Ludlow calcimicrobe-aphrosalpingid sponge-dominated communities built shallow shelf-margin clusters and barrier reefs in an island arc complex, now exposed in southeast Alaska (Soja, 1994). This assemblage also built similar carbonate buildups in bank-margin facies throughout the Urals (Antoshkina, 1996). Calcimicrobe-lithistid sponge associations were also important in patch reef growth, and formed individual reefs and the cores of composite stromatoporoid-coralgal-capped reefs in deeper subtidal ramp and foreslope settings in the Canadian Arctic Islands (Narbonne and Dixon, 1984; Brunton and Dixon, 1991a, 1994; Dixon and Graf, 1992).

Although biostromal (tabular) reefs occur through the Silurian, they are apparently best developed in middle Ludlow-Pridoli carbonate successions (Figures 1, 2). The middle Ludlow biostromal and patch reef units of the Hemse beds (Gotland) are well-documented (Kershaw, 1993; Kershaw and Keeling, 1994). Biostromes

(tabular reefs) represent habitat modifications by reef-building epibenthic metazoans in shallow, muddier shelf seas. This reef growth appears to have taken place under semi-restricted and perhaps slightly more saline conditions during prolonged stillstand and/or regressive conditions. Hemse patch reefs, up to 5–10 m-thick and approximately 100 m in diameter, occur in the central part of Gotland and contain peculiar tabulate corals, few stromatoporoids, and a specialized reef brachiopod fauna. For the brachiopods, reef associations became common by the Ludlow.

The late Ludlow reef-building episode (major episode C in Figure 2) marks the onset of thick stromatoporoid-microbial-coralgal and stromatoporoid-algal shelf-margin reefs, clusters, and barrier-like complexes. Llandovery–middle Ludlow flat-topped carbonate banks changed to partially reef-rimmed, distally-steepened banks in the late Ludlow. These bank-margin reefs are best known from Latvia and Lithuania, Canadian Arctic Islands, eastern Canada (Gaspé), Nevada, Texas, the Urals, and Novaya Zemlya (Shuiskii, 1975, 1983; Nestor, 1984; Bourque et al., 1986; Shishkin, 1986; Brunton and Dixon, 1991a; Ruppel, 1993; Figures 1, 2). This lateral differentiation of lithofacies immediately follows the Salinic-2 disturbance (Figure 3), coincides with short-lived uplift and erosion along the eastern margin of Laurentia and western margin of Baltica, and shows renewed but short-lived, laterally extensive, and rapid reef complex accretion and carbonate production.

PRIDOLI REEF-BUILDING EPISODES.—Two reef-building episodes have been noted in the Pridoli (Figures 1, 2). Biotic diversity and skeletal volume of stromatoporoids and tabulate corals were drastically reduced in Pridoli buildups. Syringoporids became the important tabulate corals in some early–middle Pridoli biostromes, and small bioherms occur with greatly reduced numbers of stromatoporoids, favositids, heliolitids, and minor halytitids. Small bryozoan-algal-dominated mounds are also known from upper Pridoli successions. Stromatoporoid-coral- and stromatoporoid-algal-dominated reefs had a restricted development in both mid- and distal-shelf settings (Figures 1, 2). Calcareous sponges and calcimicrobes built barrier-like shelf-margin reefs on late Pridoli banks in southwest Alaska (Clough and Blodgett, 1989) at a time of prolonged global sea-level stillstand conditions.

The decline in diversity of Pridoli reef-building taxa and in sizes of individual reefs and complexes was related to a combination of factors. These include climate change (reduction of evaporation-induced deposition and seafloor precipitation from Ludlow to Pridoli), with continued tectonism and associated lowering of relative

sea-levels after the second significant phase of the Salinic disturbance (Salinic-2; Figure 3).

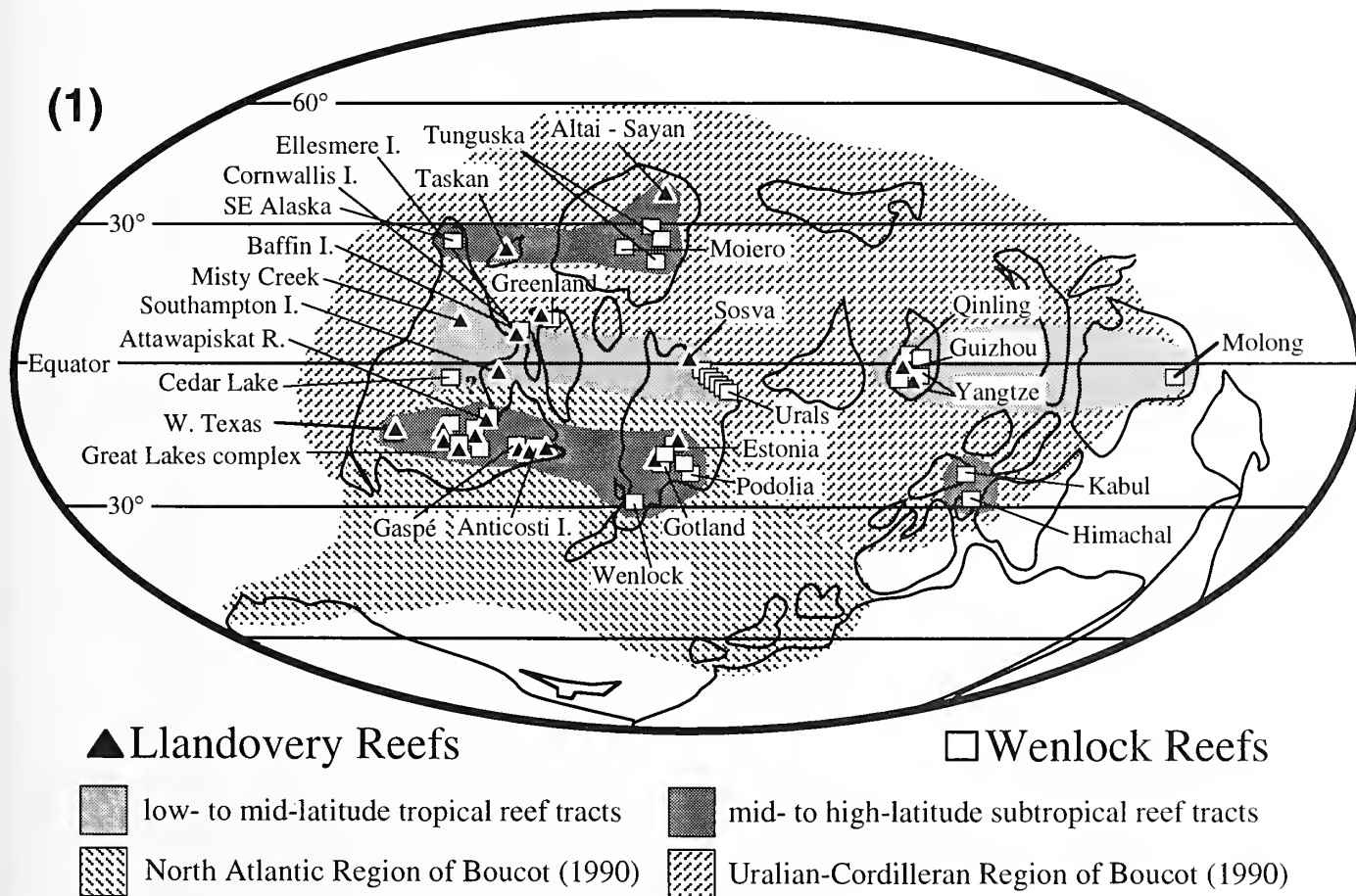
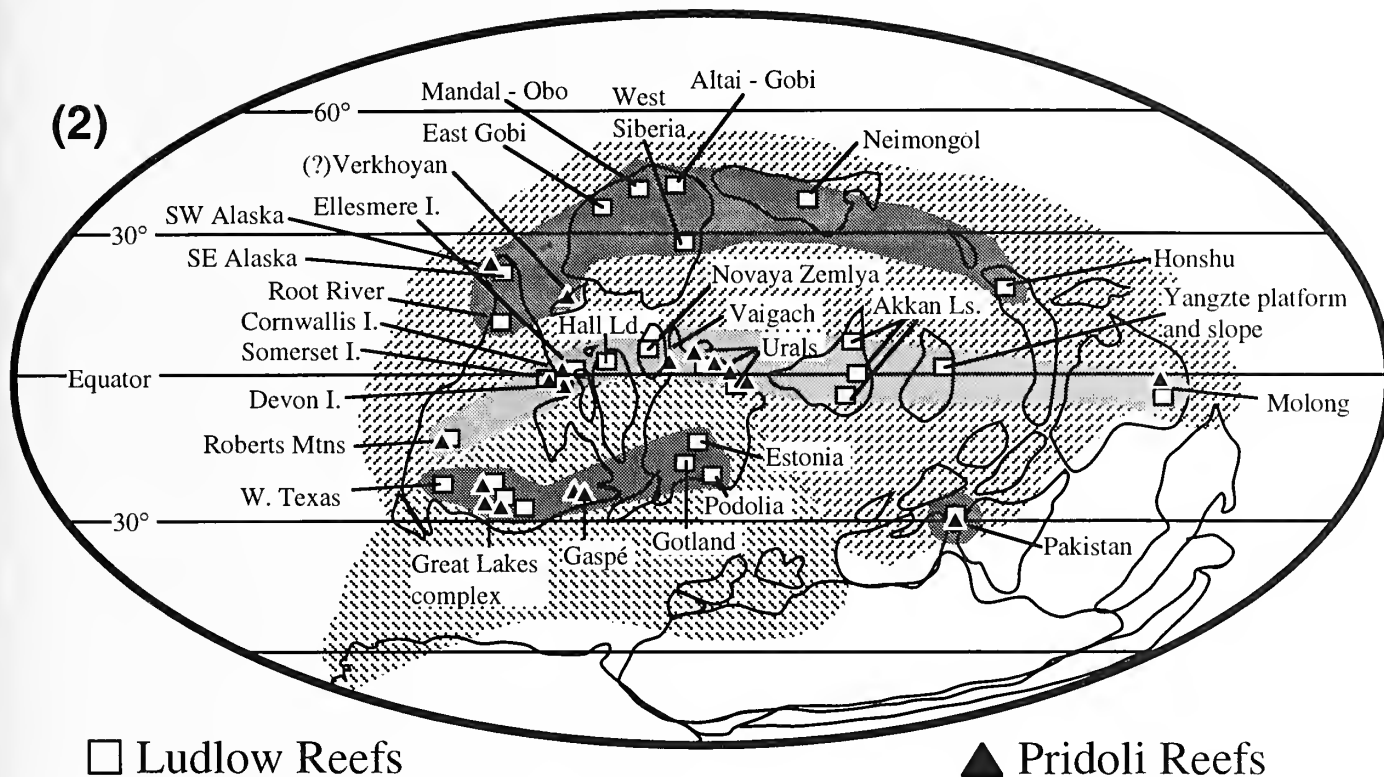
SILURIAN REEF PALEOBIOGEOGRAPHY

A number of reef tracts and possible “reef provinces” have been delineated in the latest Llandovery–Wenlock and Ludlow–Pridoli (Figure 4.1, 4.2). Reef tracts noted herein are based on our current understanding of reef and level-bottom invertebrate distributions and inferred larval distribution pathways. Most tracts occur within the North Silurian realm of Boucot (1985, 1990). Testing the validity of probable Silurian “reef provinces” will require more detailed collecting and taxonomic studies of the wide variety of metazoans and parazoans, calcareous algae, and calcimicrobes, and refinement of plate reconstructions that take biogeographic data into account.

Plotting the variety of Silurian reefs, climatically-sensitive mineral occurrences such as bauxite deposits, and level-bottom community distributions on the plate reconstructions of Scotese and McKerrow (1990) reveals that the Siberian and Kazakhstan Plates are positioned too far north and that the Siberian plate should be rotated 180° (see also Copper and Brunton, 1991). Based on modern reef positions, we have rotated and re-positioned some plates between the 30° N and S paleolatitudes to better represent the paleobiologic and environmental nature of the various reefal communities and relate them to probable oceanographic surface currents and larval distribution paths (Figure 4.1, 4.2).

Several of the proposed reef tracts appear to have been longer than modern reef tracts. The middle Wenlock Appalachian reef tract (Mesolella, 1978; Smosna et al., 1989) was approximately 800 km long, and if extended into the Gaspé region of Laurentia (Bourque et al., 1986; and references in Bourque, 1989), would have been at least 1,800 km long. The northeastern Laurentia (Canadian Arctic Islands–North Greenland) Wenlock reef tract

FIGURE 4—(opposite) Silurian reef tracts and possible “reef provinces” (plate reconstruction after Scotese and McKerrow, 1990). Extent of warm-water “level-bottom” faunas of Uralian–Cordilleran and North Atlantic regions from Boucot (1990; also Meyerhoff et al., 1996). Reefs mostly in tropical and subtropical paleolatitudes, as modern coralgal reefs. Many reef tracts were longer than the Great Barrier Reef Province of Australia. 1, Early Silurian (Llandovery–Wenlock). Wenlock reef tracts have the most diverse communities and coincided with acmes of epibenthic reef invertebrates. 2, Late Silurian (Ludlow–Pridoli). Late Ludlow reef tracts had the widest geographic extent of Silurian. Late Wenlock–Pridoli reefs suggest the Siberian and Kazakhstan Plates have been positioned too far north in most Silurian reconstructions (see also Copper, 1994, and Early Devonian brachiopod biogeography in Alekseeva, 1992).



extends for at least 1,500 km, and the Urals reef tract extends more than 2,000 km (see also Copper, 1994; Antoshkina, 1996). According to most plate reconstructions, the regions that now constitute the Ural Mountains (Baltic Plate) and the Yangtze platform (China Plate) appear to have remained within the equatorial region throughout the Silurian. Such climatic stability apparently allowed for virtually continuous reef growth (Figures 1, 4; Krasnov et al., 1986; Sharkova, 1986; Shishkin, 1986; Antoshkina, 1996). It is generally in these regions that we find the few exceptions where reef growth occurred during both P- and S-State oceanic conditions.

Smaller-scale Late Silurian reef tracts developed within the extensive carbonate banks of Laurentia (Midcontinent region of Michigan and Illinois; Lowenstam, 1950; Mesolella et al., 1974; Huh et al., 1977; Gill, 1979, 1985, 1994; Briggs et al., 1980; Bay, 1983; Droste and Shaver, 1985; Friedman and Kopaska-Merkel, 1991; Shaver, 1991). Reef tracts also developed along carbonate bank margins, now preserved in late Ludlow successions that extend from Estonia through Latvia and Lithuania and perhaps into the Podolian region of the Ukraine (Klaamann and Einasto, 1982; Nestor, 1984; Kaljo et al., 1991). The most extensive Late Silurian reef tracts continued to be paleoequatorial, and include the distal-shelf, shelf-margin, and slope reef clusters of Laurentia and Baltica (i.e., the Canadian Arctic Islands, Gaspé, and Ural Mountains).

NATURE OF REEF SUCCESSIONS AND REEF GEOMETRIES

The generally accepted view that Silurian reefs are dominated by stromatoporoids and corals is misleading. Silurian reefs reveal a wide range of epibenthic and minor cryptic organisms that generally show changes in preferred shelf position, habitat and biotic association through time (Figures 1, 5, 6). Llandovery–Wenlock bryozoan-algal- and bryozoan-algal-coral-dominated reefs with encrusting fistuliporoid cruststone fabrics and middle-late Pridoli examples with foliaceous-fistuliporoid lettuce-stone fabrics (Cuffey, 1985; Hewitt and Cuffey, 1985) are among the few exceptions. This bioherm consortium shows relative uniformity in habitat preference through the Silurian (Figure 1).

Typical community successions include the following changes: 1) from lower tabulate coral to upper stromatoporoid, stromatoporoid-algal and stromatoporoid-microbial communities; and 2) from lower tabulate coral and/or siliceous sponge-calcimicrobial communities either to upper stromatoporoid-algal or to tabulate

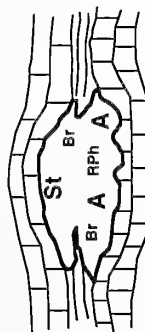
coral-algal communities (Figures 5, 6). Apparent trends in reef growth (buildup geometries) through the Silurian suggest: 1) changes in the Wenlock from biohermal to biostromal constructions—in some instances involving intervals of interrupted growth or discontinuous autosuccessional development (i.e., “keep-up” and “catch-up” styles of reef growth documented for modern and Tertiary reefs by Neumann and Macintyre, 1985); 2) coalescence of small bioherms into larger composite structures that possess low diversity, but abundant stromatoporoids and sparse tabulate corals and calcimicrobes (i.e., similar to the “expansion type” style of reef growth observed off of Belize and interpreted to represent onset of prolonged stillstand conditions by Mazzullo et al., 1992); 3) early biostrome development by monospecific or low-diversity tabulate and/or colonial rugose coral faunas, followed by establishment of overlying biohermal structures; 4) regionally extensive, thick, late Ludlow distal-shelf composite bioherm development in response to a short-lived increase in subsidence and renewed accommodation space recorded largely along the margins of Laurentia and Baltica following the Salinic-2 disturbance (Figures 1, 3, 6); and 5) an increase in biostrome development as a preferred reef geometry through Ludlow and particularly Pridoli successions, largely due to a general shallowness of most Pridolian mixed carbonate-siliciclastic banks.

Many Wenlock patch reefs show similar faunal elements and ecologic development, especially those in tectonically similar lithofacies settings (Figure 5). Wenlock bioherms in shallow epeiric seas of central Laurentia (Michigan, Illinois, and Appalachian regions) and surrounding shallow-water carbonate banks contain the same corals and stromatoporoids as pericratonic bioherms of the Gaspé and Anticosti shelves and Jaani and Jaagarahu reefs (Estonia) and Höglint reefs (Gotland) of the Baltic carbonate bank (Figure 5). The shapes and community structures or autosuccessions of these buildups differ, and demonstrate regional variability in reef shape and structure (see reef profiles in Crowley, 1973; Shaver, 1977; Shaver et al., 1978; Droste and Shaver, 1985; Gill, 1985; Bourque et al., 1986; Friedman and Kopaska-Merkel, 1991; Riding and Watts, 1991; de Freitas et al.,

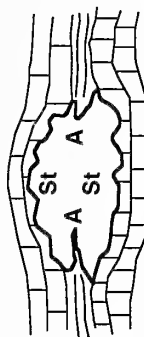
FIGURE 5—(opposite) Geometry, skeletal metazoans, succession, and lithofacies of Early Silurian (Llandovery–Wenlock) reefs from Laurentia and Baltica. Sizes of letter abbreviations for metazoans reflect skeletal volume in reefs. Geometry of some reefs varies with paleogeographic setting, especially reefs with “keep-up” style of aggradation. Biostrome development above bioherms took place preferentially in intracratonic settings (e.g., late Wenlock of New York, early Wenlock of Gotland, Sweden).

Early Silurian Pericratonic & Intracratonic reef geometries & successions

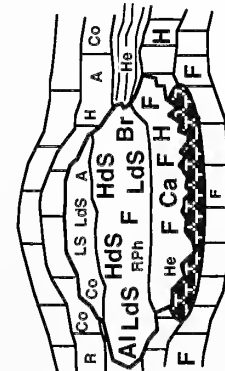
Inner-shelf reefs



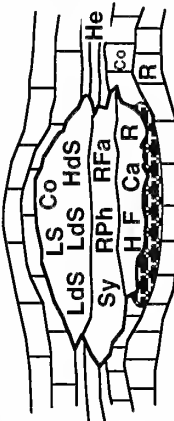
(Llandovery bioherms: Arctic I., Canada, and Baltic Region -- data in Brunton & Copper 1994)



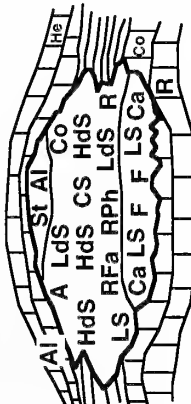
(Llandovery bioherms: Iowa -- Witzke 1983; Wisconsin, Nazbro reefs -- Soderman & Carozzi 1963; Shaver et al. 1978)



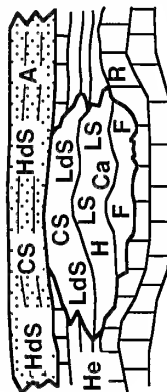
(latest Llandovery-Wenlock bioherms: Anticosti I., Baltic Region, North Greenland -- see discussion and references in Brunton & Copper 1994)



(Wenlock bioherms: Mid-continent region, U.S.A. -- Shaver 1991; Shaver et al. 1978; Shaver & Soderman 1989)



(latest Llandovery-Wenlock bioherms: Midcontinent U.S.A., Anticosti I., Baltica Region, North Greenland -- Shaver et al. 1978; Brunton & Copper 1994)

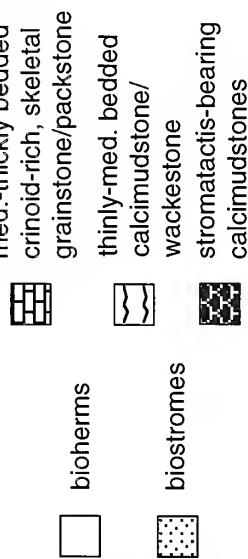


(late Wenlock: Gasport reefs, New York State, U.S.A. -- Crowley 1973; Shaver et al. 1978; Höglint reefs, Gotland, Sweden -- Kershaw 1993)

Middle-shelf and distal-shelf reefs

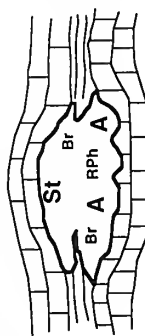
Major epibenthic metazoans involved in reef construction & lithofacies associations

TABULATE CORALS	STROMATOPORIDS	RUGOSE CORALS
H - halysitids	(clathrodictyids/ecclimadictyids)	RFa - dendroid forms
Ca - cateniporids	LS - laminar	RPh - phaceloid forms
F - favositids	LdS - low domical	Ra - arachnophyllids
Al - alveolitids	HdS - high domical	R - horn corals
Co - coenitids	CS - columnar	
He - heliolitids		
Sy - syringoporids		
	BRYOZOA	ALGAE/CALCIMICROBES
	Br - bryozoans	A - algae (green, red)
		St - stromatolites, cyanobacteria

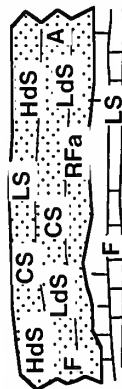


Late Silurian Pericratonic & Intracratonic reef geometries & successions

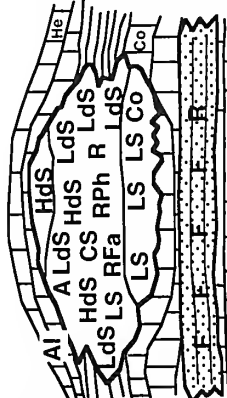
Mid-shelf reefs & shelf-margin complexes



(Ludlow-Pridoli bioherms in restricted marine settings: e.g., Arctic I. & Eastern Canada; Appalachian Basin)

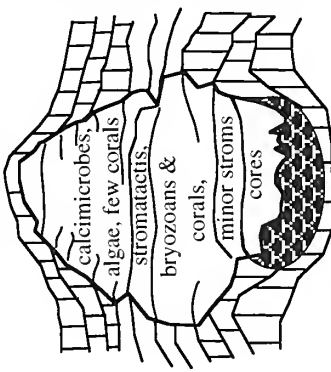


(middle Ludlow & Pridoli biostromes; well-described from Gotland -- Kershaw 1990, 1993; Kershaw & Keeling 1994; Riding 1981; also occur in Arctic I. & E. Canada, Urals, Alaska)

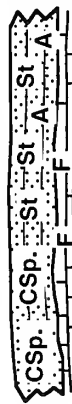


(latest Wenlock, Ludlow, Pridoli bioherms: Midcontinent region, Arctic I. & E. Canada, Estonia, Latvia, Podolia, Lithuania, Siberia, Urals; Copper & Brunton 1991)

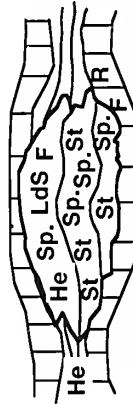
Mid- to distal-shelf & basinal-foreslope reefs



(generalized middle Llandovery to Pridoli and early Lochkov "pinnacle" reefs: buildups represent episodic biohermal accretion in distal shelf, basinal, and slope settings, possess numerous paleokarst surfaces: e.g., Michigan, Illinois, Appalachian, Gaspé, Uralian, Franklinian, and possibly Baltic basins; Smith 1990; Friedman & Kopaska-Merkel 1991; de Freitas et al. 1993a)



(middle Ludlow barrier structures: e.g., SE Alaska -- Soja 1994)



(middle to late Ludlow bioherms: Arctic Islands -- Brunton & Dixon 1994; Gaspé -- Bourque et al. 1986; Nevada -- Copper & Brunton 1991)

(note: both barrier-like and biohermal structures have been described)

Major epibenthic metazoans involved in reef construction & lithofacies associations

TABULATE CORALS	STROMATOPORIDS	RUGOSE CORALS		
H - halytitids	(densastromids, parallelotromids, plexodictyids, and simplexodictyids)	RFa - dendroid forms		med.-thickly bedded crinoid-rich, skeletal grainstone/packstone
F - favositids		RPh - phaceloid forms	bioherms	
Al - alveolitids	LS - laminar	Ra - arachnophyllids		thinly-med. bedded calcimudstone/wackestone
Co - coenitids	LdS - low domical	R - horn corals	biostromes	stromatolite-bearing calcimudstones
He - heliolitids	HdS - high domical			
Sy - syringoporids	CS - columnar			
ALGAE/CALCIMICROBES	BRYOZOA	SPONGES		
A - algae (green, red)	Br - bryozoans	Sp. demosponges (siliceous)		
St - stromatolites		CSp. calcareous sponges		

1993a; Kershaw, 1993; Kershaw and Keeling, 1994; Brunton and Copper, 1994). Variations in local paleogeographic and tectonic settings (e.g., sea-surface temperatures and bank-to-margin positions), in combination with relative sea-level fluctuations, appear to have been the main controls on reef community structure (Figures 4–6).

Calcimicrobes and algae increased in volume (and relative importance) in middle–late Ludlow shallow and deeper, medial to distal banks and deeper-water foreslope reefs (Figure 6). The thickest individual Silurian bioherms and composite reef complexes are recorded from the upper Ludlow. Dominant calcimicrobes, algae, and associated low-diversity calcareous (aphrosalpingid) sponge communities were constructors of middle Ludlow shallow-marine shelf-margin reefs off northwest Laurentia (southeast Alaska; Soja, 1991, 1994; Soja and Riding, 1993). Calcimicrobes and low-diversity siliceous sponge communities also built middle and late Ludlow deeper-water reefs that are situated on distally-steepened ramp-like banks and foreslopes of northern Laurentia (Canadian Arctic Archipelago; Narbonne and Dixon, 1984; Dixon and Graf, 1992; Brunton and Dixon, 1994).

Biostromal reefs occur through the Silurian, but are most prevalent in middle Ludlow and Pridoli carbonates that appear to have been deposited in intracratonic, shallow-marine, mid- to distal-bank settings (Figures 1, 2). Middle Llandovery (Aeronian; Figure 1) coral-stromatoporoid-dominated biostromes have been described from the Baltic carbonate bank (Estonia; Nestor, 1984). Among the most carefully documented Silurian biostromes are those of the middle Ludlow eastern facies of the Hemse beds of Gotland (Kershaw, 1993; Kershaw and Keeling, 1994). These tabular masses may represent adaptations by Silurian reef-building metazoans shallow, generally muddier carbonate-bank environments. Examples known from the Ludlow–Pridoli Barlow Inlet Formation of the Canadian Arctic Islands are up to 5 m-thick and are traceable along coastal sections for almost 10 km (Brunton and Dixon, 1991a). These bedded stromatoporoid-colonial rugose coral-dominated masses were established in an apparently normal marine environment, but were affected by prolonged stillstand or near-stillstand conditions, and possibly grew under stressed conditions. Many of these distal-shelf biostromes form the lower parts of shallowing-up cycles, and are overlain

by megalodont bivalve-rich units, which cap the biostromes and represent more restricted lagoonal environments (see also de Freitas et al., 1993b). These Ludlow and Pridoli shallowing-up packages may be regarded as Silurian “löfer-like” cyclic units.

CARBONATE BANKS, REEF POSITIONS AND TECTOPHASES

Three main carbonate bank geometries appear to be present in Silurian successions: 1) linear, fault-scarp margins with sharp transitions between sparsely reef-bearing shallow-marine carbonate bank facies and basinal, deep-water, turbiditic, muddy facies (e.g., Llandovery–Wenlock successions in North Greenland and eastern Ellesmere Island and Nevada [Hurst, 1980, 1981; Hurst and Kerr, 1982; and Hurst et al., 1985]); 2) ramp-like open (unrestricted ocean current flow) banks or distally steepened ramps, characterized by sinuous boundaries between prograding, shallow-marine, reef-bearing, bank facies and onlapping–offlapping organic-rich, graptolite-bearing, muddy basinal facies; and 3) relatively small carbonate shelves (fringing reefs?) adjacent to island arc complexes (see Soja, 1993). Carbonate “ramp-like” bank geometries are common in Silurian epeiric seas for at least Llandovery–middle Ludlow successions (e.g., Urals [Cherkesova, 1970; Antoshkina, 1996]; Midcontinent region, U.S.A. [Huh et al., 1977; Briggs et al., 1980; Droste and Shaver, 1985; Coburn, 1986]; Gaspé region, eastern Canada [Bourque et al., 1986; Lavoie et al., 1992]; Hudson Bay region [Suchy and Stearn, 1992]; Canadian Arctic Islands and North Greenland [Sodero and Hobson, 1979; Hurst, 1981; Hurst and Surlyk, 1984; Narbonne and Dixon, 1984; de Freitas, 1991]; Baltic region [Laufeld and Bassett, 1981; Kaljo et al., 1991]; Alaska [Soja, 1993]; Nevada [Hurst et al., 1985]; Texas [Ruppel, 1993]).

Extensive shelf-margin, stromatoporoid-calcimicrobial reefs in Baltica and Laurentia mark a significant change in carbonate bank geometry from ramp-like sequences to reef-rimmed in the late Ludlow (Brunton and Dixon, 1991a; Kaljo et al., 1991). The lateral differentiation of lithofacies in upper Ludlow successions reflects increased subsidence rates following the Salinic-2 disturbance (Figure 3). Deposition rates increased during the late Ludlow in Laurentia–Baltica (Christiansen and Hansen, 1989; Brett et al., 1990; Kaljo et al., 1991; Kemp, 1991).

The Ludlow appears to have been a time of extensive mixed terrigenous and carbonate mud deposition. Examples include the regionally extensive (i.e., for hundreds of kilometers) nodular limestone facies and

FIGURE 6—(opposite) Geometry, major skeletal metazoans, succession, and lithofacies of Late Silurian (Ludlow–Pridoli) reefs from Laurentia and Baltica. Sizes of letter abbreviations for metazoans in reflect skeletal volume in reefs. Geometry of some reefs varies with paleogeographic setting, especially reefs with a “keep-up” style of aggradation.

scattered sponge-coral-microbial mounds of the Douro Formation in the Canadian Arctic Archipelago, equivalent-age Greben Horizon nodular limestones and mounds (that extend for more than 1,500 km along the Urals), and the type Ludlow at Wenlock Edge, which shows mixed nodular limestone lithofacies.

Dendroid stromatoporoids (amphiporids) and favositids first appeared in the Ludlow, perhaps in response to these muddy seascapes. Amphiporids occur in some shelf-edge reefs and in inferred back-reef lagoonal settings in late Ludlow partially reef-rimmed carbonate banks of the Urals, Asia, Canadian Arctic Islands, and eastern Canada (Gaspé), and by the Pridoli were present in Podolia. This facies, in combination with bank-margin reef complexes, forms part of a suite of bank lithofacies that show a Devonian carbonate-bank archetype (Brunton and Dixon, 1991b; see Burchette, 1981).

DISCUSSION

The temporal correlation between Secundo oceanic episodes (S-States), transgressions, and major reef-building episodes suggests that climate was a major controlling factor in the paleogeographic extent and duration of Silurian reef growth. The Jeppsson (1990) oceanic model, which relates the CO₂ storage capacity of Silurian oceans to temperature changes, may partly explain the nature of plankton distribution and carbonate bank sedimentation in some Llandovery–Ludlow successions.

Reef initiation appears to match deepening phases and thus early sea-level highstand conditions. Accommodation space is vital for reef growth (i.e., aggradation and/or expansion and progradation). Regional rises in relative sea-level allow for expansion of intracratonic banks (ecospace expansion) and enable reef growth to become established. Silurian reef community shallowing-up trends and community replacements may be attributed to the skeletal precipitation of epibenthic metazoans and accumulation of their eroded particulate matter, in combination with early marine cementation (e.g., reef data in James and Macintyre, 1985; Copper and Brunton, 1991; Brunton and Copper, 1994), and to episodic growth and periodic exposure (karstification) during development of thicker (a few to tens of meters) composite-reef structures (e.g., so-called “pinnacle” reef structures). The result of prolonged stillstand conditions or shoaling conditions would likely be the establishment of extensive tabular reefs (biostromes) and decline of patch-reef growth, as observed in many Late Silurian successions.

The existence and duration of S- and P-States in the Llandovery–Pridoli have been inferred from conodont faunal turnovers, data from other fossil groups, and sedi-

mentological observations. Durations of S- and P-State oceanic conditions were highly variable through the Silurian (Figures 2, 3). S-State oceans appear to have had the longest durations in the Llandovery and Ludlow. The Wenlock shows the greatest number of oceanic state reversals, with four S- and P-State couplets in a time span of ca. 5 Ma. These short-lived (ca. 1 Ma) oceanic states are perhaps indicative of the greatest oceanic and climatic stability in the Silurian (Figure 3). The Wenlock also coincides with the acme of Silurian reef development (Figures 1, 2).

The length of the Pridoli, which has two S-State oceans, seems to be the most contentious; estimates range from 2–10 Ma (Figure 3). If the duration of the Pridoli is limited to 2 Ma, then minimum estimates for carbonate-accumulation rates exceeded 300 B (1 B [Bubnoff]=1 mm/1000 yrs). There are at least 700 m of Pridoli shallow-water carbonates in the Barlow Inlet Formation, Cornwallis Island, Canadian Arctic (Brunton and Dixon, 1991a). In the North Greenland foldbelt, estimates for Silurian carbonate bank deposition rates increased through the Silurian from a relatively slow 15–20 B in the Early Silurian to up to 150 B during the Ludlow (Christiansen and Hansen, 1989, p. 73). Deposition rates of Upper Silurian carbonates from central Laurentia (Michigan and northern Appalachians) are estimated to be ca. 25–100 B (Table 3 of Enos, 1991; presumably based on a ca. 5 Ma duration of the Pridoli), and about 13 B for so-called “pinnacle” reefs in the Michigan Basin (Sarg, 1988). The increased deposition rates along the perimeters of Laurentia and Baltica coincide with the onset of a second major tectophase in the late Ludlow. Significant lithofacies differentiation in upper Ludlow carbonate bank-margin successions reflects a biologic response to this regionally extensive but short-lived event.

CONCLUSIONS

Eight global reef-building episodes of different duration and paleogeographic extent are recognized for the Silurian. Extensive Wenlock and late Ludlow reef tracts are recognized in the various epeiric seas that spanned the paleoequatorial region. Late Silurian reef tracts show the greatest paleogeographic extent; perhaps this was a biologic response to increasing global surface ocean temperatures and, in part, to the gradual movement of additional carbonate banks and associated shallow epeiric seascapes into equatorial regions through the Silurian.

The major controls on reef development appear to have been climate and tectonism. Climatic amelioration through the early Llandovery, in conjunction with the appearance of regionally extensive shallow-marine epeiric seas in the late Telychian, facilitated the greatest diversifica-

tion of epibenthic reef-building metazoans recorded in the Silurian. This rapid increase in diversity followed the first major erosional phase associated with the Salinic disturbance (Salinic-1). Subsequent Wenlock S-State oceans, which dominated the epoch and lasted on the order of 4–5 Ma, promoted the establishment of extensive “carbonate factories” that featured diverse heterotroph-based and photoautotroph-dominated epibenthic invertebrate associations. The acme of Silurian reef growth was in the Wenlock.

Stromatoporoids became the main skeletal epibenthic invertebrates of late Ludlow and many Pridoli reefs—this trend continued and became more pronounced in the Devonian. Calcareous algae, calcimicrobes, and sponges also show evolutionary and environmental diversification through the Silurian. Physical and oceanographic changes during the late Wenlock, and associated step-down extinctions of numerous Wenlock reef invertebrates and planktic and nektonic faunas, may have enabled calcimicrobes and algae to play a much more substantial role in Late Silurian reef development. Calcimicrobes and calcareous algae helped construct the largest Silurian bank-margin complexes and bioherms. These biotic shifts or community replacements appear to have been biologic responses to continued climatic warming, increased mud and evaporation-induced deposition, a second tectophase of the Salinic disturbance, and subsequent global sea-level stillstand conditions through the Pridoli.

ACKNOWLEDGMENTS

FRB thanks Post-Doctoral Fellowship supervisor N.P. James for funding aspects of this research through an NSERC Operating Grant. Funding also came from industry and government grants and scholarships to FRB during graduate work. The Polar Continental Shelf Project and, in particular, the field operations personnel in Resolute, Cornwallis Island, are thanked for their logistic support. Sincere thanks are extended to the Silurian researchers both cited and contacted at the James Hall meeting for their help in gathering the data used to plot reef positions and biotic constituents. We also thank C.E. Brett and R.J. Elias for their constructive critiques. (The editors note the following contributions: F. Brunton and P. Copper contributed \$300; O. Dixon contributed \$500; and L. Smith contributed \$100.)

REFERENCES

ALDRIDGE, R.J., L. JEPSSON, and K.J. DORNING. 1993. Early Silurian oceanic episodes and events. *Journal of the Geological Society of London*, 150:501–513.

ALEKSEEVA, R.E. 1992. Early Devonian paleozoogeographic regions of Eurasia (based on brachiopods). *Paleontological Journal*, 26:1–14.

ANTOSHKINA, A.I. 1996. Silurian reefs in the north-east of the European platform, p. 24b. *In* The James Hall Symposium. Second International Symposium on The Silurian System, University of Rochester.

BAY, T.A. 1983. The Silurian of the northern Michigan Basin, p. 53–72. *In* P.M. Harris (ed.), *Carbonate Buildups—A Core Workshop*. Society of Economic Paleontologists and Mineralogists, Core Workshop No. 4, Dallas.

BOUCOT, A.J. 1985. Late Silurian–Early Devonian biogeography, provincialism, evolution and extinction. *Philosophical Transactions of the Royal Society, London*, B309:323–339.

———. 1990. Silurian biogeography, p. 191–196. *In* W.S. McKerron and C.R. Scotese (eds.), *Palaeozoic Palaeogeography and Biogeography*. Geological Society, Memoir 12.

BOURQUE, P.-A. 1989. Silurian reefs, p. 245–250. *In* H.H.J. Geldsetzer, N.P. James and G.E. Tebbutt (eds.), *Reefs, Canada and Adjacent Areas*. Canadian Society of Petroleum Geologists, Memoir 13.

———, G. AMYOT, A. DESROCHERS, H. GIGNAC, C. GOSSELIN, G. LACHAMBRE, and J.-Y. LALIBERTE. 1986. Silurian and Lower Devonian reef and carbonate complexes of the Gaspé Basin, Québec—a summary. *Bulletin of Canadian Petroleum Geology*, 34:452–489.

BRETT, C.E. 1984. Autecology of Silurian pelmatozoan echinoderms, p. 87–120. *In* M.G. Bassett and J.E. Lawson (eds.), *Autecology of Silurian Organisms*. Special Papers in Palaeontology 32.

———. 1991. Organism-sediment relationships in Silurian marine environments, p. 301–344. *In* M.G. Bassett, P.D. Lane, and D. Edwards (eds.), *The Murchison Symposium: Proceedings of an International Conference on The Silurian System*. Special Papers in Palaeontology 44.

———, W.M. GOODMAN, AND S.T. LODUCA. 1990. Sequences, cycles, and basin dynamics in the Silurian of the Appalachian Foreland Basin. *Sedimentary Geology*, 69:191–244.

BRIGGS, L.I., D. GILL, D.Z. BRIGGS, and R.D. ELMORE. 1980. Transition from open marine to evaporite deposition in the Silurian Michigan Basin, p. 253–270. *In* A. Nissenbaum (ed.), *Hypersaline Brines and Evaporitic Environments*. Elsevier, Amsterdam.

BRUNTON, F.R., and P. COPPER. 1994. Paleogeologic, temporal, and spatial analysis of Early Silurian reefs of the Chicotte Formation, Anticosti Island, Quebec, Canada. *Facies*, 31:57–80.

———, AND O.A. DIXON. 1991a. Latest Silurian reef, mudmound and platform development: a response to sea level changes and/or tectonics in the Boothia Uplift region, Canadian Arctic Archipelago. *Geological Society of America, Abstracts with Programs*, 23(3):5.

———, and ———. 1991b. Distribution and morphologic characters of stromatoporoids in a Late Silurian carbonate platform succession, Canadian Arctic, p. 10, 11. *In* 6th International Symposium on Fossil Cnidaria including Archaeocyatha and Porifera, Münster.

———, AND ———. 1994. Siliceous sponge-microbe biotic associations and their recurrence through the Phanerozoic as reef mound constructors. *Palaos*, 9:370–387.

BURCHETTE, T.P. 1981. European Devonian reefs: a review of current concepts and models, p. 85–142. *In* D.F. Toomey (ed.), *European Fossil Reef Models*. Society of Economic Paleontologists and Mineralogists, Special Publication 30.

CHERKESOVA, S.V. 1970. The Greben Horizon of the Silurian of Vaigach, p. 5–23. *In* S.V. Cherkesova (ed.), *Stratigrafiya i Fauna siluriiskikh Otlozhenii Vaigacha*. Nauchno Issledovatel'skii Institut Geologii Arktiki, Leningrad.

- CHRISTIANSEN, F. G., AND K. HANSEN. 1989. Timing of thermal episodes, p. 73–77. *In* F.G. Christiansen (ed.), *Petroleum Geology of North Greenland*. Grønlands Geologiske Undersøgelse, Bulletin 158.
- CLOUGH, J.G., AND R.B. BLODGETT. 1989. Silurian–Devonian algal reef mound complex of southwest Alaska, p. 404–407. *In* H.H.J. Geldsetzer, N.P. James and G.E. Tebbutt (eds.), *Reefs, Canada and Adjacent Areas*. Canadian Society of Petroleum Geologists, Memoir 13.
- COBURN, G.W. 1986. Silurian of the Illinois Basin: A carbonate ramp. *Oil and Gas Journal*, 84:96–100.
- COPPER, P. 1994. Ancient reef ecosystem expansion and collapse. *Coral Reefs*, 13:3–11.
- , AND F.R. BRUNTON. 1991. A global review of Silurian reefs, p. 225–259. *In* M.G. Bassett, P.D. Lane, and D. Edwards (eds.), *The Murchison Symposium: Proceedings of an International Conference on the Silurian System*. Special Papers in Palaeontology 44.
- CROWLEY, D.J. 1973. Middle Silurian patch reefs in Gasport Member (Lockport Formation), New York. *American Association of Petroleum Geologists Bulletin*, 57:283–300.
- CUFFEY, R.J. 1985. Expanded reef-rock textural classification and the geologic history of bryozoan reefs. *Geology*, 13:307–310.
- CUMINGS, E.R. 1932. Reefs or bioherms? *Geological Society of America Bulletin*, 43:331–352.
- DE FREITAS, T.A. 1991. Stratigraphy, mud buildups, and carbonate platform development of the Upper Ordovician to Lower Devonian sequence, Ellesmere, Hans, and Devon Islands, Arctic Canada. Unpublished Ph.D. dissertation, University of Ottawa, Ottawa, 431 p.
- , F.R. BRUNTON, AND T. BERNECKER. 1993a. Silurian megalodont bivalves of the Canadian Arctic and Australia: Palaeoecology and evolutionary significance. *Palaios*, 8:450–464.
- , O.A. DIXON, AND U. MAYR. 1993b. Silurian pinnacle reefs of the Canadian Arctic. *Palaios*, 8:172–182.
- DIXON, O.A., AND G.C. GRAF. 1992. Upper Silurian reef mounds on a shallowing carbonate ramp, Devon Island, Arctic Canada. *Bulletin of Canadian Petroleum Geology*, 40:1–23.
- DROSTE, J.B., AND R.H. SHAVER. 1985. Comparative stratigraphic framework for Silurian reefs—Michigan Basin to surrounding platforms, p. 73–93. *In* K.R. Cercone and J.M. Budai (eds.), *Ordovician and Silurian Rocks of the Michigan Basin and its Margins*. Michigan Basin Geological Society, Special Paper 4.
- ENOS, P. 1991. Sedimentary parameters for computer modeling, p. 63–99. *In* E.K. Franseen, W.L. Watney, C.G. St. C. Kendall, and W. Ross (eds.), *Sedimentary Modeling: Computer Simulations and Methods for Improved Parameter Definition*. Kansas Geological Survey, Bulletin 233.
- ETTENSÖHN, F.R. 1994. Tectonic control on formation and cyclicity of major Appalachian unconformities and associated stratigraphic sequences, p. 217–242. *In* J.M. Dennison and F.R. Ettensöhn (eds.), *Tectonic and Eustatic Controls on Sedimentary Cycles*. Concepts in Sedimentology and Paleontology No. 4.
- FAY, I., AND P. COPPER. 1982. Early Silurian bioherms in the Manitoulin Formation of Manitoulin Island. *Third North American Paleontological Convention, Proceedings*, 1:159–163.
- FORDHAM, B.G. 1992. Chronometric calibration of mid-Ordovician to Tournaisian conodont zones: a compilation from recent graphic-correlation and isotope studies. *Geological Magazine*, 129:709–721.
- FLÜGEL, E., AND E. FLÜGEL-KÄHLER. 1992. Phanerozoic reef evolution: basic questions and data base. *Facies*, 26:167–278.
- FRIEDMAN, G.M., AND D.C. KOPASKA-MERKEL. 1991. Late Silurian pinnacle reefs of the Michigan Basin, p. 89–100. *In* P.A. Catocinos and P.A. Daniels, Jr. (eds.), *Early Sedimentary Evolution of the Michigan Basin*. Geological Society of America, Special Paper 256.
- GILL, D. 1979. Differential entrapment of oil and gas in Niagara pinnacle-reef belt of northern Michigan. *American Association of Petroleum Geologists Bulletin*, 63:608–620.
- . 1985. Depositional facies of Middle Silurian (Niagara) pinnacle reefs, Belle River Mills gas field, Michigan Basin, southeastern Michigan, p. 123–139. *In* P.O. Roehl and P.W. Choquette (eds.), *Carbonate Petroleum Reservoirs: Casebooks in Earth Sciences*. Springer-Verlag, New York.
- . 1994. Niagara reefs of northern Michigan, Part 1: exploration portrait. *Journal of Petroleum Geology*, 17:99–110.
- GRADSTEIN, F.M., AND J. OGG. 1996. A Phanerozoic timescale. *Episodes*, 19 (1–2).
- GRAHN, Y., AND M.V. CAPUTO. 1992. Early Silurian glaciations in Brazil. *Palaeogeography, Palaeoclimatology, Palaeoecology*, 99:9–15.
- HARLAND, W.B., R.L. ARMSTRONG, A.V. COX, L.E. CRAIG, A.G. SMITH, AND D.G. SMITH. 1990. *A Geological Timescale 1989*. Cambridge University Press, Cambridge.
- HEWITT, M.C., AND R.J. CUFFEY. 1985. Lichenaliid-fistuliporid crust-mounds (Silurian, New York–Ontario). Typical Early Palaeozoic bryozoan reefs, p. 599–604. *In* *Proceedings of the Fifth International Coral Reef Congress, Tahiti*.
- HUH, J.M., L.I. BRIGGS, AND D. GILL. 1977. Depositional environments of the Niagara–Salina pinnacle reefs in the northern shelf of the Michigan basin, p. 1–21. *In* J.H. Fischer (ed.), *Reefs and Evaporites*. American Association of Petroleum Geologists, Studies in Geology 5.
- HURST, J.M. 1980. Paleogeographic and stratigraphic differentiation of Silurian carbonate buildups and biostromes of North Greenland. *American Association of Petroleum Geologists Bulletin*, 64:527–548.
- . 1981. Platform edge and slope relationships: Silurian of Washington Land, North Greenland and comparison to Arctic Canada. *Bulletin of Canadian Petroleum Geology*, 29:408–419.
- , AND J.W. KERR. 1982. Upper Ordovician to Silurian facies patterns in eastern Ellesmere Island and western North Greenland and their bearing on the Nares Strait lineament, 137–145. *In* P.R. Dawes and J.W. Kerr (eds.), *Nares Strait and the Drift of Greenland: A Conflict in Plate Tectonics*. Meddelelser om Grønland, Geoscience 8.
- , AND F. SURLYK. 1984. Tectonic control of Silurian carbonate-shelf margin morphology and facies, North Greenland. *American Association of Petroleum Geologists Bulletin*, 68:1–17.
- , P.M. SHEEHAN, AND J.M. PANDOLFI. 1985. Silurian carbonate shelf and slope evolution in Nevada: history of faulting, drowning and progradation. *Geology*, 13:185–188.
- JAMES, N.P., AND I.G. MACINTYRE. 1985. Carbonate depositional environments, modern and ancient, Part I: reefs, zonation, depositional facies, and diagenesis. *Colorado School of Mines Quarterly*, 80:1–70.
- , AND H.H.J. GELDSETZER. 1989. Introduction, p. 1–8. *In* H.H.J. Geldsetzer, N.P. James, and G.E. Tebbutt (eds.), *Reefs, Canada and Adjacent Areas*. Canadian Society of Petroleum Geologists, Memoir 13.
- JAMIESON, R.A., AND C. BEAUMONT. 1988. Orogeny and metamorphism: a model for deformation and pressure–temperature–time paths with applications to the central and southern Appalachians. *Tectonics*, 7:417–445.
- JEPPSSON, L. 1987. Lithological and conodont distributional evidence for episodes of anomalous oceanic conditions during the Silurian, p. 129–145. *In* R.J. Aldridge (ed.), *Palaeobiology of Conodonts*. Ellis Horwood Ltd., Chichester.

- . 1990. An oceanic model for lithological and faunal changes tested on the Silurian record. *Journal of the Geological Society of London*, 147:663–674.
- . 1996. Silurian events—a review of the knowledge in 1996, p. 59. In *The James Hall Symposium. Second International Symposium on The Silurian System*, University of Rochester.
- , V. VIIRA, AND P. MÄNNIK. 1994. Silurian conodont-based correlations between Gotland (Sweden) and Saaremaa (Estonia). *Geological Magazine*, 131:201–218.
- JOHNSON, M.E. 1996. Stable cratonic sequences and a standard for Silurian eustasy, p. 203–211. In B.J. Witzke, G.A. Ludvigson and J.E. Day (eds.), *Paleozoic Sequence Stratigraphy: Views from the North American Craton*. Geological Society of America, Special Paper 306.
- KALJO, D., A.J. BOUCOT, R.M. CORFIELD, A. LE HERISSE, T.N. KOREN', J. KŘÍŽ, P. MÄNNIK, T. MÄRSS, V. NESTOR, R.H. SHAVER, D.J. SIVETER, AND V. VIIRA. 1995. Silurian bio-events, p. 173–224. In O.H. Walliser (ed.), *Global Events and Event Stratigraphy in the Phanerozoic*. Springer-Verlag, Berlin.
- , AND T. MÄRSS. 1991. Pattern of some Silurian bioevents. *Historical Biology*, 5:145–152.
- , H. NESTOR, AND R. EINASTO. 1991. Aspects of Silurian carbonate platform sedimentation, p. 205–224. In M.G. Bassett, P.D. Lane and D. Edwards (eds.), *The Murchison Symposium: Proceedings of an International Conference on The Silurian System*. Special Papers in Palaeontology 44.
- KEMP, A.E.S. 1991. Middle Silurian pelagic and hemipelagic sedimentation and palaeoceanography, p. 261–299. In M.G. Bassett, P.D. Lane and D. Edwards (eds.), *The Murchison Symposium: Proceedings of an International Conference on The Silurian System*. Special Papers in Palaeontology 44.
- KERSHAW, S. 1990. Stromatoporoid palaeobiology and taphonomy in a Silurian biostrome on Gotland, Sweden. *Palaeontology*, 33:681–705.
- . 1993. Sedimentation control on growth of stromatoporoid reefs in the Silurian of Gotland, Sweden. *Journal of the Geological Society of London*, 150:197–205.
- . 1994. Classification and geological significance of biostromes. *Facies*, 31:81–92.
- , AND M. KEELING. 1994. Factors controlling the growth of stromatoporoid biostromes in the Ludlow of Gotland, Sweden. *Sedimentary Geology*, 89:325–335.
- KLAAMAN, E., AND R. EINASTO. 1982. Coral reefs of Baltic Silurian (structure, facies relations), p. 35–40. In *Ecostratigraphy of the East Baltic Silurian*. Academy of Sciences of the Estonian SSR Institute of Geology, Valgus, Tallinn.
- KRASOV, V.I., S.A. STEPANOV, AND L.S. RATANOV. 1986. Middle Paleozoic reef systems in Siberia, p. 237–244. In D.L. Kaljo and E. Klaamann (eds.), *Theory and Practice of Ecostratigraphy*, Valgus, Tallinn.
- LANE, N.G. 1971. Crinoids and reefs, p. 1430–1443. In *Reef Organisms through Time*. Proceedings of the North American Paleontological Convention, Part J, Field Museum of Natural History, Chicago.
- LAUFELD, S., AND M.G. BASSETT. 1981. Gotland: The anatomy of a Silurian carbonate platform. *Episodes*, 4:23–27.
- LAVOIE, D., P.-A. BOURQUE, AND Y. HÉROUX. 1992. Early Silurian carbonate platforms in the Appalachian orogenic belt: the Sayabec-La Vieille formations of the Gaspé-Matapédia basin, Quebec. *Bulletin of Canadian Petroleum Geology*, 34:452–489.
- LEGGETT, J.K. 1978. Eustasy and pelagic regimes in the Iapetus Ocean during the Ordovician and Silurian. *Earth and Planetary Science Letters*, 41:163–169.
- LOWENSTAM, H.A. 1950. Niagaran reefs in the Great Lakes area. *Journal of Geology*, 58:430–487.
- MAZZULLO, S.J., K.E. ANDERSON-UNDERWOOD, C.D. BURKE, AND W.D. BISCHOFF. 1992. Holocene coral patch reef ecology and sedimentary architecture, northern Belize, Central America. *Palaios*, 7:591–601.
- MÄNNIK, P., AND V. VIIRA. 1993. Events in the conodont history during the Silurian in Estonia. *Proceedings of the Estonian Academy of Sciences*, 42:58–69.
- MESOLELLA, K.J. 1978. Paleogeography of some Silurian and Devonian reef trends, central Appalachian Basin. *American Association of Petroleum Geologists Bulletin*, 62:1607–1644.
- , J.D. ROBINSON, L.M. MCCORMICK, AND A.R. ORMISTON. 1974. Cyclic deposition of Silurian carbonates and evaporites in Michigan Basin. *American Association of Petroleum Geologists Bulletin*, 58:34–62.
- MEYERHOFF, A.A., A.J. BOUCOT, D. MEYERHOFF HULL, AND J.M. DICKENS. 1996. Phanerozoic Faunal and Floral Realms of the Earth: The Intercalary Relations of the Malvinokaffric and Gondwana Faunal Realms with the Tethyan Faunal Realm. Geological Society of America, Memoir 189.
- MCKERROW, W.S., R.ST.J. LAMBERT, AND L.R.M. COCKS. 1985. The Ordovician, Silurian, and Devonian Periods, p. 73–80. In N.J. Snelling (ed.), *The Chronology of the Geological Record*. Geological Society of London, Memoir 10.
- NARBONNE, G.M., AND O.A. DIXON. 1984. Upper Silurian lithistid sponge reefs on Somerset Island, Arctic Canada. *Sedimentology*, 31:25–50.
- NESTOR, H. 1984. Autecology of stromatoporoids in Silurian cratonic seas, p. 265–280. In M.G. Bassett and J.E. Lawson (eds.), *Autecology of Silurian Organisms*. Special Papers in Palaeontology 32.
- . 1990. Biogeography of Silurian stromatoporoids, p. 215–221. In W.S. McKerrrow and C.R. Scotese (eds.), *Palaeozoic Palaeogeography and Biogeography*. Geological Society of London, Memoir 12.
- . 1994. Main trends in stromatoporoid evolution during the Silurian. *Courier Forschungsinstitut Senckenberg*, 172:329–339.
- . 1995. Ordovician and Silurian reefs in the Baltic area, p. 39–47. In B. Lathuiliere and J. Geister (eds.), *Coral Reefs in the Past, Present and Future*. Publications du Service Géologique du Luxembourg, Luxembourg, Proceedings of the Second European Regional Meeting of the International Society for Reef Studies 29.
- NEUMANN, A.C., AND I. MACINTYRE. 1985. Reef response to sea level rise: keep-up, catch-up or give-up. *Proceedings of the Fifth International Coral Reef Symposium*, 3:105–110.
- RIDING, R. 1981. Composition, structure and environmental setting of Silurian bioherms and biostromes in northern Europe, p. 41–83. In D.F. Toomey (ed.), *European Fossil Reef Models*. Society of Economic Paleontologists and Mineralogists, Special Publication 30.
- RIDING, R., AND N. WATTS. 1991. The lower Wenlock reef sequence of Gotland: facies and lithostratigraphy. *Geologiska Föreningens i Stockholm Föreläsningar*, 113:343–372.
- RUPPEL, S.C. 1993. Depositional and diagenetic character of Hunton-equivalent rocks in the Permian Basin of West Texas, p. 91–106. In K.S. Johnson (ed.), *Hunton Group Core Workshop and Field Trip*. Oklahoma Geological Survey, Special Publication 93-4.
- SARG, J.F. 1988. Carbonate sequence stratigraphy, p. 155–160. In C.K. Wilgus, B.S. Hastings, H.W. Posamentier, J.C. Van Wagoner, C.A. Ross, and C.G.St.C. Kendall (eds.), *Sea-Level Changes: An Integrated Approach*. Society of Economic Paleontologists and Mineralogists, Special Publication 42.
- SCHUHMACHER, H., AND H. ZIBROWIUS. 1985. What is hermatypic? A redefinition of ecological groups in corals and other organisms. *Coral Reefs*, 4:1–9.

- SCOTese, C.R., AND W.S. MCKERROW. 1990. Revised world maps and introduction, p. 1–21. In W.S. McKerrrow and C.R. Scotese (eds.), *Palaeozoic Palaeogeography and Biogeography*. Geological Society of London, Memoir 12.
- SHARKOVA, T.T. 1986. Principles of reef development in the Silurian and Devonian basins of south Mongolia, p. 70–77. In T.A. Grunt and T.N. Smirnova (eds.), *Problems of Paleobiogeography of Asia*. Joint Soviet-Mongolian Expedition 29.
- SHAYER, R.H. 1977. Silurian reef geometry—new dimensions to explore. *Journal of Sedimentary Petrology*, 47:1409–1424.
- . 1991. A history of study of Silurian reefs in the Michigan Basin environs, p. 101–138. In P.A. Catocinos and P.A. Daniels, Jr. (eds.), *Early Sedimentary Evolution of the Michigan Basin*. Geological Society of America, Special Paper 256.
- , AND J.A. SUNDERMAN. 1989. Silurian seascapes: water depth, clinothems, reef geometry, and other motifs—a critical review of the Silurian reef model. *Geological Society of America Bulletin*, 101:939–951.
- , C.H. AULT, W.I. AUSICH, J.B. DROSTE, A. HOROWITZ, W.C. JAMES, S.M. OKLA, C.B. REXROAD, D.M. SUCHOMEL, AND J.R. WELCH. 1978. The Search for a Silurian Reef Model: Great Lakes Area. State of Indiana Department of Natural Resources Geological Survey Special Report 15, 36 p.
- SHISKIN, M.A. 1986. Stratigraphic facies models of the Silurian, Lower and Middle Devonian of the western slope of the Polar Urals, p. 186–192. In D.L. Kaljo and E. Klamann (eds.), *The Theory and Practice of Ecostratigraphy*. Valgus, Tallinn.
- SHUISKIL, V.P. 1975. Boundary layers of the Silurian and the Devonian in the region of Belyi Nos Cape in the Pai-Khoi, p. 105–118. In *Materials on the Paleontology of the Middle Paleozoic of the Urals and Kazakhstan*. USSR Academy of Sciences, Proceedings of the Institute of Geology and Geochemistry 117 (In Russian).
- . 1983. Upper Silurian and Lower Devonian Reef Complexes of the Western Slopes of the Urals. *Voprosy Ekosistemnogo Analiza, Akademiya Nauk, Sverdlovsk*, 83 p. (In Russian).
- SMITH, L. 1990. Karst episodes during cyclic development of Silurian reef reservoirs, southwestern Ontario, p. 69–88. In T.R. Carter (ed.), *Subsurface Geology of Southwestern Ontario—A Core workshop*. Ontario Petroleum Institute Inc., London.
- SMOSMA, R., J.M. CONRAD, AND T. MAXWELL. 1989. Stratigraphic traps in Silurian Lockport Dolomite of Kentucky. *American Association of Petroleum Geologists Bulletin*, 73:874–886.
- SODERMAN, J.W., AND A.V. CAROZZI. 1963. Petrography of algal bioherms in Burnt Bluff Group (Silurian), Wisconsin. *American Association of Petroleum Geologists Bulletin*, 47:1682–1708.
- SODERO, D.E., AND J.P. HOBSON. 1979. Depositional facies of Lower Paleozoic Allen Bay carbonate rocks and contiguous shelf and basin strata, Cornwallis and Griffith Islands, Northwest Territories, Canada. *American Association of Petroleum Geologists Bulletin*, 63:1059–1091.
- SOJA, C.M. 1991. Origin of Silurian reefs in the Alexander terrane of southeastern Alaska. *Palaaios*, 6:111–125.
- . 1993. Carbonate platform evolution in a Silurian oceanic island: a case study from Alaska's Alexander terrane. *Journal of Sedimentary Petrology*, 63:1078–1088.
- . 1994. Significance of Silurian stromatolite-sphinctozoan reefs. *Geology*, 22:355–358.
- , AND R. RIDING. 1993. Silurian microbial associations from the Alexander terrane, Alaska. *Journal of Paleontology*, 67:728–738.
- SUCHY, D.R., AND C.W. STEARN. 1992. Lower Silurian sequence stratigraphy and sea-level history of the Hudson Bay Platform. *Bulletin of Canadian Petroleum Geology*, 40:335–355.
- WANG H. AND CHEN J. 1991. Late Ordovician and early Silurian rugose coral biogeography and world reconstruction of palaeocontinents. *Palaeogeography, Palaeoclimatology, Palaeoecology*, 86:3–21.
- WATKINS, R. 1993. The Silurian (Wenlockian) reef fauna of southeastern Wisconsin. *Palaaios*, 8:325–338.
- WATTS, N.R. 1988. Carbonate particulate sedimentation and facies within the Lower Silurian Höglint patch reefs of Gotland, Sweden. *Sedimentary Geology*, 59:93–113.
- WITZKE, B.J. 1988. Silurian benthic invertebrate associations of eastern Iowa and their paleoenvironmental significance. *Wisconsin Academy of Sciences, Arts and Letters*, 71:21–47.

PART IV: ISOTOPE STUDIES

HIGH-RESOLUTION SILURIAN $^{87}\text{Sr}/^{86}\text{Sr}$ RECORD: EVIDENCE OF EUSTATIC CONTROL OF SEAWATER CHEMISTRY?

STEPHEN C. RUPPEL¹, ERIC W. JAMES², JAMES E. BARRICK³, GODFREY NOWLAN⁴,
AND T.T. UYENO⁴

¹Bureau of Economic Geology, The University of Texas at Austin, Austin, Texas 78713,

²Department of Geological Sciences, The University of Texas at Austin, Austin, Texas 78712,

³Department of Geosciences, Texas Tech University, Lubbock, Texas 79409, and

⁴Geological Survey of Canada, Calgary, Alberta T2L 2A7

ABSTRACT—Comparison of Silurian seawater $^{87}\text{Sr}/^{86}\text{Sr}$ data with recent interpretations of sea-level history suggest that higher-frequency fluctuations in $^{87}\text{Sr}/^{86}\text{Sr}$ may be causally related to eustasy. $^{87}\text{Sr}/^{86}\text{Sr}$ data were derived from conodont elements from localities in North America and Europe that represent thirteen of fourteen defined Silurian conodont zones. Laboratory studies of conodont elements show that they can provide an accurate record of original seawater $^{87}\text{Sr}/^{86}\text{Sr}$, which in turn provides the first high-resolution record of seawater chemistry for the Silurian and shows several higher-frequency cycles superimposed on a gradual longer-term rise in $^{87}\text{Sr}/^{86}\text{Sr}$ for the period. Higher-frequency cycles have a duration of about one conodont zone, and many correlate with sequence boundaries known globally. Sequence bases that mark sea-level rise consistently appear to correlate with falls in $^{87}\text{Sr}/^{86}\text{Sr}$. This suggests a eustatic control of short fluctuations in sea-water strontium isotope chemistry.

INTRODUCTION

The continually changing but cyclic nature of strontium isotope ratios in the world's oceans during the Phanerozoic was well established in the 1970s and 1980s (e.g., Peterman et al., 1970; Veizer and Compston, 1974; Burke et al., 1982). Documentation of these secular changes in seawater $^{87}\text{Sr}/^{86}\text{Sr}$ has provided the basis for a powerful tool for relative age-dating of marine sedimentary deposits. In recent years, a large number of researchers have utilized published secular $^{87}\text{Sr}/^{86}\text{Sr}$ trends to define the relative age and timing of complex depositional and diagenetic events in the rock record. $^{87}\text{Sr}/^{86}\text{Sr}$ trends for the Cenozoic and much of the Mesozoic section are now par-

ticularly well known due to several detailed, high-resolution studies completed in recent years (e.g., DePaolo and Ingram, 1985; Koepnick et al., 1986; Hess et al., 1986; Hodell et al., 1990, 1991; Jones et al., 1994a, 1994b).

Until recently, $^{87}\text{Sr}/^{86}\text{Sr}$ data for the Paleozoic (the most comprehensive of which are those of Burke et al., 1982) were too imprecise for accurate age determinations. Major problems with accurately defining seawater $^{87}\text{Sr}/^{86}\text{Sr}$ curves for the Paleozoic lie in the large uncertainties in timing and strontium isotope ratio because of imprecise sample ages and the difficulty of assessing the degree of diagenetic alteration.

In the past few years, several studies have contributed to the development of better-resolved $^{87}\text{Sr}/^{86}\text{Sr}$ changes for parts of the Paleozoic (Cummins and Elderfield, 1994; Ruppel et al., 1995; Bruckschen et al., 1995; Martin and MacDougall, 1995; Diener et al., 1996). All of these studies utilized modern, high-resolution instrumentation and carefully developed analytical techniques to obtain high-precision measurements of $^{87}\text{Sr}/^{86}\text{Sr}$ largely from conodont elements or brachiopod shells. Although some studies have concluded that conodont elements may not preserve an unaltered record of seawater $^{87}\text{Sr}/^{86}\text{Sr}$ (Cummins and Elderfield, 1994; Diener et al., 1996), Ruppel et al. (1995, 1996) and others (Martin and MacDougall, 1995; Holmden et al., 1996) have argued they can. Many of these recent high resolution studies have also reported higher-frequency cycles in $^{87}\text{Sr}/^{86}\text{Sr}$ (Cummins and Elderfield, 1994; Ruppel et al., 1995, 1996; Bruckschen et al., 1995; Diener et al., 1996).

We have documented the $^{87}\text{Sr}/^{86}\text{Sr}$ record for the Silurian based on conodont elements (Ruppel et al., 1996). In that report, we noted possible correlations between tentatively defined eustatic cycles and higher-

frequency cycles in $^{87}\text{Sr}/^{86}\text{Sr}$. We compare herein our original data with recently compiled sea-level history data for the Silurian (Johnson, 1996). This comparison makes an even stronger argument for a correlation between higher-frequency fluctuations in $^{87}\text{Sr}/^{86}\text{Sr}$ and eustasy. We also present data to support our claims: 1) that conodont elements can preserve an accurate record of original $^{87}\text{Sr}/^{86}\text{Sr}$ retrievable with proper analytical techniques; and 2) that conodont elements can be excellent materials on which to base the construction of accurate curves of seawater $^{87}\text{Sr}/^{86}\text{Sr}$ for the Paleozoic.

METHODS

The $^{87}\text{Sr}/^{86}\text{Sr}$ values of this report were obtained from conodont elements recovered from Silurian carbonate rock successions in Oklahoma, Tennessee, Texas, Quebec, and western Europe (Table 1). To ensure accurate relative placement of samples in a stratigraphic framework, conodont zonal determinations were made for all samples. Because the most unequivocal stratigraphic placement of samples is based on superposition, we concentrated our initial efforts on one section in Oklahoma. The Silurian section of the Hunton Group along U.S. Rte. 77 in southern Oklahoma contains a largely continuous record of all but the lowest part of the system (Barrick and Klapper, 1976, 1992). This succession was augmented with samples from other nearby localities in Oklahoma (Barrick and Klapper, 1976, 1992). Additional samples for the Wenlock Series came from the Wayne Formation in Tennessee (Barrick, 1983). As it contains four of the same conodont zones sampled in Oklahoma, the Wayne succession provides an important basis to compare $^{87}\text{Sr}/^{86}\text{Sr}$ values from geographically separated areas. Llandovery samples came primarily from the well-constrained and stratigraphically continuous succession of the Jupiter and Chicotte Formations on Anticosti Island, Quebec (Uyeno and Barnes, 1983). Supporting data for the Llandovery were obtained from selected samples from the Gaspé Peninsula of Quebec (Nowlan, 1983), Arkansas, Ohio, Sweden, England, and oil field cores from the Texas subsurface. All samples were correlated into the U.S. Rte. 77 section in Oklahoma by conodont zonation and superposition. We obtained and analyzed more than 60 samples from thirteen of the conodont zones recognized for the Silurian (Barrick and Klapper, 1976; Nowlan, 1983; Aldridge, 1985; Sweet, 1988; Jeppsson, 1988).

For the most part, we selected single conodont elements for analysis. Because elements typically show strontium concentrations of 2,000 to 4,000 ppm, we were routinely able to analyze single elements or fragments of elements that weighed as little as 10 micrograms. This

approach reduced the risk of error due to physical mixing of specimens and generally improved precision. Because some workers have concluded that thermal alteration can increase the likelihood of Sr exchange (Bertram et al., 1992; Cummins and Elderfield, 1994), we limited our sample selection to elements with conodont alteration indices (i.e., CAI; Epstein et al., 1977) less than 2.

All samples were weighed, transferred to Teflon screw-top vials, and cleaned in several changes of quartz-distilled water. Early in the project, we noticed that some elements were incompletely cleaned by the distilled water washes. These samples typically also produced $^{87}\text{Sr}/^{86}\text{Sr}$ values that were up to 0.000153 times more radiogenic than the residual conodont element material (Figure 1). Because of this, we conducted experiments to determine the best technique for further cleaning, and determined that the highest reproducibility was obtained by leaching samples in weak acetic acid before analysis. Successive leaching of single elements indicated that radiogenic strontium was efficiently removed by leaching for 12–16 hours in 0.5% acetic acid. Leaching beyond this point showed no significant difference in $^{87}\text{Sr}/^{86}\text{Sr}$ values between the leachate and residuum. Holmden et al. (1996) conducted similar leaching experiments that also showed that pre-analysis leaching is crucial for removing radiogenic strontium from surficial layers of conodont elements and for obtaining more accurate seawater $^{87}\text{Sr}/^{86}\text{Sr}$ values. After leaching, elements were rinsed in quartz-distilled water, dried at room temperature, and reweighed to determine the amount of material lost to leaching. Weight losses typically ranged from 2–45% of the original sample weight.

All subsequent procedures were performed under laminar flow HEPA-filtered air. Samples were rinsed in quartz-distilled water, and then dissolved in 20 microliters of concentrated nitric acid. Sample-bearing vials were capped, left on a 90° C hot plate for several hours, and then cooled. For chemical separation of Sr, we used the ion exchange resin Sr-SPEC 50 from Eichrom Industries in Darian, Illinois. Ion exchange columns were constructed from disposable polyethylene "eyedropper" pipettes. Pipette tubes were trimmed to accommodate 75 microliters of cleaned resin; the bottom was plugged with a porous polypropylene frit, and the bulb of the pipette cut to form a 2 ml reservoir. The columns were cleaned for several days in baths of warm 7N HNO_3 and 6N HCl. During ion exchange, 2.2 ml of 3.3N high-purity HNO_3 was added to the column after the dissolved sample to elute ions other than Sr. Blanks for the entire analytical procedure were less than 12 picograms of total Sr, which for these samples is insignificant.

Following ion exchange, samples were loaded onto Ta single filaments with phosphoric acid and run on a Finnegan MAT 261 mass spectrometer. Data were cor-

TABLE 1—⁸⁷Sr/⁸⁶Sr data from Silurian conodont elements.

Conodont Zone	Location	Sample Number	Formation	⁸⁷ Sr/ ⁸⁶ Sr	Precision (2 σ)	Lithology
<i>Ou. elegans detorta</i>	Oklahoma	I35-2AA	Henryhouse	0.708729	0.000021	aW
<i>Ou. elegans detorta</i>	Oklahoma	77-40A	Henryhouse	0.708708	0.000012	aW
<i>Ou. elegans detorta</i>	Oklahoma	77-39	Henryhouse	0.708711	0.000011	aW
<i>Ou. elegans detorta</i>	Oklahoma	77-37	Henryhouse	0.708717	0.000028	aW
<i>O. eosteinhornensis</i>	Oklahoma	ChiC A-28	Henryhouse	0.708703	0.000014	fW
<i>O. eosteinhornensis</i>	Oklahoma	77-36	Henryhouse	0.708722	0.000010	afW
<i>O. snajdri</i>	Oklahoma	Hickory Ck-13	Henryhouse	0.708732	0.000013	fW
<i>O. snajdri</i>	Sweden	Juves 3	Hamra	0.708724	0.000011	afW
<i>O. snajdri</i>	Oklahoma	77-34A	Henryhouse	0.708711	0.000010	afW
<i>O. snajdri</i>	Oklahoma	77-27	Henryhouse	0.708731	0.000009	fW
<i>O. snajdri</i>	Oklahoma	77-310	Henryhouse	0.708699	0.000010	sM
<i>Po. siluricus</i>	Oklahoma	77-307	Henryhouse	0.708689	0.000011	sM
<i>Po. siluricus</i>	Oklahoma	77-25	Henryhouse	0.708698	0.000008	sM
<i>A. ploeckensis</i>	England	England 4.8	Leintwardine	0.708696	0.000010	sM
<i>A. ploeckensis</i>	Oklahoma	77-305	Henryhouse	0.708671	0.000011	shale
<i>A. ploeckensis</i>	Oklahoma	77-304	Henryhouse	0.708659	0.000012	shale
<i>A. ploeckensis</i>	Oklahoma	77-303	Henryhouse	0.708608	0.000015	sM
<i>K. crassa</i>	Tennessee	Clifton 13	Wayne	0.708531	0.000010	sfP
<i>K. crassa</i>	Tennessee	Clifton 13 leach	Wayne	0.708554	0.000012	sfP
<i>K. crassa</i>	Oklahoma	77-301	Henryhouse	0.708549	0.000012	sM
<i>K. crassa</i>	Oklahoma	M2-1	Clarita	0.708463	0.000011	afW
<i>K. crassa</i>	Oklahoma	77-24	Clarita	0.708489	0.000027	afW
<i>K. stauros</i>	Oklahoma	77-22	Clarita	0.708446	0.000009	afW
<i>K. stauros</i>	Tennessee	Clifton 11	Wayne	0.708432	0.000011	afP
<i>K. stauros</i>	Tennessee	Clifton 11 leach	Wayne	0.708496	0.000015	afP
<i>K. stauros</i>	Oklahoma	Haragan Ck-9	Clarita	0.708428	0.000011	afW
<i>K. amsdeni</i>	Oklahoma	77-16	Clarita	0.708474	0.000012	fW
<i>K. amsdeni</i>	Oklahoma	Haragan Ck-4	Clarita	0.708370	0.000015	fW
<i>K. amsdeni</i>	Oklahoma	77-20 A	Clarita	0.708349	0.000010	fW
<i>K. amsdeni</i>	Tennessee	Centerville-9	Wayne	0.708349	0.000012	fP
<i>K. amsdeni</i>	Tennessee	Centerville-9 leach	Wayne	0.708341	0.000016	fP
<i>K. ranuliformis</i>	Tennessee	CA-103	Clarita	0.708379	0.000018	afW
<i>K. ranuliformis</i>	Tennessee	CA-103 leach	Clarita	0.708525	0.000013	afW
<i>K. ranuliformis</i>	Oklahoma	Haragan Ck 2	Clarita	0.708349	0.000015	fW
<i>K. ranuliformis</i>	Oklahoma	Haragan Ck 2 leach	Clarita	0.708388	0.000012	fW
<i>K. ranuliformis</i>	Oklahoma	77-14	Clarita	0.708420	0.000012	fW
<i>K. ranuliformis</i>	Oklahoma	77-12A	Clarita	0.708377	0.000020	fW
<i>K. ranuliformis</i>	Oklahoma	77-11	Clarita	0.708334	0.000011	shale
<i>P. amorphognathoides</i>	England	Hughly Brook F	Purple Shales	0.708368	0.000012	shale
<i>P. amorphognathoides</i>	Tennessee	CA-102	Wayne	0.708365	0.000010	afW
<i>P. amorphognathoides</i>	Tennessee	CA-101A	Wayne	0.708363	0.000010	afW
<i>P. amorphognathoides</i>	Tennessee	CA-101A leach	Wayne	0.708399	0.000015	afW
<i>P. amorphognathoides</i>	Texas	SantaFe12656'	Fusselman	0.708319	0.000010	G
<i>P. celloni</i>	Oklahoma	M10-4	Cochrane	0.708073	0.000012	fW
<i>P. celloni</i>	Oklahoma	55-103	Cochrane	0.708064	0.000010	fW
<i>P. celloni</i>	Arkansas	Love Hollow	Brassfield	0.708153	0.000008	G
<i>P. celloni</i>	Anticosti	267	Chicotte	0.708309	0.000011	G
<i>P. celloni</i>	Anticosti	264	Jupiter	0.708267	0.000011	M-W
<i>D. staurognathoides</i>	England	Gullet 2	Wych	0.708268	0.000010	G
<i>D. staurognathoides</i>	Anticosti	260	Jupiter	0.708236	0.000011	M-W
<i>D. staurognathoides</i>	Anticosti	292	Jupiter	0.708248	0.000010	M
<i>D. staurognathoides</i>	Anticosti	281	Jupiter	0.708220	0.000012	M
<i>D. staurognathoides</i>	Anticosti	238	Jupiter	0.708172	0.000009	M
<i>D. kentuckyensis</i>	Ohio	Brassfield (Cooper)	Brassfield	0.708049	0.000008	fW
<i>D. kentuckyensis</i>	Texas	Pegasus 12005'	Fusselman	0.707986	0.000011	G

⁸⁷Sr/⁸⁶Sr ratios are corrected to a running average of NBS 987 standards analyzed before, during, and after sample runs. NBS 987 averaged 0.710255 ± 0.000029 at the 95% confidence level (n = 15). Modern seawater Sr run concurrently yielded 0.709172 ± 0.000008 at the 95% confidence level (n = 6). "leach" denotes analyses of acid leachates. Lithology codes: M, mudstone; W, wackestone; P, packstone; G, grainstone; a, argillaceous, s, silty; f, fossiliferous. Conodont genera: A. = *Ancoradella*, D. = *Distomodus*, K. = *Kockella*, O. = *Ozarkodina*, Ou. = *Oulodus*, P. = *Pteraspithodus*, Po. = *Polygnathoides*.

rected for mass fractionation with an exponential law and an $^{86}\text{Sr}/^{88}\text{Sr}$ ratio of 0.1194. At least one NBS 987 standard and a modern seawater standard were run with each turret of samples. We noted minor instrumental drift during the course of the study. During this time, NBS 987 averaged 0.710255 ± 0.000029 (at the 95% confidence level, $n=15$). To calculate analytical precision, we averaged NBS 987 standards run in previous, current, and subsequent turrets, and then corrected the sample ratios of each turret by the difference between this running average of the value for the standard and the overall average. This procedure reduced the variation in the seawater standard from 0.709171 ± 0.000021 to 0.709176 ± 0.000016 (at the 95% confidence level, $n=14$). This compares very well with 2 sigma estimates of analytical reproducibility of ± 0.000022 to ± 0.000026 cited in earlier studies (Hodel et al., 1990; Miller et al., 1991; Martin and MacDougall, 1991; Jones et al., 1994a). Duplicate analyses were performed for 22 conodont samples. Average deviation from the mean was <0.000016 , and about equal to analytical precision (Figure 2).

We plotted our data (Table 1) against conodont zones, which are in turn correlated with graptolite zones (fide Johnson, 1996). In doing so, we purposely avoided relating $^{87}\text{Sr}/^{86}\text{Sr}$ to geochronology because of the large uncertainties associated with most estimates of geologic time for the Paleozoic. Plotting $^{87}\text{Sr}/^{86}\text{Sr}$ data against time can greatly obscure the true resolution possible with $^{87}\text{Sr}/^{86}\text{Sr}$ chemostratigraphy. Jones et al. (1994a) reached the same conclusion in their study of the Lower Jurassic, and similarly plotted their $^{87}\text{Sr}/^{86}\text{Sr}$ data against ammonite zones.

DEFINING SEAWATER $^{87}\text{Sr}/^{86}\text{Sr}$ CHEMISTRY

Fundamental to any reconstruction of the chemistry of the ancient oceans is the selection and analysis of samples that are chemically unaltered. In practice, virtually all sedimentary materials (i.e., sediments, cements, and fossils) have undergone variable degrees of diagenesis. This is especially true of the carbonate, phosphate, and evaporite minerals from which most $^{87}\text{Sr}/^{86}\text{Sr}$ data have been obtained. Cathode luminescence has been used by many to screen for diagenesis in rocks and fossils, but several studies have demonstrated significant chemical diagenesis even where physical evidence is lacking (Popp et al., 1986; Rush and Chafetz, 1990; Wadleigh and Veizer, 1992; Banner and Kaufman, 1994; W.B. Ward, personal commun., 1997). Owing to the difficulty in recognizing altered sample materials, the significance of most $^{87}\text{Sr}/^{86}\text{Sr}$ data must be evaluated by comparison with other

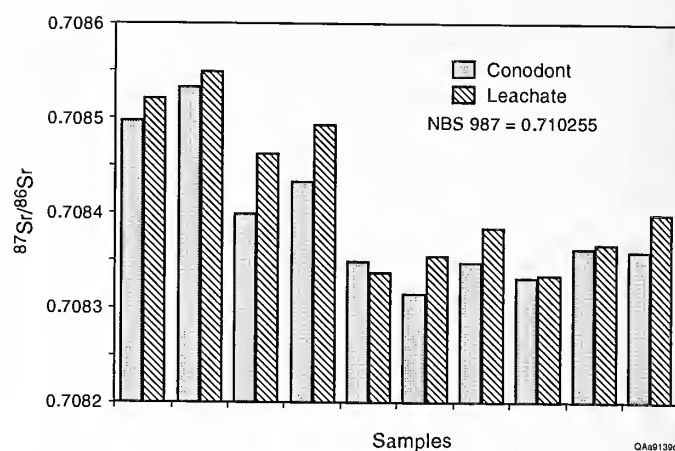


FIGURE 1—Variation in $^{87}\text{Sr}/^{86}\text{Sr}$ measurements from leachates and residual cores of conodont elements. Note that most leachates are radiogenic.

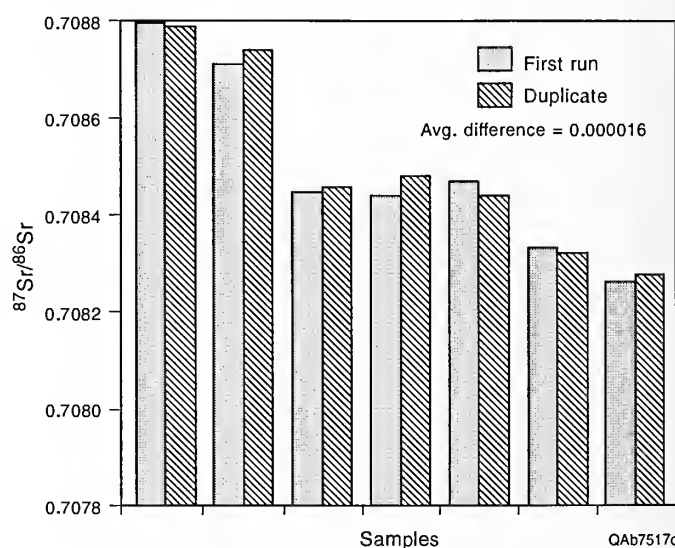


FIGURE 2—Variation among duplicate analyses of $^{87}\text{Sr}/^{86}\text{Sr}$ from conodont elements.

data. In general, it is assumed that lower $^{87}\text{Sr}/^{86}\text{Sr}$ values are closer to original sea water composition (Burke et al., 1982; Jones et al., 1994a). This is likely because shallow-water, nearshore sediments are more likely to be exposed to diagenetic fluids that carry radiogenic strontium from cratonic sources. If altered by diagenesis, these materials most commonly undergo isotopic shifts to higher or more radiogenic values. Because of the predisposition of sediments to become radiogenic, $^{87}\text{Sr}/^{86}\text{Sr}$ seawater isotope "curves" are typically drawn along the lowest $^{87}\text{Sr}/^{86}\text{Sr}$ data points in the data set, and are constantly susceptible to re-evaluation or modification as additional data become available.

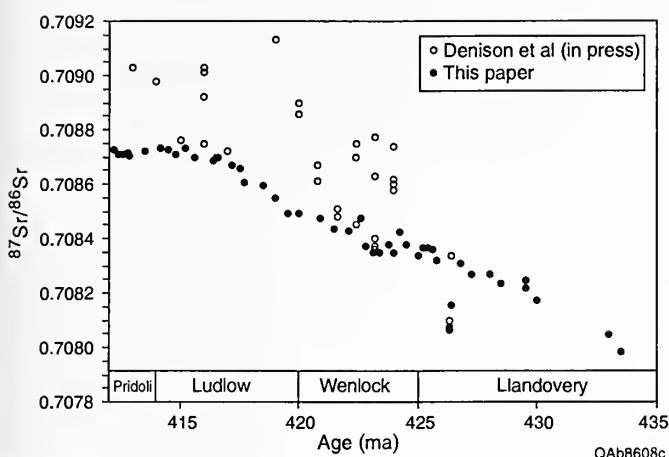


FIGURE 3—Comparison of Silurian $^{87}\text{Sr}/^{86}\text{Sr}$ data of this report with those of Burke et al. (1982) as redocumented by Denison et al. (In press).

One basis for assessing the validity of our data set is a comparison with other data sets. We have accordingly plotted our data with those of Burke et al. (1982), the only other comprehensive data set for the Silurian as recently upgraded by Denison et al. (In press; Figure 3). Although it is impossible to make an exact comparison because biostratigraphic information is absent for Burke et al.'s (1982) samples, it is nevertheless apparent that our data show less scatter and are much less radiogenic (Figure 3). Our data show an order of magnitude less variation among equivalent and adjacent samples, a variation that is typically within analytical reproducibility. The lack of scatter and lower radiogenic character of our data suggest that conodont elements have not been modified by post-depositional diagenesis, as were the predominately whole-rock limestone samples used for Burke et al.'s (1982) study, but instead preserve the original $^{87}\text{Sr}/^{86}\text{Sr}$ chemistry of Silurian seawater. Good agreement among our duplicate analyses of conodont elements (Figure 2) also supports this contention, as does the similarity of equivalent samples from different sample localities.

CONODONT RECORD OF SILURIAN SEA WATER $^{87}\text{Sr}/^{86}\text{Sr}$

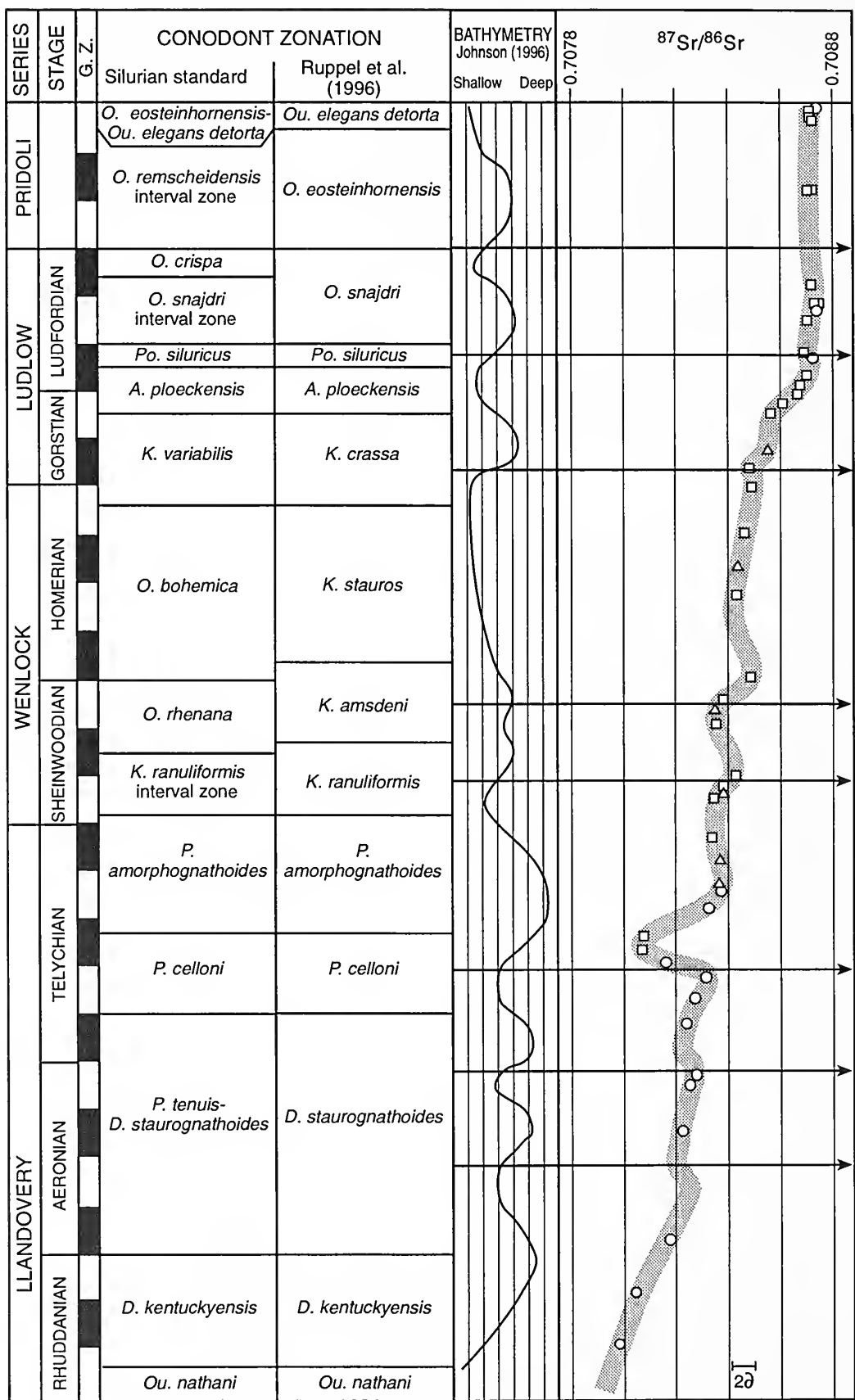
Our data reflect the general increase in $^{87}\text{Sr}/^{86}\text{Sr}$ ratios from the beginning to the end of the Silurian (Figures 3, 4) shown by earlier studies (e.g., Burke et al., 1982; Denison et al., In press) as part of a long-term cycle in $^{87}\text{Sr}/^{86}\text{Sr}$ that extends from the Late Ordovician to the Middle Devonian. Although we did not analyze samples from the lowermost Silurian *Ozarkodina nathani* Zone, our earlier

reported values from the uppermost Ordovician (Ruppel et al., 1996) imply a value of 0.7079 for the beginning of the Silurian as the approximate low point for this long-term cycle. This value is considerably lower than the approximate value of 0.7081 (adjusted to NBS 987 = 0.710255) of Burke et al. (1982). Our value of 0.7087 for the Silurian–Devonian boundary is similar to theirs. However, better correlations by conodonts suggest that the acme of the long-term Silurian–Devonian $^{87}\text{Sr}/^{86}\text{Sr}$ cycle occurs at the Silurian–Devonian boundary, not in the upper Silurian as shown by Burke et al. (1982).

As reported earlier (Ruppel et al., 1996), our data also show short-term variations in $^{87}\text{Sr}/^{86}\text{Sr}$ values during the Silurian. These variations are supported in most cases by more than one data point and, in several instances, by data from more than one locality (Figure 4). These short-term variations in $^{87}\text{Sr}/^{86}\text{Sr}$ values are cyclical with amplitudes of $1\text{--}1.5 \times 10^{-4}$, and are about an order of magnitude lower in amplitude than the long-term Silurian–Devonian $^{87}\text{Sr}/^{86}\text{Sr}$ cycle. The duration of these higher-frequency cycles cannot be determined with any precision because of uncertainties in geochronology. Most are approximately one conodont zone in duration (Ruppel et al., 1996). Although ages through the Silurian are poorly defined, recent estimates have suggested a duration of 26 Ma (Tucker and McKerrow, 1995) or 23 Ma (Johnson, 1996), and imply an average duration of about 2 Ma per conodont zone. Most higher-frequency $^{87}\text{Sr}/^{86}\text{Sr}$ cycles have amplitudes of about 1×10^{-4} , although the late Llandovery cycle has a much higher amplitude of about 3×10^{-4} . Similar higher-frequency $^{87}\text{Sr}/^{86}\text{Sr}$ cycles have recently been documented for both the Devonian (Diener et al., 1996) and the Mississippian (Cummins and Elderfield, 1994). Cycles from both of these studies appear to exhibit similar amplitudes (ca. $1\text{--}1.5 \times 10^{-4}$) and durations (ca. 1–1.5 Ma) by comparison with those reported herein. $^{87}\text{Sr}/^{86}\text{Sr}$ data reported by Diener et al. (1996; see also Bruckschen et al., 1995), which are based on analyses of brachiopods, appear to show even higher frequency fluctuations based on closer sampling through Middle Devonian conodont zones. Taken together, these studies and ours present a strong argument for the reality of higher-frequency oscillations in $^{87}\text{Sr}/^{86}\text{Sr}$ values during the Paleozoic.

HIGHER-FREQUENCY $^{87}\text{Sr}/^{86}\text{Sr}$ OSCILLATIONS AND SEA-LEVEL CYCLICITY

Based on comparisons of Silurian, Devonian, and Permian $^{87}\text{Sr}/^{86}\text{Sr}$ data with sea-level rise and fall events, Ruppel et al. (1995, 1996) suggested that higher-frequency oscillations in $^{87}\text{Sr}/^{86}\text{Sr}$ may be tied to eustasy.



QAb7566c

Sea-level fall and rise cycles are relatively well established for the Devonian (Johnson et al., 1985; Johnson and Klapper, 1992; Elrick, 1995) and Permian (Kerans et al., 1994; Kerans and Fitchen, 1995), and allow ready comparison with $^{87}\text{Sr}/^{86}\text{Sr}$ trends. The sea-level history of the Silurian, on the other hand, has been less well known. Studies based on facies and faunal patterns have indicated as many as four major worldwide sea-level-fall events in the Llandovery (Johnson et al., 1981, 1991; Aldridge et al., 1993) and at least four more for the Wenlock–Ludlow–Pridoli interval (Jeppsson 1987; Ross and Ross, 1988; Johnson et al., 1991), although there is some variation in the location of these events. Johnson (1996) has recently presented an up-to-date summary of the most widely recognized and correlative of these events for the Silurian. This scheme provides a much more rigorous basis for comparison of sea-level cycles with $^{87}\text{Sr}/^{86}\text{Sr}$ oscillations.

When conodont $^{87}\text{Sr}/^{86}\text{Sr}$ data are compared to these sea-level rise–fall cycles (Figure 4), many cycles (which are of approximately equal scale to third-order depositional sequences) appear to coincide with changes in rates of rise or fall in $^{87}\text{Sr}/^{86}\text{Sr}$ (Figure 4). Perhaps the best correlation between $^{87}\text{Sr}/^{86}\text{Sr}$ and sea-level is seen in the *Pterospirifer celloni* Zone (Figure 4). The large shift in $^{87}\text{Sr}/^{86}\text{Sr}$ to less radiogenic values in the middle *P. celloni* Zone coincides with what is interpreted to have been the largest sea-level rise during the Silurian (Johnson, 1996). This $^{87}\text{Sr}/^{86}\text{Sr}$ fall, which is recorded in our data set by two samples from different localities in Oklahoma, was also observed by Denison et al. (In press) in a whole-rock sample from another locality in Oklahoma (Figure 3). Although less striking, small $^{87}\text{Sr}/^{86}\text{Sr}$ falls are also observed at or near many of the other documented Silurian sequence boundaries. Apparent slight offsets between $^{87}\text{Sr}/^{86}\text{Sr}$ falls and sea-level rises in the *Kochelasma amsdeni*, *K. ranuliformis*, *Kochelasma crassa*, and *Polygnathoides siluricus* Zones may be explained by imprecise location of samples relative to sequence boundaries. The position of these sea-level-rise events cannot now be defined more precisely in the Oklahoma succession from which these

samples were collected. By contrast, the location of samples relative to sequence boundaries is much clearer for the *Distomodus staurognathoides* Zone, for which the samples come from the well-constrained section on Anticosti Island (Johnson et al., 1981). The sequence boundary defined in the upper part of this zone corresponds with a well-defined fall in $^{87}\text{Sr}/^{86}\text{Sr}$ (Figure 4), and the trend of the $^{87}\text{Sr}/^{86}\text{Sr}$ data at the lower sequence boundary suggests a similar fall, although sampling density is insufficient to show this conclusively.

One $^{87}\text{Sr}/^{86}\text{Sr}$ cycle is apparently not associated with a known sequence boundary. Although Ruppel et al. (1996) suggested a sequence boundary correlated with the *Pterospirifer amorphognathoides* Zone fall in $^{87}\text{Sr}/^{86}\text{Sr}$, no such sea-level rise was recognized by Johnson (1996).

Comparison of our $^{87}\text{Sr}/^{86}\text{Sr}$ data and interpreted Silurian sea-level history (Johnson, 1996) tends to suggest a pattern of more radiogenic $^{87}\text{Sr}/^{86}\text{Sr}$ at depositional sequence tops and lower values at their bases. This same pattern has been observed in Devonian and Permian carbonate successions by the authors (Ruppel et al., 1995). Data reported by Diener et al., (1996) also demonstrate increasing (although fluctuating) $^{87}\text{Sr}/^{86}\text{Sr}$ through depositional sequences followed by substantial falls at sequence boundaries.

DISCUSSION

The interpretation of higher-frequency cycles in seawater $^{87}\text{Sr}/^{86}\text{Sr}$ from our data set is based on the conclusion that the strontium isotope composition of these conodont elements has not been altered by diagenesis. This differs from the conclusions reached by Cummins and Elderfield (1994) and Diener et al. (1996). In each of those studies, conodont elements were found to be significantly radiogenic when compared to coeval brachiopods. In neither study, however, were conodont elements cleaned by leaching before analysis. As we have stated, we found leaching to be critical in achieving reproducible and non-radiogenic results. We found surface and outer layers of some conodont elements to be as much as 1.53×10^{-4} more radiogenic than the interior, residual material. In a study of Permian and Triassic conodont elements, Martin and MacDougall (1995) also found radiogenic strontium on outer layers of conodont elements and utilized a similar leaching process to remove it before analysis. Holmden et al. (1996) recently documented a very similar relationship, but also showed that probable seawater signatures do remain in internal layers, and that by leaching of surficial layers, these signals can be recorded. Thus although diagenesis and contamination by radiogenic strontium is a constant concern, we feel that our experi-

FIGURE 4—(opposite) Comparison of $^{87}\text{Sr}/^{86}\text{Sr}$ values with interpreted sea-level history of the Silurian. Plot is scaled by assigning graptolite zones (G. Z., shown by black and white bars) an equal duration. Correlations to conodont zonation and sea-level curve from Johnson (1996). Sequence boundaries shown by arrow lines. The width of the $^{87}\text{Sr}/^{86}\text{Sr}$ curve approximates the analytical reproducibility (± 0.000016 at the 95% confidence level). Locations of samples: squares, Oklahoma; triangles, Tennessee; circles, other localities. Conodonts: A., *Ancoradella*; D., *Distomodus*; K., *Kochelasma*; O., *Ozarkodina*; Ou., *Oulodus*; P., *Pterospirifer*; Po., *Polygnathoides*.

ments with leaching and duplicate analyses (Figures 1 and 2), combined with the confirmation of data points provided by samples from geographically separate sample locations, suggest that we have recorded the original Silurian seawater chemistry by following the techniques outlined above.

In addition to carefully selected and leached sample materials, development of a high-resolution record of secular change in $^{87}\text{Sr}/^{86}\text{Sr}$ that is capable of defining higher-frequency oscillations requires an accurate basis for inter-section correlation and stratigraphic location of data points. Despite recent improvements (e.g., Tucker and McKerrow, 1995), geochronologic dates for the Paleozoic are too imprecise for this purpose. Biostratigraphy offers a much more precise framework for sample correlation. However, because higher-frequency $^{87}\text{Sr}/^{86}\text{Sr}$ cycles in many cases appear to have durations of less than one faunal zone (Figure 4), recognition of these cycles depends on tying samples to physically continuous stratigraphic sections. Although data can be interrelated by superposition within such sections, correlation between sections requires a sophisticated biostratigraphic framework such as the one now provided by conodonts. Recent efforts directed at refining global conodont zonation by graphic correlation techniques promise an even higher resolution framework (Kleffner, 1989, 1995; Fordham, 1992). Only when all $^{87}\text{Sr}/^{86}\text{Sr}$ data are related to such a framework can the precise nature of higher-frequency fluctuations in $^{87}\text{Sr}/^{86}\text{Sr}$ be documented.

The improved resolution of changes in seawater $^{87}\text{Sr}/^{86}\text{Sr}$ through the Silurian allowed by our conodont-based data has important implications for the use of $^{87}\text{Sr}/^{86}\text{Sr}$ chemostratigraphy in correlating Silurian and other Paleozoic sedimentary rock successions. Better resolution of secular $^{87}\text{Sr}/^{86}\text{Sr}$ trends ostensibly means more precise relative dating and characterization of depositional and diagenetic events. In situations where the Silurian $^{87}\text{Sr}/^{86}\text{Sr}$ curve defines rapid changes in $^{87}\text{Sr}/^{86}\text{Sr}$, as during the Ludlow, for example, the correlation potential exceeds that available from conodont zones, but is probably more imprecise than that offered by graptolite zones. The potential precision suggested by the graptolite zonation (Figure 4), however, is rarely realized in shallow-water carbonate platform successions because of the scarcity of graptolites. Where the rate of $^{87}\text{Sr}/^{86}\text{Sr}$ change is less, as in the Pridoli, the potential resolution from $^{87}\text{Sr}/^{86}\text{Sr}$ chemostratigraphy is much poorer. The presence of higher-frequency cycles in the $^{87}\text{Sr}/^{86}\text{Sr}$ record also complicates the potential for high-resolution chemostratigraphy. In intervals where such fluctuations occur, the relative age of the rocks must be known to within a single conodont zone to utilize the added resolution provided by higher-frequency $^{87}\text{Sr}/^{86}\text{Sr}$ cycles. Where such biostratigraphic precision is absent,

resolution is less because of the recurrence of similar $^{87}\text{Sr}/^{86}\text{Sr}$ values in successive cycles (Figure 1).

If higher-frequency fluctuations in $^{87}\text{Sr}/^{86}\text{Sr}$ truly occurred in Paleozoic oceans, as this and other recent data sets appear to indicate, a reconsideration of models of strontium flux in marine basins during the Paleozoic may be in order. Cyclic rises and falls in seawater $^{87}\text{Sr}/^{86}\text{Sr}$ of the sort documented for the Silurian require alternating inputs from two very different reservoirs of strontium. For long-term cycles, such as those documented for Phanerozoic oceans, cyclic rise and fall of $^{87}\text{Sr}/^{86}\text{Sr}$ is accomplished primarily by changes in the relative input of non-radiogenic strontium from oceanic hydrothermal sites and radiogenic strontium from continental weathering. Higher ratios require an increase in continental erosion, whereas falls require a decrease in erosion and/or an increase in hydrothermal activity (Faure, 1986; Elderfield, 1986; Edmond, 1992). Higher-frequency rises in $^{87}\text{Sr}/^{86}\text{Sr}$ values in the Silurian may be attributable to erosion of radiogenic strontium-bearing continental land masses during times of lowered sealevel. It is highly unlikely, however, that hydrothermal flux can vary significantly at the approximately 1–2 Ma scale of these oscillations to account for short-term falls in $^{87}\text{Sr}/^{86}\text{Sr}$.

Higher-frequency $^{87}\text{Sr}/^{86}\text{Sr}$ cyclicity may be explained by periodic mixing of two discrete and isolated marine reservoirs of $^{87}\text{Sr}/^{86}\text{Sr}$. Wilde et al. (1991) interpreted the Silurian oceans to have been highly stratified, but also argued that mixing of these stratified water masses occurred episodically. It seems likely that during times of stratification, bottom waters could exhibit distinctly lower $^{87}\text{Sr}/^{86}\text{Sr}$ values because of ^{86}Sr flux from hydrothermal sources, whereas surface waters could be much more radiogenic because of an influx of craton-derived ^{87}Sr . Mixing of these water masses could produce a shift in $^{87}\text{Sr}/^{86}\text{Sr}$ values that, according to current models of the mixing rate of strontium in the world oceans, would be recorded nearly instantaneously around the globe.

Very similar, higher-frequency fluctuations in seawater $^{87}\text{Sr}/^{86}\text{Sr}$ have been documented for the Silurian (this report), Mississippian (Cummins and Elderfield, 1994), Devonian (Ruppel et al., 1995; Diener et al., 1996), and Permian (Ruppel et al., 1995). Curiously, such cycles are not as apparent in the excellent $^{87}\text{Sr}/^{86}\text{Sr}$ record of the Tertiary. Although DePaolo (1986) described changes in the rate of increase in $^{87}\text{Sr}/^{86}\text{Sr}$ during the Miocene, some of which correlate with third-order sequence boundaries, these shifts do not appear to have been supported by more recent data. Nevertheless, the increasing abundance of Paleozoic data that appear to define such cycles requires that the existence of shifts be seriously considered. If these cycles are real, they must record the occurrence of

very rapid shifts in Sr flux, or the $^{87}\text{Sr}/^{86}\text{Sr}$ ratio of contributing source areas, and/or Sr residence and mixing times very different from those observed today. This inconsistency seems to indicate that Paleozoic oceans may have been different from modern oceans in terms of strontium chemistry.

The apparent association between third-order depositional sequences and cyclic fluctuations in $^{87}\text{Sr}/^{86}\text{Sr}$ suggests a cause-and-effect relationship between changes in sea-level and seawater strontium chemistry. Third-order sea-level falls can result from tectono-eustatic or glacio-eustatic mechanisms (Vail et al., 1977; Bally, 1980; Cloetingh, 1988). Either mechanism can result in increased flux of continental siliciclastics to marine basins. There seems to be good evidence that the episode of continental glaciation that reached its peak in the Late Ordovician continued into the Early Silurian (McKerrow, 1979; Grahan and Caputo, 1992). The well-expressed cycles of sea-level and $^{87}\text{Sr}/^{86}\text{Sr}$ in the Llandovery and the Wenlock may thus be directly related to glacially induced sea-level fluctuations. It is interesting to note that higher-frequency $^{87}\text{Sr}/^{86}\text{Sr}$ cycles documented by Cummins and Elderfield (1994) are also from a period of glaciation. Silurian glacial activity is thought to have abated by the Ludlow, which may explain the more equivocal record of sea-level fluctuations and changes in $^{87}\text{Sr}/^{86}\text{Sr}$ for this part of the Silurian.

The absence of a perfect agreement between $^{87}\text{Sr}/^{86}\text{Sr}$ cycles and interpreted eustatic cycles (Figure 4) may be explained in several ways. First, sea-level-rise events are interpreted from sedimentary successions in several basins around the world. Because of the differing geometries of these basins, transgressions may occur at different times in different areas. In addition, definition of the actual sequence boundary can be equivocal. It is not always obvious which sediments were deposited during transgression and which were formed during the preceding highstand. Secondly, establishing precise position within single conodont zones can be difficult. This is principally the result of variable preservation and recovery of fossils at different localities, but can also be due to variations in faunal assemblages caused by local paleo-ecological conditions. It should be noted in Figure 4 that all of the "mismatches" between $^{87}\text{Sr}/^{86}\text{Sr}$ and eustatic cycles are still within a single conodont zone. Finally, if seawater $^{87}\text{Sr}/^{86}\text{Sr}$ values exhibited interbasinal variations during the Silurian, a situation not borne out by studies of modern oceans but one that cannot be ruled out for ancient oceans, discrepancies between the onset of sea-level rise and increases in $^{87}\text{Sr}/^{86}\text{Sr}$ may be due to local variations in the timing of the influx of radiogenic strontium in individual basins. It should also be stated here that despite our careful analysis and collection of

data that suggest the opposite conclusion, diagenesis cannot be totally ruled out as a contributing factor to the observed variations. In fact, observations of more radiogenic strontium at the tops of depositional sequences might be the expected result of diagenesis associated with sea-level fall. However, based on the data we have presented, we maintain that the increases in $^{87}\text{Sr}/^{86}\text{Sr}$ at sequence tops are not the result of such diagenesis.

As is clear from the above discussion, the recognition of higher-frequency oscillations in $^{87}\text{Sr}/^{86}\text{Sr}$ raises significant questions about the resolution and utility of secular changes in global correlation of depositional and diagenetic sedimentary events, and about the very processes that control the flux and distribution of strontium in the ocean basins. Although improvements in instrumentation, technique, and sample selection have resulted in highly accurate measurements of $^{87}\text{Sr}/^{86}\text{Sr}$ in sedimentary successions, many issues remain to be resolved before the true potential of this tool for improved correlations of these successions can be established. Especially needed to resolve these issues are detailed studies that interrelate $^{87}\text{Sr}/^{86}\text{Sr}$ values to sequence stratigraphy. Key to any study, whether based on conodonts or other carefully prepared sample materials, is a rigorously defined biostratigraphic base for correlation and comparison of data.

CONCLUSIONS

Based on laboratory experiments and comparison with other data sets, we conclude that conodont elements can preserve an excellent record of the strontium isotope composition of the world's oceans. Leaching may be necessary to remove radiogenic strontium from outer element layers, but when properly prepared, conodont elements can form the basis for substantial improvements in the quality and resolution of seawater $^{87}\text{Sr}/^{86}\text{Sr}$ changes during the Paleozoic.

The evolution of seawater during the Silurian was characterized by higher-frequency (approximately 2 Ma) oscillations in $^{87}\text{Sr}/^{86}\text{Sr}$ chemistry. Although knowledge of the sea-level history of the Silurian is still evolving, there is now good evidence that many of these oscillations correlate with eustatic cyclicity. Such a correlation requires a substantial reassessment of the controls on changes in the strontium isotope chemistry of the Paleozoic oceans.

Improvements in instrumentation and technique have greatly improved the precision and accuracy of defining seawater $^{87}\text{Sr}/^{86}\text{Sr}$ in sedimentary successions. However, evaluation of the full potential and limitations of $^{87}\text{Sr}/^{86}\text{Sr}$ chemostratigraphy for the correlation of

depositional and diagenetic events must await further high-resolution studies of secular variation in $^{87}\text{Sr}/^{86}\text{Sr}$ and of the mechanisms of strontium flux into the world oceans. These studies must be interrelated by correlations based on sophisticated biotic zonations such as those that are based on conodonts.

ACKNOWLEDGMENTS

Funding was provided by the Texas Higher Education Coordinating Board through the Advanced Research Program (#003658-040). We thank E. Landing, R.P. Major, G. Klapper, B.S. Norford, and two anonymous reviewers for their constructive comments on the manuscript. Discussions with R.E. Denison and W.B. Ward contributed to our understanding of the strontium chemistry of the Phanerozoic.

REFERENCES

- ALDRIDGE, R.J. 1985. Conodonts of the Silurian System from the British Isles, p. 69–92. In A.C. Higgins and R.L. Austin (eds.), *A Stratigraphical Index of Conodonts*. Ellis Horwood, Chichester.
- , L. JEPSSON, AND K.J. DORNING. 1993. Early Silurian oceanic episodes and events. *Journal of the Geological Society of London*, 150:501–513.
- BALLY, A.W. 1980. Basins and subsidence—a summary. *American Geophysical Union, Geodynamics Series*, 1:5–20.
- BANNER, J.L., AND J. KAUFMANN. 1994. The isotopic record of ocean chemistry and diagenesis preserved in non-luminescent brachiopods from Mississippian carbonate rocks, Illinois and Missouri. *Geological Society of America Bulletin*, 106:1074–1082.
- BARRICK, J.E. 1983. Wenlockian (Silurian) conodont biostratigraphy, biofacies, and carbonate lithofacies, Wayne Formation, central Tennessee. *Journal of Paleontology*, 57:208–239.
- , AND G. KLAPPER. 1976. Multielement Silurian (late Llandoveryan–Wenlockian) conodonts of the Clarita Formation, Arbuckle Mountains, Oklahoma, and phylogeny of *Kockelella*. *Geologica et Paleontologica*, 10:59–100.
- , AND ———. 1992. Late Silurian–Early Devonian conodonts from the Hunton Group (upper Henryhouse, Haragan and Bois D'Arc Formations), south-central Oklahoma, p. 19–66. In J. R. Chaplin and J. E. Barrick (eds.), *Special Papers in Paleontology and Stratigraphy. A Tribute to Thomas W. Amsden*. Oklahoma Geological Survey, Bulletin 145.
- BERTRAM, C.J., H. ELDERFIELD, R.J. ALDRIDGE, AND S.C. MORRIS. 1992. $^{87}\text{Sr}/^{86}\text{Sr}$, $^{143}\text{Nd}/^{144}\text{Nd}$, and REEs in Silurian phosphatic fossils. *Earth and Planetary Science Letters*, 113:239–249.
- BRUCKSCHEN, P., F. BRUHN, J. VEIZER, AND D. BUHL. 1995. $^{87}\text{Sr}/^{86}\text{Sr}$ isotopic evolution of Lower Carboniferous seawater: Dinantian of western Europe. *Sedimentary Geology*, 100:63–81.
- BURKE, W.H., R.E. DENISON, E.A. HETHERINGTON, R.B. KOEPNICK, H.F. NELSON, AND J.B. OTTO. 1982. Variation of seawater $^{87}\text{Sr}/^{86}\text{Sr}$ throughout Phanerozoic time. *Geology*, 10:516–519.
- CLOETINGH, S. 1988. Intraplate stresses: a tectonic cause for third-order cycles in apparent sea-level?, p. 19–30. In C.K. Wilgus, B.S. Hastings, C.St.G.C. Kendall, H.W. Posamentier, C.A. Ross, and J.C. Van Wagoner (eds.), *Sea-Level Changes: An Integrated Approach*. Society of Economic Paleontologists and Mineralogists, Special Publication 42.
- CUMMINS, D.I., AND H. ELDERFIELD. 1994. The strontium isotopic composition of Brigantian (late Dinantian) seawater. *Chemical Geology*, 18:255–270.
- DEPAOLO, D.J. 1986. Detailed record of the Neogene Sr isotopic evolution of seawater from DSDP Site 590B. *Geology*, 14:103–106.
- , AND B.L. INGRAM. 1985. High resolution stratigraphy with strontium isotopes. *Science*, 227:938–941.
- DENISON, R.E., R.B. KOEPNICK, W.H. BURKE, E.A. HETHERINGTON, AND A. FLETCHER. In press. Construction of the Silurian and Devonian $^{87}\text{Sr}/^{86}\text{Sr}$ curve. *Chemical Geology*.
- DIENER, A., S. EBNETH, J. VEIZER, AND D. BUHL. 1996. Strontium isotope stratigraphy of the Middle Devonian. Brachiopods and conodonts. *Geochimica et Cosmochimica Acta*, 60:639–652.
- EDMOND, J.M. 1992. Himalayan tectonics, weathering processes, and the strontium isotope record in marine limestones. *Science*, 258:1594–1597.
- ELDERFIELD, H. 1986. Strontium isotope stratigraphy. *Palaeogeography, Palaeoclimatology, Palaeoecology*, 57:71–90.
- ELRICK, M. 1995. Cyclostratigraphy of Middle Devonian carbonates of the eastern Great Basin. *Journal of Sedimentary Research*, B65:61–79.
- EPSTEIN, A.G., J.B. EPSTEIN, AND L.D. HARRIS. 1977. Conodont Color Alteration—An Index to Organic Metamorphism. U.S. Geological Survey Professional Paper 995.
- FAURE, G. 1986. *Principles of Isotope Geology*. Wiley, New York.
- FORDHAM, B.G. 1992. Chronometric calibration of mid-Ordovician to Tournaisian conodont zones: a compilation from recent graphic-correlation and isotopic studies. *Geological Magazine*, 129:709–721.
- GRAHAN, Y., AND M.V. CAPUTO. 1992. Early Silurian glaciations in Brazil. *Palaeogeography, Palaeoclimatology, Palaeoecology*, 99:9–15.
- HESS, J., M. BENDER, AND J. SCHILLING. 1986. Evolution of the ratio of strontium 87 to strontium 86 in seawater from Cretaceous to present. *Science*, 231:979–984.
- HODELL, D.A., G.A. MEAD, AND P.A. MUELLER. 1990. Variation in the strontium isotopic composition of seawater (8 Ma to present): implications for chemical weathering rates and dissolved fluxes to the oceans. *Chemical Geology*, 80:291–307.
- , P.A. MUELLER, AND J.R. GARRIDO. 1991. Variation in the strontium isotopic composition of seawater during the Neogene. *Geology*, 19:24–27.
- HOLMDEN, C., R.A. CREASER, K. MUEHLENBACHS, S.M. BERGSTROM, AND S.A. LESLIE. 1996. Isotopic and elemental systematics of Sr and Nd in 454 Ma biogenic apatites: implications for paleoseawater studies. *Earth and Planetary Science Letters*, 142:425–437.
- JEPSSON, L. 1987. Lithological and conodont distributional evidence for episodes of anomalous oceanic conditions during the Silurian, p. 129–145. In R. J. Aldridge (ed.), *Paleobiology of Conodonts*. Ellis Horwood, Chichester.
- . 1988. Conodont biostratigraphy of the Silurian–Devonian boundary stratotype at Klonk, Czechoslovakia. *Geologica et Palaeontologica*, 22:21–31.
- JOHNSON, J.G., AND G. KLAPPER. 1992. North American midcontinent T–R cycles, p. 127–135. In J.R. Chaplin and J.E. Barrick (eds.), *Special Papers in Paleontology and Stratigraphy: A Tribute to Thomas W. Amsden*. Oklahoma Geological Survey, Bulletin 145.

- , AND ———, AND C.A. SANDBERG. 1985. Devonian eustatic fluctuations in Euramerica. *Geological Society of America Bulletin*, 96:567–587.
- JOHNSON, M.E. 1996. Stable cratonic sequences and a standard for Silurian eustasy, p. 203–211. *In* B.J. Witzke, G.A. Ludvigson, and J.E. Day (eds.), *Paleozoic Sequence Stratigraphy: Views from the North American Craton*. Geological Society of America, Special Paper 306.
- , L.R.M. COCKS, AND P. COPPER. 1981. Late Ordovician–Early Silurian fluctuations in sea-level from eastern Anticosti Island, Quebec. *Lethaia*, 14:73–82.
- , RONG J.-Y., AND YANG X.-C. 1985. Intercontinental correlation by sea-level events in the Early Silurian of North America and China (Yangtze Platform). *Geological Society of America Bulletin*, 96:1384–1397.
- , D. KALJO, AND RONG J.-Y. 1991. Silurian eustasy, p. 145–163. *In* M.G. Bassett, P.D. Lane, AND D. Edwards (eds.), *The Murchison Symposium. Proceedings of an International Conference on the Silurian System*. Special Papers in Paleontology, 44.
- JONES, C.E., H.C. JENKINS, AND S.P. HESSELBO. 1994a. Strontium isotopes in Early Jurassic seawater. *Geochimica et Cosmochimica Acta*, 58:1285–1301.
- , ———, A.L. COE, AND S.P. HESSELBO. 1994b. Strontium isotopes in Jurassic and Cretaceous seawater. *Geochimica et Cosmochimica Acta*, 58:3061–3074.
- KERANS, C., AND W.M. FITCHEN. 1995. Sequence Hierarchy and Facies Architecture of a Carbonate Ramp System: San Andres Formation of Algerita Escarpment and Western Guadalupe Mountains, West Texas and New Mexico. University of Texas at Austin, Bureau of Economic Geology, Report of Investigations 235.
- , F.J. LUCIA, AND R.K. SENG. 1994. Integrated characterization of carbonate ramp reservoirs using Permian San Andres Formation outcrop analogs. *American Association of Petroleum Geologists*, 78:181–216.
- KLEFFNER, M.A. 1989. A conodont-based Silurian chronostratigraphy. *Geological Society of America Bulletin*, 101:904–912.
- . 1995. A conodont- and graptolite-based Silurian chronostratigraphy, p. 159–176. *In* K.O. Mann and H.R. Lane (eds.), *Graphic Correlation*. SEPM (Society for Sedimentary Geology), Special Publication 53.
- KOEPNICK, R.B., W.H. BURKE, R.E., DENISON, E.A. HETHERINGTON, H.F. NELSON, J.B. OTTO, AND L.E. WAITE. 1985. Construction of the seawater $^{87}\text{Sr}/^{86}\text{Sr}$ curve for the Cenozoic and Cretaceous: supporting data. *Chemical Geology*, 58:55–81.
- MARTIN, E.E., AND J.D. MACDOUGALL. 1991. Seawater Sr isotopes at the Cretaceous/Tertiary [sic, n-dash, not virgule] boundary. *Earth and Planetary Sciences Letters*, 104:166–180.
- , AND ———. 1995. Sr and Nd isotopes at the Permian/Triassic [sic, n-dash, not virgule] boundary: a record of climate change. *Chemical Geology*, 125:73–99.
- MCKERROW, W.S. 1979. Ordovician and Silurian changes in sea-level. *Journal of the Geological Society of London*, 136:137–145.
- MILLER, K.G., M.D. FEIGENSON, J.D. WRIGHT, AND B.M. CLEMENT. 1991. Miocene isotope reference section, Deep Sea Drilling Project Site 608: an evaluation of isotope and biostratigraphic resolution. *Paleoceanography* 6:33–52.
- NOWLAN, G.S. 1983. Early Silurian conodonts of eastern Canada. *Fossils and Strata*, 15:95–110.
- PETERMAN, Z.E., C.E. HEDGE, AND H.A. TOURTELOT. 1970. Isotopic composition of strontium in sea-water throughout Phanerozoic time. *Geochimica et Cosmochimica Acta*, 34:105–120.
- POPP, B.N., F.A. PODOSEK, J.C. BRANNON, T.F. ANDERSON, AND J. PIER. 1986. $^{87}\text{Sr}/^{86}\text{Sr}$ ratios in Permo–Carboniferous sea water from the analysis of well preserved brachiopod shells. *Geochimica et Cosmochimica Acta*, 50:1321–1328.
- ROSS, C.A., AND J.R.P. ROSS. 1988. Late Paleozoic transgressive–regressive deposition, p. 227–248. *In* C.K. Wilgus, B.S. Hastings, C.St.G.C. Kendall, H.W. Posamentier, C.A. Ross, and J.C. Van Wagoner (eds.), *Sea-Level Changes: An Integrated Approach*. Society of Economic Paleontologists and Mineralogists, Special Publication 42.
- RUPPEL, S.C., E.W. JAMES, AND J.E. BARRICK. 1995. Improvements in the record of secular change in sea-water $^{87}\text{Sr}/^{86}\text{Sr}$: a stronger basis for dating of Paleozoic diagenetic and depositional events, p. 84A. *In* American Association of Petroleum Geologists Annual Convention Program, Houston.
- , ———, ———, G.S. NOWLAN, AND T.T. UYENO. 1996. High-resolution $^{87}\text{Sr}/^{86}\text{Sr}$ chemostratigraphy of the Silurian: implications for event correlation and strontium flux. *Geology*, 24:831–834.
- RUSH, P.F., AND H.S. CHAFETZ. 1990. Fabric-retentive, non-luminescent brachiopods as indicators of original $\delta^{13}\text{C}$ and $\delta^{18}\text{O}$ composition: a test. *Journal of Sedimentary Petrology*, 60:968–981.
- SWEET, W.C. 1988. The Conodonta: Morphology, Taxonomy, Paleocology, and Evolutionary History of a Long-Extinct Animal Phylum. Oxford Monographs on Geology and Geophysics, No. 10.
- TUCKER, R.D., AND W.S. MCKERROW. 1995. Early Paleozoic chronology: a review in light of new U–Pb zircon ages from Newfoundland and Britain. *Canadian Journal of Earth Sciences*, 32:368–379.
- UYENO, T.T., AND C.R. BARNES. 1983. Conodonts of the Jupiter and Chicotte Formations (Lower Silurian), Anticosti Island, Quebec. *Canada Geological Survey Bulletin* 355.
- VAIL, P.R., R.M. MITCHUM, JR., AND S. THOMPSON III. 1977. Global cycles of relative change of sea-level, p. 83–97. *In* C.E. Payton (ed.), *Seismic Stratigraphy—Applications to Hydrocarbon Exploration*. American Association of Petroleum Geologists Memoir 26.
- VEIZER, J., AND W. COMPSTON. 1974. $^{87}\text{Sr}/^{86}\text{Sr}$ composition of seawater during the Phanerozoic. *Geochimica et Cosmochimica Acta*, 38:1461–1484.
- WADLEIGH, M.A. AND J. VEIZER. 1992. $^{18}\text{O}/^{16}\text{O}$ and $^{13}\text{C}/^{12}\text{C}$ in Lower Paleozoic articulate brachiopods: implications for the isotopic composition of seawater. *Geochimica et Cosmochimica Acta*, 56:431–443.
- WILDE, P., W.B.N. BERRY, AND M.S. QUINBY-HUNT. 1991. Silurian oceanic and atmospheric circulation and chemistry, p. 123–143. *In* M.G. Bassett, P.D. Lane, and D. Edwards (eds.), *The Murchison Symposium: Proceedings of an International Conference on the Silurian System*. Special Papers on Paleontology, 44.

CORRELATION OF CARBON ISOTOPE EVENTS AND ENVIRONMENTAL CYCLICITY IN THE EAST BALTIC SILURIAN

DIMITRI KALJO, TARMO KIIPLI, AND TÕNU MARTMA

Institute of Geology, 7 Estonia Avenue, EE-0001 Tallinn, Estonia

ABSTRACT—1,200 whole-rock samples were analyzed from eight cores located along a shallow–deep shelf transect that extends from the Hirnantian (Upper Ordovician) through the top of the Pridoli. The most important positive $\delta^{13}\text{C}$ excursions are in the Hirnantian (+4.1–+6.0‰), lower Aeronian (Llandovery) (+3.0–+5.2‰), middle Homerian (Wenlock) (+2.1–+4.6‰), and middle Ludfordian (Ludlow) (+4.2–+5.9‰). The last three excursions coincide with those established on Gotland; the lower Wenlock and upper Ludlow excursions correlate with events in Australia. The East Baltic data support conclusions from Gotland that deeper-water facies show lower $\delta^{13}\text{C}$ values. The most positive excursions occur after important extinctions during a low-diversity interval, which may coincide with a phase of enhanced bioproductivity. During the Early Silurian, glaciations and glacio-eustatic changes seem to play a significant role, but there is no full agreement in the sea-level curve and carbon isotope excursions.

INTRODUCTION

Cyclicity seems to be one of the most common patterns of the changing environment. Quite different features (biotic, climatic, magmatic, oceanic, sedimentological, tectonic, etc.) can be cyclic. In some cases, a cosmic influence has been suggested (e.g., Milankovich cycles; see Jepsen, 1990), among other forcing mechanisms.

Carbon cycling is one feature of environmental cyclicity. The essence of the cycling in the ocean is photosynthetic reduction of bicarbonate carbon to organic carbon. Organic carbon will mainly be oxidized and returned to the photic zone through the so-called “biological pump” (Kump, 1991; Holser et al., 1995), but will be partly buried in sediments. Under specific conditions (anoxic bottom waters, rapid sedimentation, high biological productivity), this process may result in enhanced removal of light organic carbon from surface waters, and will consequently cause higher $\delta^{13}\text{C}$ values in surface carbonates (recorded in fossils and sedimentary rocks). A

full accounting of carbon cycling also involves carbon influx from land (rivers) and interaction with the atmosphere. Our interest was in establishing the main shifts in the carbon isotope ratio of Silurian sedimentary rocks and to discover possible relationships with different environmental processes and events.

Silurian carbon isotope studies are leading to important results. Earlier results were summarized by Holser et al. (1995), but additional data have been recorded (Andrew et al., 1994; Wenzel, 1994; Heath et al., 1996; Samtleben et al., 1996; Wenzel and Joachimski, 1996), especially for the Baltic area. We commenced our work in the Wenlock and Ludlow, and now the complete Silurian of Estonia and Latvia has been covered (Kaljo et al., 1996). Our main objectives were to obtain better interfacies correlation between sections by utilizing carbon isotope excursions, and to decipher the causes of environmental changes and bioevents. Eight cores have now been investigated (Figure 1).

The methodology of this type of isotope study has been discussed elsewhere (Kaljo et al., 1997), and only the most important aspects are noted herein. Carbon isotopes were measured in whole-rock samples in order to examine facies which do not contain the brachiopod shells that earlier provided carbon isotope data. The samples were powdered to a $<10\ \mu\text{m}$ grain size and reacted with 100% phosphoric acid at 100°C for fifteen minutes. The reproducibility of the results is better than 0.1%. A comparison of our whole-rock data from the East Baltic with those of Samtleben et al. (1996) and Wenzel and Joachimski (1996) from brachiopod shells from Gotland shows a great similarity in the carbon isotope curves (Figure 2). Slight differences in $\delta^{13}\text{C}$ values that occur in the three sets of data discussed below do not detract from a clear general pattern.

1,200 samples were analyzed; the mean sampling interval was 2 m, but was greater in monotonous sequences and less in chronostratigraphic boundary intervals. Isotope studies in the Baltic area (Samtleben et al., 1996; Wenzel and Joachimski, 1996; Kaljo et al., 1997) have shown that $\delta^{13}\text{C}$ is little-affected in most Silurian

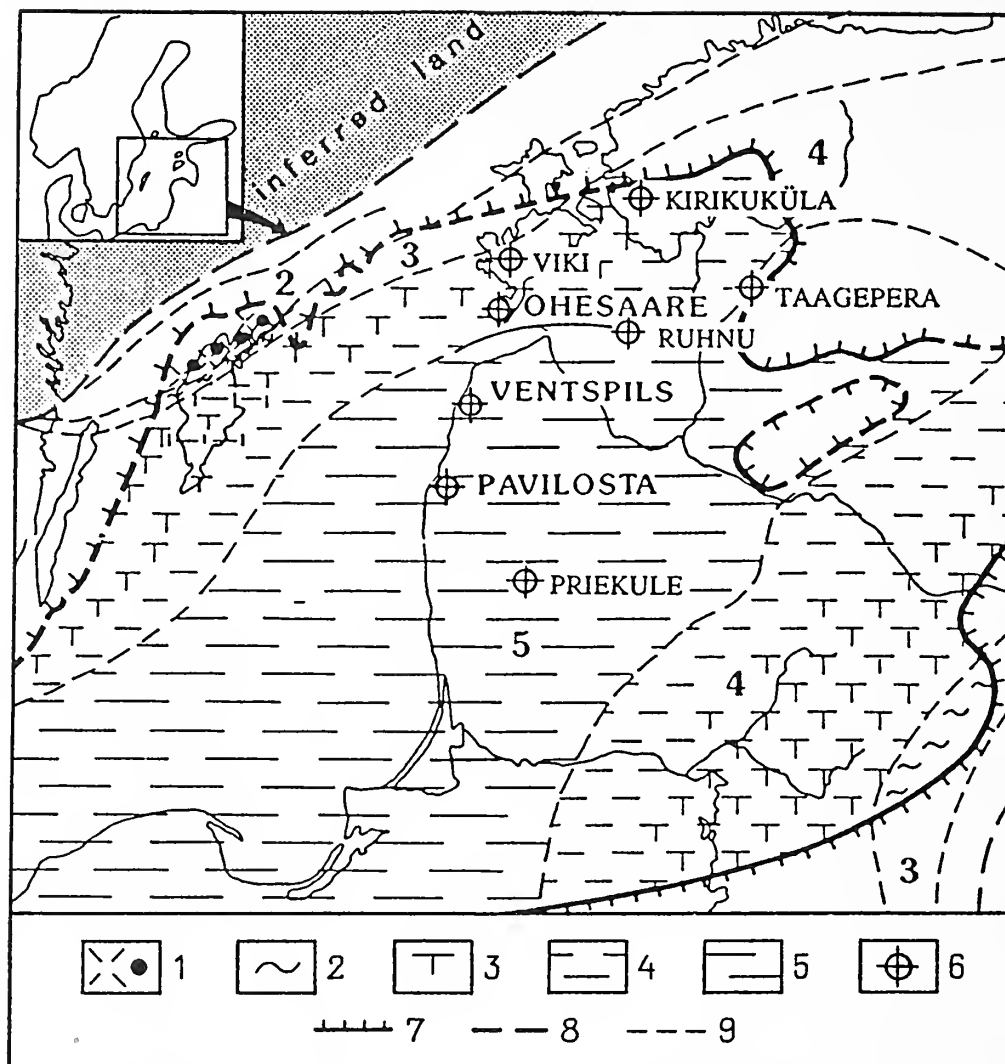


FIGURE 1—Location of cores studied in this report and distribution of early Wenlock (Sheinwoodian) rocks and facies belts across the Baltic region during the *Monograptus riccartonensis* Chron (after Bassett et al., 1989). Key: 1, skeletal grainstones with reefs; 2, skeletal pack- and wackestones; 3, marlstones; 4, green mudstones; 5, grey mudstones, sometimes silty; 6, borehole; 7, eroded margin of Sheinwoodian; 8, paleoshoreline; 9, facies boundaries. Numbers on the map mark facies belts: 2, nearshore high-energy shoals; 3, shallow mid-shelf; 4, deeper outer-shelf; 5, deep-shelf depression.

sedimentary rocks by diagenetic processes. Veins, faults, and weathered rocks may have altered $\delta^{13}\text{C}$ ratios. Oxygen isotopes are not discussed herein because the whole-rock samples we examined usually contain both calcite and dolomite with notably different fractionation factors (Kaljo et al., 1997).

The main components, and some minor and trace elements in the rocks (MgO , Al_2O_3 , SiO_2 , K_2O , CaO , Fe_2O_3 , S, Cl, Mn, Sr), were measured by X-ray fluorescence analysis (XRF). Siliciclastic material, calcite, and dolomite concentrations were recalculated from these data (Figures 3–6).

The samples were all taken from cores, which made

it easy to establish a sample succession and to correlate them in terms of the local biostratigraphy and lithostratigraphy. On the other hand, exact correlations in terms of the graptolite zonation, which was our basis for comparing data from different areas, was often rather complicated. However, occurrences of graptolites (Kaljo,

FIGURE 2—(opposite) Baltic stratigraphy and correlation. Graptolite zones after Koren' et al. (1996), but simplified in Telychian and Homerian. Other sources noted in text. Abbreviations: B, beds; U, Uduvere Beds; H, Himmiste Beds; S, Sauvere Beds. Vertical ruling shows gaps.

Series	Stages	Generalized graptolite zones	Gotland	East Baltic	N & W Latvia	S & W Estonia	
			Beds	Stages	Formations, beds		
PRIDOLI		<i>Pristiograptus transgrediens</i> - <i>Monograptus bouceki</i>		Ohesaare	Targale	Ohesaare	
		<i>Monograptus lochkovenski</i> - <i>Monograptus branikensis</i>		Kaugatuma	Minija	Lõo B.	
		<i>Monograptus ultimus</i> - <i>Monograptus parultimus</i>				Äigu B.	
LUDLOW	Ludfordian	<i>Monograptus formosus</i>	Sundre	Kuressaare	Ventspils	Kuressaare	
		<i>Neocucullograptus kozlowski</i> - <i>Bohemograptus bohemicus tenuis</i>	Hamra Burgsvik Eke		Mituva Nova B.		
		<i>Saetograptus leintwardinensis</i>	Hemse	Paadla	Dubysa		
	Gorstian	<i>Lobograptus scanicus</i>		Dubysa			
		<i>Neodiversograptus nilssoni</i>					
WENLOCK	Homerian	<i>Monograptus ludensis</i> - <i>Monograptus praedeubell</i>	Klinteberg	Rootsiküla	Siesartis	Soeginina B.	
		<i>Gothograptus nassa</i> - <i>Pristiograptus parvus</i>	Mulde Halla			Vesiku B.	
		<i>Cyrtograptus lundgreni</i>		Ancia B.		Viita B.	
	Sheinwoodian	<i>Cyrtograptus perneri</i> - <i>Cyrtograptus rigidus</i>	Slite	Jaagarahu	Riga	Sõrve	
		<i>Monograptus belophorus</i> - <i>Monograptus riccartonensis</i>	Tofta	Jaani		Jamaja	
		<i>Cyrtograptus murchisoni</i> - <i>Cyrtograptus centrifugus</i>	Höglint			Riga	
				U. Visby			
	LLANDOVERY	Telychian	<i>Cyrtograptus insectus</i> - <i>Oktavites spiralis</i>	L. Visby	Adavere	Jurmala	Velise
<i>Monoclimacis crenulata</i> - <i>Monoclimacis griestoniensis</i>			not exposed	Raikküla		Dobele	Rumba
<i>Streptograptus crispus</i> - <i>Spirograptus guerichi</i>							
<i>Monograptus sedgwickii</i>		Remte			Saarde		
<i>Demirastrites convolutus</i>				Juuru		Staciunai	
<i>Monograptus argenteus</i>					Juuru		Staciunai
<i>Demirastrites pectinatus</i> - <i>Demirastrites triangulatus</i>		Juuru					
<i>Coronograptus cyphus</i>				Juuru		Staciunai	
<i>Cyrtograptus vesiculosus</i>			Juuru		Staciunai		
<i>Parakidograptus acuminatus</i>		Juuru					Staciunai

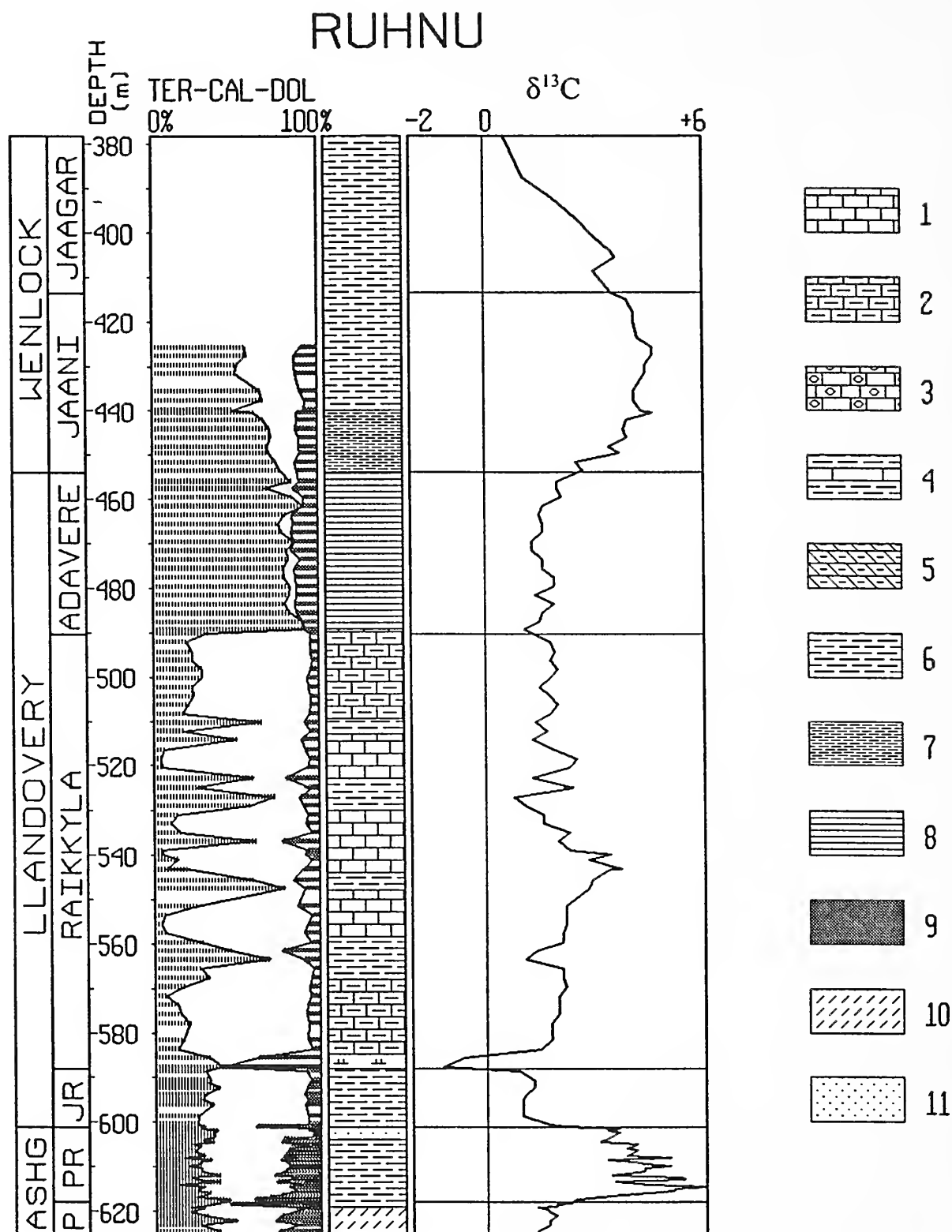


FIGURE 3—Lithology and $\delta^{13}\text{C}$ curve of the Ruhnu core. Stratigraphy in Figure 2. Gap and condensation interval in upper Aeronian (Saarde and Rumba Formations locally missing). Abbreviations: ASHG, Ashgill; P, Pingu Stage; PR, Porkuni Stage; JR, Juuru Stage; JAAGAR, Jaagarahu Stage; TER, terrigenous material; CAL, calcite; DOL, dolomite. Horizontal bars in the TER-CAL-DOL column mark geochemical samples. Carbon isotopes analyzed through the entire section of cores. Lithology: 1, undifferentiated limestone; 2, argillaceous limestone; 3, crinoidal limestone; 4, marl- and limestone intercalations; 5, argillaceous dolostone; 6, marlstone; 7, brown marlstone; 8, grey shale; 9, black shale; 10, red marlstone; 11, sandy-silty limestone.

1970; R.Z. Ulst in Gailite et al., 1987), chitinozoans (Nestor, 1994), and microvertebrates (Märss, 1986) allowed us to achieve reliable results.

GEOLOGICAL SETTING

The locations of the eight cores studied for carbon isotopes are shown in Figure 1. This figure shows the early Wenlock facies distribution in the Baltic Sea region. In general, the cores are located along a line from the north (Kirikuküla) to the south (Priekule) and coincide with a transition from shallow- to deep-shelf facies (for a more comprehensive summary, see Bassett et al., 1989). The early Wenlock reconstruction of Figure 1 is for a period of sea-level highstand, and therefore the relatively deep-water outer-shelf facies belt (number 4 in Figure 1) also occupies the northern area (Kirikuküla, Viki, and Taagepera areas). Earlier in the Rhuddanian and Aeronian, this region had nearshore and shallow-shelf facies. Due to a general shoaling of the Baltic Basin beginning in the middle Wenlock, the shallow-shelf belt moved south in a stepwise manner. As a result, the Ohesaare area in the late Wenlock and the Ventspils area in the Pridoli were covered by a shallow sea. Deep-water Ludlow sediments with graptolites are present in the Pavilosta and Priekule regions. General information on lithologies of the cores is shown in Figures 3–6. In the nearshore high-energy belt (number 2 in Figure 1), there are carbonate rocks (predominantly grainstones), often with organic buildups. In the shallow shelf or mid-shelf, different limestones (wackestones with grain- and packstone beds) that are locally nodular or intercalated with marlstones are present. Seawards on the deeper outer shelf and especially in the shelf depression (numbers 4 and 5 in Figure 1, respectively), the carbonate content of rocks decreases, and siliciclastics (clay and fine silt in some levels) increase. As a result, marlstones and mudstones dominate the outer shelf, but the basinal areas are characterized by mudstones and argillites (i.e., shales and claystones, sometimes dark or even black) with graptolites, pyrite, and high C_{org} content that indicate relatively deep-water, oxygen-deficient depositional conditions.

East Baltic stratigraphy is divisible into 1) regional stages, which are chronostratigraphic units with isochronous boundaries; and 2) formations and members, which are lithostratigraphic units, often with diachronous boundaries, usually restricted to specific facies areas (confacies belts). Figure 2 shows the stratigraphic terminology employed for the subdivision of sequences and the dating of events (see Kaljo, 1987; Nestor, 1993).

To facilitate the comparison of East Baltic and Gotland data, a column on the latter sequence, based mainly on the correlations of Jeppsson et al. (1994) and

others (Bassett et al., 1989; Kaljo, 1990; Nestor, 1994), is included in Figure 2. Despite a different stratigraphic nomenclature, both areas have a very similar geological history, especially in basin evolution, which is seen in the East Baltic in numerous cores that penetrate the Silurian.

CARBON ISOTOPE EXCURSIONS

Carbon isotopes were studied in eight East Baltic cores that represent different facies (for locations, see Figure 1). Due to geological history, the sections are more or less incomplete, but the whole set of sections has been correlated biostratigraphically. This permits a tracing of every $\delta^{13}C$ excursion that has been established between at least three sections. Comments on the sections are included in the explanations of the corresponding figures. A few additional remarks are made on the sections not figured, but which were used in this analysis.

The following intervals were studied: At Kirikuküla, the Hirnantian–lower Wenlock (beginning of the Jaani Stage), with a gap in the Aeronian (the upper Raikküla Stage, equivalent to the *Monograptus argenteus* and *Demirastrites convolutus* Zones, is missing). At Taagepera, the Hirnantian–middle Aeronian (through the middle of the Saarde Formation). At Viki, the Aeronian–Homerian (Aeronian Saarde and Rumba Formations are missing in part or somewhat condensed). At Pavilosta, the Sheinwoodian–Ludfordian. This latter section received a preliminary study for more data on a strong positive $\delta^{13}C$ peak in the Ludlow. Combined micropalaeontological and geological data place this excursion in the *Bohemograptus bohemicus tenuis*–*Neocucullograptus kozlowskii* Generalized Graptolite Zone, and we accept that there is only one positive peak in the Ludlow.

Carbon isotope values measured in these cores are relatively easily correlatable if differences in thicknesses of the stratigraphic units and the gaps in the sequences are taken into account. Precise biostratigraphic correlation is always required, but sometimes its resolution appears to be insufficient for exact comparisons.

Despite these limitations, similar carbon isotope curves occur across the Baltic Silurian, and are well developed in all of the sections (Figures 3–6) and in other available data sets (Corfield et al., 1992; Jux and Steuber, 1992; Heath et al., 1996; Samtleben et al., 1996; Wenzel and Joachimski, 1996). The most important positive and negative $\delta^{13}C$ excursions in these curves are summarized below (see Figures 3–7).

The Hirnantian (latest Ordovician) is a starting point for comparing the Silurian history of carbon cycling. In the Hirnantian, $\delta^{13}C$ values reach +4.1‰ at Taagepera, +4.8‰ at Kirikuküla, and +6.0‰ at Ruhnu

OHESAARE

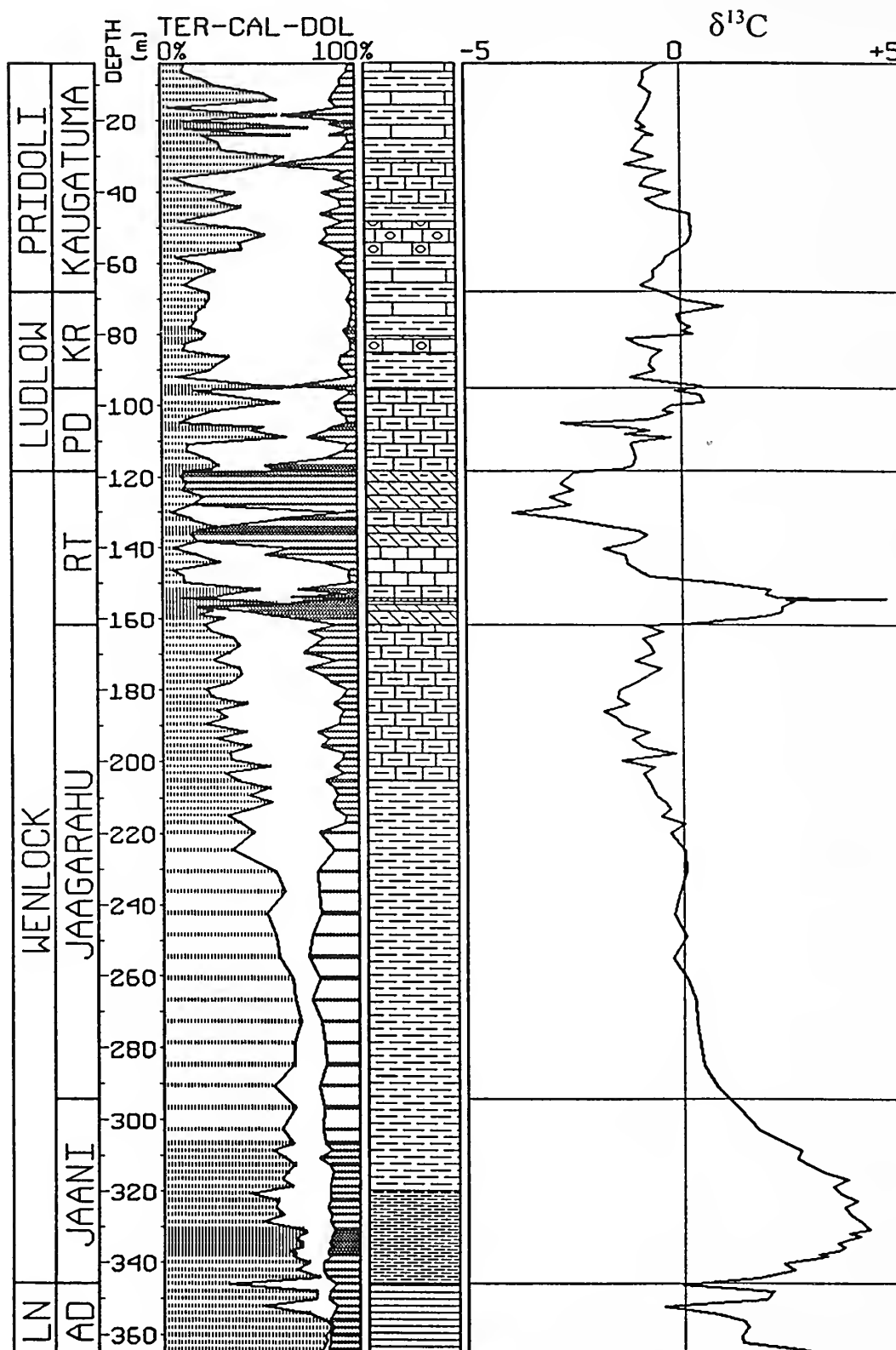


FIGURE 4—Lithology and $\delta^{13}\text{C}$ curve of Ohesaare core. Several significant gaps interrupt the sequence (see Figure 2), especially in Homerian and Ludlow. Highest part of the section (Ohesaare Stage) is missing in the Ohesaare core, which is located near the stratotype locality. Eleven samples from the stratotype were measured and added to the core data (Figure 7). Explanation in Figure 3. Additional abbreviations: LN, Llandovery. Stages: AD, Adavere; RT, Rootsiküla; PD, Paadla; KR, Kuressaare.

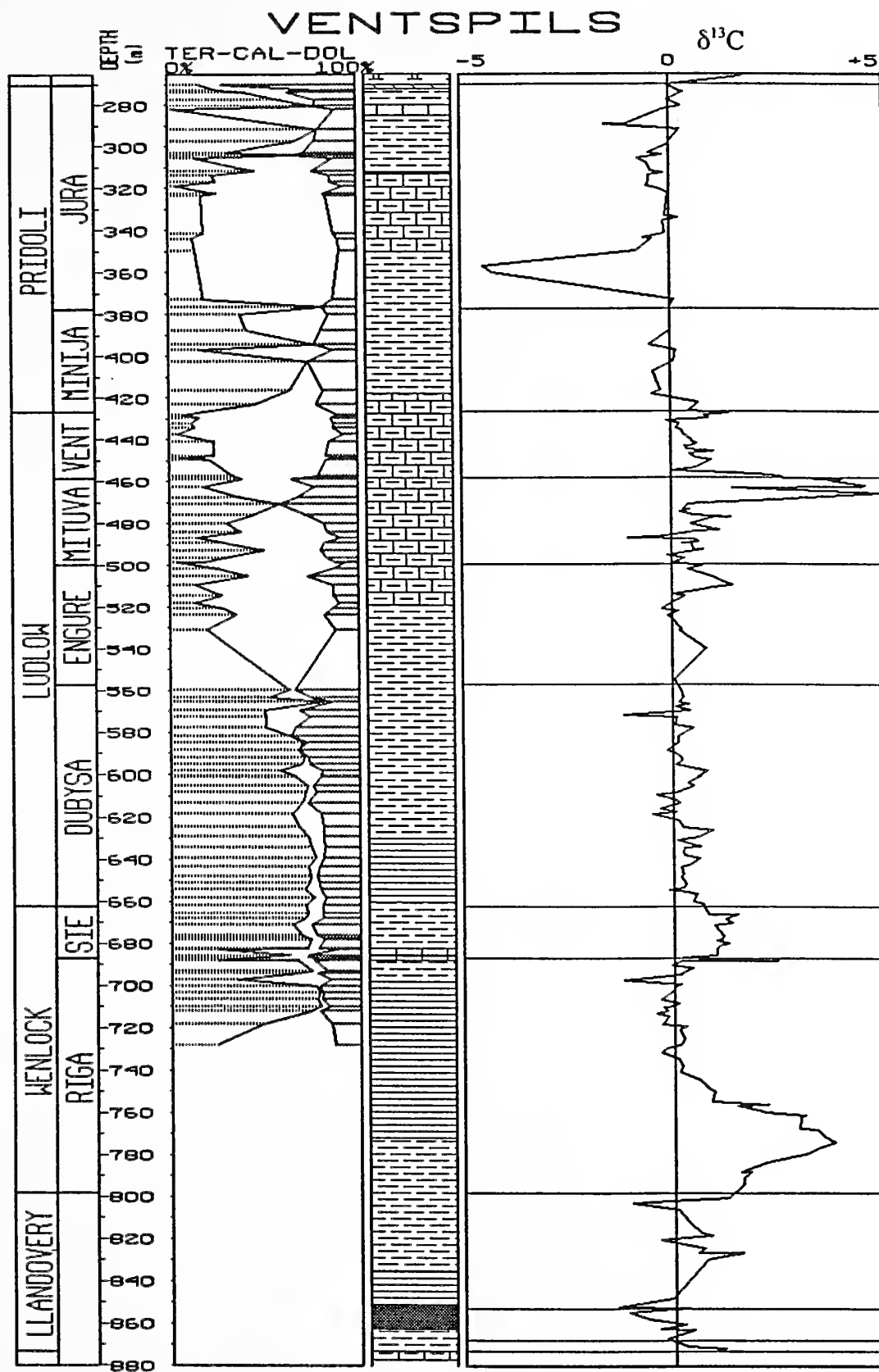
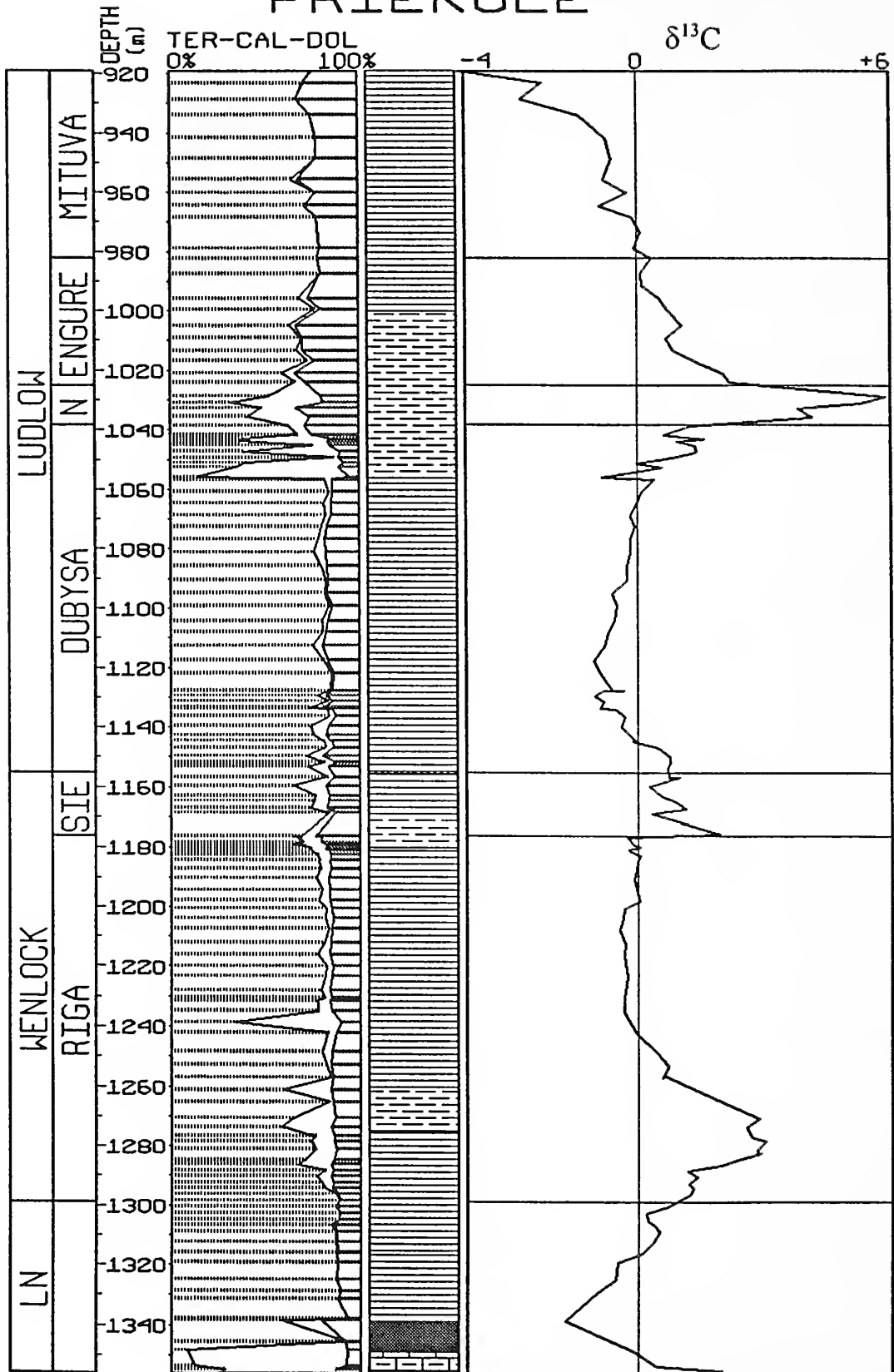


FIGURE 5—Lithology and $\delta^{13}\text{C}$ curve of Ventspils core. Rhuddanian and Aeronian are condensed by comparison with more carbonate-rich sections. Additional sampling at Ventspils is needed. Four records of very negative $\delta^{13}\text{C}$ values not confirmed by adjacent samples were excluded from this curve; these records are at (depth, ^{13}C value in ‰): 682.7 m, -9.5; 701.1 m, -5.2; 728.1 m, -9.0; 733.9 m, -10.9. These negative deviations are not yet understood. Explanation in Figure 3. Additional abbreviations: SIE, Siesartis Formation; VENT, Ventspils Formation.

PRIEKULE



(Figure 3). This isotope event was discussed by Brenchley et al. (1994, 1995).

A sudden fall of the curve followed in the lowermost Raikküla Stage (i.e., lowest *Coronograptus cyphus* Zone) with a $\delta^{13}\text{C}$ of -1.4‰ at Ruhnu (Figure 3).

A positive excursion with a peak in the *Demirastrites triangulatus*-*D. pectinatus* Zone follows in the middle of the Saarde Formation. The $\delta^{13}\text{C}$ values in the Taagepera and Ruhnu cores (Figure 3) reach +3.0‰ and +3.9‰, respectively.

Due to gaps in the cores of different duration higher in the Aeronian (see above), the carbon curve is not distinctly defined. However, data from Kirikuküla and Ventspils (Figure 5) show a -1.3‰ to -1.4‰ negative excursion of the $\delta^{13}\text{C}$ values, respectively, in the Rumba and uppermost Dobeles Formations in the *Monograptus sedgwickii* Zone.

In the Telychian, $\delta^{13}\text{C}$ values rise slowly to a broad positive excursion in the lower Sheinwoodian and a peak in the *Monograptus riccartonensis*-*M. belophorus* Zone (i.e., the Jaani Stage and the lower part of the Riga Formation). This $\delta^{13}\text{C}$ peak is established in the Viki (+5.2‰), Ruhnu (+4.6‰), Ohesaare (+4.2‰), Ventspils (+3.8‰), Pavilosta (+3.3‰), and Priekule (+3.1‰) cores. This trend to lighter $\delta^{13}\text{C}$ values (Figure 1) coincides with the currently accepted seaward-deepening of the East Baltic basin (Bassett et al., 1989), accompanied by a decreasing carbonate content of the rocks.

The peak in the *M. riccartonensis*-*M. belophorus* Zone was followed by a ^{13}C depletion that culminated in the lower Homerian *Cyrtograptus lundgreni* Zone, just below the next positive excursion in the *Pristiograptus parvus*-*Gothograptus nassa* Zone (lower Rootsiküla Stage). The latter peak is rather strong in the Ohesaare core (+4.6‰), and is followed by a rapid decrease in $\delta^{13}\text{C}$ values to -3.8‰ in the middle Rootsiküla Stage (i.e., *Monograptus praedeubeli*-*M. ludensis* Zone). Although $\delta^{13}\text{C}$ values rise slightly, they remain negative at the very beginning of the Ludlow (Soeginina Beds, i.e., lowest part of the *Neodiversograptus nilssoni* Zone). The *P. parvus*-*G. nassa* Zone positive peak is not so clearly defined in other East Baltic sections, but can still be identified by much lower $\delta^{13}\text{C}$ values at Ventspils (+2.4‰) and Priekule (+2.1‰). The negative Homerian shift is less pronounced in the latter two sections, but is well established by Corfield et al. (1992) in the Anglo-Welsh area.

In the Ludlow and Pridoli, the carbon isotope curve fluctuates within the $\pm 1\%$ limits, the only exception being a strong positive excursion in the Nova Beds of the Dubysa Formation at Priekule (+5.9‰, Figure 6) and in the Mituva Formation at Pavilosta (+4.2‰) and Ventspils (+5.0‰, Figure 5). At Ohesaare, the level of this peak is cut out at a stratigraphic gap (Kaljo et al., 1997).

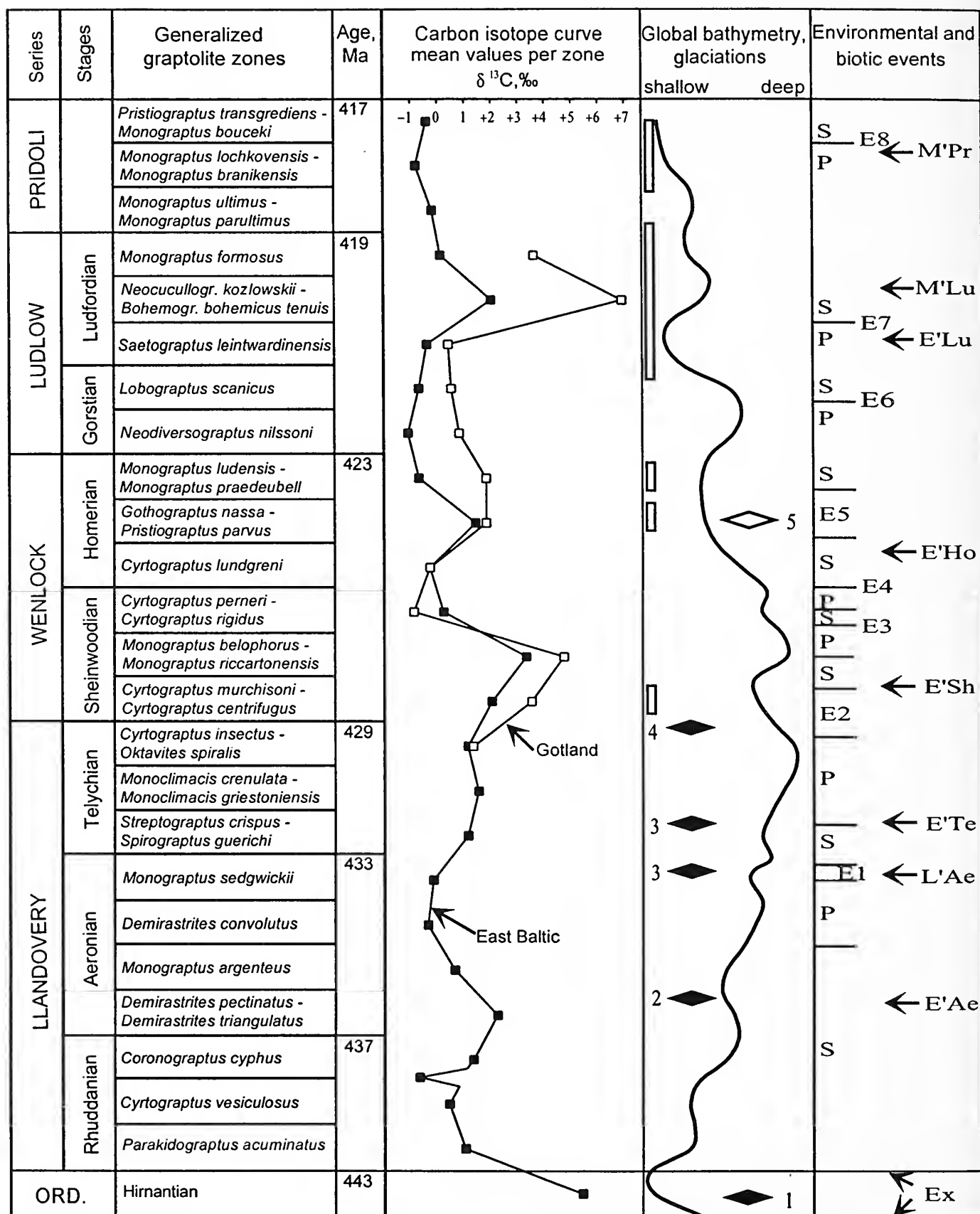
CORRELATION WITH GOTLAND CARBON ISOTOPE CURVE

Two reports on stable isotopes in the Gotland sequence (Wenzel and Joachimski, 1996; Samtleben et al., 1996) allow a comparison with the results in the East Baltic. The Gotland section is much thinner (Figure 2), but the most interesting part with three main positive peaks is well represented. The general pattern of the carbon isotope curve and inter-regional correlation show that the peaks (lower and upper Wenlock, middle Ludfordian) are clearly coincident in both areas, despite the fact that the Gotland data are based on brachiopod shells, while we utilized whole-rock samples. However, a better understanding of connections of the carbon cycling with other environmental events (sea-level curves, oceanic episodes, etc.) requires a more detailed correlation of the $\delta^{13}\text{C}$ curves.

For this purpose, we correlated two generalized curves with the standard graptolite zonation (Figure 7). The curves were compiled by the following procedure: 1) the East Baltic and Gotland sequences were correlated with each other and with the standard biostratigraphic zonation (sources mentioned above), and intervals of the generalized graptolite zones were identified in terms of the local stratigraphy; 2) mean values of $\delta^{13}\text{C}$ for every graptolite zone were calculated for the East Baltic (data from the Kirikuküla, Ruhnu, Ohesaare, and Ventspils cores and Ohesaare cliff section were used) and Gotland (data from Samtleben et al., 1996, and Wenzel and Joachimski, 1996); and (3) mean carbon isotope values and other environmental data in each zone were plotted against the graptolite zonation to produce a generalized carbon isotope curve (Figure 7).

The overall result of this procedure would be most influenced by problems in the correlation of graptolite and shelly sequences. However, we are optimistic because there are many detailed biostratigraphical studies published on the East Baltic and Gotland Silurian and because a few incorrectly dated samples do not usually strongly influence the mean carbon values (on the other hand, the narrow high peaks in Figures 3–5 are considerably lower in Figure 7). Thus, two doubtful correlations deserve to be commented upon.

FIGURE 6—(opposite) Lithology and $\delta^{13}\text{C}$ curve of Priekule core. The Nova Beds (Figure 2) are diachronous, and correlation of the related carbon isotope excursions is complicated (see Kaljo et al., 1997) and ambiguous. Explanations in Figure 3. Additional abbreviation: N, Nova Beds.



Despite the generally uniform trends of the East Baltic and Gotland carbon isotope curves (Figure 7), there is a clear discrepancy at the very end of the Homerician, where the East Baltic curve shows a rapid $\delta^{13}\text{C}$ decrease. However, the Gotland curve stays high and decreases only in the Gorstian. In addition to possible real differences between the curves, gaps in the sections, insufficient sampling, and problems of correlation should be considered.

Another source of doubt is related to the middle Ludfordian peak that is correlated (Figure 7) into the *Bohemograptus bohemicus tenuis*-*Neocucullograptus kozlowskii* Zone. This follows the correlation of Figure 2 and is also the one suggested by Jeppsson et al. (1994). According to the global sea-level curve (Figure 7), the middle Ludfordian peak coincides with an interval of eustatic rise. Bearing in mind a hiatus at this level in Estonia (Figure 2, note that the uppermost Paadla Stage is missing above the Torgu Formation), the Baltic facies interpretation conflicts with the global curve (Johnson et al., 1991). Inaccuracy in age determination might be involved in both the Baltic and global curves. On the other hand, there are many known examples of different sea-level records on various parts of continents and even in small parts of sedimentary basins. For example, the Aeronian in southern Scandinavia and western Latvia is largely represented by black graptolitic shales with a high C_{org} and a pyrite content that is typical of anoxic deep-water conditions. During the *Demirastrites convolutus* Chron and the *Monograptus sedgwickii* Chron in Scandinavia, a belt of black shales advanced toward the shore. However, in the Estonian part of the basin, there is a major gap that is also present in East Baltic sections (e.g., Kirikuküla and Ruhnu; Figure 2). A local sea-level curve describes the facies evolution of the area much better, but it contradicts the global character of the carbon isotope curve.

In conclusion, the general pattern of the carbon isotope curve seems well established in the Baltic Silurian, and it might be used for correlation purposes and interpretation of different environmental processes. Many details, however, need to be studied more thoroughly.

ENVIRONMENTAL AND BIOTIC CYCLICITY AND CARBON ISOTOPES

Figure 7 relates the carbon isotope and global sea-level curves, oceanic episodes, glaciations, biotic events, and phases of enhanced oxygenation in the ocean. The first impression from this figure is that the coincidence of these phenomena may not be accidental. We consider the coincidence persuasive if the events that are compared always occur within a zone. In Figure 7, $\delta^{13}\text{C}$ data are plotted in the middle of a zone and bioevents at the top, but it is usually unrealistic to date a glaciation or a sea-level change more precisely. All more or less proven glaciations (numbers 1–4 and the presumed glaciation 5 in Figure 7) coincide with positive excursions of the carbon isotope curve. In the early Aeronian and late Homerician, the coincidence is good. In the early Telychian, there is a clear rise of the curve, but the time of glaciation is not firmly defined beyond being “early Telychian or possibly still in the latest Aeronian” (Grahn and Caputo, 1992, p. 13). A glaciation in the latest Telychian–earliest Wenlock seems to occur before the highest peak of the excursion, clearly at the beginning of the positive shift. From this correlation, we conclude that heavy carbon isotope values are causally tied to the cooling of the climate and glaciation in the high-latitude regions.

Positive $\delta^{13}\text{C}$ peaks are usually coincident with sea-level lowstands (Brenchley et al., 1994; Wenzel and Joachimski, 1996), and some authors also point out a connection with times of reef growth and carbonate platform expansion (Samtleben et al., 1996). Although these general tendencies are supported by our data, detailed correlations are more ambiguous. In the early Aeronian and late Homerician, the suggested pattern is followed more or less well. In the early Sheinwoodian, the positive shift of $\delta^{13}\text{C}$ values began during a sea-level lowstand, but the peak followed during the next highstand. The same scenario is valid in the middle Ludfordian.

In the Early Silurian, glacial events may be the causes of sea-level lowering. Sea-level lowstands, particularly if coincident with a glaciation, are believed to be times of more vigorous circulation and thus enhanced oxygenation of ocean-bottom waters. This could explain the correlation of the so-called oxic events with sea-level lowstands (Figure 7).

FIGURE 7—(opposite) Correlation of East Baltic and Gotland carbon isotope curves and environmental and biotic events. Stratigraphy as in Figure 2. Dates mainly from Tucker and McKerrow (1995, see text). East Baltic (black squares) and Gotland (open squares) $\delta^{13}\text{C}$ curves explained in text. Vertical bars mark enhanced oxygenation of bottom waters (Kemp, 1991; Koren', 1987; Wenzel and Joachimski, 1996). Eustatic curve slightly modified from Johnson et al. (1991). Oceanic primo (P) and secundo (S) episodes and events (E) after Aldridge et al. (1993), Jeppsson (1993), and Jeppsson et al. (1995). Events: E_1 , Sandvika; E_2 , Ireviken; E_3 , Boge; E_4 , Valleviken; E_5 , Mulde; E_6 , Linde; E_7 , Lau; E_8 , middle Pridoli. Due to space limitations, a P–E–S cycle between E_2 and E_3 is not shown. Black rhombs are glaciations: 1, Hirnantian (Brenchley et al., 1994, 1995; Grahn and Caputo, 1992); 2–4 are Brazilian glaciations (Grahn and Caputo, 1992). Dating of No. 3 is problematic. White rhomb is possible glaciation (No. 5) after Johnson and McKerrow (1991). Arrows with letters show stratigraphic position of Silurian bioevents from Kaljo et al. (1995). Ex bioevent in latest Ordovician (Nestor et al., 1991) includes two phases in Pirgu (pre-Hirnantian) and Porkuni (Hirnantian) Stages.

Bioproduction has been accepted as an important factor in carbon fractionation. High primary productivity removes light carbon from ocean water and causes high $\delta^{13}\text{C}$ values. Unfortunately, we do not know much about rates of Silurian productivity, and the corresponding estimates are more or less hypothetical. We can measure diversity changes in biota (usually only a small part of it), but diversity and productivity have only a remote connection.

In spite of all the limitations noted above, we tried to understand the role of biodiversity changes in carbon cycling. For this purpose, the main biotic events known from a recent survey (Kaljo et al., 1995) were plotted in Figure 7. In the comments below, most attention is paid to planktic biota (particularly micro-organisms) that produce most of the modern biomass. From this correlation, we make the following observations:

- 1) The early Aeronian $\delta^{13}\text{C}$ peak coincides with a fourth-order radiation and closely follows the extinction event that, to some degree, affected conodonts and graptolites. The standing diversity, however, remained at a relatively high level. The first diversity low began in the *Demirastrites convolutus* Zone (acritarchs), but particularly low conodont and graptolite diversity characterizes the *Monograptus sedgwickii* Zone (Kaljo et al., 1995; Štorch, 1995).

- 2) The early Sheinwoodian $\delta^{13}\text{C}$ positive excursion began in the time interval of the Ireviken Event (Figure 7, E_2), a second-order bioevent that featured mass extinctions of conodonts and acritarchs. Chitinozoans and graptolites, which were mostly planktic organisms, were greatly affected (Melchin, 1994; Kaljo et al., 1995; Štorch, 1995). The peak of the carbon excursion was reached after this bioevent, when many of these groups of organisms had low diversities. Graptolites, conodonts, chitinozoans, and to some extent acritarchs, were characterized by a four-fold increase in the number of taxa at the Wenlock–Llandovery boundary. It should be mentioned that this subsequent low-diversity interval featured a pelagic ecotope filled with masses of *Monograptus riccartonensis*. To feed such a large quantity of graptolites, large amounts of microplankton were needed.

- 3) The middle–late Homerian positive carbon excursion coincides with the Mulde Event (a fifth-order bioevent characterized by the appearance of several new lineages). The Mulde Event includes a low-diversity interval among planktic organisms that followed a major extinction event at the end of the *Cyrtograptus lundgreni* Zone (Kaljo et al., 1995; Koren', 1987).

- 4) The middle Ludfordian $\delta^{13}\text{C}$ peak was preceded by a third-order bioevent with major extinctions of graptolites, ostracoderms, acritarchs, and conodonts in the

Saetograptus leintwardinensis Zone. It was followed by or coincident with a second-order bioevent known from profound changes in vertebrate communities and the disappearance of many graptolites, corals, and conodonts in the *Bohemograptus bohemicus tenuis*–*Neocucullograptus kozlowskii* Zone (Urbanek, 1993; Kaljo et al., 1995; Štorch, 1995). Owing to these extinctions, the latter zone is also a low-diversity interval among planktic organisms.

In summary (Figure 7), all but the early Aeronian positive carbon isotope excursions follow major (second- or third-order) bioevents and coincide with a low-diversity period of most planktic organisms. The middle Ludfordian peak also partly coincides with a major extinction event. The early Aeronian and middle Homerian positive shifts coincide with a low-order origination event.

On the other hand, all but one high-order (II–III) bioevent (extinction) are followed by or partly coincide with a major carbon positive excursion. The exception is the middle Pridolian bioevent. Correlation of the main positive excursions with some oceanic turnovers or events (Figure 7; E_2 , E_5 , E_7) suggested by Jeppsson et al. (1995; also Aldridge et al., 1993) is reliable. However, it seems very difficult to find counterparts of all other oceanic events described by Jeppsson et al. (1995), especially in the Wenlock.

DISCUSSION

In our analysis, major attention was paid to four of the most pronounced positive carbon isotope excursions. Such shifts of $\delta^{13}\text{C}$ values might be caused by different environmental and biotic factors. These factors often interact with each other, and sometimes one or several clearly dominate. Depending on the duration of a carbon isotope excursion, a steady-state or a transient model (Kump, 1991; Holser et al., 1995) should be applied for the interpretation of the $\delta^{13}\text{C}$ data. These two states are of a rather different length (1 Ma and 100 Ka, respectively), which allows a means to classify the isotope events in the Baltic.

In Figure 7, we used the absolute ages suggested by Tucker and McKerrow (1995), except for one. Instead of 428 Ma for the base of the Wenlock, we show 429 Ma because a thin volcanic ash in the uppermost graptolite zone in the Llandovery has an age of 430.1 \pm 2.4 Ma (Tucker and McKerrow, 1995) and the difference of 2 Ma seems to be too much for an interval of less than one graptolite zone. Stage boundaries in the Llandovery are interpolated from the known dates.

Absolute ages of boundaries vary little in the different time scales. Therefore, the average duration of a

graptolite zone depends mostly on the number of zones distinguished in a higher chronostratigraphic unit. For the Llandovery, Hughes (1995) calculated an average of 1 Ma per zone. We used the so-called generalized graptolite zones (Koren' et al., 1996) for correlation with non-graptolitic sections, and our average for the Telychian is 1.3 Ma per zone.

Based on this time scale, we can estimate probable ages and durations of the main isotope events:

- 1) The early Aeronian excursion at 436 Ma, with a duration clearly on the order of 1 Ma.

- 2) The early Sheinwoodian excursion at 428 Ma, with a duration of more than 1 Ma.

- 3) The middle Homerian peak at 424 Ma. The positive excursion occurs between two ^{13}C depletion intervals in the *Cyrtograptus ludgreni* and *Monograptus ludensis*-*M. praedeubeli* Zones. The actual duration of the event might be estimated as half that of the *Gothograptus nassa*-*Pristiograptus parvus* Zone (i.e., 0.5 Ma or less, but we do not know how much).

- 4) A middle Ludfordian event at 420 Ma, with a duration of the excursion of 0.5–1.0 Ma. Correlation uncertainties do not allow for a higher precision.

From the above data, we conclude that three of the Silurian isotope events are clearly of greater duration. For these, a steady-state model should be applied. The middle Homerian excursion seems to be the shortest, and the transient model is not excluded. To find confirmation for the estimates above, more detailed sampling and age identification are necessary.

In addition, a strikingly regular temporal pattern of the events is observed. Beginning with the Hirnantian event (444 Ma), there is an interval of 8 Ma until the early Aeronian event, followed by another interval of 8 Ma until the early Sheinwoodian event reaches a peak. Higher in the Wenlock and Ludlow, the positive excursions occur every 4 Ma, a time span twice as long as that in the Llandovery. The actual figures may be different, but the regular pattern of the carbon isotope changes seems obvious, although the cause of such regularity is not clear.

If the steady-state model is used in the interpretation of the Baltic Silurian $\delta^{13}\text{C}$, the dominant role of photosynthetic reduction must be modified by the impact of enhanced burial of organic carbon, higher primary productivity, changed oceanic circulation and bottom-water conditions and their influence on the burial and oxidation rates, and overall bioproduction. The effect of riverine influx on surface waters during the Silurian seems to be less pronounced (or at least indistinct) than during later geological periods, due to the scanty vegetation and soil cover on the land.

Nearly the same set of carbon isotope excursions described in this report was analyzed by Heath et al. (1996), Samtleben et al. (1996), and Wenzel and Joachimski (1996). A good starting point for discussion is the latest Ordovician isotope event dealt with by Brenchley et al. (1994, 1995). For comparison, we have included our Ordovician data (Figures 3, 7) that show a major positive carbon isotope shift (ca. +4‰ in the Hirnantian Porkuni Stage above the pre-event level), substantial sea-level fall, and two major extinctions before and during Porkuni time. We have suggested the influence of a Gondwana glaciation (Kaljo et al., 1991; Nestor et al., 1991). These data are in agreement with those of Brenchley et al. (1994, 1995).

The effects noted by Brenchley et al. (1994, 1995) that are of prime interest in analyzing the effects of high-latitude glaciation are: 1) sinking of cool, well-oxygenated waters and their replacement by warm, saline-bottom waters in the lower latitudes; 2) growth of the ice cap led to glacio-eustatic fall; and 3) an up-welling of nutrient-rich waters that led to enhanced productivity, especially by planktic organisms, as part of a eutrophication of earlier oligotrophic ecosystems and consequent extinction of numerous biotic elements not prepared for such changes of conditions. The latter idea was also advocated by Loydell (1994) in a discussion of early Telychian changes in graptolite diversity.

Two additional comments should be made. First, the wide distribution of black shales marks an enhanced burial of organic carbon. Second, anoxic or dysaerobic conditions in bottom waters needed for organic carbon burial were usually confined to sea-level highstands (Wilde et al., 1991).

Using these more or less generally accepted conclusions, we have tried to analyze the situation in the Baltic Silurian. The first strongly positive carbon isotope excursion in the early Aeronian is close to the middle of the *Coronograptus gregarius* Zone glaciation event (number 2, in Figure 7). This event did not cause serious changes in biota (although a possible radiation should be noted) while sea-level was still high or had only begun to drop. The correlation of the listed events is not precise, and therefore this positive shift could best be tied to the wide distribution of black shales and anoxic or dysaerobic conditions in the Aeronian. These developments do not reveal anything about the causes of the positive shift in the early Aeronian. We may only guess that the glaciation did have some influence on ocean circulation and bioproduction, but the data are controversial. Aldridge et al. (1993) regarded the early Aeronian as a time of a warm secundo episode. This fits well with high sea-level and black shale distribution. We can see some signs of glacial

influence (sea-level lowering and change of lithology due to increased oxygenation) only higher in the section, but this change is diachronous in different areas.

The early Sheinwoodian isotope event seems to fit with the glaciation model described above. This event is associated with sea-level fall, changed oceanic circulation, better oxygenation of the bottom waters, and severe extinctions in the initial phase of the event. These are followed by a low-diversity interval, abundance of opportunistic species, and increased planktic bioproduction and burial of C_{org} (see also Kaljo et al., 1997) in the second phase of the event. The first phase coincides well with the Ireviken Event (Aldridge et al., 1993; Jeppsson et al., 1995).

The middle Homerian positive isotope excursion cannot be interpreted so clearly. The glaciation (number 5, Figure 7) is not proven by sedimentary rocks, but mainly deduced from a eustatic lowstand at the end of the Wenlock (Johnson and McKerrow, 1991). However, we do have eustatic and biodiversity lows, an interval with better oxygenation of the bottom waters, and some signs of the abundance of a few opportunistic species (Kaljo et al., 1997). On the other hand, no black shale accumulation has been recorded, and Jeppsson et al. (1995) defined this interval as a warm *secundo* episode.

The last major carbon isotope event is in the middle Ludfordian and shows the highest $\delta^{13}C$ values (see above). This event is associated with two severe extinction events. It coincides with a low-diversity interval and oxic bottom waters. Sea-level rose after a strong fall in the early Ludfordian. There is no significant black shale accumulation, and Jeppsson's (1993) Lau P-S Event (Figure 7, E₂) developed just prior to the $\delta^{13}C$ peak.

The middle Homerian and middle Ludfordian isotope events discussed herein are not related to a known glaciation, and the sea-level curve has different trends at these event levels. However, the biotic changes are clearly important. Therefore, we propose that a severe extinction was often followed during the resultant low-diversity period by a considerable increase in bioproduction in planktic communities. This may have caused differences in fractionation of carbon isotopes between surface and deep water (Samtleben et al., 1996) and burial of light carbon if conditions allowed. Such increase seems to have two causes: changes in ocean circulation (better ventilation and nutrient flow), and appearance of unoccupied niches in ecotopes.

The Baltic data corroborate carbon isotope records from Australia (Andrew et al., 1994). The Australian Silurian records three events (note that parentheses bracket maximum $\delta^{13}C$ values in ‰): Ireviken (+3.5), Pentamerid (+13), and Silurian-Devonian boundary (+8). The first

one can be correlated well with the Baltic early Sheinwoodian excursion; the second is not precisely dated, but seems to be close to our middle Ludfordian peak; the last one occurs in the lowermost Devonian but was not studied by us. Andrew et al (1994) clearly showed that each carbon isotope excursion followed a biotic event, as is primarily the case in the Baltic.

CONCLUSIONS

In the East Baltic Silurian, four main positive excursions in carbon isotopes are recorded. Three of these occur in the Wenlock and Ludlow and coincide with those established on Gotland. Two excursions coincide with trends in Australia. These seem to be true global events.

The general pattern of both the East Baltic and Gotland carbon isotope curves is the same. This shows sufficient authenticity of the East Baltic whole-rock data.

The East Baltic data support the observations made on Gotland (Samtleben et al., 1996; Wenzel and Joachimski, 1996) that deeper-water sediments show lower $\delta^{13}C$ values. It is true also for one positive excursion measured in different facies, and agrees with a similar conclusion made by Grossmann (1994).

Most of the Silurian carbon isotope positive peaks occur after important extinctions of organisms (mainly planktic). They occur during a low-diversity interval, which supposedly coincided with a phase of enhanced bioproduction and led to a corresponding differentiation in carbon fractionation in the water column.

During the Early Silurian, glaciations in the southern hemisphere and glacio-eustatic changes seem to have played a significant role in ocean circulation that influenced oxidation of bottom waters and bioproduction. However, there is no full coincidence or relationship of the sea-level curve with carbon isotope excursions. Therefore, other factors should be considered, because they probably interacted.

ACKNOWLEDGMENTS

The authors thank E. Kiipli, Ü. Männik, A. Noor, and K. Ronk for technical and linguistic help. We acknowledge with thanks the constructive criticism by J. Veizer and an anonymous reviewer, and suggestions by E. Landing that greatly improved our manuscript. The study was supported in part by Estonian Science Foundation grants No. 1935 and 2186. This report is a contribution to IGCP Project No. 386.

REFERENCES

- ALDRIDGE, R.J., L. JEPPSSON, AND K.J. DORNING. 1993. Early Silurian oceanic episodes and events. *Journal of the Geological Society of London*, 150:501–513.
- ANDREW, A.S., P.J. HAMILTON, R. MAWSON, J. TALENT, AND D.J. WHITFORD. 1994. Isotopic correlation tools in the mid-Palaeozoic and their relation to extinction events. *Australian Petroleum Explorers Association Journal*, 34:268–277.
- BASSETT, M.G., D. KALJO, AND L. TELLER. 1989. The Baltic region, p. 158–170. *In* C.H. Holland and M.G. Bassett (eds.), *A Global Standard for the Silurian System*. National Museum of Wales, Geological Series 9.
- BRENCHLEY, P.J., J.D. MARSHALL, G.A.F. CARDEN, D.B.R. ROBERTSON, D.F.G. LONG, T. MEIDLA, L. HINTS, AND T.F. ANDERSON. 1994. Bathymetric and isotopic evidence for a short-lived Late Ordovician glaciation in a greenhouse period. *Geology*, 22:295–298.
- , G.A.F. CARDEN, AND J.D. MARSHALL. 1995. Environmental changes associated with the “first strike” of the Late Ordovician mass extinction. *Modern Geology*, 20:69–82.
- CORFIELD, R.M., D.J. SIVETER, J.E. CARTLIDGE, AND W.S. MCKERROW. 1992. Carbon isotope excursion near the Wenlock–Ludlow (Silurian) boundary in the Anglo-Welsh Area. *Geology*, 20:371–374.
- GAILITE, L.K., R.Z. ULST, AND V.I. YAKOVLEVA. 1987. *Stratopicheskie i Tipove Razrezy Silura Latvii*. Zinatne, Riga (In Russian).
- GRAHN, Y., AND M.V. CAPUTO. 1992. Early Silurian glaciation in Brazil. *Palaeogeography, Palaeoclimatology, Palaeoecology*, 99:9–15.
- GROSSMANN, E.L. 1994. The carbon and oxygen isotope record during the evolution of Pangea: Carboniferous to Triassic, p. 207–228. *In* G.D. Klein (ed.), *Pangea: Paleoclimate, Tectonics, and Sedimentation During Accretion, Zenith and Breakup of a Supercontinent*. Geological Society of America, Special Paper 288.
- HEATH, R.J., P.J. BRENCHLEY, AND J.D. MARSHALL. 1996. A carbon and oxygen stable isotope stratigraphy for the early Silurian of Estonia, p. 58. *In* The James Hall Symposium: Second International Symposium on the Silurian System. Programs and Abstracts. University of Rochester.
- HOLSER, W.T., M. MAGARITZ, AND R.L. RIPPERDAN. 1995. Global isotopic events, p. 63–88. *In* O.H. Walliser (ed.), *Global Events and Event Stratigraphy in the Phanerozoic*. Springer Verlag, Berlin.
- HUGHES, R.A. 1995. The durations of Silurian graptolite zones. *Geological Magazine*, 132:113–115.
- JEPPSSON, L. 1990. An oceanic model for lithological and faunal changes, tested on the Silurian record. *Journal of the Geological Society of London*, 147:663–674.
- . 1993. Silurian events, the theory, and the conodonts. *Proceedings, Estonian Academy of Sciences, Geology*, 42:23–27.
- , V. VIIRA, AND P. MÄNNIK. 1994. Silurian conodont-based correlations between Gotland (Sweden) and Saaremaa (Estonia). *Geological Magazine*, 131:201–218.
- , R.J. ALDRIDGE, AND K.J. DORNING. 1995. Wenlock (Silurian) oceanic episodes and events. *Journal of the Geological Society of London*, 152:487–498.
- JOHNSON, M.E., AND W.S. MCKERROW. 1991. Sea level and faunal changes during the latest Llandovery and earliest Ludlow (Silurian). *Historical Biology*, 5:153–169.
- , D. KALJO, AND RONG J.-Y. 1991. Silurian eustasy, p. 145–163. *In* M.G. Bassett, P.D. Lane, and D. Edwards (eds.), *The Murchison Symposium. Special Papers in Palaeontology*, 44.
- JUX, U., AND T. STEUBER. 1992. C_{carb} - und C_{org} -Isotopenverhältnisse in der silurischen Schichtenfolge Gotlands als Hinweise auf Meeresspiegelschwankungen und Krustenbewegungen. *Neues Jahrbuch für Geologie und Paläontologie. Monatshefte*, 7:385–413.
- KALJO, D. 1970. Graptolity, p. 179–185. *In* D. Kaljo (ed.), *Silurian of Estonia*. Valgus, Tallinn (In Russian).
- . 1990. The Silurian of Estonia, p. 21–26. *In* D. Kaljo and H. Nestor (eds.), *Field Meeting Estonia 1990. An Excursion Guidebook*. Tallinn.
- (ED.). 1987. *Resheniya Mezvedomstvennogo Soveshchaniya po Ordoviku i Siluru Vostochno-Evropejskoj Platformy 1984 g.s. Regional'nyimi Stratigraficheskimi Skhemami*. Leningrad.
- , H.E. NESTOR, L.J. POLMA, AND R.E. EINASTO. 1991. Pozdneordovskoe oledenenie i ego otrazhenie v osadkonakoplenii Paleobaltiiskogo bassejna, p. 68–78. *In* D. Kaljo, T. Modzalevskaya, and T. Bogdanova (eds.), *Major Biological Events in Earth History*. Estonian Academy of Sciences, Tallinn.
- , A.J. BOUCOT, R.M. CORFIELD, T.N. KOREN', J. KØI, A. LEHERISSE, P. MÄNNIK, T. MÄRSS, V. NESTOR, R.H. SHAVER, D.J. SIVETER, AND V. VIIRA. 1995. Silurian bio-events, p. 173–224. *In* O.H. Walliser (ed.), *Global Events and Event Stratigraphy in the Phanerozoic*. Springer-Verlag, Berlin.
- , T. KIIPLI AND T. MARTMA. 1996. Summary of the first carbon studies in the East Baltic Silurian. *Acta Geologica Hungarica*, 39(suppl.):94, 95.
- , ———. *In press*. Carbon isotope event markers through the Wenlock–Pridoli sequence at Ohesaare (Estonia) and Priekule (Latvia). *Palaeogeography, Palaeoclimatology, Palaeoecology*.
- KEMP, A.E.S. 1991. Mid-Silurian pelagic and hemipelagic sedimentation and palaeoceanography, p. 261–299. *In* M.G. Bassett, P.D. Lane, and D. Edwards (eds.), *The Murchison Symposium. Special Papers in Palaeontology*, 44.
- KOREN', T. 1987. Graptolite dynamics in Silurian and Devonian time. *Bulletin of the Geological Society of Denmark*, 35:149–159.
- , A.C. LENZ, D.K. LOYDELL, M.J. MELCHIN, P. ŠTORCH, AND L. TELLER. 1996. Generalized graptolite zonal sequence defining Silurian time intervals for global paleogeographic studies. *Lethaia*, 29:59–60.
- KUMP, L.R. 1991. Interpreting carbon-isotope excursions: Strangelove oceans. *Geology*, 19:299–302.
- LOYDELL, D.K. 1994. Early Telychian changes in graptoloid diversity and sea level. *Geological Journal*, 29:355–368.
- MÄRSS, T. 1986. *Silurian Vertebrates of Estonia and West Latvia*. Valgus, Tallinn (In Russian with English summary).
- MELCHIN, M.J. 1994. Graptolite extinction at the Llandovery–Wenlock boundary. *Lethaia*, 27:285–290.
- NESTOR, H. 1993. *Catalogue of Silurian Stratigraphic Units and Stratotypes in Estonia and Latvia*. Estonian Academy Publishers, Tallinn.
- , E.R. KLAAMANN, T.R. MEIDLA, P.E. MÄNNIK, R.P. MÄNNIL, V.V. NESTOR, J.R. NOLVAK, M.P. RUBEL, L.I. SARV, AND L.M. HINTS. 1991. *Dinamika fauny v Baltijskom bassejne na granitse ordovika i silura*, p. 79–86. *In* D. Kaljo, T. Modzalevskaya, and T. Bogdanova (eds.), *Major Biological Events in Earth History*. Valgus, Tallinn.
- NESTOR, V. 1994. Early Silurian Chitinozoans of Estonia and North Latvia. *Estonian Academy Publishers*, Tallinn.
- SAMBTLEBEN, C., A. MUNNECKE, T. BICKERT, AND J. PÄTZOLD. 1996. The Silurian of Gotland (Sweden): facies interpretation

- based on stable isotopes in brachiopod shells. *Geologische Rundschau*, 85:278–292.
- ŠTORCH, P. 1995. Biotic crises and postcrisis recoveries recorded by Silurian planktonic graptolite faunas of the Barrandian area (Czech Republic). *Geolines*, 3:59–70.
- TUCKER, R.D., AND W.S. MCKERROW. 1995. Early Paleozoic chronology: a review in light of new U-Pb zircon ages from Newfoundland and Britain. *Canadian Journal of Earth Sciences*, 32:368–379.
- URBANEK, A. 1993. Biotic crises in the history of Upper Silurian graptoloids: a paleobiological model. *Historical Biology*, 7:29–50.
- WENZEL, B. 1994. Carbon and oxygen isotopic variations of brachiopods from Gotland (Sweden): possible indicators of large scale climatic oscillations. *Erlanger Geologische Abhandlungen*, 122:65.
- , AND M.M. JOACHIMSKI. 1996. Carbon and oxygen isotopic composition of Silurian brachiopods (Gotland/Sweden) [sic, n-dash, not virgule]: palaeoceanographic implications. *Palaeogeography, Palaeoclimatology, Palaeoecology*, 122:143–166.
- WILDE, P., W.B.N. BERRY, AND M.S. QUINBY-HUNT. 1991. Silurian oceanic and atmospheric circulation and chemistry, p. 123–143. *In* M.G. Bassett, P.D. Lane, and D. Edwards (eds.), *The Murchison Symposium. Special Papers in Palaeontology*, 44.

EARLY SILURIAN CARBON AND OXYGEN STABLE-ISOTOPE STRATIGRAPHY OF ESTONIA: IMPLICATIONS FOR CLIMATE CHANGE

RACHEL J. HEATH, PATRICK J. BRENCHLEY AND JAMES D. MARSHALL

Department of Earth Sciences, University of Liverpool, Brownlow Street, P.O. Box 147, Liverpool L69 3BX, U.K.

ABSTRACT—Early Silurian recovery followed the Ashgill extinction; however, there were smaller episodes of extinction of Llandovery plankton and benthos. Recent studies of Late Ordovician events have shown that the Ashgill extinction was associated with major glaciation, glacio-eustatic changes, and a large positive excursion in $\delta^{18}\text{O}$ and $\delta^{13}\text{C}$ in marine carbonates. It has been suggested that Early Silurian events are also related to changes in ocean state, or sea-level fluctuations associated with climatic change. To test this model, a carbon and oxygen stable-isotope stratigraphy is established for the Llandovery and lowermost Wenlock. Data was obtained from brachiopod calcite from Estonian shelf-carbonate sequences with shallow burial history and low thermal maturity.

A gradual trend towards more negative and constant $\delta^{18}\text{O}$ values through the Llandovery and nearly constant values of $\delta^{13}\text{C}$ exists, with two small excursions that are based on limited data. In the early Wenlock, a large positive excursion in oxygen (nearly 2‰) and carbon (>2‰) persists for five graptolite zones, and is associated with extinctions of planktic faunas.

Gradual decrease in $\delta^{18}\text{O}$ through the Llandovery is interpreted to reflect a progressive warming, and the $\delta^{13}\text{C}$ data suggest relatively stable oceanic conditions without major changes in carbon cycling. The magnitude of the positive isotopic excursion in the early Wenlock may indicate major cooling, possibly associated with growth of ice caps, and the carbon excursion reflects major changes in carbon cycling.

The isotope data suggest relatively stable oceanic conditions that are consistent with progressive recovery of ecosystems after the Ashgill extinction. The isotope data do not confirm proposals of four glacio-eustatic changes, nor do they identify major perturbations of the carbon cycle during planktic extinction events in the Llandovery or show any systematic variation with proposed P and S states.

INTRODUCTION

The early Silurian was a time of biotic recovery after extinction events associated with the Ashgill (Ordovician)

glaciation; however, smaller extinctions in plankton and benthos have been identified in the Llandovery (see Kaljo et al., 1995, for a review). Recent work has successfully used oxygen and carbon stable-isotope trends of biogenic carbonate to improve the resolution of climatic and oceanic changes, particularly for end-Ordovician events (Brenchley et al., 1995a). Brenchley et al. (1995b) have shown that large positive excursions of $\delta^{18}\text{O}$ and $\delta^{13}\text{C}$ that correlate with glacio-eustatic fluctuations in the Ashgill are also closely associated with extinction events. This report presents a carbon and oxygen stable-isotope stratigraphy for the Lower Silurian of Estonia, which is part of a continuing project to investigate whether faunal changes, particularly among planktics, are related to oceanic changes recorded in the isotopic record. It also aims to investigate the possibility of establishing a global stable-isotope stratigraphy for the Early Silurian.

The oxygen stable-isotopic composition of biogenic calcium carbonate precipitated in equilibrium with surrounding water depends on the isotopic composition of that water and the temperature of precipitation (Epstein et al., 1951). Similarly, the carbon isotopic composition of biogenic carbonate reflects that of the ambient water, but fractionation is not strongly temperature-dependent. Therefore, changes in carbon isotope values are taken as an indicator of changes in the flux of the marine carbon reservoir. Because of the success of isotopic studies in interpretation of Quarternary and Tertiary environments and climate (e.g., Shackleton and Boersma, 1981; Prentice and Matthews, 1988), isotopes have been used to investigate earlier geological epochs (Veizer et al., 1986; Grossman et al., 1991; Wadleigh and Veizer, 1992). Brachiopod shells appear to be the most suitable sediment component for isotopic studies of the Paleozoic, and have been used commonly for that purpose, although their use as indicators of the isotopic composition of ancient seawater is still controversial (Rush and Chavetz, 1990; Land, 1995). Factors mitigating in their favor are their mineralogy, relative abundance in Paleozoic sediments,

and ease of identification and extraction. Articulate brachiopods secrete shells of low-magnesium calcite (Lowenstam, 1961; Morrison and Brand, 1986), which is relatively stable in the diagenetic environment and more resistant to alteration than such carbonates as high-magnesium calcite and aragonite. Several methods are available to assess the extent of diagenetic alteration. These include cathodoluminescence and trace-element determinations to reveal chemical alteration, and scanning electron microscopy and petrography to show textural alteration. Analysis of a single component, such as a brachiopod shell, from a carbonate rock is an advantage over sampling bulk rock, as the latter gives isotope values which are an average of all the diagenetic and depositional carbonate phases in the sample; whereas a well-preserved shell will have an isotopic signal that reflects the isotopic composition of the ambient water. The main factor mitigating against the use of biogenic carbonates are vital effects, which may give disequilibrium fractionation (Carpenter and Lohmann, 1995; Wefer and Berger, 1991). Brachiopods, however, exert smaller vital effects than other marine organisms, and their oxygen isotope vital effects are not thought to be significant (Lepzelter et al., 1983; Wefer and Berger, 1991). Carbon generally shows a slightly larger range of values that arise from vital effects (Wefer and Berger, 1991), but it is possible to assess these effects through studies of inter- and intra-taxonomic variations, and so avoid giving significance to isotopic shifts which are an artifact of the biological variability.

GEOLOGY AND STRATIGRAPHY

The Early Silurian succession of Estonia was deposited in the intra-cratonic East Baltic Basin. This sequence of carbonates, argillaceous carbonates, and calcareous mudstones overlies similar Ordovician sedimentary rocks. The region is tectonically undeformed and has not been deeply buried (Kaljo et al., 1988). During the Ordovician, a relatively shallow epicontinental sea existed in the Baltic region. This developed into a gulf-like basin with a comparatively deep basin depression rimmed by a carbonate shelf in the Caradoc to middle Llandovery (Nestor, 1990a). Five confacies belts that reflect depth and distance from shore have been recognized in the Silurian (Kaljo et al., 1988). The basin was generally stable until the early Ludlow, with a transgressive maximum in the late Llandovery–early Wenlock. However, a regressive phase is recorded in the middle Llandovery (Nestor, 1990a).

Brachiopods for analysis were obtained from the “Ruhnu core”, which was taken from a borehole on the

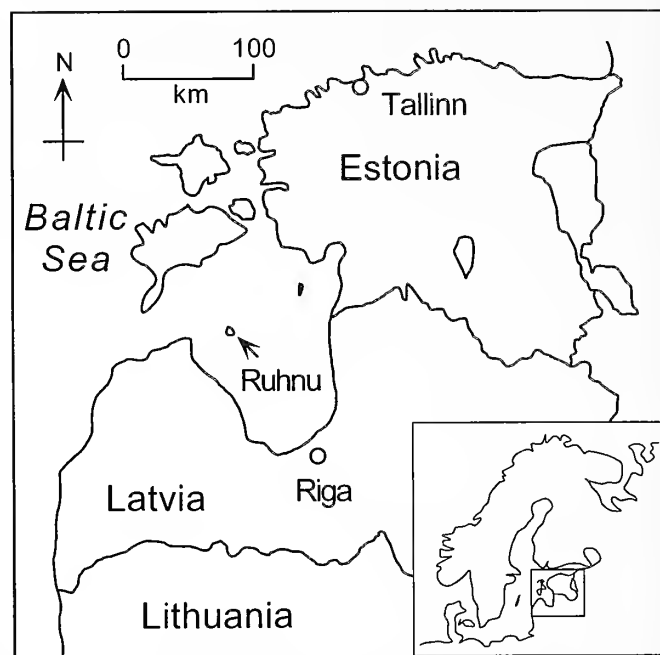


FIGURE 1—Map of Estonia with location of Ruhnu borehole.

island of Ruhnu in the Bay of Riga (Figure 1). The Ruhnu core includes Early Silurian rock that represents confacies belts 3 and 4, which were deposited in a deep-shelf to shelf-basin transitional setting.

The history of sea-level change in this part of the basin is inferred from lithological and faunal evidence from the Ruhnu core and is shown as a relative sea-level curve in Figure 2. Relatively uniform facies and brachiopod assemblages in the Ruhnu core indicate that locally there were no major sea-level falls in the lower Llandovery after a shallowing at the base of the Saarde Formation (lower Rhuddanian). The occurrence of *Dicoelosia* in the Lemme Member and younger units denotes benthic assemblage 5, which has been estimated as representing a paleobathymetry of >90 m (Brett et al., 1993). The increasing abundance of graptolites and trilobite material and increasingly argillaceous sediment from the Velise to the Jamaja Formations indicates continued deepening through the Telychian and lower Wenlock to shelf-edge depths (ca. 200m; see Brett et al., 1993). *Dicoelosia* is not recorded below the Lemme Member (late Aeronian), but the preservation of graptolites and the similarity of brachiopod assemblages to those of much of the earlier sequence indicates that it was not significantly shallower. There is lithological evidence for a marked shallowing in the *Monograptus sedgwickii* Zone (late Aeronian). This regressive unit is only 1.0 m-thick in the Ruhnu core, and has been assigned to benthic assemblage depth 3–4 (Johnson et al., 1991a), the shallowest assemblage identi-

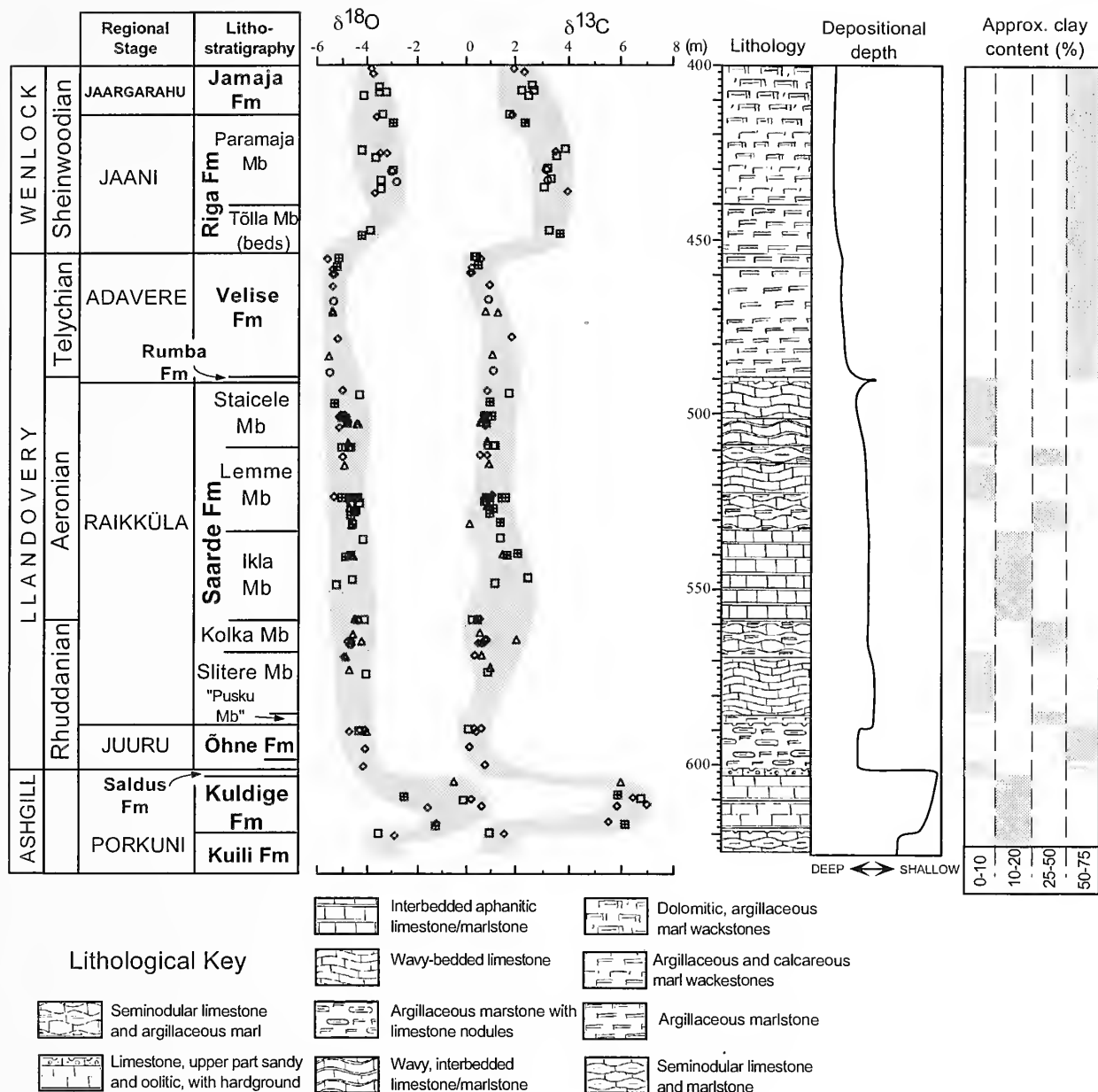


FIGURE 2—Relationship of brachiopod $\delta^{13}\text{C}$ and $\delta^{18}\text{O}$ values from Ruhnu core with stratigraphy, lithology, and local sea-level changes. Symbols represent brachiopod orders: diamond, Orthis; circle, Pentamerida; triangle, Spiriferida; open square, indeterminate; crossed square, Strophomenida. Shaded area encloses range of isotopic data. Approximate clay content of sediment from Nestor (1990b). Scale gives depth in core (meters).

fied in this core sequence. There are two pyritized surfaces separated by 2 cm at the base of the Rumba Formation; these are interpreted as hiatal. There are similar pyritized laminae at the bases of the Saarde and Õhne Formations. Only the latter, which corresponds with the Ordovician–Silurian boundary, is considered to represent a major hiatus. There is no indication that any of the surfaces were ever subaerially exposed.

SAMPLING AND ANALYTICAL TECHNIQUES

Whole brachiopod shells and fragments were extracted from the rock matrix. Generally, the shells were less than 5 mm across and 0.5 mm thick. Brachiopods were sampled at stratigraphic intervals that depended on their

occurrence through 220 m of core. With the exception of a gap of 16 m in the Slite Member, samples were collected at 2–7 m intervals. The brachiopods range stratigraphically from the upper Ashgill to the lower Wenlock. The shells were removed from the matrix by wet sieving, freeze-thawing with sodium sulphate solution, and drilling. The specimens were cleaned mechanically in an ultrasonic bath until all adhering sediment was removed. Preservation of representative samples was assessed by scanning electron microscopy and by determination of trace-element concentrations. Due to the small size of many of the shells and shell fragments, it was not possible to evaluate preservation in every sample analyzed.

Specimens for stable-isotope analysis were powdered if larger than 5 mg, but were otherwise used whole. Samples of 1.5–4 mg were baked in an E2000 Biorad Plasma Asher for two hours to remove organic components. The carbonate was dissolved in 100% phosphoric acid at 50 C. The CO₂ evolved was analyzed with a modified VG Isogas SIRA 12 isotope-ratio mass spectrometer at the University of Liverpool. The results were corrected by standard methods (Craig, 1957) and are expressed in "delta" (δ) notation as per mil (‰) relative to the V-PDB international standard. The analytical precision (1 σ) based on multiple analysis of an internal standard (run as an unknown) is better than ± 0.05 ‰ for $\delta^{13}\text{C}$ and ± 0.1 ‰ for $\delta^{18}\text{O}$.

An assessment of shell preservation was by determination of trace elements and scanning electron microscopy. The shells for SEM examination were selected from samples that yielded sufficient material. Unetched gold-palladium-coated fracture surfaces were examined with a Phillips XL30 with an accelerating voltage of 10–15 kV. In addition, concentrations of the trace elements Fe, Mn, Mg, and Sr were determined by inductively coupled, plasma atomic-emission spectroscopy (ICP-AES) at the University of Liverpool.

RESULTS

The analytical data are presented in Appendices 1 and 2. Graphic representations are in Figures 2 and 3.

PRESERVATION.—Under the SEM, the specimens were seen to be generally well preserved and clearly show secondary layer ultrastructure and well-preserved crystal-lites. This good preservation of shell ultra-structures is taken as evidence that diagenetic alteration has not significantly affected the isotopic signature of the shell.

Trace elements (Fe, Mg, Sr, and Mn) showed no significant correlations with each other, and none correlated with either $\delta^{13}\text{C}$ or $\delta^{18}\text{O}$. The lack of systematic variation of

trace-element concentrations with isotope values precludes their use as indicators of preservation in this study.

VARIABILITY.—The sensitivity of the isotope record (i.e., the level at which isotopic events can be resolved) depends on the range of variation in the brachiopods sampled. Studies of modern and Recent brachiopods show that biological control of isotopic fractionation (i.e., vital effects) can result in inter- and intra-taxonomic differences (Lepzelter et al., 1983; Carpenter and Lohmann, 1995). Single specimens may also show variations as great as 1‰, which probably reflect ontogenic differences or seasonality. The assessment of intra-specimen variation in brachiopods from the Ruhnu core was not possible, as the shells were generally too small to allow multiple samples from a single specimen. Intra-genus variation was investigated at two horizons. Specimens of the strophomenid *Leangella* sp. from a horizon in the Staicele Member showed ranges of 0.2‰ and 0.1‰ for $\delta^{13}\text{C}$ and $\delta^{18}\text{O}$, respectively ($n=4$), whereas *Leangella* sp. from a Lemme Member sample gave slightly larger ranges of 0.7‰ for $\delta^{13}\text{C}$ and 0.6‰ for $\delta^{18}\text{O}$ ($n=6$). Statistically valid numbers of brachiopods for the study of inter-taxon variation could not be collected from single beds due to restrictions posed by sampling core. Because of this, data were pooled from different horizons within a lithological unit (Appendix 1). Appendix 1 shows that within a unit, differences in mean $\delta^{13}\text{C}$ and $\delta^{18}\text{O}$ between genera are small (<0.3 ‰), and do not suggest major inter-taxon differences. However, given the small amount of data available on intra- and inter-taxon variability, it seems prudent to take a conservative approach in interpreting the isotopic data, and to give significance only to those stratigraphic shifts that are substantially greater than the observed range of values for an individual horizon (i.e., 0.7‰).

STABLE ISOTOPES.—Large positive shifts are recorded in $\delta^{13}\text{C}$ and $\delta^{18}\text{O}$ in the lower Wenlock (Silurian) and in the Ashgill (Upper Ordovician) (Figure 2). In the stratigraphic interval between these peaks, the oxygen isotope record shows a gradual trend towards more negative values. The carbon isotope signal grossly parallels the oxygen isotopic trends, but shows more small-scale variability, particularly through the Llandovery. Values of $\delta^{13}\text{C}$ in the Llandovery show no long-term directional change, but include two possible minor excursions that are based on limited data (Figure 2). The minor perturbations include a 1‰ negative shift in $\delta^{13}\text{C}$ in the top of the Velise Formation (late Telychian) and a 1‰ positive shift in the Ikla Member (early Aeronian), but their significance is uncertain as these shifts are not significantly larger than observed intra-taxon variations.

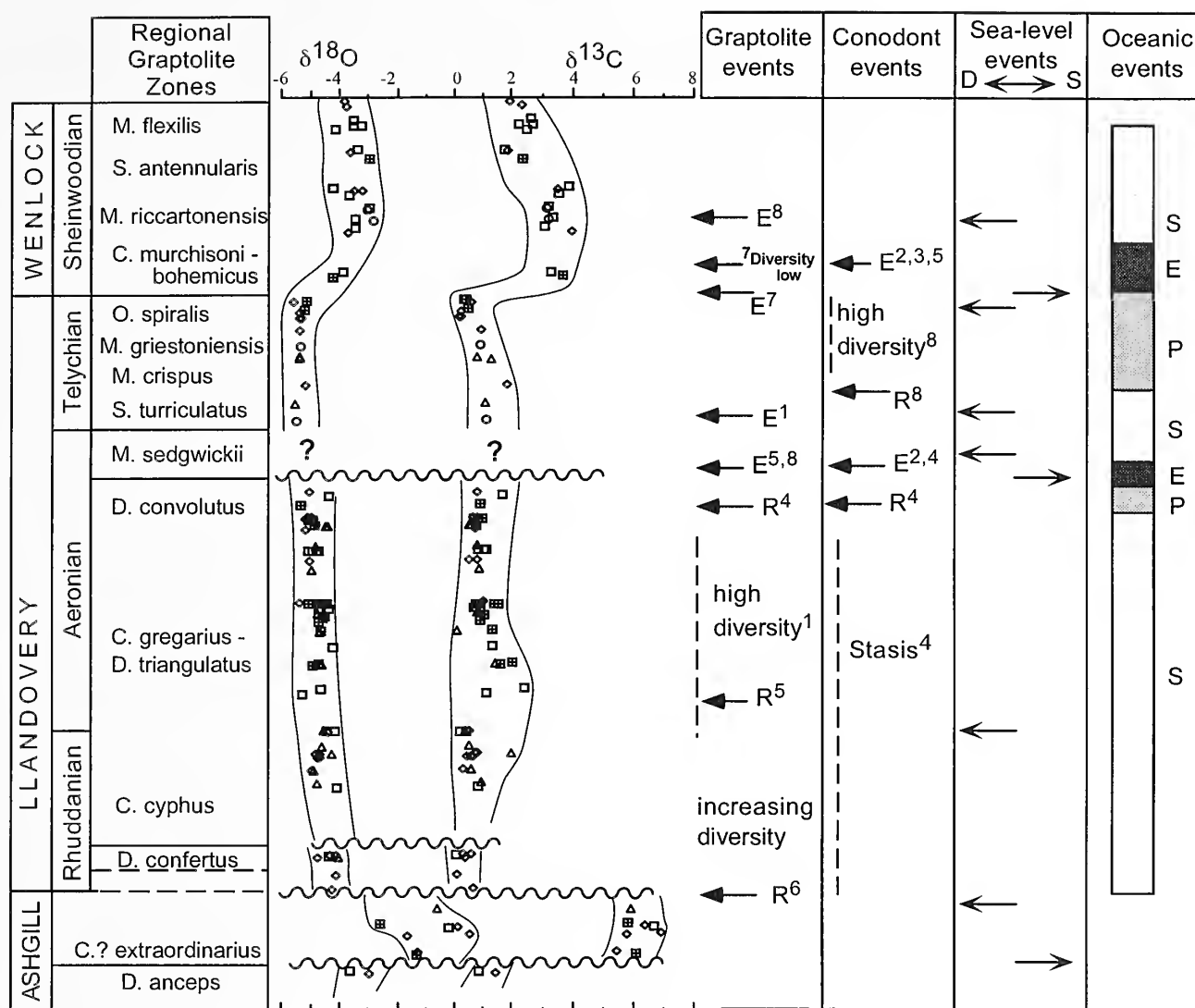


FIGURE 3—Relationship between stable isotope changes and faunal, oceanic and global sea-level events. Isotope data symbols as Figure 2. Faunal events: E, extinction; R, radiation. Oceanic events of Aldridge et al. (1993) and Jeppsson et al. (1995): E, event; P, Primo episode; S, Secundo episode. Sea-level events of Johnson et al. (1991b): D, deepening event (to left); S, shallowing event (to right). Sources of faunal data: ¹Loydell (1994), ²Chatterton et al. (1990), ³Jeppsson (1987) ⁴Aldridge et al. (1993), ⁵Leggett et al. (1981), ⁶Melchin and Mitchell (1991), ⁷Melchin (1994), and ⁸Kaljo et al. (1995).

Oxygen values rise from a mean of -5.3‰ in the Velise Formation (upper Llandovery–Wenlock boundary), by 1‰ in the 5 m sequence across the Llandovery–Wenlock boundary, to a mean of -3.5‰ in the Riga Formation (lower Wenlock). This is a total shift of 1.8‰ (Figure 2). Similarly, mean carbon values increase by 2.3‰ from +0.8‰ to +3.1‰. The isotopic variation between the Velise Formation and the Riga Formation (the Llandovery–Wenlock transition) is not associated with any notable lithological changes. The most pronounced lithological change occurs lower in the sequence at the base of the Adavere Stage, between the bioturbated nodular micrites and marls of the Staicele

Member and Rumba Formation and the laminated argillaceous marls of the Velise Formation (Figure 3). There is no corresponding significant isotopic shift that corresponds to this, and this suggests that the isotopic signal does not simply reflect changes in the depositional environment, type of sediment, or differences in diagenesis between lithologies. This is further supported by the evidence that the most lithologically varied units (Lemme and Staicele Members) do not have correspondingly varied isotopic signals.

In the Ashgillian isotope shift, $\delta^{18}\text{O}$ increases from nearly -3.5‰ to almost +1‰ in the Kuldiga Formation

and returns to previous levels in the Öhne Formation (lowermost Llandovery). Carbon values show a parallel trend, but, the shift is slightly larger, and values rise from +1.5‰ to a maximum of +7‰ before returning in the Öhne Formation to values that are slightly more negative than those of the pre-shift conditions of the Kuili Formation. The precise timing of the negative shift is not clear as no samples were recovered from the intervening Saldus Formation.

DISCUSSION

THE ISOTOPIC RECORD.—Stratigraphic variation in isotopic values is commonly interpreted as a reflection of changing paleoceanography and environment, but may also reflect differences in diagenetic overprint (Brand, 1987; Bates and Brand, 1991; Grossman et al., 1991; Banner and Kaufman, 1994). Although it remains possible that the texturally pristine brachiopod shells could have been affected by diagenesis, there are several aspects of the Estonian Silurian sequences which favor the conservation of a primary isotopic signal. The Baltic sequences have not been deeply buried or metamorphosed, and there has been no major tectonic deformation of the succession (Kaljo et al., 1988). Paleokarst surfaces are absent in the Ruhnu core succession; there is consequently no need to consider the effects of local meteoric diagenesis which commonly result in stratigraphic trends in isotope values (Allan and Matthews, 1982; Rush and Chavetz, 1990).

The large positive shifts in $\delta^{13}\text{C}$ and $\delta^{18}\text{O}$ apparent in the late Ashgill from the Ruhnu core have previously been identified in other Baltic core sequences (Brenchley et al., 1995a; Carden, 1995), and are also seen in carbonate sequences from North America (Carden, 1995) and Sweden (Marshall and Middleton, 1990). Large positive shifts in $\delta^{13}\text{C}$ are also recorded from organic carbon in deep-water graptolitic shales at Dob's Linn in Scotland (Underwood et al., In press) and China (Wang et al., 1993). The isotopic record of carbonates from Argentina (Marshall et al., In press) indicates that these shifts occurred over a wide range of latitudes. This can be taken as evidence that the Ruhnu brachiopod signal reflects global effects. The changes in $\delta^{13}\text{C}$ and $\delta^{18}\text{O}$ in the Ashgill correlate well with the glacio-eustatic changes of the Late Ordovician glaciation, and have been causally related (Brenchley et al., 1995a). Later isotope shifts from the same sequence may also be related to significant climatic and oceanic events. The largest oxygen and carbon isotope shift in the Early Silurian occurs near the Llandovery–Wenlock boundary, with elevated isotope values persisting into the Sheinwoodian, at least into the *Monograptus flexilis* Zone. There is evidence for oceanic and faunal changes at

this time (discussed below). At present, this event has been recorded only in the Baltic region. Independent isotope studies of brachiopods from the Wenlock of Gotland, Sweden, show positive shifts in $\delta^{13}\text{C}$ and $\delta^{18}\text{O}$ of the same style and magnitude as the Estonian data (Samtleben et al., 1995; Wenzel and Joachimski, 1995).

The Wenlock isotope record from Gotland has been interpreted to reflect paleosalinity shifts that relate to changes in the input of fresh water (Samtleben et al., 1995). This is because shifts in the oxygen isotope record correlate with facies changes in the Gotland succession. By this interpretation, more negative oxygen isotope values are associated with increased runoff that led to the formation of marly sediments and, it is suggested, inhibited reef formation as a result of greater turbidity (Samtleben et al., 1995). More positive values are associated with reef growth and less clayey sediments, which reflect a decreased input of fresh water. There is no apparent correlation between the isotopic record and lithological change in the Ruhnu core. Ruhnu sediments were deposited in deep water towards the center of the basin and at some distance from the point of entry of any fresh-water runoff at the basin margins. The faunal evidence suggests that normal marine conditions prevailed. The isotope signal from such an environment is unlikely to reflect paleosalinity changes. If intra-basinal effects had significantly influenced isotope values, then a strong association between lithology and the isotopic record would be expected, but this is not the case for the Ruhnu core data (Figure 2). The lack of correlation between lithology and intra-basinal sea-level fluctuations with $\delta^{18}\text{O}$ suggests that local changes in precipitation and runoff were not the dominant cause of isotopic variation.

Alternatively, the isotopic signal may reflect extra-basinal changes. The direction and magnitude of the Wenlock oxygen isotope shifts suggest ice volume changes as a possible external control factor. In the absence of salinity changes, changes in $\delta^{18}\text{O}_{\text{ocean water}}$ ($\delta^{18}\text{O}_{\text{ow}}$) are the effect of ice volume. Rainfall and snow at high latitudes have more negative $\delta^{18}\text{O}$ values than ocean water; consequently, high-latitude ice sheets are a reservoir for ^{16}O (Anderson and Arthur, 1980). When ice sheets build up and extend during glaciation, $\delta^{18}\text{O}_{\text{ow}}$ is shifted towards more positive values. Decrease in ocean temperature during glaciation will also increase $\delta^{18}\text{O}_{\text{carbonate}}$ as isotopic fractionation during precipitation is temperature-dependent. In this way, the onset of ice sheet growth and related cooling could produce a positive oxygen isotope shift of the magnitude seen at the Llandovery–Wenlock boundary.

Positive $\delta^{18}\text{O}$ shifts in the Cenozoic isotope record, which have been interpreted as the result of ice volume

effects as described above, are often associated with negative $\delta^{13}\text{C}$ shifts. This is because organic matter is incorporated into sediment at below-normal rates during regression (Berger and Vincent, 1986), and this increases the relative abundance of ^{12}C in total dissolved carbon. Contrary to this, the Ruhnu core carbon values are shifted in a positive direction, roughly in parallel with the oxygen curve. This suggests that organic carbon was being sequestered at this time. The size of the shift indicates major changes in the carbon cycle, and may reflect changes in planktic productivity and rate of organic carbon sequestration.

In the discussion below, isotopic trends will be related to oceanographic change, eustasy, and their effect on biotas. A current model for Early Silurian climate will be summarized.

RELATIONSHIP TO SEA-LEVEL.—Deepening events for which a glacio-eustatic cause has been suggested are identified at the Rhuddanian–Aeronian transition and in the middle Aeronian (lowest *Monograptus sedgwickii* Zone), early Telychian (*Spirograptus turriculatus* Zone), and late Telychian (Johnson et al., 1991b; Figure 3). They have been defined on the basis of benthic assemblages, and have been identified from analysis of sequences from a number of paleocontinents (Johnson and McKerrrow, 1991; Johnson et al., 1991a) including Baltica. The rate of change of these sea-level fluctuations is consistent with their proposed glacio-eustatic origin. Glacial sediments of Early Silurian age have been described in Brazil (Grahn and Caputo, 1992), but there is no other evidence for the extent of glaciation.

Although several cores from Estonia were included in the study by Johnson et al. (1991a), sedimentological and paleontological evidence from the Ruhnu core do not reflect the sea-level rises proposed therein. This may be because the depth range of the benthic assemblages in the core is greater than the amount of sea-level change which took place. However, if the sea-level changes were glacio-eustatic, they could be expected to correlate with changes in the isotopic record.

A comparison of the isotopic signal with sea-level events (Figure 3) shows that the proposed deepening phases are not reflected in the Ruhnu core oxygen isotope data. However, a eustatic regression identified near the Llandovery–Wenlock boundary (Johnson and McKerrrow, 1991, fig. 1) does appear to coincide with the onset of high $\delta^{18}\text{O}$ and $\delta^{13}\text{C}$ values. Although the general trend of Llandovery oxygen isotopes towards more negative values could be compatible with gradual glacio-eustatic rise, there are no isotopic events that would be compatible with the rapid deepening phases identified by Johnson and McKerrrow (1991) and Johnson et al. (1991a, 1991b).

The absence of any correlation between sea-level rises and the isotopic record for the Llandovery could indicate that sea-level fluctuations were of relatively low magnitude. Proposed Llandovery deepening events are estimated on the basis of benthic assemblage depths to represent sea-level rises of 30–50 m (Johnson and McKerrrow, 1991) and more recently, based on the relief on coastal paleotopography, of 60–70 m (Johnson et al., this volume). The amount of water sequestered to produce this amount of sea-level change may not be sufficient to produce an isotope shift of a magnitude greater than the internal variability of the isotope signal ($\pm 0.7\text{‰}$), in which case the Llandovery deepening events could not be identified from the Ruhnu core data. However, the Llandovery–Wenlock isotope excursion is resolved by isotope data that suggest that the regression at this time was greater than earlier sea-level changes. Although there is no local evidence for shallowing, a eustatic fall at the Llandovery–Wenlock transition and the occurrence of glacial sediments in the lower Wenlock (Grahn and Caputo, 1992) support the interpretation of this isotope shift as a reflection of changes in $\delta^{18}\text{O}_{\text{ocean water}}$ by ice sheet growth with climatic cooling. Elevated isotope values through the early–middle Sheinwoodian suggest a longer cool period than indicated by the sea-level curve, which depicts fairly rapid deepening (deglaciation?) in the *Cyrtograptus murchisoni*–*Bohemograptus bohemicus* Zone (Figure 3).

RELATIONSHIP TO ICE VOLUME AND TEMPERATURE.—If it is accepted that the Ruhnu core isotope signal reflects changes in $d^{18}\text{O}_{\text{ow}}$, then inferences can be made about the nature of the climatic fluctuations that these isotopic changes represent. As noted above, salinity is not likely to be a principal component of the Ruhnu isotope signal. This leaves ice-volume and temperature-variation effects to account for the major oxygen isotope excursion at the Llandovery–Wenlock boundary. Major temperature changes at low latitudes in the early Wenlock are not supported by faunal evidence; stable, diverse, typical carbonate-shelf faunas persisted at this time (Kaljo et al., 1988; Nestor, 1994), but minor changes cannot be ruled out. This has implications for the amount of sea-level change which can be inferred from the isotope signal (see discussion below).

The relative contributions of ice volume and temperature change to the isotope shift (and hence to eustatic change) are not easily determined, as the two are not simply related. Models for more recent climate shifts give varying estimates of the amount of temperature change in the tropics during glaciation. The CLIMAP reconstruction describes small changes (less than 2°C) in sea-surface temperatures (SST) in the tropics between glacial

and interglacial times (Broeker and Denton, 1989). If this model is taken as an analogue for the Early Silurian, then ice volume changes would be expected to have had a greater influence than temperature changes on the isotopic record. Alternatively, a more recent report (Guilderson et al., 1994) suggests that SSTs in the tropics may have been cooler by as much as 6° C during the Last Glacial Maximum. The deep-shelf environment represented by the Ruhnu core succession would have been above the ocean thermocline and in the mixed layer. For this reason, it would be affected by variation in SST. If a large shift of tropical SST in response to glaciation as described by Guilderson et al. (1994) is applicable to the Early Silurian, then a substantial part of the isotope shift could be due to temperature change.

The estimate of the amount of sea-level change from the size of the isotope shift is also subject to error. The temperature effect is not proportional to ice volume change, which means that the oxygen record is not a perfect proxy for ice volume (Broeker and Denton, 1989). Attempts to quantify possible sea-level changes from the magnitude of the isotope shift are based on estimates of the volume of water that must be removed from the oceans to produce a certain amount of sea-level fall, and on estimates of the isotopic composition of the sequestered water. For instance, an isotope shift of 0.0133‰ for every meter of sea-level change would result if the water sequestered to produce the sea-level fall had an isotopic composition as extreme as modern snow from the interior of Antarctica (Appendix 3, column [a]) (Emiliani and Shackleton [1974] in Rowley and Markwick, 1992). Appendix 3 shows the amount of sea-level change that would be expected from the observed positive 2‰ oxygen isotope shift with varying combinations of ice volume and temperature effects for three different estimates of the change in $\delta^{18}\text{O}_{\text{ow}}$ per meter of sea-level change. Values for the change in $\delta^{18}\text{O}$ per meter of sea-level change have been calculated by different workers for the sea-level change since the Last Glacial Maximum. These range from 0.0133 m⁻¹ (Emiliani and Shackleton [1974] in Rowley and Markwick, 1992), which assumes that the sequestered water has extremely negative $\delta^{18}\text{O}$ values, to as low as 0.008‰ m⁻¹ (Schrage et al., 1992), which is based on less negative values for the water sequestered. It is clear from Appendix 3 that the calculated sea-level fluctuations are unrealistically large if the isotopic shift is due only to ice-volume effects (row 1), especially for scenario (c). The cases in which the values are 1‰ or less are attributed to ice volume effects and give more reasonable sea-level changes, but invoke tropical sea temperature changes of 4.5°C or more. The observed excursion can be accounted for with an equal contribution from both sea-level and temperature change (rows 3 and 4). However,

this requires a minimum sea-level fall of 75 m. This is within the bounds of possibility, but exceeds the most recent estimate of sea-level fluctuations for the Llandovery (i.e., 60–70 m, see Johnson et al., this volume).

These calculations suggest a sea-level fall similar to or in excess of that of the Hirnantian, which has been estimated as 50–100 m (Brenchley and Newall [1980] in Brenchley et al., 1995b) or ~60 m (Crowley and Baum [1991] in Brenchley et al., 1995a). In this respect, estimates of end-Ordovician sea-level change conflict with those of the Early Silurian. The sedimentological changes at the Llandovery–Wenlock boundary are not as severe as the end-Ordovician, are associated with smaller oxygen and carbon isotope shifts, and consequently suggest that the sea-level change was smaller.

RELATIONSHIP TO FAUNAL EVENTS.—Planktic organisms, such as graptolites and conodonts, are sensitive to changes in ocean stratification, upwelling, and flux of nutrients. Consequently, episodes of extinction followed by radiations identify particularly significant times of environmental disturbance. The records of turnover in graptolites and conodonts through the Early Silurian are compared with the isotope record in Figure 3. This shows episodes of extinction or decreased diversity near the Aeronian–Telychian boundary and at the Llandovery–Wenlock boundary. There are no significant extinction events reported in the Rhuddanian and early-middle Aeronian for graptolite or conodont faunas. For the graptolites, this is a period of increasing diversity and radiation after the Hirnantian extinctions, which began in the *Parakidograptus acuminatus* Zone and continued with a number of radiation events (Leggett et al., 1981; Kaljo et al., 1995). Conodont faunas took longer to recover and were in stasis through the early Llandovery (Aldridge et al., 1993). Ruhnu core isotope values through this interval are relatively constant, which reflects stable environmental conditions with no dramatic oceanographic disturbances. Both graptolites and conodonts underwent a radiation in the *Demirastrites convolutus* Zone (late Aeronian). However, this is followed by a decrease in diversity of conodont and graptolite faunas in the *Monograptus sedgwickii* Zone. Unfortunately, no isotope data were recovered from this interval, so it is not known whether the biotic turnover is associated with isotopic changes. A graptolite-diversity low in the *Stimulograptus utilis* Subzone (lower *Spirograptus turriculatus* Zone) has been related to the sea-level fall after the second Llandovery deepening (Loydell, 1994). The most significant biotic crisis in the Early Silurian occurs at the beginning of the Wenlock. There is a graptolite diversity low in the *Cyrtograptus murchisoni* Zone, but the highest extinction rate occurs between the *Monoclimacis crenulata* and

Cyrtograptus centrifugus Zones and corresponds to the Llandovery–Wenlock boundary (Melchin, 1994). The faunal events are correlated with the eustatic regression at this time and with a positive excursion in $\delta^{18}\text{O}$ and $\delta^{13}\text{C}$ in the Ruhnu core (Figure 3). The diversity low appears to correlate with the time of greatest rate of sea-level change, whereas the highest extinction rate may occur at the maximum lowstand. Conodonts are also severely affected by the early Wenlock extinction event (Jeppsson, 1987; Chatterton et al., 1990; Aldridge et al., 1993), with the general disappearance of genera with platform elements (Jeppsson, 1987). Some benthic groups also show diversity changes, (e.g., trilobites in North America [Chatterton et al., 1990] and brachiopods [Kaljo et al., 1995]).

RELATIONSHIP TO OCEANIC EVENTS.—Jeppsson (1990) proposed a model for oceanic cycles to explain lithological and faunal changes in the Silurian. He identified alternations in climate states between P episodes (or times when the climate was cool at high latitudes and humid at low latitudes) and S episodes (or times when the climate was warm at high latitudes and dryer at low latitudes). A third state occurs briefly at the transition from a P episode to an S, and is termed an "event". According to the model, an episode is identified by characteristic lithologies and faunas that reflect the ocean state and climate of that time. The model describes a number of oceanic and lithological changes and includes changes in the carbon isotope record. It is suggested that positive shifts in $\delta^{13}\text{C}$ would occur during P episodes, with burial of organic carbon in black shales that form in shallow waters; conversely, S episodes would be associated with lower $\delta^{13}\text{C}$ values that result from lower planktic productivity. As the model also includes sea-level changes, one would expect this to be reflected in the oxygen isotope record if the changes were glacio-eustatic. The model states that severe P episodes could become cold enough for the growth of ice sheets, which means that some P episodes would be expected to coincide with positive shifts in $\delta^{18}\text{O}$. S episodes, being relatively warm, might be expected to be associated with decreased $\delta^{18}\text{O}$ values with local temperature increase, and melting of the ice sheets thought to exist at that time in the Gondwanan highlands. The model has been applied to the Early Silurian, and the resulting pattern of episodes has been described (Aldridge et al., 1993; Jeppsson et al., 1995).

The pattern of P and S episodes is related to the Ruhnu isotope stratigraphy in Figure 3. There are two proposed oceanic cycles in the Early Silurian, with P–S transition events in the late Aeronian and at the Llandovery–Wenlock boundary. According to the model, negative shifts in $\delta^{13}\text{C}$ would be expected at P to S transi-

tions, but these are not recorded in the Ruhnu core. There is no relationship between trends in $\delta^{13}\text{C}$ and $\delta^{18}\text{O}$ from Ruhnu and the proposed P and S episodes. This may indicate that climatic differences between P and S episodes are not great enough to be resolved by the isotopic record. As with sea-level events, the isotopic record can resolve only those climatic changes greater than a certain magnitude. Although minor differences cannot be ruled out, large differences in organic carbon production and burial and carbonate deposition between S and P episodes are not inferred for the Early Silurian.

The positive isotope shifts in $\delta^{13}\text{C}$ and $\delta^{18}\text{O}$ between the Velise and Riga Formations coincide with the Ireviken Event of Jeppsson et al. (1995), a P–S transition event which is defined by conodont faunal event horizons in Gotland. This occurs in the *Pterospiriferus amorphognathoides* (conodont) Zone and spans the Llandovery–Wenlock boundary. The interpretation of the positive oxygen isotope shift as an indication of cooling in the early Wenlock conflicts both with the model of S state ("greenhouse") conditions at this time, which was inferred by Jeppsson (1987), and with the association of increased basin oxygenation with the Llandovery–Wenlock regression (Kemp, 1991).

A cluster of faunal events recorded in the published literature may correspond to the late Aeronian oceanic event identified by Aldridge et al. (1993). Unfortunately, there is no isotope data available in the Ruhnu core for the critical interval, and this report cannot contribute to a discussion of the significance of these events.

CONCLUSIONS

This report confirms a large isotopic shift associated with Hirnantian sedimentary rocks in the Baltic and a positive shift in $\delta^{13}\text{C}$ and $\delta^{18}\text{O}$ values in the early Wenlock that is regional in extent and associated with extinctions in graptolites and conodonts and glacio-eustatic changes. The isotope data point to stable environmental conditions in the Llandovery. This is consistent with progressive recovery following Late Ordovician deglaciation. The Wenlock isotope excursions may be related to the growth of ice caps. The Llandovery–Wenlock boundary isotopic shifts are associated with extinctions in planktic faunas that were sensitive to environmental change.

An association of biotic events with proposed eustatic change occurs in the *Monograptus sedgwickii* Zone (Figure 3), an interval for which no brachiopod isotope data are available. An isotopic study of this interval would be valuable.

The brachiopod isotopic record of the Ruhnu core does not provide evidence for the P and S ocean states

proposed by Aldridge et al. (1993) and Jeppsson et al. (1995), but does indicate major oceanographic events in the Early Silurian. The isotopic data do not confirm the four eustatic deepening events which have been proposed for the Llandovery (Johnson et al., 1991b). These data suggest that brachiopod isotope records can be used to investigate major climate shifts, but are not sufficiently sensitive to discriminate less severe environmental changes. The record of isotopic events fits a model where glacio-eustatic changes are the dominant cause of oceanographic change, rather than a model in which switches between P and S episodes are the main cause of oceanic events.

More isotopic studies of other Llandovery–Wenlock boundary successions are needed to confirm the significance of the boundary event. Detailed isotopic studies, in which the contribution of biogenic fractionation, lithology, and regional climate change to the isotope record are evaluated for each study area, are required before global isotope events can be identified.

ACKNOWLEDGMENTS

Fieldwork in Estonia was made possible by D. Kaljo, L. Hints, T. Martma, and T. Kipli. Many brachiopod specimens used for analysis were donated and identified by M. Rubel. We thank S.F. Crowley, D.F. Steele, and J.D. Ball for invaluable technical assistance. The manuscript benefited from reviews by L. Derry and an anonymous reviewer and from comments by the editors. This study was supported by a University of Liverpool Postgraduate Studentship to RJH and by NERC operating grants to the Stable Isotope Laboratory at the Department of Earth Sciences, University of Liverpool. This work is a contribution to IGCP Projects 335 and 386.

REFERENCES

- ALDRIDGE, R.A., L. JEPSSON, AND K.J. DORNING. 1993. Early Silurian oceanic episodes and events. *Journal of the Geological Society, London*, 150:501–513.
- ALLEN, J.R., AND R.K. MATTHEWS. 1982. Isotope signatures associated with early meteoric diagenesis. *Sedimentology*, 29:797–817.
- ANDERSON, T.A., AND M.A. ARTHUR. 1980. Stable isotopes of oxygen and carbon and their application to sedimentologic and paleoenvironmental problems, p. 1.1–1.151. *In* *Stable Isotopes in Sedimentary Geology*, SEPM Short Course 10. Society of Economic Paleontologists and Mineralogists, Dallas.
- BANNER, J.L., AND J. KAUFMAN. 1994. The isotopic record of ocean chemistry and diagenesis preserved in non-luminescent brachiopods from Mississippian carbonate rocks, Illinois and Missouri. *Geological Society of America Bulletin*, 106:1074–1082.
- BATES, N.R., AND U. BRAND. 1991. Environmental and physiological influences on isotopic and elemental compositions of brachiopod shell calcite: implications for the isotopic evolution of Palaeozoic oceans. *Chemical Geology (Isotope Geoscience Section)*, 94:67–78.
- BERGER, W.H., AND E. VINCENT. 1986. Deep sea carbonates: reading the carbon-isotope signal. *Geologische Rundschau*, 75:249–269.
- BRAND, U. 1987. Depositional analysis of the Breathitt Formation's marine horizons, Kentucky, U.S.A.: trace elements and stable isotopes. *Chemical Geology (Isotope Geoscience Section)*, 65:117–136.
- BRENCHLEY, P.J., J.D. MARSHALL, G.A.F. CARDEN, D.B.R. ROBERTSON, D.G.F. LONG, T. MEIDLA, L. HINTS, AND T.F. ANDERSON. 1995a. Bathymetric and isotopic evidence for a short-lived Late Ordovician glaciation in a greenhouse period. *Geology*, 22:295–298.
- , G.A.F. CARDEN, AND J.D. MARSHALL. 1995b. Environmental changes associated with the "first strike" of the Late Ordovician mass extinction. *Modern Geology*, 20:69–82.
- BRETT, C.E., A.J. BOUCOT, AND B. JONES. 1993. Absolute depths of Silurian benthic assemblages. *Lethaia*, 26:25–40.
- BROEKER, W.S., AND H. DENTON. 1989. The role of ocean-atmosphere reorganisations in glacial cycles. *Geochimica et Cosmochimica Acta*, 53:2465–2501.
- CARDEN, G.A.F. 1995. Stable isotope changes across the Ordovician–Silurian boundary. Unpublished Ph.D. dissertation, University of Liverpool, 284 p.
- CARPENTER, S.J., AND K.C. LOHMANN. 1995. $\delta^{18}\text{O}$ and $\delta^{13}\text{C}$ values of modern brachiopod shells. *Geochimica et Cosmochimica Acta*, 59:3749–3764.
- CHATTERTON, B.D.E., G.D. EDGEcombe, AND P. TUFFNELL. 1990. Extinction and migration in Silurian trilobites and conodonts of northwestern Canada. *Journal of the Geological Society, London*, 147:703–715.
- CRAIG, H. 1957. Isotopic standards for oxygen and carbon and correction factors for mass-spectrometric analysis of carbon dioxide. *Geochimica et Cosmochimica Acta*, 12:133–149.
- EMILIANI, C., AND N.J. SHACKLETON. 1974. The Bruhnes Epoch: isotopic paleotemperatures and geochronology. *Science*, 183: 511–514.
- EPSTEIN, S., R. BUCHSBAUM, H. LOWENSTAM, AND H.C. UREY. 1951. Carbonate–water isotopic temperature scale. *Bulletin of the Geological Society of America*, 62:417–426.
- FAIRBANKS, R.G., AND R.K. MATTHEWS. 1978. The marine oxygen isotope record in Pleistocene coral, Barbados, West Indies. *Quaternary Research*, 10:181–196.
- GRAHN, Y., AND M. CAPUTO. 1992. Early Silurian glaciations in Brazil. *Palaeogeography, Palaeoclimatology, Palaeoecology*, 99:9–15.
- GROSSMAN, E.L., ZHANG C., AND T.E. YANCEY. 1991. Stable isotope stratigraphy of brachiopods from Pennsylvanian shales in Texas. *Geological Society of America Bulletin*, 103:953–965.
- GUILDERSON, T.P., R.G. FAIRBANKS, AND J.L. RUBENSTONE. 1994. Tropical temperature variations since 20,000 years ago: modulating interhemispheric climate change. *Science*, 263:663–665.
- JEPSSON, L. 1987. Lithological and conodont distributional evidence for episodes of anomalous oceanic conditions during the Silurian, p. 129–145. *In* R.J. Aldridge (ed.), *Palaeobiology of Conodonts*. Ellis Horwood, Chichester.
- . 1990. An oceanic model for lithological and faunal changes tested on the Silurian record. *Journal of the Geological Society of London*, 147:663–674.
- , R.A. ALDRIDGE, AND K.J. DORNING. 1995. Wenlock (Silurian) oceanic episodes and events. *Journal of the Geological Society of London*, 152:487–498.

- JOHNSON, M.E., AND W.S. MCKERROW. 1991. Sea-level and faunal changes during the latest Llandovery and earliest Ludlow (Silurian). *Historical Biology*, 5:153–169.
- , B.G. BAARLI, H. NESTOR, M. RUBEL, AND D. WORSLEY. 1991a. Eustatic sea level patterns from the Lower Silurian (Llandovery Series) of southern Norway and Estonia. *Geological Society of America Bulletin*, 103:315–335.
- , D. KALJO, AND RONG J.-Y. 1991b. Silurian eustasy. *Special Papers in Palaeontology*, 44:145–163.
- KALJO, D., H. NESTOR, AND L. PÖLMA. 1988. East Baltic region. *Bulletin of the British Museum, Natural History (Geology)*, 43:85–91.
- , A.J. BOUCOT, R.M. CORFIELD, A. LE HERISSE, T.N. KOREN', J. KRÍŽ, P. MANNIK, T. MÄRSS, V. NESTOR, R.H. SHAVER, D.J. SIVETER, AND V. VIIRA. 1995. Silurian bioevents, p. 173–226. *In* O.H. Walliser (ed.), *Global Bioevents and Event Stratigraphy in the Phanerozoic*. Springer-Verlag, Berlin.
- KEMP, A.E.S. 1991. Mid Silurian pelagic and hemipelagic sedimentation and palaeoceanography. *Special Papers in Palaeontology*, 44:261–299.
- LAND, L.S. 1995. Comment on "Oxygen and carbon isotopic composition of Ordovician brachiopods: implications for coeval seawater" by H. Qing and J. Veizer. *Geochimica et Cosmochimica Acta*, 59:2843–2844.
- LEGGETT, J.K., W.S. MCKERROW, L.R.M. COCKS, AND R.B. RICKARDS. 1981. Periodicity in the marine realm. *Journal of the Geological Society of London*, 138:167–176.
- LEPZELTER, C., T.F. ANDERSON, AND P.A. SANDBERG. 1983. Stable isotope variation in modern articulate brachiopods (abs). *Association of American Petroleum Geologists*, 67:500, 501.
- LOWNSTAM, H.A. 1961. Mineralogy $^{18}\text{O}/^{16}\text{O}$ ratios and strontium and magnesium contents of Recent and fossil brachiopods and their bearing on the history of the oceans. *Journal of Geology*, 69:241–260.
- LOYDELL, D.K. 1994. Early Telychian changes in graptoloid diversity and sea-levels. *Geological Journal*, 29:609–613.
- MARSHALL, J.D., AND P.D. MIDDLETON. 1990. Changes in marine isotopic composition and the Late Ordovician glaciation. *Journal of the Geological Society of London*, 147:1–4.
- , P.J. BRENCHLEY, P. MASON, G.A. WOLF, R.A. ASTINI, L. HINTS, AND T. MEIDL. *In press*. Palaeogeography, Palaeoclimatology, Palaeoecology.
- MELCHIN, M.J. 1994. Graptolite extinction at the Llandovery–Wenlock boundary. *Lethaia*, 27:285–290.
- , AND C.E. MITCHELL. 1991. Late Ordovician extinction in the Graptoloidea, p. 143–156. *In* C.R. Barnes and S.H. Williams (eds.), *Advances in Ordovician Geology*. Geological Survey of Canada, Paper 90-9.
- MORRISON, J.O., AND U. BRAND. 1986. Geochemistry of recent marine invertebrates. *Geoscience Canada*, 13:237–254.
- NESTOR, H. 1990a. Basin development and facies models, p. 33–36. *In* D. Kaljo and H. Nestor (eds.), *Field Meeting, Estonia: An Excursion Guidebook*. Estonian Academy of Sciences, Tallinn.
- . 1990b. Some aspects of lithology of the Ordovician and Silurian rocks, p. 27–32. *In* D. Kaljo and H. Nestor (eds.), *Field Meeting, Estonia: An Excursion Guidebook*. Estonian Academy of Sciences, Tallinn.
- NESTOR, V. 1994. Early Silurian Chitinozoans of Estonia and Northern Latvia. *Academia*, 4, Tallinn.
- PRENTICE, M.L., AND R.K. MATTHEWS. 1988. Cenozoic ice-volume history: development of a composite oxygen isotope record. *Geology*, 16:963–966.
- ROWLEY, D.B., AND P.J. MARKWICK. 1992. Haq et al. eustatic sea-level curve: implications for sequestered water volumes. *Journal of Geology*, 100:703–715.
- RUSH, P.F., AND H.S. CHAVETZ. 1990. Fabric-retentive, non-luminescent brachiopods as indicators of original $\delta^{13}\text{C}$ and $\delta^{18}\text{O}$ composition: a test. *Journal of Sedimentary Petrology*, 60:968–981.
- SAMTLEBEN, C., A. MUNNECKE, AND T. BICKERT. 1995. The Silurian of Gotland (Sweden): facies interpretation based on stable isotopes in brachiopod shells. *Geologische Rundschau*, 85:278–292.
- SCHRAG, D.P., G. HAMPT, AND D.W. MURRAY. 1992. Pore fluid constraints on the temperature and oxygen isotopic composition of the glacial ocean. *Science*, 183:1930–1932.
- SHACKLETON, N., AND A. BOERSMA. 1981. The climate of the Eocene ocean. *Journal of the Geological Society of London*, 138:153–157.
- UNDERWOOD, C.J., S.F. CROWLEY, J.D. MARSHALL, AND P.J. BRENCHLEY. *In press*. High resolution carbon isotope stratigraphy of the basal Silurian stratotype (Dob's Linn, Scotland) and its global correlation. *Journal of the Geological Society of London*, 154.
- VEIZER, J., P. FRITZ, AND B. JONES. 1986. Geochemistry of brachiopods: oxygen and carbon isotopic records of Paleozoic oceans. *Geochimica et Cosmochimica Acta*, 50:1679–1696.
- WADLEIGH, M.A., AND J. VEIZER. 1992. $^{18}\text{O}/^{16}\text{O}$ and $^{13}\text{C}/^{12}\text{C}$ in Lower Paleozoic articulate brachiopods: implications for the isotopic composition of seawater. *Geochimica et Cosmochimica Acta*, 56:431–443.
- WANG K., C.J. ORTH, M.A. ATTREP, B.D.E. CHATTERTON, WANG X., AND LI J. 1993. The great latest Ordovician extinction on the South China Plate: chemostratigraphic studies of the Ordovician–Silurian boundary interval on the Yangtse Platform. *Palaeogeography, Palaeoclimatology, Palaeoecology*, 104:61–79.
- WEFER, G., AND W.H. BERGER. 1991. Isotope paleontology: growth and composition of extant calcareous species. *Marine Geology*, 100:207–248.
- WENZEL, B., AND M.M. JOACHIMSKI. 1995. Carbon and oxygen isotopic composition of Silurian brachiopods (Gotland/Sweden): palaeoceanographic implications. *Palaeogeography, Palaeoclimatology, Palaeoecology*, 122, 143–166.

APPENDIX 1

COMPARISONS OF MEAN OXYGEN AND CARBON STABLE-ISOTOPE VALUES OF SELECTED GENERA IN THREE MEMBERS OF THE SAARDE FORMATION (LLANDOVERY).

Member	Taxon	n=	$\delta^{18}\text{O}\text{‰}$		$\delta^{13}\text{C}\text{‰}$		Range(‰)	
			x	l σ	x	l σ	$\delta^{18}\text{O}$	$\delta^{13}\text{C}$
Staicele	<i>Onniella</i>	7	-4.90	0.12	0.88	0.03	0.30	0.11
	<i>Leangella</i>	5	-4.88	0.06	0.90	0.08	0.16	0.22
Lemme	<i>Leangella</i>	13	-4.60	0.17	1.09	0.22	0.66	0.67
	<i>Meifodia</i>	6	-4.54	0.13	0.77	0.26	0.36	0.74
Kolka	<i>Meifodia</i>	5	-4.31	0.19	0.82	0.7	1.77	0.38
	<i>Onniella</i>	6	-4.57	0.13	0.75	0.12	0.34	0.47

APPENDIX 2

$\delta^{13}\text{C}$ AND $\delta^{18}\text{O}$ VALUES OF RUHNU CORE BRACHIOPODS. "INDETERMINATE" REFERS TO SHELL FRAGMENTS THAT COULD NOT BE IDENTIFIED. SAMPLE NUMBER IS DEPTH IN METERS (SEE SCALE IN FIGURE 2).

Sample No.	Stratigraphic Unit	Order	Family	Genus	$\delta^{13}\text{C}$ (‰)	$\delta^{18}\text{O}$ (‰)
401.4	Jamaja Formation	Orthida	Dalmanellidae	Onniella	1.94	-3.792
402.6	Jamaja Formation	Orthida	Dalmanellidae	Resserella	2.313	-3.754
405.9	Jamaja Formation	Indeterminate			2.597	-3.527
407.5	Jamaja Formation	Indeterminate			2.197	-3.264
407.75	Jamaja Formation	Indeterminate			2.64	-3.557
408.8	Jamaja Formation	Indeterminate			2.485	-4.138
414.3	Paramaja Formation	Indeterminate			1.73	-3.389
415.2	Paramaja Formation	Orthida	Dalmanellidae		1.873	-3.632
416.75	Paramaja Formation	Strophomenida		cf. Eoplectodonta	2.298	-2.986
424.3	Paramaja Formation	Indeterminate			3.838	-4.215
425.5	Paramaja Formation	Orthida	Dalmanellidae	Resserella sabrinae	3.51	-3.178
425.5	Paramaja Formation	Orthida	Dalmanellidae	Resserella sabrinae	3.545	-3.463
426.5	Paramaja Formation	Indeterminate			3.542	-3.685
430	Paramaja Formation	Indeterminate			3.219	-2.982
430.5	Paramaja Formation	Pentamerida		cf. Clorinda	3.139	-3.038
432.85	Paramaja Formation	Indeterminate			3.353	-3.469
433.3	Paramaja Formation	Pentamerida		cf. Clorinda	3.186	-2.795
435.2	Paramaja Formation	Indeterminate			3.054	-3.466
436.8	Paramaja Formation	Orthida	Dalmanellidae	Resserella sp.	3.97	-3.649
447.5	Tolla Member	Indeterminate			3.229	-3.891
448.6	Tolla Member	Strophomenida			3.671	-4.236
455.1	Velise Formation	Indeterminate			0.401	-5.185
455.1	Velise Formation	Strophomenida			0.432	-5.142
455.9	Velise Formation	Orthida	Skenidiidae	Skenidioides	0.659	-5.551
457.85	Velise Formation	Strophomenida	Sowerbyellidae	Eoplectodonta	0.532	-5.252
458.85	Velise Formation	Orthida	Dalmanellidae	Onniella	0.352	-5.346
460.1	Velise Formation	Orthida	Skenidiidae	Skenidioides	0.274	-5.348
460.1	Velise Formation	Orthida	Skenidiidae	Skenidioides	0.311	-5.312
463.6	Velise Formation	Orthida	Dalmanellidae	Visbyella	1.019	-5.346
467.5	Velise Formation	Pentamerida			0.93	-5.33

APPENDIX 2 (CONTINUED)

Sample No.	Stratigraphic Unit	Order	Family	Genus	$\delta^{13}\text{C}$ (‰)	$\delta^{18}\text{O}$ (‰)
470.78	Velise Formation	Spiriferida	Indet atrypid		0.879	-5.385
471.3	Velise Formation	Spiriferida	Lissatrypidae	Glassia	1.336	-5.332
478.7	Velise Formation	Orthida	Skenidiidae	Skenidioides	1.845	-5.121
483.5	Velise Formation	Spiriferida	Lissatrypidae	Glassia	1.129	-5.493
488	Velise Formation	Pentamerida			1.145	-5.507
493.6	Staicele Member	Orthida	Dalmanellidae		0.93	-4.93
494.4	Staicele Member	Indeterminate			1.69	-4.325
496.7	Staicele Member	Strophomenida	Leptellinidae	Leangella	1.01	-5.282
500.6	Staicele Member	Orthida	Dalmanellidae	Onniella	0.808	-5.026
500.6	Staicele Member	Orthida	Dalmanellidae	Onniella	0.924	-4.887
500.85	Staicele Member	Orthida	Dalmanellidae	Onniella	0.895	-4.778
500.85	Staicele Member	Orthida	Dalmanellidae		0.905	-4.897
500.85	Staicele Member	Orthida	Dalmanellidae		0.919	-5.06
500.85	Staicele Member	Strophomenida	Leptellinidae	Leangella	0.904	-4.869
500.85	Staicele Member	Strophomenida	Leptellinidae	Leangella	0.807	-4.974
500.85	Staicele Member	Strophomenida	Leptellinidae	Leangella	0.925	-4.861
500.85	Staicele Member	Strophomenida	Leptellinidae	Leangella	1.027	-4.919
502.6	Staicele Member	Orthida	Dalmanellidae		0.885	-4.752
502.6	Staicele Member	Strophomenida			0.852	-4.813
502.9	Staicele Member	Spiriferida	Lissatrypidae	Meifodia	0.628	-4.39
502.9	Staicele Member	Spiriferida	Lissatrypidae	Meifodia	0.709	-4.333
503.7	Staicele Member	Orthida	Dalmanellidae		0.845	-5.048
508.2	Staicele Member	Spiriferida	Lissatrypidae	Meifodia	0.92	-4.743
509.4	Staicele Member	Indeterminate			1.147	-5.009
509.4	Staicele Member	Indeterminate			1.19	-4.727
509.4	Staicele Member	Indeterminate			1.11	-4.89
509.4	Staicele Member				0.921	-4.661
512.3	Staicele Member	Orthida	Dalmanellidae	Onniella	0.914	-4.927
512.3	Staicele Member	Orthida	Dalmanellidae	Onniella	0.677	-4.967
514.9	Ikla Member	Spiriferida	Lissatrypidae	Meifodia	0.975	-4.899
523.5	Ikla Member	Orthida	Dalmanellidae		1.107	-5.275
523.95	Ikla Member	Indeterminate			0.866	-4.52
523.95	Ikla Member	Strophomenida	Leptellinidae	Leangella	0.913	-4.526
523.95	Ikla Member	Strophomenida	Leptellinidae	Leangella	1.437	-5.012
523.95	Ikla Member	Strophomenida	Leptellinidae	Leangella	1.575	-4.845
523.95	Ikla Member	Strophomenida	Leptellinidae	Leangella	0.984	-4.435
523.95	Ikla Member	Strophomenida	Leptellinidae	Leangella	1.017	-4.664
523.95	Ikla Member	Strophomenida			0.993	-4.464
523.95	Ikla Member	Strophomenida			0.95	-4.349
523.95	Ikla Member	Strophomenida	Leptellinidae	Leangella	0.901	-4.592
525.2	Ikla Member	Indeterminate			0.824	-4.624
525.2	Ikla Member	Indeterminate			0.99	-4.282
525.2	Ikla Member	Indeterminate			0.799	-4.595
526.6	Ikla Member	Spiriferida	Lissatrypidae	Meifodia	0.914	-4.651
527.3	Ikla Member	Strophomenida	Leptellinidae	Eoplectodonta	1.136	-4.478
527.8	Ikla Member	Strophomenida			0.997	-4.516
528.6	Ikla Member	Strophomenida		cf. Eoplectodonta	0.977	-4.685
528.6	Ikla Member	Strophomenida		cf. Eoplectodonta	1.021	-4.635
531.02	Ikla Member	Strophomenida			1.383	-4.605
531.5	Ikla Member	Spiriferida	Lissatrypidae	Meifodia	0.242	-4.591
535.4	Ikla Member	Indeterminate			1.401	-4.168
540.2	Ikla Member	Strophomenida	Leptellinidae	Leangella	2.07	-4.628
540.45	Ikla Member	Spiriferida	Lissatrypidae	cf. Meifodia	1.542	-4.546
540.45	Ikla Member	Strophomenida	Sowerbyellidae	Eoplectodonta	1.679	-4.892

APPENDIX 2 (CONTINUED)

Sample No.	Stratigraphic Unit	Order	Family	Genus	$\delta^{13}\text{C}$ (‰)	$\delta^{18}\text{O}$ (‰)
547.1	Ikla Member	Indeterminate			2.422	-4.589
548.55	Ikla Member	Indeterminate			1.197	-5.224
558.6	Kolka Member	Indeterminate			0.301	-4.351
558.6	Kolka Member	Indeterminate			0.555	-4.076
558.6	Kolka Member	Spiriferida	Lissatrypidae	Meifodia	0.54	-4.432
559	Kolka Member	Orthida	Dalmanellidae	Onniella	0.682	-4.326
562.9	Kolka Member	Spiriferida	Lissatrypidae	Meifodia	0.652	-4.548
564.8	Kolka Member	Orthida	Dalmanellidae	Onniella	0.924	-4.579
564.8	Kolka Member	Orthida	Dalmanellidae	Onniella	0.856	-4.711
564.8	Kolka Member	Spiriferida	Lissatrypidae	Meifodia	2.071	-4.168
565.7	Kolka Member	Orthida	Dalmanellidae	Onniella trigona	0.785	-4.668
566	Kolka Member	Orthida	Dalmanellidae	Onniella	0.577	-4.612
566	Kolka Member	Orthida	Dalmanellidae	Onniella	0.707	-4.562
569.2	Slitere Member	Orthida	Dalmanellidae	Onniella	0.448	-4.834
569.2	Slitere Member	Spiriferida	Lissatrypidae	Meifodia	0.729	-4.768
572.9	Slitere Member	Spiriferida	Lissatrypidae	Meifodia	1.071	-4.636
573.6	Slitere Member	Indeterminate			0.922	-4.035
590.2	Ohne Formation	Orthida	Dalmanellidae		0.439	-4.049
590.2	Ohne Formation	Indeterminate			0.206	-4.285
590.3	Ohne Formation	Orthida	Dalmanellidae		0.71	-4.223
590.5	Ohne Formation	Spiriferida	Lissatrypidae	Meifodia	0.06	-3.936
590.9	Ohne Formation	Orthida	Dalmanellidae		0.511	-4.629
595.4	Ohne Formation	Orthida	Dalmanellidae		0.273	-3.989
600.5	Ohne Formation	Orthida	Skenidiidae	Skenidioides	0.87	-4.081
605.3	Kuldiga Formation	Spiriferida		Hindella? sp.	6.023	-0.429
609	Kuldiga Formation	Strophomenida			5.95	-2.465
609.9	Kuldiga Formation	Rhynchonellida		Plectothyrella	6.502	0.276
610	Kuldiga Formation	Indeterminate			6.757	-0.09
611.8	Kuldiga Formation	Rhynchonellida		Plectothyrella	7.057	0.676
612.5	Kuldiga Formation	Orthida		Hirnantia sp.	5.909	-1.483
616.9	Kuldiga Formation	Rhynchonellida		Plectothyrella	5.591	-1.105
617.25	Kuldiga Formation	Strophomenida	Leptaenidae	Leptaena	6.198	-1.188
619.7	Kuili Formation	Indeterminate			1.016	-3.501
620.4	Kuili Formation	Orthida	Dalmanellidae		1.598	-2.794

APPENDIX 3

ESTIMATED SEA-LEVEL FALL FOR A 2‰ OXYGEN ISOTOPE SHIFT FOR FIVE COMBINATIONS OF ICE VOLUME AND TEMPERATURE EFFECTS AND FOR THREE ESTIMATES OF $\delta^{18}\text{O}_{\text{OCEANWATER}}$. VALUES FOR CHANGE IN $\delta^{18}\text{O}$ PER METER OF SEA-LEVEL CHANGE ARE FOR DIFFERENT ESTIMATES OF GLACIAL-INTERGLACIAL CHANGES BASED ON DATA FROM THE LAST INTERGLACIAL AND ASSUME A GLACIAL-INTERGLACIAL SEA-LEVEL CHANGE OF 120 M. THIS CALIBRATION MAY NOT BE DIRECTLY APPLICABLE TO NON-GLACIAL TIMES OR TO NON-GLACIAL-GLACIAL TRANSITIONS, BUT PROVIDES A USEFUL COMPARISON. VALUES (A), (B), (C) AFTER EMILIANI AND SHACKLETON (1978 IN ROWLEY AND MARKWICK, 1992), FAIRBANKS AND MATTHEWS (1978), AND SCHRAG ET AL. (1992), RESPECTIVELY.

	Component due to change in ice volume (‰)	Component due to change in temperature (‰)	Temperature change (°C)	(a) 0.0137‰ m ⁻¹	(b) 0.0 11‰m ⁻¹	(c) 0.008‰m ⁻¹
(1)	2	0	0	150	182	241
(2)	1.5	0.5	2.25	113	136	181
(3)	1	1	4.5	75	91	120
(4)	0.5	1.5	6.75	36	45	60
(5)	0	2	9	—	—	—



ISSN: 0278-3355

ISBN: 1-55557-206-5

The New York State Museum is a program of
The University of the State of New York
The State Education Department